

Rothamsted Repository Download

PhD Thesis

Heard, S. 2014. *Plant Pathogen Sensing for Early Disease control*. PhD Thesis Rothamsted Research

The output can be accessed at: <https://repository.rothamsted.ac.uk/item/8wq13>.

© 9 February 2014, Please contact library@rothamsted.ac.uk for copyright queries.

Plant Pathogen Sensing for Early Disease Control

A thesis submitted to the University of Manchester for the
degree of Doctor in Philosophy in the Faculty of Engineering
and Physical Sciences

2013

Stephanie Heard

School of Electrical and Electronic Engineering

Table of Contents

Table of Contents	2
List of Figures	10
List of Tables	13
List of abbreviations	16
Abstract.....	18
Declaration.....	19
Copyright	19
Acknowledgements.....	20
Chapter 1: General Introduction.....	21
1.1 The challenges of securing food for a growing global population	21
1.2 The use of crop protection in agricultural systems.....	22
1.3 The role of fungal pathogens in agriculture	24
1.4 Fungal infection modes	28
1.5 Technological advances in fungal pathogen forecasting systems, detection and diagnosis in agricultural systems.....	29
1.6 Detection and diagnosis of plant pathogens	30
1.6.1 DNA-based detection methods.....	30
1.6.2 Immunology-based/ Antibody-based detection methods	31
1.6.3 Antibodies for metabolite sensing.....	33
1.6.4 Biosensor for pathogen detection	34
1.6.4.1 Surface plasmon resonance (SPR).....	35
1.6.4.2 Electrochemical biosensors	35
1.6.4.3 Wireless biosensor networks.....	36
1.7 The SYield biosensor consortium	38
1.8 <i>Sclerotinia sclerotiorum</i> : the pathogen of choice for the SYield Biosensor	39
1.8.1 <i>Sclerotinia sclerotiorum</i> : Taxonomy.....	39
1.8.2 Advances in the genome sequencing of <i>Sclerotinia sclerotiorum</i>	40
1.8.3 <i>Sclerotinia sclerotiorum</i> : Life cycle and infection strategy	40
1.8.4 Oxalic acid and its role in <i>Sclerotinia sclerotiorum</i> infection	44
1.8.5 Biosynthesis of OA	46
1.8.6 <i>Sclerotinia sclerotiorum</i> : a necrotroph, a biotroph or something in between?.....	49
1.8.7 Control of <i>Sclerotinia sclerotiorum</i> in the field	49
1.8.8 Forecasting systems available for <i>S. sclerotiorum</i>	50
1.9 Project objectives	51
1.9.1 Hypotheses to be tested:	52
Chapter 2: General Experimental Procedures.....	53

2.1 <i>S. sclerotiorum</i> sclerotia and ascospore production	53
2.2 <i>S. sclerotiorum</i> mycelial cultures	53
2.3 Bioassay to test different complex media to induce oxalic acid production by <i>S. sclerotiorum</i> ascospores	55
2.4 Sigma high throughput spectrophotometric determination of oxalic acid in liquid media	56
2.6 Calculation of the concentration of oxalic acid in samples	57
2.7 Statistical analysis	58
2.8 DNA extraction	58
2.8.1 Hyphae DNA extraction	58
2.8.2 <i>S. sclerotiorum</i> ascospores DNA extraction	58
2.9 RNA extraction	59
2.10 Amplification of DNA targets using Polymerase Chain Reaction	59
2.11 Quantitative Polymerase Chain Reaction	60
Chapter 3: The development of an electrochemically compatible biological matrix for the specific induction of <i>S. sclerotiorum</i> ascospore germination and oxalic acid secretion to be used within an infield automated detection biosensor.	61
3.1.1 Introduction	61
3.1.2 Considerations for the biological matrix design and biosensor detection success	64
3.2 Experimental Procedures	67
3.2.1 Bioassay for the quantification of OA produced by ascospores in on solid media made from plant extracts	67
3.2.2 Preliminary experiments	69
3.2.2.1 Detection limits of Sigma OxOx enzymatic spectrophotometric assay	69
3.2.2.2 Preliminary work to determine whether any additions to assay can inhibit enzyme activity	69
3.2.2.3 Storing medium for later OA detection and electrochemical analysis.	69
3.2.2.4 <i>The effect of temperature, shaking and a flotation membrane on OA production.</i>	70
3.2.3 OA production induction via Tricarboxylic Acid Cycle intermediates combined with a baseline nutrient	70
3.2.4 Complex media (Soytone and Yeast) combined with TCA cycle intermediates and their effect on OA production	70
3.2.5 The influence of different glucose concentrations on OA production in a complex medium. .	71
3.2.6 TCA cycle intermediate additions	71
3.2.7 Comparison four electrochemical compatible media for OA induction	72
3.2.8 Limits of detection.	72

3.2.9 The relationship between <i>S. sclerotiorum</i> ascospore number, biomass and oxalic acid production	72
3.2.10 Buffering Capacity of the medium	73
3.2.11 Competition assays.....	74
3.2.12 High throughput fungicide sensitivity testing	74
3.3 Results.....	76
3.3.1 The used of host plant extracts within a solid matrix	76
3.3.2 Liquid medium is better than solid medium for the quantification of OA	77
3.3.3 Preliminary experiments	79
3.3.3.1 <i>Detection limits of Sigma OxOx enzymatic spectrophotometric assay</i>	79
3.3.3.2 <i>Preliminary work to determine whether any additions to assay can inhibit enzyme activity</i>	80
3.3.3.3 <i>Storing medium for later OA detection and electrochemical analysis</i>	81
3.3.3.4 <i>The effect of temperature, shaking and a flotation membrane on OA production</i>	82
<i>Figure 18: The effect of different environmental conditions on OA production.</i>	82
3.3.3.5 <i>Creating a more defined medium which induces OA secretion and is compatible with both the enzymatic spectrophotometric assay and the biosensor electrochemistry</i>	83
3.3.3.6 <i>OA production induction via Tricarboxylic Acid Cycle intermediates combined with a baseline nutrient</i>	84
3.3.4 Complex media (Soytone and Yeast) combined with TCA cycle intermediates and their effect on OA production.....	86
3.3.5 The influence of glucose concentration on OA production in a complex medium	87
3.3.6 TCA cycle intermediate additions	90
3.3.7 Electrochemical-compatibility of the defined medium for biosensor development	93
3.3.8 Comparison four electrochemical compatible media for OA induction	95
3.3.9 Limits of detection	97
3.3.10 Verifying spore counts using DNA quantification	98
3.3.11 The relationship between <i>S. sclerotiorum</i> ascospore number, biomass and oxalic acid production	99
3.3.12 Buffering Capacity of the medium	104
3.3.13 The effect of competing fungi on oxalic acid production.....	109
3.3.14.1 <i>Competition assays</i>	109
3.3.14.2 <i>Fungicide additions to the medium</i>	111
3.4 Discussion	115
3.4.1 Optimising OA secretion from ascospores in a liquid matrix	115
3.4.2 pH and Buffering of complex media to maintain OA production	116
3.4.3 The relationship between <i>S. sclerotiorum</i> ascospore number, biomass and oxalic acid production	117
3.4.4 Selectivity of the medium	119

Chapter 4: The testing of an electrochemically compatible nutrient medium for detection of oxalic acid produced by <i>S. sclerotiorum</i> ascospores within an oilseed rape system.	120
4.1.1 Introduction	120
4.1.2 Objectives of field trials:	120
4.2 Experimental Procedures	121
4.2.1 Field trial set up.....	121
4.2.2 Medium testing.....	124
4.2.3 Electrochemical Measurement of oxalic acid production	126
4.2.4 Daily spore counts of qPCR of field trial samples	128
4.2.5 ITS identification of other fungi present in field samples	128
4.3 Results	128
4.3.1 Field trial results 2011	128
4.3.1.1 Apothecia development and visible signs of <i>S. sclerotiorum</i> disease in the field, 2011..	128
4.3.1.2 OxOx spectrophotometer assay, 2011	129
4.3.1.3 Validation of <i>S. sclerotiorum</i> DNA using qPCR 2011	129
4.3.2. Field trial Results 2012	132
4.3.2.1 Apothecia development in the field 2012	132
4.3.2.2 OxOx spectrophotometer assay and electrochemical detection of OA 2012	132
4.3.2.3 Validation of <i>S. sclerotiorum</i> DNA using qPCR 2012	133
4.3.2.4 Disease Assessment 2012.....	134
4.3.2.5 Rooftop sampling for both field trials.	138
4.3.2.6 Isolation of other fungal species present within the field samples.....	140
4.4 Discussion	143
4.4.1 Summary of field trials.....	143
4.4.2 Fungal contaminants	143
4.4.3 The use of an electrochemical biosensor to detect OA.....	145
4.4.4 Positioning of sampling equipment	146
4.4.5 Equipment failures	146
4.4.6 Future of SYield	147
Chapter 5: Predicting the secretome of <i>Sclerotinia sclerotiorum</i> to identify novel detection targets and candidate genes that play a role during infection.	150
5.1 Introduction	150
5.2 Experimental Procedures	151
5.2.1 Bioinformatics.....	151
5.2.2 Stage 1: Predicting the total secretome	152
5.2.4 Genes coding for proteins with a known function.....	153

5.2.5 <i>S. sclerotiorum</i> genome map	153
5.2.6 Blast2Go analysis	154
5.2.7 EST support.....	154
5.2.8 Multispecies Comparison	154
5.3 Results.....	155
5.3.1 The predicted secretomes of <i>S. sclerotiorum</i> and <i>B. cinerea</i>	155
5.3.2 Distribution of the genes coding for the refined secretome across the <i>S. sclerotiorum</i> genome	157
5.3.3 Identifications of RxLR-dEER motifs and Y/F/WxC motifs in the <i>S. sclerotiorum</i> refined secretome.	164
5.3.4 EST support analysis for the secretome	166
5.3.5 EST support for unannotated sequences.....	168
5.3.6 Further analysis of unannotated sequences	168
5.3.7 PFAM abundance within predicted secreted proteins with a potential plant cell degrading function	170
5.3.8 Further analysis of PFAM abundance across the <i>S. sclerotiorum</i> refined secretome.....	173
5.3.9 Biological, functional and compartmental analysis of the <i>S. sclerotiorum</i> secretome	175
5.3.10 Proteome support for the refined secretome.....	177
5.3.11 Known virulence factors identified in the refined secretome	179
5.3.12 Multispecies comparison analysis	181
5.3.12.1 <i>Uniquely secreted proteins</i>	181
5.3.12.2 <i>Shared proteome homology between species</i>	182
5.3.12.3 <i>Multispecies comparison of gene copy</i>	185
5.4 Discussion	187
Chapter 6: Using the <i>S. sclerotiorum</i> secretome to identify uniquely secreted protein targets for infield disease detection.	192
6.1 Introduction	192
6.2 Experimental Procedures.....	195
6.2.1 Bioinformatics.....	195
6.2.2 GPI Anchors.....	195
6.2.3 Primer design used for PCR screening and RT-qPCR	196
6.2.4 First Strand cDNA synthesis	197
6.2.5 Generating GFP tagged protein targets	197
6.2.6 Transformation of competent cells with pBluntNAT-Odc2GFP vector:.....	198
6.2.7 Restriction Digests	199
6.2.7.1 <i>Verification of construct</i>	199
6.2.7.2 <i>Restriction digest of construct template inserts</i>	199
6.2.8 Primer design for construct template insert	199

6.2.9 Amplification of insert	200
6.2.10 Ligation of the digested inserts and plasmid.	200
6.2.11 Methods for Fungal Transformation	201
6.2.11.1 Protoplast production	201
6.2.11.2 Transformation of <i>S.sclerotiorum</i> protoplasts	202
6.2.11.3 DNA extraction for southern and PCR	205
6.2.11.4 Polymerase chain reaction for verification of gene integration	206
6.2.11.5 Southern Blot	206
6.2.11.5.1 DNA digestion.....	206
6.2.11.5.2 Probe synthesis	207
6.2.11.5.3 Southern blot and hybridisation.....	207
6.2.11.5.4 Washing and detection.....	208
6.2.11.5.5 Chemiluminescent detection film development.....	208
6.2.11.5.6 Film development.....	208
6.2.12 GFP fluorescence under different environmental growth conditions	208
6.2.12.1 Solid growth.....	209
6.2.12.2 Liquid medium	209
6.2.12.3 In planta infection.....	209
6.3 Results.....	210
6.3.1 Bioinformatics.....	210
6.3.1.2 Gene selection method 2.....	210
6.3.1.3 GPI Anchor analysis.....	211
6.3.2 Screening of isolates.....	212
6.3.3 EST support and relative gene expression of unique putative secreted proteins.	214
6.3.4 RNA sequencing expression	215
6.3.5 GFP transformation: construct development	216
6.3.6 <i>S. sclerotiorum</i> transformation	216
6.3.7 Southern Blot	218
6.3.8 GFP fluorescence of secreted proteins under different growth conditions.	219
6.3.9 Updated BlastP results	230
6.4 Discussion	230
6.4.1 The use of a bioinformatics pipeline to select protein targets for pathogen detection.....	230
6.4.2 Protein expression verification.....	231
6.4.3 GFP as a reporter tag for secreted proteins	233
Chapter 7: A comparative investigation into the transcriptomes of wild type and an oxalic acid deficient <i>S. sclerotiorum</i> mutant during <i>in vitro</i> growth and infection of <i>Arabidopsis</i> leaves.....	235
7.1 Introduction	235

7.2 Experimental Procedures	236
7.2.1 Plant varieties, fungal strains and infection conditions.	236
7.2.2 RNA extraction	237
7.2.3 TruSeq RNA Library Construction (ICBR Experimental procedure)	238
7.2.4 Illumina GAIIx Sequencing (ICBR Experimental procedure)	238
7.2.5 Bioinformatics Analysis	238
7.3 Results	241
7.3.1 Challenges with using Δoah mutant to obtain high quality RNA.....	241
7.3.2 Calculation of the percentage of reads aligned to each reference genome	241
7.3.3 The most abundant transcripts in each library.....	246
7.3.4 Comparison of significant differential putative secreted protein gene expression events across the different conditions.....	248
7.3.5 Expressed putative secreted proteins.....	249
7.3.6 Comparison of significantly expressed secreted proteins during WT in vitro conditions and in planta infection.....	251
7.3.7 Comparison of significantly expressed secreted proteins during WT and Δoah in vitro conditions	256
7.3.8 The botcinic acid biosynthesis cluster.....	257
7.3.9 Expression of appressoria associated genes	260
7.3.10 Expression of documented virulence genes.....	261
7.3.11 Polygalacturonase expression.....	263
7.3.12 Genes with similar expression patterns as <i>oah</i>	265
7.4 Discussion	268
7.4.1 Genes with the highest abundance	268
7.4.2 Expression of the putative refined secretome.....	269
7.4.3 Botcinic acid gene cluster expression.....	271
7.4.4 Proposed virulence genes	273
7.4.5 Polygalcturonases expression.....	276
7.4.6 Genes with a similar expression pattern as <i>oah</i>	277
Chapter 8: General Discussion	279
8.1 Summary of key findings and developments	279
8.2 Development of a robust method for ascospore production	281
8.3 Advances in Decision Support Systems for monitoring <i>S. sclerotiorum</i> disease outbreaks and the future of the SYield biosensor	282
8.4 Advances in pathogenomics	286
8.5 Advances in the understanding of <i>S. sclerotiorum</i> biology through genomics	287
List of References	293

Appendices	312
Appendix 1: The 432 genes which make up the refined <i>S. sclerotiorum</i> secretome.	312
Appendix 2: The 499 genes which make up the refined <i>B.cinerea</i> secretome	319
Appendix 3: Secretome sequence sets mapped across the <i>S. sclerotiorum</i> refined secretome.....	327
Appendix 4.1: Plant polysaccharide degrading proteins.....	329
Appendix 4.2: Lipid degrading proteins.....	331
Appendix 4.3: Protein degrading proteins.....	332
Appendix 5: The proteomes used in the cross species comparison.....	333
Appendix 6: The cross species comparison between the 432 protein sequences in the <i>S. scleroriotum</i> refined sectrome and the homologous	336
Appendix 7: Field Trials results 2011.	342
Appendix 8: Field Trial results 2012.....	343

List of Figures

Figure 1: Estimated disease loss in oilseed rape.	25
Figure 2: The DAS-ELISA assay.	32
Figure 3: Positive and negative detection of pathogens using handheld lateral flow devices.	33
Figure 4: The basic components of a biosensor system.	34
Figure 5: The life cycle and disease strategy of <i>S. sclerotiorum</i> in oilseed rape systems.	42
Figure 6: A visible cloud- like puff of ascospores released from <i>S. sclerotiorum</i> apothecia.	43
Figure 7: The Tricarboxylic Cycle taken from Kegg.	48
Figure 8: The 12 well plate used to test various liquid media for oxalic acid production by <i>S. sclerotiorum</i> ascospores.	55
Figure 9: Oxalic acid concentration determined using a high throughput spectrophotometric assay.	57
Figure 10: Schematic of the basic principles of electrochemistry used in the SYield biosensor.	64
Figure 11: The standard OA concentration agar plates.	68
Figure 12: Plate set up for fungicide sensitivity assay.	75
Figure 13: BPB bleaching caused by three <i>S. sclerotiorum</i> different spore solutions.	77
Figure 14: Different amounts of sclerotia formation on different agars containing BPB.	77
Figure 15: Detection limits of the Sigma OxOx enzymatic spectrophotometric assay.	79
Figure 16: Absorbance readings of known concentrations of OA in PDB media containing different concentrations of the malate.	80
Figure 17: Storing medium for later OA detection and electrochemical analysis.	81
Figure 18: The effect of different environmental conditions on OA production.	82
Figure 19: The effect of different additions to minimal nutrient media on OA production.	85
Figure 20: The effects of soytone and yeast media on OA production.	86
Figure 21: The effect of adding glucose to complex growth media to induce OA production by <i>S. sclerotiorum</i> ascospores.	87
Figure 22. The effect of increasing glucose concentrations on OA production.	89
Figure 23. The effect of adding different TCA cycle intermediates on OA production.	92
Figure 24: The effect of different media on the efficiency of the electrochemical assay.	94
Figure 25: Oxalic acid production by <i>S.sclerotiorum</i> ascospores in different, electrochemical compatible media.	96
Figure 26: The effects of different ascospore number on OA production.	97
Figure 27: Using qPCR to determine accurate ascospore numbers and OA production.	99
Figure 28: The relationship between OA production, pH change and dry biomass accumulation of different ascospores dilutions.	102
Figure 29: Predicted means generated by the REML analysis.	103
Figure 30: Buffering capacity of MES buffer.	105
Figure 31: Buffering capacities of HEPES and succinate buffers.	107
Figure 32: The change in pH monitored in buffered media.	108
Figure 33: Oxalic acid produced by different fungal species isolated from field trial samples.	110

Figure 34: The effect of fungal contaminants on oxalic acid production by two different spore dilutions.	110
Figure 35: The effect of combined fungicide treatment on <i>S. sclerotiorum</i> fungal competitors.	114
Figure 36: Air sampling devices used during field trials.	122
Figure 37: Field set up for 2011 and 2012.	123
Figure 38: Pot incubation assay.	125
Figure 39: Electrochemical set up.	127
Figure 40: Field trial results 2011.	130
Figure 41: Field trial results 2011.	131
Figure 42: Oilseed rape with <i>S. sclerotiorum</i> disease symptoms.	134
Figure 43: Field trial 2012 field results.	135
Figure 44: Field trial result 2012.	136
Figure 45: Disease assessment.	137
Figure 46: Rooftop <i>S. sclerotiorum</i> detection.	139
Figure 47: The 2013 automated SYield device.	148
Figure 48: <i>S. sclerotiorum</i> secretome pipeline.	158
Figure 49: <i>B. cinerea</i> secretome pipeline.	159
Figure 50: The <i>S. sclerotiorum</i> refined secretome distribution across the 16 mapped chromosomes.	162
Figure 51: The physiological process that the proteins within the refined secretome are involved in. ...	176
Figure 52: The pBluntNAT-Odc2GFP construct generated at JRL.	198
Figure 53: Primer design of construct inserts.	200
Figure 54: The pBluntNAT-GFP construct.	203
Figure 55: Onion infection assay.	209
Figure 56: The relative quantification of putative secreted proteins.	214
Figure 57: Sequencing of the final re-ligated pBluntNAT-Odc2GFP construct.	217
Figure 58: PCR verification of transformed cultures.	218
Figure 59: Southern blot of the <i>S. sclerotiorum</i> transformants generated.	219
Figure 60: Transformant growth on PDA, 12 dpi.	221
Figure 61: GFP fluorescence in <i>S. sclerotiorum</i> transformants grown on cellophane sheets over PDA. ...	222
Figure 62: Transformants grown in YP sucrose broth for four days.	223
Figure 63: GFP fluorescence in <i>S. sclerotiorum</i> transformants grown on water agar.	224
Figure 64: GFP fluorescence in <i>S. sclerotiorum</i> transformants grown on water agar covered with Lilly pollen.	225
Figure 65: <i>S. sclerotiorum</i> transformant infection of onion epidermis.	226
Figure 66: <i>S. sclerotiorum</i> transformant infection of onion epidermis, 1 day post inoculation.	227
Figure 67: Alignments of successfully integrated SP1 and SP4 protein sequences.	229
Figure 68: Bioinformatics workflow for RNAseq alignments.	240
Figure 69: <i>A. thaliana</i> infection with <i>S. sclerotiorum</i> agar plugs inoculated with WT strain and <i>Δoah</i> strain.	243
Figure 70: <i>A. thaliana</i> leaf infection progression over two time points.	244

Figure 71: Leaf staining of fungal infection.....	245
Figure 72: Patterns of secreted protein expression.	255
Figure 73: Botcinic acid cluster.	258
Figure 74: Three subgroups of putative polygalacturonases expressed in during WT <i>in vitro</i> and <i>in planta</i> condition.....	264
Figure 75: Three groups of genes which exhibited similar expression profiles to <i>oah</i>	266
Figure 76: Spore dispersal events of fungal pathogens.	285
Figure 77: Comparison of <i>in planta</i> and <i>in vitro</i> infection/ growth of <i>S. sclerotiorum</i>	291

List of Tables

Table 1: Example of the main fungicide groups and their modes of action	27
Table 2: <i>S. sclerotiorum</i> and <i>B. cinerea</i> isolates used throughout this project	54
Table 3: Methods for detecting OA in clinical samples and for the investigation of OA production by plant pathogens.....	66
Table 4: The baseline minimal salts required for <i>S. sclerotiorum</i> fungal growth.....	83
Table 5: ANOVA results for three experiments testing the effect of succinate, malate and fumarate on OA production.....	91
Table 6: The four media selected for electrochemical compatibility	93
Table 7: The spore counts of different spore solutions determined using qPCR.....	101
Table 8: The REML output for the effects of spore treatment on the production of OA measured in the liquid medium over 11 days.	101
Table 9 : The REML output for the effects of spore treatment on pH of the liquid medium measured over 11 days.	101
Table 10: The REML output for the effects of spore treatment on the <i>S. sclerotiorum</i> biomass monitored over 11 days.	101
Table 11: The different fungicides tested for efficacy against fungi identified in field samples.....	111
Table 12: The concentration of fungicide required to inhibit growth and development of different fungal spores.	112
Table 13: A combined fungicide treatment.	114
Table 14: Batches of samples collected over field trials to be incubated with the medium being tested and then tested for OA.	126
Table 15: OA positive events 2012.	133
Table 16: The different fungal species isolated from the cyclone field samples incubated with medium.	141
Table 17: Seven EST Libraries downloaded from the Broad.....	154
Table 18: Distribution of secreted proteins across the 16 chromosomes of <i>S. sclerotiorum</i>	161
Table 19: Description of the 31 gene clusters distribution across the <i>S.sclerotiorum</i> refined secretome.	163
Table 20: <i>S. sclerotiorum</i> secretome proteins which contain an RXLR motif.	165
Table 21: <i>S. sclerotiorum</i> secretome protein sequences which encode Y/F/WxC motif containing proteins.....	165
Table 22: 28 secretome genes with 40 or more EST counts in at least one EST library.	167
Table 23: <i>S. sclerotiorum</i> small, cysteine rich proteins identified in the refined secretome.....	170
Table 24: The most common PFAM domains involved in degradation of host plant substrate.	172
Table 25: Predicted secreted proteins involved in plant cell wall degradation.....	172
Table 26: The most abundant PFAM domains within the <i>S. sclerotiorum</i> secretome that have non plant cell hydrolytic properties.....	175
Table 27: Secreted proteins involved in general Kegg Pathways.	176
Table 28: The proteins identified in liquid medium after incubation with <i>S. sclerotiorum</i> for several days.	177

Table 29: The 32 proteins identified from sclerotial liquid samples that were found in the <i>S. sclerotiorum</i> refined secretome.	178
Table 30: The proteins known in <i>S. sclerotiorum</i> to be required for virulence during plant infection. ...	180
Table 31: Proteins unique to the <i>S. sclerotiorum</i> refined secretome.	181
Table 32: Proteins unique to the <i>B. cinerea</i> refined secretome.	182
Table 33: Unique <i>S. sclerotiorum</i> and <i>B. cinerea</i> proteins.	183
Table 34: Genes found in <i>S. sclerotiorum</i> and <i>B. cinerea</i> that are also present in only a limited number of other fungi.	185
Table 35: Sequence characteristics for detection targets.	194
Table 36: Primer sets designed for the amplification of unique <i>S. sclerotiorum</i> protein DNA sequences.	196
Table 37: PCR conditions for the different polymerase systems used to amplify the sequences of interest.	201
Table 38: Primer sets designed to amplify construct inserts of putative secreted proteins.	204
Table 39: Three sequences unique to <i>S. sclerotiorum</i>	210
Table 40: Five sequences unique to <i>S. sclerotiorum</i> found that are not in the <i>B. cinerea</i> genome.	211
Table 41: <i>S. sclerotiorum</i> sequences containing GPI anchor motifs with no homologues in the <i>B. cinerea</i> genome.	212
Table 42: Set of putative <i>S. sclerotiorum</i> detection targets.	213
Table 43: The FPKM values for the 8 putative secreted protein gene sequences.	215
Table 44: NCBI BlastP result performed after transformants were made.	228
Table 45: RIN values calculated using an Agilent 2100 Bioanalyser.	242
Table 46: The total reads for each library aligned to both the <i>A. thaliana</i> and <i>S. sclerotiorum</i> reference genome.	242
Table 47: The most abundant <i>S. sclerotiorum</i> transcripts in each RNAseq library.	246
Table 48: The combined genes with the highest FPKM values from each of the five conditions analysed.	247
Table 49: Four comparisons of libraries analysed and the number of statistically significant gene expression events calculated in each comparison.	248
Table 50: The 20 genes with no annotation identified in the secretome which had expression.	249
Table 51: The 68 genes with annotation identified in the secretome which had expression support.	249
Table 52: Forty secreted proteins identified in the <i>S. sclerotiorum</i> refined secretome that account for the 60 statistically significant gene expression events across the comparison of <i>in vitro</i> and <i>in planta</i> conditions.	252
Table 53: Four secreted proteins identified in the refined secretome with significant gene expression between the <i>in vitro</i> WT and <i>Δoah</i> samples.	256
Table 54: The <i>S. sclerotiorum</i> homologue gene identified in <i>B. cinerea</i> which are responsible for the synthesis of botcinic acid.	259
Table 55: The ortholog genes in <i>S. sclerotiorum</i> known to be associated with appressoria formation. .	260
Table 56: Expression of documented virulence genes.	262

Table 57: Seventeen <i>S. sclerotiorum</i> genes identified in the refined secretome as putative polygalacturonases.	264
Table 58: The expression of the top 20 genes with most similar expression profiles to oxaloacetate acetylhydrolase gene across the five libraries.	267

List of abbreviations

µg	microgram
µl	microlitre
µM	micromolar
Avr	Avirulence gene
BLAST	Basic Local Alignment Search Tool
cAMP	Cyclic adenosine monophosphate
cm	centimetre
CO ₂	Carbon dioxide
d.f.	Degrees of Freedom
DNA	Deoxyribonucleic acid
ETI	Effector triggered susceptibility
GFP	Green Fluorescent Protein
GR	Green Revolution
H ₂ O ₂	Hydrogen peroxide
hpi	hours post infection
HR	Hypersensitive Response
hr(s)	hour(s)
JRL	Jeffrey Rollins Laboratory
KEGG	Kyoto encyclopaedia of genes and genomes
km	kilometre
L	litre
M	Molar
mABs	Monoclonal antibodies
MAPK	Mitogen Activated Protein Kinase
mg	milligram
mins	minutes
ml	millilitre
mm	millimetre
mM	millimolar
mU	milliunits
ng	nanogram
NGS	Next generation Sequencing
O ₂	Oxygen
OA	Oxalic acid
°C	Degrees Celsius
OxOx	oxalate oxidase
pABs	Polyclonal antibodies
PAMP	Pathogen associated molecular patterns
PCR	Polymerase Chain Reaction
PCWDEs	Plant cell wall degrading enzymes
PDA	Potato dextrose agar
PDB	Potato dextrose broth
pg	picogram
PGs	Polygalacturonases

PTI	PAMP Triggered Immunity
qPCR	Quantitative PCR
R	Resistance gene
RNA	Ribonucleic acid
RNASeq	Ribonucleic acid sequencing
ROS	Reactive oxygen species
RT	Reverse Transcriptase
SDB	Sabouraud dextrose broth
secs	seconds
seqs	sequences
SNA	Synthetic nutrient agar
SPR	Surface Plasmon Resonance
UV	Ultra Violet

Abstract

The University of Manchester

Stephanie Heard

Degree of Doctor in Philosophy

Thesis Title: Plant Pathogen Sensing for Early Disease Control

September 2013

Sclerotinia sclerotiorum, a fungal pathogen of over 400 plant species has been estimated to cost UK based farmers approximately £20 million per year during severe outbreak (Oerke and Dehne 2004). *S. sclerotiorum* disease incidence is difficult to predict as outbreaks are often sporadic. Ascospores released from the fruiting bodies or apothecia can be dispersed for tens of kilometres. This makes disease control problematic and with no *S. sclerotiorum* resistant varieties available, growers are forced to spray fungicides up to three times per flowering season in anticipation of the arrival of this devastating disease.

This thesis reports the development of the first infield *S. sclerotiorum* biosensor which aims to enable rapid detection of airborne ascospores, promoting a more accurate disease risk assessment and fungicide spraying regime. The sensor is designed to detect the presence of oxalic acid, the main pathogenicity factor secreted during early *S. sclerotiorum* ascospore germination. Upon electrochemical detection of this analyte in the biosensor, a binary output is relayed to farmer to warn him of a disease risk. This project focused on the development of a nutrient matrix which was designed to be contained within the biosensor. The role of this matrix was to promote the growth of captured airborne *S. sclerotiorum* ascospores and induce high levels of oxalic acid secretion. The use of the designed biological matrix to promote oxalic acid production was tested during three field trials in *S. sclerotiorum* artificially inoculated fields.

This thesis describes the use of contemporary pathogenomics technologies to further investigate candidate genes involved in pathogenicity alongside the secretion of oxalic acid. A pre-described bioinformatics pipeline was used to predict the *S. sclerotiorum* secretome to identify potential effector proteins as well as explore proteins which are unique to *S. sclerotiorum* to be used as other novel targets for detection. GFP tagged constructs were designed to investigate the expression of the putative targets for *S. sclerotiorum* detection.

The transcriptomes of wild type and oxalic acid deficient *S. sclerotiorum* strains during infection as well as during a saprotrophic stage were investigated. This study provided expression support for not only some of the unannotated genes identified in the putative secretome, but some candidate genes speculated to be involved in infection.

Declaration

I declare that no portion of the work referred to in the thesis has been submitted in support for another degree or qualification of this or any other university or other institute of learning.

Copyright

- i. The author, Stephanie Heard, of this thesis (including any appendices and/or schedules to this thesis) owns certain copyright or related rights in it (the “Copyright”) and she has given The University of Manchester certain rights to use such Copyright including for administrative purposes.
- ii. Copies of this thesis, either in full or in extracts and whether in hard or electronic form, may be made only in accordance to Copyright, Designs and Patents Act 1988 (as amended) and regulations issued under it or, where appropriate, in accordance with licensing agreements which the University has from time to time. This page must form part of any such copies made.
- iii. The ownership of certain Copyright, patents, designs, trade marks, and other intellectual property (the “The Intellectual Property”) and any reproductions of copyright works in the thesis for example graphs and tables (“Reproductions”), which may be described in this thesis, may not be owned by the author and may be owned by third parties. Such Intellectual Property and Reproductions cannot and must not be made available for use without the prior written permission of the owner(s) of the relevant Intellectual Property and/or Reproductions.
- iv. Further information on the conditions under which disclosure, publication and commercialisation of this thesis, the copyright and any Intellectual Property and/ or Reproductions described in it may take place is available in the University IP Policy (see <http://documents.manchester.ac.uk/DocuInfo.aspx?DocID=487>), in any relevant Thesis restriction declarations deposited in the University Library, the University Library Regulations (see <http://www.manchester.ac.uk/library/aboutus/regulations>) and in the University’s policy on the Presentation of Theses.

Acknowledgements

This Ph.D. would not have been possible without the help from many individuals over the past four years. Firstly I am grateful to my two brilliant supervisors Kim Hammond-Kosack and Jon West. Their doors were always open and they have provided constant advice, guidance, and support. Thank you to Kim for mentoring me through many complex situations throughout the project.

It was a privilege to work in a place like Rothamsted Research and I'd like to thank the numerous people in the former Plant Pathology Department who have helped along the way. These include Gail Canning for her amazing molecular biology tuition and Wing Sam-lee, Martin Urban and Neil Brown for giving their time to provide fundamental lab training and sharing their plant pathology knowledge. Many thanks to Jason Rudd, Hans Cools, Helen Carter and Helen Brewer for their assistance and willingness to help whenever I needed it. I would like to thank John Lucas for his support and manuscript preparation and to thank Leanne Freeman for her hard work during the summers. A big thank you to John Antoniw, David Hughes, Ambrose Andongabo and Keywan Hassani-Pak for their assistance during the bioinformatics analyses. I would like to thank Stephen Powers for his statistical expertise. And to the Visual Communications Unit for all their help in preparing the many posters for conferences.

I would like to extend my gratitude to John Pickett and the Society of General Microbiology for awarding the travel bursaries which allowed me to carry out a short project at the University of Florida. Thank you to Jeffrey Rollins for being such an excellent collaborator and to Xiaofei Liang who is a *S. sclerotiorum* transformation genius.

I am grateful to have worked with such a dynamic group of people on the SYield project, especially Sophie Weiss, Shradha Singh and my industrial supervisor, Sarah Perfect who all provided invaluable support and advice throughout the project. I would also like to thank my university supervisor, Bruce Grieve for his assistance.

I am grateful to my family for their unfailing encouragement. To my brilliant housemates for their humour and friendship and the Rothamsted Ph.D. students who made 11am coffee entertaining every day. And finally to Dr Jones who was there to make me smile throughout.

Chapter 1: General Introduction

1.1 The challenges of securing food for a growing global population

The world's population is predicted to grow from the current 7.2 billion people to a staggering 9.6 billion people by the year 2050 (United Nations, 2013). The ability to sufficiently feed this number of people relies on modern agriculture increasing current production by between 60 and 110% (Tilman et al. 2011, *OECD-FAO Agricultural Outlook 2012-2021* 2012). This is a colossal challenge as there are multiple factors which will affect the global community's ability to achieve this goal. How productive our agricultural systems are is dependent on our ability to cope with factors including climate change resulting in unpredictable weather patterns and changes in pest and disease outbreaks, insufficient fertile land, availability of water and expensive and limited energy supplies. The global shift towards a meat based diet, whether land is used for food, feed or biofuel production, excessive food wastage in developed countries and uneven distribution of food across the globe add to the problem and make it difficult to assess how and where food production would be best increased.

Some studies suggest that improving crop yields will be the answer in creating sustainable, intensive agricultural systems capable of the necessary outputs while preserving valuable natural ecosystems (Matson and Vitousek 2006, Phalan et al. 2011). The Royal Society published a report in 2009 describing how 'growth in production must be achieved for the most part without the cultivation of additional land' as 'the environmental consequences of increasing cultivated areas are undesirable' (Society 2009). Other studies suggest that improving crop yields is not enough to achieve secure food supplies and the only way to achieve this is through the clearing and use of *all* suitable land for agriculture whether it is already used for production or not (Ray 2013). A study which analysed the current increase in production of the world's top four crops; maize, rice, wheat, and soybean (which are responsible for two thirds of the world's global calories), found that crop production is only increasing at 1.6%, 1.0%, 0.9%, and 1.3% per year, respectively. This is less than the projected 2.4% per year rate required to double global production by 2050. At these rates, global production in these crops would increase by approximately 67%, 42%, 38%, and 55%, respectively. This is lower than will be required to feed the population by 2050 (Ray 2013). As the population steadily grows, the clock ticks for a decision to be made on the global strategy for future food production while considering precious natural resources that are vital to the health and wellbeing of the planet.

Modern agricultural practises have changed enormously as a result of the Green Revolution (GR), which occurred between 1966 and 1985 (Pingali 2012) . During this period, crop production tripled even with only a 30% increase in the use of cropable land (Pingali 2012). Gross world food production (cereals, grains, roots, tuber, pulses and oil crops) increased by 138%, from 1961 to 2007. That is an increase from 1.84 billion tonnes of food to 4.38 billion tonnes (Society 2009). This dramatic increase was a result of high rates of investment in scientific crop research to set up publicly funded crop breeding programs to develop biotic and biotic-stress tolerant plants, policy support, market development and infrastructure growth (Pingali 2012). Significant developments in synthetic fertiliser production and the discovery of chemical pesticides and herbicides changed smaller scale market garden style food production to intensive, monoculture systems used today to produce cheap food that the governments of the world promised its citizens after suffering food shortages during the war years. However, the benefits from the GR have not been seen everywhere and low income countries, mainly in sub-Saharan African countries, still experience low food productivity resulting in poverty and chronic food shortages. Food price spikes in the mid-2000s have highlighted how the pressures of unstable economies, increases in fuel prices and the effects of climate change can dramatically affect food security. As a result a call for renewed interest in agricultural investment has been a main concern for many policy makers and other stakeholders. Chemical discovery and managed pesticide resistance programs are key to improving farming systems as well as the development of precision farming equipment and sustainable energy solutions. A clear lesson learnt from the 1960's GR is that success can only be achieved with vast investment into scientific research on a global scale which will ultimately lead to innovative scientific solutions which will allow growers to secure the yields required to feed our growing population while reducing the negative effects on the environment.

1.2 The use of crop protection in agricultural systems.

Successful yield outputs rely heavily on a range of energy-intensive inputs into agricultural systems. Large-scale farming would not be possible without the use of synthetic nitrogen fertilisers, herbicides, pesticides and fungicides. Artificially synthesised nitrogen fertilisers improved crop yields significantly because providing there are no other limitations in soil, there is a linear relationship between available nitrogen and crop biomass accumulation (Society 2009). Application of nitrogen is

essential to exploit the full genetic potential of improved crop cultivars. The ability of growers to protect large monocultures from pests, pathogens and weeds significantly improves yields. Pests (which include insects, fungal pathogens, viruses and nematodes) have been estimated to account for 50% global potential loss in wheat and 80% potential global loss in cotton production (Oerke 2006). For this reason, the global use of pesticides rose to 3 million tonnes per year in 2000. Although pesticide use has been controversial for many years, primarily because they are blamed for causing environmental damage, chemical pesticides have often been the most effective in controlling pests. However the unmanaged, overuse of chemical sprays over the last four decades has resulted in many pest species becoming resistant to pesticides, reducing the efficacy of the chemicals. Resistance is the decreased susceptibility of a pest to a pesticide. Resistance can evolve within a pest population if it is exposed to a high selection pressure, in this case the chemical pesticide. If one individual pest contains a trait which allows it to be less susceptible to that pesticide, it will survive and that trait will spread throughout the pest population rendering the chemical ineffective (FRAG-UK). It has been observed that within one to two decades of the seven major herbicides being introduced, herbicide- resistance weeds were visible in grower's fields (Palumbi 2001). Insects can often evolve resistance within one decade of exposure to a chemical, whereas bacterial pathogens evolve resistance much quicker. This can occur within 3 years of intensive exposure to antibiotics (Tilman et al. 2002) as a result of the ease of transmission of genes between bacterial species, i.e. by horizontal gene transfer. In the past, growers had no guidance or restrictions on the numbers of sprays to apply to crops. As a result resistance spread rapidly. More recently considerable research has gone into developing pesticide spraying regimes which decrease the incidence of resistance. Growers are advised not to overspray and given guidance on the time of year and the most appropriate product to apply.

As a result of the EU Directive 91/414/EEC, around 75% of some 1000 active ingredients used in pesticide products have been removed from the market since 1993 (Postnote 2009). This is because they have been tightening the cut-off criteria which chemistries must pass in order to be registered for pesticide use. This again will challenge the farming community's ability to prevent resistance developing against the ever decreasing crop protection products available. Other methods of crop protection include the use of resistant cultivars, crop rotations, the use of pest free seed or plants, attracting natural enemies to control insect pests or the use of biocontrol agents for some fungal pathogens and nematodes.

1.3 The role of fungal pathogens in agriculture

Fungal pathogens cause a variety of diseases within crops. Fungal pathogens use plant material as a substrate for nutrient acquisition. Different species will use specific host plant tissue to acquire nutrients. For example, Take-all disease, caused by *Gaeumannomyces graminis* var *tritici*, results in the formation of patches of blackened roots in wheat crops. This prevents the infected wheat plant from efficient removal of nutrients and water from the soil. *Botrytis cinerea* on the other hand is a broad host disease but is extremely problematic on soft fruit and causes decay which affects the quality of the produce. Fungal pathogens are difficult to control within crops because their microscopic size poses a challenge detection before symptoms appear on the crop. Usually once disease symptoms are visible, to achieve effective control is difficult. This is because many fungal pathogens have the ability to produce and disseminate millions of spores during sporulation.

Fungal

pathogens in particular account for the loss of approximately 16% of yield globally (Oerke and Dehne 2004). *Septoria tritici*, (recently renamed *Zymoseptoria tritici*) a fungal pathogen which cause Septoria blotch disease of wheat was responsible for £35.5 million of economic loss globally in 1998 (Innes 2010). In the same year, Take all disease, was estimated to have caused approximately £55 million worth of damage (Oerke and Dehne 2004). Figure 1 highlights the UK yield losses to winter oilseed rape crops as a result of the main four oilseed rape fungal pathogens; *Leptosphaeria maculans* which causes phoma stem canker, *Pyrenopeziza brassicae*, the causal agent of light leaf spot, *Sclerotinia sclerotiorum*, the causal agent of stem rot and *Alternaria brassicae*, the cause of dark pod spot (Fitt et al. 2006) (Fitt et al. 1997)

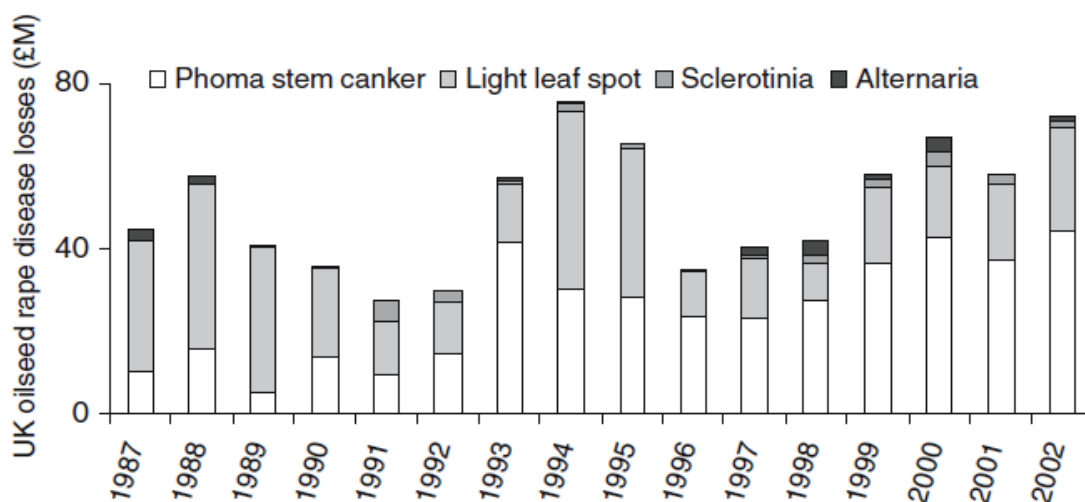


Figure 1: Estimated disease loss in oilseed rape.

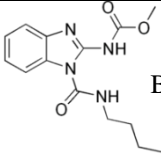
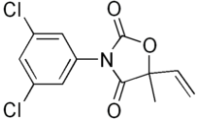
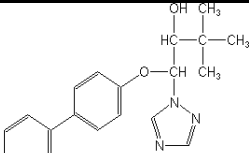
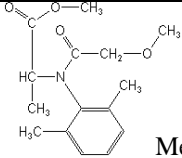
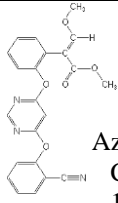
Figure taken from (Fitt et al. 2006). The estimated losses from diseases (phoma stem canker, light leaf spot, Sclerotinia stem rot and Alternaria pod spot) in winter oilseed rape in England and Wales for harvest years 1987-2002, calculated from disease survey data (www.cropmonitor.co.uk).

Fungal disease not only causes yield loss, many fungi also produce mycotoxins during plant infection. Mycotoxins are secondary metabolites secreted by the fungus during infection. Many of these toxins, if consumed by humans and/or animals, can cause many harmful effects including sickness and diarrhoea, gastrointestinal problems, kidney damage and in some cases are carcinogenic. Mycotoxins are produced by some fungi to assist with disease induction or pathogenicity. For example deoxynivalenol or DON mycotoxin is produced by *Fusarium culmorum* and *F. graminearum* through primary isoprenoid metabolism (Kimura et al. 2003). This toxin inhibits protein translation in eukaryotes and is required for the infection of wheat ears but not maize cobs (Hammond-Kosack and Rudd 2008). However, some phytopathogenic fungi produce toxins, but their precise function is not known (Lowe et al. 2012). Mycotoxin production can be particularly damaging post-harvest. If grain for example is not stored correctly and any residual fungal spores germinate and colonise the grain, there is a risk that the stored grain may subsequently become contaminated with the mycotoxin. It is therefore of vital importance that growers are able to prevent or minimise fungal disease in their crops, to maximise the harvested yields but also to reduce losses occurring during storage or transportation.

As with insect pests, fungal pathogens are predominately controlled with the use of fungicides. Table 1 lists a few of the main fungicide groups and their modes of action.

Fungicides are classed as preventative if the chemistry prevents the pathogen from developing or curative if the chemistry interrupts the growth of an already established pathogen prior to symptom development. Fungicides can also be eradicated and will disrupt the development of a pathogen that has already established disease symptoms. However most fungicides are not curative or eradicated so it is extremely difficult to control the disease once symptoms are visible. Although fungicide applications have been shown to improve yields significantly over the last forty years, reports of fungicides becoming less effective due to resistance is now a common occurrence (FRAG-UK). In fungi there are four main mechanisms of resistance. Firstly, there is a change in the chemical target site due to a mutation in the DNA sequence at a specific location. Secondly, the organism may produce more of the target site and the chemistry becomes less effective. This has been seen in *Mycosphaerella graminicola*, a fungal pathogen of wheat. This pathogen has showed reduced sensitivity to fungicides as a result in an increase in the cytochrome P450 target site, Cyp51. Some resistant strains may increase the rate of removal or breakdown of the compound to detoxify the cell. Finally there may be underlying naturally resistant individuals within a population. When a chemical is sprayed repeatedly into the same environment, resistance strains will spread quickly throughout the population. Often resistance has developed as a direct result of the intensive overuse of single site mode of action fungicides (**Table 1**) (Russell 2005). Over the last 10 years there has been considerable research into developing strategies for reducing resistance to new fungicides in the anticipation of prolonging the effectiveness of newer compounds. Research bodies such as the Fungicide Resistance Action Group (FRAG-UK) and the HGCA (HGCA) as well as agrochemical companies work closely together to educate fungicide users about the risk of pathogen resistance and suggest specific management strategies. These include reducing the number of applications per season and applying the chemicals only at certain times or life stages of the crop. It is also essential that fungicide mixtures used must have different modes of action. Growers are encouraged to use fungicidal mixtures where possible and to use disease-resistant crop varieties to decrease selection pressure and reliance on fungicides. Growers need to be prepared to use new fungicides with different modes of action and finally longer crop rotations should be chosen.

Table 1: Example of the main fungicide groups and their modes of action

Fungicide Group	Target Site	Mode of action	Target species	Chemical structure
Benzimidazole Fungicides (Methyl Benzimidazole Carbamates fungicide) (Group 1),	β -tubulin assembly in mitosis	Blocks the polymerisation of tubulin which prevents the nuclear division of fungal cells. Systemic	Works on a broad spectrum of powdery mildews, <i>Botrytis</i> blights, leaf spots and blights. (FRAG-UK)	 <p>Benomyl CAS Number: 17804-35-2</p>
Dicarboximide Fungicides (Group 2)	MAP/Histidine-Kinase in osmotic signal transduction (<i>os-1, Daf1</i>)	Prevents mycelia growth and reduces spore germination. Protectant	<i>Works on a broad spectrum including Botrytis, Monilinia and Sclerotinia.</i> (FRAG-UK)	 <p>Vinclozolin: CAS Number: 50471-44-8</p>
Sterol Biosynthesis Inhibitors (SBI's) (formerly DeMethylation Inhibitors DMI's) Fungicides (Group 3)	C14-demethylase in sterol biosynthesis (<i>erg11/cyp51</i>)	Inhibit sterol biosynthesis in membranes. (includes pyrimidines and triazoles and can be curative) Systemic	Broad spectrum including powdery mildews, rusts and many leaf spotting fungi including apple scab. (FRAG-UK)	 <p>Bitertanol (triazole) CAS Number: 55179-31-2</p>
Phenylamide Fungicides (Group 4)	RNA polymerase I	Inhibits nucleic acid synthesis- RNA polymerase I Systemic	Potato and tomato late blight and grape downy mildew. (FRAG-UK)	 <p>Metalaxyl CAS Number: 57837-19-1</p>
QoI or Strobilurin Fungicides (Group 11)	complex III: cytochrome bc1 (ubiquinol oxidase) at Qo site (<i>cyt b gene</i>)	Inhibits mitochondrial electron transport complex III enzyme which prevents respiration. Protectant	Works on broad spectrum including <i>Septoria tritici</i> and Powdery mildew (Bartlett et al. 2002)	 <p>Azoxystrobin CAS Number: 131860-33-8</p>

1.4 Fungal infection modes

Many of the most destructive agricultural pathogens have been described as necrotrophs which are fungal pathogens which rely on killing host cells to live off the nutrients once the cell is dead. Other fungi can exhibit biotrophic lifestyles which obtain nutrients from cells without killing the cell for long periods of time and without causing problematic disease symptoms. There has been a recent re-classification of many traditional fungal necrotrophs which exhibit a biotrophic life stage before inducing necrotrophy. These have been re-defined as hemi-biotrophic fungi. Advances in sequencing technologies have made the study of pathogen genomes and the interactions between host plants and pathogens more accessible. Both experimental approaches based on sequencing are foreseen to facilitate the discovery of new targets for the control of pathogen.

In 1971, Flor and colleagues put forward the gene-for-gene hypothesis (Flor 1971). Flor hypothesised that for every dominant avirulence (Avr) gene in the pathogen, there is a matching resistance (R) gene in the host. It was assumed that a direct interaction between the products of these genes would lead to the stimulation of the host defence response including the hypersensitive response (HR) which arrests fungal growth. Since then, molecular plant pathologists have been trying to identify these Avr and R genes to understand plant-pathogen interactions. Subsequent research led to the isolation of several Avr proteins, now termed effector proteins, many of which are small secreted proteins which manipulate host cell structure and function (Birch et al. 2006, Kamoun 2003). Throughout the co-evolutionary arms race between a plant and an adapted pathogen, plant hosts have developed effector-triggered immunity (ETI) as the host R proteins are able to perceive the presence of specific effector proteins directly or indirectly. Detection by the host, forces the pathogen to mutate and develop new effectors to suppress the activation of plant defences and so the cycle continues (Stergiopoulos and de Wit 2009, Jones and Dangl 2006).

Chitin is a principle building block of fungal cell walls but it can also act as a signalling molecule to elicit plant defence if it is detected by plant cells. Chitin and other pathogen associated compounds including glycan and xylanase are known as PAMPs or pathogen associated molecular patterns. PAMPs will binds to PAMP recognition receptors (PRRs) localised on plant cell walls. The binding event will facilitate PAMP triggered immunity (PTI) and allow the plant to induce plant defence mechanisms to prevent progression of disease. In the case of chitin, the PRR have already been identified in some

plant hosts. The LysM receptor kinase CERK1 mediates bacterial perception in *Arabidopsis* by binding chitin (Gimenez-Ibanez et al. 2009). Rice requires both a LysM receptor-like kinase, OsCERK1, alongside CEBiP (chitin elicitor binding protein) to induce PTI (Shimizu et al. 2010).

Pathogens have evolved a counter attack strategy to PTI. Recently effector proteins have been discovered in a variety of bacterial and fungal pathogens which prevent PTI. Avr2 and Ecp6 (van Esse et al. 2008) secreted by the tomato pathogen *Cladosporium fulvum* and the Mg3LysM effector secreted by wheat infecting pathogen *Mycosphaerella graminicola* (Marshall et al. 2011) act against plant chitinases or bind chitin, preventing the plant from recognising fungal chitin which would normally elicit plant defence.

1.5 Technological advances in fungal pathogen forecasting systems, detection and diagnosis in agricultural systems

Forecasting systems which give early warning predictions of fungal outbreaks can help growers target their sprays more efficiently. Correct targeting of fungicides will reduce the risk of fungicide resistance as it will prevent overuse of the chemistry. It will also benefit the environment and reduce the growers' costs. There are a variety of Decision Support Systems (DSS) which are based on mathematical models which incorporate meteorological data for the prediction of pathogen outbreaks (Evans et al. 2006, Magarey et al. 2005, Smith et al. 2007). Many knowledge transfer bodies such as DEFRA, the HGCA or research institutes can provide advice on which forecasting systems to follow for a particular disease. Some agrochemical companies also provide growers with free online disease forecasting systems to assess the risks of disease outbreak which may influence a grower's need for sprays. For example, Rothamsted Research has an online prediction tool which predicts the risk of light leaf spot outbreaks on different oilseed rape cultivars across the UK. The Syngenta BlightCast system is available on-line; to give potato growers and agronomists a five-day advance warning of localised blight risks caused by the oomycete *Phytophthora infestans*. This online tool was developed to enable risk based selection of appropriate fungicides and ensure application at the right time to prevent infection. However many of these forecasting systems are usually dependent on local weather conditions and cannot be used in other countries where the weather patterns may be significantly different. What could be suitable as a multi-country forecasting system is one which combines weather based predictions with real time automated monitoring of the pathogen. Some prediction systems require monitoring of certain aspects of the disease including leaf wetness, appearance of apothecia or the appearance of lesions

on leaves for example to calculate whether there is a disease risk. This can be a challenge for growers who may not be experts in disease diagnosis. As a result there have been major advances in disease diagnosis and detection which may contribute to the future of disease forecasting systems when combined with meteorological data. Detection and diagnosis of fungal pathogens are key to select the correct control measures and forecasting is key for optimising efficiency.

1.6 Detection and diagnosis of plant pathogens

The identification of the many pathogens which may attack a crop during a growing season is a challenge for most growers. Growers do not always have the expert taxonomic skills they need to diagnose a disease symptom and this may compromise their ability to provide accurate crop protection. Rapid detection and diagnosis of plant pathogens is key to implementing correct control strategies for containment or elimination of plant diseases which would otherwise have serious economic consequences. As farms become larger and growers become more reliant on mechanised equipment, the need for automated and user friendly diagnosis tools increases. Grower- friendly methods of pathogen detection need to be practical, readily available and cost effective. They also need to be specific to a certain pathogen or ideally as multiplexed systems capable of detecting a range of pathogens accurately. The following sections will discuss the current technologies used by growers and researchers to diagnose and detect plant pathogens as well as looking to the future of this rapidly expanding sector of agricultural technology.

1.6.1 DNA-based detection methods

Advances in fungal genomics has revolutionised our ability to identify genomic sequences which can be used as unique detection targets for disease diagnosis. Polymerase Chain Reaction (PCR) has facilitated many plant disease clinics across the world to rapidly identify disease samples without the need to culture a sample for spore identification. Spore trapping devices can be used to capture air samples which contain airborne spores. The DNA can then be extracted for testing. Potentially contaminated plant tissue, soil and water samples can also be used in DNA extraction. The extracted DNA can then be used in species specific PCR to determine the species of pathogen and the amount of inoculum in the air or in other sample substrates. This has been successfully done for *S. sclerotiorum* (Rogers et al. 2009). The detection test involves the use of 7-day Burkard spore trap, which traps airborne spores on a wax film. DNA is extracted from the wax strip and the quantity of *S. sclerotiorum* determined through qPCR by amplifying a unique DNA sequence to *S.*

sclerotiorum. Alongside these detection studies it has also been necessary to relate the amount of spores in the air to give an indication of disease epidemics. For example, 25-35 *Botrytis squamosa* conidia/ m⁻³ air were found to cause 2.5 lesions per leaf (Carisse et al. 2005). It was also found that when detection of this inoculum was used to indicate disease potential, a fungicide reduction of 75% and 56% in 2002 and 2003 was documented (Carisse et al. 2005). This sort of monitoring is important for sporadic diseases such as *S. sclerotiorum* where a very low number of ascospores (12 spores/ m⁻³) measured by spore-trapping related to disease incidence (Rogers et al. 2009).

1.6.2 Immunology-based/ Antibody-based detection methods

Advances in rapid and cost effective antibody production over the last 10 years have allowed the development of antibody based detection systems for plant disease diagnosis. Antibody based diagnosis / detection systems have been designed to be used in the laboratory as well as in hand held devices at point of use. These systems are based on the use of antibodies as high affinity ligands which will bind to cell surface fragments or antigens or even whole cell substrates. Antibodies that can be used in various detection systems can be either monoclonal or polyclonal. Monoclonal antibodies (mAb) will bind to a single site or epitope of the target fragment whereas polyclonal antibodies (pAb) will bind to multiple epitopes on a single antigen allowing more specificity for target detection. mAbs and pAbs are routinely produced by the injection of the whole cell / pathogen or surface fragment into a suitable animal. Another increasingly popular production method is the use of bacterial expressed recombinant fragments which include single chain variable fragments (scFv) (Skottrup et al. 2008). These fragments are a sixth of the size of standard antibodies (Lamberski et al. 2006) and maintain high specificity to the parental mAb. Using bacterial cultures for production ensures an infinite supply of genetically stable scFvs which is cost effective, and more attractive than using animal systems.

Antibody based kits for plant disease diagnosis were originally developed in 1977 (Clark and Adams 1977) but are now commercially available for laboratory use. Most companies supply a DAS-ELISA kit (double antibody sandwich enzyme-linked immunosorbent assay) for disease diagnosis. This test involves the use of multi well microtiter plates which have a specific antibody adsorbed to the surface of the microtiter wells. A plant extract is incubated for a period of time in an extraction buffer in the well. The incubation allows the binding of the antigen to bind to the antibody. A conjugate buffer containing an enzyme-labelled antibody is then added to the wells and incubated. After a final washing step, another buffer reacts with the conjugated enzyme labelled

antibody that is bound to the target fragment. The wells which contained samples with the pathogen of interest will change colour and can be visualised using a spectrophotometer (

Figure 2). There are many commercial ELISA kits available for the detection of plant viruses as specific antibodies can be raised easily against such organisms, however there are fewer kits available for fungal pathogen diagnosis to a species level. This is partially because of cross reactivity between different species and in the case of most spores, due to low allergenicity of the surface coat. ELISA kits have been developed for fungi and oomycetes including, *Botrytis cinerea*, *Pythium spp*, *Phytophthora spp* and *Septoria spp* (Agdia, Bioreba, Neogen). ELISA kits will allow for quantitative and accurate diagnosis of the disease however the tests require skilled technicians and specialised equipment. There is also usually a time delay for the grower to obtain results which may limit the time window for disease treatment. ELISA technology, although not thought of as traditional biosensor technology, can be classified as a biosensing technique. This is because it transforms the biological response of the antibody binding event and relays the response optically with the use of a spectrophotometer to detect changes in chemiluminescence or fluorescence.

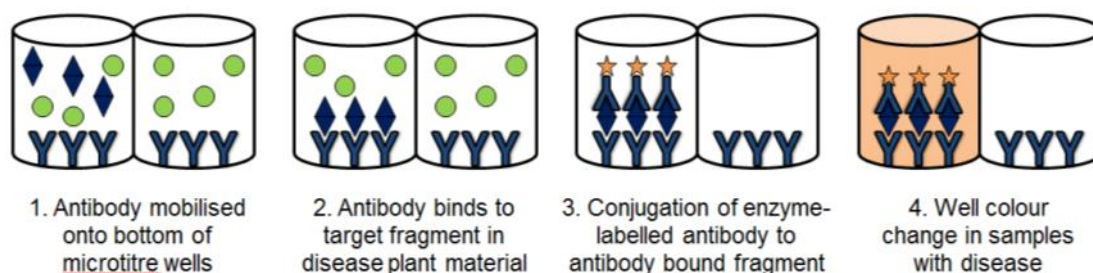


Figure 2: The DAS-ELISA assay.

Multiwells contain antibodies which are used to bind to pathogen specific antibodies

Handheld lateral flow devices (LFD) have been developed so that growers can carry out rapid disease assessments in the field as opposed to waiting for results from a diagnostics laboratory. One step LFDs are similar to ELISA assays as they use pAbs and mAbs to bind to a fragment or antigen which is specific to a certain pathogen, however this method is not quantitative. A LFDs commercially available from Pocket Diagnostics™ (www.pocketdiagnostic.com) contains antibody-coated latex beads which will bind the specific pathogen antigen absorbed from the plant extract (Ward et al. 2004). The user will crush up and incubate the infected plant sample in a buffer. After incubation, the buffer

solution is dropped onto a release pad on the bottom of the LFD which contains specific antibody-coated latex beads which will bind to the target antigen from the plant extract. The solution containing the conjugated antibodies will migrate along an absorbent pad to a test strip where latex beads containing the bound antigen will be trapped forming a visible line on the pad. Surplus unbound antibodies migrate further along the pad and are trapped onto a second strip. This acts as a control indicating that the test worked correctly (**Figure 3**). There are a variety of LFDs which are capable of identifying a many plant viruses although some can diagnose some fungal pathogens including *B. cinerea*, oomycete pathogens such as *Pythium* and *Phytophthora sp* and bacterial pathogens including *Ralstonia solanacearum* and *Erwinia amylovora*.

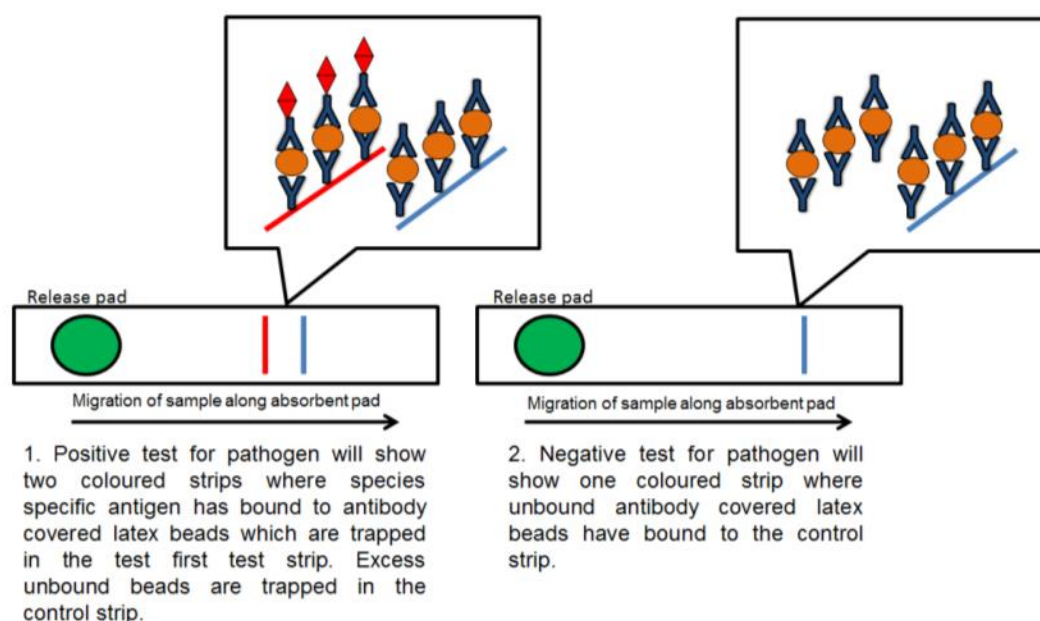


Figure 3: Positive and negative detection of pathogens using handheld lateral flow devices.

1.6.3 Antibodies for metabolite sensing

Plant pathogen detection devices can also target secreted metabolites rather than cell surface proteins for accurate diagnosis. A rapidly expanding example of this is the need for detection methods for fungal and bacterial toxins which are secreted into substrates. Many species of fungi including *Penicillium spp* and *Aspergillus spp* secrete mycotoxins during growth in or on food substrates. Manufactures and sellers of perishable foods have to follow strict legislation to ensure their food does not contain mycotoxin levels above a certain threshold outlined by the EU Commission Regulation (EC) No. 1881/2006). On site diagnosis kits made by companies including Neogen Europe Ltd, for many toxins including aflatoxins, ochratoxins and DON using LFD have been developed.

However more accurate laboratory based ELISA and HPLC testing is used to quantify the amounts of the different toxins more accurately.

1.6.4 Biosensors for pathogen detection

Since the invention and success of the blood glucose biosensor (Clark and Lyons 1962), research into using biosensing as a way to monitor and quantify elements of biological systems at point of care (POC) has flourished in medical professions. Biosensing applications to detect plant pathogens in an agricultural system are an expanding field because there is the potential to develop devices which detect pathogens rapidly. In addition, this fully automated format can be easily used with very little technical skill. There is also the potential to combine biosensor outputs with wireless networks to enable data of detection events to be sent to a central monitoring and processing unit which can then incorporate the information into a disease forecasting system. However much of the technology is laboratory based and remains to be translated into handheld or automated devices.

A biosensor takes a biological response and translates it into an electrical signal (Turner 2000) (**Figure 4**). It is an analytical device which integrates a biological sensing element or bioreceptor within a physicochemical transducer and is required to produce an electronic signal proportional to the specific analyte that it is measuring (Nierman et al. 2005). Bioreceptors include antibodies, enzymes, whole cells and DNA. These are usually immobilised onto some form of sensor surface. The transducer, which can be optical or electrochemical, takes the biological response and changes it into an electrical signal. An example of optical transducers includes surface plasmon resonance (SPR) or fibre optics. Electrochemical transducers make use of changes in current, potential, impedance and conductance across an electrode surface for detection events (Velusamy et al. 2010).

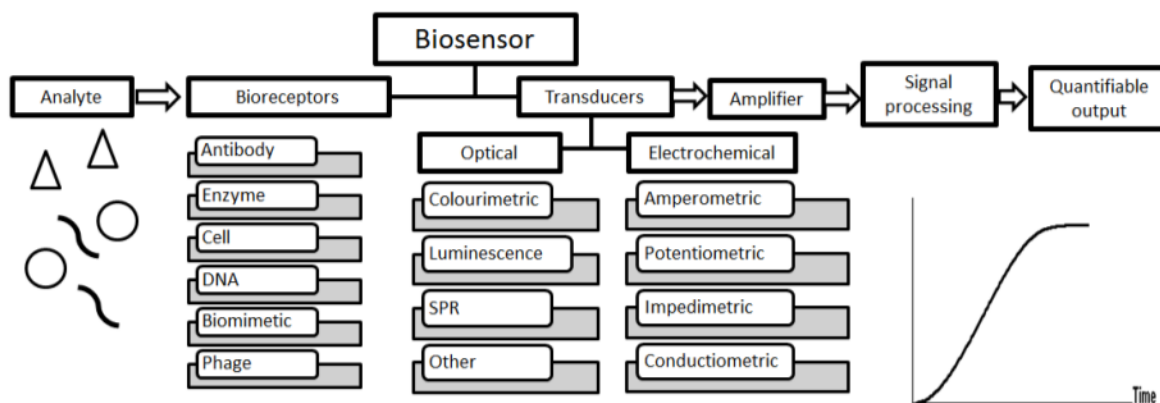


Figure 4: The basic components of a biosensor system.

1.6.4.1 Surface plasmon resonance (SPR)

A popular technique to characterise the interactions of small molecules such as proteins, polysaccharides and nucleic acids is SPR (Skottrup et al. 2008). It is a label free, optical biosensing technique which can be used to detect molecular binding events. SPR incorporates the use of a light source which passes through a prism and impacts on a gold surface sensor chip. The light bounces off the sensor chip and is received by a detector. At a certain angle known as resonance angle, light is absorbed by the sensor film, causing electrons or surface plasmons to resonate (Skottrup et al. 2008). This causes a loss in intensity in the reflected beam and this change can be detected by a reflectivity curve (Biosensing Instrument Inc ©). Antibodies can be immobilised onto sensor chip surfaces and the binding events at the sensor surface will cause a change in the refractive index, which is then monitored. This is a real-time method of detection and can also be used to calculate rates of binding events. SPR is still very much a laboratory based method of detection but has been used to detect a variety of viruses including Cowpea mosaic virus (Torrance et al. 2006) and Lettuce mosaic virus (Candresse et al. 2007). Fungal pathogens including *Fusarium culmorum* (Zezza et al. 2006) and *Aspergillus niger* (Nugaeva et al. 2007) and the oomycete *Phytophthora infestans* (Skottrup et al. 2007) have been detected by SPR in a laboratory. Many of these detection systems use a Biacore SPR sensor surface onto which species specific antibodies are immobilised. The most commonly exploited surface chemistry used to mobilise the antibodies onto the sensor surface is called CM5 (Johnsson et al. 1991). This sensor surface consists of a SiCO₂ base layer mobilised on top of a gold film. Long chain hydroxyalkyl thiols are also attached to the gold film. Carboxymethylated dextran (CM5) is then mobilised onto the surface which creates a hydrogel on the gold film. The CM5 has carboxylic side groups which can attach to other biomolecules. Although SPR technology has its advantages as a real time, label free detection method, the main disadvantage is that it lacks sensitivity for measuring small molecules.

1.6.4.2 Electrochemical biosensors

Electrochemical transduction is a popular choice for biosensor systems and has been researched thoroughly. This form of transduction was used in the original glucose biosensor system. These biosensors can be classified into amperometric, potentiometric, impedimetric and conductometric biosensors, based on the observed factors such as current, potential, impedance and conductance, respectively (Velusamy et al. 2010). For example an amperometric biosensor will consist of an oxidoreductase enzyme which is

stabilised onto an electrode. The enzyme is specific to a particular analyte which is specific to the pathogen being detected. Upon arrival of the analyte, the enzyme will oxidise the analyte and the electrons generated in the reaction are shuttled to the electrode through artificial electron acceptors or mediators such as ferrocene or hexacyanoferrate. The mediation of electrons produces a current that is directly proportional to the concentration of the analyte (Turner 2000). Antibodies can also be stabilised onto electrode surfaces so that the binding event of target antigen to antibody can be detected. Electrochemical biosensors have been successfully used to diagnose many food borne pathogens including *E-coli* and *Salmonella* which can cause significant harm to human and animals if ingested (Muhammad-Tahir and Alocilja 2003, Muhammad-Tahir and Alocilja 2004, Yang et al. 2001). One study used an amperometric biosensor to detect *S. typhimurium* cells. The bacterial cells were bound by magnetic- beads which were conjugated to antibodies and then subsequently detected by an alkaline-phosphatase (AP)-labelled anti-*Salmonella* antibody. The AP antibody catalysed the breakdown of *para*-aminophenyl phosphate into electro-active *para*-aminophenol. This generates an electrochemical signal and measures over 8×10^3 bacterial cells / mL (Gehring et al. 1996). Microbes have also been used for over a decade within sensors as they can be used to catalyse certain amperometric reactions. Some examples include ethanol yeast-based bio electrodes, based on the activity of alcohol dehydrogenase in yeast (Miyamoto et al. 1991). Yeast and vitamin K3 were used in the preparation of bioelectrodes sensitive to ethanol and glucose (Miki et al. 1994) . This technology can be further expanded to detect crop pathogens by exploiting certain biological or metabolic reactions during pathogen growth and then using these biological signals to potentially generate an electrical signal which can measure the presence of that pathogen in a field. However for the diagnosis of plant diseases, the field is still lead by antibody based devices such as the LFD and laboratory based assays including ELISA and PCR. There is still a large need for infield diagnostics that can use the above technologies to detect pathogenic species automatically.

1.6.4.3 Wireless biosensor networks

There has been a shift within agricultural industries to harness biosensor technology which was originally developed for indoor wireless sensor networks (WSN) and medical professions. Biosensor technology is being used with WSN and radio frequency identification (RFID) (Ruiz-Garcia et al. 2009). Both have promising uses in environmental monitoring, irrigation, livestock, greenhouse, cold chain control or traceability. A main advantage of the WSN technology is that it allows multiple networks

to communicate whereas RFID has no cooperative capabilities. RFID can either come in an active or semi-passive form. Semi-passive RFID only has enough power to sense and record data. An active RFID system can broadcast data and communicate with other nodes in its network within a range of 100 meters. The power required for active RFID is ten times more expensive than semi-passive RFID devices. Currently semi-passive and active-RFID tags have been developed, no bigger than a credit card, which can record temperature and are used in industry (Amador 2008). Semi-passive tags to record humidity, light, shock/vibration and gas accumulation such as ethylene (which accumulates during plant stress) are also becoming commercially available. Current examples of sensors include environmental monitors in food containers which monitor the temperature and humidity of a space which can then be equated to stresses which food will undergo when being transported during the journey from the grower to the supermarket (Ruiz-Garcia et al. 2009). In greenhouse environments, WSN can also be used to monitor and control temperature, relative humidity and light (Wang 2008).

A biosensor wireless network consists of many nodes, each one comprising of a sensing, processing and communicating unit (Akyildiz et al. 2002). In a wireless network, each sensor node can change information with a gateway unit which can communicate with other sensors from other networks. Designing a wireless network has the added benefit of not requiring any wiring which makes installation much more economic and reduces any problems that wiring installation creates. Wireless network nodes have to be placed correctly in the field to ensure the data sensor devices are able subsequently to transmit through very challenging environments. Crop canopy and climatic variability may be a problem for many sensors as well as sufficient power supplies. These all add to problems of erroneous data collection and all need to be taken into account when designing a network. Packet Reception Rate which refers to how much of the recorded message is lost in a network must be evaluated in each system. It may be improved by simply increasing the number of nodes, changing the position of one or reducing the range of monitored area (Ruiz-Garcia et al. 2009).

There has been successful applications of WSN within a closed environment in the monitoring of potato blight disease caused by *Phytophthora infestans* by using temperature and humidity sensors (Baggio 2005). This network uses 150 sensor boards to be used directly in the field (Baggio 2005). These boards are equipped with sensors for registering temperature and relative humidity. The network also contains 30 nodes which act as communication relays. The sensors were placed at a range of heights (20-60 cm above ground). There are also a number of sensors measuring soil humidity. The data is collected

by nodes at the edge of the field called a 'gate-way' and transferred via Wi-Fi to a PC where the data is logged. This PC is connected to the internet and can be uploaded to a server. The data collected can be used to monitor whether the field conditions are conducive for plant infection, and allow simulations for algorithms for other WSNs.

1.7 The SYield biosensor consortium

The research described in this thesis contributed to the work of a consortium that aimed to develop a network of infield biosensors for the real-time detection of airborne ascospores from the fungal pathogen *Sclerotinia sclerotiorum*. This project required an array of different disciplines including electrical engineers, computer specialists, biochemists, biologists, satellite image surveyors, mathematical modellers, field trial managers and business managers. As a result, the consortium consisted of a range of small, medium enterprises (SMEs) (Burkard Engineering, DMCii, Uniscan, and Gwent Group) and academic partners (Rothamsted Research and The University of Manchester). The consortium was led by the agrochemical company, Syngenta and was assembled in November 2010 to take on the challenge of building the biosensor. The project received approximately £1.5 million over three years from the Technology Strategy Board (TSB) and Syngenta combined.

The original biosensor network design aimed to unite local farm networks of infield biosensors which would interact all over the UK to warn oilseed rape growers of any emerging *S. sclerotiorum* disease threat to their crop. This early warning system is designed to help growers choose the best crop protection to reduce the risk of *S. sclerotiorum* disease. This enables growers to save money on fungicide inputs and produce more food from fewer inputs by developing an integrated farm management strategy. *S. sclerotiorum* was the chosen pathogen for detection as it causes sporadic outbreaks which are very difficult to predict. Currently farmers will spray to protect crops against the disease even when there is very little risk of outbreaks. An electrochemical detection method was chosen as a result of the electrochemical expertise available to the project and that this pathogen secretes the organic acid, oxalic acid (OA). OA is easily broken down by the oxidoreductase enzyme, oxalate oxidase (OxOx) and has similar activity to the glucose oxidase enzyme used in the blood glucose biosensor. The blood glucose technology has developed over many years of research and in theory could be easily applied to similar enzyme systems. After three years of work on the project, an automated biosensor has been developed to detect *S. sclerotiorum*; however the integration of a network of biosensors across the UK is still a work in progress.

1.8 *Sclerotinia sclerotiorum*: the pathogen of choice for the SYield Biosensor

1.8.1 *Sclerotinia sclerotiorum*: Taxonomy

S. sclerotiorum is a fungal pathogen which has a broad host range of more than 400 plant species (Boland and Hall 1994) globally, predominantly dicotyledonous. It has been estimated that this disease can cause the loss of up to 60 million dollars per year in the combined oilseed crops; sunflower, canola and soybean (Lu 2003). This pathogen poses a threat to economically important crops including sunflower, soybean, oilseed rape, chickpea, peanut, lentils, carrots, lettuce. Monocotyledonous plants such as onion and tulip are also at risk (Boland and Hall 1994). In the UK, oilseed rape, carrot and lettuce crops are the most affected (Clarkson et al. 2007). This disease has been called by a variety of other names including cottony rot, watery soft rot, crown rot, stem rot, blossom blight and white mould (Bolton et al. 2006). It was first officially described as *Sclerotinia sclerotiorum* de bary in 1884 (De 1884) and has been taxonomically characterised as being part of the Sclerotiniaceae fungal family, in the order Helotiales and in the Ascomycota phylum (Bolton et al. 2006). This family is associated with the production of melanised hyphal aggregates called sclerotia. From these stipitate apothecia develop and from these structures, ascospores are released. *S. sclerotiorum* is a homothallic fungus and so to produce ascospores from apothecia, sexual reproduction arises from self-fertilisation (Clarkson et al. 2013). This has resulted in clonal population structures across the world, with a few clones being sampled at high frequency but more interestingly there are many different diverse clones too. This highlights that *S. sclerotiorum* has a very diverse population structure. DNA fingerprinting and microsatellite studies have shown that generally within a population there is one or very few clones sampled with high regularity. This has been shown in the same locations over multiple years of sampling (Clarkson et al. 2013). An example of this was evident in Canadian oilseed rape isolates which had similar DNA fingerprinting to isolates sampled from soybean in Ontario and Quebec (Hambleton et al. 2002). In many cases the DNA fingerprinting or microsatellites are closely related to mycelial compatibility groups (MCGs). MCG testing is a phenotypic, macroscopic assay which is based on the self / non self-recognition mechanism controlled by many loci within the fungal genome (Carbone et al. 1999).

1.8.2 Advances in the genome sequencing of *Sclerotinia sclerotiorum*

The Broad Institute has sequenced the *S. sclerotiorum* genome and a comparative study of this genome and the closely related sequenced *Botrytis cinerea* genome has been conducted (Amselem et al. 2011). The *S. sclerotiorum* genome is predicted to contain 14,522 genes. The *S. sclerotiorum* genome contains 16 linkage groups which correspond to an estimated 16 chromosomes (Amselem et al. 2011). Also available for bioinformatics analysis is an estimated 17th ‘waste bin’ chromosome containing the concatenated unmapped sequences. Having this resource available publically has allowed further investigation into the infection strategies and mechanisms of pathogenicity which will be further covered in this thesis.

1.8.3 *Sclerotinia sclerotiorum*: Life cycle and infection strategy

S. sclerotiorum derives its nutrients from dead or decaying plant cells. For the purpose of this thesis and the SYield project, the infection strategy adopted by this pathogen to infect oilseed rape was studied; however infection strategies used against other host plants including carrots and lettuce are the same. *S. sclerotiorum* has evolved a lifecycle which is synchronous with the flowering stage of oilseed rape (**Figure 5**). Petals or senescing tissue play an extremely important role during the infection process as airborne ascospores which land on petal/ senescing tissue are able to obtain nutrients during early spore germination without having to combat any host plant defence mechanisms (Bolton et al. 2006, Lumsden 1979). This ascomycete fungus, produces melanised resting structures called sclerotia which can survive for several years in the soil making it particularly difficult to eradicate from fields (Hegedus and Rimmer 2005). Sclerotia which are found naturally in an area respond specifically to the environmental cues of that region. Slight differences in climates will affect the optimum germination conditions required by sclerotia of different isolates. For example, in temperate regions such as the UK, sclerotia require a period of cold conditioning (over wintering) in the soil which has a high moisture content. Sclerotia will undergo carpogenic germination which is the development of fruiting bodies or apothecia which release ascospores. Apothecia germination will occur after a period of increased temperature during springtime, which generally coincides with oilseed rape flowering. This is because the sclerotia respond to the same environmental cues as the plant during flowering. After periods of rainfall which create a soil water potential of 100 KpA for one to two weeks coincident with increases in temperature between 25- 30 °C, the fruiting bodies or apothecia can develop. Under the surface of the mushroom shaped apothecia, rows of asci develop. These are cylindrical-sac

like zygote cells which contain 8 hyaline, ellipsoid binucleate ascospores (Kohn 1979). Ascospores are released continually when pressure builds up within the asci. Clouds of ascospores are sometimes visible when there is a change in air pressure, a gust of wind or physical disturbance of the apothecia (Figure 6).

Most of the ascospores will remain in the field where they were released, however it has been shown that some ascospores can travel for several kilometres in air currents (Li et al. 1994). Continuous rainfall and dry periods allow apothecia to maintain moisture and re-release ascospores. A viable spore may be blown onto a senescing part of the host plant such as a petal. The spore will then colonise the petal and once the petal is abscised from the plant and falls onto healthy plant tissue, the fungal hyphae have sufficient energy to infect. The mode of infection involves the penetration directly through the waxy cuticle of the leaf rather than through the stomata. The apex of hyphae forms either an appressoria or a pad of short hyphae which are perpendicularly attached to the host surface by mucilage (Hegedus and Rimmer 2005). Penetration of the cuticle involves both mechanical and enzymatic digestion, most noticeably a hyphal fan which grows over the subcuticular wall of the epidermis (Hegedus and Rimmer 2005). The secretion of the organic acid; oxalic acid, cell wall degrading enzymes (CWDEs) and pectin degrading enzymes are released subsequently. Once the pathogen has scavenged all the available nutrients, hyphae begin to form sclerotia in the stem of the plant. When the stem of the plant falls to the ground, the sclerotia fall into the soil and overwinter until the conditions are correct again for apothecia development.

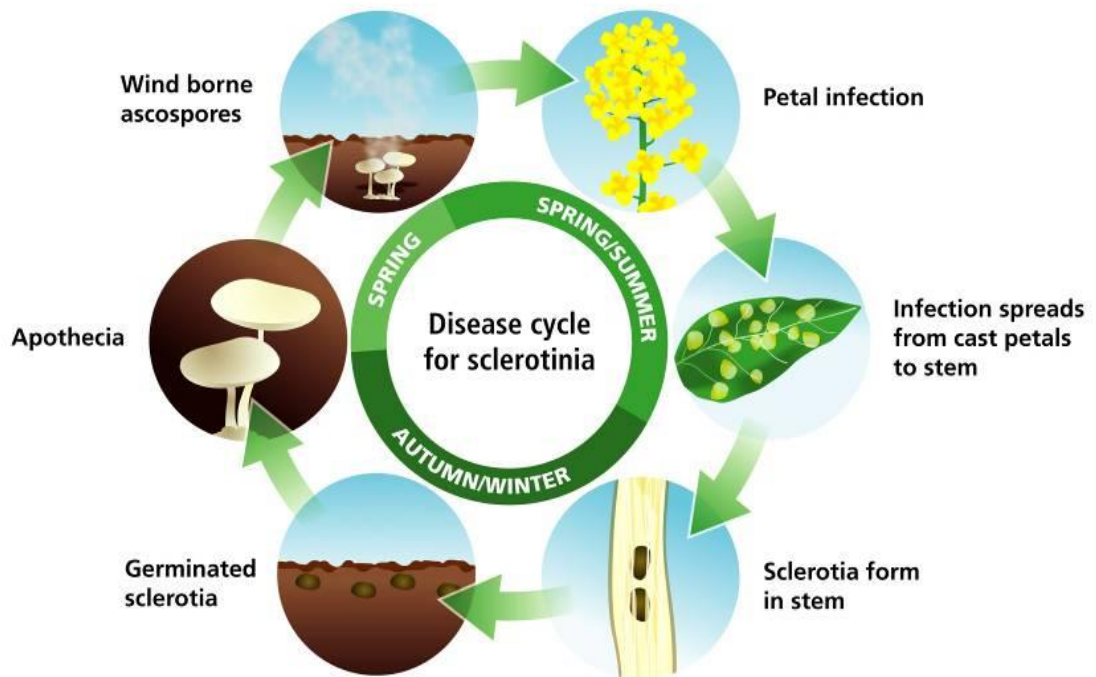


Figure 5: The life cycle and disease strategy of *S. sclerotiorum* in oilseed rape systems.

(Courtesy of Syngenta).

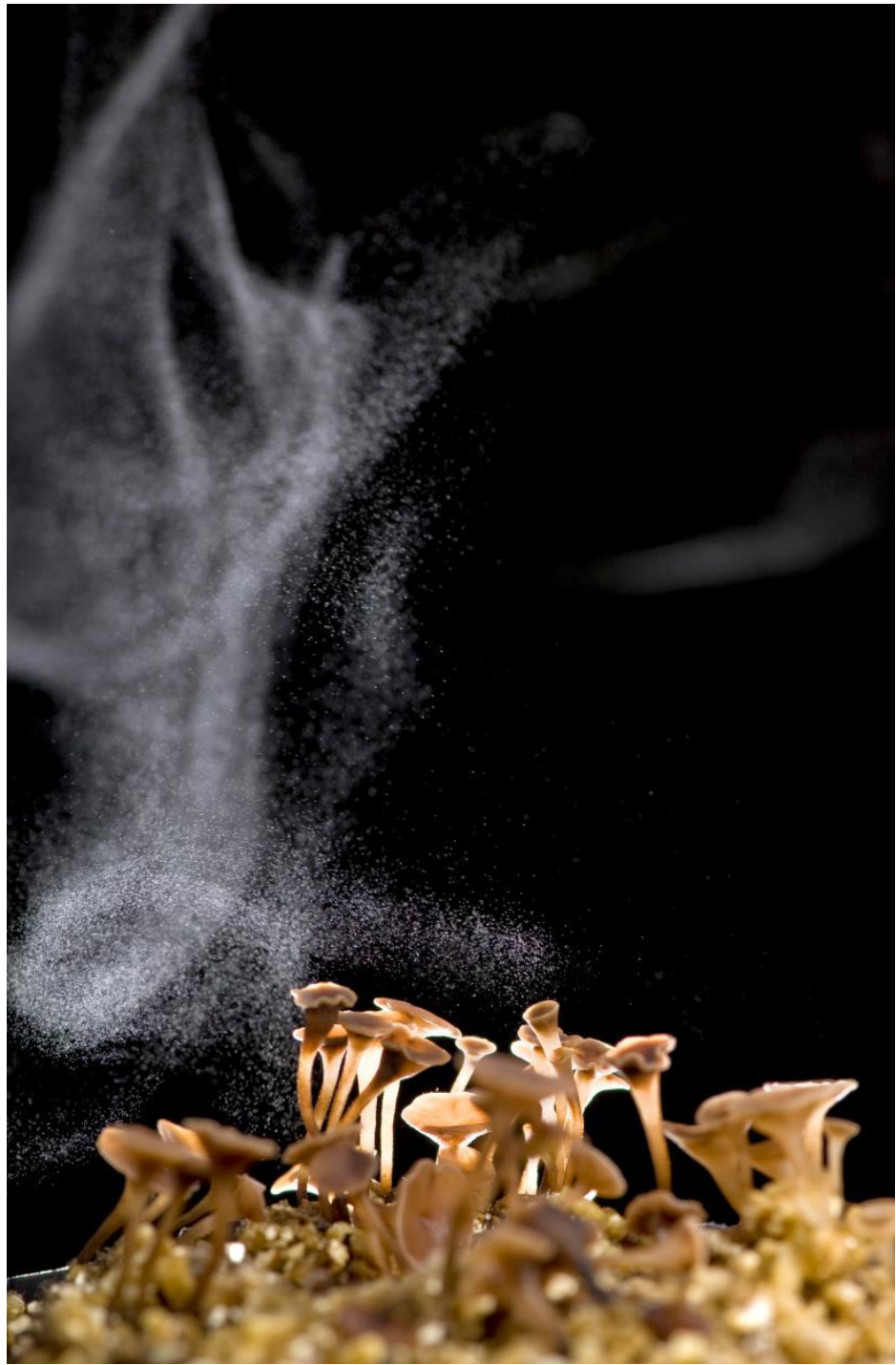


Figure 6: A visible cloud- like puff of ascospores released from *S. sclerotiorum* apothecia. *S. sclerotiorum* sclerotia were potted up in containers of damp vermiculite and conditioned for a period of 6 weeks in the dark in a 5 °C room. The containers were re-located into a light box with a 12hr near UV/ white light regime at 18 °C. Fruiting bodies or apothecia germinated and were kept moist in cloched boxes. Upon removal of the cloche lid, ascospores were released into the surrounding air as a result in the change in pressure.

1.8.4 Oxalic acid and its role in *Sclerotinia sclerotiorum* infection

The secretion of oxalic acid during early plant infection has been described as the main pathogenicity factor for *S. sclerotiorum* (Maxwell and Lumsden 1970, Magro et al. 1984, Dutton and Evans 1996, Godoy et al. 1990, De 1884). Oxalic acid has been detected within host plant tissue during and after fungal infection. It is principally detected in its conjugate base form, oxalate which occurs when oxalic acid loses two protons. Although oxalic acid been described as a phytotoxin it also has a variety of functions during infection including the mediation of a range of pH dependent processes during the infection process (Rollins and Dickman 2001), and as a result creates optimum conditions for CWDEs (Bateman and Beer 1965). Oxalic acid also disrupts cell wall integrity by chelating calcium within the plant cell wall. It's other documented functions include deregulation of stomatal guard cell closure (Guimaraes and Stotz 2004), suppression of the induced plant oxidative burst (Cessna et al. 2000), elicitation of plant programmed cell death (Kim et al. 2008) and changing the cellular redox-status in the plant (Williams et al. 2011).

A neutral pH environment activates the secretion of oxalic acid. Bateman (1965) describes the importance of lowering the pH of the plant tissue to create a more favourable environment for enzymes such as Polygalacturonases (Bateman and Beer 1965) and pectin methylesterases which breakdown pectin within plant cells (Riou et al. 1991) thereby releasing stored starch which the fungus will then utilise. It has been shown by quantifying the expression levels of specific gene transcripts, that there is differential expression of certain genes coding for CWDEs during pathogenesis (Bolton et al. 2006). Polygalacturonases (PGs) are important enzymes that are expressed the most during the early phase of colonisation of healthy plant tissues at 36 hours post inoculation (hpi) but not during the later phase at 96 hpi (Kasza et al. 2004). RT-qPCR showed that some PG transcripts (*pg6* and *pg7*) were detected from 24 hpi until the end of the time course experiment at 96 hpi. This highlights that different enzymes potentially have different roles at different time points following infection.

Oxalic acid production is a self-limiting mechanism. As oxalic acid accumulates, the pH decreases further and subsequent OA production is inhibited. This process is regulated by the *pac1* gene in *S. sclerotiorum* which is a pH responsive gene. The *pac1* protein, originally characterised in *A. nidulans*, is positively regulated under alkaline conditions. It actively promotes transcription of alkaline-expressed genes (Rollins 2003) and under a neutral pH may be involved in the upregulation of genes involved in

oxalic acid synthesis (Rollins 2003). *Pac1* is also involved in the regulation of sclerotia development which occurs during the final stages of infection when pH would be less acidic.

An increase in production of cyclic AMP (cAMP), an intracellular signal transducer, which activates ion channels and MAP kinases, has been linked to the increase in oxalic acid production (Jurick et al. 2004). Once the pathogen has successfully used up all the nutritional reserves from the plant, there is a decrease in cAMP production which is linked to the decrease in the amount of glucose available. This decrease in cAMP prevents the production of oxalic acid and activates sclerotial formation (Rollins 2003).

Oxalic acid is a strong chelator of divalent cations such as Ca^{2+} (Godoy et al. 1990) and it is thought that it sequesters calcium in the form of insoluble calcium oxalate crystals which disrupts cell integrity (Bateman and Beer 1965). Once the oxalate has combined with calcium ions found in the host cell wall, polygalacturonase can more readily hydrolyse pectates found in the middle lamella which thereby further enhances the tissue maceration process (Bateman and Beer 1965).

Oxalic acid has also been shown to reduce the oxidative burst within the host plant (Cessna et al. 2000). An oxidative burst involves a highly controlled localised release of reactive oxygen species (ROS) caused by the reduction of molecular oxygen into hydrogen peroxide (H_2O_2), superoxide radicals ($\cdot\text{O}_2^-$) and hydroxyl radicals ($\cdot\text{OH}$) and is produced as part of the early plant defence response at the site of infection. ROS are directly toxic to fungi, by damaging membranes and proteins and also by inducing programmed cell death (PCD) in the pathogen (Hegedus and Rimmer 2005). In plants, localised PCD is frequently triggered by the detection of the presence of PAMPS/ MAMPS, effectors or other signal molecules which initiate a PTI or ETI mediated response in the host plant (Wojtaszek 1997). Once ROS are detected, a cascade of downstream signalling pathways and networks, which activate plant stress responses to combat infection, are activated. The plant oxidative burst is suppressed at low pH and when there is a decrease of Ca^{2+} ions within plant cells. It has been demonstrated that oxalate-deficient strains of *S. sclerotiorum* allow unrestricted H_2O_2 production in the soybean host cells. When adding oxalic acid directly to soybean cells, there was an inhibited production of H_2O_2 (Cessna et al. 2000) indicating that OA suppresses the oxidative burst. A reduction in the pH in the absence of oxalic acid production was found not to be sufficient to suppress the oxidative burst. Therefore the production of oxalic acid is required for complete suppression (Cessna et al. 2000).

S. sclerotiorum also produces a zinc-superoxide dismutase (Li et al. 2004a). This

enzyme scavenges ROS and depletes the ROS signal to reduce the impact of the plant oxidative burst to the pathogen and reduce downstream signalling within the plant.

As previously described, *S. sclerotiorum* has a very broad host range *S. sclerotiorum* which includes over 400 plant (principally dicotyledonous) species. Non-host species, for example, i.e. barley and wheat, are able to evade infection through the production of oxalate oxidase or germin which catabolises OA and so enables the plant to remove apoplastic oxalate and maintain the oxidative burst and cell integrity as well as reducing enzyme action (Cessna et al. 2000).

1.8.5 Biosynthesis of OA

The biosynthesis of this compound in *S. sclerotiorum* has not been fully characterised however the principle way in which oxalic acid is produced includes the direct hydrolysis of oxaloacetate into acetate and oxalate (Lenz et al. 1976) by a relatively well characterised enzyme oxaloacetate acetylhydrolase (OAH) (EC 3.7.1.1) (Han et al. 2007). This enzyme is active during the Tricarboxylic Acid Cycle (TCA) or the Citrate Cycle (Cessna et al. 2000) which is an important aerobic pathway for the final steps during the oxidation of carbohydrates and fatty acids, which generates NADH and linked to other metabolic cycles which produce ATP (**Figure 7**).

OAH was initially purified in *Aspergillus niger* (Han et al. 2007) and homologues of this protein have been identified in both *S. sclerotiorum* (SS1G_08218) and *B. cinerea* (BC1G_03473). *S. sclerotiorum* mutant strains deficient in this enzyme are unable to produce oxalic acid and its ability to induce disease is severely impaired (Rollins, JA unpublished, (Amselem et al. 2011)). Current research shows that oxaloacetate is also associated with other metabolic cycles including glyoxylate and dicarboxylate metabolism and pyruvate metabolism. Oxaloacetate is also a component of Glycolysis or Gluconeogenesis which is a key pathway involved in the generation of small amounts of ATP and NADH as a reducing power as well as the conversion of glucose into pyruvate (Han et al. 2007). These mechanisms vary depending on the organism. The ability to convert pyruvate to oxaloacetate by the gluconeogenic enzyme, pyruvate carboxylase (EC:6.4.1.1) will play a key role in the production of OA. Similarly the upstream conversion of acetyl-CoA to pyruvate using pyruvate dehydrogenase (EC 1.2.1.51) directly affects the amount of OA produced. An increase in flux through both these steps leads to increased OA production.

The two other suggested routes for production of oxalate in fungi (Han et al. 2007) include the oxidation of glyoxylate by Glyoxylate dehydrogenase (EC1.2.1.17) (

Culbertson et al. 2007 a & b) and glyoxylate oxidase (EC1.2.3.5). Glyoxylate dehydrogenase was crudely purified from *Sclerotinia rolfii* (Maxwell and Lumsden 1970, Bateman and Beer 1965, Balmforth and Thomson 1984) but has not since been further studied in *S. sclerotiorum*.

Finally the production of oxalate was studied during the oxidation of glycolaldehyde by the GLOX enzyme, glyoxal oxidase. This was explored during lignin decomposition with the enzyme isolated from the white rot fungi *Phanerochaete chrysosporium* (Hammel et al. 1994).

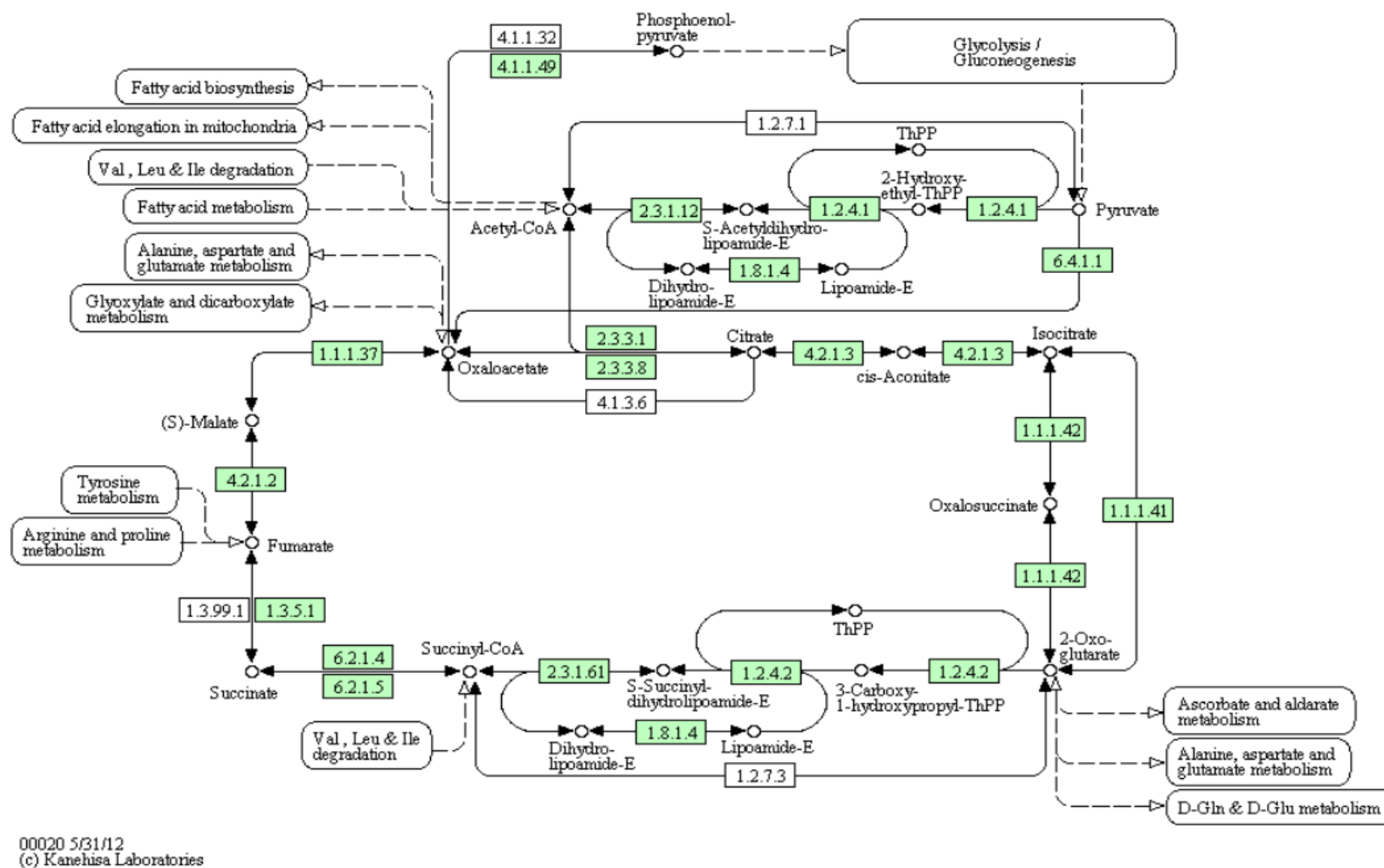


Figure 7: The Tricarboxylic Cycle taken from Kegg. <http://www.genome.jp/kegg>

The TCA cycle is the principle proposed pathway that generates excess oxalic acid. However other pathways including glycolysis may also be responsible for the production of this organic acid. Green boxes highlight the ortholog enzymes identified in *S. sclerotiorum* which play a role in the TCA cycle.

1.8.6 *Sclerotinia sclerotiorum*: a necrotroph, a biotroph or something in between?

For many years *S. sclerotiorum* has been described as a true necrotroph. Recently the use of bioimaging and a fluorescently labelled strain has revealed that *S. sclerotiorum* may exhibit a very short initial biotrophic phase. This was demonstrated by Kabbage and colleagues (Kabbage et al. 2013) who have shown an interplay between autophagy and apoptosis during the initial hours post infection. Programmed Cell Death (PCD) can determine what lifestyle *S. sclerotiorum* is exhibiting at different infection stages. PCD is an intrinsic programme for cell suicide. These cell programmes sense and monitor multiple internal and external cues and instruct the cell to eliminate itself from the organism for the overall survival of the animal, plant or microbe. Cells can undergo apoptosis which is characterised by a cascade of tightly controlled checks which are successfully negotiated prior to reaching a point-of-no-return life. Or they can undergo autophagy which is a catabolic process in which proteins and damaged organelles are engulfed and sequestered in characteristic double membrane vesicles termed autophagosomes. Kabbage and colleagues hypothesised that the type of induced host PCD is important in determining resistance or susceptibility to a fungal pathogen. They compared infection of *Arabidopsis thaliana* plants, transformed with a *C. elegans* CED-9 anti-apoptotic gene, with a wild type *S. sclerotiorum* strain (WT) and an oxalic acid deficient mutant strain (A2). WT infection resulted in a resistant phenotype and disease formation was completely inhibited. The authors concluded that the WT strain induces a runaway apoptotic cell death in the host plant whereas the oxalate deficient strain induces autophagy cell death which is responsible for the restricted growth phenotype of the mutant fungus. They showed that during the initiation of pathogenesis, the WT fungus hyphae do not kill cells; there is also no evidence for oxidative stress and fungal growth is observed in living plant tissue. *S. sclerotiorum* then switches to a necrotrophic lifestyle inducing apoptosis to induce disease formation when the hyphae live off dead plant cells. The authors also identified an effector-like protein in *S. sclerotiorum* called SsCm1 that has strong similarity (structural and functional) to the *Ustilago maydis* effector Cmu1, which codes for a secreted chorismate mutase. Cmu1 serves to maintain biotrophy during the establishment of smut infections in maize leaves, by maintaining low levels of salicylic acid at the site of infection (Djamei et al. 2011). A similar function is speculated for SsCm1 (Kabbage et al. 2013).

1.8.7 Control of *Sclerotinia sclerotiorum* in the field

Many methods recommended for *S. sclerotiorum* control involve prophylactic fungicide spraying. The HGCA provides advice on the use of a combination of prochloraz,

tebuconazole, azoxystrobin, prothiaconazole, iprodione and boscalid fungicides which can all provide effective control against *S. sclerotiorum*. However there have now been cases of resistance to MBC chemistry (**Table 1**) in France and so this needs to be addressed with better spray programmes and integrated pest management strategies. The Canola Association of Australia (CAA) (Australia 2008) also recommend that as well as fungicide use other measures can be taken to protect the oilseed rape crop against *S. sclerotiorum*. This includes the use of good quality seed during sowing, using sufficiently long crop rotations and avoiding planting susceptible crops in or around infected fields. The CAA also insists that growers use a range of fungicides and carry out the right number of sprays per season. There is also a biocontrol product which is commercially available called Constans. This product incorporates the fungal mycoparasite *Coniothyrium minitans* into a spray which is applied to the soil prior to the growing of high value vegetable crops (de Vrije et al. 2001). Once the inoculum has built up within soil, the biocontrol agent is very effective in breaking down the sclerotia in the soil which prevents further apothecia formation and reduces disease incidence significantly.

1.8.8 Forecasting systems available for *S. sclerotiorum*

Sporadic fungal disease outbreaks are difficult to forecast as they rely heavily on very particular environmental conditions. There are some forecasting methods developed for predicting outbreaks of *S. sclerotiorum* in economically important crops such as peanut, lettuces and oilseed rape (Clarkson et al. 2007, Smith et al. 2007, Twengstrom and Sigvald 1996, Twengstrom and Sigvald 1993, Twengstrom et al. 1998). BASF (agrochemical company) and ADAS (agricultural and environmental agency) have combined forces to implement a *Sclerotinia* germination tool for UK based growers. This tool is based on the direct observations of sclerotia at sclerotial depots and is monitored on a weekly basis throughout June to August. This helps gauge the germination pattern of natural sclerotia within carrots buried in areas which have been previously affected by the disease. Growers are advised to continually check published information on the website to be ready to take action against disease outbreaks. A predictive model for carpogenic germination of sclerotia to forecast sclerotinia disease on lettuce has also been developed. Again this model is dependent on the close observation of apothecia development from sclerotia found in the soil of previously contaminated fields, soil moisture temperature, climatic temperature and canopy density of the crop (Clarkson et al. 2007). The monitoring of apothecia development can be difficult due to the small size of the mushroom-like structures. The predictive model may also vary as the temperature at which sclerotia

germinate is based on a particular climate and temperature ranges cited vary from 16 °C to 30 °C (Clarkson et al. 2007). One study showed 20 isolates from different regions which all required different temperatures for germination (Huang and Kozub 1991). This makes it difficult to generate prediction models for an outbreak during a season across different climates. Soil water content measurements also differ between studies. One study used theta probes which measure the top 6cm of soil and then convert the measurement to soil water potential. This is a challenge as these values vary greatly within a single field and this makes it difficult to gauge accurate readings across even a single farm.

One way to monitor *S. sclerotiorum* inoculum in a field is to use semi-selective agar plates. This method involves placing the agar plates, open, under the canopy to allow *S. sclerotiorum* ascospores to drop onto the plates (Steadman et al. 1994). The semi-selective agar contains a bromophenol blue pH indicator dye which will change from blue to yellow as *S. sclerotiorum* ascospores germinate and secrete oxalic acid. Sclerotia production on the plate is then monitored for confirmation of species. This method may be effective for studying whether *S. sclerotiorum* is present in a field but it does not give a rapid enough result as to whether the disease is present or not before an outbreak will occur.

Disease models are extremely important in generating predictions to help forecast disease risks and they are an important life line for growers who are trying to implement good pest control management strategies. More automated ways to monitor the arrival of the disease in combination with the already useful prediction models available would be a significant improvement in controlling this and other fungal pathogens.

1.9 Project objectives

This project is very much focused on the development of an automated infield biosensor to detect the presence of the fungal pathogen *S. sclerotiorum*, in particular the selective growth surface or the biological matrix within the biosensor that *S. sclerotiorum* ascospores will be sampled into. The matrix will need to induce rapid growth for specifically this species of fungi and induce secretion of an analyte (oxalic acid) to be quantified and detected with an electrochemical assay. This project also aims to investigate other important aspects of pathogen biology so that information from these investigations can contribute to the development of an accurate detection system. Methods to investigate the biology and the underlying molecular mechanisms of infection included the use of RNA sequencing to look at the transcriptome during infection processes as well as using

bioinformatics tools to predict the suit of proteins secreted during early infection. This will not only help identify potential effector candidates but also potential protein targets which can be applied to other diagnostic techniques.

1.9.1 Hypotheses to be tested:

1. The number of *S. sclerotiorum* ascospores is positively correlated with OA concentrations after incubation in an appropriate medium.
2. A biological matrix which is conducive to the growth of *S. sclerotiorum* can be used in combination with an electrochemical assay for OA to detect the presence of ascospores.
3. The use of a bioinformatics pipeline to predict secreted proteins can be used to identify potential new nucleotide or protein targets for the detection of *S. sclerotiorum*.
4. The lack of oxaloacetate acetylhydrolase secretion by a mutant strain of *S. sclerotiorum* compromises the expression of other genes important for disease development.

Chapter 2: General Experimental Procedures

2.1 *S. sclerotiorum* sclerotia and ascospore production

To obtain *S. sclerotiorum* ascospores throughout this PhD, it was necessary to obtain large sclerotia that would produce large numbers of apothecia. Sclerotia were generated using carrot agar as this was observed to generate the largest sclerotia. Carrot agar was prepared by boiling and then blending 400 g of carrots in 400 ml of deionised H₂O and subsequently increasing the final volume to 1L with deionised H₂O before adding 20 g/L of agar to prepare the solid media. Plates were poured after autoclaving liquid medium under a sterile flow hood. *S. sclerotiorum* sclerotia for apothecia production were generated by inoculating carrot agar plates with a 6 mm² *S. sclerotiorum* mycelial plug placed in the centre of the plate. The plates were incubated at 18 °C for 3 weeks until mature black sclerotia had formed at the edge of the plates. Plate lids were removed and sclerotia air dried for two days. Sclerotia were picked off the plate and the same isolates consolidated. Harvested sclerotia were surface sterilised in 10 % sodium hypochlorite and 95% ethanol and washed with sterile water. Sclerotia were dried under a sterile flow hood. Sclerotia were stored in bags placed in boxes with silica gel at 5 °C.

The following apothecia production protocol was adapted from the method used by Dr. John Clarkson, University of Warwick. Containers were filled with medium sized particle vermiculite and soaked thoroughly with water. The sclerotia were buried in the containers and a fine layer of vermiculite placed on top. The pots were soaked once more. The containers were kept at 5 °C for 8 weeks and then kept for 4 weeks at 18 °C under near UV and white light in cloched containers until they produced apothecia. Cloched lids were lifted from boxes and ascospores harvested from apothecia by vacuuming the spores onto sterile filter paper on a daily basis.

Ascospore suspensions were made by placing a section of spore-coated filter paper into sterile water and shaking vigorously from time to time over a period of several minutes. A 20 µl 0.1% Tween solution was added to 1ml of ascospore solution to prevent spore clumping. Ascospore numbers were estimated using a haemocytometer. 10 µl of spore solution was placed under the cover slip of a haemocytometer and observed under a Leica 20x compound light microscope. Ascospores were counted and the ascospore solution calculated.

2.2 *S. sclerotiorum* mycelial cultures

Sterilised sclerotia were halved using a sterile scalpel under a flow hood. The sclerotia halves were placed face down onto PDA plates. Plates were incubated in the dark at 18° C for 2 days. Agar plugs were taken from the advancing hyphal edge.

Table 2: *S. sclerotiorum* and *B. cinerea* isolates used throughout this project.

Species	Isolate name	Plant host	Origin
<i>S. sclerotiorum</i>	L2003	Lettuce	John Clarkson, Warwick, UK
<i>S. sclerotiorum</i>	L6	Lettuce	John Clarkson, Warwick, UK
<i>S. sclerotiorum</i>	L17	Lettuce	John Clarkson, Warwick, UK
<i>S. sclerotiorum</i>	L44	Lettuce	John Clarkson, Warwick, UK
<i>S. sclerotiorum</i>	GFW 1	OSR	Rothamsted, UK
<i>S. sclerotiorum</i>	GFW 2	OSR	Rothamsted, UK
<i>S. sclerotiorum</i>	GFW 3	OSR	Rothamsted, UK
<i>S. sclerotiorum</i>	GFW 6	OSR	Rothamsted, UK
<i>S. sclerotiorum</i>	GFR 1	OSR	Rothamsted, UK
<i>S. sclerotiorum</i>	GFR 2	OSR	Rothamsted, UK
<i>S. sclerotiorum</i>	GFR 3	OSR	Rothamsted, UK
<i>S. sclerotiorum</i>	GFR 4	OSR	Rothamsted, UK
<i>S. sclerotiorum</i>	GFR 10	OSR	Rothamsted, UK
<i>S. sclerotiorum</i>	GFR 11	OSR	Rothamsted, UK
<i>S. sclerotiorum</i>	GFR 12	OSR	Rothamsted, UK
<i>S. sclerotiorum</i>	GFU1	OSR	Rothamsted, UK
<i>S. sclerotiorum</i>	BF	OSR	Rothamsted, UK
<i>S. sclerotiorum</i>	BF1	OSR	Rothamsted, UK
<i>S. sclerotiorum</i>	BF3	OSR	Rothamsted, UK
<i>S. sclerotiorum</i>	BF4	OSR	Rothamsted, UK
<i>S. sclerotiorum</i>	BF7	OSR	Rothamsted, UK
<i>S. sclerotiorum</i>	81(A)	OSR	Rothamsted, UK
<i>S. sclerotiorum</i>	M1/448	OSR	Rothamsted, UK
<i>S. sclerotiorum</i>	M448	OSR	Rothamsted, UK
<i>S. sclerotiorum</i>	b1/31 1992	OSR	Rothamsted, UK
<i>S. sclerotiorum</i>	1992B	OSR	Rothamsted, UK
<i>S. sclerotiorum</i>	S14	Lettuce	Bristol, UK
<i>S. sclerotiorum</i>	S4	Lettuce	Bristol, UK
<i>S. sclerotiorum</i>	SS Polish LL15	OSR	Poland, UK
<i>S. sclerotiorum</i>	SS Polish Sco50	OSR	Poland, UK
<i>S. sclerotiorum</i>	US 1980	Nebraska bean	Jeffrey Rollins, Broad sequenced strain, US
<i>Sclerotinia trifoliorum</i>	R316	Grass	Rothamsted, UK
<i>Botrytis cinerea</i>	181038	Soft fruit	Rothamsted, UK
<i>Botrytis cinerea</i>	967	Soft fruit	UK, Syngenta
<i>Botrytis cinerea</i>	978	Soft fruit	UK, Syngenta
<i>Botrytis cinerea</i>	1305	Soft fruit	UK, Syngenta
<i>Botrytis cinerea</i>	1430	Soft fruit	UK, Syngenta

2.3 Bioassay to test different complex media to induce oxalic acid production by *S. sclerotiorum* ascospores

Different liquid media were tested for improved secretion of oxalic acid by *S. sclerotiorum* ascospores in 12 well plates (**Figure 8**). Media was made up according to manufacturer's instructions. Additions to media including Glucose, malate, fumarate, succinate and buffers including MES (2-(*N*-morpholino) ethanesulfonic acid) and HEPES (4-(2-hydroxyethyl)-1-piperazineethanesulfonic acid) (Sigma Aldrich, UK) were made up to the required concentrations and filter sterilised before adding to the medium. Media pH was altered using a pH meter and probe (Hanna Instruments, USA). pH of solutions was adjusted using 1M NaOH or HCL. Media were autoclaved before use. Wells were filled with 2 ml of the medium of choice for testing and then seeded with ascospore solutions. Three wells were used for three biological replicates. Three wells per plate were used as control wells which were seeded with water. Plates were incubated in the dark, on the bench top at 20 °C.



Figure 8: The 12 well plate used to test various liquid media for oxalic acid production by *S. sclerotiorum* ascospores.

Each well within the twelve well plate was dosed with 2 ml of the liquid medium being tested for to determine its ability to induce oxalic acid production by *S. sclerotiorum* ascospores which were seeded into the medium. Nine wells contain ascospores which have been incubated for 4 days. Three wells were used as control wells which were seeded with sterile water to ensure the medium contained no oxalic acid or was contaminated.

2.4 Sigma high throughput spectrophotometric determination of oxalic acid in liquid media.

This assay was optimised with the help of Prof. Nicola Tirelli and Dr. Cong Duan-Vo at the University of Manchester. Solution A was made up with 50 mM Succinate buffer (Sigma Prod. No. S-7501), 0.79 mM N,N Dimethylaniline (Sigma Prod. No. D-8509) and 0.11 mM 3-Methyl-2- Benzothiazolinone Hydrazone MBTH (Sigma Prod. No. M-8006) which were dissolved in 100 ml of deionised water. The pH was adjusted to pH 3.8 at 37°C with 1 M NaOH. 100 mM Ethylenediaminetetraacetic Acid Solution (EDTA) was made up in deionised water (Sigma Stock No. ED2SS). 1 mg / ml aliquots of Horseradish Peroxidase (HRP) (Sigma Prod. No. P-8375) was made up in cold deionised water immediately before use. A 0.25 - 0.50 unit/ml aliquot of Oxalate Oxidase (OxOx) (Sigma/Syngenta in house production) was dissolved in cold deionised water immediately before use. A master mix solution containing 12.6 ml Solution A, 0.5 ml 100 mM EDTA, 1 mg / ml HRP, 0.35 unit / ml OxOx and 1.5 ml water was mixed together.

In a 96-well flat-bottom tissue culture plate (TPP®), 10 µl of liquid medium to be tested for OA concentration was pipetted into a single well. At least two technical replicates per sample were used. 10 µl of un-inoculated medium was used as blank. A set of standards included a ranged of OA concentrations (0, 25, 50, 100, 200, 400, 1000, 1500, 2000, 2500, 3000 µM) were set up on each plate to generate a standard curve to enable prediction of the oxalate concentrations. These standards were used. These were made from the 100 mM stock oxalic acid concentration and using a dilution factor 14 to ensure the correct working concentration in the final sample volume (150 µl) and also made up in the same medium being tested. A 140 µl aliquot of the master mix was pipetted into each well of a 96 well and incubated at 37°C for 5 hr (**Figure 9**). The plates were read in a Varioskan Flash spectral scanning multimode reader (Thermo Scientific™) at 590nm (light path 1cm, 37°C). The plate was read at time 0 and then 5hrs later.

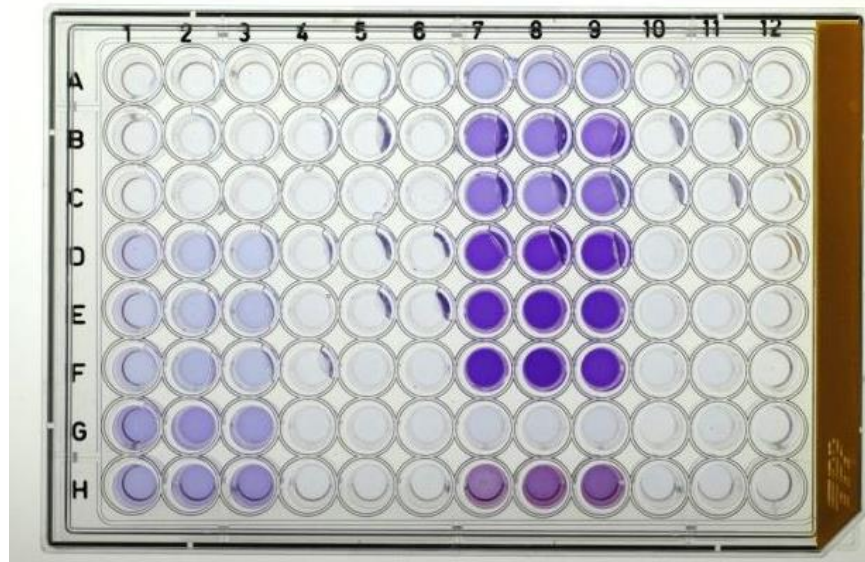


Figure 9: Oxalic acid concentration determined using a high throughput spectrophotometric assay.

A 96-well flat-bottomed tissue culture plate used to quantify oxalic acid concentration of media samples. Ten microliter of medium was added to 140 μ l of the master mix solution. Increasing oxalic acid concentrations of solutions can be observed with increasing purple intensity in the wells. The absorbance of each aliquot was read in a plate Varioskan spectrophotometer.

2.6 Calculation of the concentration of oxalic acid in samples

The results from the Varioskan software were imported into Microsoft Excel and the value of OA determined using the Genstat asymptote script written by Stephen Powers based at the Rothamsted Statistics department. The script was based on the following equation:

$$y = a + bR^{conc}$$

This script predicted the OA values using the equation used to fit the known standard concentrations of OA to an asymptotic curve. The OA concentration average of the three biological replicates which contained known concentrations of OA was used to create the concentration bar graphs. Absorbance values greater than the standard concentration could not be estimated. In this case the test had to be repeated by either increasing standard concentrations or by diluting the 10 μ l sample with water.

Script used in Genstat to determine OA concentrations by applying the equation to known absorbance values of the known concentrations of OA:

```

express e1; valu=!e(y=a +b*R**Conc)
model Absorb;fit=y
rcyc a,b,R; init=0.932,-0.6926,0.99;step=*,*,*
fitn [calc=e1;print=s,e,m,mon]
rgraph Conc
scalar abs1
read abs1
value xxxx
scalar C1
variate [nv=1; val=*] se1
express e2; valu=!e(C1=log((abs1-a)/b)/log(R))
rfunc [calc=e2;se=se1] C1
vari CforANOVA; valu=! (#C1)
vari SEforANOVA;valu=! (#se1)
print CforANOVA,SEforANOVA

```

2.7 Statistical analysis

General ANOVA analysis was done to assess whether there was any significant difference between the effects of different treatments of media on the amount of OA produced in the different experiments. GenStat 2011, version 14, (c) VSN International, Ltd, Hemel Hempstead, UK was used for the analysis.

2.8 DNA extraction

2.8.1 Hyphae DNA extraction

DNA extraction was done by growing up a range of fungal isolates either in PDB liquid medium for 1 week or on sterile cellophane discs on top of PDA plates. Cultures were vacuum filtered and freeze dried to remove excess liquid. A Plant DNeasy mini kit (Qiagen, Manchester UK) was used to extract DNA. The manufacturer's protocol was followed.

2.8.2 *S. sclerotiorum* ascospores DNA extraction

An ascospore solution made up in 2 ml tubes. The tubes were frozen at -20 °C and freeze dried to remove any moisture. Alternatively Burkard wax tape strips were cut into strips corresponding to a single day of air sampling. The strips were coiled into 2 ml screw cap tubes. One scoop of ballotini beads (0.5 g x 400-455 µm diameter) we placed in the same 2 ml tubes. 440 µl of Extraction Buffer consisting of; 400 mM Tris-HCl; 50 mM

EDTA pH 8; 500 mM sodium chloride; 0.95 % sodium dodecyl sulphate (SDS); 2 % polyvinylpyrrolidone and 5 mM 1,10-phenanthroline monohydrate, was added to each tube. 0.1% β -mercaptoethanol was added to each 2 ml tube. The tubes were processed in a FastPrep machine. They were shaken 3 times at 6.0 m/s for 40 sec, with a 2 minute cooling period between each cycle. During this period, the tubes were placed on ice. After shaking, 400 μ l of 2 % SDS was added to each tube. The tubes were inverted several times and incubated at 65 °C in a water bath for 30 mins. Eight hundred microlitres of the bottom phase of phenol: chloroform (1:1) was added to each tube and then vortexed. Tubes were centrifuged at 4 °C at 13 krpm for 10 mins. In a 1.5ml flip-top Eppendorf tube, 30 μ l of 7.5 M ammonium acetate and 480 μ l of isopropanol was added. The top layer of the supernatant from the original tube was pipetted up carefully and placed into the 1.5 ml Eppendorf tube containing the ammonium acetate mixture. The tubes were inverted several times and centrifuged at -20 ° at 13 krpm for 30 mins. The supernatant was removed leaving a DNA pellet. The pellet was washed with 200 μ l of 70 % ethanol and the tube centrifuged again at 13 krpm for 15 mins. The ethanol was removed and the pellet dried. The pellet was re-suspended in 30 μ l of sterile deionised water and mixed. All DNA was stored in a freezer at - 20 °C.

2.9 RNA extraction

To obtain RNA from *S. sclerotiorum* ascospores grown in vitro, ascospores were germinated in 1 ml PDB in Eppendorf tubes for 5 days. Material was collected by centrifuging the tubes for 2 min at 4°C. The supernatant was pipetted off. The mycelium was washed with RNase free water and snap frozen in liquid nitrogen. The mycelium was then freeze dried to remove moisture.

To obtain RNA from *S.sclerotiorum* infected leaf tissue, leaves were collected into 2 ml tubes and immediately frozen in liquid nitrogen. The tubes were freeze dried to remove moisture.

In both instances, RNA was extracted using a RNeasy Plant mini kit (Qiagen, Manchester UK) following the manufacturer's instructions. RNA/ DNA quantified on a NANodrop ND-1000 spectrophotometer (NanoDrop Technologies).

2.10 Amplification of DNA targets using Polymerase Chain Reaction

Polymerase Chain Reaction (PCR) amplification was performed with REDTaq readymix (Sigma-Aldrich). For each 25 μ l reaction; a total of 10 mM of each primer and 25-100 ng of DNA template was used. 12.5 μ l REDTaq ready mix and 10 μ l sterile water, were added. Sterile water was used in place of DNA templates as a negative control. A

GS4 thermocycler (G-storm, Somerset, UK) was used for the PCR. Cycling parameters included a denaturing step of 95 °C for 2 mins followed by 35 cycles of 95°C for 30 secs, 55°C for 30 secs, 72°C for 45 secs and a final extension step of 72°C for 5 mins. PCR products were run on a 0.8% molecular biology grade agarose (Fisher Scientific, Loughborough, UK) gel with 1 X TBE buffer (0.89 M Tris Borate, 20mM Na₂EDTA). Gels were stained with ethidium bromide (Sigma-Aldrich, UK) at a final concentration of 0.78 µg ml⁻¹. Typically, 10 µl of PCR product and 4 µl of 1 kb or 100 bp Gene Ruler ladder (Fermentas, Thermo scientific, UK) were loaded onto gels. Gels were electrophoresed at 120V for 20 – 40 mins. DNA fragments were visualised under a 302 nm transilluminator (Syngene, MD, USA) using the Gene Genius BioImaging System.

2.11 Quantitative Polymerase Chain Reaction for the specific identification of *S. sclerotiorum*.

A high throughput Roche Taqman qPCR protocol for the specific identification *S. sclerotiorum* DNA was optimised by Jon West and Gail Canning (method pending publication; Calderón-Ezquerro et al. Molecular Detection Of Airborne Sclerotinia Sclerotiorum Spores On Mexican Crops). ABGENE 96 well plates were used for the assay. A master mix was prepared with 10 µl 2x FastStart universal probe ROX Master mix (Roche Diagnostics GmbH), 0.04 µl Taqman Probe (100 µM) (TCG TAC CTT GGC AAC ACC TAC TTC) (Applied Biosystems), 0.75µl Carman Ss Forward Primer (100µM) (TGT CAG AAA TAA TGA GAT CAA AAG), 0.25µl Carmen Ss Reverse Primer (100µM) (CCG ACC TCT ATT CAT ACC CT), 4.96µl dH₂O. Standard concentrations of *S. sclerotiorum* DNA were used to generate a standard curve (0.00005-5 ng/ µl) on each plate. 4 µl DNA template or dH₂O (non-template control) was pipetted into the wells before the master mix was added. 3 technical replicate wells per sample were used. Plates were sealed and centrifuged in a SpeedVac. A Mx3000P (Startagene) qPCR machine was used. Thermal cycling parameters: 95°C 10mins and 40 cycles of 95°C for 15 secs, 56°C for 45 secs and 72°C for 45secs. Spore number can be calculated as 1 spore is the approximate of 0.1 pg DNA detected.

Chapter 3: The development of an electrochemically compatible biological matrix for the specific induction of *S. sclerotiorum* ascospore germination and oxalic acid secretion to be used within an infield automated detection biosensor.

3.1.1 Introduction

Chapters 3 and 4 report an investigation into the development of an infield automated biosensor for the detection of the fungal pathogen *S. sclerotiorum* in oilseed rape fields, the first of its kind in the world. The SYield consortium which was assembled in November 2010 to take on this challenge, received three years of funding from the Technology Strategy Board (TSB) and Syngenta. The consortium consists of a range of small, medium enterprises (SMEs) and academic partners.

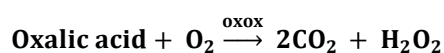
S. sclerotiorum was the pathogen of choice for this project as a result of its sporadic lifestyle which makes it difficult to predict. Outbreaks only occur every few years but when they do, they can be severe, reducing yield by up to 50%. There are some climate based forecasts to predict potential outbreaks for this pathogen, however as they are predominantly weather based, they only work on a regional scale and some rely on being able to identify the fruiting bodies in the field or by physically monitoring petal stick (Clarkson et al. 2007, Parker et al. 2009). Both methods remain a challenge for many growers because of the need to provide such continuous monitoring for a single disease. Currently growers can spray fungicide protectants up to three times per flowering season to protect crops being infected with *S. sclerotiorum* even though there may be no risk of disease. This may also increase the selection pressure for resistance to develop in other pathogen populations. For example, Boscalid a SDHI fungicide, is not only used to control *S. sclerotiorum* but is used against *Alternaria sp*, *Botrytis cinerea*, *Blumeria graminis* and *Rhizoctonia solani* in leafy vegetables. Overuse of this single fungicide without using other chemistries with different modes of action, could lead to less resistance fungal populations.

S. sclerotiorum ascospores are released from apothecia which develop from sclerotia found in the soil. The ascospores are wind dispersed upon release. Although most ascospores are dispersed locally, they can be moved tens of kilometres from the source. This poses a potential disease threat to host crops within a large area in the vicinity of the inoculum source. The aim of this project is to detect the presence of *S. sclerotiorum* ascospores within a field and combine this information with climatic information, to provide a more accurate disease risk assessment. This will provide a more accurate spray window for growers. This will potentially benefit the environment, reduce selection

pressures for resistance and help growers save thousands of pounds per growing season if they can avoid applying a second or third spray each growing season if this detection system can accurately determine that there is no disease risk.

The basic design of this detection system combines an air sampling unit which actively draws air into the device and deposits the air particles onto a biological matrix which is attached to an electrochemical biosensor. The electrochemical biosensor consists of an enzyme which is stabilised onto a carbon electrode. The enzyme is specific to a particular analyte which is specific to the pathogen being detected. Upon arrival of the analyte, the enzyme will hydrolyse the analyte. The products of this reaction will then physically react with the electrode causing a change in potential across the matrix which is then detected using a potentiostat. This detection event can then be transmitted wirelessly to the end user.

This chapter focuses on the development of the biological matrix within the biosensor which is a selective nutrient liquid medium which actively encourages *S. sclerotiorum* ascospores which are sampled from the air into the device, to germinate and grow within the matrix. As previously described, *S. sclerotiorum* produces oxalic acid (OA) during development. The secretion of this organic acid regulates a whole range of virulence functions. OA was chosen as the analyte to be detected within the biosensor as firstly it is secreted at an early stage of ascospores germination and secondly, oxalate oxidase (OxOx), readily hydrolyses OA to release carbon dioxide (CO₂) and hydrogen peroxide (H₂O₂).



Once the ascospores have been incubated with the liquid medium and secreted oxalic acid, the liquid will then be applied to a carbon electrode which contains two enzyme, OxOx and horse radish peroxidase (HRP). The detection of *S. sclerotiorum* will actually be based on a coupled enzyme reaction. During this process OxOx will hydrolyse any OA present in the liquid medium, releasing hydrogen peroxide and carbon dioxide. Hydrogen peroxide will then be hydrolysed by HRP and measured using an electrochemical process described as cyclic voltammetry. This technique involves the application of a potential to an electrode which is ramped linearly between two voltage points at a scan rate of 0.05 V/s. The measurement starts with a specific condition, for example everything in the sample is fully reduced. As the potential changes from the starting conditions, the active chemical species in the sample will become oxidised. The detection principle in this biosensor is based on the electrochemical oxidation of hydrogen

peroxide which is generated from the activity of OxOx (**Figure 10**). This system is based on the blood glucose biosensor which was invented in 1962 and originally determined the glucose concentration by applying a negative potential to a platinum cathode containing stabilised glucose oxidase (Gox). The reductive detection of the oxygen consumption which was released from the breakdown of glucose was then measured (Clark and Lyons 1962). The electrochemistry used in the SYield biosensor was optimised and fixed to measure only the release of hydrogen peroxide and not any other electrochemical-active chemical species that may be in the matrix. This part of the project was carried out by Dr. Sophie Weiss at the University of Manchester. The positive detection of OA (termed ‘a positive event’) will be relayed through a network as a wireless signal to be picked up by a central processing unit. The positive event will then be integrated with climatic information and fed into a real time disease prediction model. If a risk is predicted then the farmer will be notified and advised to spray his crop to protect against *S. sclerotiorum*.

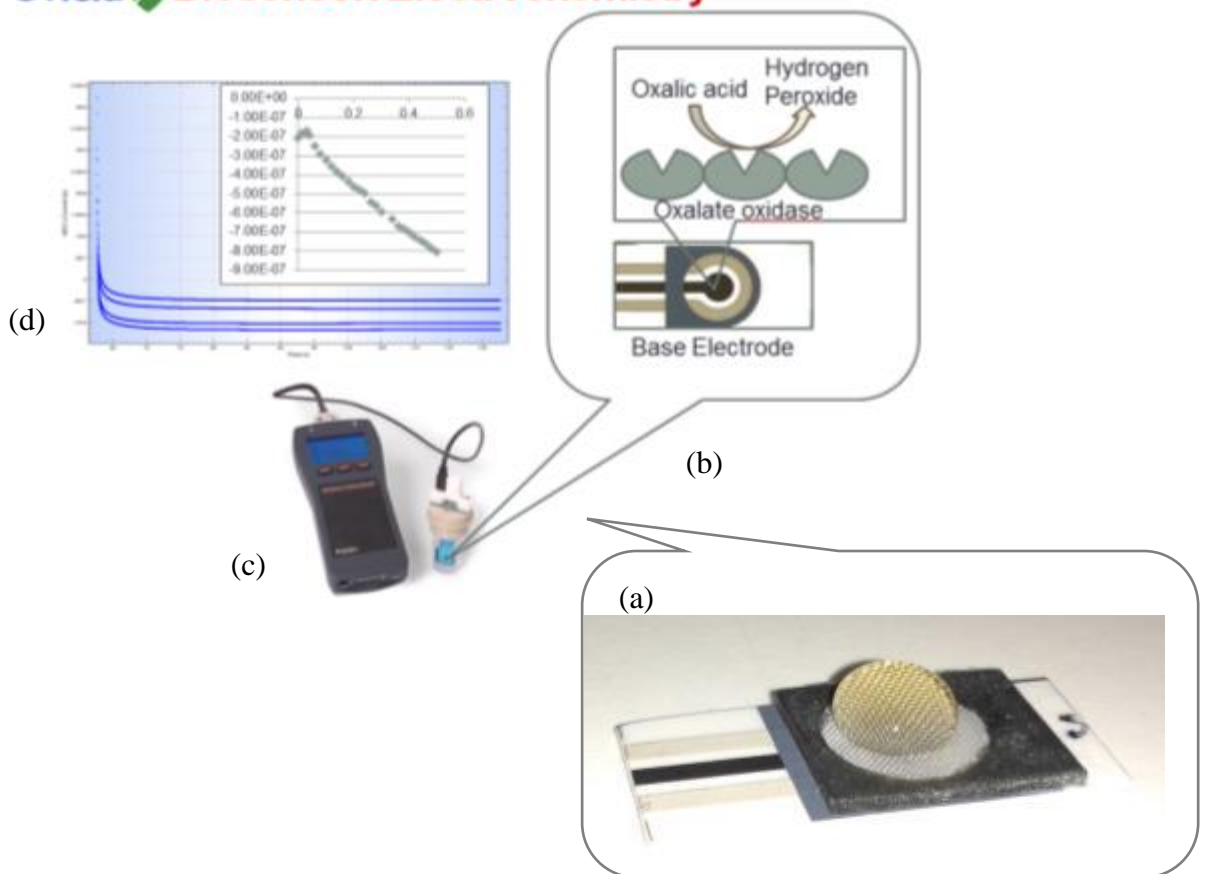


Figure 10: Schematic of the basic principles of electrochemistry used in the SYield biosensor.

a) The biological matrix (liquid medium) contains the analyte to be detected, OA. b) The electrode contains OxOx stabilised enzyme which hydrolyses OA in the biological matrix, releasing hydrogen peroxide, which directly reacts with the electrode. c) A potentiostat is connected to the working and reference electrodes and monitors the change in current as the hydrogen peroxide becomes oxidised. d) The output of the change in current can be monitored and reported using software connected to the potentiostat. The change in current increases as the amount of OA in the biological matrix increases.

3.1.2 Considerations for the biological matrix design and biosensor detection success

There were certain challenges which required consideration throughout the development of the biological matrix to ensure that the detection of *S. sclerotiorum* ascospores was as accurate as possible. It was of paramount importance that the matrix was able to:

- Induce rapid growth of fungal hyphae post ascospore germination.
- Induce rapid secretion of OA.

- Induce high levels of OA production.
- Be selective for *S. sclerotiorum* growth and not the many other fungi which may be present in the air sample which either produce OA themselves or could out-grow the *S. sclerotiorum* hyphae.
- Detect low ascospore numbers.
- Must be compatible with the electrochemistry and not inhibit any of the chemistry within the sensor system

Other fundamental questions to be solved during the formulation of the matrix for accurate sensor development included:

- Does the change in pH of the biological matrix have an effect on the pathogen growth or biosensor performance?
- What is the effect of temperature on fungal growth and enzyme activity?
- Is oxalic acid quantifiable in the biosensor and how does this relate to spore number?
- Does the OA level correlate to disease risk in the field?
- Does the sensor rapidly detect early germ tube growth post spore germination to maximise the window of opportunity for successful crop protection?

This chapter reports the development stages of the nutrient matrix that will address the above considerations and questions. There have been other studies in the past exploring how to optimise OA production from *S. sclerotiorum*. However all these previous investigations have only explored OA production from mycelial plug inoculations and not ascospores which makes this work novel. OA secretion from a range of plant pathogens has been investigated previously however no previous studies have investigated the compatibility of a nutrient matrix coupled to an electrochemical for the detection of *S. sclerotiorum* ascospores. Other OA detection methods have been previously used in medical studies which use quantification of OA in human urine to monitor kidney stone development (**Table 3**).

The investigations into developing a nutrient medium began with the use of host plant extracts to germinate the ascospores and initiate hyphal growth. However a more defined medium was eventually developed that was compatible with the electrochemical assay. The effect of different glucose concentrations and other additions/ subtractions to the medium was investigated as well as the buffering capacity. Investigations into the typical fungal community which may be present within the biosensor air sample were also undertaken. Other fungal competitors were identified and medium specificity was addressed through the use of fungicidal additions. Chapter 4 will report how the biological matrix developed in this chapter performed during field trials.

Table 3: Methods for detecting OA in clinical samples and for the investigation of OA production by plant pathogens.

Detection methods for OA in urine as an indicator for kidney stones	Detection methods for OA in fungal pathogens/host plants
High-performance liquid chromatography (Holloway et al.1989)	KMnO ₄ titration (Bateman and Beer 1965)
Gas chromatography (Gelot et al. 1980)	Thin-layer chromatography (Vega et al. 1970)
Ion chromatography (Schwille et al. 1989)	Enzymatic detection in a HPLC eluate (Rassam and Laing 2005)
Spectrophotometric methods based on oxalate oxidase (Kohlbecker and Butz 1981)	Bromophenol blue, quenching reaction. Absorbance measured (Durman et al. 2005)
Oxalate decarboxylase (Beutler et al.1980)	
pH-electrode determination coupled with an enzymatic reaction (Boer et al. 1984)	
Chemiluminescence detection (Balion and Thibert 1994)	

3.2 Experimental Procedures

3.2.1 Bioassay for the quantification of OA produced by ascospores in on solid media made from plant extracts.

Various host plant extracts were used to make different solid agar media to test the best medium for the quickest, most reliable oxalic acid induction from *S. sclerotiorum* ascospores:

PDA (Potato Dextrose Agar)	20 g potato dextrose agar (Difco) added per 500 ml deionised water and autoclaved.
Carrot Agar	400 g of chopped fresh carrots autoclaved in 400 ml deionised water. Carrots blended. Carrot solution made up to 500 ml with deionised water and mixed with 10 g agar before re-autoclaving.
V8 juice	0.8 g CaCO ₃ , 8 g agar and 80 ml V8 juice mixed (company add) with 320 ml deionised water and autoclaved.
Sunflower Seed agar	25 g sunflower seeds were pulverised in a blender. The seeds were boiled in 500 ml deionised water for 30 mins. The seed extract was cooled and filtered through gauze. The filtrate was mixed with 5 g glucose and 7.5 g agar. The solution was made up to 500 ml with distilled water and autoclaved.
SNA (Synthetic nutrient poor agar)	20 x stock solution of made up using 0.1 % KH ₂ PO ₄ , 0.1 % KNO ₃ , 0.1 % MgSO ₄ ·7 H ₂ O, 0.05 % KCl, 0.02 % glucose, 0.02 % saccharose, 2 % Agar. 20 ml 20 X SNA stock added to 500 ml deionised water.

Bromophenol blue pH indicator dye was added to the different plant extract agars. A stock solution of bromophenol blue was made up by diluting 0.1 g powder in 4 ml 95 % ethanol. A 1 ml aliquot of this stock solution was added to 500 ml liquid agar media. Bromophenol blue will change a substrate from blue to yellow during the acidification of the substrate. Sodium succinate (56 mM) which has been previously shown to increase OA production in *S. sclerotiorum* cultures, was added to duplicate bottles of all media. All the media was titrated to pH 6 using hydrochloric acid or sodium hydroxide before autoclaving the solution. Three replicate plates for each treatment were used. Three ascospore solutions (L6 isolate) were made up using ascospore covered filter paper. Sixteen spots of 20 µl ascospore solution were pipette onto each plate in sterile conditions. The plates were stored in 18 °C incubator and regularly checked for signs of bleaching or mycelia growth. Yellowing circles around growing colonies were compared to known concentrations and volumes of OA dropped onto the same type of plate (**Figure 11**).

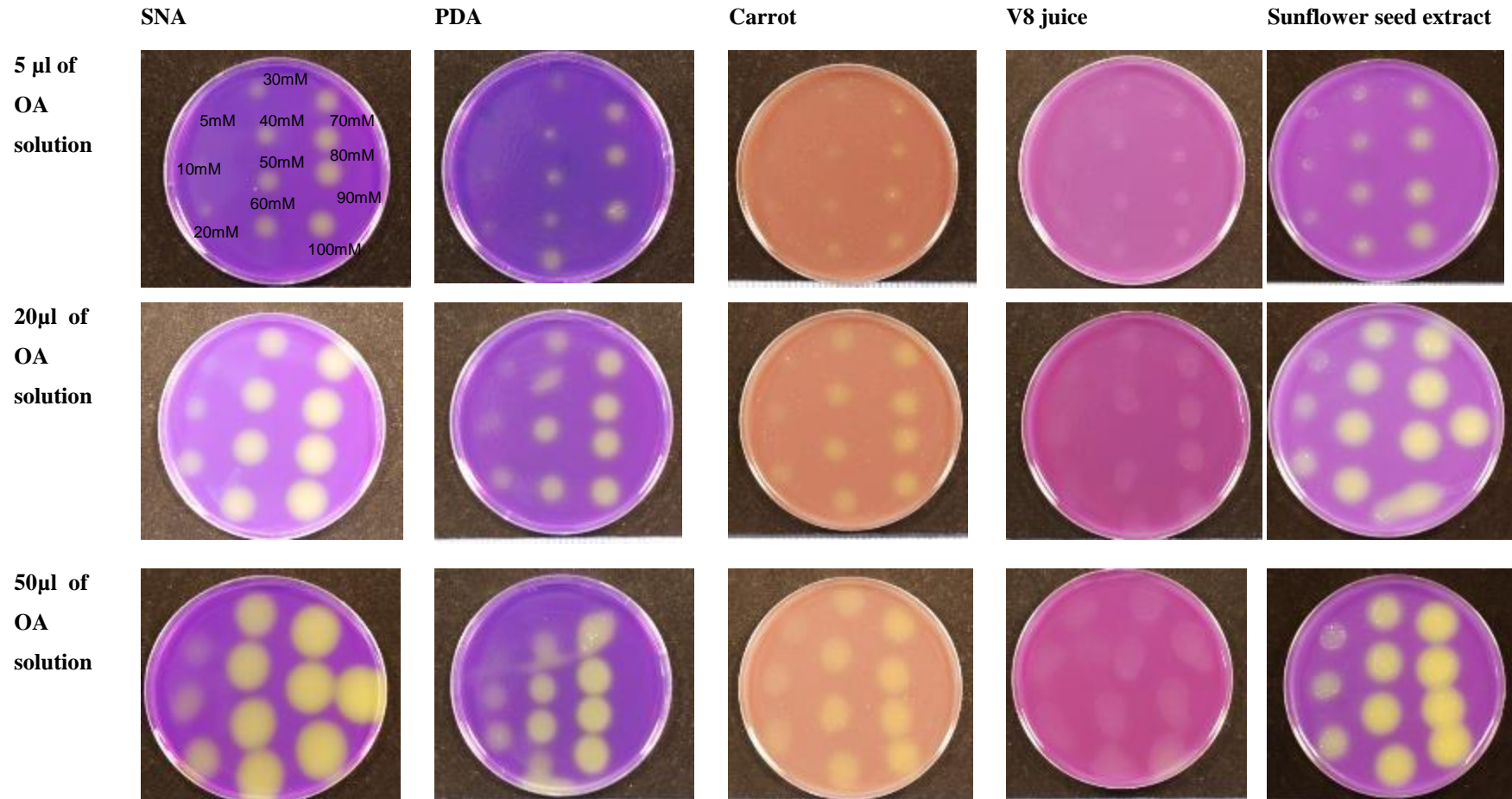


Figure 11: The standard OA concentration agar plates.

Plates used to quantify OA secreted by *S. sclerotiorum* ascospores grown on different plant extract agars. Agar contained a bromophenol blue pH dye which changes the agar colour from blue to yellow during acidification of the agar, during the release of OA. Each type of agar tested had 5, 10 and 50 μ l of different solutions containing different concentrations of OA dropped onto the different plates. Colour changes in carrot and V8 agars were difficult to assess due to lack of blue colour change.

For details on how ascospore solutions were made up for testing and how bioassays for media testing were carried out refer to General Experimental Procedures (Chapter 2).

3.2.2 Preliminary experiments

3.2.2.1 Detection limits of Sigma OxOx enzymatic spectrophotometric assay

Preliminary experiments were completed to determine the OA detection limits of the enzymatic spectrophotometric tests. Twenty six wells of a 96 well plate were filled with 20 μ l potato dextrose broth (PDB) (Sigma Aldrich, 24g/L). The wells were then spiked with different OA concentrations to achieve working OA concentrations of 0, 2, 5, 10, 15, 20, 25, 50, 100, 200, 400, 500 and 800 μ M. The absorption of two replicates per concentration was measured using the spectrophotometric assay (see Chapter 2) and the experiment was repeated twice.

3.2.2.2 Preliminary work to determine whether any additions to assay can inhibit enzyme activity.

A second experiment was completed to determine whether different chemical additions to the medium, for example; malic acid, succinic acid and fumarate, could affect the activity of the OxOx and HRP enzymes or inhibit these enzyme used in the optical enzymatic assay and as a result affect the accuracy of the absorbance readings and oxalate concentrations calculated with the use of the standard curves. These additions are intermediates of the Tricarboxylic acid cycle which has been described as the principal OA biosynthesis pathway ([Culbertson et al. 2007](#)). They were chosen as they had been previously used to induce OA secretion (explained in detail later on). OA standards were made up with the addition of different concentrations of malate in PDB medium. Two replicates for each concentration were tested.

3.2.2.3 Storing medium for later OA detection and electrochemical analysis.

The wells of a 12 well plate were filled with 2 ml of PDB. The PDB was spiked with 100 mM stock solution of oxalic acid to reach a working concentration of 140 μ M or 100 μ M oxalic acid. 12 replicates per concentration were used. Six replicates for each concentration were frozen at either -20°C or -80°C. The concentration of OA was measured using the spectrophotometer assay (see Chapter 2) after 7 days of being in the respective freezers.

3.2.2.4 The effect of temperature, shaking and a flotation membrane on OA production.

PDB was made up following manufactures instructions and adjusted to pH 5 before autoclaving. Six wells of eight 12 well plates were filled with 2 ml of PDB. Three wells per plate were seeded with 100 μ l ascospore solution (approximately 45 000 *S. sclerotiorum* L6 ascospores per well). 3 wells on the plate were used as a negative control and were seeded with 100 μ l water. Four of the plates were kept at 20 °C and the other 4 plates were kept at 25 °C. A disc of sterile miracloth (Merck Millipore, UK) was placed into the wells of two plates incubated at 20 °C and the wells of two plates incubated at 25. The membrane was added to the medium by cutting a miracloth disc the size of the well and then dropping it on top of the medium before adding in the ascospores. Plates with and without miracloth discs were either shaken at 150RPM or kept still under both temperatures. All experiments were carried out in the dark. The plates were incubated for 4 days and the OA concentrations calculated using the spectrophotometer assay (see Chapter 2).

3.2.3 OA production induction via Tricarboxylic Acid Cycle intermediates combined with a baseline nutrient

Media were made by adding 25 mM malate, 25 mM succinate, 25mM ammonium acetate, 1% pectin, 25mM glucose or PDB (24 g/ L) to the baseline minimal salts (Culbertson et al 2007). The wells of a 12 well plate were filled with 2 ml of different media. Each treatment was replicated using 3 wells. 100 μ l ascospore solutions (4000 spores / well) of L6 and L2003 *S. sclerotiorum* isolates were added to the each well and incubated in the different growth media for six days. Negative control wells were seeded with 100 μ l sterile spectrophotometer assay (see Chapter 2)water. The OA concentrations calculated using the spectrophotometer assay (see Chapter 2).

3.2.4 Complex media (Soytone and Yeast) combined with TCA cycle intermediates and their effect on OA production.

1% Soytone medium(Fisher Scientific) and 1% Yeast medium (Sigma-Aldrich) were made up with baseline nutrient salts (Culbertson et al 2007). The media were adjusted to pH 5 before autoclaving. 2 ml of each medium was added to the wells of 12 well plates. 1M stock solutions of glucose, malic acid, ammonium acetate or succinate were sterile filtered and added to each type of media, and adjusted to make a working concentration of 25 mM glucose, malic acid, ammonium acetate or succinate . Each individual treatment was replicated in three wells. An L6 isolate *S. sclerotiorum* ascospore solution was made up in sterile water. 100 μ L spore solution was added to each well (approximately 3000

spores). 100 µL sterile water was added to negative control wells. The plates were incubated for 4 days. The OA concentration of each well was calculated using the spectrophotometer assay (see Chapter 2).

3.2.5 The influence of different glucose concentrations on OA production in a complex medium.

1% Soytone medium was made up with baseline nutrient salts and adjusted to pH 5. The wells of 12 well plates were filled with 2 ml of medium. A stock solution of 500 mM glucose solutions was sterile filtered and added to each well to make media with either 0, 25, 50 or 100 mM additional glucose concentrations. Each treatment was replicated 3 times in 3 wells. A *S. sclerotiorum* L6 ascospore solution was made. Approximately 2900 ascospores were added to each well. Negative control wells contained no ascospores. The plates were incubated for 4 days at 20 °C in the dark. The OA concentration of each well was calculated using the spectrophotometer assay (see Chapter 2).

On three separate occasions lower glucose concentrations (0, 5, 10, 15, 20, 25 mM) were also tested with 1% soytone medium as described above on three. The first experiment 900 *S. sclerotiorum* L6 isolate ascospores were used per well. The second repeat of the experiment used varying numbers of L6 isolate ascospores ranging from 175, 750, 1050, 2100 and 7500 ascospores per well. The third repeat experiment used a single ascospore dose per well of 175 L6 *S. sclerotiorum* isolate ascospores. All treatments were repeated in three wells. Plates were incubated for 7 days at 20 °C in the dark.

3.2.6 TCA cycle intermediate additions

TCA cycle intermediates were tested for their effect on OA production in a similar format to how the effects of different glucose concentrations on OA production was investigated. 1% soytone medium was made up with baseline nutrient salts and 25 mM glucose and adjusted to pH 5 before autoclaving. 2 ml of the medium was added to the wells of a 12 well plate. 1M stock solutions of fumarate, malate and succinate were made up with sterile water and sterile filtered. Working concentrations of 0, 5, 15 and 25mM of the intermediates were added to the wells separately. Three replicate wells were used per treatment. The experiment was repeated on 3 separate occasions. There The OA concentration of each well was measured at day 3, 4 and 7 of incubation using the spectrophotometer assay (see Chapter 2). Ascospore concentrations used for each separate experiment were approximately 1750, 900 and 4860 ascospores per well of the L6 *S. sclerotiorum* isolate. Sterile water was added to wells for a negative control. Plates were incubated for 7 days at 20 °C in the dark.

3.2.7 Comparison four electrochemical compatible media for OA induction

The four electrochemical compatible media were tested for their ability to promote OA production from *S. sclerotiorum* L6 isolate ascospores. 1% Potato dextrose broth, 1% Yeast Nitrogen base with no added amino acids (Sigma Aldrich), 1% Sabouraud Dextrose Broth (Sigma-Aldrich) and 1% Czapeks Dox (Oxoid, Thermo Scientific) media were made up separately with baseline nutrient salts and adjusted to pH 5. Sterile filtered 25mM glucose was added to a second batch of the same media after autoclaving. In each well of a 12 well plate, 2 ml of the medium was added. Six wells were used for each type of medium. Three wells contained ascospores and 3 wells acted as negative controls with no ascospores added. Approximately 9250 ascospores were added to each well. Plates were incubated for 7 days at 20 °C in the dark and the OA concentrations of each well checked on day 3, 4, 5 and 6 of incubation.

3.2.8 Limits of detection.

1% Sabouraud Dextrose Broth (SDB) was made up with minimal baseline salts and adjusted to pH 5 before autoclaving. 500 µl plastic field pots were cleaned with 95 % Ethanol and dried in sterile conditions. Each single pot was placed in a single well of a 12 well plate so that the pots remained under sterile incubation conditions. 400 µl of the medium was pipette into each pot. Three spore dilutions were tested to determine the lowest number of ascospores that could be detected by the amount of OA measured. 0, 4, 16, 67, 135, 543, 1087, 4350 *S. sclerotiorum* L6 isolate ascospores were added to separate pots. Three pots were used per ascospore dilution. The plates were incubated in the dark at 20 °C and the OA concentrations of each pot measured after 3, 4 and 5 days incubation in sterile conditions by using the spectrophotometer assay (see Chapter 2).

3.2.9 The relationship between *S. sclerotiorum* ascospore number, biomass and oxalic acid production

1% SDB medium was made up with baseline salts and adjusted to pH5 before autoclaving. 2 ml of the medium was added to the wells of 12 well plates. Three *S. sclerotiorum* L6 isolate ascospore dilutions were made up in sterile water so that each well contained either a high spore dose of 2366 spores, a medium spore dose of 291 spores or a low spore dose of 50 spores. Each spore dose was replicated in three wells. Negative control wells contained no spores. The plates were incubated in the dark at 20 °C for 11 days The plates were set up so that at days 1, 2, 3, 4, 5, 6 and 11 incubation, three wells of each spore dose were destructively sampled. These samples were used to measure the average biomass of the fungal cultures growing for each spore dose. All liquid and any

visible fungal biomass from these wells was pipetted into a pre-weighed 2ml tube. The tube was frozen at -20 °C and freeze dried to remove any liquid. The tubes were then re-weighed and the difference between the pre and post weight calculated.

Over 11 days of incubation, the pH of the liquid medium was tested using a micro pH probe (Hanna Instruments, UK) which is capable of measuring volumes as small as 100 µl as the medium volume decreases significantly after 11 days incubation. The OA content of the wells were also measured on day 1, 2, 3, 4, 5, 6 and 11 of incubation.

As a result of the destructive sampling structure of the experiment and the repeated measures aspect of the experiment, the method of Residual Maximum Likelihood (REML) was used to fit a linear mixed model to the pH and oxalate data, accounting for the design of the experiment (plates, wells within plates and time points within wells) as random terms in the model. As part of this structure, the effect of the correlation over time for the wells was accounted for. The overall effect of treatment compared to control and then the effects of low, medium and high treatment, nested within this comparison were taken as fixed terms in the model, along with the main effect of time and the interaction of time with these other terms. The GenStat (2011, version 14, (c) VSN International, Ltd, Hemel Hempstead, UK) was used for the analysis.

The model used was based on the following equation:

$$y = \underbrace{\text{constant} + \text{Treatment}_i + \text{Time}_i + (\text{Treatment} \cdot \text{Time})_{ij}}_{\text{Fixed Terms}} + \underbrace{\text{Plate}_k + (\text{Plate} \cdot \text{Wells})_{kc}}_{\text{Random Terms}} + E$$

(Where terms in the model are as stated and with E as the error term)

3.2.10 Buffering Capacity of the medium

50 mM MES (2-(N-morpholino)ethanesulfonic acid), 50 mM Succinate and 50 mM HEPES (4-(2-hydroxyethyl)-1-piperazineethanesulfonic acid) were added to separate bottles of 1% SDB. SDB was also tested without an additional buffer. Separate buffered media were adjusted to pH 4, 5, 6 or 7 and then autoclaved. 2 ml of each treatment was added to 9 wells. A low ascospore dose was added to 3 wells, a high ascospore dose added to 3 wells and the final three wells were used as negative control wells with no ascospores added. The low *S. sclerotiorum* L6 isolate ascospore dose used in the MES buffered medium was 30 ascospores per well and the high dose was 290 ascospore per well. The low *S. sclerotiorum* L6 isolate ascospore dose used in the HEPES and Succinate buffered

media was 38 ascospores and the high dose was 2366 ascospores per well. The plates were incubated in the dark, 20 °C for 5 to 11 days. The OA concentration and the pH was measured for each well on day 1, 2, 3, 4, 5, 6, 7 and 11.

3.2.11 Competition assays

Trichoderma, *Botrytis*, *Alternaria* and *Epicoccum* species isolated from the field (See Chapter 4) were cultured on PDA plates to obtain spores. Spore solutions were obtained for each fungal species by pipetting 1ml sterile water onto the surface of the plate. Using an L-shaped spreader, the spores were mixed with the water. Water and spore solution was pipette off the plate. *S. sclerotiorum* ascospore solution (L6 isolate) was made as mentioned previously.

To test whether any of these species secreted oxalic acid within the medium, the wells of 12 well plates were filled with 2 ml SDB medium, pH. All fungal spore solutions were adjusted so that 1000 spores were added to each well. Each fungal spore type was repeated in 3 wells. The plates were incubated over 7 days in the dark at 20 °C and the OA concentration of each well measured on day 4, 5 and 7 of incubation.

To determine the competition between different fungal species, the wells from 12 well plates were filled with 2 ml SDB, pH 5. *Botrytis* and *Trichoderma* spores were germinated separately and together with high and low doses of *S. sclerotiorum* L6 isolate ascospores. The high spore dose was adjusted so that 290 ascospores were added to each well and the low dose added to the well was 30 ascospores. 100 spores of *Botrytis* and *Trichoderma* were added to each well separately. Each species of fungal spore was incubated individually too. Each treatment was replicated in three wells. The plates were incubated over 5 days in the dark at 20 °C and the OA concentration of each well measured on day 3, 4 and 5 of incubation. Observations of fungal growth were also recorded on these days.

3.2.12 High throughput fungicide sensitivity testing

Fungicide sensitivity assays were adapted from the methods published by Pijls et al (1994) (Pijls et al. 1994). Dimethylsulfoxide (DMSO) or acetone was used to dissolve fungicide powders to make stock concentrations of fungicides. Potato dextrose broth (2X) was amended with decreasing concentrations of fungicides to ensure that a final working concentration across the columns of the plates of each fungicide in the medium was determined at 60, 30, 15, 7.3, 3.75, 1.875, 0.9375, 0.469, 0.234, 0.117, 0.059, 0 $\mu\text{g ml}^{-1}$. A 100 μl aliquot of fungicide amended PDA was added to each well of a flat bottomed 96 well microtitre plate (**Figure 12**). The 100 μl aliquot of ascospore suspension (1×10^6) of each fungal isolate was added to each well. Plates were incubated in the dark, at room

temperature. After three days of incubation, fungal growth was measured using a FLUOstar OPTIMA microplate reader (BMG Labtech, Offenburg, Germany) in end point mode. The optical density of colonies was measured at 630nm. The concentration of fungicide which inhibited growth was measured.

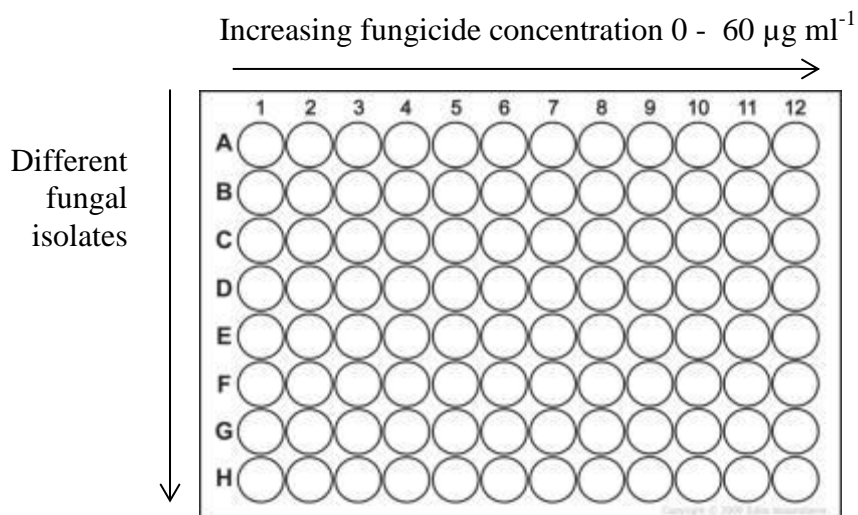


Figure 12: Plate set up for fungicide sensitivity assay.

A single fungal isolates was applied to each row of the plates. The different fungicide concentrations increased across the rows.

3.3 Results

3.3.1 The used of host plant extracts within a solid matrix

Host plant extracts including potato dextrose agar (PDA), carrot agar, sunflower seed extract and V8 juice agar (pureed tomatoes and carrots), were initially chosen for testing in a solid agar form to investigate the best medium for OA secretion from *S. sclerotiorum* ascospores. These substrates were selected as it was hypothesised that host plants would contain substrates that would induce rapid OA secretion. Bromophenol Blue (BPB), a pH indicator dye was added to the solid agar to monitor OA secretion by monitoring the change from blue to yellow upon acidification of the medium (**Figure 11**). A second set of plates contained bromophenol blue and sodium succinate as it has previously been shown that succinate can increase OA production (Pierson and Rhodes 1992). Three different spore solutions were tested per treatment. After four days of incubation, the highest spore dilutions on the PDA and sunflower seed plates were the first plates to show yellowing of the dye indicating OA was being produced and secreted.

This method provided a time scale of OA production however determining the amount of OA produced was extremely challenging. Areas of bleaching and the bleaching intensity were compared to plates of media with known concentrations and volumes of OA. It was difficult to compare inoculated plates with the OA standard plates as bleached areas of the plate would soon fade after addition of the oxalic acid standards. The different colours of the media also affected the bleaching intensity. Another challenge with this method was that the yellowing could be caused by any secreted acid which lowered the substrate pH and so was not specific to OA.

Although OA could not be accurately quantified from this experiment, these experiments did demonstrate that the sunflower seed and potato dextrose agars promoted the quickest OA production out of all the media as yellowing in these two media was seen first (**Figure 13**). It also highlighted that carrot agar was the best medium for sclerotia production as the sclerotia were consistently the largest on this type of medium (**Figure 14**). This method for producing sclerotia was adopted throughout the Ph.D.

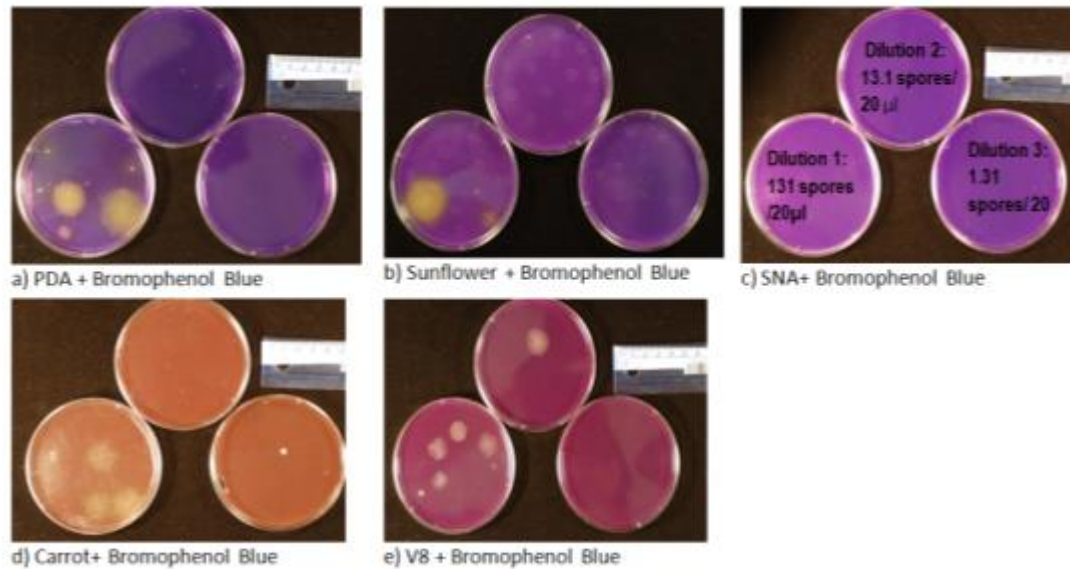


Figure 13: BPB bleaching caused by three *S. sclerotiorum* different spore solutions.

Ascospores grown on different media for four days. Bleaching first seen in PDA and sunflower agar plates (a,b). No bleaching was observed in SNA plates (c) and less bleaching was observed in carrot and V8 agars (d, e).

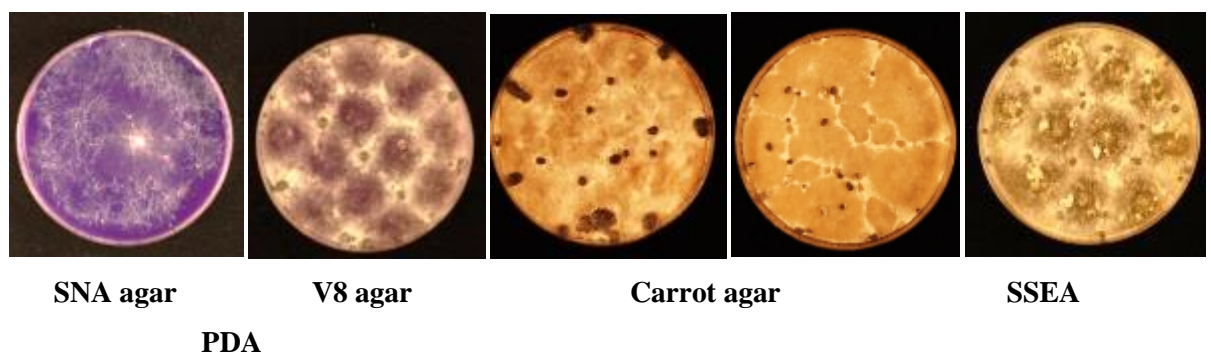


Figure 14: Different amounts of sclerotia formation on different agars containing BPB.

Carrot agar induced the largest sclerotia which are the black stone-like structures visible on the plates. SNA agar did not support / supported the smallest sclerotia formation.

3.3.2 Liquid medium is better than solid medium for the quantification of OA

The purpose of the next strategy was to increase the accuracy of OA quantification from germinating *S. sclerotiorum* ascospores. An optical enzymatic assay used to detect OA using spectrometry was found to be commercially available (Sigma-Aldrich, UK) (See Chapter 2). This assay has been utilised in medical professions to monitor oxalic acid in urine as an indicator of kidney stones (Kohlbecker and Butz 1981). This assay was optimised with the help of Prof. Nicola Tirelli and Dr. Cong Duan-Vo at the University of Manchester. This assay was used to measure the amount of OA in liquid aliquots of media.

Initially the PDB (the liquid form of PDA) and liquid sunflower seed extract were tested in for successful OA induction by *S. sclerotiorum* ascospores. The sunflower seed extract promoted OA production however oxalate concentrations varied as a result of the solid seed particles in the medium which interfered with the spectrophotometer readings (data not shown). In addition, during the testing of this medium in the pre-optimised electrochemical assay, the particles in the sunflower seed medium burnt onto the electrode. From this point onwards it was decided to choose a more defined medium that would allow reproducible oxalate production from ascospores. Also the medium was required to be compatible with both the spectrophotometer and the electrochemical assay being developed at the University of Manchester. PDB induced OA secretion and was compatible with the Sigma high throughput optical enzymatic assay and as a result was used as a control medium to determine whether other media were better inducers of OA secretion by *S. sclerotiorum* ascospores.

3.3.3 Preliminary experiments

3.3.3.1 Detection limits of Sigma OxOx enzymatic spectrophotometric assay

Preliminary experiments were completed to determine the OA detection limits of the enzymatic spectrophotometric tests. Two millimetre aliquots of potato dextrose broth (PDB) were spiked with different OA concentrations to achieve working OA concentrations of 0, 2, 5, 10, 15, 20, 25, 50, 100, 200, 400, 500 and 800 μM . The absorption of two replicates per concentration was measured and the experiment was repeated twice. The results highlight that below 25 μM , there is a lot of background noise which prevents an accurate quantification of OA. Therefore any measurements made below this concentration were not quantifiable (**Figure 15**)

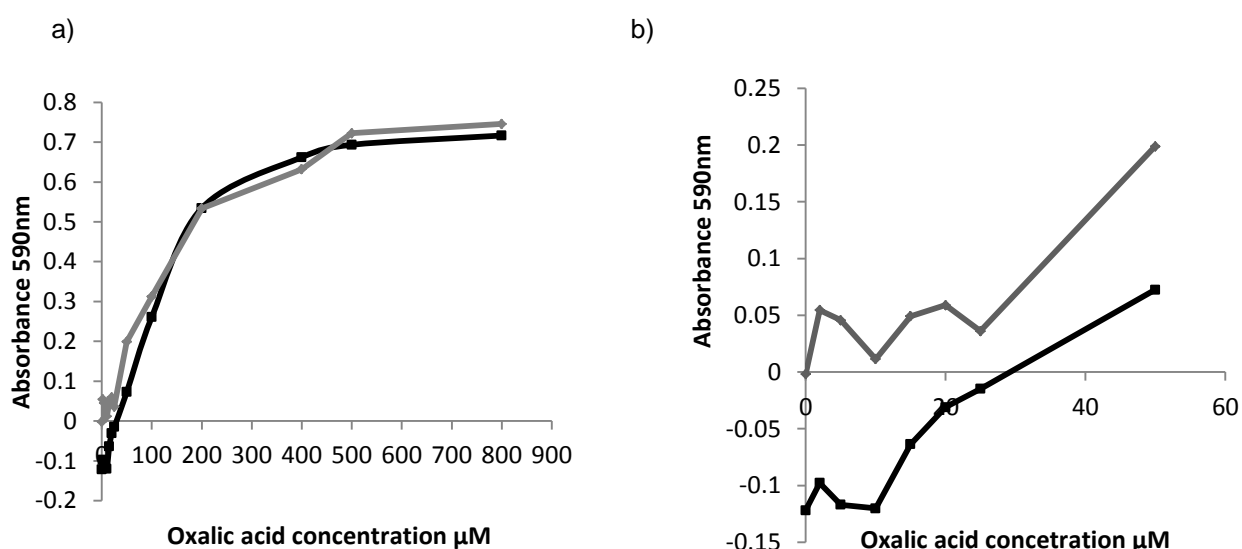


Figure 15: Detection limits of the Sigma OxOx enzymatic spectrophotometric assay.

a) Two biological replicates used to test a range of OA concentrations within the optical spectrophotometric assay and to determine the lowest level of OA detectable. Constant values can be read above 25 μM , anything below this will be considered a negative OA event. b) The enlarged area standard OA values from 0-50 μM which highlight the noise in readings below 25 μM .

3.3.3.2 Preliminary work to determine whether any additions to assay can inhibit enzyme activity

A second experiment was completed to determine whether different chemical additions to the medium, for example; malic acid, succinic acid and fumarate, could affect the activity of the enzymes or inhibit the enzyme used in the optical enzymatic assay and as a result affect the absorbance readings of the standard curves. These additions are intermediates of the Tricarboxylic acid cycle which has been described as the principal OA biosynthesis pathway (Culbertson et al. 2007). They were chosen as they had been previously used to induce OA secretion (explained in detail later on).

OA standards were made up using different concentrations of malate in PDB medium. Two replicates for each concentration were tested. The results highlight that the absorbance readings for media containing different malic acid concentrations were markedly lower than the medium which contained PDB only with no additional malate (0 mM malic acid) (**Figure 16**). This highlights that the malate may inhibit the activity of some component of the enzymatic assay. As a result a separate set of standards were generated for the specific type of medium being tested.

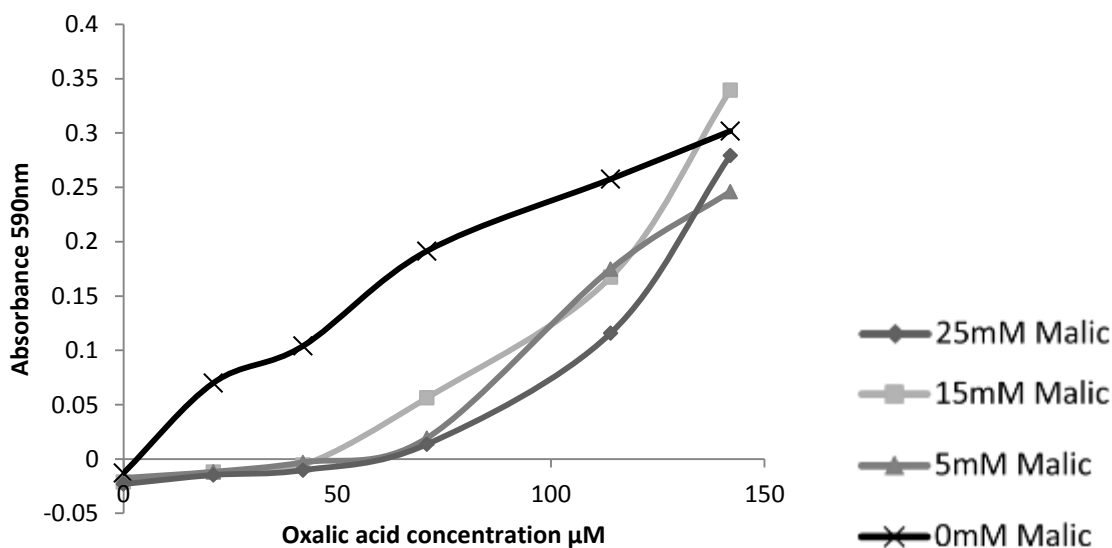


Figure 16: Absorbance readings of known concentrations of OA in PDB media containing different concentrations of the malate.

The absorbance values for those containing malate are similar compared with the absorbance values of those samples with 0mM malate. This highlights the need for standards to be made up in the same medium to the samples being tested.

3.3.3.3 Storing medium for later OA detection and electrochemical analysis

Freezing appears to have an effect on the detectable concentration of OA (**Figure 17**). In both instances the OA measurements were between 10 and 21 % lower post freezing.

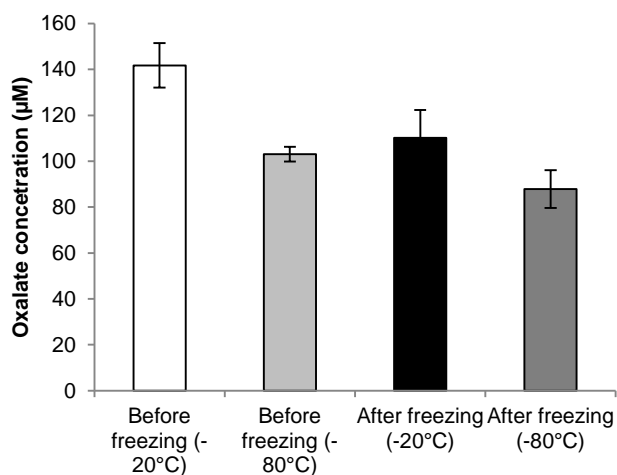


Figure 17: Storing medium for later OA detection and electrochemical analysis.

The OA levels in spiked PDB samples measured before and after freezing highlighted that there was an effect of freezing at both temperatures. Bars represent the average OA production of six biological replicates.

3.3.3.4 The effect of temperature, shaking and a flotation membrane on OA production

PDB was used to establish whether other environmental effects could affect OA production. These included external temperature, aerating the culture by shaking and whether a floating miracloth membrane would make a difference to OA production. The membrane was tested to determine whether it supported the mycelia network which forms following ascospore germination. All the experiments were carried out in the dark because previous studies have shown that exposure to UV light can inhibit of OA production (Rollins and Dickman 2001). Furthermore, when the samples are incubated in the biosensor device, this will be in an enclosed environment with no light allowed to filter through. Unfortunately two treatments were missing from the results due to bacterial contamination of the cultures. The data set lacks the results for the plates kept still at 25 °C because these plates were contaminated after 2 days growth. After four days of incubation, samples kept at 20 °C induced higher levels of OA compared with at 25 °C, regardless of the presence of a membrane or whether the culture was shaken (**Figure 18**). It was decided for future medium testing, experiments would be maintained at room temperature in the dark, with no membrane or no shaking. In the final biosensor, having to shake the sample would require a large amount of energy.

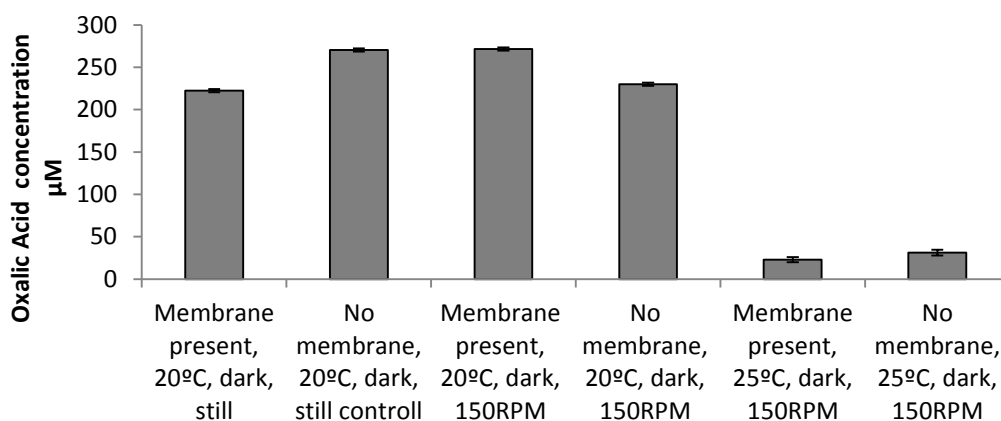


Figure 18: The effect of different environmental conditions on OA production.

Oxalic acid production by *S. sclerotiorum* L6 ascospore after four days growth under different environmental conditions. Ascospores added to 12 multi well plates with each well containing 2ml PDB. Bars represent the average OA production of three biological replicates. Ascospore concentration: 45 000 spores/well.

3.3.3.5 Creating a more defined medium which induces OA secretion and is compatible with both the enzymatic spectrophotometric assay and the biosensor electrochemistry

Fungi have relatively simple nutritional requirements in comparison to larger, more complex animal systems however they still require a range of macro elements which include carbon, nitrogen, oxygen, hydrogen, sulphur and phosphate which are significant for carbohydrate, lipid and protein assimilation. Other micro-elements which are still vital for fungal development but required in much small amounts, include calcium, zinc, copper, iron and manganese. Micro and macro-elements are key components of any medium used to culture fungi. Culbertson et al (2007a&b) has defined a baseline nutrient medium which can be used as the main source of micronutrients for *S. sclerotiorum* growth (Culbertson et al. 2007a, Culbertson et al. 2007b). This baseline was used as the basis of the defined medium (Table 4).

Table 4: The baseline minimal salts required for *S. sclerotiorum* fungal growth.

Defined by Culbertson et al 2007

Micro nutrient		Company obtained	Mg / litre
$(\text{NH}_4)_2\text{SO}_4$	Ammonium sulphate	Sigma Aldrich A4418	1000
KH_2PO_4	Potassium phosphate	Sigma Aldrich P9791	500
NaCl	Sodium chloride	Sigma Aldrich S7653	450
$\text{MgSO}_4 \cdot 7\text{H}_2\text{O}$	Magnesium sulfate heptahydrate	Sigma Aldrich 230391	250
$\text{FeCl}_3 \cdot 6\text{H}_2\text{O}$	Iron (III) chloride, hexahydrate	Sigma Aldrich	0.5
$\text{C}_6\text{H}_9\text{NO}_6$	Na nitrilotriacetate	Sigma Aldrich	5
$\text{CuSO}_4 \cdot 5\text{H}_2\text{O}$	Copper sulphate	Sigma Aldrich C1297	1
ZnCl_2	Zinc chloride	Sigma Aldrich 96468	1
$\text{MnSO}_4 \cdot \text{H}_2\text{O}$	Manganese (II) sulphate monohydrate	Sigma Aldrich M7634	1
$\text{Na}_2\text{MoO}_4 \cdot 2\text{H}_2\text{O}$	Sodium molybdate dehydrate	Sigma Aldrich 71756	1

3.3.3.6 OA production induction via Tricarboxylic Acid Cycle intermediates combined with a baseline nutrient

Once the essential micro nutrients required by *S. sclerotiorum* were selected (Culbertson et al. 2007a, Culbertson et al. 2007b), other nutrient additions were tested to see if single additions to the baseline medium would instantly induce OA secretion. OA biosynthesis or oxalogenesis, is believed to be predominantly formed in fungi via the Tricarboxylic Acid Cycle through the hydrolysis of oxaloacetate into oxalic acid and acetate (Han et al. 2007). The TCA cycle is an essential aerobic pathway during the oxidation of carbohydrates and fatty acids. This cycle has been exploited in fungi to produce excess citric acid as a bi-product of the pathway which can then be used in many food and beverage industries. Intermediates which are considered to feed into the Tricarboxylic Acid Cycle (TCA), for example glucose, malate and succinate have been previously tested to determine whether OA production can be optimised through the addition of these intermediates (Culbertson et al. 2007a, Culbertson et al. 2007b).

In this investigation glucose, malate and succinate were combined with the basic baseline nutrient medium to test whether OA production could be induced in germinating ascospores of two different *S. sclerotiorum* isolates (L6 and L2003). An ammonium nitrate source and pectin source were also tested to see if these could induce OA just in combination with the basic salt mixture as these have been shown to induce OA production (Culbertson et al. 2007a, Culbertson et al. 2007b). The effect of these compounds combined with the baseline salts was compared to the OA production in PDB as it was established as a good OA inducer. The medium was adjusted to pH 5. The effect of pH will be discussed later on in the chapter.

The results indicate there was no OA induction by ammonium nitrate, malic acid, pectin and succinate (**Figure 19**). PDB induced the highest amount of OA from the spores and glucose also had some effect. These results highlight that a complex medium as well as potentially an addition of a simple sugar such as glucose are required for ascospore germination, hyphal growth and high OA induction.

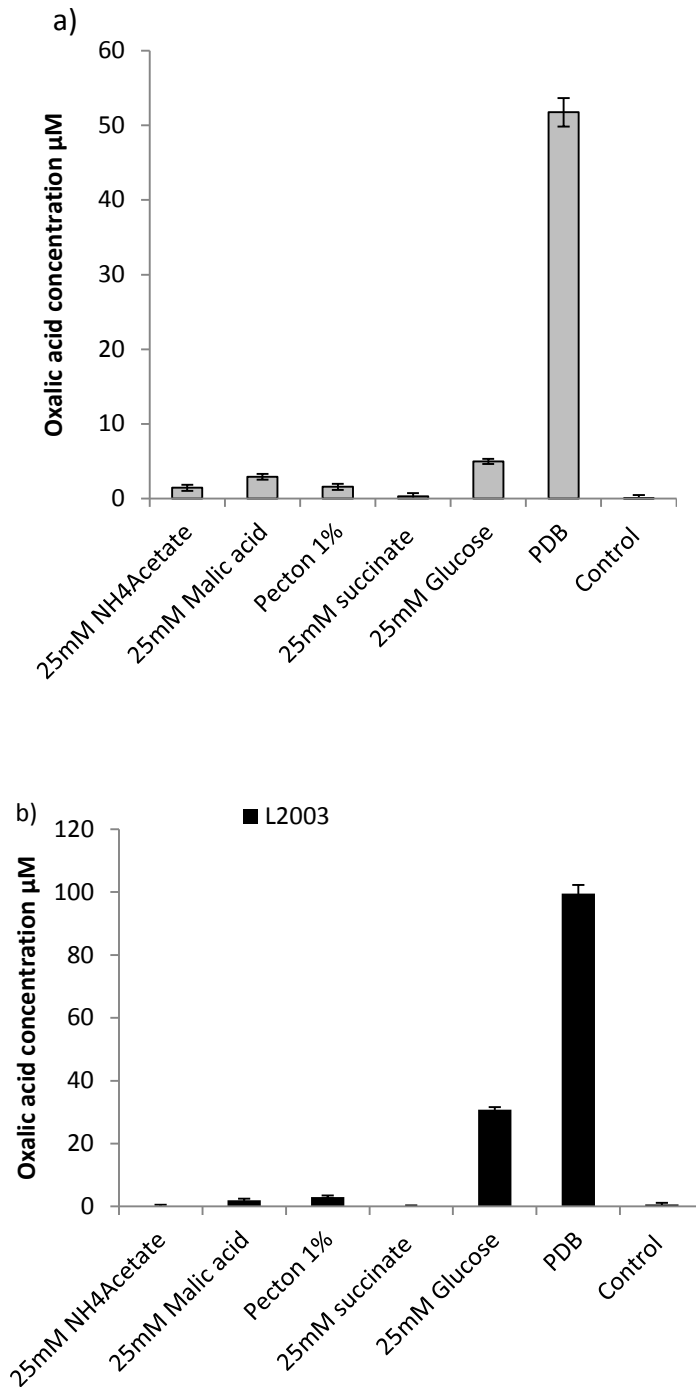


Figure 19: The effect of different additions to minimal nutrient media on OA production. 25 mM malate, succinate, ammonium acetate, pectin, glucose or PDB were combined with the baseline micronutrients. L6 (a) and L2003 (b) isolates were incubated in the different growth media for six days. Ascospores were grown in 12 multi well plates, each well containing 2 ml medium. Ascospore concentration: 4000 spores/ well. The bars represent the average OA production of three biological replicates. a) OA production by L6 *S. sclerotiorum* isolate. b) OA production by *S. sclerotiorum* isolate L2003.

3.3.4 Complex media (Soytone and Yeast) combined with TCA cycle intermediates and their effect on OA production.

Many of the off-the-shelf media used to culture fungi can be described as complex media because they contain a rich mix of carbohydrates, amino acids and fatty acids. Culbertson et al (2007) studied the effect of different complex media including soytone (pancreatic enzyme digest of soybean, which is a *S. sclerotiorum* plant host), tryptone (a peptide mixture obtained from the digestion of casein by the protease trypsin) and yeast extract. In previous experiments (Culbertson et al. 2007a, Culbertson et al. 2007b) mycelial plugs were used to inoculate flasks containing different complex media with the addition of glucose and other TCA cycle intermediates. In this study the OA concentrations of ascospores germinated in 1% soytone and 1% yeast complex carbohydrate media along with intermediates of the TCA were compared. In all cases the soytone medium out-performed the yeast media except in the presence of the ammonium nitrate source. The addition of 25mM glucose to the soytone appeared to be the best inducer of OA (**Figure 20**).

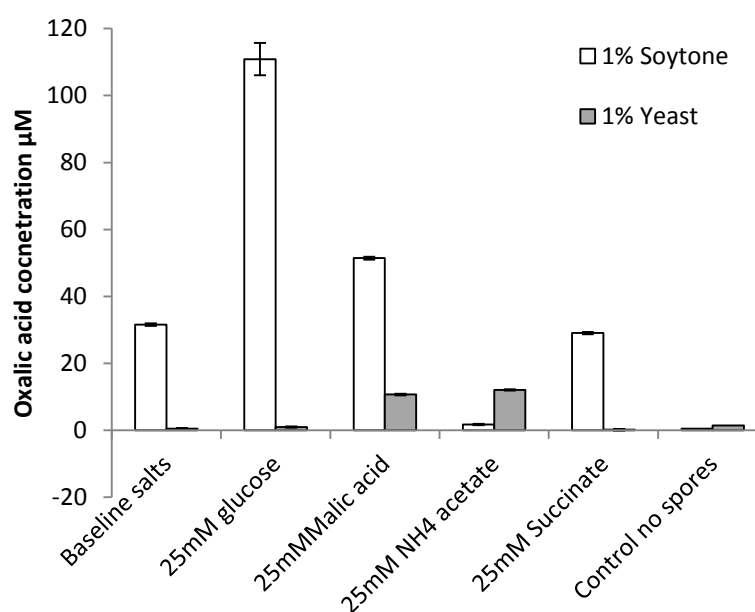


Figure 20: The effects of soytone and yeast media on OA production.

Oxalate production by *S. sclerotiorum* from ascospore derived hyphae grown in 1% soytone and yeast extract media. Each medium contains the baseline salt, pH 5. OA was measured after 4 days of growth. Bars represent the average OA production of three biological replicates. Ascospore concentration 3000 spores/ biological replicate.

3.3.5 The influence of glucose concentration on OA production in a complex medium.

The 25 mM glucose combined with 1% Soytone medium was investigated further to determine if additional OA could be induced. Initially it was hypothesised that larger glucose additions to the medium would increase OA production however this was not the case. The 1% Soytone media was combined with 0, 25, 50 and 100 mM glucose (**Figure 21**) and incubated with ascospores for four days. Additions of glucose above 25 mM appeared to have a detrimental affect and inhibited the production of OA. An ANOVA was performed to determine if there was any statistical significance between different treatments. There was no significant difference between the the treatments ($P= 0.074$, $df=3$).

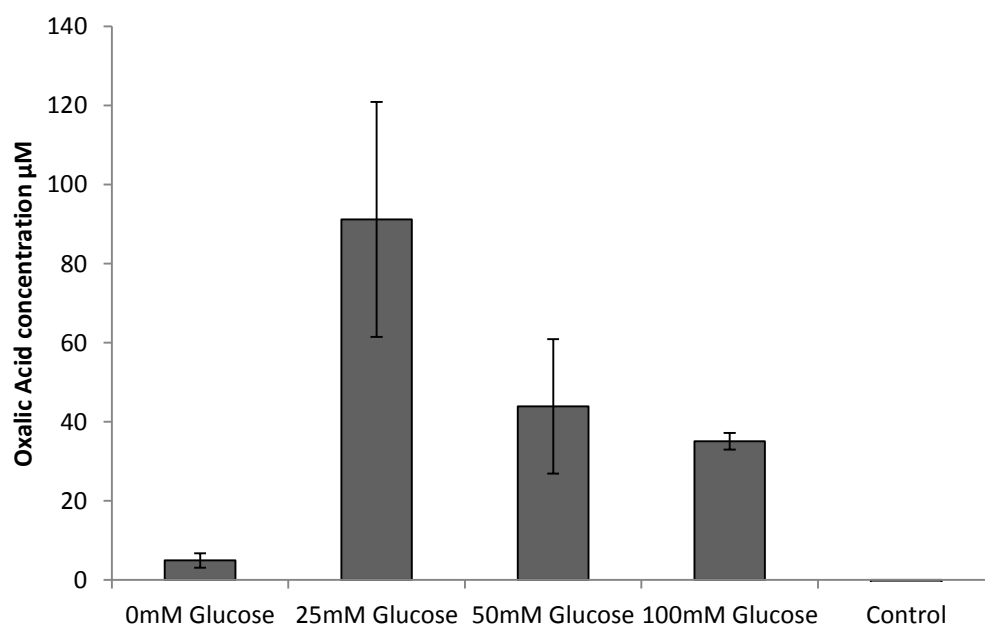


Figure 21: The effect of adding glucose to complex growth media to induce OA production by *S. sclerotiorum* ascospores.

Oxalic acid production from *S. sclerotiorum* L6 isolate ascospore seeded cultures grown in 1 % soytone with increasing concentrations of glucose. OA concentration measured after 4 days of growth. Bars represent the average OA production of three biological replicates. Ascospore concentration: 2900 spores/biological replicate.

OA production after a longer incubation period was investigated. A range of glucose concentrations, from 0-100 mM (**Figure 22a**) was then tested up to seven days post incubation. This revealed that the higher glucose concentrations (50-100mM) appear to be utilised after four days of growth, whereas the lower glucose concentrations made a greater difference to OA production at 4 days of growth. However there was no significant differences between the different glucose concentrations on any particular day ($P=0.117$, $df=6$). The ANOVA revealed no significant interaction of treatment and day ($P=0.14$, $df=12$). There was a highly significant difference with regards the affect of different day which was expected ($P<0.001$, $df=2$) as OA production is significantly upregulated between day 3 and 4.

Glucose concentrations were further investigated to determine if low levels of glucose increased OA secretion at 4 days of incubation (**Figure 22b, c**). Different concentrations of spores were tested on separate occasions in the same baseline medium (1% soytone with minimal salts, pH 5). There was a significant difference between all the different treatment structures (Glucose treatment, $p<0.001$, $df=5$; spore treatment, $p<0.001$, $df=4$; glucose.spore $p<0.001$, $df=20$). However it is very difficult to determine whether any changes to the glucose concentration made a considerable difference to the OA production. In this experiment, it was also observed that the different spore dilutions did not correspond to OA secretion, for example the highest starting ascospore dose did not result in the highest OA level. This suggests that OA production is extremely variable and certain additions to the medium cannot be guaranteed to increase OA production.

The effect of glucose concentrations lower than 25mM on OA production measured over several days of incubation (**Figure 22c**) showed some significance differences between glucose concentrations ($p=0.05$, $df=5$) and was very significant between OA measurements on different days ($p<0.001$, $df=2$). When the interaction between glucose concentration and day were evaluated there was a significant difference ($p=0.014$, $df=10$). Although there are significant statistical differences, as in previous experiments, there is no considerable visual difference between the glucose concentrations. At day 7 there was no difference in OA production between the 20 mM glucose and 0 mM additions. However at day 4 the lower glucose concentrations do increase OA production compared with the 0mM. For the purpose of the biosensor development, the samples will be tested for OA at a maximum of 4 days post sample incubation. Therefore with the defined complex medium (1% soytone and base nutrient source), a 5-25 mM addition of glucose may assist in promoting OA production from ascospores within this medium.

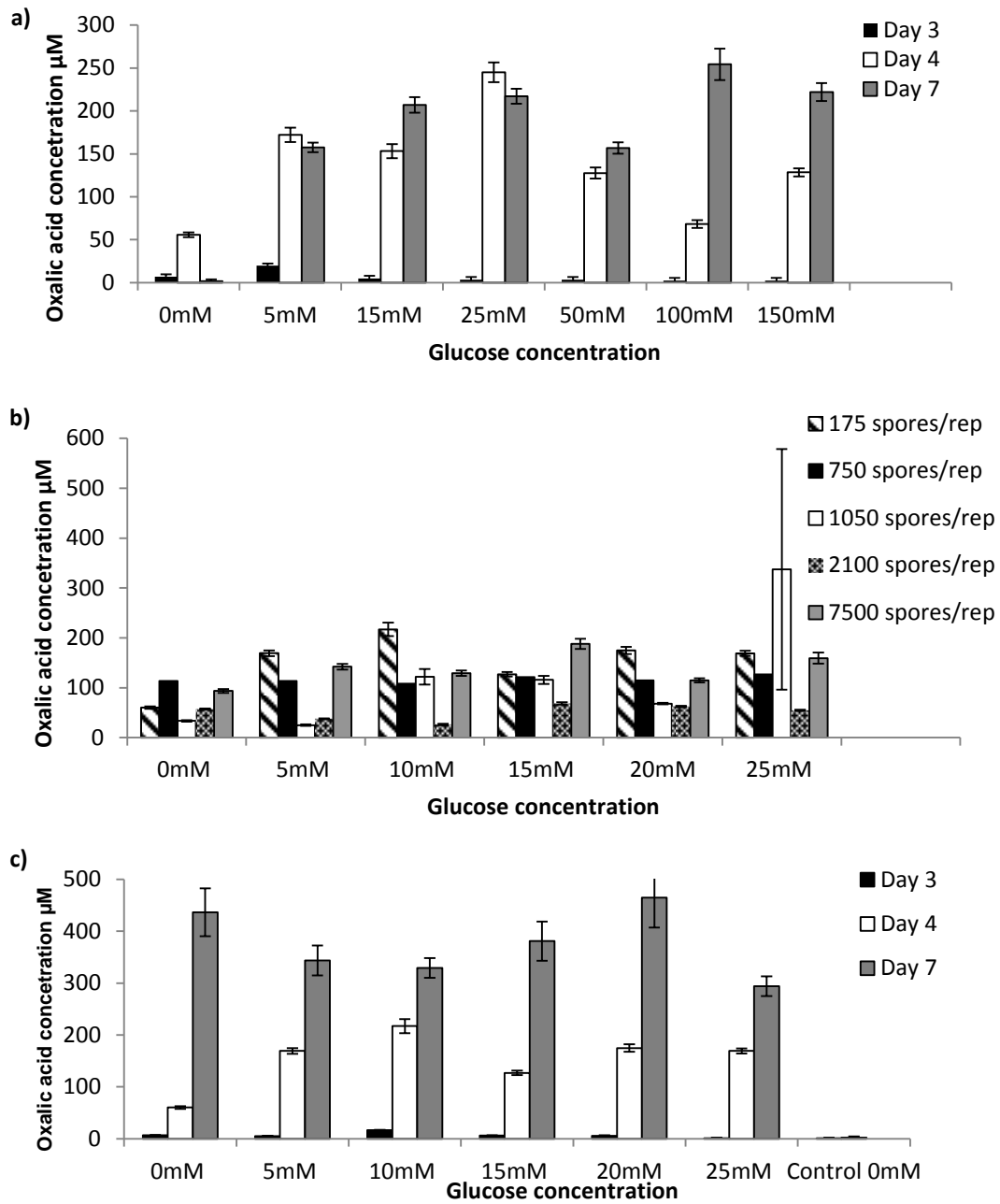


Figure 22. The effect of increasing glucose concentrations on OA production.

a) Oxalic acid production of *S. sclerotiorum* L6 isolate ascospores grown in 1% soytone and baseline minimal salts with increasing concentrations of glucose, all media at pH5. a) OA concentration measured at 3, 4 and 7 day intervals. The spore dose used was 900 spores / biological replicate. Bars represent the average OA production of three biological replicates. b) OA production after four days incubation. Different ascospore numbers grown in 1% soytone and baseline minimal salts with decreasing glucose concentrations. Bars represent the average OA production of three biological replicates. c) Oxalic acid production of ascospores grown in 1% soytone and baseline minimal salts with decreasing concentrations of glucose. OA concentration measured at 3, 4 and 7 day intervals. The spore dose used was 175 spores / biological replicate. Bars represent the average OA production of three biological replicates.

3.3.6 TCA cycle intermediate additions

After determining the complex defined medium (25 mM glucose, 1 % Soytone, minimal baseline salts, pH5), the effect of adding different TCA intermediates was addressed once more. Fumarate, malate and succinate are all considered as potential OA inducers and all are pre-cursors of oxaloacetate within the TCA cycle (See Chapter 1). The effect of adding malate, fumarate and succinate at different concentrations to the 1% soytone medium with glucose, was investigated on three separate occasions. When used within the biosensor system, this medium will be used to test OA production within a 4 day incubation range, therefore OA amount measured on day 4 of incubation was the main focus to match the needs of the field measurements. There was little, if any after 3 days of incubation in all three experiments (data not shown).

Analysis of the first experiment (**Figure 23a**) revealed statistical significance for all levels of treatments, including the concentration of TCA cycle intermediate, the type of treatment and the day of measurement (**Table 5**). At day 4, 5mM and 15mM fumarate and malate were the best OA inducing treatments.

The second experimental repetition (**Figure 23b**) showed no statistical significance between different treatments and the different concentrations. There was a large affect between the different days ($p < 0.001$, $df = 2$) as well as between the interaction between the concentration of the TCA cycle intermediate and the different days ($p = 0.033$, $df = 6$). The standard error between the different types of treatments (succinate, malate or fumarate) overlaps with the 0mM treatments. This suggests again that the additions did not give repeatable OA induction. However, 15mM fumarate again showed the greatest mean OA induction at 4 days incubation, but had a very large standard error.

The experiment was repeated a third time (**Figure 23c**) and OA production was measured at 3, 4 and 5 days of incubation. 15 mM and 5 mM fumarate had the greatest induction for OA at day 4, but was only marginally larger than the 0 mM fumarate treatment. The concentration of the TCA cycle intermediates was significant ($p < 0.001$, $df = 2$) as was the interaction between the different day and the different concentrations ($p = 0.002$, $df = 4$) (**Table 5**). At day 5, OA levels for all treatments had increased to similar concentrations. There was little difference between the different treatments compared to the OA levels in just the baseline medium (0 mM). Even though the differences were only very slight there has been some statistical significance that fumarate does increase OA levels at day 4 of incubation. As a result, a 15 mM fumarate addition to the medium was considered for future medium testing. The OA levels for this experiment were much higher than for the first experiment even though the spore concentration was lower. This

highlights once again that an increasing ascospore number cannot be directly correlated with an increase in OA concentration. This could be accounted for because of the viability of spores or the accuracy of calculating spore number in the solution.

Table 5: ANOVA results for three experiments testing the effect of succinate, malate and fumarate on OA production.

1st Experiment	d.f.	F pr.	2nd Experiment	d.f.	F pr.	3rd Experiment	d.f.	F pr.
ANOVA			ANOVA			ANOVA		
Sample stratum								
Treatment	2	<.001	Treat	2	0.08	Treat	3	0.003
Conc	3	<.001	Conc	3	0.341	Conc	2	<.001
Treat.Conc	6	<.001	Treat.Conc	6	0.656	Treat.Conc	6	0.135
Residual	24		Residual	24		Residual	24	
Sample Day stratum								
Day	2	<.001	Day	2	<.001	Day	2	<.001
Day.Treatment	4	<.001	Day.Treat	4	0.303	Day.Treat	6	0.091
Day.Conc	6	<.001	Day.Conc	6	0.033	Day.Conc	4	0.002
Day.Treat.Conc	10	<.001	Day.Treat.Conc	12	0.814	Day.Treat.Conc	12	0.349
Residual	42		Residual	40		Residual	47	

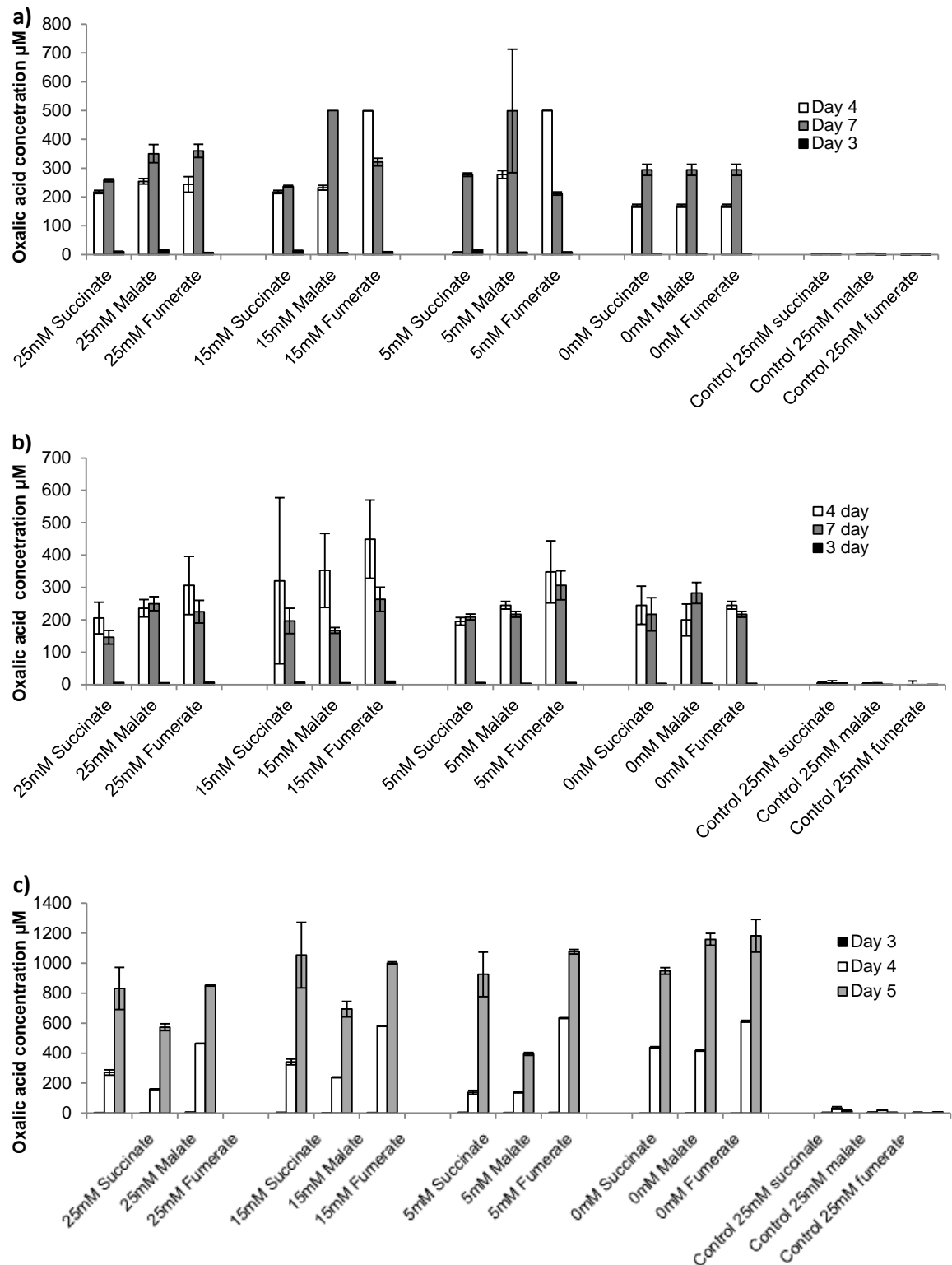


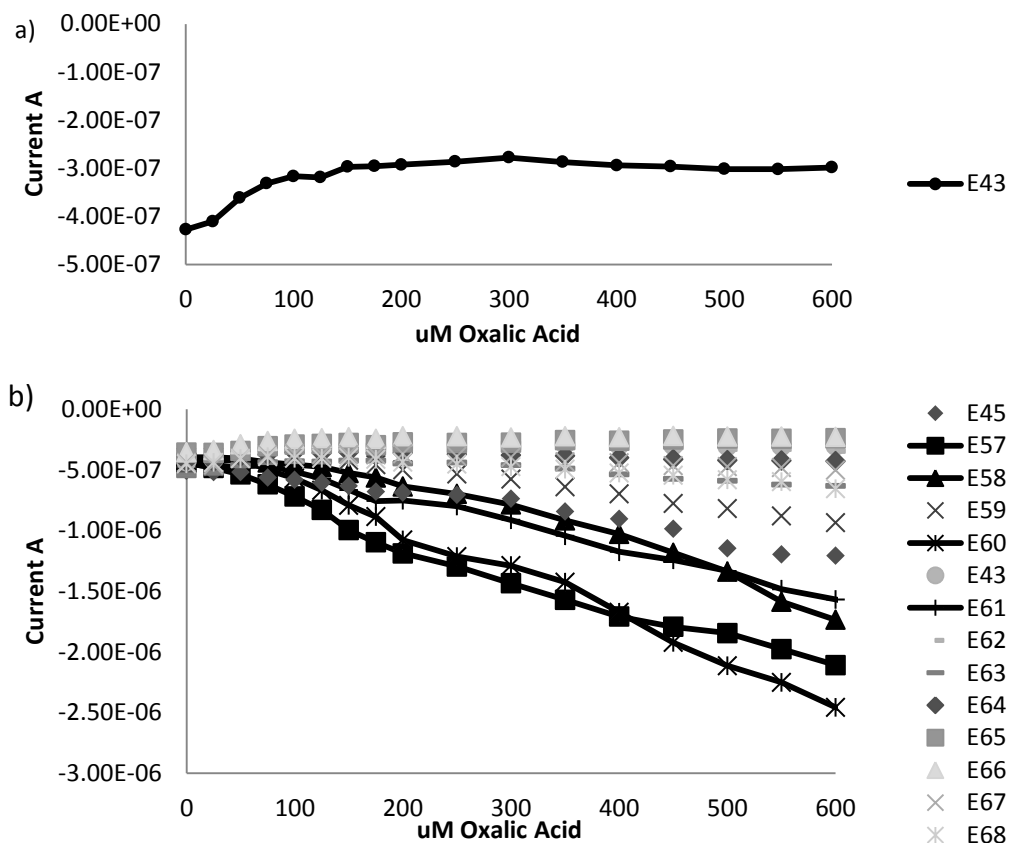
Figure 23. The effect of adding different TCA cycle intermediates on OA production. Three independent biological experiments to assess the effect of succinate, malate and fumarate on OA production from ascospores measured at different time intervals. All media contains 1% Soytone, 25mM Glucose, baseline salts, pH 5 and the additional intermediate. Bars represent the average OA production of three biological replicates. The estimations for 15mM fumarate and malate OA values were outside the standard concentrations used, so predictions made in Genstat have no standard error. The ascospore concentrations used to seed each biological replicated were (a) 1750 ascospores, (b) 900 ascospores and (c) 4860 ascospores.

3.3.7 Electrochemical-compatibility of the defined medium for biosensor development

Up to this point in the development of the medium (1 % soytone, 25 mM glucose, baseline minimal salts at pH 5) the electrochemical biosensor had not been fully optimised. Therefore no medium samples had been tested for compatibility with the electrochemical assay prior to the fungal growth experiments. When the electrochemical assay had been optimised by Dr. Sophie Weiss, at the University of Manchester, the soytone medium was tested and found not to be compatible with the system. Known amounts of OA were spiked into the 1% soytone medium and pipetted onto the electrode containing the stabilised OxOx. However there was no enzymatic activity and no OA detected (**Figure 24a**). This result highlighted one or several components in this medium inhibited some part of the electrochemical assay. To find a medium with suitable electrochemical compatibility before the second field trials, a range of standard laboratory media samples were sent to the University of Manchester to be tested for compatibility with the electrochemistry, by Dr Weiss (**Figure 24b**). The media were tested at pH 3.8 as this is the predicted after 4 days incubation with *S. sclerotioeum* ascospores. Four of the 13 samples tested were electrochemically compatible. These four media were tested for the growth of ascospores and to determine whether suitable levels of OA could still be detected using both optical and electrochemical methods of OA detection (**Table 6**).

Table 6: The four media selected for electrochemical compatibility

Medium compatible with electrochemistry	Component of medium
1% Potato dextrose broth	Potato Starch (from 200g Potato infusion) Dextrose
1% Yeast nitrogen base	Yeast base to which carbon and amino acid source can be added.
1% Sabouraud dextrose broth	Peptic Digest of Animal Tissue Pancreatic Digest of Casein (phosphoproteins) Dextrose
1% Czapeks dox liquid	Saccharose, Sodium Nitrate, Dipotassium Phosphate Magnesium Sulfate, Potassium Chloride, Ferrous Sulfate.



Legend	Growth media tested
E45	50mM succinic acid 100mM KCl pH 3.8
E57	1% potato dextrose broth minimal media pH 3.8
E58	1% yeast nitrogen base without a minimal media pH 3.8
E60	1% Sabouraud dextrose broth medium min media pH 3.8
E61	1% Czapeks dox liquid medium in minimal media pH 3.8
E59	1% YPD broth in minimal media pH 3.8
E43	1% soytone in minimal media pH 3.8
E62	1% yeast tryptone broth in minimal media pH 3.8
E63	1% LB lennox broth in minimal media pH 3.8
E64	1% yeast extract in minimal media pH 3.8
E65	1% mycological peptone in minimal media pH 3.8
E66	1% tryptone soya broth in minimal media pH 3.8
E67	1% beef extract in minimal media pH 3.8
E68	1% granulated tryptone in minimal media pH 3.8

Figure 24: The effect of different media on the efficiency of the electrochemical assay. a) The lack of compatibility of the soytone medium with electrochemical assay. b) Activity of OxOx in 1% nutrient media electrolyte tested in 13 different growth media. E57, E58, E60 and E61 show the greatest changes in current with increasing OA concentration. Soytone (E43) by comparison has no activity within this assay. Samples tested at pH 3.8 as this is the optimum working pH for OxOx. Data courtesy of Dr. Sophie Weiss, University of Manchester.

3.3.8 Comparison four electrochemical compatible media for OA induction

Ascospores were grown in each of the four electrochemically compatible media to determine their abilities to induce high OA production from *S. sclerotiorum* L6 isolate ascospores. This experiment was repeated on three separate occasions with consistent results for each experiment. Only one set of experimental results is shown to reduce repetition (**Figure 25**). The highest OA standards used in the calibration curve for this experiment was 3000 μM . Some wells contained more than 3000 μM OA after 6 days of incubation and therefore the actual OA content could not be calculated. These samples were plotted at 3000 μM and no standard variation could be calculated. Sabouraud dextrose broth (SDB), containing minimal salts with no glucose addition, was the most consistent OA inducer with high levels of OA detected at day 3 (**Figure 25b**). Soytone and PDB also promoted oxalic acid at day 3 but at significantly lower levels. The addition of glucose had no significance on oxalic acid production. The yeast base medium induced OA production but only much later in the time course and only with the glucose addition. SDB with baseline minimal salts, pH5 was used from this point on to carry out further testing.

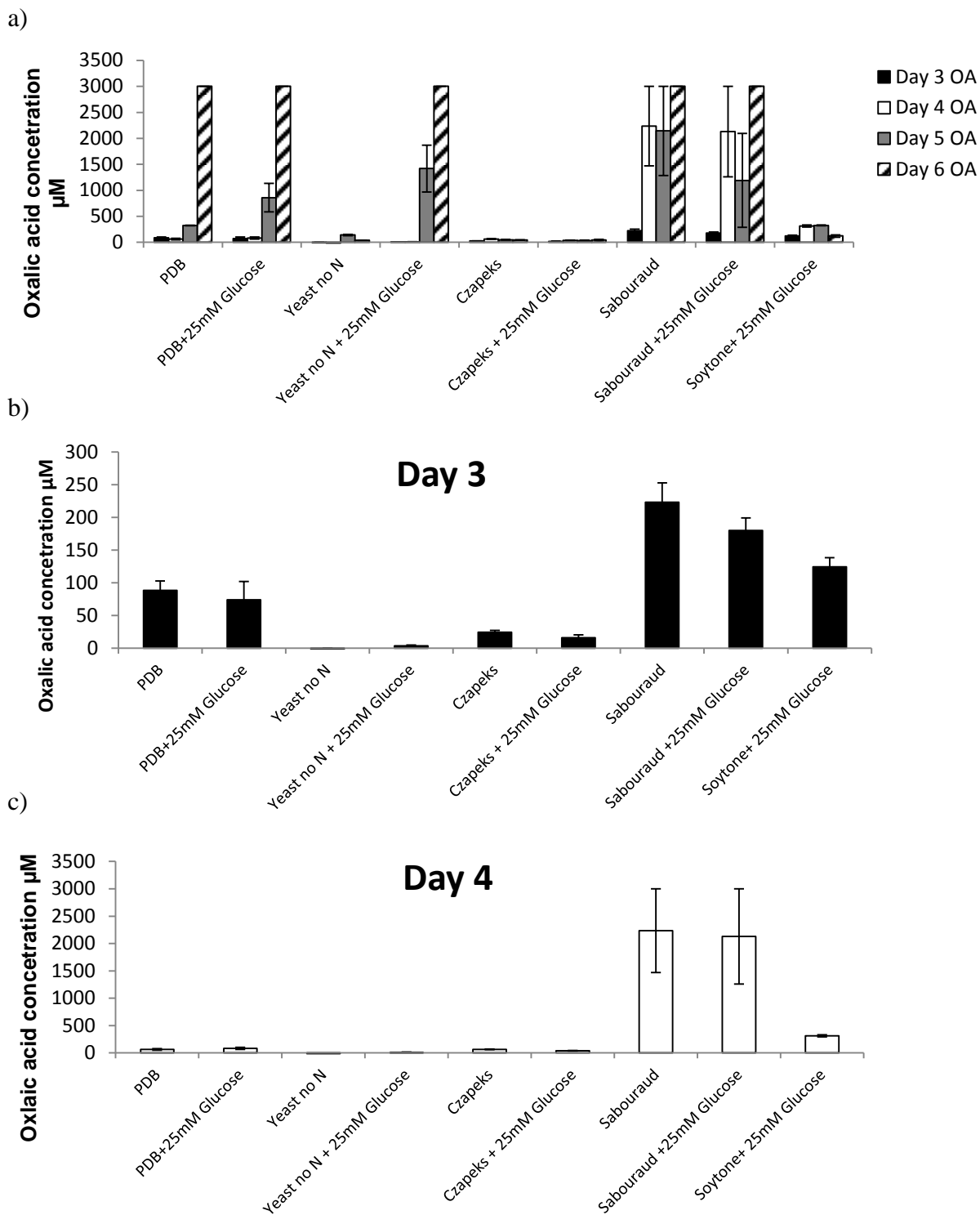


Figure 25: Oxalic acid production by *S.sclerotiorum* ascospores in different, electrochemical compatible media.

Ascospores incubated in different media over 6 days. Bars represent the average OA production of three biological replicates. 9250 spores/ biological replicate. a) OA production over 6 days. b) OA production at day 3 of incubation. c) OA production at day 4.

3.3.9 Limits of detection.

During biosensor sampling within a field environment, air will be sampled directly into the pots which will contain the medium to induce OA production. Therefore, it was necessary to test whether the ascospores would germinate and produce oxalic acid within a smaller medium volume and within a bespoke 400 µl pot made of a different plastic to the previously used 12 well plates. It was also necessary to determine the lowest number of spores which could be sampled that would still grow and produce detectable levels of OA.

Different ascospore concentrations were incubated in 400 µl of SAB medium. After 3 days of incubation, all spore dilutions had secreted OA (**Figure 26**). Statistically, there is a significant difference between some of the spore dilutions ($p= 0.002$, d.f.= 6) and the different days ($p< 0.001$, d.f.= 2) as well as the interaction between day and ascospore dilution ($p< 0.001$, d.f.=12). Visually it is difficult to pick out a trend especially on day 4 when most of the ascospore dilutions are secreting high OA amounts. What is noticeable is the lowest spore doses (67, 16, 4 spores per pot) have a longer time lag until they produce their highest amounts of oxalic acid compared with higher ascospore doses. OA concentrations are most likely higher than previously tested because of the smaller volume of liquid which the spores are grown in, which would concentrate the OA in the pots.

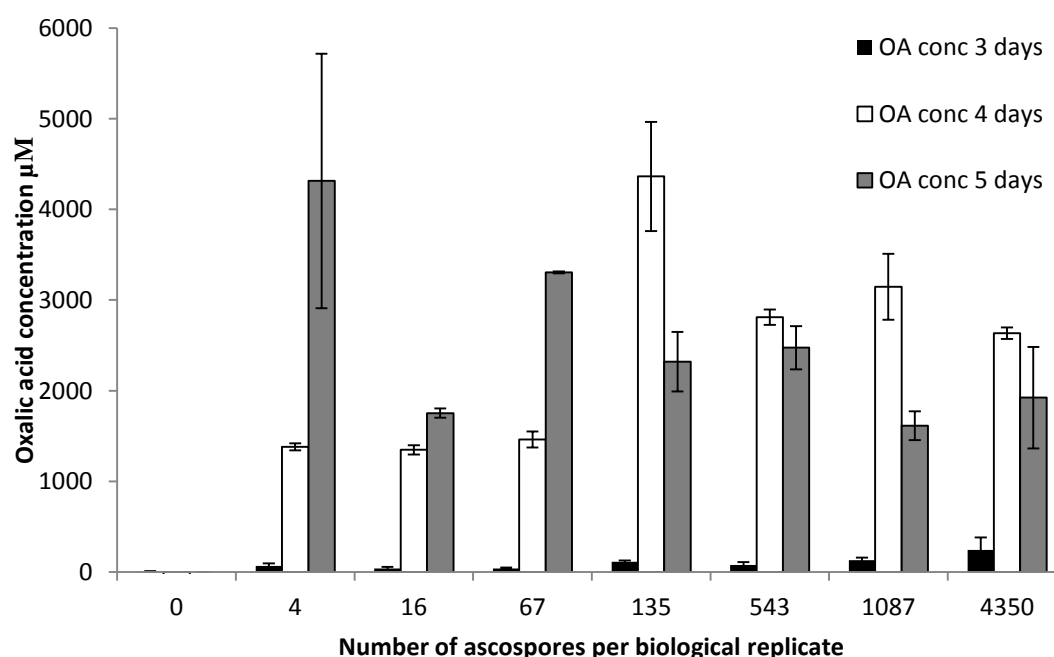
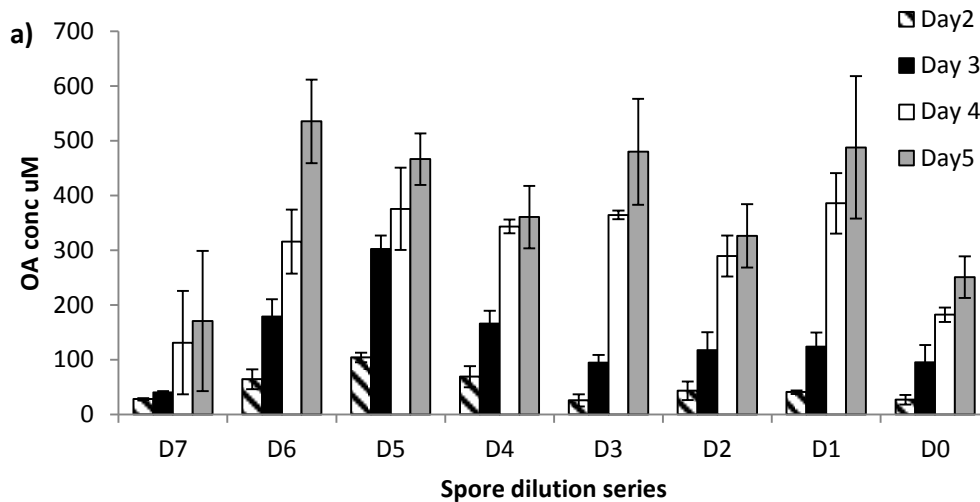


Figure 26: The effects of different ascospore number on OA production.

Oxalic acid production from different ascospore dilutions over 5 days of incubation in 400 µl SAB and minimal base salts, pH5. Spore solution LSD: 688, Day LSD: 450, Residual: 42.

3.3.10 Verifying spore counts using DNA quantification

Quantitative PCR was used to check whether the ascospore numbers calculated with the aid of a haemocytometer could be verified by quantifying *S. sclerotiorum* DNA within the spore doses being used to inoculate the SDB medium (**Figure 27**) (see General Experimental Procedures). DNA from three replicates per spore dose was extracted and were tested. The qPCR spore counts were much lower than the haemocytometer counts (**Figure 27b**). However, the qPCR counts were still dropping by 50% per dilution and this confirms that even though the ascospore counts were doubling (i.e the original count of 4 spores, was by PCR analysis now considered to be 8 spores), the OA concentrations were still not positively correlated with ascospore number. This discrepancy in spore number could be a result of the filter paper particles which are present in all spore solutions after the filter paper is added to sterile water to make up the spore solution. This could easily cause spore clumping, even though a 0.1% tween solution was added to the spore solution before spore counts were taken. Solutions were also vortexed vigorously to break up clumps. As previously noted, lower spore solutions resulted in the production of similar amounts of oxalic acid comparable with the higher spore numbers at day 3, 4 and 5. As a recommendation from these pot testing experiments, the limit of detection for this assay can be set at 10 spores in up to 500µl of medium.



b)

Dilution	Haemocytometer spore counts	Average qPCR spore counts
D7	4	10
D6	8	12
D5	16	21
D4	66	18
D3	132	19
D2	527	104
D1	856	222
D0	1000	426

Figure 27: Using qPCR to determine accurate ascospore numbers and OA production.

a) OA production from different spore dilutions incubated for 5 days in 500ul SAB, minimal salts, pH5. b) Comparison of the spore counts from a haemocytometer counted under a light microscope (20X) and the number of spores in the same volume calculated using qPCR.

3.3.11 The relationship between *S. sclerotiorum* ascospore number, biomass and oxalic acid production

Previous experiments have demonstrated that there is no consistent positive correlation between the number of *S. sclerotiorum* ascospores and an increasing amount of OA measured during incubation tests. It was hypothesised that there may be an initial starting biomass required to initiate OA production and this initial biomass may be influenced by the initial spore number. An experiment which monitored the relationship between ascospores number (high (2366), medium (291), low (50) ascospore), biomass, OA and pH carried out over 11 days (**Figure 28**). The average ascospore concentration per spore dose was calculated using qPCR (**Table 7**).

Once again it was observed that lower spore doses (below 1000 spores per replicate) produced OA at four days of incubation, whereas the higher spore doses

produced OA during the third day of incubation. To perform the REML analysis these data required log transformation as it ensured a normal distribution for the data. There were a few negative values of OA for the control sample so to adjust the values for transformation, 9.6 was added to all oxalate values. The control oxalate values were nested within the treatment (spore dilution) so that all values for each ascospore dilution and the control were compared against each other (**Figure 29**). The REML model creates a predicted table of means which fits the model. The measure of fit was then used to calculate whether there is any statistical significance of the effect of treatment. The output from the REML model indicates that there is a highly significant interaction between treatment (spore dilution) nested within control vs. treatment and time. This translates that on a particular day, there was an effect of spore dilution on oxalate production (**Table 8**). This can be seen on day 3 where OA is positively correlated with higher spore numbers, but at day 5 the higher spore concentration is negatively correlated with OA production.

The overall change in pH followed a similar pattern across the three ascospore dilutions however the higher spore dose exhibited a more rapid pH drop between day 2 and 5 compared with the medium/low ascospore doses which exhibited this change between day 3 and 6. By day 6 the higher spore dilutions had reached their lowest pH and began to increase once more. A day later the medium and low spore dilutions followed this pattern. Once more, the REML analysis showed a highly significant interaction between the treatment of spore dilution nested within the control vs the treatment and time, highlighting that there is a significant effect of spore dose treatment on pH of the sample (**Table 9**).

The biomass did not differ greatly between larger and smaller spore doses but the higher spore dose was marginally higher at day 3 compared with the two other spore doses. This could possibly account for the early increase in OA production by this spore dose at this time point. This experiment was repeated a second time and the results are comparable suggesting that it is not biomass only that accounts for the increase in OA, there may be other factors. The REML output indicates that there was no significant effect of spore dose on the biomass but there was a main effect of time only (**Table 10**). It is important to note that by 11 day of incubation there was significantly reduced liquid medium in the culture pots.

Table 7: The spore counts of different spore solutions determined using qPCR. The spore number is the average of 3 biological replicates.

Spore dose treatment	Average of 3 biological replicates	Standard error
High spore	2366	150
Medium spore	291	25
Low Spore	50	29

Table 8: The REML output for the effects of spore treatment on the production of OA measured in the liquid medium over 11 days.

CvsT= control (with no spores) versus treatment (with spores).

Fixed term (OA)	Waldstatistic	n.d.f.	F statistic	d.d.f.	F pr
Time_day	3332.38	7	459.84	118.0	<0.001***
CvsT	96.22	1	96.22	80.2	<0.001***
Time_day.CvsT	3221.07	7	444.51	118.2	<0.001***
CvsT.Treatment	11.34	2	5.67	18.3	0.012
Time_day.CvsT.Treatment	425.90	14	29.26	156.4	<0.001***

Table 9 : The REML output for the effects of spore treatment on pH of the liquid medium measured over 11 days.

CvsT= control (with no spores) versus treatment (with spores).

Fixed term (pH)	Wald statistic	n.d.f.	F statistic	d.d.f.	F pr
Time_day	13067.46	7	1803.38	118.3	<0.001***
CvsT	209.82	1	209.82	66.6	<0.001***
Time_day.CvsT	4441.23	7	612.91	118.3	<0.001***
CvsT.Treatment	23.09	2	11.54	14.3	0.001***
Time_day.CvsT.Treatment	600.62	14	41.27	157.0	<0.001***

Table 10: The REML output for the effects of spore treatment on the *S. sclerotiorum* biomass monitored over 11 days.

CvsT= control (with no spores) versus treatment (with spores).

Fixed term (Biomass)	Waldstatistic	n.d.f.	F statistic	d.d.f.	F pr
Treatment	0.38	2	0.19	1.8	0.841
Time_day	194.72	7	24.85	19.5	<0.001***
Treatment.Time_day	9.55	14	0.61	20.0	0.828

*** Statistical significance

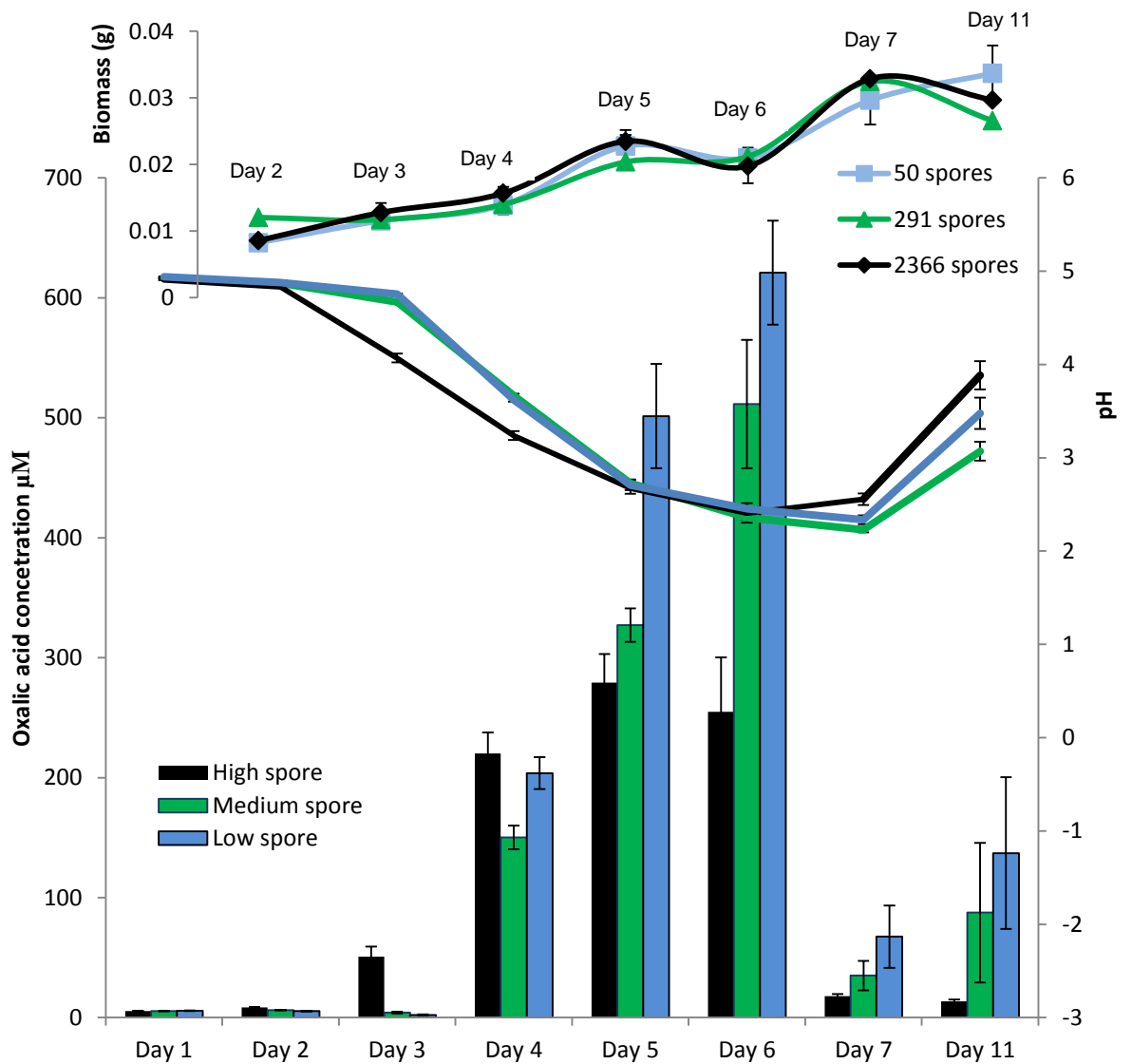


Figure 28: The relationship between OA production, pH change and dry biomass accumulation of different ascospores dilutions.

S. sclerotiorum L6 isolate ascospores incubated in 2 ml SDB with minimal salts. Bars represent the average OA production of three biological replicates. pH values the average of the three biological replicates. The values are untransformed. High ascospore: 2366 spores/ biological replicate. Medium ascospore: 291 spores/ biological replicate. Low ascospores: 50 spores / biological replicate.

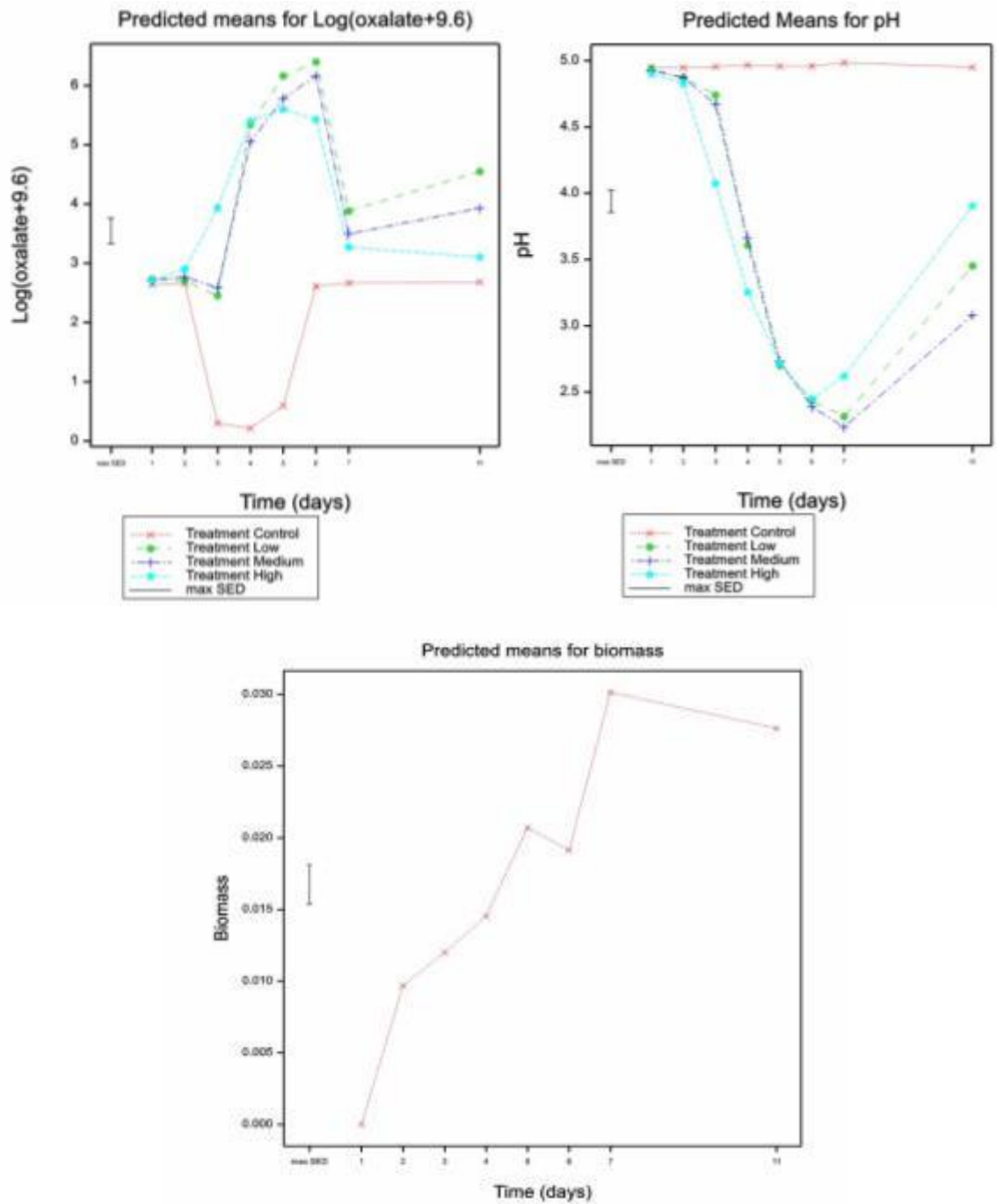


Figure 29: Predicted means generated by the REML analysis.

The values are generated by fitting a linear fixed model to the pH, OA and biomass values. The OA original data was increased by adding 9.6 to eliminate negative values and then log transformed.

3.3.12 Buffering Capacity of the medium

The environmental pH has been shown to be important for the induction of OA. Secreted OA decreases the pH of the surrounding environment which in turn creates the optimal pH for secreted polygalacturonase and other acid acting enzymes required during infection. Rollins and Dickman (2001) reported that OA production may be a self-limiting mechanism, so that increasing OA levels decreases pH which restricts further OA secretion and so OA levels may actually fall after a period of time. Culbertson et al (2007) reported a trend of decreasing OA levels after 5 days incubation with mycelia plugs incubated in media in flasks. Medium pH was observed to increase after 5 days incubation. There is speculation that the increasing pH could be the result of a proton-consuming reaction, where secreted oxalate decarboxylase catalyses the breakdown of oxalate into formate and carbon dioxide which may increase the medium pH if the formate is subsequently secreted into the medium (Magro et al. 1984).

Different additions to the medium may also act as buffers to prevent the medium pH dropping rapidly. Culbertson hypothesised that the intrinsic buffering capacity of each medium will affect the amount of OA secreted. If the pH drops too much this inhibits OA production (Rollins and Dickman 2001) however oxalate production could possibly be maintained if the medium was kept above pH 3.5 (Maxwell and Lumsden 1970, Culbertson et al 2007a & b).

To investigate whether the SDB medium could be buffered to increase OA production within the biosensor, three routinely used biological buffers were tested to measure whether the medium can be buffered sufficiently over at least 4 days of incubation and whether maintaining a higher pH stimulates further oxalic acid production (**Figure 30**).

Initially, MES (2-(N-morpholino)ethanesulfonic acid) buffer (50 mM) was used to make up the SDB at pH 4, 5, 6 and 7. Two ascospore doses were used to see if there was any difference between the amount of ascospores and the ability to buffer a medium. The media buffered at pH 5 had the highest oxalic acid concentrations for both spore dilutions at day 4 (**Figure 30a**). The pH dropped rapidly in samples with the higher OA concentrations. Media with a starting pH of 7 contained less OA and exhibited less of a pH drop. It is interesting that there is minimal oxalic acid production at day 2 and 3, compared to previous experiments when oxalic acid production was measured at least at day 3. This could be an effect of the MES buffer. The pH measurements indicate that there was no buffering of the medium.

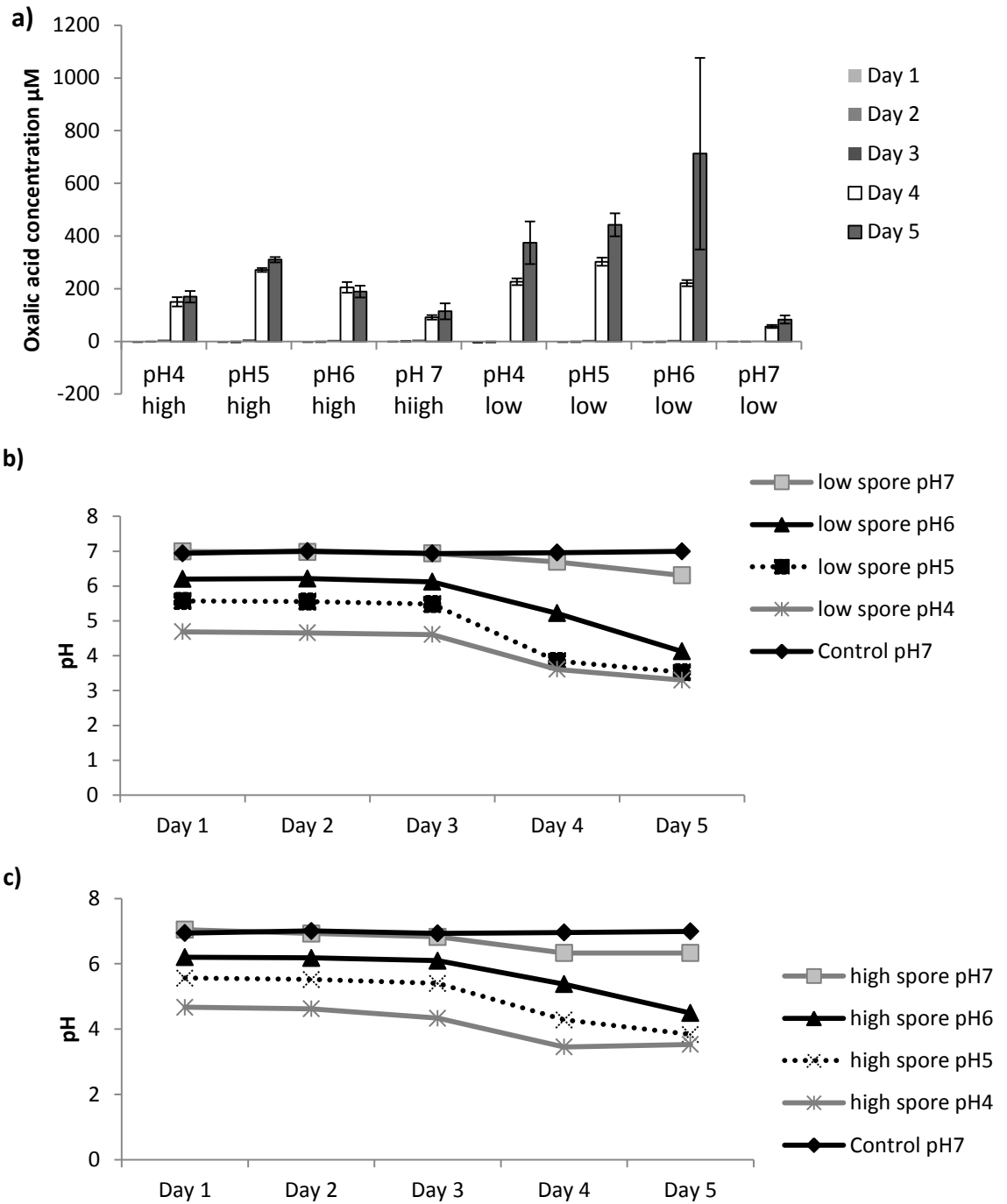


Figure 30: Buffering capacity of MES buffer.

a) Oxalic acid production by two spore dilutions of ascospores grown in SDB medium at different pH over five days. Media buffered using MES buffer. Bars represent the average OA concentration of three biological replicates. High spore: 290 spore/replicate. Low spore: 30 spore/well. b-c) The change in medium pH over the time course for the two different spore dilutions. c) The control medium which was non-inoculated.

Succinate (50 mM) and HEPES (4-(2-hydroxyethyl)-1-piperazineethanesulfonic acid) (50 mM) buffers were then tested for medium buffering abilities (**Figure 31**). The buffers were added to SDB at a range between pH 4.9 - 6.5. A pH above pH 7 was not included as the previous experiment highlighted that lower OA was induced when ascospores were grown in media at this pH. The succinate buffer reduced the oxalic acid output considerably (**Figure 31 e,f**). The HEPES buffer did promote oxalic acid production compared with the SDB control but only at later stages in the time course, day 6 and 7 (**Figure 31 c,d**). The control SDB had the highest oxalic acid concentrations at the earliest time points (**Figure 31 a,b**) which for the biosensor would be the most appropriate time points to assess. The highest OA production was observed in the SDB control at day 4 which will be the date for measuring samples in the biosensor in the field. It is difficult to determine what the best pH would be required as low spore dose have a better OA output when the environment is at pH5, whereas for higher spore dose pH 5.9 was a better OA inducer.

The pH of media was measured over time (**Figure 32**). Both HEPES and succinate have some ability to buffer the medium with higher ascospore doses when compared with the un-buffered control medium. However, the lower spore doses incubated in both buffered media showed a similar change in pH to the un-buffered control. The two spore dilutions generally followed a similar pH drop, however the lower spore dose lagged behind by 1 day.

For all three treatments, high ascospore doses produced oxalic at day 3 and low ascospore doses produced oxalic acid at day 4. At day 4 the levels of oxalic acid between the two ascospore doses are comparable. The OA concentrations did decrease after 6 days, which suggests the OA was broken down/ re-metabolised and after this point the pH values do begin to increase which is in keeping with what has been observed for mycelial plug inoculations previously (B. J. Culbertson et al. 2007, Bryan J. Culbertson et al. 2007)

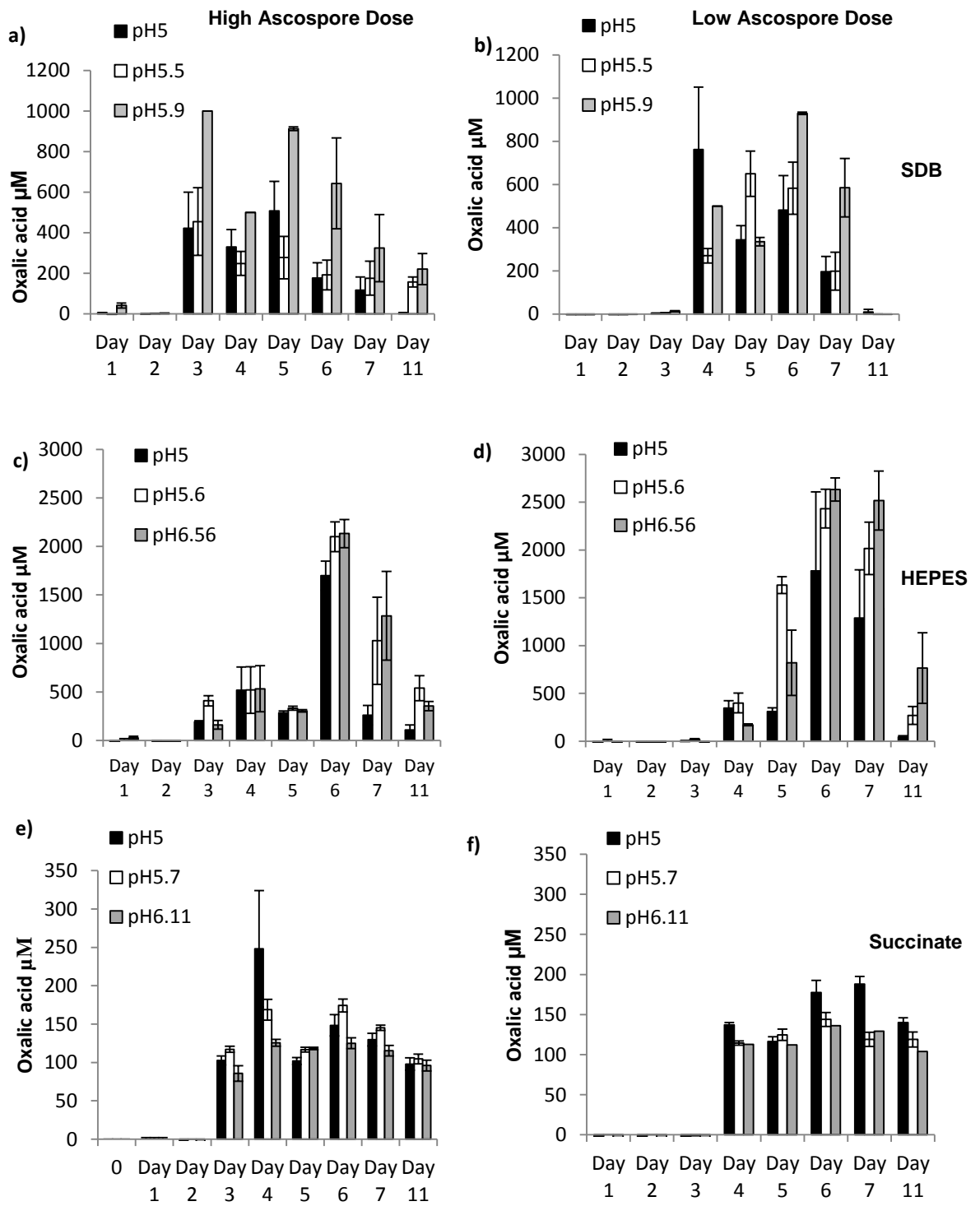


Figure 31: Buffering capacities of HEPES and succinate buffers.

Oxalic acid production by two spore dilutions of ascospores grown in buffered SDB media over 11 days. a,c,e) high ascospore dilution: 2366 spores / biological replicate. b,d,f) low ascospore dilution: 38 spores/ biological replicate. Bars represent the average OA production per 3 biological replicates. a-b) control SDB medium with no buffer addition. c-d) 50 mM HEPES buffer in SDB. e-f) 50 mM succinate in SDB.

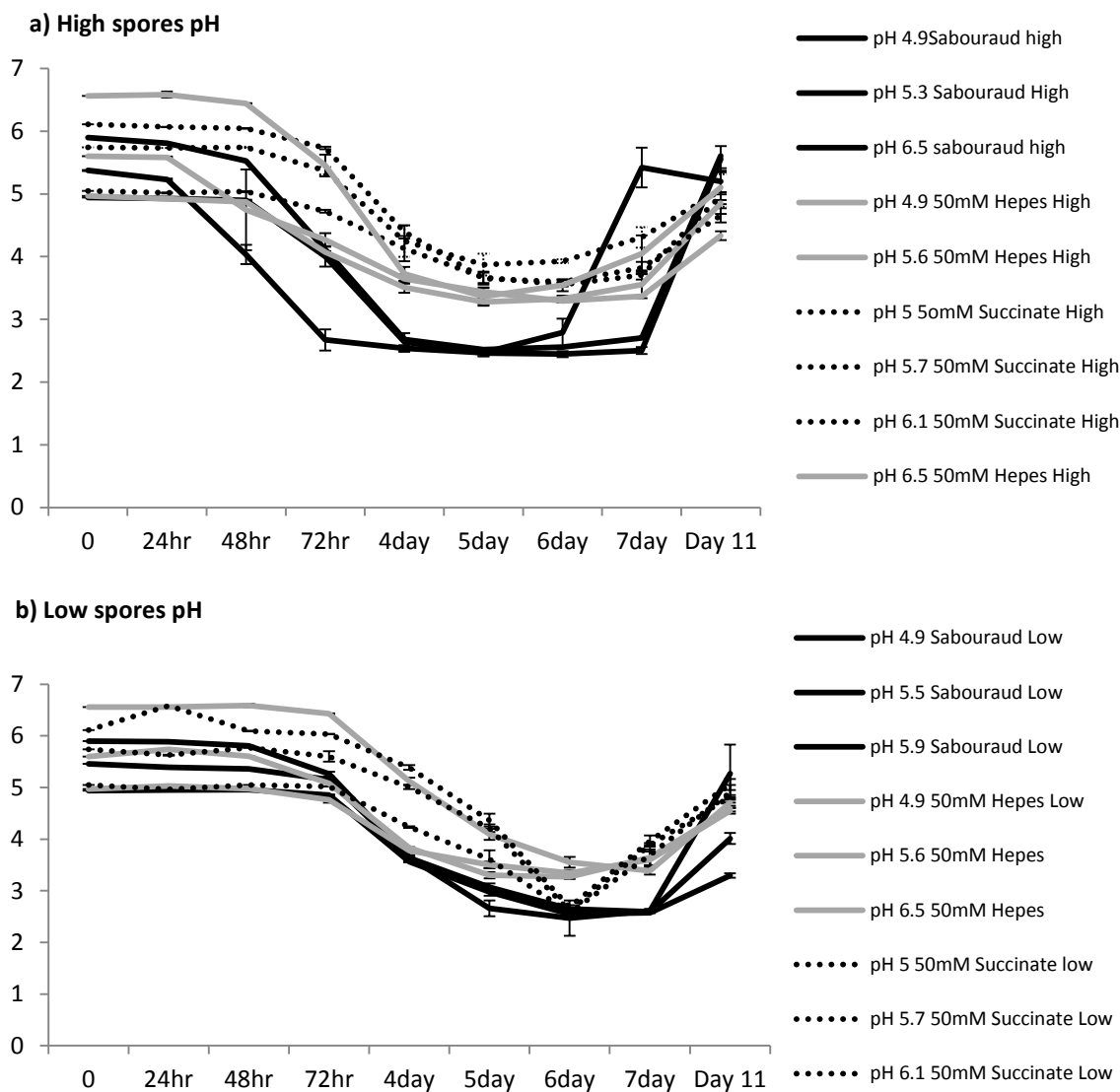


Figure 32: The change in pH monitored in buffered media.

Time course over 11 days of ascospores incubation. Values are the average pH of three biological replicates. a) High ascospore dilution: 2366 spores / biological replicate. b) low ascospore dilution: 38 spores/ biological replicate

3.3.13 The effect of competing fungi on oxalic acid production

Once an electrochemically compatible medium had been identified (SDB, base minimal salts, pH5), it was necessary to investigate the effects of other fungal species which may be sampled into the biosensor along with *S. sclerotiorum* ascospores. Other fungi sampled into the medium may out-compete *S. sclerotiorum* or secrete oxalic acid which would potentially generate false positives. During field testing of the medium, other fungal species which were isolated from media which had been used to incubate air samples from the field were investigated (Chapter 4). These species included a variety of *Trichoderma spp* and *Epicoccum nigrum* which have been reported as bio control agents of *S. sclerotiorum* (Elad 2000, Inbar et al. 1996, Huang et al. 2000, Zhou et al. 1991). Both groups of fungi could be responsible for false negatives in the biosensor if they prevented *S. sclerotiorum* from growing and /or producing OA. *Botrytis cinerea* which is also documented to secrete oxalic acid was isolated from the field samples (Blanco et al. 2006). It was therefore necessary to investigate the effects of these fungi on the ability of *S. sclerotiorum* to produce OA and test a range of fungicides which may prevent the growth of these species.

3.3.14.1 Competition assays

During two field trials (Chapter 4), a variety of fungal species were isolated and identified from air samples which were incubated with the medium. Attempts were initially made to optimise published qPCR methods for the detection of *Trichoderma sp*, *E. nigrum* and *B. cinerea*. This would enable the accurate quantification of spore numbers in the air samples to identify the potential risk. However all three methods continually amplified *S. sclerotiorum* DNA as well as the other fungi. Subsequently, this area of research had to be abandoned due to time constraints.

Growth competition assays were developed to see how detrimental these other fungal species could be for the biosensor system. *Trichoderma*, *Botrytis*, *Alternaria* and *Epicoccum* species isolated from the field were cultured to obtain spores. Spores were grown in SDB either independently or mixed in with *S. sclerotiorum* ascospores and OA concentrations were measured every day for 7 days (**Figure 33**). Oxalic acid was produced by *S. sclerotiorum* and *B. cinerea* when grown independently or together in the medium. However, when *S. sclerotiorum* was mixed with *Trichoderma*, *Alternaria* and *Epicoccum* isolates, OA production was significantly impaired. It is very difficult to know how the distribution of the other species spores will change in the field and how this will affect *S. sclerotiorum* oxalic acid production.

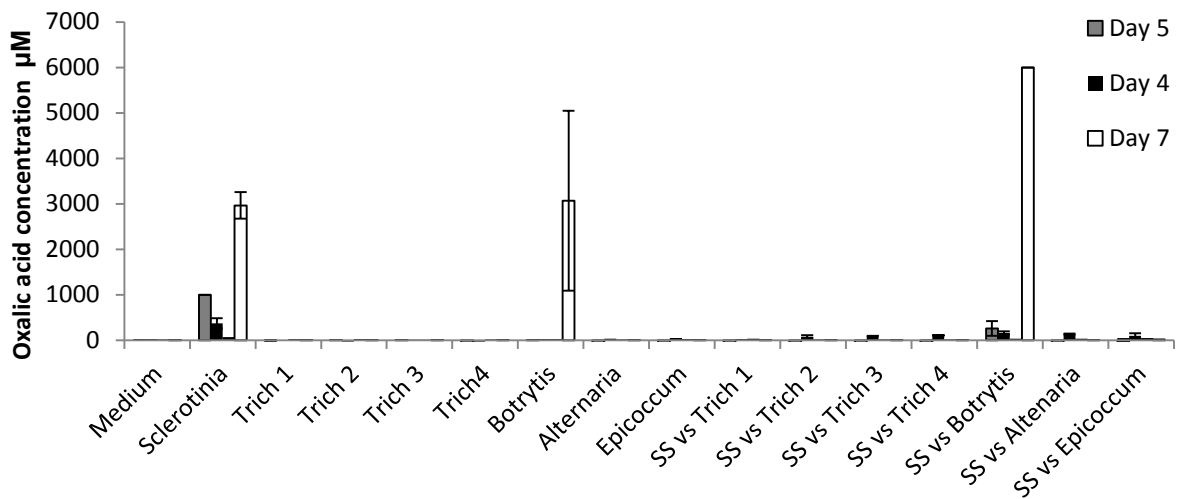


Figure 33: Oxalic acid produced by different fungal species isolated from field trial samples.

The spores from different species were grown with and without *S.sclerotiorum* spores in SDB medium over 7 days. Bars represent the average OA production of three biological replicates. 1000 spores / biological. Ss: *S. sclerotiorum*. Trich: *Trichoderma sp.*

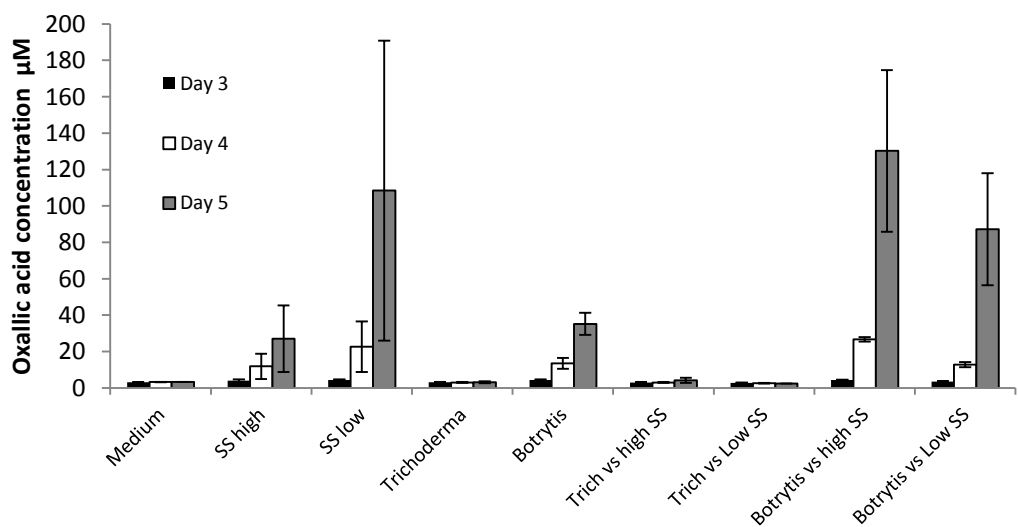


Figure 34: The effect of fungal contaminants on oxalic acid production by two different spore dilutions.

Ascospores incubated over 5 days in 2 ml SDB medium. Bars represent the average OA production of three biological replicates. High Ss ascospore spore dilution: 290 spores / biological replicate. Low ascospore spore count approximately 30 spores / biological replicate. *Botrytis* and *Trichoderma* spore counts were diluted to 100 spores / biological replicate. Ss: *S. sclerotiorum*. Trich: *Trichoderma sp.*

The number of *S. sclerotiorum* ascospores present in the biosensor assay may affect whether other species can outcompete it or not. A high and low *S. sclerotiorum* spore dose was used in another competition assay just with *Trichoderma sp* and *B. cinerea* (**Figure 34**). At day 4, *Trichoderma sp* had significantly suppressed *S. sclerotiorum* oxalate production. *B. cinerea* produced equivalent amounts of oxalic acid to *S. sclerotiorum* in this assay. Both could pose a significant risk in the field but this risk will vary depending on how frequent spores from these other pathogens are sampled into the biosensor. This is still unknown.

3.3.14.2 Fungicide additions to the medium

To create a selective medium that will encourage the growth of only *S. sclerotiorum*, a range of fungicides were tested for their activity against the identified competing fungi. A variety of fungicides were tested to find a discriminatory dose of chemistry that would suppress all other fungi except *S. sclerotiorum* (**Table 11**). These fungicides were chosen as they were the chemicals available in the laboratory. These fungicides were tested at different concentrations using a high throughput fungicide sensitivity assay to determine whether there is any fungicide which may make the medium selective for the target species.

Table 11: The different fungicides tested for efficacy against fungi identified in field samples

Mixed Fungicide Groups	DMI Group- effects Sterol biosynthesis in membranes	MBC Group- effects β -tubulin assembly in mitosis
Chlorothalonil (Chloronitriles-Multi-site contact activity)	Prochloraz	Thiabendazole
Etridiazole (AH-fungicides-Lipid synthesis and membrane integrity)	Prothioconazole	Thiophanate-methyl
Iprodione (Dicarboximides-MAP/Histidine-kinase in osmotic signal transduction)	Propiconazole	Zoxamide
Pentachloronitrobenzene (PCNB)	Imazalil	Fuberidazol
		Diethofencarb Carbendazim (used to control <i>S. sclerotiorum</i>)

Table 12: The concentration of fungicide required to inhibit growth and development of different fungal spores. Twelve serial dilutions of the different fungicides were dosed into 100 ml 2 x medium across the rows of 96 well plates. The density of the fungal biomass assessed using an optical spectrophotometer after 24hrs incubation. Ss= *S. sclerotiorum*. BC = *B. cinerea*. Tri= *Trichoderma sp.*

Fungal species	Fungicide concentration (ug /ml) required to kill the pathogen											
	Chlorothalonil	Etridiazole PCNB Diethofencarb	Carbendazim	Thiabendazole	Thiophanate- methyl	Prochloraz	Prothiocon azole	Propico nazole	Imazalil	Iprodione	Zoxamide	Fuberi dazol
<i>SS1 L44</i>		>60	No growth	0.1	1.9							
<i>SS2 GFR10</i>		>60	0.1	0.2	1.9 (0.9)							
<i>SS3 US</i>		>60	0.1	0.2	1.9		3.6	0.9	0.5	0.9		0.5
	73.15849			21.5	15.7	0.6	1.6		0.7	0.5		
<i>Ss GFW5</i>					0.9		1.9	1.9	3.8	0.9	0.9	0.5
<i>SS1 L6</i>	0.19540			0.1	1.1	155	0.1	0.0	0.6	0.5		0.6
<i>SS2 GFR1</i>	0.00361			0.2	40	88.3	0.3	1.2	1.0	0.4		0.7
<i>BC 1 B798</i>	7.5	>60	0.1	0.2	0.9	0.2	7.5	0.9	1.9	0.9	1.9	1.9
	0.25131			0.1	1.3	0.04	0.8	0.001	0.7	0.3		0.5
<i>BC2 18 1038</i>		>60	0.1	0.2	0.9	0	15	1.9	7.5	0.9	1.9	1.9
	0.00011			0.1	0.4	0.5	0.1	0.2	0.0	0.1		0.1
<i>Tri1 T.koningii C2729</i>	15	>60	0.5	0.5	15	0.1	15	15	15	7.5	>120	3.8
	0.58012			0.1	10	0.02		0.3	1.8	1.3		1.5
<i>Tri2 Field isolate K -77b</i>	15	>60	0.2	0.2	15	1.9	15	60	60	15	>120	7.5
	0.43237			0.1	11.3	1		2.9	5.8	1.1		1.5
<i>Tri 3 T. harzianum 72.1</i>	>60	>60	0.2	0.5	15							
<i>Tri 4 T. harzianum C2679</i>	>60	>60	0.5	0.9	60<x<120	3.8	15	60	>120	7.5	>120	30
	0.43535			0.2	18	0.4		58.51	>120	1.5		3.4

After testing a range of concentrations of the listed fungicides, it was extremely difficult to determine the concentration of fungicides to add to the medium that would kill other fungal contaminants but allow *S. sclerotiorum* ascospores to continue to germinate and produce oxalic acid. This is principally because the *Trichoderma spp* requires a much higher concentration of all the fungicides tested to inhibit growth compared to *S. sclerotiorum* (**Table 12**). The concentrations required to inhibit *S. sclerotiorum* growth vary between different isolates so it would be a risk to set the highest fungicide concentration tested which still allows spore germination as some isolates might be sensitive and inhibit growth.

A fungicide mixture combining the most effective fungicides against the competing fungi was developed by mixing in the doses of fungicide which had not inhibited *S. sclerotiorum* growth in the previous assay (**Table 13**). *Trichoderma sp*, *S. sclerotiorum* and *B. cinerea* ascospores were added to the SDB medium with and without the fungicide mix. The species were mixed as well as incubated individually. The oxalic acid concentration was measured over 7 days to assess whether *S. sclerotiorum* could withstand the fungicide treatment (**Figure 35**). The oxalic acid produced by *B. cinerea* and *S. sclerotiorum* was seriously reduced when grown in the presence of fungicides compared to the medium without. Little growth of *S. sclerotiorum* and *B. cinerea mycelium* was visible. *Trichoderma sp* growth was also reduced when treated with this fungicide mixture however not as severely as the two fungi.

The results highlight that it may not be feasible to kill *Trichoderma spp* effectively using appropriate fungicides without inhibiting growth of *S. sclerotiorum* ascospores in the medium. Therefore a better strategy would be to focus on trying to inhibit *B. cinerea* spore germination because this fungus will cause an increased risk of false positives. Thiophanate-methyl and Fuberidazol could potentially be used in the medium as most of the *S. sclerotiorum* isolates tested were able to continue to grow in higher concentrations of these fungicides compared with *B. cinerea*.

Table 13: A combined fungicide treatment.

Amounts of fungicide based on the lowest doses of fungicides required to inhibit *S. sclerotiorum* ascospore growth was mixed in SDB. *Trichoderma spp*, *S. sclerotiorum* and *B.cinerea* ascospores were grown separately and together in the medium and the growth and oxalate concentration of the medium measured over 7 days.

Fungicide	Non-lethal dose to Ss ug/ml	Added to 20ml Sabouraud medium (ul)
Prochloraz	0.47	189 (106x dilution)
Prothioconazole	3.75	1.5ml (13.3diltuion)
Propiconazole	0.9375	426 (46x dilution)
Imazil	0.47	189 (106x dilution)
Iprodione	0.9375	426 (46x dilution)
Fuberidazol	0.469	189 (106x dilution)
Chloranothil	0.47	189 (106x dilution)
Thionphanale-methyl	0.95	426 (46x dilution)
Thiabendazole	0.117	49 (427x dilution)

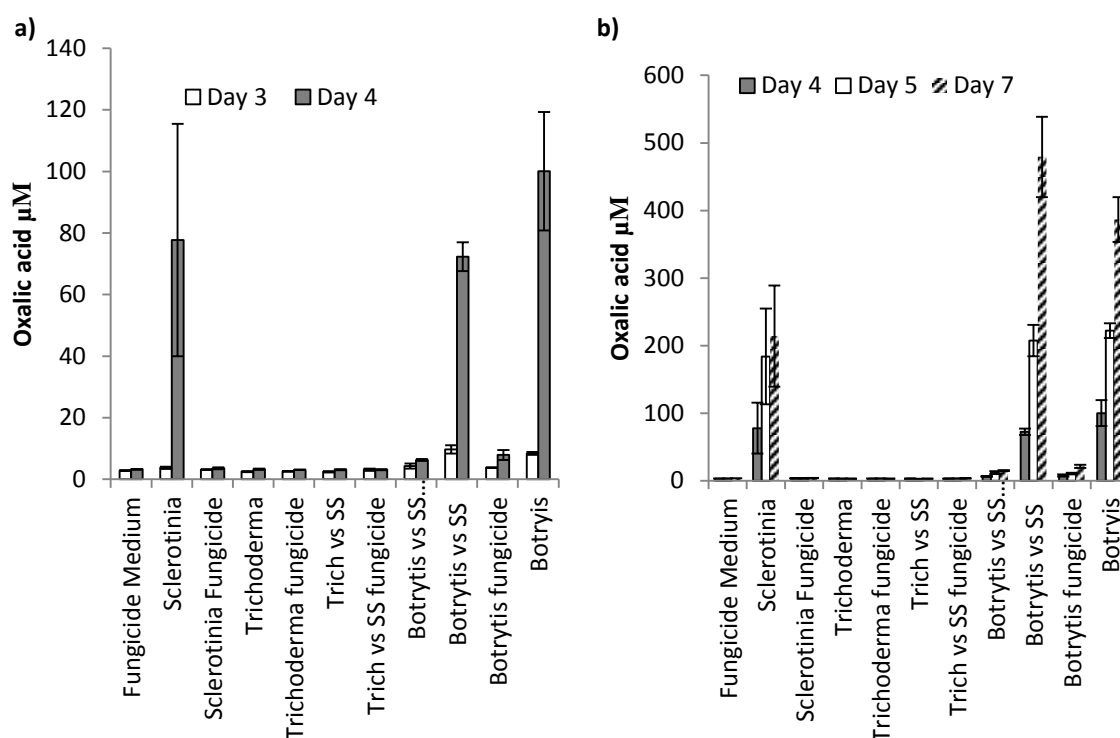


Figure 35: The effect of combined fungicide treatment on *S. sclerotiorum* fungal competitors.

Trichoderma sp, *S.sclerotiorum* and *B.cinerea* ascospores were incubated with and without the fungicide mixture. OA production was measured over 7 days of growth. Bars represent the average OA of 3 biological replicates. Spores were grown in 2 ml of medium with fungicide mix. Fungicide= the medium contains the mix of fungicides.

3.4 Discussion

3.4.1 Optimising OA secretion from ascospores in a liquid matrix

The use of a liquid based matrix as opposed to a solid based matrix has shown to be more suitable for the induction of OA and quantification of OA from germinating ascospores. The use of a defined media induced more reliable and reproducible OA production from ascospores compared with host plant extracts which is necessary for accurate detection of this pathogen within the biosensor. Sabouraud dextrose broth was not only the best inducer of OA which has been tested but is also electrochemically compatible with the biosensor which has been optimised to detect the presence of OA.

Previously published studies have shown that additions of TCA cycle intermediates to a carbon source can optimise OA secretion by *S. sclerotiorum* ascospores (Culbertson et al. 2007, Maxwell and Lumsden 1970, Godoy et al. 1990). However, the results presented in this chapter did not always support these conclusions. Additions of succinate to the minimal baseline medium or to a complex medium consistently induced lower OA production from ascospores compared with a complex medium such as PDB. This is different to other studies that reported an increase in OA production after the addition of succinate. Additions of other TCA cycle intermediates such as 5-15 mM malate and fumarate to complex media were observed to increase OA amounts secreted by ascospores, but only at a later point during incubation, after 4 days incubation. It is questionable whether *S. sclerotiorum* is actually capable of metabolising succinate directly from exogenous substrates. There is no evidence that external sources of succinate, malate or fumarate are bioavailable organic acids which filamentous fungi will uptake directly. There are no reports of any succinate, malate or fumarate receptors within fungal extracellular membranes, however if these could be broken down by secreted enzymes, then the products may be re-absorbed. Other fungal secreted organic acids such as citric acid can be re-metabolised as they act as siderophores which help to make essential nutrients principally iron bioavailable by chelating to free iron in the surrounding environment. The chelated iron is then transported into the cell (Plessner et al. 1993). However this is not the case for the three TCA cycle intermediates tested within this study. The use of ascospores rather than mycelial plugs which were used in all other studies and the use of different isolates may also account for the differences seen in the effects of TCA cycle intermediates between the different studies

Additions of glucose to the baseline minimal nutrients did increase OA production, but it was continually the use of a complex medium which contains a high carbohydrate

and protein content which induced the highest OA induction. Higher amounts of glucose additions to complex media induced lower OA secretion during incubation under 4 days but after this point the higher glucose levels induced marginally higher OA production. This supports other studies which have shown that OA and growth of mycelial plugs of *S. sclerotiorum* are dependent on the availability of simple and complex carbohydrates. (Maxwell and Lumsden 1970, Vega et al. 1970, Marciano et al. 1989, Rollins and Dickman 2001). It is more likely that the availability of suitable carbohydrate sources which can be broken down into simple sugars by the plethora of fungal enzymes and then utilised in the glyoxylate pathway to provide the intermediates for the TCA cycle will affect OA production. Glucose transport in *Saccharomyces cerevisiae* has been well studied and two glucose uptake systems have been defined. One system is a constitutive low-affinity system and the second is a glucose-repressed high-affinity system (Lagunas 1993). Other similar glucose transport systems have been defined for the ascomycetes *Neurospora crassa* and *Trichoderma harzianum* (Scarboro.Ga 1970a, Scarboro.Ga 1970b, Schneide and Wiley 1971, Delgado-Jarana et al. 2003). If there are two glucose affinity systems in *S. sclerotiorum*, this could account for the higher glucose concentrations only making a difference later on in the incubation time course, when the available carbon sources would become more depleted. This may induce a putative high affinity glucose system, however this is a speculation and requires further investigation.

One way in which this work and the previous published studies could be improved is by radioactively labelling the intermediates added to the media to determine whether they are directly taken up by the fungus. Without this information it is very difficult to determine whether the intermediate or other compounds within the complex media are affecting OA production. The expression of genes involved in transport of exogenous nutrients into the fungal cell and the enzymes involved in different metabolic cycle could also be investigated to determine which pathway(s) may be the most critical for maximising OA production.

3.4.2 pH and Buffering of complex media to maintain OA production

Environmental pH has been shown to be important for regulating OA production by *S. sclerotiorum* ascospores. Principally pH substrates above pH 5 have been shown to induce OA production (Maxwell and Lumsden 1970, Rollins and Dickman 2001, Culbertson et al. 2007). This was observed when SDB was buffered at pH 5 there was a reduction in the amount of OA produced and as a result pH 5 was chosen as the optimum starting pH for the medium used within the biosensor.

pH has been shown to strongly regulate the *pac* homologue gene in *S. sclerotiorum* which in turn regulates a range of pH dependent developmental genes in the fungus. The more oxalic acid secreted, the lower the pH which activates many developmental genes. However once a certain acidic pH is reached, oxalic acid production is inhibited (Rollins and Dickman 2001). It has been suggested that by buffering the medium, prolonged OA could be achieved. This was certainly observed for the 50mM HEPES buffer added to SDB which had prolonged high levels of OA production (**Figure 31 c-d**). At day 6 and 7, the OA amounts were nearly double that of the control SDB for both high and low spore dilutions. However for the biosensor, 6 days for sample incubation is too long a period and instead 4 days is a better incubation time frame to allow a suitable fungicide spray window for growers. At day 4 there was very little difference between the amounts of OA produced in the control SAB medium or the HEPES buffered medium. As a result, no buffer was added to the final medium.

3.4.3 The relationship between *S. sclerotiorum* ascospore number, biomass and oxalic acid production.

In this series of experiments, no evidence was obtained that ascospore number positively correlated to increases in OA concentration or biomass. This finding supports other published studies, where the highest biomass of a mycelial plug inoculated culture did not correspond to the highest amount of OA measured (Culbertson et al. 2007). Instead it was observed in this study that a baseline biomass was required before OA production was induced. This is observed as the lower ascospore doses only reached this required biomass a day later compared with the highest ascospore doses and only then was OA secreted. It is important to note that biomass did not differ significantly between the three spore doses and this is most likely because once the spores germinate, the wells can only support so much biomass as there is a limited nutrient supply, principally the glucose supply, which was not replenished. The 2 ml of medium will only support the growth and development of a finite number of fungal cells and it was also observed that by 11 days there was very liquid remaining in the wells. In addition, it was difficult to assess out of the 2000 spores, for example, how many were actually viable.

Biomass reduced later on during the infection course probably due to a combination of pH environmental signals and reduced availability of nutrients for biomass growth. By 11 days growth, the pH had increased and cultures began to synthesise sclerotia, a process which is linked to gene regulation by the alkaline dependent *pac1* gene. This gene actively promotes transcription of alkaline-expressed genes (Rollins 2003). This occurs when *pac1*

recognises alkaline expressed genes which contain multiple copies of a 5'GCCARG-3' binding site situated in a zinc finger DNA-binding domain (Espeso et al. 1997). Under alkaline conditions this gene is activated and so ensures that only pH responsive genes are activated under the right pH conditions (Espeso et al. 1997). The production of sclerotia may account for the decrease in biomass in the older colonies as the fungus potentially recycles biomass to make the sclerotia.

Obtaining accurate biomass measurements was a challenge during this experiment as it was not possible to gather 100% of the biomass from the plastic wells for freeze drying which will make the data more variable.

During the first few days of incubation, the OA concentration increased for all three ascospore doses and the pH dropped which was an expected result. The OA concentrations eventually reduced in all spore concentrations which correlated with an increase in pH. This could be a result of putative oxalate decarboxylase enzymes which are secreted into the medium, and hydrolyse OA into formate and carbon dioxide. Secretion of formate oxidases may then be involved in the breakdown of formate. Formate oxidases have been shown to be part of glucose-methanol-choline oxidoreductase family (Doubayashi et al. 2011). Two putative oxalate decarboxylase enzymes as well as ten putative secreted glucose-methanol-choline oxidoreductase family proteins were predicted in the refined *S. sclerotiorum* secretome (Chapter 5). These genes could be investigated for further extracellular function. Another possibility is that *S. sclerotiorum* may possess oxalate:formate transporters which are present in other fungi including *Saccharomyces cerevisiae* and *Aspergillus fumigatus* (Cheng et al. 2007, Nierman et al. 2005). These may assist in the efflux of oxalate and influx of formate but this has not been identified yet and so requires further information.

From the above experiments there remains little understanding about why the OA concentrations vary so much between different ascospore doses and different biomasses. For the purpose of the biosensor this is not a problem as even the smaller amounts of ascospores captured within the sensor will be able to produce detectable levels of OA. From an academic perspective it may be interesting to repeat this experiment but monitor the expression of pH-dependent genes to determine at which point specific genes are expressed and how these might further induce growth.

3.4.4 Selectivity of the medium

The medium designed for testing during field trials (Chapter 4) did not contain any fungicides because the experimental data generated in this chapter did not identify either a single fungicide agent or a fungicide mixture which could control other potential competitors without killing *S. sclerotiorum*. *Trichoderma sp* were particularly difficult to control with fungicides. Routine antibiotics were added to the medium to reduce contamination from bacteria. Field results show that this medium, without the use of fungicides was still able to encourage oxalate production from *S. sclerotiorum* ascospores. However, further fungicide testing could be carried out test find a fungicide that could kill *B. cinerea* without inhibiting *S. sclerotiorum* growth.

In conclusion, this chapter has shown the successful development of a liquid biological matrix which is able to promote the germination of approximately 10 to over 2000 spores and induce detectable levels of secreted OA after four days of incubation. The OA in this medium can be successfully detected by both a commercially available high throughput spectrophotometric enzymatic OA detection assay as well as an optimised electrochemical OA detection biosensor.

Chapter 4: The testing of an electrochemically compatible nutrient medium for detection of oxalic acid produced by *S. sclerotiorum* ascospores within an oilseed rape system.

4.1.1 Introduction

An electrochemically compatible biological matrix was developed to be used within the SYield biosensor for the detection of oxalic acid (OA) secreted from germinated *S. sclerotiorum* ascospores (Chapter 3). The matrix comprised a liquid nutrient medium consisting of baseline minimal salts, Sabouraud Dextrose Broth and antibiotics, at pH 5. In a laboratory environment, the medium was able to induce high amounts of OA secretion from viable *S. sclerotiorum* ascospores. OA secreted from spore doses above approximately 1000 spores per liquid aliquot was detected at three days of incubation however OA secreted from lower spore doses could be detected only after four days of incubation. It was necessary to test the liquid medium ability to detect specifically *S. sclerotiorum* secreted OA from field air samples which could potentially contain a range of other fungal spores, dust and other organisms. These ‘dirty’ air samples have the potential to inhibit *S. sclerotiorum* growth and in doing so, reduce the positive OA detection events. Another possibility is that there are other fungal species in the ‘dirty’ air samples which also secrete OA and would induce false positives. To ensure that ascospores were present within a field environment for testing the SYield biosensor, sclerotia were artificially buried within an oilseed rape field to allow natural production of apothecia and ascospores release during the flowering stage of the oilseed rape. A variety of air sampling equipment was then used to sample the air for ascospores to test for OA production as well as to extract DNA to verify that *S. sclerotiorum* was responsible for OA detection events.

4.1.2 Objectives of field trials:

Two out of the three field trials which have been carried out to test the SYield biosensor at different developmental stages are described in this chapter. The objectives of these field trials were to:

- investigate whether the OA inducing liquid media described in Chapter 3 can be used to induce *S. sclerotiorum* ascospores in ‘dirty’ field air samples to secrete detectable levels of OA.
- investigate the use of the optimised electrochemical assay to detect OA accurately in the liquid medium.

- determine whether the OA detection events can be verified by the presence of *S. sclerotiorum* DNA sampled on the same days as the OA positive events.
- observe apothecia development in the field to ensure that this coincides with OA detection events and the detection of *S. sclerotiorum* DNA.
- test the efficiency of new air sampling machinery that is to be used with the biosensor.
- gather climatic data which will be incorporated into a disease prediction model.
- understand how the positioning of air sampling equipment may affect the sampling of ascospores.
- assess the power requirements of the sampling equipment.
- carry out disease assessments of the oilseed rape.
- correlate the OA detection events to disease incidence in the field.

4.2 Experimental Procedures

4.2.1 Field trial set up

Two sets of independent field trials over two field seasons were carried out to test the efficiency of the biological matrix reported in Chapter 3 (**Figure 37**). In the September of both 2010 and 2011, sclerotia of four UK isolates (L6, L44, L17 and RRes mixed, see Chapter 2 for sclerotia production method) were buried approximately 1-2 cm deep in the soil of oilseed rape fields; New Zealand (2011) and Geescroft (2012) situated on the Rothamsted farm. This allowed the sclerotia to undergo a period of winter conditioning so that they produced apothecia during the following flowering season. The field sampling period was from the 11 April to 28 June in 2011 (78 days) and the 21 March - 6 June 2013(77 days) which coincided with the flowering period of oilseed rape. The aim was for the apothecia to develop from the buried sclerotia and the ascospores to be released in synchrony with the flowering oilseed rape. This occurred in 2012 field trials however the 2011 field was very dry and the sclerotia had to be artificially watered to induce apothecia formation.

Within the area of buried sclerotia, different spore sampling systems were used to sample the ascospores released into the air from the apothecia. The set up for 2011 and 2012 are represented in **Figure 36 d-e**. During the two field sampling seasons, two cyclone samplers and two Burkard 7 day air samplers were placed in the middle of the inoculated site. The cyclone sampler captured air into a sterile 1.5 ml Eppendorf tube (**Figure 36b**) and the Burkard sampler impacted air samples onto a wax-coated plastic strip which was

then used to extract DNA and assess, the amount of *S. sclerotiorum* DNA sampled per day using qPCR (**Figure 36a**). In the 2012 field trial, a new sampling device developed by Burkard, called a SYield Virtual Impactor (SVI) which sampled air into 500 μ l pots was tested (**Figure 36c**). A modified version of this pot system would be used in the automated biosensor which was developed for the 2013 field trials. The different samplers collected air continuously from 8 am to 8 pm on a daily basis, with the cyclone Eppendorf tubes and wax strip changing position every 24 hrs so that daily air samples were obtained. A meteorological station was also placed alongside samplers in both field trials to collect data on the hourly rainfall amount, wind speed and direction and atmospheric temperature. A soil temperature meter was also buried in the centre of the inoculated sites.

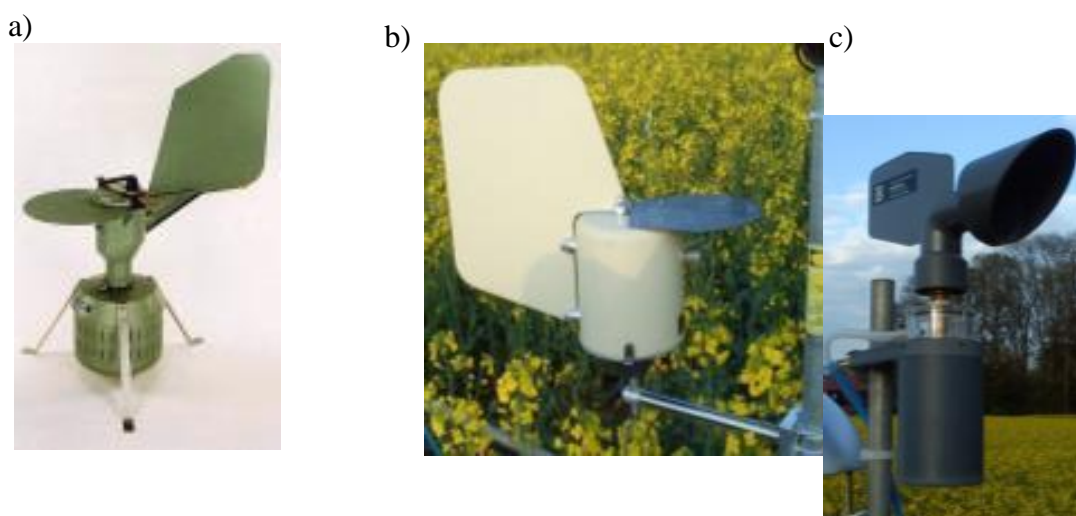


Figure 36: Air sampling devices used during field trials.

Burkard 7 day air samplers for DNA extraction. b) Cyclone air sampler, sampled air into 1.5 ml Eppendorfs. c) SYield Virtual Impactor (SVI) air sampler which sampled air into 500 μ l pots. The air volume that each sampler can sample is as follows:

Burkard 7 day = 10L/min (collection is very efficient for particles above 2 microns)

Cyclone = 24L/min (collection efficiency about 25% for particles above 2 microns)

SYield automated = 20L/min (collection efficiency about 80% for particles above 2 microns)

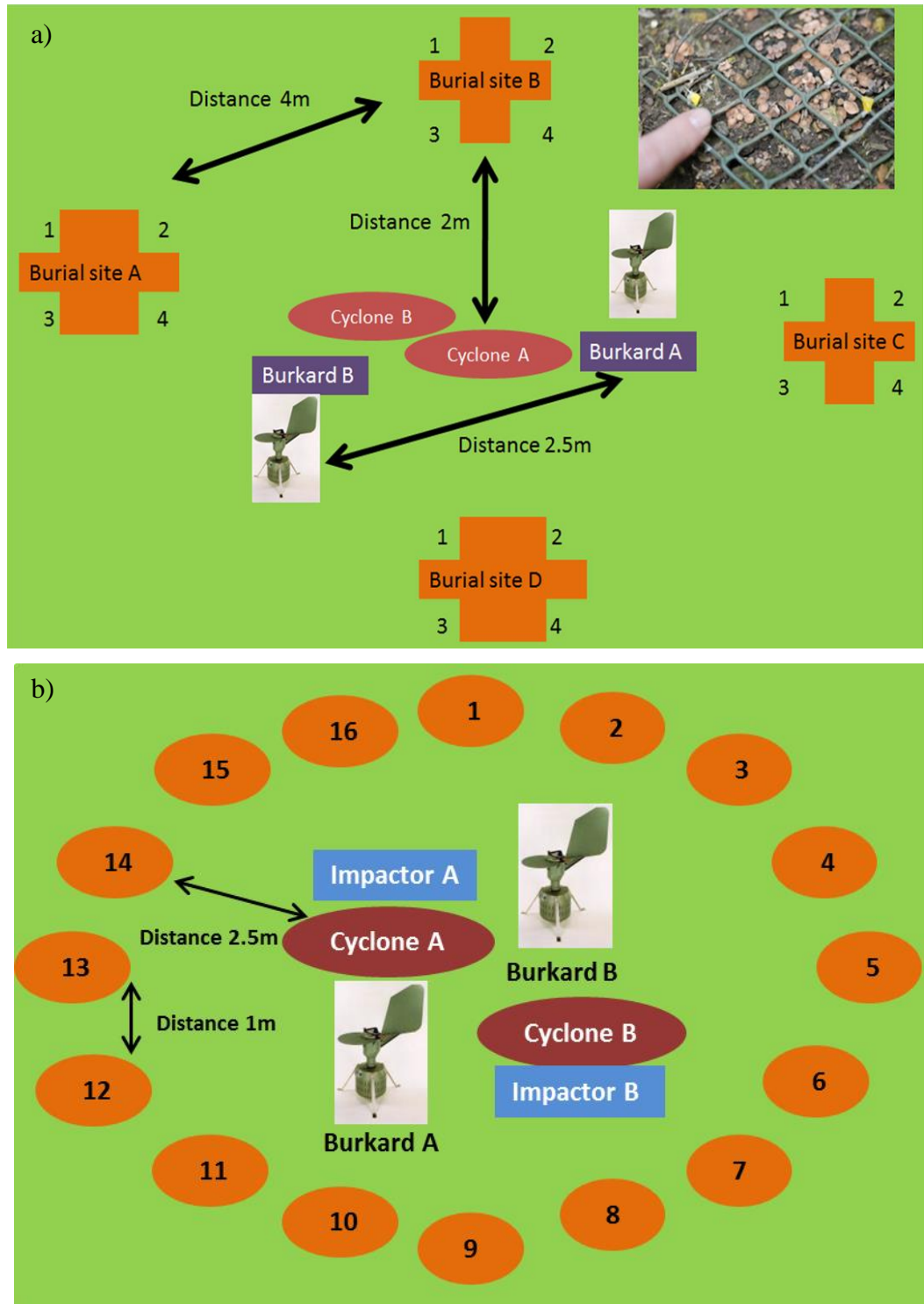


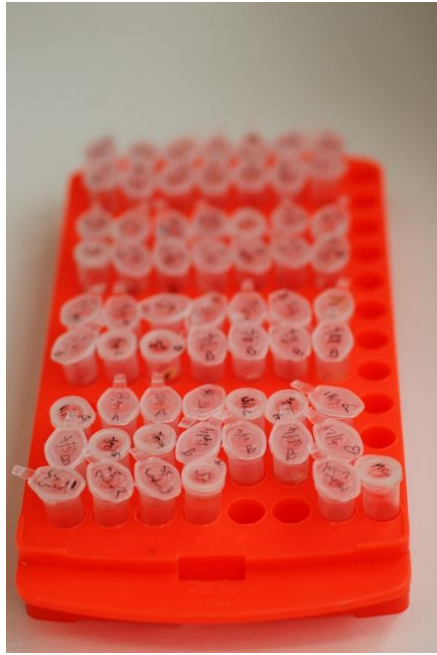
Figure 37: Field set up for 2011 and 2012.

a) The field trial set up in the Rothamsted ‘New Zealand’ oilseed rape field, 2011. Air sampling equipment including two cyclones and two Burkard 7 day air samplers were placed in the centre of four sclerotial burial sites. At each burial site, four different isolates were buried: 1- L6, 2- L17, 3- L44, 4- RRes mixed. Top right picture demonstrates the size of apothecia germinating during flowering of the oilseed rape. e) The field trial set up in the Rothamsted ‘Geescroft’ oilseed rape field, 2012. Air sampling equipment including

two cyclones, two Burkard 7 day wax strip samplers and two SVI samplers were placed in the centre of a ring of 16 sclerotial burial sites, a pattern of L6, L17, L44 and RRes mixed isolates.

4.2.2 Medium testing

Samples were collected weekly from the field cyclone samplers (2011,2012) and daily from the SVI samplers (2012 only). All samples were stored at 4 °C until a batch of approximately 10-20 samples for each sampler had been collected (**Table 14**). In 2011, the 1 % soytone medium with glucose and baseline salts was tested by pipetting 1 ml of the medium into the cyclone Eppendorfs. In 2012, 400 µl or 1 ml of SDB medium (Sabouraud Dextrose Broth, baseline minimal salts and 150 mg / L PenStrep antibiotics) was added to the SVI pots or 1.5 ml cyclone Eppendorf tubes respectively. All samples were incubated with the media at room temperature (approx. 20 °C) in the dark (**Figure 38**). In 2011 the samples were tested for oxalic acid production after day 3, 4 and 7 days of incubation using the high throughput OxOx spectrophotometer assay (see General Experimental Procedures). As two cyclones and SVI's were used, there were two samples for each day (A and B). In 2012, the A and B samples for the cyclones as well as SVI pots were tested with both the high throughput OxOx spectrophotometer assay (see General Experimental Procedures) and the optimised electrochemical measurements after 4 days of incubation. For all batches, a set of controls were included in the testing. One positive control consisted of the same medium being tested in the field seeded with known *S. sclerotiorum* ascospores to ensure that the medium would induce ascospore growth if ascospores were present in the dirty field air samples. A second control included the medium inoculated with water to ensure the medium itself was not giving any OA readings.



a)

b)

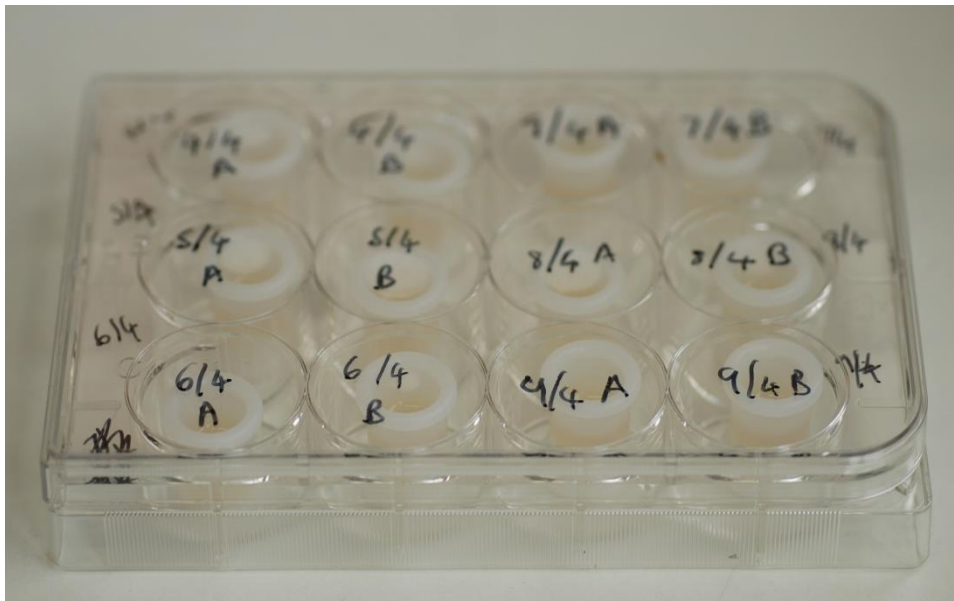


Figure 38: Pot incubation assay.

a) The Eppendorf tubes collected from the cyclone samplers in the field which were filled with medium and incubated in the dark at 20 °C. b) The SVI pots collected from the field SVI samplers and incubated with SDB medium in the laboratory.

Table 14: Batches of samples collected over field trials to be incubated with the medium being tested and then tested for OA.

2011 cyclone samples were tested at day 3, 4 and 7 of incubation using the OxOx spectrophotometer assay 2011. 2012 cyclone and SVI samples were tested for OA after 4 days of incubation using the OxOx spectrophotometer assay and electrochemical assay.

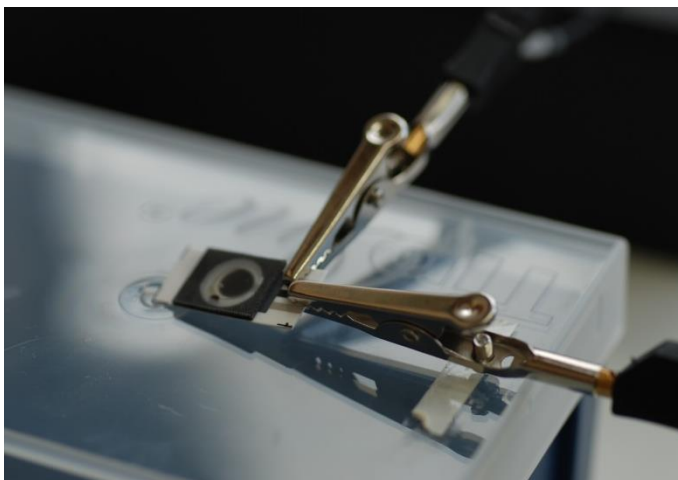
Batch	Sample Number	Date 2011
A	1-23 A/B	11/04- 03/05
B	24-45 A/B	04/05 - 25/05
C	46-71 A/B	26/05- 20/06
D	72- 79 A/B	21/06 -28/06

Batch	Cyclone	Sampling date	SYield virtual impactor	Sampling date 2012
A	C1-C28	21/03 - 17/-4	S1-S14	04/04 - 17/04
B	C29-C42	18/04 - 01/05	S15-S32	18/04 - 05/05
C	C43- C56	02/05 - 15/05	S33-S44	06/05 - 17/05
D	C57-C63	16/05 - 22/05	S45-S59	15/05 - 01/06

4.2.3 Electrochemical Measurement of oxalic acid production

Electrochemical measurements were performed by Dr. Sophie Weiss. Two 40 µl aliquots from the SVI sample pots were tested during batch testing sessions. One aliquot was used on a carbon electrode with oxalate oxidase (OxOx) and horseradish peroxidase (HRP) enzyme stabilised onto the surface of an electrode (**Figure 39**). The HRP is used to reduce hydrogen peroxide released from the breakdown of oxalic acid by OxOx. The second 40 µl aliquot was used on a Prussian Blue (PB) electrode. PB electrodes have both the stabilised OxOx on the surface and ferric hexacyanoferrate which will catalyse the oxidation of hydrogen peroxide when the PB is in an oxidised form. Both cyclic voltammetry and chronoamperometric measurements were performed with the two electrodes. Liquid aliquots were incubated on the electrode surface for 2 mins before a measurement was taken using a potentiostat connected to the electrode with crocodile clips.

a)



b)



c)

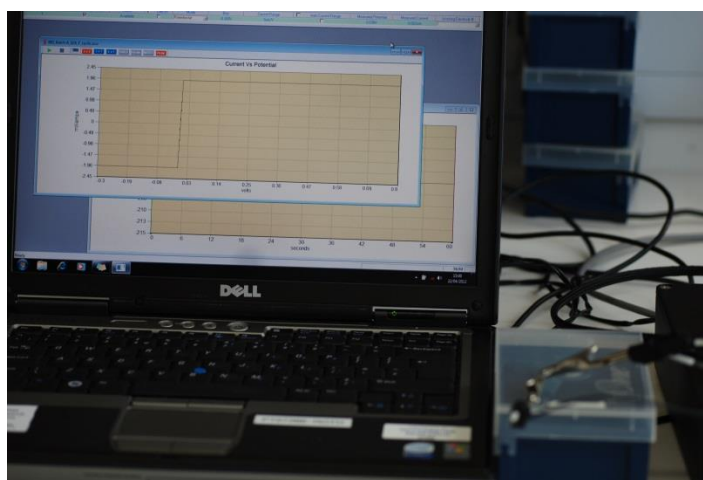


Figure 39: Electrochemical set up.

a) Crocodile clips connected to the working and reference electrodes. Liquid medium aliquots were placed onto the centre of the electrode mesh, under which the stabilised enzymes were contained. b) Crocodile clips connected to a potentiostat. c) The potentiostat was connected to a computer with the software to monitor the change in current during oxidation of the electrode.

4.2.4 Daily spore counts of qPCR of field trial samples

See General Experimental Procedures (Chapter 2)

To determine how many spores were sampled daily into the Burkard 7 day air sampler, the wax tapes from the spore trap were cut into daily strips, 48 mm x 20 mm and then subdivided longitudinally into two subsections, each 48 mm x 10 mm. These (a working subsample and a duplicate) were each placed into 2 ml screw cap tubes and frozen at -20°C by a summer student, Leanne Freeman.

4.2.5 ITS identification of other fungi present in field samples

After testing the liquid for oxalic acid incidence, the fungal biomasses from both the cyclone and SVI samples were cultured on PDA plates to isolate out individual species to identify what other fungi are captured in the air samples. Steph Heard (2011) and Leanne Freeman (2012) performed the rounds of culturing and sub culturing to obtain pure cultures on PDA plates. Mycelium obtained from pure cultures was freeze dried and DNA extracted using a QIAGEN PLANT DNeasy mini plant kit. The manufacturer's protocol was followed. ITS5 F (GGA AGT AAA AGT CGT AAC AAG G) and ITS4 R (TCC TCC GCT TAT TGA TAT GC) (White et al. 1990) primers were used to amplify the ITS region using RedTaq ready mix and thermal cycling parameters described in General Experimental Procedures, Chapter 2. Sequences were sent off to MGW Operon for sequencing analysis. Returned sequences were blasted in NCBI for species identification at a Genus level.

4.3 Results

4.3.1 Field trial results 2011

4.3.1.1 Apothecia development and visible signs of *S. sclerotiorum* disease in the field, 2011

This field season was extremely dry and warm. Initial apothecia development was observed in the inoculation sites on the 13 May 2011. As a result of the lack of rain throughout the field season, sclerotia inoculation sites required artificially watered to

induce apothecia development. Apothecia were kept damp for prolonged spore release by light watering throughout the sampling period. Three weeks after the field sampling, the oilseed rape surrounding the sclerotia burial sites was assessed for disease symptoms. Symptoms were observed only in plants directly near where the apothecia had developed.

4.3.1.2 OxOx spectrophotometer assay, 2011

In total, 200 samples were retrieved from the cyclone A and B samplers. These samples were incubated with the 1% soytone medium. These included A and B samples 1.5 ml Eppendorf tubes collected from the two cyclones. All samples were tested for OA production at 3, 4 and 7 days incubation using the OxOx spectrophotometer assay. Any measurements below 25 μM were considered as negative oxalate events due to the insensitivity of the assay to define a concentration of OA accurately below this threshold. In total, 9 samples across both A and B samples tested positive for OA (**Figure 40a**). The biomass from these 9 samples was freeze dried and the DNA extracted. qPCR identified 5 out of the 9 OA positive sample contained *S. sclerotiorum* DNA (**Figure 41**).

4.3.1.3 Validation of *S. sclerotiorum* DNA using qPCR 2011

DNA was extracted from the daily tape sections obtained from the Burkard 7 day wax strip sampler and qPCR analysis carried to detect the presence of *S. sclerotiorum* ascospores for each day during the sampling period. These data were obtained by Gail Canning and Jon West. In total *S. sclerotiorum* DNA was detected on 52 days of the 78 day sampling period in at least one of the two Burkard samplers (**Figure 40b**). Of these 52 *S. sclerotiorum* DNA positive samples, only four of the corresponding medium incubated cyclone samples tested positive for OA (Appendix 7). The last two OA positive samples could not be verified using the spore trap qPCR because these traps did not sample during this time due to mechanical failure. The other 3 OA positive OA events measured by the spectrophotometer could have been induced by other OA producing fungi.

The wax tape samples collected on the same day as the five OA positive samples did not contain *S. sclerotiorum* DNA, although 3 of these events were verified by the qPCR of the medium incubated tube contents. It is also important to note that there was some mechanical failure of the Burkard spore traps which means there is no qPCR data for some of the days.

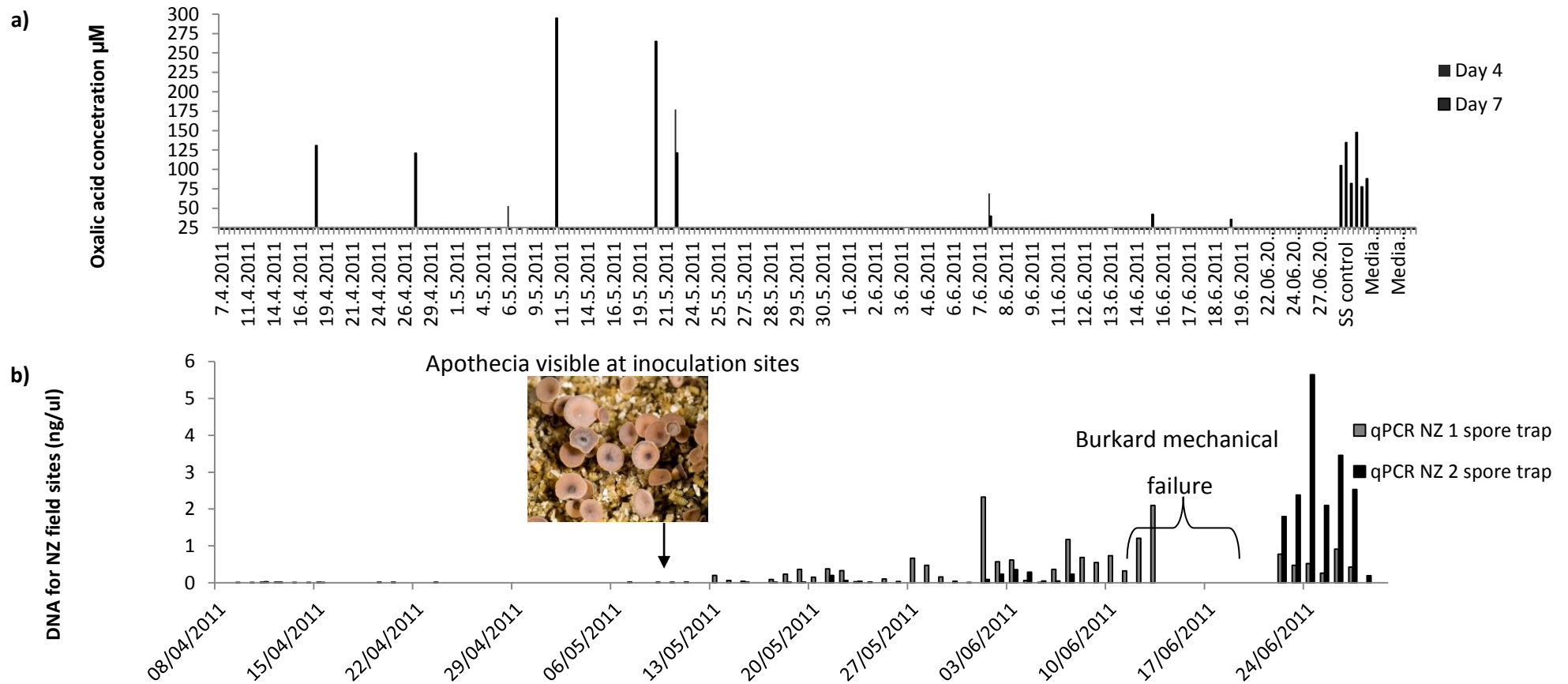


Figure 40: Field trial results 2011.

a) Cyclone samples incubated in 1% soytone medium which tested positive for oxalic acid positive. All samples were tested at day 3, 5 and 7 post incubation. Only 9 tested positive for OA b) Two Burkard 7 day wax strip samples (A and B) which tested positive for *S. sclerotiorum* DNA. 0.1 pg DNA corresponds to 1 ascospore.

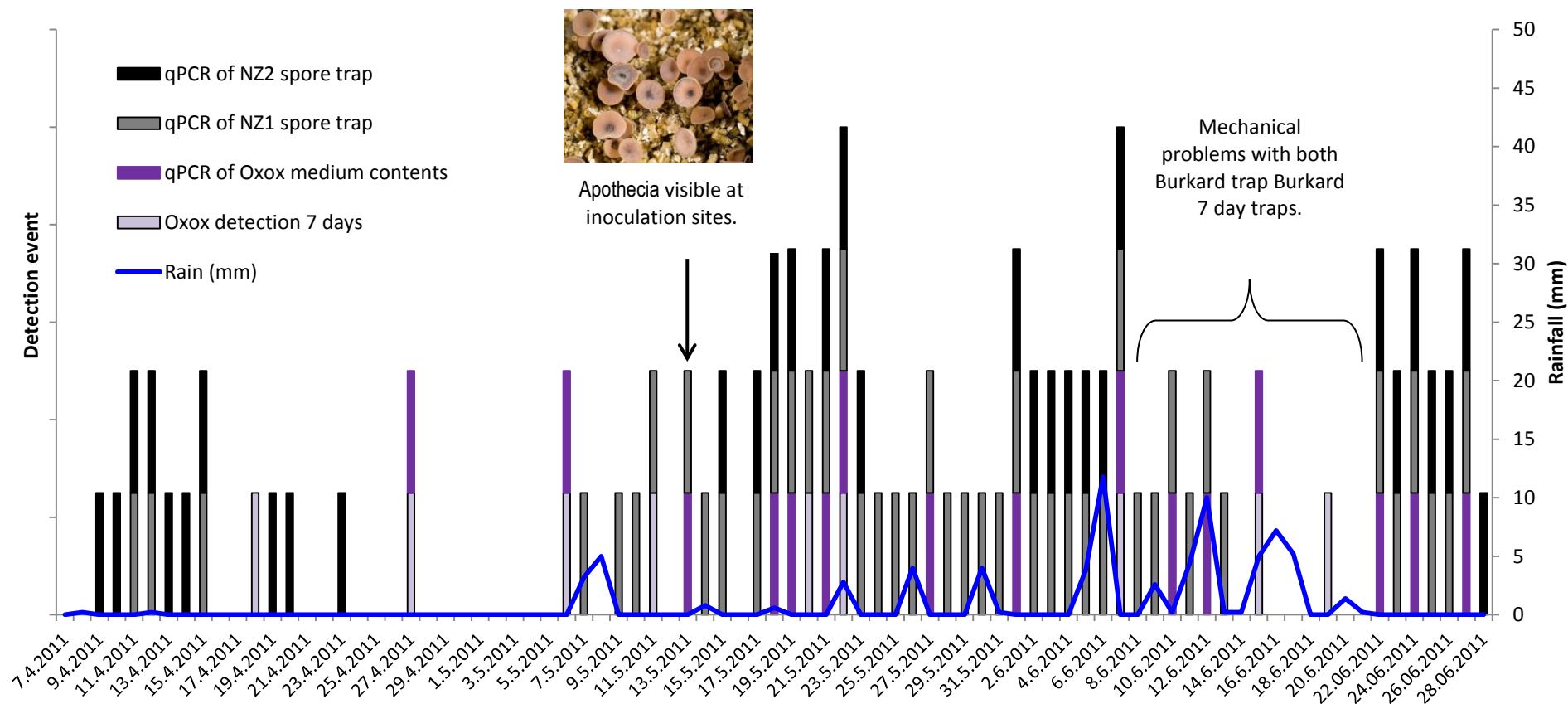


Figure 41. Field trial results 2011.

Non-quantitative combined positive events for the detection of DNA using qPCR from both Burkard 7 day air samplers and the positive OA events from the cyclone medium incubated samples. Each block represents a positive event rather than quantification. Rainfall (mm) during this period is denoted on the left scale bar (mm). Apothecia were first observed on the 10/5/2011. Mechanical failures for the Burkard traps were noted between the 8/6/2011 – 21/6/2011.

4.3.2. Field trial Results 2012

4.3.2.1 Apothecia development in the field 2012

This field season was much wetter compared with 2011, with a maximum 38 mm of rainfall being measured on a single day compared with the maximum being 12 mm on a single day in 2011. On most rainy days there was above 2mm of rain per day measured. The beginning of apothecia development in the burial sites in Geescroft was observed in one isolate (Mixed RRes) on the 18 April 2012. The 3 other isolates were later in development and were only observed on the 3 May 2012. There was no need for artificial watering due to frequent rain showers.

4.3.2.2 OxOx spectrophotometer assay and electrochemical detection of OA 2012

The cyclone air sampler has been described as having a lower particle capture efficiency (25%) compared with the Burkard and SVI traps with have about 80% capture efficiency. As a result the cyclone OA results were not compared to the SVI results. One hundred and twenty sample pots from the A and B SVI samplers, were collected over the field trial from the 4 April to the 6 June 2012. After 12 hrs of air being sampled into the two SVI pots (A and B), the pots were collected from the field and in the laboratory 400 µl SDB medium pipetted into to the pots. Pots were incubated for 4 day. Aliquots of liquid were tested for OA concentration using both the OxOx spectrophotometer assay and the electrochemical assay. Electrochemical measurements were made with two different electrodes, HRP and PB electrodes. Overall, there were 20 positive OA events detected by both A and B samplers for both the electrochemical detection (both type of electrode) and spectrophotometer detection of OA detection (**Figure 43, Appendix 6**). All 20 events were detected after the 3 May, when most of the apothecia had developed. Individually over the sampling period, the Prussian Blue electrode detected 24 OA positive events in one or both of the samplers, the Horseradish Peroxidase enzyme detected 28 positive OA events in one or both of the samplers and finally the spectrophotometer assay detected 25 positive OA events. The PB electrode gave similar OA readings compared with the HRP electrode and the spectrophotometer assay.

Table 15: OA positive events 2012.

The number of positive OA events detected in the SVI pots by both electrodes and the spectrophotometer methods.

Measurement type	SVI sampler A Positive OA events		SVI sampler B Positive OA events	
	Pre observed apothecia development	Post apothecia development	Pre observed apothecia development	Post apothecia development
All 3	0	15	0	9
HRP electrode	3	21	0	12
PB electrode	6	29	1	15
Spectrophotometer	0	19	0	12

4.3.2.3 Validation of *S. sclerotiorum* DNA using qPCR 2012

S. sclerotiorum DNA was detected on 74 days (21 March - 6 June, 77 days) over the sampling period in one or both of the Burkard 7 day traps (A and B) (**Figure 44**). However the SVI sampler started sampling at a later date taking the sampling period down to 61 days. Out of these 61 days, *S. sclerotiorum* DNA was detected on 59 days in either one or both Burkard 7 day traps. The DNA results were compared to OA positive events detected using the spectrophotometer data. There were 24 positive OA positive events (41 %) which overlapped with the DNA positive events. 27 (46%) and 23 (39%) positive OA events detected with the HRP and PB electrode respectively overlapped with the presence of *S. sclerotiorum* DNA (**Appendix 7**). This means that during the sampling period roughly 96% of the OA positive events were correlated with the presence of that *S. sclerotiorum* ascospores which were in the air. There was one day when there was a positive OA event (30 April) for both the electrode assays and the spectrophotometer data which could have been a potential false positive as there was no *S. sclerotiorum* DNA detected.

4.3.2.4 Disease Assessment 2012

A disease assessment was undertaken to monitor any *S. sclerotiorum* disease. In 2012, there were more visible disease symptoms in the inoculated field sites compared with the 2011 field site but nationally it was not a bad *S. sclerotiorum* year probably as a result of the heavy rainfall during apothecia development. This would probably prevent ascospores travelling as far and prevent any colonised petal tissue from sticking on leaf tissue to induce disease.

In 2012, two weeks after the last date of burkard spore trap sampling, disease symptoms were clearly visible in oilseed rape directly by the sclerotia burial sites as well as further away (**Figure 45**). Sclerotia could be seen developing in the stems of some infected plants (

Figure 42). Approximately 8 infections per m² were observed directly around the burial sites. Disease incidence tailed off to 1 infection per m² approximately 30 m away from the burial sites (Fig). Two weeks after this observation, the visible symptoms observed had doubled (data not shown).



Figure 42: Oilseed rape with *S. sclerotiorum* disease symptoms.

Visible symptoms of *S. sclerotiorum* infection on the stems of oilseed rape. Stems appear white and on some stems, sclerotia are visible.

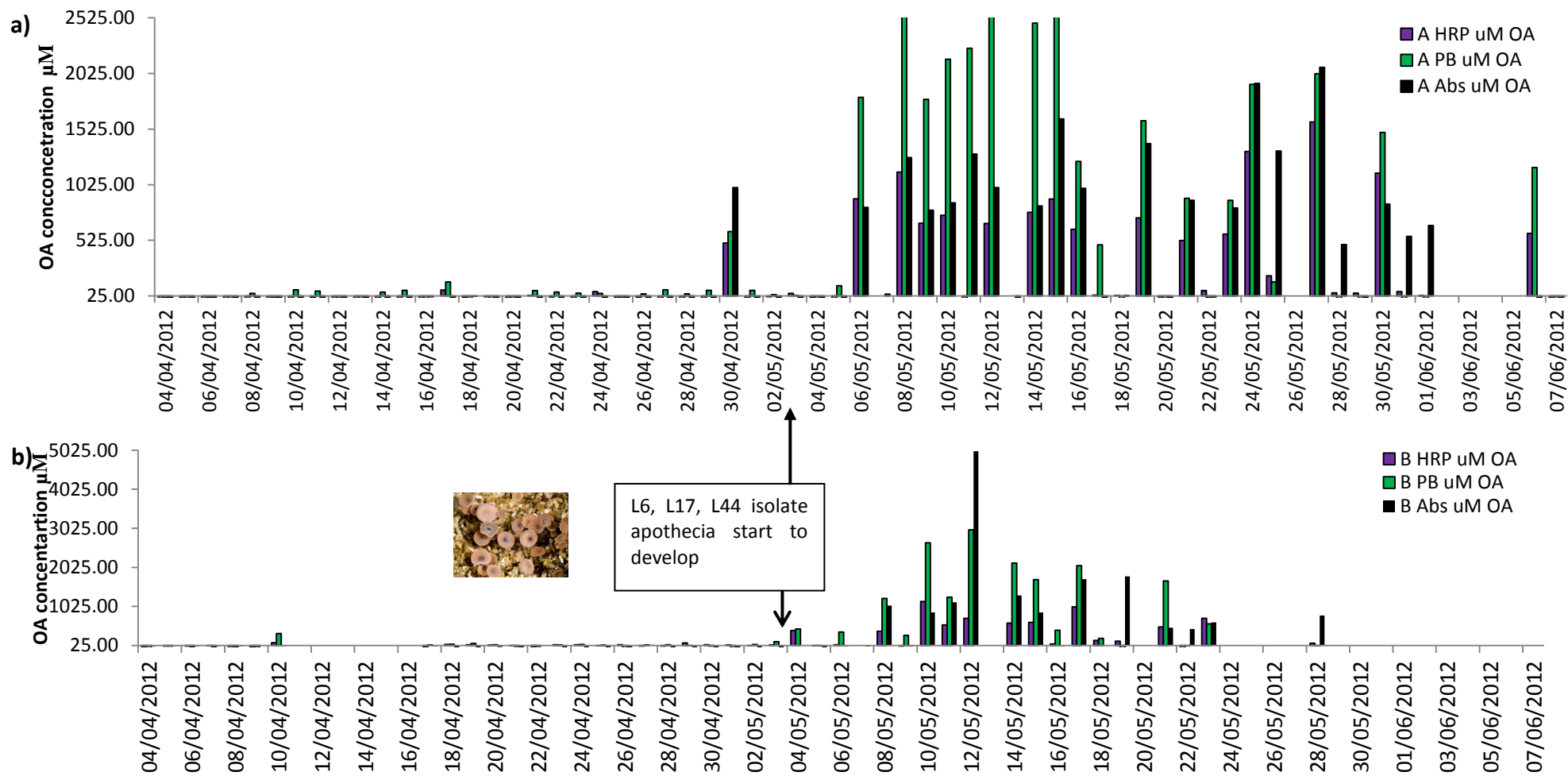


Figure 43: Field trial 2012 field results.

The OA concentrations measured by spectrophotometer OxOx assay (Abs) and both HRP and PB electrode types for both SVI samplers, A (a) and B (b). Initial apothecia were observed on the 18 April, with all isolates forming apothecia by the 3 May.

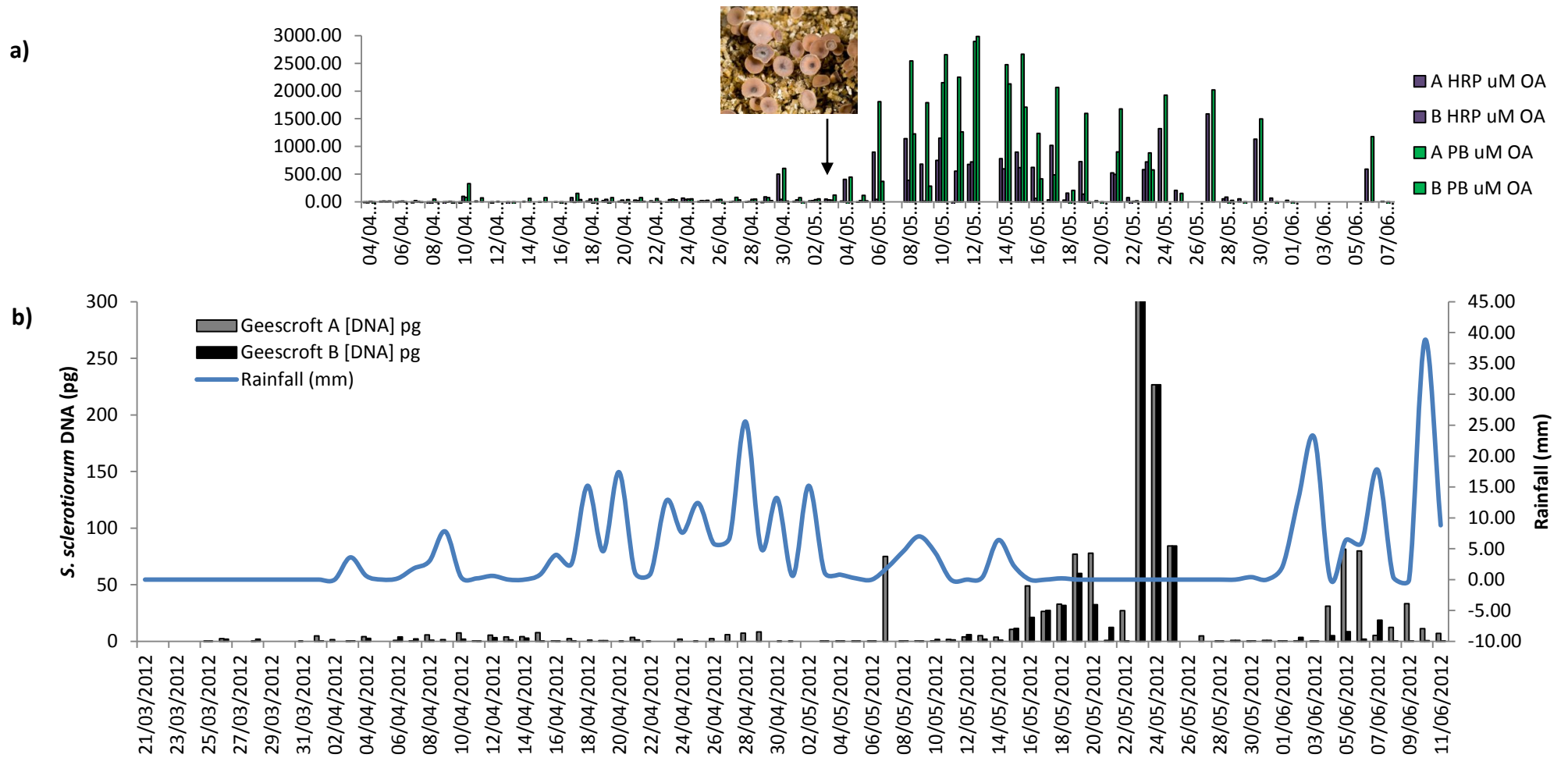


Figure 44: Field trial result 2012.

a) The OA concentrations measured by both HRP and PB electrodes for both SVI samplers. b) The daily *S. sclerotiorum* DNA sampled by the Burkard 7 day traps, A and B. The daily rainfall was measured with a weather station.

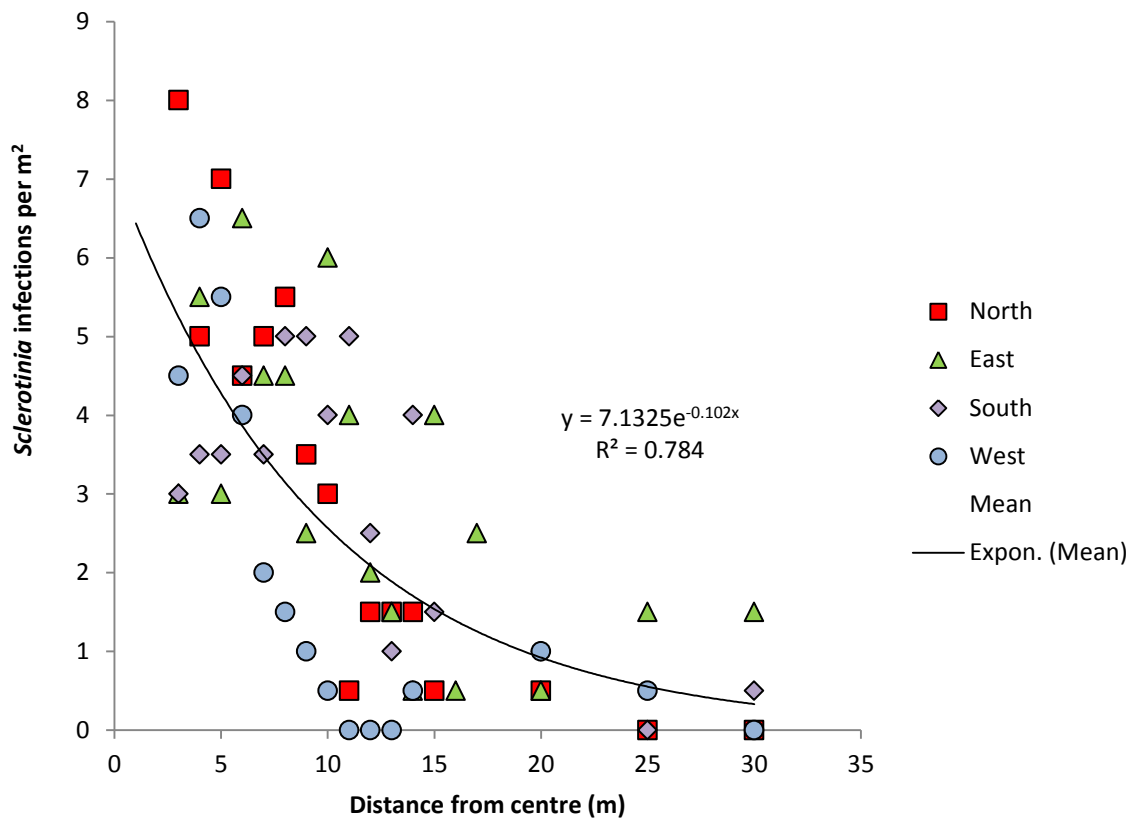


Figure 45: Disease assessment.

Disease was assessed by looking *S. sclerotiorum* infection on all stems within a 1m² area along 30 m transect in a north, south, east and westwards from the sclerotia burial sites in the RRes Geescroft oilseed rape field.

4.3.2.5 Rooftop sampling for both field trials.

For both field trials, a Burkard 7 day sampler was placed on the roof of a 3 storey building (8 m height), approximately 1-2 km from the field testing sites. The positioning of these samplers on a rooftop allowed the assessment of how much *S. sclerotiorum* DNA could be detected at a larger distance from the site of ascospore inoculum. Overall, as expected, the roof top sampler detected a much lower amount of DNA on the roof compared with the samplers at the field sites (**Figure 46**). In 2011, the rooftop sampler shows a similar pattern of DNA detection as the field site but diluted by about 1/20th. In 2012, the rooftop sampler, detected DNA in a similar pattern and also diluted by about 1/20th, however the largest peak of DNA detect in the field, was not really detected on the rooftop. There was reduced DNA levels in 2012 in both the field and on the roof primarily because of the wet summer which probably kept the ascospores from moving as far as they would have done.

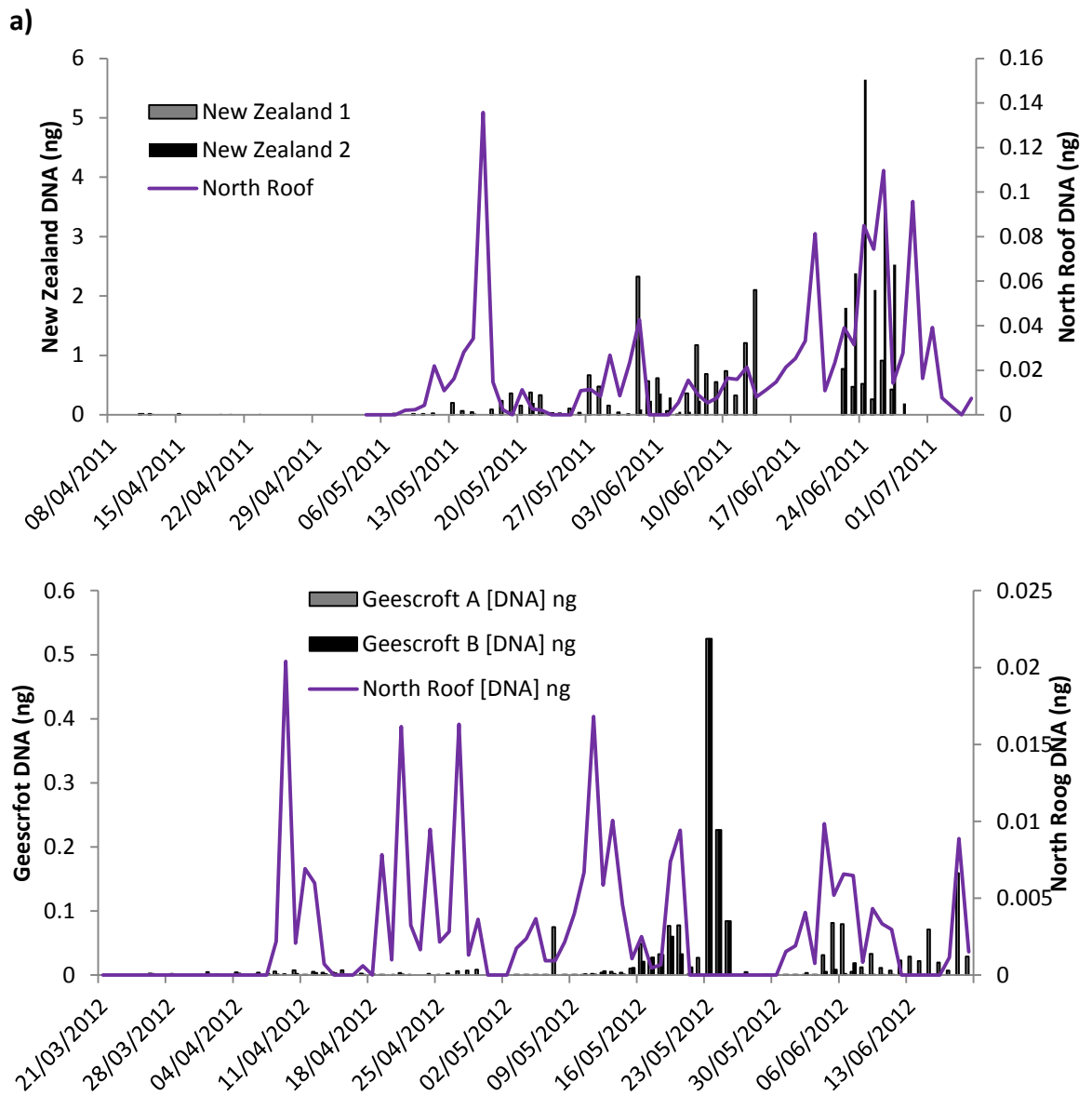



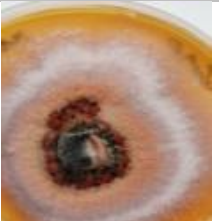






Figure 46: Rooftop *S. sclerotiorum* detection.

a) Comparison of the quantity of *S. sclerotiorum* DNA detected in the RRes New Zealand Fields by both A and B Burkard samplers and the DNA detected on the roof in 2011. b) Comparison of the quantity of *S. sclerotiorum* DNA detected in the RRes Geescroft fields, with both Burkard A and B and the DNA detected with the Burkard sampler on the roof in 2012. 0.1 pg DNA corresponds to 1 ascospore.








4.3.2.6 Isolation of other fungal species present within the field samples

During both field trials, the fungal biomass which had grown in the cyclone Eppendorfs incubated with liquid media was cultured on PDA plates to isolate other species that may be growing alongside *S. sclerotiorum*. After several rounds of sub-culturing, a range of pure fungal cultures containing 1 species were isolated. The DNA from the culture was extracted and a second plate of the same culture was sent to the fungal taxonomist Dr. Hanna Kwasna, Department of Forest Pathology, University of Life Sciences in Poznań, Poland for identification. The DNA from the ITS4/5 region was amplified and sent for sequencing. The identification by Dr. Kwasna and the identification of the ITS region was similar but it was difficult to define species level with the IT analysis (Table 16). Some of the fungi isolated included *Trichoderma*, *Epicoccum*, *Alternaria* which are all common genera and have all been used as biocontrol agents against other plant pathogens. The only isolated fungus capable of secreting OA was *B. cinerea*. *Rhizopus spp* was also identified on some plates but this was not cultured due to the ease of it contaminating other plates.

Table 16: The different fungal species isolated from the cyclone field samples incubated with medium. Cultures were identified by sequencing the ITS4/5 region of extracted DNA for each species and sending plates to Dr. Kwasna for identification at the University of Poland.

Taxon	Lifestyle	Photograph	Taxon	Lifestyle	Photograph
<i>Trichoderma fasciculatum</i>	Resides in soil and woody material. Biocontrol agent of many plant soil pathogens.		<i>Epicoccum nigrum</i>	Saprophytic ascomycete potential biocontrol agent.	
<i>Aureobasidium pullulans</i>	Yeast-like fungus. Epiphyte occurring in many environments.		<i>Myceliophthora thermophila</i>	Thermophilic phaeoid fungus found in soils.	
<i>Botrytis cinerea</i>	Ubiquitous broad spectrum necrotroph found, infects most fruits.		<i>Trichoderma sp</i>	Potential biocontrol agent.	
<i>Sclerotinia sclerotiorum</i>	Appearance is very close to <i>B.cinerea</i> however there are no asexual spores (conidia) in <i>S. sclerotiorum</i> cultures.		<i>Trichoderma fasciculatum</i> Bissett	Potential biocontrol agent.	

Continuation of Table

Taxon	Lifestyle	Photograph	Taxon	Lifestyle	Photograph
<i>Penicillium brevicompactum</i>	Ubiquitous ascomycete saprophyte.		<i>Phoma glomerata</i>	Plant pathogen.	
<i>Humicola grisea</i>	Found in soils and plant material.		<i>Alternaria sp</i>	One of the most abundant plant necrotrophs found in the field.	
<i>Fusarium sp</i>	Plant Pathogen of wheat (previous crop in field was wheat).		<i>Myceliophthora thermophila</i>	Thermophilic phaeoid fungus found in soils.	
<i>Geotrichum candidum</i>	Plant pathogen causing rot on various fruits and is used in cheese making.				

4.4 Discussion

4.4.1 Summary of field trials

2011	2012
OxOx spectrophotometer assay	OxOx spectrophotometer assay Electrochemical assay
Manual sample collection	Manual sample collection
9 positive oxalic acid events	20 positive oxalic acid events detected by all spectrophotometer and electrochemical assays
Oxalic acid event at day 7 incubation	Oxalic acid event day 4 incubation
Very dry	Mix of wet and dry
Late apothecia development and required artificial watering	Apothecia during flowering
No disease	Disease symptoms

The field trial results for 2011 and 2012 show a clear progression and improvement in the choice of medium for the induction of OA secretion by *S. sclerotiorum* ascospores sampled within oilseed rape fields. In 2012, not only were the weather conditions conducive for disease progression in the oilseed rape fields, but the improved medium used to incubate the field samples demonstrated an improvement in OA detection after a significantly reduced incubation period. The rainfall data also demonstrated the importance in frequent rain showers and short drier periods for apothecia formation and maintenance as well as continued ascospore release. It is not enough just to detect the arrival of ascospores within the field, but it is essential that this information is combined with the collected climatic data so that an accurate risk of disease can be made.

4.4.2 Fungal contaminants

There were concerns that the contaminating species isolated in the 2011 field samples had outcompeted *S. sclerotiorum* ascospore growth and reduced the amount of OA positive events. There were further concerns that *B. cinerea* which is ubiquitous in most environments may generate false positive OA signals. It was considered that this could again be a problem in

the 2012 field trial. *B.cinerea* and competing species such as *Trichoderma spp*, *Epicoccum spp* and *Alternaria spp* were isolated again in the 2012 field trial samples, however it is assumed that these other fungal species did not cause significant problems as there was an increase in OA positive detection events which coincided with the development of *S. sclerotiorum* apothecia. If *B. cinerea* had caused false OA events then there would have been higher amounts of OA observed before the development of the apothecia in the field. Instead most of the positive detection events are after the majority of apothecia were developed and during a drier period after rain showers which is the perfect climatic conditions for ascospores release. These data suggests that the ascospores were not outcompeted by other fungi, as there was good correlation between the detection of *S. sclerotiorum* DNA (96%) and high levels of OA detected on the same days as well as the higher peaks of DNA been detected after the formation of most apothecia. It is still curious that there were low levels of *S. sclerotiorum* DNA being detected before the visual observation of the apothecia. This could be accounted for by the sampling of ascospores from further afield, however this was not picked up by our OA detection assay. One possibility for this result is that it is only on the sampling of larger gusts of ascospores is there capture of ascospores. A second result is that there needs to be a threshold for the DNA/ spore number before it is considered a positive DNA detection event. However previous work in the lab (Chapter 3) has revealed that as low as 10 ascospores can generate measureable levels of OA after incubation for 4 days in the medium. It is very difficult to determine the abundance of the other fungal species within the liquid samples without carrying out an optimised qPCR for each of the species isolated in the field samples. This makes it difficult to speculate the extent these other species may pose a risk to *S. sclerotiorum* growth. The isolation was carried out on PDA plates which is a different environment to liquid and so may have encouraged the growth of species that may have grown differently in a liquid environment. This may also have skewed the representation of which species pose a risk within the growth medium. The amount of *Trichoderma* spores, for example, being sampled into the biosensor compared to a potential disease causing gust of *S. sclerotiorum* ascospores would most likely be relatively low. Therefore if there is likely to be any disease caused by the *S. sclerotiorum* ascospores then it could be proposed that there would be many viable ascospores being sampled into the medium which would outcompete other fungi. To ensure that there are no false positive OA detection events, further work

should be carried out to address the use of fungicides to inhibit *B. cinerea* growth rather than the other fungal species which could differ from field to field.

4.4.3 The use of an electrochemical biosensor to detect OA

The electrochemical detection assay proved to detect the presence of OA successfully. On 22 days during the field trial, both the electrochemical and spectrophotometer tested positive for OA. All of these coinciding detection events were after the development of apothecia. The low levels of OA detection by predominately the Prussian blue electrode before apothecia formation is thought to be simply background noise. It is therefore important to determine the background level noise for each assay. Based on the 2012 field trial data, it was decided that the HRP electrodes would be selected for the 2013 field trials as most of the optimisation work was done with this type of electrode and there were more positive events detected with this electrode. From the result it was also decided to set a threshold for OA detection for the HRP electrode as well as setting a range of low, medium and high values which corresponds to different amounts of OA so that the levels of OA being detected during future field trials could be semi quantitative. It was determined in Chapter 3 that OA cannot be correlated with spore number, however it would still be useful to have some quantification of OA levels being detected in future field trials in order to adjust detection sensitivity. Further investigation is required to determine whether we can get this semi-quantitative measurement to work with the wireless signalling. The following current thresholds have been set for future OA detection upon by the electrochemist Dr. Sophie Weiss:

Detection level of OA	Amp reading	OA amount from 2012 field trials
Negative	readings less than -1.5×10^{-6} Amps	
Low	readings greater than -1.5×10^{-6} Amps	corresponds to roughly to 700uM oxalic acid . Roughly 50% of positive field trial samples ranged from 550uM-750uM oxalic acid)
Medium	readings greater than -5.75×10^{-6} Amps	700- 1400 μ M
High	Readings approx -1.48×10^{-5} Amps	1500 μ M (the highest HRP value we recorded)

4.4.4 Positioning of sampling equipment

The field results for all sampling devices highlight that samplers a maximum of 2 m apart may not yield the same results even though there were hundreds of apothecia releasing ascospores only a couple of meters from the equipment. This was evident for the 2012 SVI pots, which had fewer OA positive events from sampler pot B than A. This was the same for 2011, for the cyclone samplers, as a Positive OA event in tube A did not necessarily mean there was a positive OA detection in tube B for the same day. This highlights the need for multiple nodes in one area. All samplers had wind veils to turn the sampling head into the wind, however there may have been one part of the inoculated ring releasing ascospores and not another part of the site.

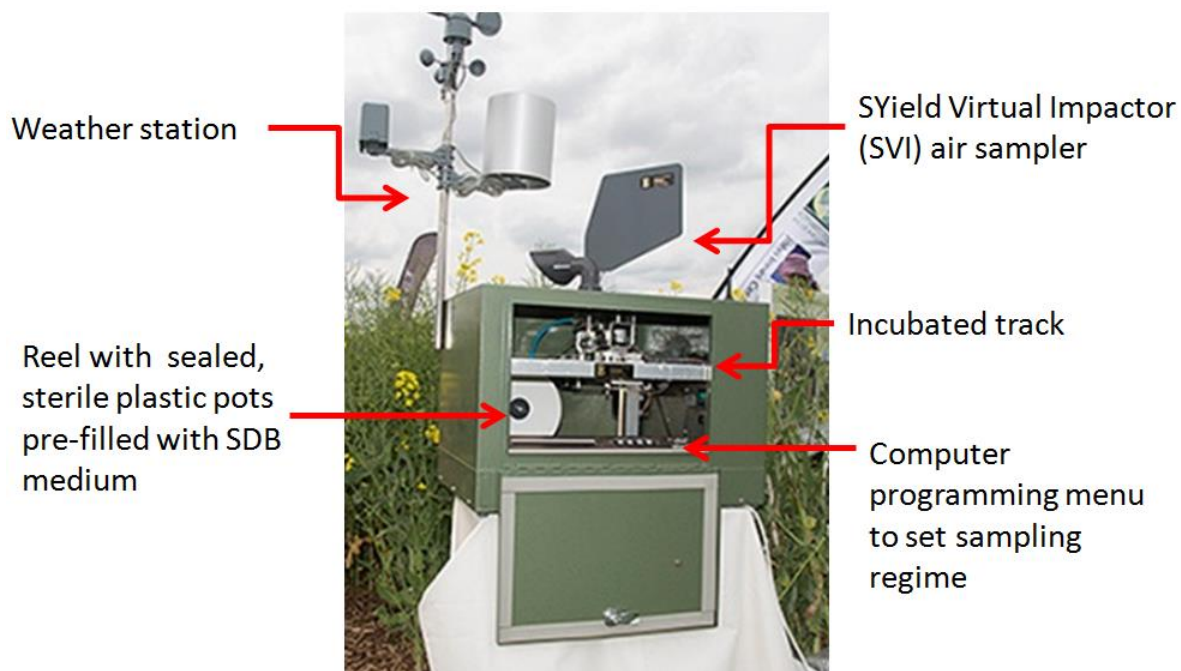
The DNA results obtained from the Burkard 7 day sampler placed on the rooftop, highlight that DNA can still be detected at a height but at much lower levels. Unlike the Burkard 7 day traps placed in the field by the buried sclerotia, DNA for *S.sclerotiorum* was also detected in small amounts on the roof before the apothecia were observed in the field. In particular , it is thought that although air sampled on a rooftop is more diluted from local sources, it is also more well-mixed and therefore comprises spore production from many fields upwind in the local region. Therefore the rooftop sample may be a more robust indication of spore presence at a regional scale. This highlights that the rooftop sampler may be capturing air samples containing ascospores from natural inoculum sources further afield. The smaller amounts of DNA may still be detectable using the growth medium and OA detection as even just 10 spores would produce detectable amount of OA and because 0.1 pg DNA corresponds to 1 ascospore, there are still tens of spores beings detected at this height. Combining biosensors on the roof as well as in the field may give a good overview of *S. sclerotiorum* ascospore on a large scale. This requires further testing.

4.4.5 Equipment failures

A serious setback for the field trials was the incidence of mechanical failures which occurred for most of the sampling equipment at some point during sampling. Although the samplers were set up in pairs during both field trials, mechanical failures would prevent some samples being collected on a certain day. This makes it difficult to analyse the data, however this is something which cannot be rectified however having more than two of the same samplers in one site sight may be an option in the future.

4.4.6 Future of SYield

Since the field trials in 2012, the SYield consortium has developed an automated infield sampling unit which is capable of measuring OA from *S. sclerotiorum* airborne ascospores. The unit which was predominantly built by Burkard and combines the SVI air sampling device, sealed, medium-prefilled pots and the electrochemical OA detection biosensor in one box which can be left in the field and requires no manhandling (**Figure 47**). The device works by sampling air in the field with the SVI sampler. Air is sampled directly into pots which are pre-filled with 400 µl SDB medium which is described in Chapter 3. After 12 hours of air being sampled into the pot, the pot is then moved along an incubation track for 4 days which is heated at 20 °C. At the end of incubation, the pot is punctured and the liquid contents drain over an electrode which has the OxOx and HRP enzymes stabilised onto the surface. The potentiostat in the unit is connected to the electrode as well as a central processing unit. Upon making a measurement, a signal is then relayed wirelessly to a mobile phone. The signal will either read negative if there was no OA detected, or have low to high readings if OA was detected. The unit can hold up to 60 pots, which will allow a daily sample to be made for 60 days which will cover the flowering stage of most oilseed rape crops. From 15 May to 17 June 2013, the automated unit was tested within *S. sclerotiorum* artificially inoculated oilseed rape fields at Rothamsted as well as on the rooftop. After a series of mechanical problems, the units were able to work without interference and did detect the presence of OA and send these messages directly back to the user. Hourly met data was also sent by the same mobile phone signal. The DNA data collected in Burkard 7 day samplers alongside these biosensors are still being analysed.



12-13th June 2013
Boothby Graffoe, Nr Lincoln, Lincs



Figure 47: The 2013 automated SYield device.

a) The components of the SYield detection device. b) SYield exhibiting at Cereals 2014.

The biosensor was exhibited at Cereals 2013 (**Figure 47**), the largest Arable cereal exhibition event in Europe and was received positively by the farming community however there are many challenges that this sampling device needs to overcome before it will be utilised as an accurate farming tool. Firstly the incidence of oxalic acid detected by the biosensor still needs to be linked to disease risk. The amount of OA detected cannot be linked to the number of spores sampled into the device. So there is no way of knowing if the OA measured is a result of a single spore or thousands of spores. This is mainly because by day 4 of incubation, the ascospores will have germinated and formed a multi cellular colony of significant biomass as was shown in Chapter 3. It has been discussed that if there are multiple positive detection events from multiple nodes and on a few days consecutively then that could be a good disease risk indicator. Although as mentioned previously the success of *S. sclerotiorum* disease incidence relies on optimal weather conditions which include periods of rainy showers and dry periods to allow spore release and dispersal. Another important factor is whether petals colonised with ascospores will actually fall and stick onto healthier plant tissue to allow the disease to spread to the rest of the plant. The ability to measure this factor automatically is very difficult but is an important part of the disease epidemiology due to complete disease escape if infected petals do not stick. Therefore this is a multifactor disease and an accurate disease risk model does not just rely on the detection of OA but needs to incorporate all these levels. Finally it is crucial that more field trials are carried out with this equipment to determine the correct height to locate the unit nodes as well as how many nodes are required in an area for accurate detection of ascospores. The rooftop DNA data suggests that nodes placed at considerable height with track incoming spores from a larger distance, however this will require further testing.

Chapter 5: Predicting the secretome of *Sclerotinia sclerotiorum* to identify novel detection targets and candidate genes that play a role during infection.

5.1 Introduction

Commercially available fungal pathogen diagnostic systems are based primarily on the use of antibodies to detect pathogen specific antigens. Other systems use nucleic acid detection targets for example in qPCR based diagnostic methods. The SYield biosensor described in Chapters 3 and 4 is based on the detection of the organic acid, oxalic acid, which is secreted during early *S. sclerotiorum* ascospore germination. However oxalic acid is not completely specific to *S. sclerotiorum*. Other fungi including *B. cinerea* and some wood decaying fungi also secrete oxalic acid (Dutton and Evans 1996). *B. cinerea*, a close relative to *S. sclerotiorum*, is a ubiquitous opportunistic pathogen in the environment. Chapter 3 reported that *B. cinerea* conidia were able to produce significant levels of OA when seeded in the same liquid medium as *S. sclerotiorum*. This could potentially cause false positives within the sensor system which would reduce the effectiveness of the disease risk model.

For future development of a truly species specific *S. sclerotiorum* detection system, this Chapter and Chapter 6 reports the use of a pre-existing bioinformatics pipeline to explore the *S. sclerotiorum* genome to identify the suite of proteins which are secreted extracellularly. This set of genes is defined as a fungal secretome. This set of genes can be explored to identify those unique, putative, secreted proteins which if actually expressed extracellularly during early ascospore germination could potentially be used as novel detection targets in an adapted biosensor system.

Bioinformatics tools allow scientists to explore the genome of a pathogen to identify those sequences which have a specific gene profile and a high probability being translated into a protein which may have effector functionality. Previously published studies (Brown et al. 2012, do Amaral et al. 2012) combine several bioinformatics software to create a pipeline workflow which is able to predict fungal secretomes. Classified effector proteins including the Mg3LysM protein in *M. graminicola* and SNODPROT 1 homologues potentially required for virulence in *Fusarium graminearum* were identified in the recently published secretomes of these pathogens (Brown et al. 2012, do Amaral et al. 2012). In this study, a similar bioinformatics pipeline was used to identify the secretome of *S. sclerotiorum* and compared with the predicted secretome of *B. cinerea* to ensure that the gene targets selected in *S. sclerotiorum* were not present in *B. cinerea*. In addition the publically downloadable

proteomes of 115 other fungi and oomycetes were compared to the *S. sclerotiorum* secretome to ensure the exclusivity of the target.

Not only does this analysis permit the detection of potentially novel targets but additional aspects of *S. sclerotiorum* infection can be investigated. The mechanism of how this pathogen infects such a wide range of plant hosts has been investigated for over 40 years. Central to its pathogenicity strategy is the secretion of oxalic acid during infection (Chapter 1). Although the organic acid oxalic acid is the key player during this infection cycle, several proteins have been identified alongside this metabolite to contribute to pathogenicity. By investigating the arsenal of proteins secreted by this pathogen, a greater understanding of this process may be gained and potential effector candidates may be identified.

This chapter reports the use of a bioinformatics analysis to define and investigate the secretome of the necrotroph *S. sclerotiorum*. The same pipeline was used to look at a close relative of this pathogen, *B. cinerea*, which shares many genomic similarities although their infection strategy slightly differs. A cross species comparison was also undertaken to compare the proteomes with this plant pathogen.

5.2 Experimental Procedures

5.2.1 Bioinformatics

For the first stage of the analysis the total secretome was predicted for the two fungi , *S. sclerotiorum* and *B. cinerea*, by Rothamsted Research bioinformatician John Antoniw with the previously used listed software (Brown et al. 2012, do Amaral et al. 2012). The second stage of analysis was done by myself to define the refined secretome by carefully sorting and interrogating John Antoniw's predictions and then identifying the candidate genes which are unique to both species with no homology in other species. In addition, the interspecies distribution of the genes present within the entire refined secretome defined by John Antoniw in a 115 species comparison was further explored by myself.

Both the *S. sclerotiorum* (WT1980) and *B. cinerea* (B05.10) genomes used in this investigation were downloaded from the Broad Institute. *Sclerotinia sclerotiorum* and *Botrytis cinerea* Sequencing Project, Broad Institute of Harvard and MIT.

(http://www.broadinstitute.org/annotation/genome/sclerotinia_sclerotiorum/MultiHome.html)

(http://www.broadinstitute.org/annotation/genome/botrytis_cinerea/MultiHome.html).

5.2.2 Stage 1: Predicting the total secretome

The first stage of the analysis followed the method described by *Amaral et al* (2012) (do Amaral et al. 2012) which is described here for clarity. An automated pipeline based on the original secretome prediction procedure described by Muller et al (2008) (Mueller et al. 2008) using Bash shell, awk and python scripts on a PC running Red Hat Enterprise Linux 5.2.

Initially all proteins from downloaded genomes with a Target P Loc = S (TargetP v1.1; http://www.cbs.dtu.dk/cgi-bin/nph-sw_request?targetp) or a Signal P D-score = Y (SignalP v3.0; http://www.cbs.dtu.dk/cgi-bin/nph-sw_request?signalp) were combined (Emanuelsson et al. 2007, Emanuelsson et al. 2000) to predict the refined secretome. These were then scanned for transmembrane (TM) spanning regions using TMHMM (TMHMM v2.0; http://www.cbs.dtu.dk/cgi-bin/nph-sw_request?tmhmm) and all proteins with 0 TMs or 1 TM, if located in the predicted N-terminal signal peptide, were retained.

GPI-anchor proteins were predicted by big-PI (http://mendel.imp.ac.at/gpi/cgi-bin/gpi_pred_fungi.cgi) (Eisenhaber et al. 2004). ProtComp was also used to predict localisation of the remaining proteins using the LocDB and PotLocDB databases (ProtComp v8.0; <http://www.softberry.com>).

WoLF PSORT analysis was done using “runWolfPsortSummaryfungi” in the WoLF PSORT v0.2 package, which estimates where proteins are located after secretion with a sensitivity and specificity of approximately 70% (Horton et al. 2007).

PFAM analysis was done using the PFAM database (<ftp://ftp.ncbi.nih.gov/pub/mmdb/cdd/>) and the rpsblast program in the NCBI blast+ software package (<ftp://ftp.ncbi.nlm.nih.gov/blast/executables/blast+/>). <http://pfam.sanger.ac.uk/> was also accessed for direct inspection of protein domains.

The number of cysteine residues within the mature peptide and the search for degenerative YFWxC and RXLR motifs were computed using custom python scripts. The number of internal sequence repeats was found using RADAR (<http://www.ebi.ac.uk/Tools/Radar/>) (Heger and Holm 2000).

The detection of RNA transcripts for the *S. sclerotiorum* genes of interest was explored by BLASTN analysis (e-100) of the 7 designated EST libraries available from the Broad website: (http://www.broadinstitute.org/annotation/genome/sclerotinia_sclerotiorum/MultiDownloads.html).

All nucleotide and amino acid sequences were aligned in Geneious Pro5.5.6 created by Biomatters. Available from <http://www.geneious.com/>. ClustalW and MUSCLE alignments were used for the analysis.

5.2.3 Stage 2: The refined secretome

The second stage analysis generated the refined secretome for both species from which uniquely secreted proteins for both genomes could be identified. A comparison between the refined genomes was made to explore the relatedness and evolution of the two pathogens. Initially only sequences starting with a methionine were selected. Then sequences predicted with an extracellular Wolf-PSORT score of 18 and above were kept in the final secretome dataset. This selection ‘cut-off’ point has been tested using a range of experimentally verified secreted fungal proteins from other pathogens including *F. graminearum* (Brown et al. 2012) and *M. graminicola* (do Amaral et al. 2012). Any mature proteins shorter than 20 amino acids were removed and sequences with 1TM were excluded from the refined set. A comparison between those sequences containing a PFAM domain were analysed and the protein family for each domain identified using <http://pfam.sanger.ac.uk>.

5.2.4 Genes coding for proteins with a known function

Those genes identified in the refined secretome with a PFAM domain were inspected for gene function and grouped into the four CAZY classes; glycoside hydrolases, glycosyl transferases, polysaccharide lyases and carbohydrate esterases listed on the Carbohydrate-Active EnZymes database (CAZy) (<http://www.cazy.org/>) (Cantarel et al. 2009). Enzyme identification was carried out using the Kegg database (<http://www.kegg.jp/>) and Brenda (<http://www.brenda-enzymes.info/>).

5.2.5 *S. sclerotiorum* genome map

A genome map for *S. sclerotiorum* was generated by John Antoniw using the free software, OmniMapFree (<http://www.omnimapfree.org>) (Antoniw et al. 2011). This allowed easy mapping of different gene groups to inspect visually the distribution of genes across the chromosomes. This was not done for *B. cinerea* due to time constraints.

5.2.6 Blast2Go analysis

The refined secretome protein set was analysed using Blast2Go to explore whether any very recent extra gene annotation existed (<http://www.blast2go.com/b2glaunch>)(Conesa et al. 2005). From this tool, the InterPro website was accessed to further explore the IPO entries discovered (<http://www.ebi.ac.uk/interpro/>) (Hunter et al. 2012, Quevillon et al. 2005).

5.2.7 EST support

Seven *S. sclerotiorum* EST libraries were downloaded from the Broad Institute online database to explore whether there was also expression data to support the gene models of interest (**Table 17**). The gene models were derived from the following biological materials and culture conditions:

Table 17: Seven EST Libraries downloaded from the Broad

Library name	Material used to make library	cDNA library source	Library size
G781	Developing sclerotia		11.6 MB
G786	Growing mycelia tissue at neutral pH	Jeffrey Rollins, University	12.9 MB
G787	Developing apothecia	of Florida	14.8 MB
G865	Infected <i>Brassica</i> leaf	Dave Edwards , Adrienne	1.0 MB
G866	Infection cushion/ appressoria	Sexton and Barbara Howlett (University of Melbourne in Australia)	306.5 KB
G2118	<i>Sclerotinia</i> tomato leaf infection	(http://www.broadinstitute.org/annotation/genome/sclerotinia_sclerotiorum/MultiDownloads.html)	3.2 MB
G2128	<i>Sclerotinia</i> oxidative stress		3.3 MB

5.2.8 Multispecies Comparison

A multispecies cross comparison was done between the refined secretome of *S.sclerotiorum* and the genomes of 115 proteomes from other fungal, oomycete, plant pathogenic nematode and plant infecting aphid species. The species were chosen based on the diverse range of lifestyles and host ranges. Genomes were downloaded (November 2012) from

the Broad, JGI and other websites which are used primarily by the research community for the species in question (Appendix 5). Conservation, absence or expansion of the homologous genes from the total secretome for *S. sclerotiorum* and *B. cinerea* were found in the other species using BLASTP analysis. The levels of confidence used were $p < e^{-5}$ or $p < e^{-100}$. The multispecies cross comparison allowed the identification of unique proteins in both species that were not found in any other species. These genes were then inspected for a cysteine number greater than 5, a Wolf P-SORT score of 18 or greater and no PFAM or other annotation.

5.3 Results

5.3.1 The predicted secretomes of *S. sclerotiorum* and *B. cinerea*

The first stage of the analysis combined SignalP and TargetP softwares to predict first the total unrefined secretome for both pathogens (**Figure 48a, Figure 49a**). All the possible secreted proteins with signal peptides were included in stage 1 of the secretome analysis (1,430 *S. sclerotiorum* seqs (9.8% of total genome), 1,640 *B. cinerea* seqs (9.9% of total genome sequences). Within this set, 75 of the *S. sclerotiorum* and 82 *B. cinerea* proteins were predicted to contain GPI anchors. The remaining mature proteins which contained one or more transmembrane domains (TM) were removed. Only proteins with a TM in the signal peptide sequence or just beyond it were kept for further analysis. A ProtComp analysis screened those proteins which are predicted not to be located in the extracellular space, these sequences were removed. This predicted a total secretome size of 1,060 proteins for *S. sclerotiorum* (7.3% of total genome) and a total secretome size of 1,262 proteins for *B. cinerea* (7.7% of total genome). The sequences containing GPI anchors are included in these figures.

The second stage of the analysis identified the ‘refined secretome’ for both species which were selected using more rigorous prediction tools (**Figure 48b, Figure 49b**). These sets included only those sequences which started with a methionine. All *S. sclerotiorum* 1,060 sequences were retained whereas 3 sequences were removed from the *B. cinerea* sequence set (BC1G_16273, BC1G_16321, BC1G_16430). Wolf-PSORT software was then used to predict the eventual location of this subset of proteins. This stringent search selects only those proteins with a score of ‘extr 18’ or greater which are predicted to be truly secreted extracellularly. This identified 472 sequences and 565 sequences had a predicted value of ‘extr 18’ or greater for *S. sclerotiorum* and *B. cinerea*, respectively. Any mature proteins shorter

than 20 amino acids with a Wolf-PSORT score 18 or greater were removed from the set (BC1G_15835 and SS1G_08160). The remaining sequences with TM=0 were included in the final sequence set (432 *S. sclerotiorum* seqs, 499 *B. cinerea* seqs). These final sets of sequences were defined as the refined secretomes. Out of 14 522 proteins predicted within the *S. sclerotiorum* genome, 3% of the proteome is predicted to be truly secreted. The *B. cinerea* refined secretome comprises 3.03% of the entire predicted proteome.

The original secretome pipeline was carried out a few months in advance of the full multispecies secretome analysis. For completeness, the set of refined secretome *S. sclerotiorum* genes was analysed using Blast2Go to retrieve updated annotations for the *S. sclerotiorum* predicted proteins ($e < 10^{-5}$). The Blast2Go search analysis revealed 310 protein sequences (72%) that have some form of annotation, including an InterPro (IPO) entry, Gene3D, SUPERFAMILY or PFAM entry. 122 sequences had no recognised InterPro entry (no IPS) or PFAM domain. The 122 sequences will be classified as the unannotated refined secretome. As a comparison, the *B. cinerea* refined secretome contains secretome 328 sequences with some form of functional annotation, i.e. PFAM, CDD domain. The other remaining 171 proteins had no functional annotation assigned. These unannotated sequences are predicted to be hypothetically secreted proteins that have not previously been analysed for gene function.

5.3.2 Distribution of the genes coding for the refined secretome across the *S. sclerotiorum* genome

The *S. sclerotiorum* genome contains 16 linkage groups which correspond to an estimated 16 chromosomes ([Amselem et al. 2011](#)). Also available for bioinformatics analysis is an estimated 17th ‘waste bin’ chromosome containing the concatenated unmapped sequences. The distribution of the refined secretome genes, unannotated genes, gene families and all other *S. sclerotiorum* gene groups investigated during this analysis, were mapped across the 16 chromosomes and 17th pseudochromosome using the OmniMapFree software (Table 18, Figure 50). The refined secretome showed no obvious spatial pattern of distribution. The genes appear to be evenly spaced across all chromosomes. There was a single gene found within the unmapped ‘wastebin’ chromosome, SS1G_14515, a unique hypothetical protein consisting of 494 nucleotide base pairs with no functional annotation. Most chromosomes have a very similar refined secretome gene density in the range 10.66 to 13.76 secreted genes per MB (Table 18). The overall density on chromosome 8 and 9 appeared to be slightly lower than on the other chromosomes, while chromosome 12 had the lowest observed density.

Figure 1A

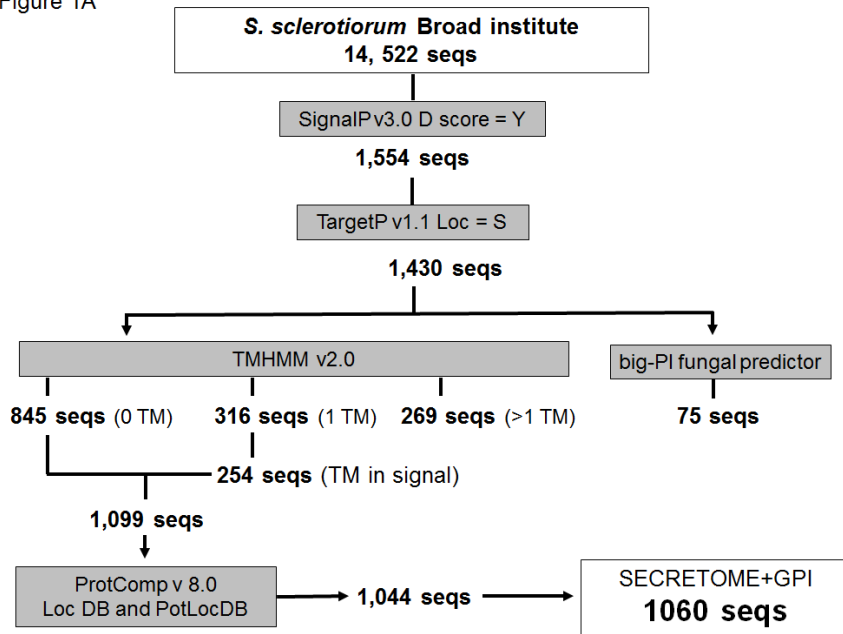


Figure 1B

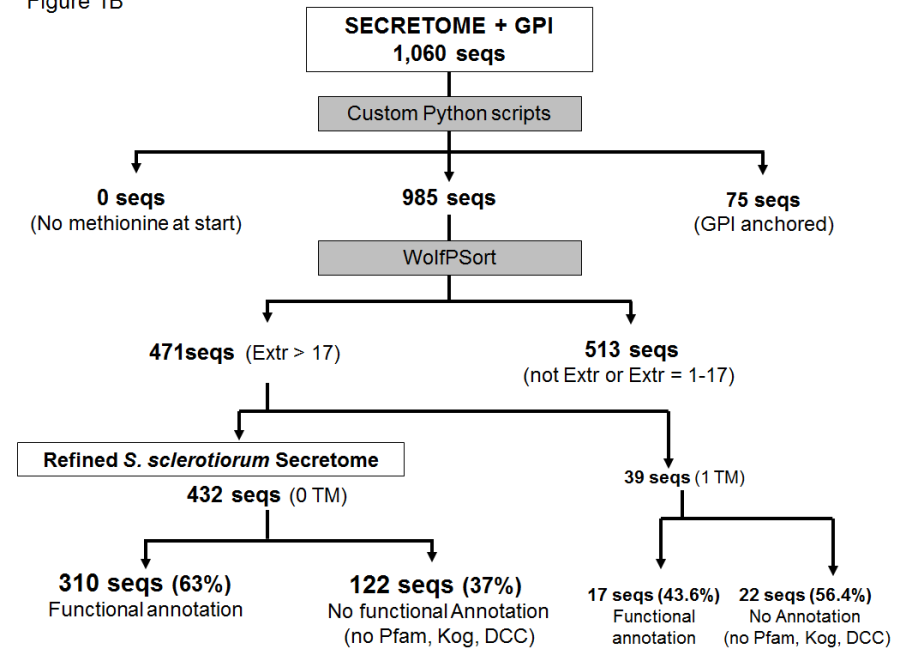


Figure 48: *S. sclerotiorum* secretome pipeline.

The bioinformatics pipeline used to predict the total secretome (A) and the refined secretome (B) of *S. sclerotiorum*.

Figure 2A

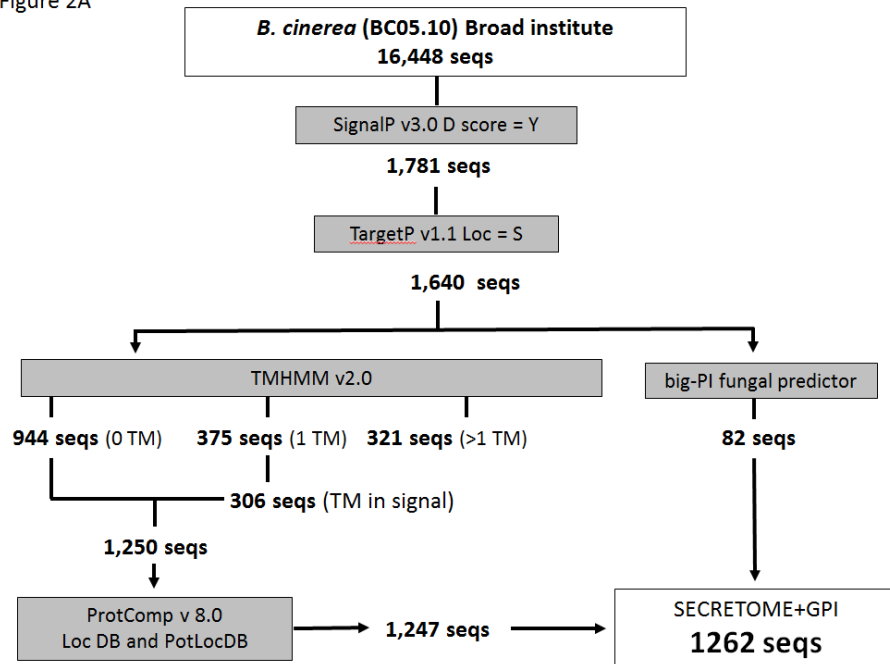


Figure 2B

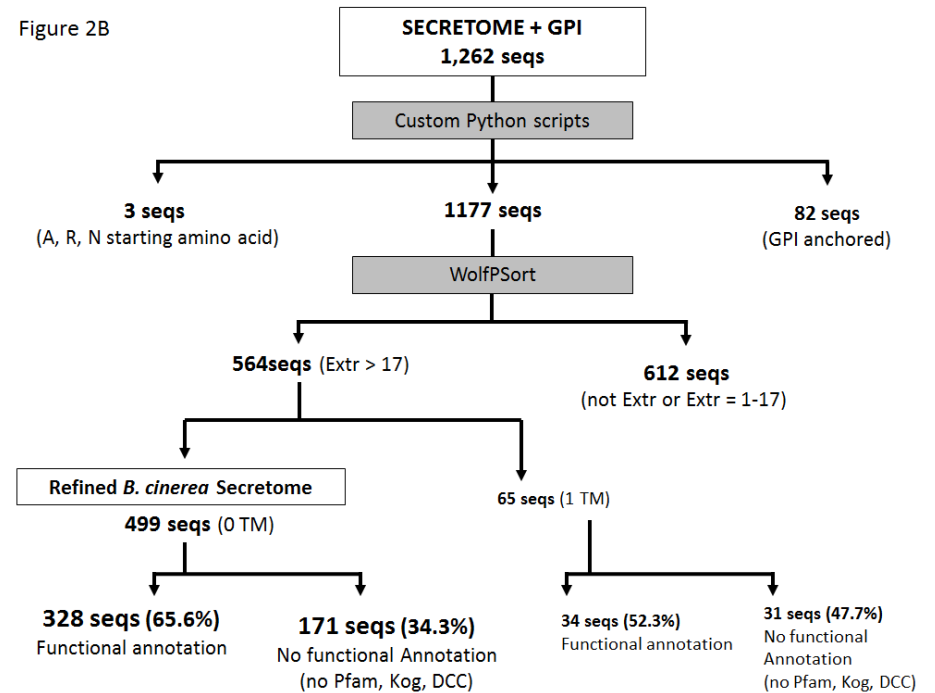


Figure 49: *B. cinerea* secretome pipeline.

The bioinformatics pipeline used to predict the total secretome (A) and the refined secretome (B) of *B. cinerea*.

There is a larger number of *S. sclerotiorum* unique genes coding for secreted proteins on chromosome 2 however there is no clustering of these four genes as they are evenly distributed across the chromosome

The refined secretome gene distribution pattern was inspected more closely to identify small gene clusters where two or more sequences were located directly next to each other or within a three gene proximity. In the Basidiomycete maize infecting pathogen *Ustilago maydis* and in the Ascomycete cereal infecting pathogen *Fusarium graminearum* small gene clusters coding for secreted proteins have previously been reported (Mueller et al. 2008, Brown et al. 2012). When entire clusters were deleted in *U. maydis*, virulence was affected in five cases indicating the importance of identifying small secreted proteins to understand fungal pathogenesis (Mueller et al. 2008). In total, 31 small gene clusters were identified across the genome map (**Figure 5, Table 19**). Most of these predicted proteins were also of a considerable size > 200 amino acids. Interestingly, five clusters were located in close proximity to the ends of the chromosomes (clusters 003, 025, 028, 030 and 031) and a further two were located in the sub-telomeric regions (008 and 015).

The nucleotide sequences making up these 31 clusters were aligned to determine whether the genes were related or duplicated. Nucleotide sequences were aligned using ClustalW alignments in Geneious. None of the nucleotide alignments shared more than 45% identity indicating that the clusters did not consist of duplicated genes. Common PFAM domains were found in two gene clusters. SS1G_12499 and SS1G_12500 in cluster 017 both contain a serine carboxypeptidase domain (PF00450) which indicates these proteins are involved in cleaving peptide bonds. SS1G_00891 and SS1G_00892 both have endoglucanase annotation. Both proteins are part of glycoside hydrolase families and contain the same carbohydrate binding module (PF00734). Both have EST support in the tomato infection library suggesting they may be co-ordinately regulated under these infection conditions. Six other gene clusters had EST support in the same libraries suggesting that under the same environmental conditions and / or during a specific physiological process, gene expression is upregulated simultaneously for all these genes. The predicted genes SS1G_01426 and SS1G_01428 in gene cluster 002 had very strong EST support in the developing apothecia library (G787) associating these proteins with this reproductive process. No *S. sclerotiorum* unique secreted proteins were found in the 31 clusters.

Table 18: Distribution of secreted proteins across the 16 chromosomes of *S. sclerotiorum*.

Chromosome	Size (nt)	Proteins			Secreted proteins per Mb	Annotation of proteins		Unique to <i>S.sclerotiorum</i>
		Predicted genes	Gene density per MB	Secreted proteins		Yes	No	
1	3964102	1479	373.1	44	11.10	27	17	1
2	3702977	1365	368.6	42	11.34	30	12	4
3	3347368	1278	381.8	40	11.95	33	7	0
4	2886255	1077	373.1	32	11.09	20	10	0
5	2826797	1040	367.9	30	10.61	23	7	0
6	2472283	908	367.3	25	10.11	17	10	1
7	2321737	876	377.3	27	11.63	20	7	0
8	2121402	800	377.1	20	9.43*	15	5	1
9	2098208	780	371.7	20	9.53*	15	5	1
10	2058163	773	375.6	24	11.66	17	6	0
11	1876643	696	370.9	20	10.66	14	6	1
12	1840947	684	371.5	14	7.60*	8	6	0
13	1812400	668	368.6	22	12.14	14	8	1
14	1774723	649	365.7	24	13.52	14	6	0
15	1431160	549	383.6	14	9.78	15	4	0
16	2398866	892	371.8	33	13.76	28	5	0
17**	54754	8	146.1	1	18.26*	0	1	1
Total	38988785	14522	373.1	432		310	122	11

* Denotes those chromosomes which have above or below average number of secreted proteins per Mb.

** 17 chromosome is a pseudochromosome

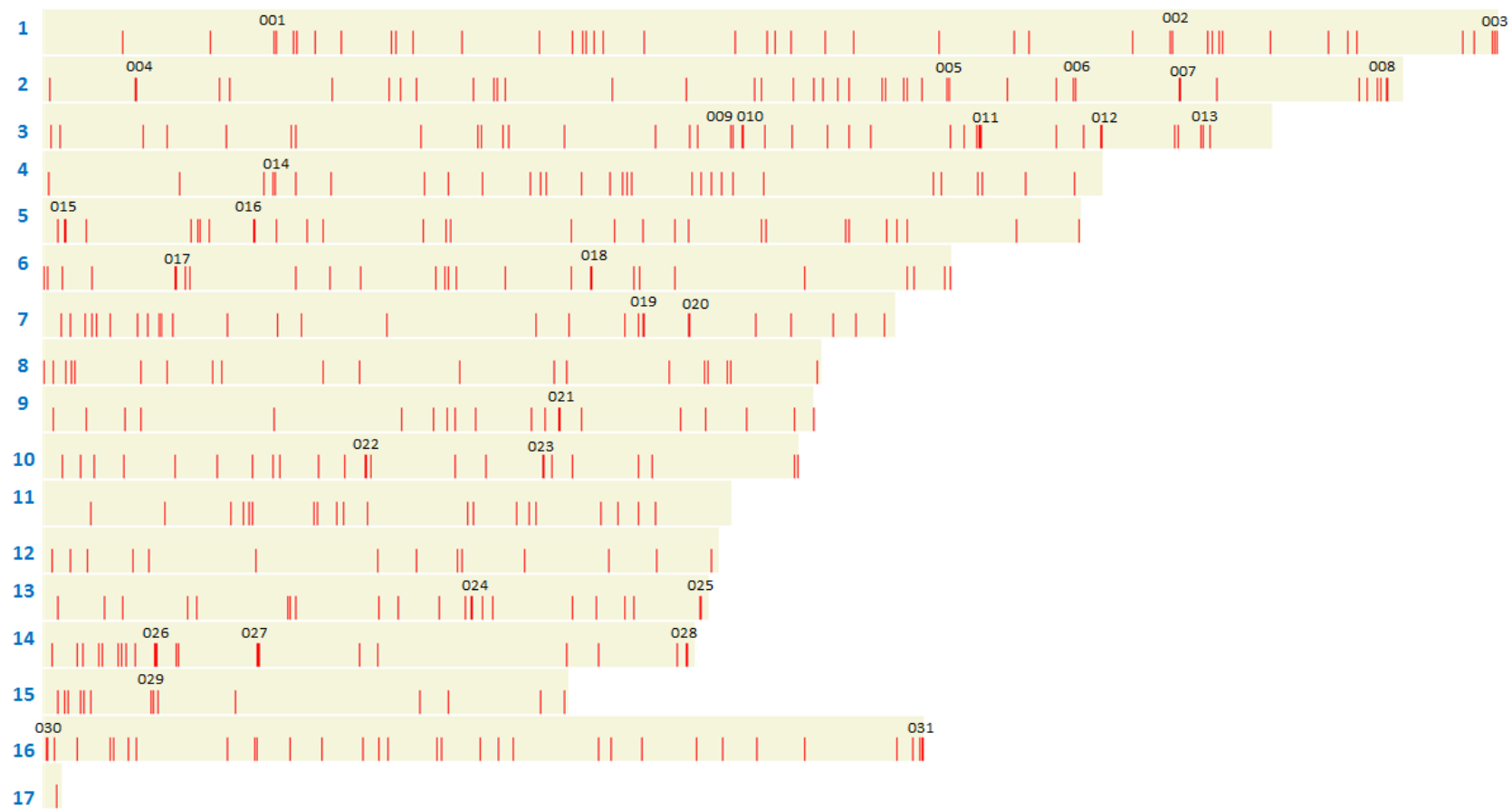


Figure 50: The *S. sclerotiorum* refined secretome distribution across the 16 mapped chromosomes. Numbers correspond to the 31 gene clusters investigated for duplications and relatedness.

Table 19: Description of the 31 gene clusters distribution across the *S.sclerotiorum* refined secretome.

Cluster	Genes	Description from Blast2Go	from	Cluster	Genes	Description from Blast2Go	Cluster	Genes	Description from Blast2Go	from
1	SS1G_09841	PP		11	SS1G_00772	HP similar to LysM domain-containing protein	22	SS1G_07656	GHF 61 protein	
1	SS1G_09844	PP		11	SS1G_00773	ankyrin repeat domain-containing protein 44	23	SS1G_07836	acidic protease	
2	SS1G_01426	PP		12	SS1G_00891	endoglucanase III	23	SS1G_07837	PP	
2	SS1G_01428	pan domain protein		12	SS1G_00892	exoglucanase-6A	24	SS1G_08889	glutaminase	
3	SS1G_01081	catalase		13	SS1G_01003	PP	24	SS1G_08892	PP	
3	SS1G_01083	GHF 31 protein		13	SS1G_01005	alpha-glucosidase precursor	24	SS1G_08894	alpha beta-hydrolase	
3	SS1G_01086	PP		14	SS1G_02345	PP	25	SS1G_09129	6-phospho-beta-galactosidase	
4	SS1G_13035	PP		14	SS1G_02347	alpha- -glucanase mutanase	25	SS1G_09130	CHP	
4	SS1G_13036	multicopper oxidase		15	SS1G_12057	polygalacturonase 1 precursor	26	SS1G_09248	hydrophobin	
5	SS1G_04662	alpha-galactosidase A precursor		15	SS1G_12059	HP similar to endoglucanase B	26	SS1G_09250	iron-sulfur cluster-binding rieske family domain protein	
5	SS1G_04664	cell surface spherulin 4-like protein		16	SS1G_12262	allergen Asp f 4 precursor	26	SS1G_09251	HP similar to endoglucanase II	
6	SS1G_04786	CHP		16	SS1G_12263	carboxypeptidase	27	SS1G_09363	-	
6	SS1G_04790	acid phosphatase		17	SS1G_12499	Serine carboxypeptidase	27	SS1G_09365	glucan 1,3-beta-glucosidase precursor	
7	SS1G_12721	PP		17	SS1G_12500	carboxypeptidase	27	SS1G_09366	beta-glucosidase	
7	SS1G_12724	CHP		18	SS1G_07183	PP	28	SS1G_13385	actin patch protein 1	
8	SS1G_12930	glucan 1,3-beta-glucosidase precursor		18	SS1G_07184	GHF 32 protein	28	SS1G_13386	cutinase	
8	SS1G_12937	glycosyl hydrolase		19	SS1G_05449	carboxypeptidase cpdS	29	SS1G_10165	CE family 8 protein	
8	SS1G_12938	extracellular proline-serine rich protein		19	SS1G_05454	chitotriosidase-1	29	SS1G_10167	polygalacturonase 1	
9	SS1G_00501	endoglucanase A		20	SS1G_05493	tannase and feruloyl esterase family protein	30	SS1G_03610	CHP	
9	SS1G_00505	CHP		20	SS1G_05494	wsc domain-containing protein	30	SS1G_03611	CFEM domain protein	
10	SS1G_00513	PP		21	SS1G_08644	lipase 5 precursor	31	SS1G_11700	chitinase 1 precursor	
10	SS1G_00514	GHF 26 protein		21	SS1G_08645	fad binding domain-containing protein	31	SS1G_11703	GPI transamidase	
11	SS1G_00768	PP		22	SS1G_07655	subtilisin-like protein	31	SS1G_11706	CHP	

*CHP: Conserved hypothetical protein, PP: Predicted Protein, GHF glycoside hydrolase family CE carbohydrate esterase

5.3.3 Identifications of RxLR-dEER motifs and Y/F/WxC motifs in the *S. sclerotiorum* refined secretome.

The *S. sclerotiorum* refined secretome was inspected for protein sequences containing RxLR dEER motifs. It has been demonstrated that the presence of this signature motif enables proteins in oomycete pathogens to cross the host plant plasma cell membrane autonomously and then to suppress host defence once inside the host cell (Tyler 2009). In total 21 protein sequences from the refined secretome were found to contain RxLR motifs. The positioning of the motifs was then examined for proximity to the N-terminal of the signal peptide. Four sequences containing a RxLR motif within 55 base pairs of the N-terminal of the signal peptide warranted further inspection. These were SS1G_00624 a predicted aspartate protease, SS1G_03160, a predicted triglyceride lipase, SS1G_03653; no IPS entry and SS1G_14321 a predicted dioxygenase (**Table 20**). When these four sequences were inspected for the presence of dEER motifs downstream of RXLR domain, no direct motif matches were identified. None of these genes were found in the clusters across the genome map.

Powdery mildew and rust fungi have been shown to secrete effector proteins which contain a Y/F/WxC motif which enables the protein to be transported across the plant cell-derived extrahaustorial membrane where they then suppress plant cell defence (Godfrey et al. 2010). Eight protein sequences from the refined secretome were found to contain Y/F/WxC motifs within 16 base pairs of the N-terminal of the signal peptide (**Table 21**). These mature proteins all vary in length, ranging from 232 to 1020 amino acids. Each sequence contains 6 or more cysteines. Six of the sequences were annotated. The 2 unannotated proteins (SS1G_02025 and SS1G_03268) are discussed in more detail below. The 6 annotated proteins consist of different enzymes including, glycoside hydrolases which are involved in plant polysaccharide degradation (GH45), an aspartate protease which cleave bonds in peptides and a histidine acid phosphatase which has a conserved catalytic core centring on a histidine that becomes phosphorylated during the course of reaction (Rigden 2008). Of these SS1G_04662, an alpha-galactosidase, was found in gene cluster 005 (**Table 19**). When mapped across the genome, there were no genes coding for proteins containing either a RxLR or Y/F/WxC motifs found on chromosomes 11, 12, 13 and 14.

Table 20: *S. sclerotiorum* secretome proteins which contain an RXLR motif.

No.	Gene ID	position	motif	PFAM	Function
1	SS1G_00624*	53	RRLR	26	Aspartate protease
2	SS1G_01811	397	RNLR	732, 5199	glucose-methanol-choline oxidoreductase family;
3	SS1G_02399	147	RLLR	295	GHF 28
4	SS1G_02553	135	RGLR	295	GHF 28
5	SS1G_03160*	82	RRLR	1764	Triglyceride lipase
6	SS1G_03420	278	RSLR	-	-
7	SS1G_03653	36	RMLR	-	-
8	SS1G_04725	536	RNLR	264	Tyrosinase
9	SS1G_04934	159	RVLR	-	-
10	SS1G_05368	793	RDLR	00933, 1915	GHF 3
11	SS1G_05784	501	RGLR	3659	GHF 71
12	SS1G_06235*	202	RMLR	295	GHF 28
13	SS1G_07847	685	RQLR	00734, 1915, 00933,	carbohydrate-binding module, GHF 3
14	SS1G_08229	150	RILR	295	GHF 28
15	SS1G_09366	179	RELRL	00933,	GHF 3
16	SS1G_12499	562	RELRL	450	Serine carboxypeptidase
17	SS1G_12724	355	RYLR	-	-
18	SS1G_14321*	75	RSLR	775	Dioxygenase

*Gene amino sequences inspected for dEER downstream of RXLR domain, however no direct motif matches were identified.

Table 21: *S. sclerotiorum* secretome protein sequences which encode Y/F/WxC motif containing proteins.

	Signal Length	position	motif after signal	Y/F/WxC	PFAM	Function	
1	SS1G_01828	21	33	12	WDC	00734, 02015	GHF 45 protein
2	SS1G_02025	20	35	15	FSC	-	candidate effector 5 protein
3	SS1G_03268	21	30	9	FSC	-	adhesin protein mad1
4	SS1G_03941	20	28	8	YAC	00026	eukaryotic aspartyl protease
5	SS1G_04662	25	40	15	FMC	00652, 02065	alpha-galactosidase A precursor
6	SS1G_09959	18	34	16	YYC	00328	histidine acid phosphatase
7	SS1G_12263	21	29	8	WYC	10287, 10290	protein tos1 precursor
8	SS1G_13860	20	32	12	WDC	02015	GHF 45 protein

5.3.4 EST support analysis for the secretome

The seven EST libraries downloaded from the Broad *S. sclerotiorum* database (**Table 17**) were inspected to identify those genes in the refined secretome which had EST support (in file S1, Tab 6). Out of the 432 genes in the refined secretome, 58 genes (13%) had at least one in hit in G781 library, 66 genes had hits in G786 library, 95 genes in G787, 20 genes in G865, 21 genes in G866, 146 genes in G2118 and 118 genes in G2128. SS1G_03361 was the only gene with EST support identified in all 7 libraries and codes for, a conserved hypothetical protein which contains the PF05577 domain corresponding to a serine carboxypeptidase S28. Carboxypeptidases have diverse functions which range from protein maturation to metabolism. Therefore expression of this during many physiological processes might be anticipated (Skidgel and Erdos 1998). Collectively, this EST analysis revealed that 246 genes present in the refined secretome (57%) had EST support.

Protein sequences with hits above 40 in any of the EST libraries were investigated further to determine which genes were the most expressed proteins under the seven different conditions explored. Twenty eight genes were identified with 40 or more hits in at least one EST library (**Table 22**). For comparison, *sspg1* (SS1G_10167) a documented secreted virulence protein with polygalacturonase activity (Dallal Bashi et al. 2012) had a count of 76 EST hits in the Tomato infection library (G2118). Fifteen of the predicted protein sequences have PFAM annotation. SS1G_00730, a protein with a glucose-methanol-choline oxidoreductase domain had EST support only in library G2128 highlighting its potential role in oxidative stress. SS1G_03326, had 97 EST hits in the sclerotia development library (G781). This protein is part of the CAP protein family (cysteine-rich secretory proteins, antigen 5 and pathogenesis-related 1 protein). This protein family has been shown to have many roles in regulation of extracellular matrix, branching morphogenesis and cell wall loosening, potentially as either proteases or protease inhibitors which have possible antifungal activity (Niderman et al. 1995). All of these described physiological processes would occur during sclerotia formation.

SS1G_03611, only had EST support in the plant infection libraries G865, G2118 and the Infection cushion library G866. This gene was found in gene cluster 030. This predicted protein has a CFEM domain which is a specific cysteine rich domain found in some proteins with proposed roles in fungal pathogenesis or conserved fungal effector domain (Kulkarni et

al. 2003). SS1G_03611 is predicted to encode a mature protein of 101 amino acids in length with 7.93% cysteine residue content.

Table 22: 28 secretome genes with 40 or more EST counts in at least one EST library.

(PP: Predicted protein).

	Broad Gene ID	G781	G786	G787	G865	G866	G2118	G2128	Gene description
1	SS1G_00263*	0	1	0	2	0	61	3	PP
2	SS1G_00730	0	0	0	0	0	0	55	choline dehydrogenase
3	SS1G_01426*	3	0	113	0	0	0	0	PP
4	SS1G_01428	0	0	90	0	0	0	0	pan domain containing protein
5	SS1G_02250*	17	2	0	0	1	39	49	PP
6	SS1G_02345*	0	0	54	0	0	0	0	PP
7	SS1G_03181	5	0	4	8	8	87	18	aspartic endopeptidase pep1
8	SS1G_03326	97	2	9	0	0	4	3	YFW12 protein
9	SS1G_04196	40	0	0	0	0	0	0	laccase-1 precursor
10	SS1G_04725	0	0	46	0	0	0	0	tyrosinase 2
11	SS1G_04857*	45	2	4	0	0	0	53	PP
12	SS1G_05337	8	66	6	0	0	2	10	malate dehydrogenase
13	SS1G_05794	0	0	3	0	0	0	42	beta-propeller-like protein
14	SS1G_05917*	186	0	0	0	0	0	4	PP
15	SS1G_06412*	0	0	96	0	0	0	0	PP
16	SS1G_07554	43	0	0	2	0	14	2	subtilisin-like protein
17	SS1G_07655	60	0	4	0	15	18	0	tripeptidyl-peptidase 1
18	SS1G_07836	0	0	0	0	0	83	8	acidic protease 1
19	SS1G_08110*	2	4	0	7	0	404	6	PP
20	SS1G_09232*	0	2	1	4	0	44	24	PP
21	SS1G_10167	0	0	0	3	1	76	4	polygalacturonase 2
22	SS1G_11239	60	0	0	0	0	2	0	WSC domain-containing protein
23	SS1G_11468	0	2	0	0	174	0	4	protein similar to ASG1
24	SS1G_12262*	13	13	49	0	3	10	17	PP
25	SS1G_12361*	2	4	0	7	0	405	6	PP
26	SS1G_12500	13	5	55	4	0	12	18	carboxypeptidase KEX1
27	SS1G_13599*	675	2	0	2	2	5	20	PP
28	SS1G_14133	10	13	1	0	9	25	60	FG-GAP repeat protein

*Those proteins sequences with no protein domains or other annotation

5.3.5 EST support for unannotated sequences

Across the secretome, those proteins with hits above 40 counts in any of the EST libraries were investigated to determine whether any hypothetical proteins with no current annotation can be assigned further information regarding their role during secretion. Twelve sequences with 40 or more hits in an EST library were found to have no PFAM domains or IPS entry (**Table 22**). Of these 12, SS1G_00263, SS1G_08110, SS1G_09232, SS1G_12361 had very high EST counts in the tomato infection library (G2118) suggesting their increased activity during infection of some but not all host species and /or a specific phase of infection. By contrast, the genes SS1G_01426, SS1G_02345, SS1G_06412 and SS1G_12262 had no EST support in the plant infection libraries but are were present in high abundance in the apothecia development library (G787). SS1G_06412 is of specific interest as this gene is unique to *S. sclerotiorum* and only had EST support in in the apothecia development library (G787). Possibly the function of this protein is specific to *S. sclerotiorum* apothecia development. SS1G_13599 had 675 EST hits in the developing sclerotia library G781. This extremely high hit count is highly suggestive of a role in this process.

5.3.6 Further analysis of unannotated sequences

No recognised PFAM domains or IPS entries were identified in 122 and 171 sequences in *S. sclerotiorum* and *B. cinerea* refined secretomes respectively. The unannotated *S. sclerotiorum* sequences were mapped across the genome. No obvious distribution patterns were observed (**Appendix 3**).

Further inspection of *S. sclerotiorum* unannotated sequences found only one sequence, SS1G_03653, with a RxLR motif close to the signal peptide sequence, however this protein currently has no EST support (**Table 20**). As previously noted, 2 unannotated sequences contain a Y/F/WxC motifs; SS1G_02025 and SS1G_03268 (**Table 21**). SS1G_02025 may be of interest as it is 232 amino acids in length, so it is a relatively small protein and although it has no PFAM domain, IPS entry or EST support, it shares homology with candidate effector proteins in other fungal pathogens including the apple scab fungus *Venturia inaequalis* (E=1.88897E-44) and the grapevine dieback pathogen *Eutypa lata* (E=3.03625E-75) (Bowen et al. 2009). SS1G_03268, has some homology with adhesin protein MAD1 found in other fungi such as *B. cinerea* (E=1.68152E-119). Adhesin proteins have been shown to contribute to fungi adhere to insect and plant surfaces (Wang and St. Leger

2007). This predicted *S. sclerotiorum* protein had 12 EST hits in the G781 developing sclerotia library suggesting its role in adhesion which is plausible as sclerotia do stick to necrotic plant material. Both sets of unannotated sequences were inspected for small (smaller than 200 amino acids), cysteine rich proteins (5% or greater), a sequence profile that has previously been used to predict candidate effector genes (Bolton et al. 2008b, do Amaral et al. 2012). Effectors previously discovered which fit this sequences profile include CfECP6, an effector which binds chitin during *C. fulvum* plant infection and prevents PAMP triggered recognition by the plant chitin receptors (Bolton et al. 2008b). Three putative homologues were found in the wheat infecting fungus *Mycosphaerella graminicola* (Marshall et al. 2011). In the *S. sclerotiorum* refined secretome, 38 genes were found with a 5% or more cysteine content in the mature amino acid sequence. Out of this group, 22 are less than 200 amino acids in length and have 6 or more cysteine residues in the mature protein (**Table 23**). None of these small cysteine rich proteins were found to contain either an RxLR or Y/F/WxC motif. Eighteen of these proteins have no annotation. When all 22 *S.sclerotiorum* cysteine rich proteins were mapped to the genome, no genes were present on chromosomes 10, 11, 12, 13 and 15 (Appendix 3) a similar distribution pattern to that of the RxLR and Y/F/WxC motif containing proteins. The genes coding for the cysteine rich proteins SS1G_01003, SS1G_02345, SS1G_03611 and SS1G_09248 were found in gene clusters 013, 014, 030 and 026, respectively. For comparison the predicted *B. cinerea* refined secretome contains 26 protein sequences rich in cysteine residue content (>5%) that are smaller than 200 amino acids.

Table 23: *S. sclerotiorum* small, cysteine rich proteins identified in the refined secretome.

	Broad ID	Length	No. Cysteine	%C	WoLFP-SORT	PFAM/IPRO	Function
1	SS1G_00534	91	8	8.79	extr=20	-	predicted protein
2	SS1G_01003	89	8	8.99	extr=25	IPR010636	predicted protein
3	SS1G_01226	144	10	6.94	extr=27	-	predicted protein
4	SS1G_01867	102	6	5.88	extr=23	-	predicted protein
5	SS1G_02068	146	8	5.48	extr=26	-	predicted protein
6	SS1G_02345	124	7	5.65	extr=27	-	hypothetical protein
7	SS1G_02800	57	6	10.53	extr=20	-	predicted protein
8	SS1G_03611	101	8	7.92	extr=21	PFAM05730	predicted protein
9	SS1G_03897	106	8	7.55	extr=26	-	predicted protein
10	SS1G_04618	137	8	5.84	extr=22	-	predicted protein
11	SS1G_04857	122	8	6.56	extr=26	-	hypothetical protein
12	SS1G_05103	83	6	7.23	extr=22	-	hypothetical protein
13	SS1G_06068	73	10	13.7	extr=27	-	predicted protein
14	SS1G_08128	71	11	15.49	extr=21	-	predicted protein
15	SS1G_08163	69	8	11.59	extr=22	-	signal peptide-containing protein
16	SS1G_09175	108	10	9.26	extr=22	-	predicted protein
17	SS1G_09248	76	8	10.53	extr=19	PFAM06766	hydrophobin
18	SS1G_10956	96	5	5.21	extr=25	-	protein
19	SS1G_11673	108	7	6.48	extr=18	IPR003609	predicted protein
20	SS1G_11706	59	5	8.47	extr=26	-	predicted protein
21	SS1G_12648	134	8	5.97	extr=26	-	predicted protein
22	SS1G_13126	129	8	6.2	extr=20	-	hypothetical protein

5.3.7 PFAM abundance within predicted secreted proteins with a potential plant cell degrading function

Out of the 432 gene sequences which make up the refined secretome for *S. sclerotiorum* and the 499 *B.cinerea* refined secretome gene sequences, 289 and 302 protein sequences respectively contain at least 1 PFAM domain. A total of 114 PFAM domains are common to both species. The most abundant PFAM domains were identified in enzymes involved in the breakdown of host plant cell walls.

A large portion of any fungal secretome will consist of enzymes which are vital for the degradation of host substrate. Glycoside hydrolase protein families are extremely important as

proteins with these domains are usually involved in hydrolysing the glycosidic bond between two or more carbohydrates (CAZY). There are key enzymes involved in the degradation of polysaccharides, specifically cellulose, hemicellulose and pectin. In the *S. sclerotiorum* refined secretome, 29 glycoside hydrolase families were identified in 94 genes (22% of refined secretome) (**Appendix 4.1**). In comparison, 25 glycoside hydrolase families were found in 92 gene sequences in the *B.cinerea* refined secretome (18% of refined secretome). When all genes containing glycoside hydrolase domains were mapped to the *S. sclerotiorum* chromosome map, the distribution was evenly spread across the genome.

One of the most abundant PFAM domains in both secretomes was the glycoside hydrolase family 28 (PF00295). This domain was found in 17 protein sequences in both refined secretomes. These 17 proteins all have polygalacturonase activity and so are heavily involved in the degradation of cell wall polysaccharides. One of these proteins (SS1G_10167) with the PF00295 domain is the characterised pathogenicity factor (*sspg1*). A *S. sclerotiorum* mutant strain lacking this gene was shown to exhibit a significantly reduced virulence phenotype (Dallal Bashi et al. 2012, Li et al. 2004b).

Further investigation into degradative enzymes revealed that the *S. sclerotiorum* refined secretome contains 30 genes involved in lipid degradation (Appendix 4.2) and 37 genes involved in protein degradation (Appendix 4.3), the same number of plant cell degrading proteins found in the *Fusarium graminearum* secretome (Brown et al. 2012). The most abundant PFAM domain implicated in lipid degradation is Carboxylesterase, type B (PF00135) (**Table 24**). This domain was more abundant in the *B.cinerea* refined secretome with 18 protein sequences containing the domain compared to 10 sequences in the *S.sclerotiorum* refined secretome. This is a family of esterases which act on carboxylic esters and have lipase activity (Donaghy and McKay 1992). The most abundant protein degrading PFAM is Peptidase S53, propeptide (PF09286) of which 8 copies were found in both fungal refined secretomes (**Table 24**). This enzyme has an acidic pH optimum which is necessary if it is to maintain activity within the extremely acidic environment generated by the secretion of oxalic acid (Amselem et al. 2011) .

Table 24: The most common PFAM domains involved in degradation of host plant substrate. Domains identified in both *S. sclerotiorum* and *B. cinerea* refined secretomes.

PFAM	Ss	Bc	Description	PFAM	Bc	Ss	Description
00295	17	17	Glycoside hydrolase, family 28	00135	18	8	Carboxylesterase, type B
00734	17	6	Carbohydrate-binding module (associated with glycoside hydrolases)	00295	17	17	Glycoside hydrolase family 28
00150	9	6	Glycoside hydrolase, family 5	01915	9	5	Glycoside hydrolase family 3
01915	8	9	Carboxylesterase, type B	00933	8	5	Glycoside hydrolase family 3
09286	8	8	Peptidase S53, propeptide	07519	8	2	Tannase and feruloyl esterase
00082	7	2	Peptidase S8/S53 domain	09286	8	8	Peptidase S53
03443	7	7	Glycoside hydrolase, family 61	14310	8	5	Fibronectin type III-like domain (associated with glycoside hydrolases)
00026	6	7	Peptidase A1	00026	7	6	Glycoside hydrolase family 28
00450	6	7	Peptidase S10	01083	7	4	Cutinase
00657	6	2	Lipase, GDSL	03443	7	7	Glycoside hydrolase family 61
00933	5	8	Glycoside hydrolase, family 3, N-terminal	00150	6	9	Glycoside hydrolase family 5
14310	5	8	Fibronectin type III-like domain (coupled with glycoside hydrolase family 3)	00734	6	17	Carbohydrate-binding module (associated with glycoside hydrolases)

In total, 94 *S. sclerotiorum* secreted enzymes found to be directly involved in degrading plant cell walls were identified (**Table 25**). Twenty genes had good EST support in both the infected Brassica library (G865) and the Tomato infection library (G2118) compared to 11 genes which had only low EST support in the neutral pH mycelia library (G786). This result highlights the possible specific role of these 20 proteins in plant infection rather than just fungal growth and development.

Table 25: Predicted secreted proteins involved in plant cell wall degradation.

	No putative secreted proteins
Glycoside hydrolases	80
Pectate lyases	4
Carbohydrate esterase	4
Lipases	6

5.3.8 Further analysis of PFAM abundance across the *S. sclerotiorum* refined secretome

To explore other expanded gene families within the *S. sclerotiorum* refined secretome that are not involved in the direct degradation of plant polysaccharides, proteins or lipids, PFAM domains with copy numbers greater than 2, not implicated in plant substrate hydrolysis were investigated (**Table 26**). A glucose-methanol-choline (GMC) oxidoreductase domain (PF00732) was present in 10 and 12 proteins in the *S. sclerotiorum* and *B. cinerea* secretomes, respectively. These proteins catalyse the transfer of electrons from one molecule to another and are involved in a range of processes (Cavener 1992). SS1G_00730 which contains a PF00732 domain had 55 hits in the oxidative stress library suggesting its key role during this process. There are 5 multi copper oxidases in *S. sclerotiorum* and 3 copies in *B. cinerea*. These enzymes have laccase activity and are involved in the oxidation of phenolic lignin units (Levasseur et al. 2010). These proteins may also have other function during fungal development, melanin synthesis and detoxification, and human and plant pathogenesis.

There are 6 FAD linked oxidase, N-terminal domains (PF01565) within the *S. sclerotiorum* secretome. These enzymes use FAD as a co-factor and are mainly oxygen-dependent oxidoreductases (IPR006094). Oxidoreductases are a large protein family generally involved in the catalysis of oxidation-reduction reactions but are involved in many processes. For example, SS1G_01116 which contains this domain is homologous to isoamyl alcohol oxidase in *Aspergillus fumigatus* (E=0) which catalyses the formation of isovaleraldehyde (Yamashita et al. 2000). GO ontology from the Blast2Go analysis describes 29 of the *S. sclerotiorum* refined secretome proteins to be involved in oxidation- reduction processes (sup table). A Berberine-like domain was found with 3 of the FAD linked oxidase genes as it is involved in the biosynthesis of numerous isoquinoline alkaloids (Kutchan and Dittrich 1995).

Tyrosinase domain (PF00264), another enzyme involved in oxidation reactions, is found in 3 genes in *S. sclerotiorum* refined secretome. In fungi, this enzyme is involved in many processes including the formation and stability of spores, in defence and virulence mechanisms, and in browning and pigmentation, mainly melanin production (Halaouli et al. 2006, SolerRivas et al. 1997). SS1G_01576, a tyrosinase has 7 hits in the sclerotia development library (G781) and SS1G_04725 had 46 EST hits in the developing apothecia library (G787). During both processes browning pigments such as melanin would be made and strengthen cell walls and aid survival.

The histidine phosphatase (PF00328) superfamily, clade-2 domain is present in 5

proteins within the secretome. Phosphatases are responsible for the process of dephosphorylation, or the removal of phosphate groups from an organic compound. This family of histidine phosphatases have a conserved His residue in the catalysis centre which is transiently phosphorylated during the catalytic cycle (Rigden 2008).

Three copies of Chloroperoxidase (PF01338) were identified in the *S. sclerotiorum* secretome. Two of the genes with this domain (SS1G_05925, SS1G_12609) have EST support in the oxidative stress library (G2128). This protein is a heme-containing glycoprotein that is secreted by various fungi (IPR000028) and performs a range of diverse functions including facilitating the decomposition of hydrogen peroxide to oxygen and water and catalysing chloroperoxidase P450-like oxygen insertion reactions (IPR000028). These enzymes have also been described to have lignin degradation activity as they are potential chlorinators of lignin (Islam et al. 2012, Ortiz-Bermudez et al. 2003).

Two copies of the necrosis inducing protein (PF05630) were found in both secretomes. This secreted protein is a known virulence protein secreted by *Phytophthora sojae*, an oomycete that causes stem and root rot on soybean plants (Qutob et al. 2002). SS1G_11912 which contains this domain has 8 EST hits in the Tomato infection library highlighting its potential role in plant necrosis.

Two copies of the cupin domain (PF00190) were found in both secretomes. These domains are present in the two oxalate decarboxylase enzymes which are crucial for the degradation of oxalic acid which is secreted at very high levels by both fungi and could be potentially toxic if this enzyme was not secreted to hydrolyse this pathogenicity metabolite (Khuri et al. 2001, Dutton and Evans 1996, Magro et al. 1988). The degradation of oxalic acid is important for the regulation of pH dependent genes which need to be expressed during a later stage of the infection process.

A single hydrophobin domain (PF06766) was found in one gene in both the *S. sclerotiorum* (SS1G_09248) and *B. cinerea* (BC1G_01012) secretomes. A second copy was found in the *S. sclerotiorum* genome (SS1G_01214). These proteins both belong to the small, cysteine rich sub-class of secreted proteins (<200 amino acids, >5 % cysteine residues). This is typical of most hydrophobins which are unique to filamentous fungi and are hydrophobic proteins usually involved in spore coat formation (Bayry et al. 2012).

Table 26: The most abundant PFAM domains within the *S. sclerotiorum* secretome that have non plant cell hydrolytic properties.

No.	PFAM domain	Gene copy number in refined secretomes		Description
		Ss	Bc	
1	00732, 05199	10	12	Glucose-methanol-choline oxidoreductase,
2	328	5	4	Histidine phosphatase superfamily, clade-2
3	1565	6	7	FAD linked oxidase, N-terminal
4	00394, 07731, 07732	5	3	Multicopper oxidase
5	1822	5	3	Carbohydrate-binding WSC
6	187	4	1	CBM Chitin-binding, type 1 (coupled with other domains)
7	264	3	3	Tyrosinase
8	1328	3	5	Chloroperoxidase
9	8031	3	4	Berberine/berberine-like
10	1476	3	0	LysM
11	5730	2	0	Extracellular membrane protein, CFEM domain
12	24	2	0	PAN-1 domain
13	149	2	0	Metallophosphoesterase domain
14	188	2	2	CAP domain
15	190	2	2	Cupin 1 (oxalate carboxylase)
16	5630	2	2	Necrosis inducing protein

5.3.9 Biological, functional and compartmental analysis of the *S. sclerotiorum* secretome

The refined *S. sclerotiorum* secretome was subjected to a Blast2Go analysis to assess on a general level the biological processes covered by this set of proteins and their principal molecular functions using GO annotation . Most of the sequences are involved in some form of catalytic activity which encompasses the many hydrolysing enzymes and oxidases which are present in high numbers. Apart from carbohydrate, peptide and lipid catabolism which is associated with hydrolysis and plant cell degradation, there are other vital biological processes which may be associated with plant infection including protein associated with oxidative stress and dephosphorylation (**Figure 51**).

Enzymes in the secretome were selected for their roles in different general metabolic pathways (**Table 27**). The starch and sucrose metabolism pathway and the pentose and glucuronate pathways contained the most enzymes from the secretome. Again this is expected

as these enzymes primarily act on different polysaccharide substrates which these pathogens are required to breakdown and incorporate into required sugars and amino acids.

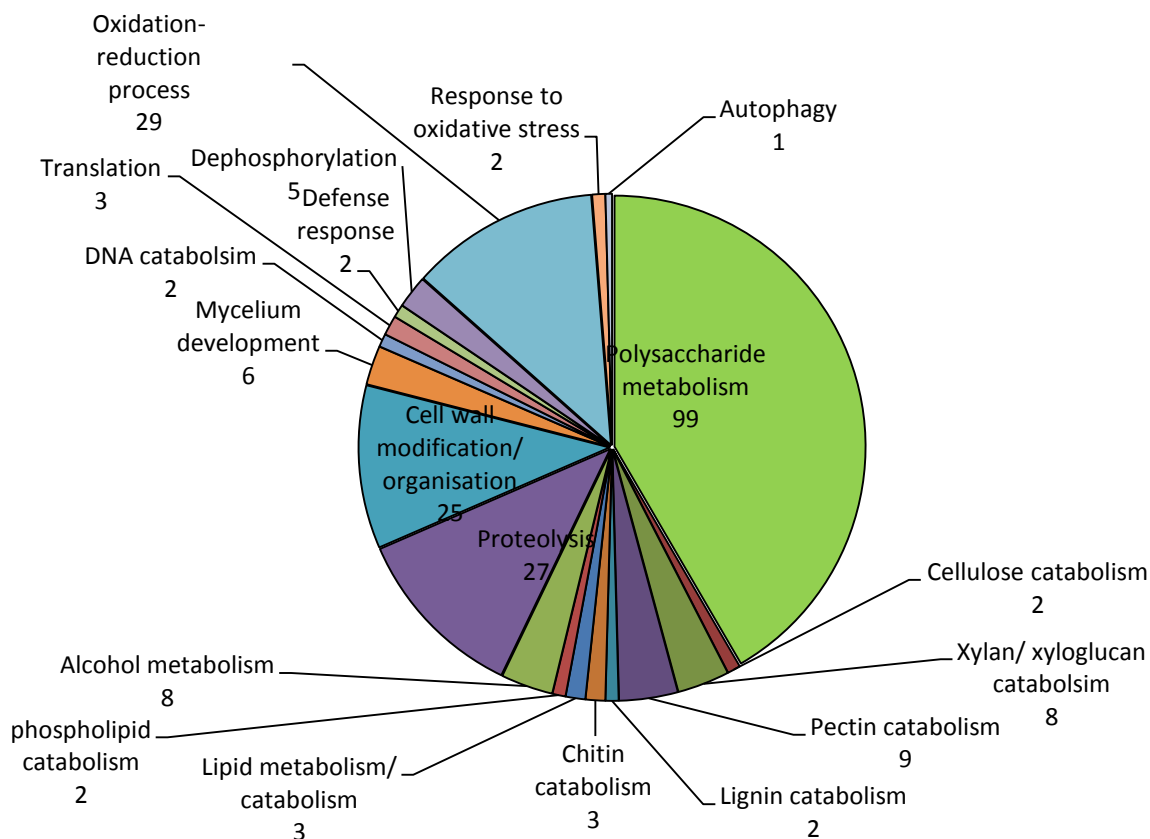


Figure 51: The physiological process that the proteins within the refined secretome are involved in. Process categorised using GO annotation levels.

Table 27: Secreted proteins involved in general Kegg Pathways.

Metabolism	No. Seqs in Pathway
Starch and sucrose metabolism	35
Pentose and glucuronate inter-conversions	22
Glycine, serine and threonine metabolism	8
Methane metabolism	6
Aminobenzoate degradation	6
Riboflavin metabolism	6
Amino sugar and nucleotide sugar metabolism	5
Other glycan degradation	5

5.3.10 Proteome support for the refined secretome

The predicted *S. sclerotiorum* refined secretome was compared to two studies which used ESI-q-TOF MS/MS and LC-MS/MS to identify secreted *S. sclerotiorum* proteins. Yajima (2006) (Yajima and Kav 2006) investigated the proteins secreted by *S. sclerotiorum* in liquid culture and Liang and colleagues (2010) (Liang et al. 2010) identified protein exudates found in the sclerotial liquid which encases immature sclerotia. Out of the 14 protein exudates identified in the liquid culture, 10 proteins were identified in the refined secretome (71 %) (**Table 28**). The later Liang proteomics study classified 56 proteins in the sclerotial liquid, 32 of these were sequences predicted in the refined secretome (57%) (**Table 29**). The predicted refined secretome so far contains 46 proteins that have been experimentally confirmed to be secreted.

Table 28: The proteins identified in liquid medium after incubation with *S. sclerotiorum* for several days.

Spot	Protein function from Yajima 2006 article	GI number	Broad ID	E value in Broad blast	Found in refined secretome
1	Neutral endopolygalacturonase SSPG1d	gi)20453991	SS1G_10167 SS1G_04177 SS1G_01009	0	Y
13	Endopolygalacturonase	gi)2196886	SS1G_10698 SS1G_11057		
3	Exopolygalacturonase	gi)32454433	SS1G_04207	0	Y
5		gi)1483221	SS1G_05832		
10					
6	Hypothetical protein Y41D4A (glutamyl-trna amidotransferase)	gi)14574316	SS1G_00271	2.4E-11	Y
11	Cellobiohydrolase 1 catalytic domain	gi)20986705	SS1G_09020	0	Y
			SS1G_04945		Y
			SS1G_02334		Y
12	Aspartyl proteinase	gi)12002205	SS1G_03181	0	Y
14	Pectin methyl esterase	gi)12964194	SS1G_03286		Y
			SS1G_10165		Y
16	Acid protease	gi)6984107	SS1G_07836	0	Y
18	Cyclohex-1-ene-1-carboxylate CoA ligase	gi)39932995	SS1G_12801	2.74E-22	N
4	Alpha-L-arabinofuranosidase	gi)11991221	SS1G_02462	0	N
2	Unnamed protein product	gi)49650592	SS1G_12749	0	N
9	Isopropylmalate/homocitrate/citra malate synthases	gi)23470424	SS1G_14205	0	N
7	Unnamed protein product	gi)49651714	no homology found in <i>S.sclerotiorum</i> genome		

Table 29: The 32 proteins identified from sclerotial liquid samples that were found in the *S. sclerotiorum* refined secretome.

	Gene ID	Spot	Description	Function
1	SS1G_00458	21	endo-beta- -glucanase precursor	Carbohydrate Metabolism
2	SS1G_01576	16	tyrosinase protein	Amino Acid Metabolism
3	SS1G_01776	15	glycoside hydrolase family 13 protein	Carbohydrate Metabolism
4	SS1G_02014	45	chitin- domain 3 protein	Unkown
5	SS1G_03181	22	aspartic endopeptidase pep1	Amino Acid Metabolism
6	SS1G_03602	7	alpha-l-arabinofuranosidase a	Carbohydrate Metabolism
7	SS1G_03629	17	aspartyl partial	Amino Acid Metabolism
8	SS1G_04085	27	extracellular cellulase allergen asp f7-	Carbohydrate Metabolism
9	SS1G_04200	3	alpha- -mannosidase family protein	Carbohydrate Metabolism
10	SS1G_04468	10	glycoside hydrolase family 47 protein	Carbohydrate Metabolism
11	SS1G_04473	8	extracellular serine-rich protein	Unknown
12	SS1G_04541	6	alpha-l-rhamnosidase	Carbohydrate Metabolism
13	SS1G_04857	19	hypothetical protein SS1G_04857	Unknown
14	SS1G_05337	27	malate dehydrogenase protein	Energy
15	SS1G_06037	17	glucan 1,3-beta-glucosidase precursor	Carbohydrate Metabolism
16	SS1G_07162	2	beta-glucosidase 1 precursor	Carbohydrate Metabolism
17	SS1G_07393	4	glycoside hydrolase family 55 protein	Carbohydrate Metabolism
18	SS1G_07639	14	acid phosphatase	Lipid and Secondary Metabolism
19	SS1G_07655	19	subtilisin-like protein	Amino Acid Metabolism
20	SS1G_07863	1	cellobiose dehydrogenase	Carbohydrate Metabolism
21	SS1G_08110	2	binding protein	Unknown
22	SS1G_08645	14	fad binding domain-containing protein	Unknown
23	SS1G_08889	6	glutaminase	Amino Acid Metabolism
24	SS1G_09143	13	amidohydrolase 2	Hydrolysis
25	SS1G_09270	28	hydrophobic surface binding protein a protein	Unknown
26	SS1G_09965	10	sphingomyelin phosphodiesterase	Lipid and Secondary Metabolism
27	SS1G_10096	9	ep11 protein	Lipid and Secondary Metabolism
28	SS1G_11912	25	necrosis and ethylene inducing peptide 2 precursor	Carbohydrate Metabolism
29	SS1G_12017	10	beta- -glucanosyltransferase	Carbohydrate Metabolism
30	SS1G_12917	19	uncharacterized serine-rich protein	Unknown
31	SS1G_12930	26	glycoside hydrolase family 17 protein	Carbohydrate Metabolism
32	SS1G_14133	23	fg-gap repeat	Signal Transduction

5.3.11 Known virulence factors identified in the refined secretome

Three proteins, Sscuta, sspg1 and a novel hypothetical protein, ssv263, which have been documented as virulence factors during *S. sclerotiorum* infection were identified in the refined secretome (**Table 30**). Four proteins containing a LysM domain were identified in the *S. sclerotiorum* genome. Three of these were identified in the refined secretome, one of which (SS1G_00772) was also found in gene cluster 011 across the genome map and has some EST support in the sclerotia and apothecia development libraries. SS1G_12509 and SS1G_12513 LysM domain containing proteins are also located quite closely together on chromosome 6. Interesting SS1G_12509 sits next to a chitinase which may be important as LysM domain containing effector proteins are involved in suppressing chitin-mediated plant defences. SS1G_12509 which has a single EST hit in the developing sclerotia (G781) and two hits in the developing apothecia library (G787). SS1G_03535, was identified in the total secretome but not the refined secretome as it has a Wolf-P-SORT score of extracellular, 12 which is lower than the cut off score of 18. This protein has been described as similar to the cfECP6 effector protein (Bolton et al. 2008b). There are no studies on the function of these 4 LysM proteins identified in the refined secretome and there is very little EST support for these predicted proteins either.

Table 30: The proteins known in *S. sclerotiorum* to be required for virulence during plant infection.

Broad ID	Gene name	Function	Virulence decreased?	Refined secretome	Reference
SS1G_07355	pac 1	Development and maturation of sclerotia.	Y	N	Rollins JA. 2003
SS1G_00699	SsSod1	Cu/Zn superoxide: detoxification of reactive oxygen species during host-pathogen interactions	Y	N	Xu L, Chen W. 2013
SS1G_01788	cna1	Calcineurin, a Ser/Thr phosphatase linked to several signal-transduction pathways, the regulation of cation homeostasis, morphogenesis, cellwall integrity, and pathogenesis in fungi.	Y	N	Harel A, Bercovich S, Yarden O. 2006
SS1G_14127	Ss-ggt1	Enzyme involved in glutathione recycling during key developmental stages of the <i>S.sclerotiorum</i> life cycle. Not required for host colonization and symptom development.	N	N	Moyi Li, Xiaofei Liang, Jeffrey A. Rollins. 2011
SS1G_00263	ssv263	Hypothetical protein unique to <i>S.sclerotiorum</i> and <i>B.cinerea</i>	Y	Y	Liang and Yajima et al. 2013
SS1G_07661	Sscuta	Cutinase enzyme	Y	Y	Dallal Bashi, Zafer. 2012
SS1G_10167	sspg1	Polygalacturonase	Y	Y	Dallal Bashi, Zafer. 2012
SS1G_05917	Ss-S12	Involved in sclerotial development of <i>S. sclerotiorum</i>	N	N	Yu, Jiang, et al. 2012
SS1G_02462	abx	arabinofuranosidase/beta-xylosidase	Y	N	Yajima et al. 2009
SS1G_08218	OAH	Enzyme catalysing the breakdown of oxaloacetate into oxalic acid, the main pathogenicity factor for <i>S. sclerotiorum</i>	Y	N	no publication currently
SS1G_03535 SS1G_00772* SS1G_12509 SS1G_12513	LysM domain	Contains a LysM domain (e=0.024) (similar to ECP6- but WolfPsort= ext12 in total secretome) Contains a LysM domain (e=0.0028) Contains a LysM domain (e=0.12) Contains a LysM domain (e=0.03)	-	N Y	Bolten et al 2008 Reported to be similar to ECP6 currently
SS1G_07626	Velvet	Contains a Velvet domain- homologue to BC1G_02977, Bcvel1 involved in Bc sclerotial development and oxalic acid production.	Y	N	no publication currently
SS1G_10796 SS1G_08814	oxalate decarboxylase	Involved in the breakdown of oxalate during infection	Y	Y	no publication currently

* SS1G_00772 identified in cluster 011

5.3.12 Multispecies comparison analysis

A multispecies comparison was done to explore the relatedness of the predicted refined secretome of *S. sclerotiorum* to the predicted proteomes of 115 other species including other plant pathogens, Oomycetes, and animal pathogens and some free living eukaryotic organisms (Appendix 5).

5.3.12.1 Uniquely secreted proteins

The 115 species proteomes were compared to the refined secretomes for *S. sclerotiorum* and *B. cinerea*. Eleven protein sequences are found only in the *S. sclerotiorum* secretome (**Table 31**) and 31 protein sequences were found to be unique to the *B. cinerea* secretome (**Table 32**). The BlastP results were determined based on protein sequences with $e <^{-5}$ value similarity. All genes had only single copies in the genomes except BC1G_12747 which had two copies. There were no significant PFAM domains in any of these protein sequences. Three of the unique *S. sclerotiorum* proteins had EST support. As mentioned previously, SS1G_06412 had 96 gene reads in the EST library for developing apothecia. SS1G_12961 had one hit in the mycelial EST library and SS1G_13126 had 5 hits in the sclerotia developmental EST library. SS1G_13126 is also a small cysteine rich protein. None of these unique genes were found in the 31 gene cluster across the *S. sclerotiorum* genome. Six of the 32 proteins sequences unique *B. cinerea* also had small, cysteine rich protein profiles.

Table 31: Proteins unique to the *S. sclerotiorum* refined secretome.

Broad ID	Protein length amino acids	Cysteines	WoLF P SORT	PFAM
SS1G_01325	30	1	extr=23	-
SS1G_03537	88	3	extr=26	-
SS1G_04611	127	4	extr=21	-
SS1G_06412	237	7	extr=18	-
SS1G_07230	63	0	extr=25	-
SS1G_10581	82	2	extr=19	-
SS1G_11065	190	5	extr=18	-
SS1G_12927	151	3	extr=21	-
SS1G_12961	78	0	extr=18	-
SS1G_13126	129	8	extr=20	-
SS1G_14515	45	0	extr=20	-

Table 32: Proteins unique to the *B. cinerea* refined secretome.

Broad ID	Protein length amino acid	Cysteines	WoLF PSORT	PFAM
BC1T_00514	121	3	extr=18	-
BC1T_00958	148	0	extr=20	-
BC1T_01077*	180	11	extr=19	-
BC1T_01886	61	2	extr=18	-
BC1T_02388	174	6	extr=20	-
BC1T_02701	147	6	extr=25	-
BC1T_03065	293	1	extr=26	-
BC1T_03412	30	0	extr=21	-
BC1T_04280	137	2	extr=26	-
BC1T_04347	371	0	extr=27	-
BC1T_05590*	68	8	extr=22	-
BC1T_05976	11	0	extr=25	-
BC1T_07477	163	4	extr=25	-
BC1T_07778*	200	7	extr=18	-
BC1T_08414	28	0	extr=19	-
BC1T_08580	41	0	extr=24	-
BC1T_08904	203	8	extr=23	-
BC1T_08911*	117	10	extr=22	-
BC1T_09968	41	3	extr=21	-
BC1T_10445	71	0	extr=18	-
BC1T_10861	40	1	extr=19	-
BC1T_11606	153	4	extr=26	-
BC1T_12450	261	0	extr=24	-
BC1T_12732	33	0	extr=21	-
BC1T_12747	142	2	extr=24	-
BC1T_12766	457	7	extr=25	-
BC1T_13846	37	1	extr=19	-
BC1T_13879*	140	7	extr=23	-
BC1T_14014	70	3	extr=24	-
BC1T_14418	95	4	extr=22	-
BC1T_15646*	86	8	extr=25	-

* Small, cysteine rich protein profile

5.3.12.2 Shared proteome homology between species

S. sclerotiorum and *B. cinerea* secretomes were compared against all 115 proteomes to identify those proteins that are common and have a high level of sequence similarity across a wide taxonomic distribution. The *S. sclerotiorum* and *B. cinerea* refined secretomes contain at least one gene homologue (e^{-100}) in 110 and 111 of the 115 species' proteomes, respectively.

When the *S. sclerotiorum* refined secretome was compared to all other proteomes at a lower level of stringency (e^{-5}) (Appendix 5), the *B. cinerea* proteome shared the highest number of common protein sequences (92%). This result was anticipated because these two

species share 84% of their total proteomes (Amselem et al. 2011). The entire multispecies dataset was explored for unique *S. sclerotiorum* and *B. cinerea* proteins not found in the other species proteomes using a threshold of e^{-5} . This revealed 30 proteins uniquely shared by these two species (**Table 33**). Four of the *S. sclerotiorum* proteins are small, cysteine rich proteins identified earlier (SS1G_02068, SS1G_03897, SS1G_09175 and SS1G_12648). Most genes had single copies within the genomes except SS1G_00263, SS1G_01086, and SS1G_04312 where 2 copies are found in both species. SS1G_09841 and SS1G_01086 were in the identified gene clusters 001, 003 and 011 respectively (**Table 19**).

To explore further the 30 *S. sclerotiorum* proteins potentially shared with *B. cinerea* a BlastN search was done using the 30 *S. sclerotiorum* gene nucleotide sequences to find the homologous gene in the *B. cinerea* genome. The predicted amino acid sequences for the two IDs were then aligned to ensure that these were gene homologues. Six proteins had maximum identity values above 40% and 24 genes had a maximum identity value above 50%. This is a confident level of homology between the two protein sequences to ensure they are homologues.

Table 33: Unique *S. sclerotiorum* and *B. cinerea* proteins.

Thirty genes identified in the *S. sclerotiorum* refined secretome which are unique to *S. sclerotiorum* and *B. cinerea*. The *S. sclerotiorum* nucleotide sequences were blasted within the Broad *B. cinerea* genome Browser. The amino acid sequences were then aligned to assess homology.

	<i>S. sclerotiorum</i> gene ID	<i>B. cinerea</i> ortholog	Identity between two nucleotide sequences (BlastN)		Identity between two amino acid alignments.	
			e value	max ID	e value	max ID
1	SS1G_00263	BC1G_00896	3.00E-74	76%	3.00E-75	73%
2	SS1G_00768	BC1G_02060	1.00E-09	82%	2.00E-29	41%
3	SS1G_01086	BC1G_12867	4.00E-86	80%	9.00E-78	78%
4	SS1G_01107	BC1G_12892	3.00E-113	77%	1.00E-74	75%
5	SS1G_01235	BC1G_03977	2.00E-90	76%	1.00E-92	75%
6	SS1G_01966	BC1G_02670	4.00E-105	77%	1.00E-60	76%
7	SS1G_02068*	BC1G_02834	2.45E-43	51%	2.00E-56	55%
8	SS1G_02690	BC1G_05658	2.00E-20	66%	2.00E-17	63%
9	SS1G_02714	BC1G_05632	0	100%	7.00E-41	44%
10	SS1G_03897*	BC1G_04521	3.00E-24	76%	3.00E-25	64%
11	SS1G_04312	BC1G_12229	0	89%	0	69%
12	SS1G_05013	BC1G_09803	4.00E-26	77%	2.00E-78	49%
13	SS1G_06747	BC1G_03293	0.035	69	9.00E-07	76%
14	SS1G_06890	BC1G_14733	4.00E-26	92%	6.00E-25	58%

15	SS1G_07027	BC1G_08442	7.00E-157	87%	3.00E-110	88%
16	SS1G_07224	BC1G_05097	1.00E-71	75%	1.00E-110	53%
17	SS1G_07571	BC1G_14520	1E-45	75%	5.00E-37	53%
18	SS1G_09175*	BC1G_01059	1.00E-57	77%	6.00E-53	68%
19	SS1G_09693	BC1G_16071	1.5	91%	2.00E-39	46%
20	SS1G_09841	BC1G_08638	4.00E-65	70%	3.00E-93	62%
21	SS1G_10082	BC1G_12529	3.00E-34	71%	1.00E-41	66%
22	SS1G_10266	BC1G_08459	1.00E-32	87%	2.00E-37	44%
23	SS1G_11120	BC1G_08106	2.00E-86	70%	3.00E-105	67%
24	SS1G_11202	BC1G_09789	3.00E-21	89%	8.00E-20	66%
25	SS1G_12648*	BC1G_04660	1.00E-90	79%	8.00E-88	81%
26	SS1G_13394	BC1G_06376	8.00E-04	68%	8.00E-31	42%
27	SS1G_13682	BC1G_14145	0	71%	4.00E-121	59%
28	SS1G_13965	BC1G_14535	1.00E-89	80%	5.00E-61	85%
29	SS1G_14007	BC1G_11588	8.00E-36	81%	1.00E-17	68%
30	SS1G_14041	BC1G_03205	3.00E-123	77%	2.00E-79	76%

* Small, cysteine rich protein profile

Many ascomycete plant pathogens which infect different mono and dicotyledonous plants were in the top most homologous proteome's (Appendix 5). These species were investigated to look at the range of homology between their proteomes and the *S. sclerotiorum* refined secretome. The ascomycete plant pathogens, share between 42% and 76% of their proteome's with the *S. sclerotiorum* refined secretome. Curiously, alongside these homologous plant pathogen proteome's, there is a single plant saprobe which shares many proteins with the *S. sclerotiorum* refined secretome. *Hysterium pulicare*, a dothideomycete found to live in decaying woody material shares 319 proteins (73%). A second saprophyte, *Rhizidhysterium rufulum*, shares 308 proteins (71%) with the *S. sclerotiorum* secretome alongside other true monocotyledonous infecting pathogens such as *Fusarium verticillioides*, *Pyrenophora tritici-repentis* and *Gaeumannomyces graminis*. This is interesting as both *S. sclerotiorum* and *B. cinerea* are predominately dicotyledonous infecting pathogens.

The *S. sclerotiorum* refined secretome shares approximately 67% homology with *Aspergilli* and 75% with *Fusarium oxysporum* proteomes. *F. oxysporum* is an opportunistic invaders of immuno-compromised animal hosts and *Aspergillus* species can cause allergy and disease in healthy animal hosts. These lifestyles are very different to the lifestyle of *S. sclerotiorum*. Although *Aspergilli* and *Fusarium oxysporum* produce oxalic acid in large quantities *in vitro* (Dutton and Evans 1996), similarly to *S. sclerotiorum* and *B. cinerea*, the role of this secreted metabolite in animal pathogenicity is unclear in these animal pathogens (Ruijter et al. 1999). There was no relationship between the homology of the proteomes between other oxalic acid producing fungi and the *S. sclerotiorum* and *B. cinerea*, refined

secretomes.

Other phyla of fungi including basidiomycetes share much less homology with *S. sclerotiorum* (less than 60%). The chromalveolata phyla which contain Oomycete plant pathogens such as *Phytophthora spp* share no greater than 36% proteome homology with the *S. sclerotiorum* refined secretome.

A comparison between the refined secretome of *S. sclerotiorum* and the proteome's of *Alternaria brassicicola* and *Leptosphaeria maculans* was made to explore putative secreted proteins common to only these three fungal species which are all economically important pathogens of oilseed rape. No proteins unique to only these three species were found. A second specific investigation was made to explore plant pathogens that infect numerous dicotyledonous and monocotyledonous species. No gene set to this entire group could be identified.

Although no specific genes associated with a specific fungal lifestyle could be found, three unique genes in the initial *S. sclerotiorum* and *B. cinerea* intercomparison were subsequently detected only in a limited number of other fungi (**Table 34**).

Table 34: Genes found in *S. sclerotiorum* and *B. cinerea* that are also present in only a limited number of other fungi.

Gene	Function	Species containing orthologue protein sequence	Lifestyle	Host
SS1G_00849	Conserved hypothetical protein	<i>Chaetomium globosum</i>	Sord-sap/animal	Woody/soil
		<i>Colletotrichum graminicola</i>	Sord-plant path	Dicot
		<i>Colletotrichum higginsianum</i>	Sord-plant path	Dicot
		<i>Magnaporthe oryzae</i>	Sord-plant path	Monocot
		<i>Magnaporthe poae</i>	Sord-plant path	Monocot
		<i>Magnaporthe grisea</i>	Sord-plant path	Monocot
		<i>Fusarium spp</i>	Sord-plant path	Mono/Dicot
SS1G_09196	Hypothetical protein similar to enoyl- hydratase isomerase	<i>Colletotrichum higginsianum</i>	Sord-plant path	Dicot
		<i>Fusarium graminearum</i>	Sord-plant path	Mono/Dicot
SS1G_12262	Allergen Asp f 4 precursor	<i>Blastomyces dermatitidi</i>	Saprophyte/ animal pathogen	
		<i>Histoplasma capsulatum</i>		
		<i>Paracoccidioides brasiliensis</i>		
		<i>Penicillium chrysogenu</i>		

5.3.12.3 Multispecies comparison of gene copy

The 115 species intercomparison revealed 47 genes with at least 10 or more gene copies in the *S. sclerotiorum* proteome at e^{-5} . The genes with the most copies were gmc

oxidoreductase, polygalacturonases and beta-glucosidases and other enzymes which are integral to cell wall degradation. Species which had either 1 or none of these gene types include; *Batrachomyces dendrobatidis* (the *Chytrid* fungus), *Caenorhabditis elegans* (a non-pathogenic nematode), *Meloidogyne spp* (a plant parasitic root-knot nematode), *Candida spp* (a human pathogen), *Saccharomyces cerevisiae*, *Allomyces macrogynus*, *Spizellomyces punctatus* and *Schizosaccharomyces cryophilus*. These species have very different lifestyles to *S. sclerotiorum* and a need for such specialised secreted enzymes for their free living and /or pathogenic lifecycles is unlikely.

The gene SS1G_06534 which encodes for a trypsin serine protease (pfam00089), has one copy in the *S. sclerotiorum* secretome however it was present in high copy number in *Drosophila melanogaster* (291 copies), *Myzus persicae* (67 copies), *Phytophthora infestans* (23 copies) and *Pythium ultimum* (15 copies). These species are either in the Animalia or Chromalveolata Kingdoms. The gene SS1G_09060, a single gene in *S. sclerotiorum* coding for another type of secreted serine protease, a subtilase (PF00082) was also found above 15 copies found in *Aspergillus oryzae*, *Gaeumannomyces graminis*, *Neurospora tetrasperma*, *Magnaporthe grisea*, and *Melampsora laricis-populina* and *Pythium ultimum*.

5.4 Discussion

The identification and analysis of a plant pathogen secretome is now an essential tool to further our understanding of how the fungal infection process is regulated and how pathogens can evade host plant defence systems. Many secreted proteins have already been identified and shown to act as effector proteins which manipulate host plant machinery for a range of fungal and Oomycete pathogens (Bolton et al. 2008b, Bowen et al. 2009, Godfrey et al. 2010, Marshall et al. 2011, Mueller et al. 2008, Tyler 2009). Not only is this a fundamental area of research but the scientific community anticipates that the identification of these candidate proteins and their function will ultimately lead to the discovery of new targets for detection and control of economically destructive pathogens including *S. sclerotiorum* and *B. cinerea*.

The use of a powerful bioinformatics pipeline as described here and in previous studies (Brown et al. 2012, do Amaral et al. 2012) allows the stringent selection of putative secreted proteins which can be further investigated *in silico*. Analyses such as these allow more informed choices to be made when selecting effector protein candidates to be tested in the laboratory, a process that can be costly and time consuming. Although the secretion of oxalic acid has been championed as the principal infection strategy for *S. sclerotiorum*, an in-depth analysis of all other putative secreted proteins was undertaken to reveal other candidate proteins potentially important in the infection process. The secretome for the closely related fungus, *B. cinerea* was investigated alongside *S. sclerotiorum* to investigate similarities and any contrasts amongst the secreted protein profiles.

A refined secretome size of 432 proteins for *S. sclerotiorum* and 499 proteins for *B. cinerea* was predicted using the bioinformatics pipeline described. Both the secretomes make up approximately 3% of their total predicted genomes. This figure is relatively small compared with the secretome size of the wheat infecting pathogens *Fusarium graminearum* and *Mycosphaerella graminicola* which represents approximately 4.1% and 4.46% of their total genomes respectively (Brown et al. 2012, do Amaral et al. 2012). Approximately, 310 and 328 protein sequences within the *S. sclerotiorum* and *B. cinerea* secretomes respectively contain some form of annotation. This highlights that approximately 30% of both secretomes require further functional investigation and some of these proteins are likely to be involved in pathogenesis.

Several notable results were identified during the analysis. Firstly the *S. sclerotiorum* secretome was evenly distributed across the 16 chromosomes and although small clusters of

secreted proteins were found, they were never found in clusters containing more than 3 genes unlike the clusters of small secreted proteins identified across the *U. maydis* genome (Kaemper et al. 2006). The clusters did not consist of any duplicated genes and in only two cases did the clusters contain similar protein families (cluster 012 & 017). There was no evidence that the documented secreted virulence associated proteins found in the *S. sclerotiorum* secretome (including *Sscuta*, *sspg1*, *ssv263pac1*), are found in clusters across the *S. sclerotiorum* genome either. However 2 of the LysM domain containing proteins sit very close to one another on chromosome 6 and sandwiched in between is a chitinase (*SS1G_12510*). The expression of this group of genes requires further investigation to demonstrate whether they have any known effector function such as the cfECP6 or MGLysM3 protein effectors (Bolton et al. 2008b, Marshall et al. 2011). The other known *S. sclerotiorum* virulence factors such as *pac1* and *ssSod1* were not identified in the secretome protein set. An explanation for this is that although they are essential for virulence, they may not actually be secreted extracellularly but instead are required for intracellular gene regulation.

Secondly, the multispecies comparison confirmed that the *B. cinerea* proteome shared closest homology with the *S. sclerotiorum* secretome across all 432 proteins. This was an expected result as it is well documented that these two pathogens are closely related (Amselem et al. 2011) however it is interesting as these two fungi do have slightly different infection strategies. *S. sclerotiorum* secretes primarily oxalic acid at very high levels during infection whereas *B. cinerea* secretes oxalic acid (van Kan 2005) as well as botcinic acid, a highly substituted lactone (Cutler et al. 1993) and botrydial acid, a tricyclic sesquiterpene (Colmenares et al. 2002). It is tempting to assume there may be a larger difference between the two secretomes to account for the difference in infection strategy, however the *B. cinerea* proteome shares 92% of the *S. sclerotiorum* secretome.

A third interesting result is that while the multispecies analysis highlighted that there are 30 seemingly unique proteins found in only *S. sclerotiorum* and *B. cinerea*, no putative unique secreted proteins were associated with groups of fungal pathogens with specific hosts or lifestyles including oilseed rape infecting fungi or more generally ascomycete plant pathogens of dicotyledonous plants. This is unlike the *M. graminicola* secretome analysis in which nine unique proteins were identified only in fungal pathogens infecting wheat (*Triticum spp*) or other cereals (do Amaral et al. 2012). One explanation could simply be that not enough oilseed rape or dicot infecting plant pathogens were compared within this study. A second

explanation could be due to the host diversification of the plant pathogens compared. Many of the dicotyledonous plant infecting fungal pathogens investigated have wide host ranges and so may require a general set of proteins for infection which may be conserved between a range of pathogens with the ability to infect both monocots and dicots. According to the tree of life (<http://tolweb.org/angiosperm>), monocotyledonous plants are grouped as a single taxon of Angiosperms whereas the plants we now know as Dicotyledonous are spread across a range of different taxons. It is tempting to speculate that the fungal pathogens with a wide host range would require a large arsenal of secreted proteins, some of which would be conserved or overlap with pathogens with more specific host ranges. This may explain why the proteome of *Botryosphaeria dothidea*, a woody dicot infecting plant pathogen may share such a large set of proteins with the secretome of *S. sclerotiorum*.

The analysis of the *S. sclerotiorum* EST libraries was extremely valuable when trying to assign some form of function to the unannotated putative secreted proteins. EST support was available for 57% of the putative proteins within the *S. sclerotiorum* secretome in a range of infection conditions and developmental stages. Two secreted proteome studies confirmed the physical secretion of 46 proteins identified in the *S. sclerotiorum* refined secretome which is of significant importance when validating the pipeline. The other secreted proteins which were not identified in these studies may be expressed during different conditions compared to those which were investigated. Some protein secretion will only be induced during specific *in planta* infection conditions or at an earlier stage of spore germination for example. In both proteome studies, a different fungal strain was used to that which has been sequenced by the Broad which may also account for any protein differences in the computational search. The *S. sclerotiorum* secretome was explored for small, cysteine rich proteins which is a protein profile typically identified in other pathogen effector proteins. This study revealed 22 proteins with this profile which could be responsible for interfering with the activation of plant defence. Ten of these have support in at least one library in particular. Interestingly, a small protein with a CFEM domain which has been implicated in plant pathogenesis had strong EST support in the infected plant libraries (G865, G2118, G866) and should be investigated further. Other unannotated proteins in this set with no known function were also identified and explored for EST support. Those with support in the *in planta* infection libraries require further study to see if they are regulating any of the infection process.

The search for RxLR or Y/F/WxC motifs within the secretome revealed that none of the proteins containing these domains have small, cysteine rich features. In contrast, the *M. graminicola* secretome contained 10 cysteine rich proteins < 150 amino acids in length which contained a Y/F/WxC motifs. Interestingly the SS1G_02025 proteins did have homology with a candidate effector 5 protein found in other fungal pathogens, *Venturia inaequalis* and *Eutypa lata* and requires further investigation.

Unsurprisingly, both secretomes analysed consist of a large battery of hydrolysing enzymes which degrade different plant host substrates. The PFAM inspection and GO functional analysis for the *S. sclerotiorum* refined secretome revealed that 37 % (161 proteins) of the secretome protein set is responsible for the degradation of plant polysaccharides, proteins and lipids. For comparison the *F. graminearum* and *M. graminicola* secretomes contains 29 % (171 proteins) and 27 % (132 proteins) plant host substrate degrading enzymes respectively (Brown et al. 2012, do Amaral et al. 2012). These are very similar figures even though these two wheat attacking fungi attack a much smaller host range. With a range of glycoside hydrolases, peptidases, lipases, cutinase and laccases, *S. sclerotiorum* is able to fully degrade all parts of the plant cell similarly to *F. graminearum* (Brown et al. 2012). As suggested in previous studies (Amselem et al. 2011), many of these polygalacturonases and proteases identified have optimum activities at an acidic pH which would be necessary in plant substrate where oxalic acid would have been secreted ahead of fungal cell colonisation (Williams et al. 2011). The polygalacturonase gene family is the largest family of polysaccharide degrading proteins within the *S. sclerotiorum* secretome compared with *B. cinerea* of which the carboxylesterases are the largest gene family expansion. This may highlight some differences between the infection strategy of the two similar fungi.

The next largest group of proteins in the *S. sclerotiorum* secretome according to the GO analysis are enzymes involved in oxidation-reduction interactions. Although these enzymes are part of a large family of oxidase proteins which are involved in multiple processes including melanin production (tyrosinase) (Halaouli et al. 2006), lignin oxidation (laccases) (Levasseur et al. 2010) and isoamyl alcohol oxidase (Yamashita et al. 2000), the redox state of the host substrate has been shown to be extremely important in the ability of *S. sclerotiorum* to cause disease. The secretion of oxalic acid has been shown to suppress the host plant oxidative burst by inhibiting the production of H₂O₂ (Cessna et al. 2000). However later during the infection, oxalic acid promotes ROS production in the plant host and is

followed by programmed cell death (Williams et al. 2011). Isoamyl alcohol oxidase catalyses the reaction between alcohol and O₂ which then releases aldehyde and H₂O₂, an important signalling molecule in the REDOX balance. GMC oxidoreductase of which there are 10 enzymes in the secretome would also play a role during this host REDOX balance. This enzyme has also been implicated in the biocontrol of other fungal species such as *Fusarium oxysporum* (Kawabe et al. 2011) and this domain was found in 9 proteins in the secretome of *M. graminicola* so may also be involved in outcompeting other fungi within the environment. With such a considerable proportion of enzymes involved in oxidation reactions, they are most likely to be fundamental to the process of infection. The significance of these oxidase proteins could be further investigated using gene knockout constructs.

The two secreted oxalate decarboxylase enzymes identified in this analysis are also integral to the infection process as they will be induced/regulated by the acidic environment created by secreted oxalic acid. These enzymes prevent direct toxicity to the fungus by hydrolysing excess oxalic acid. This will then allow a pH shift which then triggers the downstream regulation of other genes involved in other important processes such as sclerotia formation.

The identification of the *S. sclerotiorum* secretome has provided insights into how other secreted proteins alongside secreted oxalic acid may contribute to the infection cycle. Although no direct associations can be made, many candidate proteins have now been identified which need further experimental investigation to explore whether they truly are secreted proteins with an effector role.

The use of this bioinformatics pipeline and molecular biology to identify unique protein targets for *S. sclerotiorum* detection will be further discussed in Chapter 6.

Chapter 6: Using the *S. sclerotiorum* secretome to identify uniquely secreted protein targets for infield disease detection.

6.1 Introduction

Within a growing season, multiple pathogens may attack a single crop. It is sometimes very difficult for growers/crop advisors to be experts in fungal identification for all these diseases. This may compromise their ability to provide accurate disease control if they cannot recognise a particular disease symptom. If growers are unsure of the particular disease which has infected their crop, they can send infected plant material to disease diagnostic labs. These labs use a range of diagnostic tools to provide disease identification. These include using microscopy to identify a fungal species based on the specific spore structure or by using molecular based technologies including qPCR and ELISA assays. Although extremely specific and sensitive, these methods are time consuming, require specialised equipment or highly trained staff and are often very expensive.

For growers and plant health officials monitoring emerging diseases, infield detection systems or handheld devices could be used to detect a variety of pathogens accurately and quickly within the field. Currently on the market, there are handheld devices that can detect some fungal diseases. These tend to be devices based on immunological methods of detection which contain antibodies specific to plant virus or fungal pathogen proteins. One company, Pocket Diagnostics, offer a range of handheld lateral flow devices (LFDs) which are used to identify many plant viruses and some fungal pathogens including Tomato mosaic virus (ToMV), Cucumber mosaic virus (CMV), *Ralstonia solanacearum*, *Pythium*, *Erwinia amylovora*, *Phytophthora spp* and *B. cinerea* to name a few. The *B. cinerea* LFD will however test positive for *S. sclerotiorum* within a sample as these two closely related fungi share a high proportion of their proteomes. These tests work by crushing up infected plant extracts in the field and placing them in an extraction buffer. The buffer extract is placed onto a LFD. The LFD contains antibody-coated latex beads which bind to the specific pathogen antigen absorbed from the plant extract. A coloured line is then left on the device to indicate the presence of that specific pathogen (see General Introduction).

The use of oxalic acid as a detection target for *S. sclerotiorum* has been shown to be a potentially successful way to monitor the arrival of this pathogen within a field (see Chapter 3 and 4). The SYield automated, infield machinery can capture and incubate air samples within

a liquid medium and detect the secretion of oxalic acid from growing *S.sclerotiorum* ascospores with an electrochemical biosensor. A warning of the pathogen threat can be supplied within 3 to 4 days of sampling *S. sclerotiorum* ascospores which allows growers to target their fungicide sprays more efficiently and improve protection against this disease. However, within the liquid medium in this device, there are no selective fungicides to kill off other spores of competitive fungi that may be present in the air sample. As a result there remains a risk that other fungi, for example *B. cinerea*, which will grow in this medium and also secrete oxalic acid during spore germination may cause false positive detection events. Another possibility is that there may be other fungal species in the air sampled which may outcompete *S. sclerotiorum* growth in the medium resulting in missing detection all together. For this reason, this chapter reports the identification of other unique detection targets to *S. sclerotiorum* which could be used in lateral flow devices or adapted SYield biosensors.

As there are already handheld devices available based on antibody and protein detection of fungal pathogens, it seems plausible that a new protein target could be found to identify *S. sclerotiorum* specifically. This chapter reports a novel approach to identify unique protein targets secreted by using the *S. sclerotiorum* putative secretome pipeline described in Chapter 5. A secreted protein detection target ensures that the fungal organism being detected is a living pathogen as opposed to a non-viable spore for example, which nucleic acid detection targets cannot differentiate. A potential problem with using the qPCR assays developed for the quantification of *S. sclerotiorum* DNA specifically is that the DNA from both non-viable spores as well as viable ones will be amplified.

Potential protein targets were chosen based on the probability that they would be secreted extracellularly. This also allows easier detection of the fungus in the field as there is no need for sophisticated engineering to lyophilise the fungal cells or spores which may be difficult to achieve by an automated sampling device.

This study involved the inspection of gene sequences to identify certain characteristics typical of secreted proteins. It is important that these sequences firstly have no annotation and very little homology to other eukaryotic proteins so they can be potentially patented for commercial purposes and secondly will not identify other fungal species except the species of interest.

Table 35: Sequence characteristics for detection targets.

List of sequences characteristics to include and discount when choosing novel protein sequences for selection.

Characteristics to include	Characteristics to discount
<ul style="list-style-type: none">• Amino-terminal secretory signal peptide	<ul style="list-style-type: none">• No transmembrane domain
<ul style="list-style-type: none">• Protein length ≥ 20 amino acids	<ul style="list-style-type: none">• A member of a multigene family
<ul style="list-style-type: none">• Rich in cysteine confers extracellular stability	<ul style="list-style-type: none">• Function annotated (PFAM domain)
<ul style="list-style-type: none">• Predicted proteins start with a methionine.	<ul style="list-style-type: none">• If the sequence is present in any other organism
<ul style="list-style-type: none">• Presence of a host nuclear target domain	
<ul style="list-style-type: none">• A high second extracellular prediction using WoLF PSORT	

Once protein targets were identified using the bioinformatics pipelines described in the previous chapter, molecular biology techniques were used to validate protein target secretion. Initially a range of *S. sclerotiorum* isolates and *B. cinerea* isolates were screened using PCR to check for the presence or absence of the protein gene sequences. Gene expression levels of the predicted protein gene targets *in vitro* using RT-qPCR was examined. Previously published EST libraries were explored for any EST support for the protein targets as was the RNA sequencing data presented in Chapter 8. Finally this chapter reports the generation of Green Fluorescent Protein (GFP) tagged *S. sclerotiorum* transformants which enabled the observation of the tagged proteins to validate protein expression and observe protein localisation in the fungus.

Rothamsted Research does not hold the FERA licence required to transform isolates of *S. sclerotiorum*. For this reason, two travel studentships (The John Pickett Travel Fellowship and the Society for General Microbiology President's Fund) were secured so that the transformations could be carried out in the Jeffrey Rollins Laboratory (JRL) at the University of Florida, Gainesville over a period of 3 months. This research group specialises in *S. sclerotiorum* transformation protocols.

6.2 Experimental Procedures

6.2.1 Bioinformatics

The total secretome or set of 1,060 *S. sclerotiorum* protein sequences generated in the first stage secretome analysis in Chapter 5 was used to find putative secreted protein detection targets for *S. sclerotiorum* specifically. These unique proteins were found using two methods.

Method 1

Out of the 1,060 proteins in the unrefined predicted secretome, protein sequences with a cysteine number greater than 5, a WolfP Sort score of 18 or greater and no PFAM or other annotation were selected. The sequences were subjected to blast analysis using the NCBI nucleotide Blast query to search nucleotide and EST databases. Those results with any level of confidence lower than $p < e^{-40}$ were removed. If there was any relation to other fungal species in the Blast result the sequence was disregarded from the final set.

Method 2

To identify protein sequences found only in the *S. sclerotiorum* genome and not in the *B. cinerea* genome with a significant level of confidence, Dr. John Antoniw performed a Blast comparison of the *B. cinerea* and *S. sclerotiorum* genomes using transcript sequences. These sequences were used to generate DNA blast databases. The first search used the Blastn in Blast+ to search for *B. cinerea* sequences in the *S. sclerotiorum* database and collected all sequences with e values ≤ 10 . The results with e values $\leq e^{-5}$ were extracted from the set. The gene IDs were sorted and unique IDs extracted. Comparing this with all *B. cinerea* gene IDs identified, the *S. sclerotiorum* transcripts with no hits in the *B. cinerea* transcript database were selected as unique genes to *S. sclerotiorum*. Out of this set of sequences, those found in the total secretome were extracted. This set of protein sequences were inspected and only those sequences with a cysteine number greater than 5, a Wolf P-Sort score of 18 or greater, no PFAM or other annotation were chosen. This set of genes was subjected to a Blastn analysis to find those sequences with no homologues in other fungal species.

6.2.2 GPI Anchors

GPI anchor proteins were predicted by big-PI (http://mendel.imp.ac.at/gpi/cgi-bin/gpi_pred_fungi.cgi) (Eisenhaber et al. 2004). From the set of GPI anchored proteins in the total *S. sclerotiorum*, those not found in the *B. cinerea* genome were selected for analysis.

6.2.3 Primer design used for PCR screening and RT-qPCR

Primers used to PCR screen different *S. sclerotiorum* and *B. cinerea* isolates for the presence of the predicted secreted protein targets were designed to be used for relative quantification of gene transcripts using RT-qPCR. Gene sequences were imported from the Broad *S. sclerotiorum* genome browser (www.broadinstitute.org) and primers designed in Vector NTI® (Life Technologies) to the following specifications; 20 bp in length with product sizes of approximately 150 bp, a T_m between 56 and 58 °C, 45-50 % GC content and a 50 mM salt concentration (**Table 36**). Intron spanning primers were used to ensure introns were removed during reverse transcription. *S. sclerotiorum* actin was used as the gene to compare relative expression to during RT-qPCR analysis.

Table 36: Primer sets designed for the amplification of unique *S. sclerotiorum* protein DNA sequences.

Primers to screen different *S. sclerotiorum* and *B. cinerea* isolates for the presence or absence of putative secreted protein sequences. Primers were also designed for the RT-qPCR analysis.

Gene name	Gene ID	Primer	Primer sequences for PCR screening/ RT-qPCR	PCR Product length bp
SP1	SS1G_01003	F R	CCTCCATCCTCATTCTTTCA GAACATCTAGTTGAGGAATACAGC	150
SP2	SS1G_01749	F R	TGACACGAGTTTTAACTTTGC GATGTAGAGCATGTAGTAGGAACG	151
SP3	SS1G_06412	F R	GGAAACATCTTTCCTCTCACTACT CTAACTATCAGCTCGGAGTCTG	150
SP 4	SS1G_00564	F R	GCTTCTGCCTTCTAGCTTTG CGGAAGTCTTTGGATAAGCA	107
SP 12	SS1G_10452	F R	CTTCGCAGTCACAACAATTC AGTAACTGCCGTGTTGAAGG	119
GPI 1	SS1G_03000	F R	AGTCACTCTTCTTGCTGCCT CTTCCAGAGTAGGCGTTGAC	153
GPI 2	SS1G_04875	F R	ATGATCTTCTCACGCTTGAC ATGGTGCTTTGAGAAGGTTC	134
GPI 3	SS1G_07678	F R	GGTGGAGTTTCCAAGTTGAA AGAAGCGTTGCAAGAATTTG	104
<i>S. sclerotiorum</i> specific primer set	ITS 4/5 region	F R	GCTGCTCTTCGGGCCTTGTATGC TGACATGGACTCAATACCAAGCTG	278
Intron spanning gene	SS1G_01003	F R	CATTCTGCTGTATTCTCAACT CCTTAATTAACCACGCACA	253
Actin house-keeping gene (Freeman et al. 2002)	SS1G_08733	F R	CCCCAGCGTTCTACGTCT CATGTCAACACGAGCAATG	154

* F: Forward primer. R: Reverse primer

DNA/ RNA extraction (See General Experimental Procedures)

Polymerase Chain Reaction for isolate screening (See General Experimental Procedures)

6.2.4 First Strand cDNA synthesis

S. sclerotiorum RNA was treated with DNase to remove DNA using the DNA-free™ Kit (Invitrogen, Life Technologies). DNA-free cDNA was synthesised using Superscript™ III Reverse Transcriptase (Invitrogen, Life technologies, Paisley, UK). 1 µg of total RNA per sample was used for reverse transcription according to manufacturer's protocol. cDNA was checked for gDNA contamination using intron spanning primers using RedTaq PCR.

Quantitative RT-qPCRs were carried out using SYBR Green Jumpstart Taq Ready Mix (Sigma, MO, US). ROX was used as the reference dye. cDNA was diluted 10 x with RNA free water. Per reaction: 2.5 µl of each primer (1.2 µM), 10 µl Readymix and 5 µl diluted cDNA template or water were mixed per reaction tube. Reactions were carried out using the ABI 7500 real-time PCR system (Applied Biosystems, CA, US) with ABGENE 96 well plates. Three technical replicates per template were used as well as a non-template control per gene used. Cycling parameters include a 95 °C stage for 2 minutes, then 35 cycles of 95 °C for 30 seconds, 55 °C for 30 seconds and 72 °C for 45 seconds. A dissociation step was included to check for secondary products. *S. sclerotiorum* actin gene (SS1G_08733) was used as the house keeping gene to which relative gene expression was compared.

6.2.5 Generating GFP tagged protein targets

The GFP fusion construct, pBluntNAT-Odc2GFP, was sent from the Dr. Jeffrey Rollins laboratory (JRL), University of Florida to generate GFP fusion constructs with the protein sequences of interest (**Figure 52**). This construct was designed by a PhD student Xiaofei Liang at this laboratory and has successfully been used in the past to transform *S. sclerotiorum*. The GFP codon has been optimised with the GFP intron and contains the selection marker Nourseothricin for *S. sclerotiorum* transformation and Kanamycin for *E-coli* cell selection (Leroch et al. 2011). The genes of interest were under regulation of their own promoter.

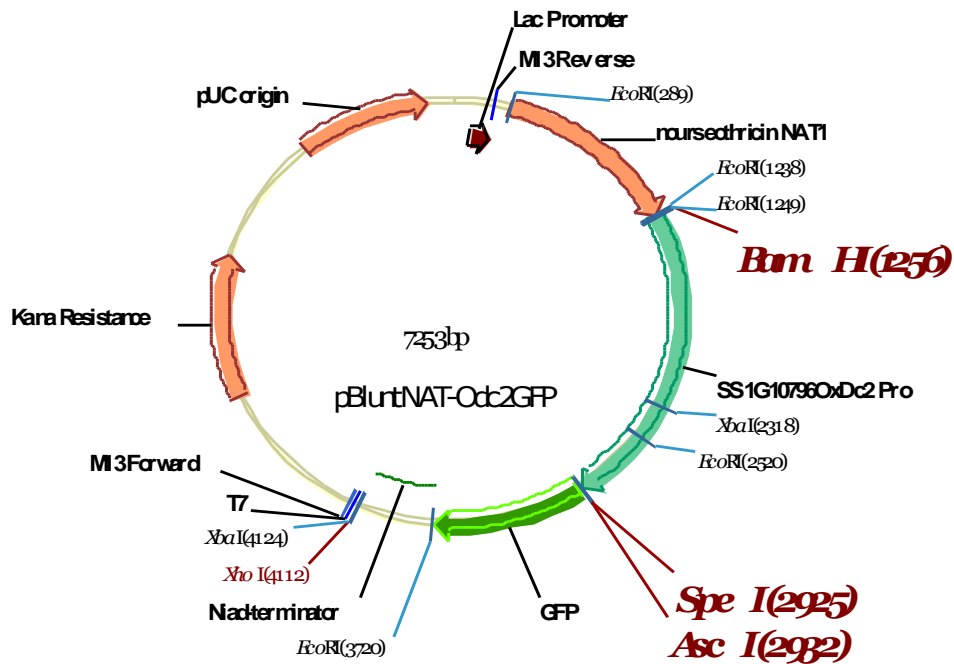


Figure 52. The pBluntNAT-Odc2GFP construct generated at JRL.

Restriction enzymes *Bam*HI and *Asc*I used to remove SS1G10796OxDc2Pro insert and then ligate the *S. sclerotiorum* protein of interest with the appropriate restriction sites. The ligated insert was designed without the gene stop codon sequence to allow continued transcription of the green fluorescent protein.

6.2.6 Transformation of competent cells with pBluntNAT-Odc2GFP vector:

3 µg of pBluntNAT-Odc2GFP construct was spotted onto the centre of a paper circle and sent from the Jeffrey Rollins laboratory, University of Florida. The paper was cut out and soaked in 300 µl sterile distilled water. After vigorous shaking, the solution was nanodropped with a concentration of 10 ng/ µl. 50 µl XL-Blue Competent cells (Agilent Technologies) were placed into to a 15 ml falcon tube using a pipette. The remaining cells were frozen at -80 °C. 0.85 µl β-mercaptoethanol (1.42 M) was added to the cells on ice. 2 µl of the plasmid was added to the cells (20 ng). The cell vector mixture was left on ice for 30 mins. The tube was then placed in a water bath for 42 °C for 45 seconds and then placed back on ice for 2 mins. 250 µl SOC was added to the mixture. The tube was incubated at 37°C for 1 hr, shaking 250 rpm. The cells were plated and streaked onto Yeast tryptone (YT) agar plates containing selective antibiotic Kanamycin (50 µg / ml).

The following day single clones were picked off the plate grown up overnight in 5ml LB medium containing Kanamycin. The cells were pelleted using a centrifuge and plasmid

minipreps made using QIAprep Spin Miniprep (Qiagen, Manchester UK) following the manufacturer's instructions. This process was repeated when constructs were re-ligated with the new template insert.

6.2.7 Restriction Digests

6.2.7.1 Verification of construct

An *Eco*-R1 digest was performed to ensure that the correct vector had been transformed into the competent cells. Per 20 μ l digest reaction, 16.3 μ l sterile, deionized water, 2 μ l restriction enzyme 10 X buffer, 0.2 μ l Acetylated BSA (10 μ g/ μ l), 1 μ l of miniprep DNA (1 μ g/ μ l) and 0.5 μ l Restriction Enzyme *Eco*RI (10u/ μ l) (Promega R6011, Southampton, UK) were added to the tube. The solution was mixed gently by pipetting, and centrifuged for a few seconds in a microcentrifuge. The solution was incubated at 37 °C for 1–4 hr. 1X Loading buffer was added to 10 μ l of digest product and run on a 1% agarose gel.

6.2.7.2 Restriction digest of construct template inserts

A double digest using *Bam*HI and *Asc*I (Fermentas, Thermo scientificTM, UK) was carried out on template inserts after DNA purification. Promega recommended the use of *Bam*HI buffer E with a 2-fold excess of the *Asc*I enzyme. Per 50 μ l reaction ; 30 ng/ μ l DNA, 4 μ l buffer E, 0.4 μ l BSA, 2 μ l *Bam*HI enzyme, 3 μ l *Asc*I enzyme and 20.6 μ l sterile water was incubated at 37 °C for 2 h. Products were run on a 1% agarose gel and bands of appropriate size excised from the gel and purified using the Promega Wizard clean up. After digestion of the vector construct, there were two bands. The largest band (5584bp) was excised from the gel which was re-ligated with the new inserts.

6.2.8 Primer design for construct template insert

Geneious 5.5.6 software (Biomatters Ltd, New Zealand) was used to carry out primer design for the protein sequence insert (**Table 38**). A maximum of 1000 bp upstream of the gene was included in the template insert to encompass the gene's promoter where possible. A shorter length of base pairs was included if the upstream gene was reached. This was checked using the Broad *S.sclerotiorum* database. The amplified insert template included a *Bam*HI restriction site at the 5' end of the gene and an *Asc*I restriction site at the 3' end (**Figure 53**). Care was taken in designing the *Asc*I site to ensure an in frame fusion with the GFP coding

sequence. The stop codon was removed to prevent immature stopping of gene expression before the GFP is expressed. There were no additional *Bam*HI / *Asc*I restriction sites within the amplified gene as this will cause further restriction of the entire gene.

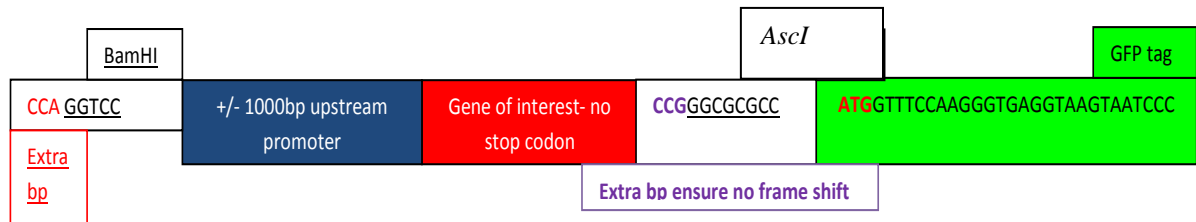


Figure 53. Primer design of construct inserts.

The amplified region must incorporate a BamHI restriction site before the promoter region, the upstream promoter region (max 1000bp), no gene stop codon and the AscI restriction site before the GFP reporter protein sequence. Extra base pairs were added into the design to keep sequence in frame with GFP fusion sequence.

6.2.9 Amplification of insert

PCR conditions using Redtaq (Sigma-Aldrich), high fidelity Phusion DNA polymerase (New England Biolabs, USA), or a Long PCR mix (Invitrogen) for larger sequences were optimised for each gene of interest. Previously used Redtaq PCR conditions were used to amplify inserts for SP1, SP4, GPi1, GPi2, GPi3 (**Table 37**). Phusion PCR system was used for SP3 (**Table 37**). Five microliter of the PCR product was run on 0.8% agarose gels to ensure that the correct single products had been amplified. If single bands were present, PCR product were directly purified using Promega Wizard clean up system by following the manufacturer's protocol. If other bands were present, the products were excised from gel first and then purified using the same system.

6.2.10 Ligation of the digested inserts and plasmid.

The Promega T4 DNA ligase protocol was followed to ligate the insert templates with the linearised construct. A 3:1 molar ratio of insert to vector was used.

Table 37. PCR conditions for the different polymerase systems used to amplify the sequences of interest.

Gene IDS	Polymerase system	Cycling conditions
SP1, SP4, GPi1, GPi2, GPi3	RedTaq	95°C/ 2mins. 35 cycles: 95°C/30sec, 55°C /30 sec, 72°C/ 45secs. Final extension 72°C/ 5mins
SP3	Phusion	98°C/ 30secs. 30 cycles: 98°C/10sec, 55°C /30 sec, 72°C/ 30secs. Final extension 72°C/ 10mins

6.2.11 Methods for Fungal Transformation

The following procedures were adopted from procedures used by the scientists at the Jeffrey Rollins Laboratory (JRL), Department of Plant pathology, University of Florida (Rollins 2003).

6.2.11.1 Protoplast production

S. sclerotiorum 1980 isolate was grown and maintained on PDA Petri dishes. A glass Petri dish containing 25 ml of PDB was inoculated with hyphae from the actively growing culture. The hyphae were harvested after 3-5 days once the plate was covered but before sclerotia initials were observed. The hyphal mass was washed with sterile water and 1x protoplast buffer (0.8 M Magnesium sulphate, 0.2 M Sodium citrate, pH 5.5) over a funnel lined with sterile cheesecloth. The mycelium was then chopped up in sterile conditions and transferred to a 125 ml Erlenmeyer flask. 200 mg Glucanex was dissolved in 3 ml Novozyme buffer (1 M Sorbitol, 50 mM Sodium citrate, pH 5.8) and sterile filtered using a 0.45 µm filter. This was added to 17 ml protoplast buffer and poured over the mycelium. The flask was incubated at 28 °C while being shaken continuously for 3 hours. The protoplasts were separated from the residual hyphae by filtering through autoclaved nylon mesh over a sterile 125 ml flask. 30 ml of 0.6 M KCl was poured over the protoplasts. The protoplasts were centrifuged in 50 ml disposable conical tubes at 3000 xg (AB50.10 5000 rpm) at 4 °C for 10 min. The protoplasts were washed with 10 ml 2x STC and centrifuged as above. The pellet was suspended in 800 µl 1x STC (1 M Sorbitol, 50 mM Tris, 50 mM Calcium chloride, pH 8) and the protoplasts counted. The concentration of protoplasts was adjusted to 1×10^8 / ml and kept on ice. 12.5 µl DMSO, 62.5 µl Heparin (5 mg/ ml in STC) and 250 µl 40 % PEG (mix 2

parts 60 % PEG in water and 1 part KTC; 1.8 M KCl , 150 mM CaCl₂,150 mM Tris, pH 8,) were added to 1 ml protoplasts. Protoplasts were routinely frozen at -80°C.

6.2.11.2 Transformation of *S.sclerotiorum* protoplasts

Constructs made at Rothamsted Research, were transformed back into competent cells (cell stock previously made in JRL) along with a control constitutive GFP expressing construct, p-BluntNAT-OliC-GFP (GFP) (**Figure 54**). Filter paper discs containing the transported constructs were cut up and placed in 200 µl sterile water. 10 µl was added to 100 µl cells and incubated on ice for 30 mins. The cells were then incubated for 1 hr at 37 °C in LB liquid. The cell mixture was plated evenly onto LB agar plates containing 400 µg/ ml Nourseothricin selection agent. Visible colonies were picked off the plates the following day and grown up in 20 ml LB medium. Plasmid preps of the cells were made. PCR was used to check whether colonies contained the inserted gene using original primers used to make the insert (**Table 38**).

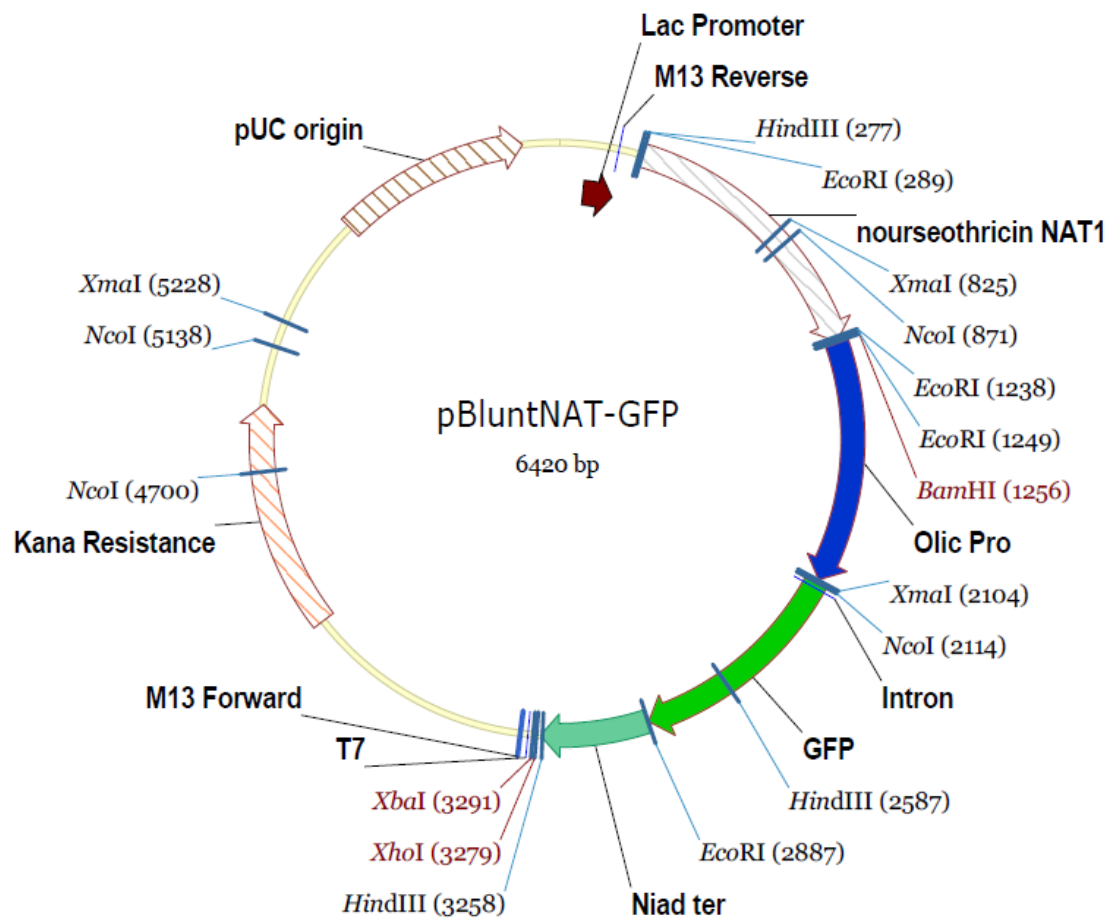


Figure 54. The pBluntNAT-GFP construct.

Used as a constitutive GFP control during transformation of *S. sclerotiorum*. Construct generated by Dr. Matthias Hahn, Department of Biology, University of Kaiserslautern, Kaiserslautern, Germany (Leroch et al. 2011).

Table 38: Primer sets designed to amplify construct inserts of putative secreted proteins.

The forward primers include a BamHI restriction site (purple) and the first 21 bases of the upstream promoter (blue). Reverse primers include the reverse complement of the end of the secreted protein sequence, without the stop codon but include an AscI restriction site (purple) which links to the GFP insert (blue). In both primers, 3 extra bases were added to prevent frame shifts (red).

Name	Position on Locus	Position of upstream gene	Distance from previous gene	Forward primer with BamHI site (first 21 bp with restriction site)	Reverse primer with AscI site (reverse complement without the stop codon in the sequences to keep it in frame!)	upstream promoter bp	Length of PCR product
SP1	Supercontig 1: 2579461-2579910	SS1G_01002.3, ends at 2576438	3023	CCAGGATCCAAATGGCTCTGAATCG TAAAA	CCGGGCGCGCCATGTTGAACTGCCT CACT	1000	1470
SP2	Supercontig 2: 1757253-1758640	SS1G_01748, ends at 1755526	1727	CCAGGATCCTATATAATTAATAATCA AAATC	CCGGGCGCGCCATCCACCACGCTA CCAAAGT	1000	2408
SP3	Supercontig 8: 245616-246633	SS1G_06411, ends at 243865	1751	CCAGGATCCATGATGTTCAAGGAAA CATCT	CCGGGCGCGCCATCGACTCTGTAC TAAGAAT	1000	2038
SP4	Supercontig 1: 1470162-1471188	SS1G_00563, ends at 1469714	448	CCAGGATCCAGCTGTGATACCTACA GCTTCAAG	CCGGGCGCGCCTCTACCTGGGAATG GAACTTT	300	1347
Gpi1	Supercontig 3: 2333058-2333486	SS1G_02999.3 ends at 2329017	4041	CCAGGATCCGGCATGCCCGTTTGT ATTTA	CCGGGCGCGCCGATTGAACAGAG ACTGAA	1000	1449
Gpi2	Supercontig 6: 123166-123596	SS1T_04874 ends at 121890	1276	CCAGGATCCAGCGGCAGGTCAACA TACA	CCGGGCGCGCCAAAAACATCAAA CCCAAAC	1000	1451
Gpi3	Supercontig 10: 432214-432589	SS1T_07677 ends at 431327	887	CCAGGATCCGCTGGTAGATAAGCTG ATAA	CCGGGCGCGCCTATAAGAAGCGTTG CAAG	700	1096
GFP	Based on HQ423138.1 GFP sequences			GTTGAAGGGCATCGATTTC AAGGAA	TTCCTTGAAATCGATGCCCTTCAAC	Only reverse primer used to reverse sequence constructs	

6.2.11.2 Continuation of transformation of *S.sclerotiorum* protoplasts

5×10^6 protoplasts (50 μ l) in STC were added to each chilled DNA (1-5 μ g) suspension and incubated on ice for 30 min. 1 ml of PEG solution was added to the protoplast-DNA suspension gently mixed. The tubes were incubated at room temperature for 20 min. Each suspension was evenly spread on the surface of a RM bottom agar plate (Modified Fries Medium / L: 239.6 g Sucrose, 5 g NaNO_3 , 1 g KH_2PO_4 , 0.51 g $\text{MgSO}_4 \cdot 7\text{H}_2\text{O}$, 0.5 g NaCl , 0.065 g $\text{CaCl}_2 \cdot 2\text{H}_2\text{O}$, 15 g/L Agar). The suspension was spread by pipetting the solution to the center of the plate and tilting the plate in a circular fashion. Petri dishes were incubated overnight at room temperature. The following day the plates were overlaid with 5 ml of RM top agar (RM agar adjusted with 8 g/L Agar) containing 400 μ g/ml Nourseothricin. Regenerating colonies were observed after 5 days. Plates were observed under GFP fluorescence filter under a Leica compound microscope and individual colonies showing evidence of fluorescence were picked and transferred to 3 compartmental Petri dishes containing PDA with 400 μ g/ml Nourseothricin. The growing hyphal tips were cut under a dissecting microscope and transferred to a new compartment on the petri dish at least 3 times to purify the genetic material. This also enabled selection of stable lines or a culture that had more uniform fluorescence.

6.2.11.3 DNA extraction for southern and PCR

Cultures of transformants (SP1B/E, SP4B/D, Gpi2a, GFP1/2) were grown on cellophane discs over PDA until it covered the plate. Fungal tissue was collected, lyophilised, frozen and ground up into a fine powder using a bead beater. 100 μ l of powder by volume was added to a 1.5 ml microfuge tube with 1 ml extraction buffer (50 mM EDTA, 0.2 % SDS) and vortexed. Tubes were incubated for 15 min at 68 °C and vortexed. Tubes were centrifuged for 5 min at 20'000 x g at room temperature. The supernatant was transferred to a clean 1.5 ml tube containing 60 μ l KAC buffer (60 ml 5 M potassium acetate, 11.5 ml glacial acetic acid, 28.5 ml distilled water).

Tubes were inverted tube 4-6 times and placed on ice for 5 min. Tubes were spun at room temperature for 5 min at 20 000 x g. The supernatant was transferred to a 2 ml round bottom microfuge tube containing 1.2 ml isopropanol and mixed vigorously. The tubes were centrifuged at room temperature for 5 min at 16 000 x g and the liquid decanted. Tubes were drained by inverting on paper towel and transferred to a vented hood for 15

min. 400 µl TE containing 10 µl RNase to 1ml TE was added to each tube and incubated for 30 min at 37 °C. Tubes were then placed on a bench top rotisserie (Labquake, Thermo Scientific™, USA) for 30 min. 20 µl 10 M LiCl to was added to each tube and mixed. 1 ml 95 % ethanol was added to each tube and then spun at 16 000 xg for 5 min. Liquid was removed and the pellet washed with 1ml 70 % ethanol. The tubes were centrifuged for 2 min to secure the pellet in tubes dried as previously described. The pellets were dissolved in 100 µl TE and incubated for 15 min at 55 °C. Tubes were placed on the rotisserie overnight for thorough mixing. 2 µl of sample with loading dye was run on 0.8 % 0.5 x TBE agarose gel containing ethidium bromide (EtBr) to estimate concentration. DNA was also quantified using Nanodrop 1000 spectrophotometer.

6.2.11.4 Polymerase chain reaction for verification of gene integration

To verify the integration of the gene of interest, PCR assays were completed using the original primers designed to amplify the template insert as well as primers designed to amplify a small section of the GFP tag, (GFP F; ATCTTGGTCGAACTCGATGG, GFP R: AGGCAATTTACCTGTGGTGC). The PCR was carried out in a 25 µl reaction containing 10 ng of DNA, 10 µM of each primer, 2.5 µl PCR buffer (Promega), 2 µl MgCl₂, 0.5 µl dNTPs, 0.2 µl Taq polymerase (NEB). The thermocycler parameters; 4 min at 94 °C, 30 cycles of 1 min at 94 °C, 1min at 55 °C, 1 min at 72 °C and a final extension step of 7min at 72 °C. 2 µl of sample with loading dye was run on 0.8 % 0.5x TBE agarose gel containing ethidium bromide (EtBr).

6.2.11.5 Southern Blot

6.2.11.5.1 DNA digestion

Transformant DNA (SP1B, SP1E, SP4B, SP4D, Gpi2a, GFP1, GFP2 and a control untransformed strain UF-70) were digested using *EcoRI* enzyme and Buffer 2 (NEB, USA) system. The enzyme cut the construct in 4 places resulting in band sizes; 949 bp, 1271 bp, 1200 bp and 3533 bp. Per 50 µl digest reaction; 5 µl buffer 2, 2 µl *EcoRI* enzyme and 10 µg DNA were mixed in a 1.5 ml tube. Samples were incubated at 37 °C overnight. The enzyme was deactivated by heating at 65 °C for 15 min. Digestion products were separated overnight by electrophoresis on a 0.8 % gel containing EtBr.

6.2.11.5.2 Probe synthesis

A probe was designed to hybridise with approximately 292 bp of the GFP tag for all of transformants. Primers (GFP Southern F: TTCCAATCTTGGTCGAACTC, GFP southern R: CGAGTCTTATAATTTCCGTC) were designed to amplify from 50 to 380 bp of the GFP insert in order to generate a probe using DIG labelling PCR. Genomic DNA isolated from the original SP1 plasmid prep used to transform *S. sclerotiorum* protoplasts was used as a template during PCR. For a single 25 µl probe reaction, 2.5 µl buffer, 1.5 µl 10 x MgCl₂, 1µl DIG labelling PCR Mix (Roche, Germany), 0.3 µl 10 mM dNTPs, 0.15 µl Taq (NEB, USA), 2 µl of each 10 mM primer, 1 µl DNA template and 10.45 µl water were added to PCR tubes. PCR conditions: 94 °C for 4 mins, 30 cycles of 94 °C for 1 min, 55 °C for 1 min and 72 °C for 1 min. Final extension step at 72 °C for 7 mins.

6.2.11.5.3 Southern blot and hybridisation

The gel containing the digested products was soaked in 0.25 N HCL for 10 mins while gently shaking. HCL was removed and the gel soaked for 30 min in Denaturing buffer (0.4 N NaOH, 0.8 M NaCl). After removal of the buffer, the gel was soaked in Neutralisation buffer (1.5 M NaCl, 0.5 M Tris-HCl, pH 7.6) for 30mins.

A 4 cm pile of paper towels were stacked up and overlaid with several sheets of 3 mm filter paper the same size as the gel. A nylon membrane (Roche, Germany), cut to the size of the gel was placed over the upside of the gel. The membrane and gel were placed over the filter paper. Another stack of five gel sized 3 mm filter papers were stacked over the gel. A filter paper bridge was placed over the gel paper stack linking it to a tray containing transfer solution (20X SPPE: 3.6 M NaCl, 0.2 M NaH₂PO₄.H₂O, 0.02 M EDTA). The stack was left overnight.

The membrane was rinsed briefly with 2X SSPE. A prehybridization buffer (6 X SSPE, 1% skim milk, 0.5% SDS) was dissolved in water at 65 °C and the membrane washed in prehybridization buffer for at least 2 hours at 65 °C. 500-600 ng of probe was added to the Hybridization buffer and boiled for 20 mins. The membrane was then washed in hybridization buffer (6 X SSPE, 1% blocking reagent, 0.5% SDS) at 65 °C in a heated rotisserie.

6.2.11.5.4 Washing and detection

The membrane was then washed 3 times for 20 mins at 65 °C in a solution containing 2X SSPE, 0.1 % SDS and 0.1 % sodium pyrophosphate in a heated rotisserie. The membrane was washed in a 100 ml rotisserie glass tube. The membrane was then further washed in a solution of 0.2X SSPE, 0.1 % SDS and 0.1 % sodium pyrophosphate, for 20 min, 3 times at 65°C.

6.2.11.5.5 Chemiluminescent detection film development

The membrane blot was equilibrated for 5 mins in 30 ml Buffer 1 (0.1 M Tris, 0.15 M NaCl). It was then incubated in 30 ml buffer 2 (Skim milk and Buffer1 which had been previously heated to 75 °C), for 1 hr. The blot was then incubated for 30 min in 20 ml buffer 2 containing Anti-Digoxigenin-AP Ab 1:20,000 to a final concentration of 37.5 mU /ml. The blot was then washed in 30 ml Buffer 1 for 15 mins four times to remove traces of antibodies. The blot was then equilibrated for 5 mins in 20 ml buffer 3 (0.1 M Tris, 0.1 M NaCl, 50 mM MgCl₂).

6 µl of CSPD was added to 10 ml of Buffer 3. 500 µl of Buffer 3 was pipetted into the centre of cling film placed on a bench top. The membrane was placed DNA side down onto the buffer solution. The membrane was covered to prevent it drying out and then placed in a freezer bag. The bag was sealed using a heat sealer and then incubated. The membrane was then exposed to an x-ray film (Kodak) overnight in a light tight box.

6.2.11.5.6 Film development

The film was developed in a dark room using a safe light. The film was washed in trays containing development solution for 10 secs, then in Stop solution for 1 min and then in Fixing solution for 1 min. The film was then rinsed in running water and hung up to dry.

6.2.12 GFP fluorescence under different environmental growth conditions

The successfully tipped transformants were grown under a range of conditions to determine whether the protein expression of interest was induced *in planta*, *in vitro* or was constitutive. The transformants were kept under Nourseothricin selection during the media growth tests. They could not be kept under selection during the onion infection assay.

6.2.12.1 Solid growth

Transformant agar plugs were used to inoculate a variety of media. Plugs were grown on PDA plates (30 g/ L) on the agar surface and on top of sterile cellophane discs. Transformant agar plugs were grown on water agar plates and water agar plates overlaid with lily pollen (*Lilium candidum*). Plates were observed using a GFP fluorescent filter on a Leica compound microscope on a daily basis over a period of 20 days.

6.2.12.2 Liquid medium

Transformant agar plugs were transferred to flasks containing 50ml of YP sucrose liquid medium (/L; 4 g yeast extract , 1 g K₂HPO₄, 0.5 g Mg₂SO₄, 15 g sucrose, pH to 6.5) and 50 ml PDB liquid medium and incubated at room temperature, unshaken. Filtered mycelium was observed using a GFP fluorescent filter on a Leica compound microscope at day 4 and 7 of incubation.

6.2.12.3 In planta infection

Yellow onions were cut into segments. Three single onion segments were inoculated with an agar plug per transformant (**Figure 55**). The segments were misted with sterile water and placed in a sealed container to increase humidity. After 24 hr the top epidermis layer of infected onion was peeled off and placed on a microscopy slide for observation using GFP fluorescent filter on a Leica compound microscope.



Figure 55. Onion infection assay.

Three onion segments inoculated with agar plugs per transformant. Segments incubated in a misted box overnight at 22 °C. The top epidermal observed under green fluorescence filter.

6.3 Results

The initial gene search for unique proteins targets for this study was performed before the multispecies proteome comparison was completed (Chapter 5). As a result, some protein targets originally chosen for analysis, were found at a later date to have homologous protein sequences in other fungi. This is principally a result of more genomic information being added to the public domain over the past three years of this study. The amount of annotation information which is added to the NCBI is continually growing.

6.3.1 Bioinformatics

6.3.1.1 Gene selection method 1

Out of the 1,061 protein sequences in the total secretome, 344 protein sequences were selected which have 5 or more cysteine residues in the mature protein. From this set 247 proteins have a Wolf-P-Sort score of 18 or more. Eight of these sequences contain no PFAM domain or other annotation. These 8 sequences were subject to a blast analysis to find those sequences with no homology with any other fungal species in the NCBI nucleotide and EST databases. From this group three sequences (**Table 39** **Table 39**) appear to be unique to *S. sclerotiorum*.

Table 39. Three sequences unique to *S. sclerotiorum*.

Gene name	Gene ID	Mature length of protein	Wolf-P SORT score	No.of cysteines	E-value	Organism with sequence similarity (top hit) NCBI Blastn
SP1	SS1G_01003	89	25	8	0.38	<i>Amphidinium carterae</i>
SP2	SS1G_01749	401	20	15	0.46	<i>Coffea arabica</i>
SP3	SS1G_06412	237	18	7	0.95	<i>Torpedo californica</i>

6.3.1.2 Gene selection method 2

The *S. sclerotiorum* genome was compared to the *B.cinerea* genome. A total of 4,722 gene sequences appear to be found in the *S. sclerotiorum* genome but not in the *B. cinerea*. Of these sequences 39 were found in the *S. sclerotiorum* refined secretome. These sequences have a Wolf P-Sort of 18 or greater and no transmembrane domains. Fourteen of these sequences contain six or more cysteines. Out of this set, five of these have no annotation and have no homology with any other proteins found in other fungi (**Table 40**).

Of these five, three of the sequences were found in the gene selection Method 1 and taken forward for further screening to find those sequences with no homology with any other fungal species in the NCBI nucleotide and EST databases

Table 40: Five sequences unique to *S. sclerotiorum* found that are not in the *B.cinerea* genome.

Gene names	Gene ID	Mature length of protein	Wolf-P SORT score	No. of cysteines	E-value	Organism with sequence similarity (top hit) NCBI Blastn
SP1	SS1G_01003	89	25	8	0.38	<i>Amphidinium carterae</i>
SP2	SS1G_01749	401	20	15	0.46	<i>Coffea arabica</i>
SP3	SS1G_06412	237	18	7	0.95	<i>Torpedo californica</i>
SP 4	SS1G_00564	283	27	12	4.2	<i>Mus musculus</i>
SP 12	SS1G_10452	174	26	8	0.75	<i>Arabidopsis thaliana</i>

6.3.1.3 GPI Anchor analysis

Sequences from the total *S. sclerotiorum* secretome containing a Glycosyl Phosphatidyl Inositol (GPI) anchor were investigated as these proteins may not be fully secreted but remain tethered to the exterior of a hyphal cell. These sequences usually do not possess a transmembrane domain and no cytoplasmic tail so that although they are not fully secreted but are always tethered to the extracellular side of the plasma membrane (Brown and Waneck 1992). If these proteins are expressed early enough they could be used as a suitable detection target. Out of the 1061 sequences in the unrefined secretome, 75 contain a GPI Anchor. Of these sequences, three had no homology in the *B. cinerea* genome. Only SS1G_03000 was found in the refined *S. sclerotiorum* secretome. The other two proteins had a Wolf P-Sort score of 16 which is a prediction that that these proteins are to be secreted or be anchored in the plasma membrane. Blastn and Blastp analysis revealed that none of the sequences had any homology with any sequences in other fungal species. All three proteins were taken forward for further analysis including PCR and gene expression testing (**Table 41**).

Table 41: *S. sclerotiorum* sequences containing GPI anchor motifs with no homologues in the *B. cinerea* genome.

Gene name	Gene ID	GPI Anchor	Protein length	WoLFP SORT	No. Cysteine	TM domain	E-value	Top hit) NCBI Blastn
Gpi1	SS1G_03000	Y	107	extr=25	6	0	0.45	<i>Leptosphaeria maculans</i>
Gpi2	SS1G_04875	Y	89	plas=16	4	1	0.17	<i>Aspergillus fumigatus</i>
Gpi3	SS1G_07678	Y	32	plas=10	1	1	0.25	<i>Ehrlichia chaffeensis</i>

6.3.2 Screening of isolates

The presence/absence of the selected gene sequences were screened across a variety of *S. sclerotiorum* isolates using PCR (See General Experimental Procedures for isolate list). The majority of genes were PCR screened across at least 12 isolates of mixed origins (English, Polish and American). The gene sequences were also screened across five *B.cinerea* isolates to check there is no sequence present in this related species. If the PCR results were negative the first screen they were re-screened a second time to confirm the negative result. A control primer set was used which amplifies only *S. sclerotiorum* DNA. These primers are designed based on the fungal Internal Transcribed Sequences (ITS) 4 / 5 region of *S. sclerotiorum* (Freeman et al. 2002). This region of the fungal genome is highly variable and surrounds the 5.8 S-coding sequence between the Small SubUnit-coding sequence (SSU) and the Large SubUnit-coding sequence (LSU) of the ribosomal operon (White et al. 1990).

Only sequences present in more than 80% of the *S. sclerotiorum* isolates tested and not in the *B. cinerea* isolates were taken forward gene expression analysis (**Table 42**). SP12 was not taken forward after screening because the sequence was only detected in 75% of the isolates tested. Most of the sequences were found in another *Sclerotinia* species, *S. trifoliorum*. These sequences were still used for the analysis as both *Sclerotinia* species cause a similar in many of the same host plants although *S. trifoliorum* is mainly a problematic disease on legumes, (perennial clover and alfalfa) in North Temperate regions (Lithourgidis et al. 2007). It would still be useful to be able to have a detection system for both.

Table 42. Set of putative *S. sclerotiorum* detection targets.

The final group of proteins taken forward for PCR screening to look for presence in at least 12 *S. sclerotiorum* isolates and absence in 5 isolates of *B. cinerea*.

Gene IDS	WoLF-PSORT score*	No.of cysteines	Present in <i>S. sclerotiorum</i> isolates		Present in <i>B. cinerea</i> (5 isolates)	Present in <i>S. trifoliorum</i> R316 isolate
SP1	extr=25	8	12/13	94%	No	Yes
SP2	extr=20	15	12/13	100%	No	Yes
SP3	extr=18	7	13/13	97%	No	Yes
SP 4	extr=27	12	16/16	100%	No	Yes
SP 12	extr=26	8	12/16	75%	No	No
GPI 1	extr=25	6	16/17	94%	No	Yes
GPI 2	plas=16	4	16/19	84%	No	Yes
GPI 3	plas=10	1	12/12	100%	No	Yes

*WoLF-P SORT score is the prediction of where that protein sequence is predicted to localise with or out of the cell. extr ; extracellular localisation of the protein. plas = protein localise in the plasma membrane.

6.3.3 EST support and relative gene expression of unique putative secreted proteins.

The expression of the putative secreted proteins was investigated using RT-qPCR. The expression of the selected genes was investigated *in vitro*. Ascospores were grown in 1 ml PDB medium and the mycelium harvested after five days of incubation. Two biological replications were used in the experiment. The expression of the selected secreted proteins was normalised against the *S.sclerotiorum* actin gene (SS1G_08733). At this particular time point, there was minimal expression of SP1, SP2, SP3, Gpi1 and Gpi2. SP4 and Gpi3 had the highest relative expression (**Figure 56**). Although SP3 (SS1G_06412) did not have high relative expression in this experiment, this gene had 96 EST counts in the developing apothecia EST library (G787) downloaded from the Broad Sclerotinia sclerotiorum genome. This gene probably requires fungal material for RNA extraction to be collected at a different developmental stage, when the apothecia develop from sclerotia rather than during hyphal growth. There was no EST support for the other genes of interest. These genes may also require different environmental stimuli or developmental conditions to be expressed. It is for this reason that it was decided to GFP tag the proteins of interest to find out when the proteins were expressed, if at all, instead of doing many more RT-qPCRs which would have become very costly.

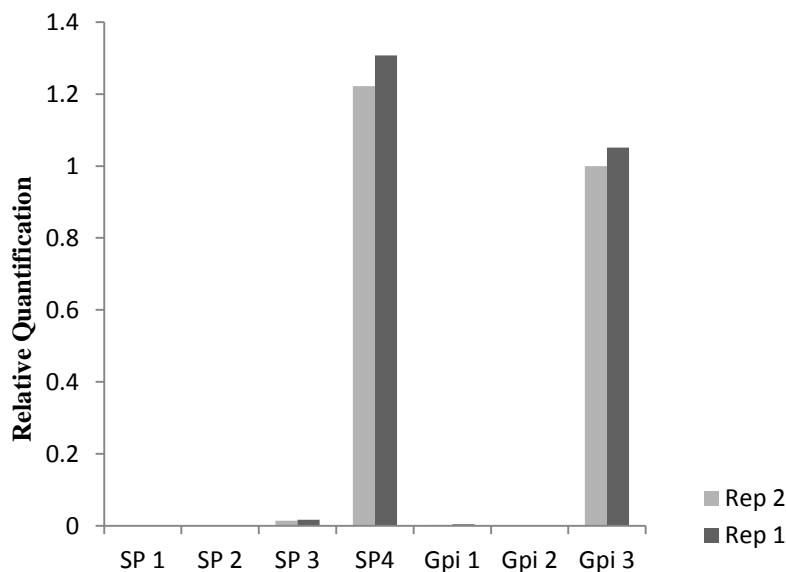


Figure 56. The relative quantification of putative secreted proteins.

RNA collected after five days of incubation after spore germination in liquid media. Transcripts normalised against actin .

6.3.4 RNA sequencing expression

The eight genes of interest were assessed for expression in the five libraries submitted for RNA sequencing (see Chapter 7 for further information on methods and how sequencing was performed). The Fragments Per Kilobase of transcript per Million mapped reads (FPKM) for the selected genes was calculated for each of the libraries sequences. There was extremely low FPKM values and this suggests that in these libraries there was nearly no expression of these genes (**Table 43**).

Table 43.The FPKM values for the 8 putative secreted protein gene sequences.

FPKM** values						
RTqPCR	Gene ID	WT T0*	WT T1*	WT T2*	OAH T0*	OAH T1*
Gene ID						
SP1	SS1G_01003	0.052853	0.336168	0.130108	0.712253	0.336168
SP2	SS1G_01749	0	0	0.085446	0	0
SP3	SS1G_06412	0	0	0.565262	0.110515	0
SP 4	SS1G_00564	0	0	0	0	0
SP 12	SS1G_10452	0.963025	0.510434	2.76577	0	0.510434
GPI 1	SS1G_03000	0	0	0	0	0
GPI 2	SS1G_04875	0	0	0	0	0
GPI 3	SS1G_07678	0.098281	0.156277	0	0	0.156277

*** Sequenced library conditions:**

WT T0: Wild type *S. sclerotiorum* grown on PDA and cellophane disc. Mycelium was taken from expanding edge of plate.

WT T1: Arabidopsis leaves infected with Wild type *S. sclerotiorum*, collected at 12hr PI.

WT T2: Arabidopsis leaves infected with Wild type *S. sclerotiorum*, collected at 24hr PI.

OAH T0: Oxalic acid deficient mutant grown on PDA + cellophane disc. Mycelium was taken from expanding edge.

OAH T1: Arabidopsis leaves infected with Oxalic acid deficient mutant, collected at 24hr PI.

**FPKM: Fragments Per Kilobase of transcript per Million mapped reads

6.3.5 GFP transformation: construct development

Attempts were made to make GFP fused constructs for all seven putative secreted proteins at Rothamsted Research. However due to time constraints only three constructs (SP1, SP4 and Gpi2) were successfully generated to be later transformed at the JRL. These three constructs were sequenced by Eurofins MWG Operon (UK), to ensure the fusion junctions of the insert and the GFP were accurate and no frame shifts had occurred during insert amplification (**Figure 57**)

6.3.6 *S. sclerotiorum* transformation

S. sclerotiorum isolate UF70 (the original WT 1980 strain sequenced by the Broad Institute) was successfully transformed with three constructs separately. After successive rounds of hyphal tipping to purify the genetic material, two stable transformant strains (which continued growing after subsequent hyphal tipping) were isolated for the SP1:GFP constructs (SP1b, SP1e), two stable transformant strains were isolated for SP4:GFP (SP4b, SP4d) and one stable line was generated for Gpi2:GFP (Gpi2a). With each separate *S. sclerotiorum* transformation, the constitutive GFP expressing construct (BluntNAT-OliC-GFP) was transformed as a positive control. Two of these transformations were stable (GFP1, GFP2) and enabled qualitative comparison of GFP fluorescence in the other transformants.

PCR was used to amplify the protein sequence insert and the GFP insert to ensure the presence of the full fusion construct (**Figure 58**). The original construct insert primers and GFP primers were used to amplify the two regions of the insert (**Table 38**). These confirmed that the amplified insert was present in the transformant DNA.

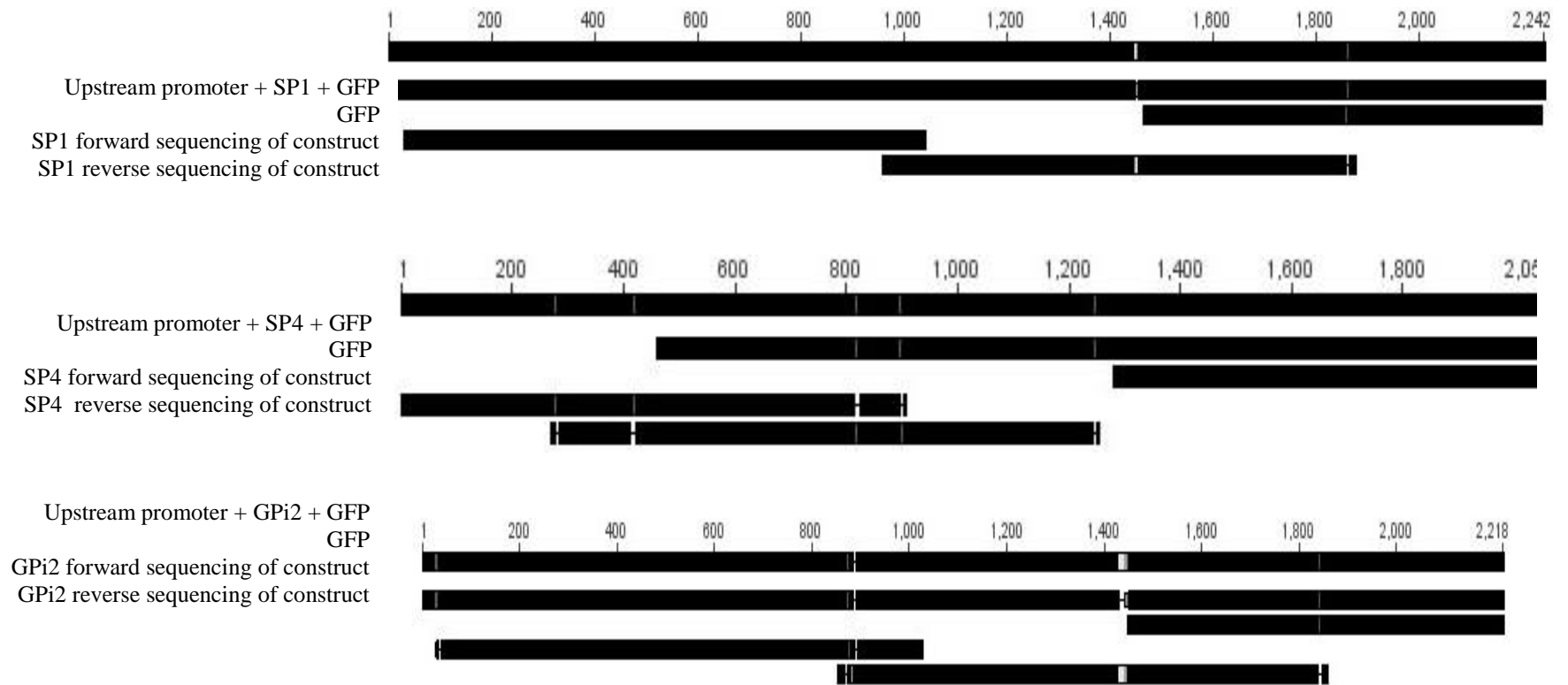


Figure 57. Sequencing of the final re-ligated pBluntNAT-Odc2GFP construct.

Construct contained inserted protein sequences fused to GFP reporter sequence for transformation. Forward sequencing of the upstream promoter starts with the *Bam*HI restriction site. Reverse sequencing across the GFP protein contains some of the GFP protein sequence, the *Asc*I restriction and the end of the secreted protein sequence. The breaks between the end of the insert and the GFP reporter are the extra base pairs added into the sequences to keep it in-frame.

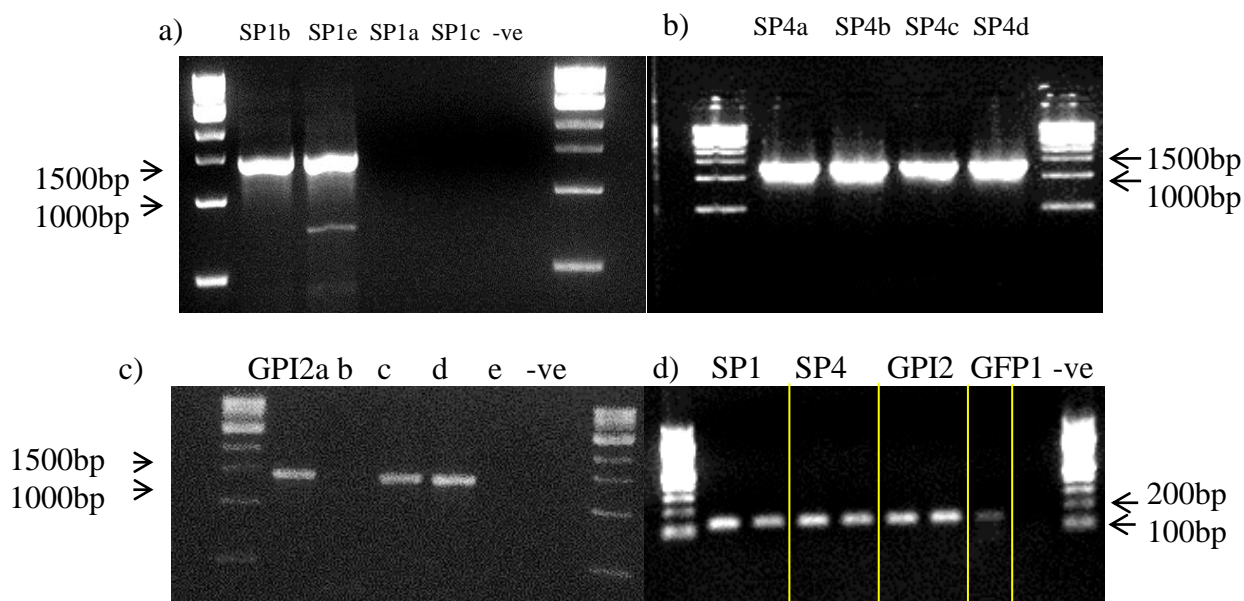


Figure 58. PCR verification of transformed cultures.

a) Four different SP1 transformants isolated during hyphal tipping. 1470 bp band in SP1b and SP1e. b) Four SP4 transformants isolated during hyphal tipping 1347 bp band seen in all four transformants. SP4b and SP4d used in further characterisation tests. c) Five GPI2 transformants isolated after hyphal tipping. 1451 bp band seen in GPI2a, c and d. GPI2a used in further characterisation tests. d) GFP insert amplified in all transformants for further testing.

6.3.7 Southern Blot

Southern blot hybridization was used to screen integration events in all transformants used in further growth characterisation tests (**Figure 59**). The strongest band at roughly 300 bp indicates that there was a successful integration event in 6 of the 7 transformants as there is a definite band at in lanes 1 to 6. There was no band present in the control untransformed control fungal strain as expected. The GFP1 transformant had the appropriate band however the band in GFP2 is very faint suggesting that the transformation event may not have worked efficiently and so was not used in growth tests. The other banding pattern in the background is a result of the partial digests and overexposure of the photographic paper.

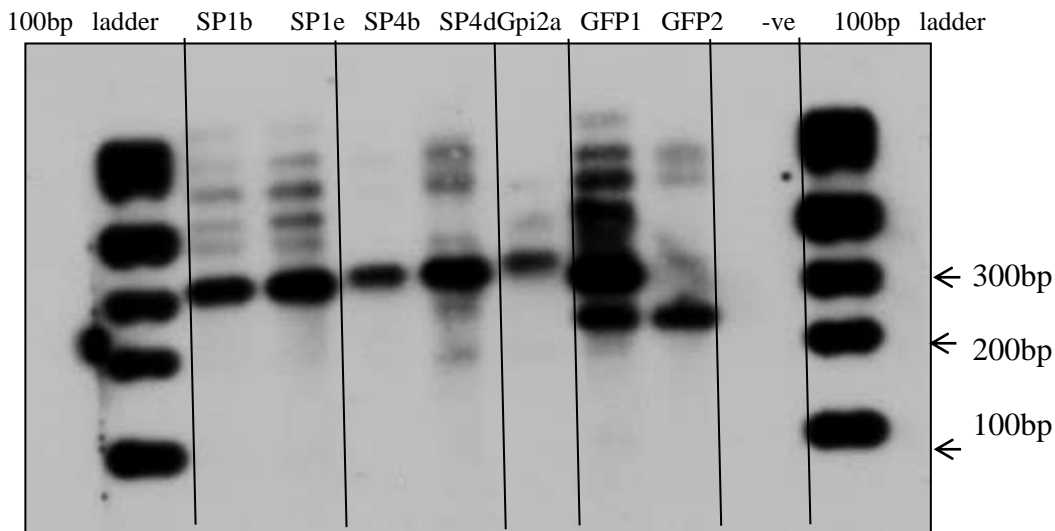


Figure 59. Southern blot of the *S. sclerotiorum* transformants generated.

The hybridisation probe was designed to bind to 300 bp of the GFP insert for all the transformants. Transformants SP1b, SP1e, SP4b, SP4d, Gpi2a and GFP1 have been successfully transformed. GFP2 constitutive expressing strain does not have a clear band of this size so transformation may not have been efficient

6.3.8 GFP fluorescence of secreted proteins under different growth conditions.

All transformants were grown under different conditions to assess what environmental conditions or developmental stages induce putative protein expression and secretion. The transformants were kept under Nourseothricin selection when possible, except during the onion infection assay. All transformed strains displayed normal growth compared to the untransformed wild type (WT) strain when grown on PDA (**Figure 60**). All transformants produced sclerotia after 12 days of growth on the plates comparable to the WT strain. The only differences in sclerotia size were seen in SP1e, SP4b, SP4d and Gpi2a which had smaller sclerotia compared with the WT sclerotia.

When strains were grown on cellophane discs on top of PDA (**Figure 61**), a strong GFP signal was observed in the constitutive GFP1 transformant and a lower GFP signal in SP1b and SP1e transformants. SP4 and Gpi2 transformants had no GFP fluorescence. The SP1 GFP fluorescence was not uniformly observed in all hyphae as with the constitutive GFP1 strain. Under the microscope the fluorescence appeared to localise more to the growing edge of the colony, although sometimes the signal would appear randomly in a localised section of a single hyphae.

When transformants were grown in flasks of YP sucrose broth at room temperature, without shaking, only the GFP1, SP1b and SP1e strains grew (**Figure 62**). Hyphae was filtered from the liquid, thinned and observed under a GFP filter. SP1b and SP1e had strong GFP signals, comparative to the constitutive expressing strain GFP1 at four and seven days incubation suggesting this protein can be induced to express for a prolonged period of hyphal growth. The GFP fluorescence was more uniformly spread across the hyphae unlike the GFP signals observed for the same transformants grown on PDA plates. Fluorescence in the SP1 transformants appeared slightly blurred compared to GFP1 fluorescence which suggests that this protein was extracellularly secreted rather than maintained in the hyphal cells. Submerging this transformant in a liquid growth medium may be the trigger for this protein to be switched on and secretion.

When transformants were grown on water agar plates the transformants appeared to grow as the wild type; an expanding colony with less hyphal biomass. GFP fluorescence was only observed in the constitutive GFP1 transformant (**Figure 63**). Lilly pollen was spread over water agar and the transformants grown on the plates. Lilly pollen was used to see whether any metabolites within the pollen may stimulate protein production. There was some GFP fluorescence in the hyphae of SP1e and SP4d (**Figure 64**) grown under this condition. This expression was seen at both the expanding edge of the colony and in other hyphae in the main body of the colony. There was no expression observed in SP4d and GPi2a.

Agar plugs taken from the edge of expanding transformant colonies grown on PDA plates were used to infect onion segments. SP1b and SP1e had good GFP fluorescence in the onion epidermis infection assay (**Figure 65**). The signal is not as strong as the GFP constitutive transformant GFP1 or as uniform across the hypha, but there was clear GFP expression. The signal was again slightly blurred as with the liquid grown cultures suggestive of possibly a secreted protein still attached to the GFP tag in the extracellular environment. SP4 and Gpi2 transformants both displayed considerably less GFP signal during this assay (**Figure 66**). It was very difficult to distinguish between GFP signal for these two transformants and background autofluorescence which is seen surrounding the onion cell walls. It was difficult to get Gpi2a infection established compared with SP1 transformants, which could account for increase in background plant autofluorescence. However, when the bright field image is compared with the GFP filter image some GFP

fluorescence tracking along the fungal hyphae was observed. The third panel on Figure 65 and Figure 66 highlights the calcium-oxalate crystals which form as oxalic acid is secreted by the fungus and chelates with plant calcium. The JRL have previously quantified increasing crystals observed under a polarised filter with increasing oxalate concentrations secreted by a fungal culture (data not shown). The polarised images indicate that all the strains were secreting oxalic acid required for pathogenicity. However Gpi2a did appear to have reduced oxalate crystals which may explain the difficulty in establishing infection.

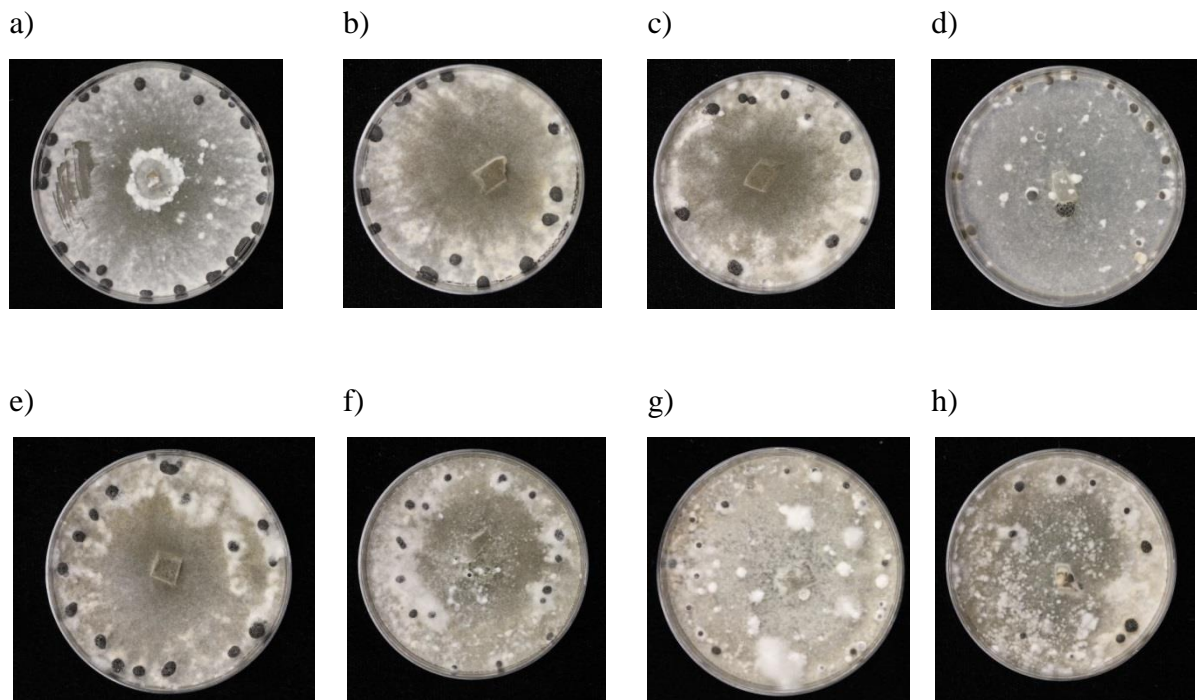


Figure 60. Transformant growth on PDA, 12 dpi.

a) WT190. b) GFP1 c)SP1B. d) SP1E. e) SP4A. f) SP4B. g) SP4D. h) Gpi2a. All transformants demonstrated normal growth rates and physiology compared with WT 1980 strain (a). All transformants developed sclerotia after 12 days on PDA plates, however SP4B (f), SP4D (g), SP1D (d) and Gpi2a (h) produced smaller sclerotia than WT 1980 (a).

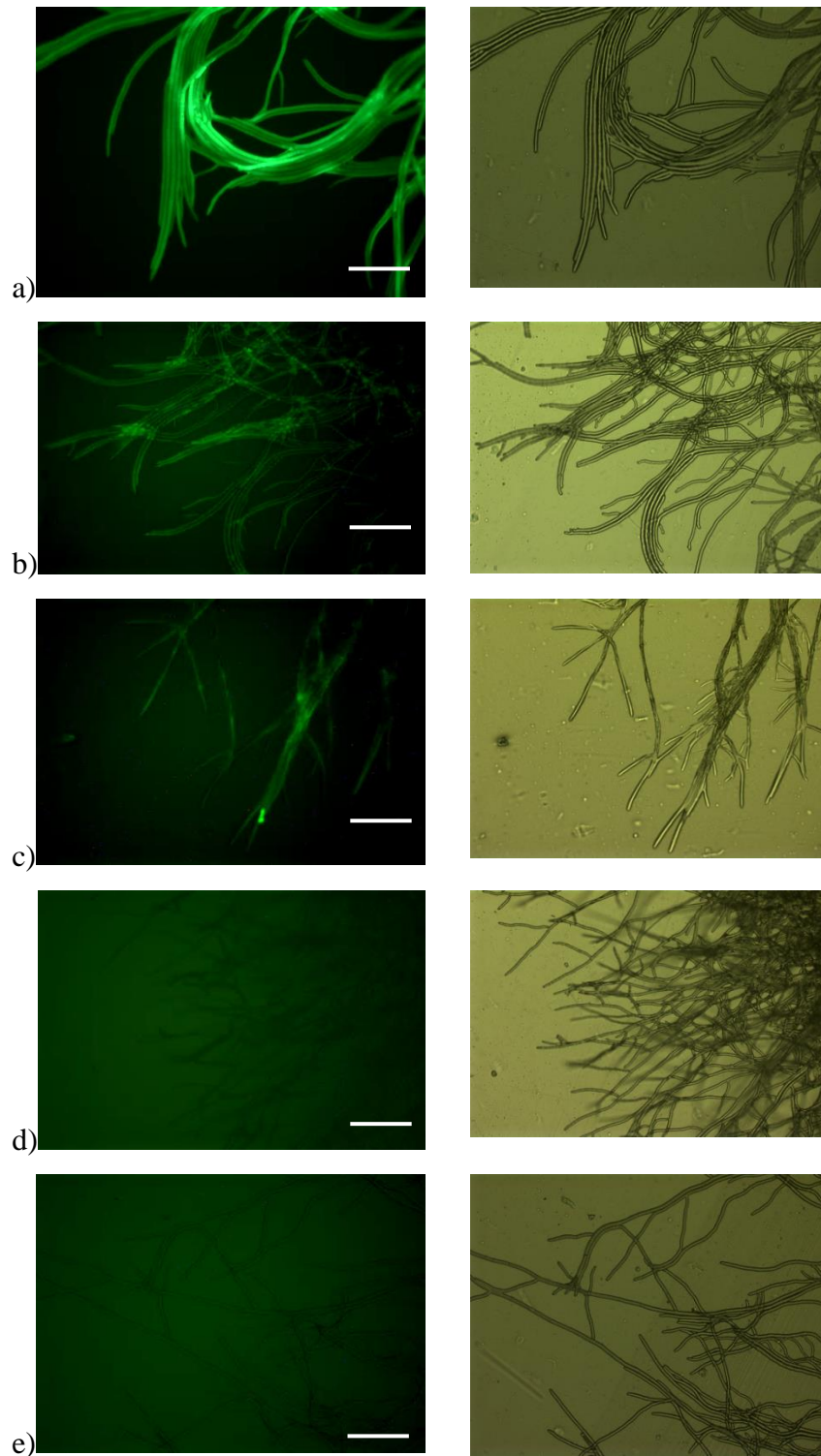


Figure 61. GFP fluorescence in *S. sclerotiorum* transformants grown on cellophane sheets over PDA. Plates observed under GFP fluorescence filter (left column) and under bright field on Leica compound microscope, 100X magnification (right column), two days after plate inoculation. a) Constitutive GFP1. b) SP1b some GFP expression. c) SP1e some GFP expression. d) SP4 transformants, no expression observed. e) GPI2a, no fluorescence was observed.

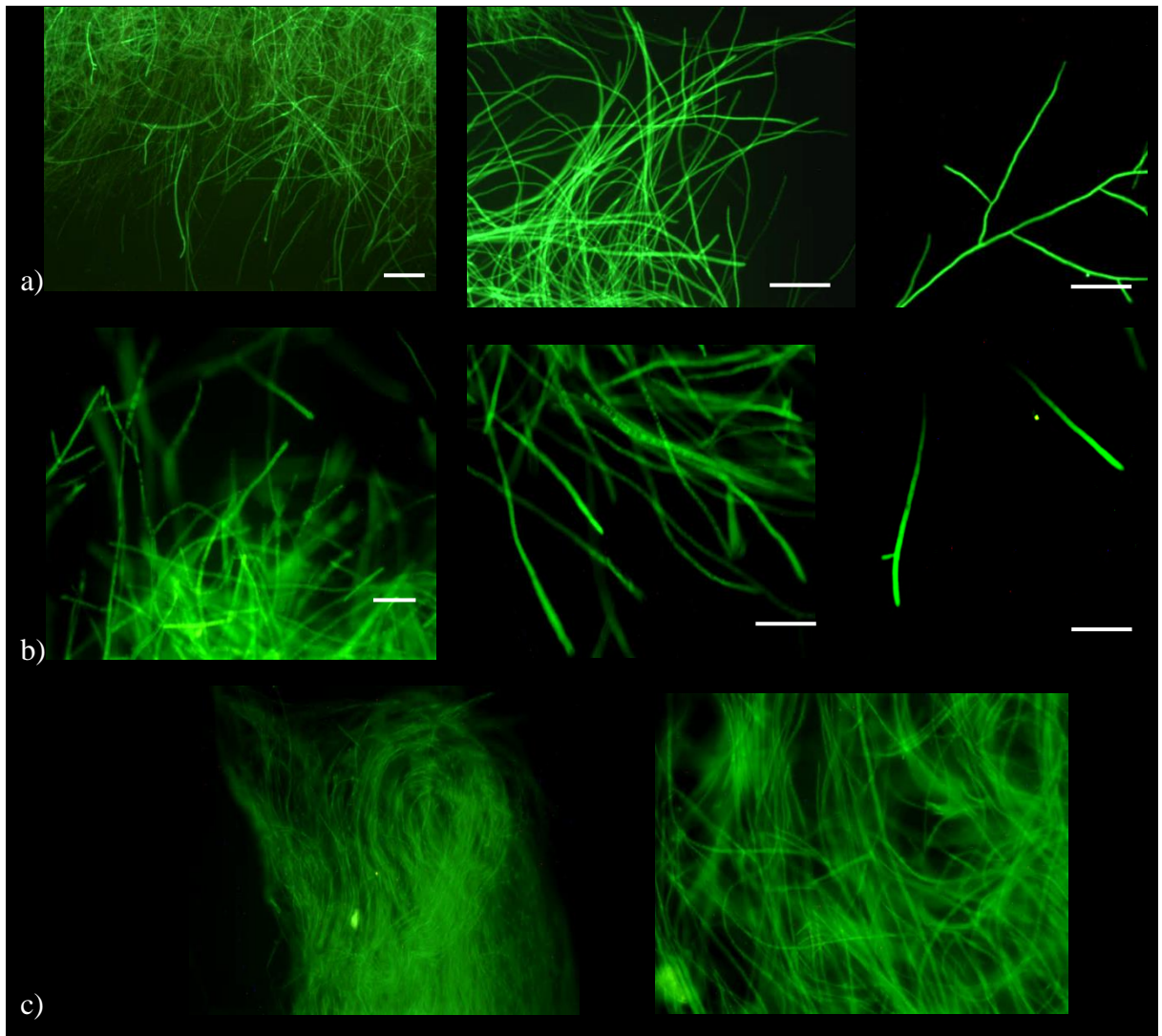


Figure 62. Transformants grown in YP sucrose broth for four days.

Only constitutive GFP1 and SP1 transformants grew in liquid medium. GFP fluorescence seen in both SP1 transformants. Mycelium observed under GFP fluorescence filter on a Leica compound microscope, 100X magnification. a) GFP1. b) SP1e. c) SP1b.

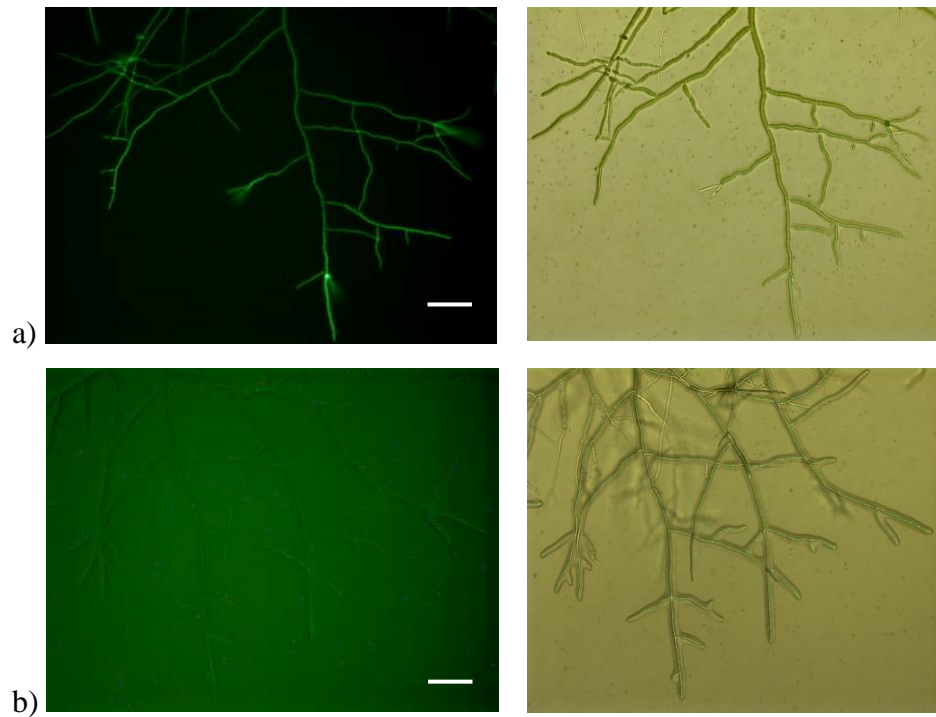


Figure 63. GFP fluorescence in *S. sclerotiorum* transformants grown on water agar .

Plates were observed on Leica compound microscope 100X magnification. Plates observed under GFP fluorescence filter (column 1 &3) and under bright field (column 2 &4) three days after plate inoculation. a) Constitutive GFP1. b) SP1b, SP1e, SP4b, SP4d, GPi2a no GFP . observed. Scalebars = 100 μ m.

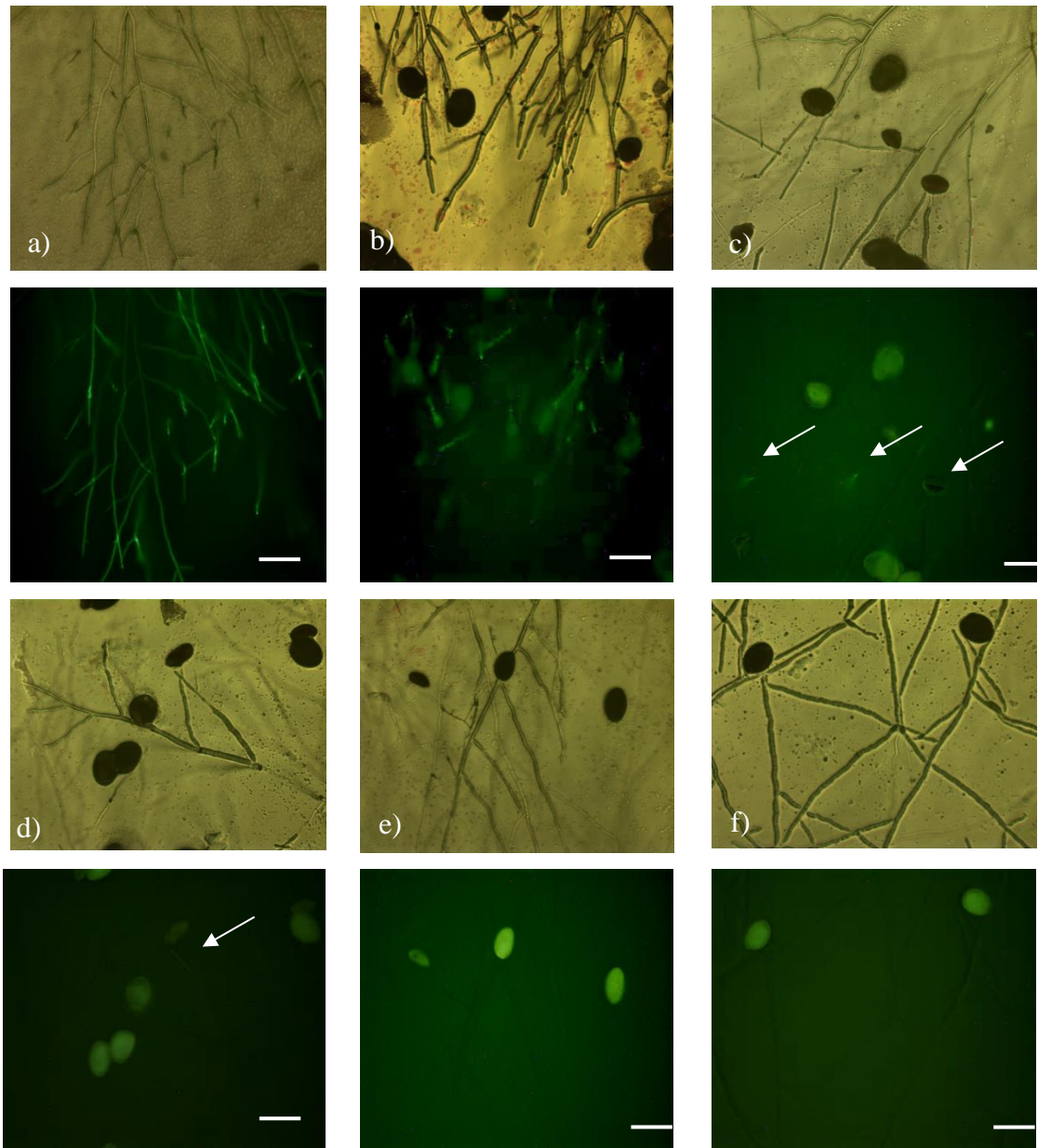


Figure 64. GFP fluorescence in *S. sclerotiorum* transformants grown on water agar covered with Lilly pollen.

Plates were observed on Leica compound 100X magnification. Plates observed under bright field (row 1 & 3) and under GFP fluorescence filter (row 2 & 4) and three days after plate inoculation. a) Constitutive GFP1. b) GFP expression observed in SP1b. c) Very low level of GFP expression observed in SP1e (white arrows). d) Very Slight GFP expression observed in SP4b (white arrow). e) No GFP observed in SP4d. f) No GFP observed in GPi2a. Scalebars = 100µm.

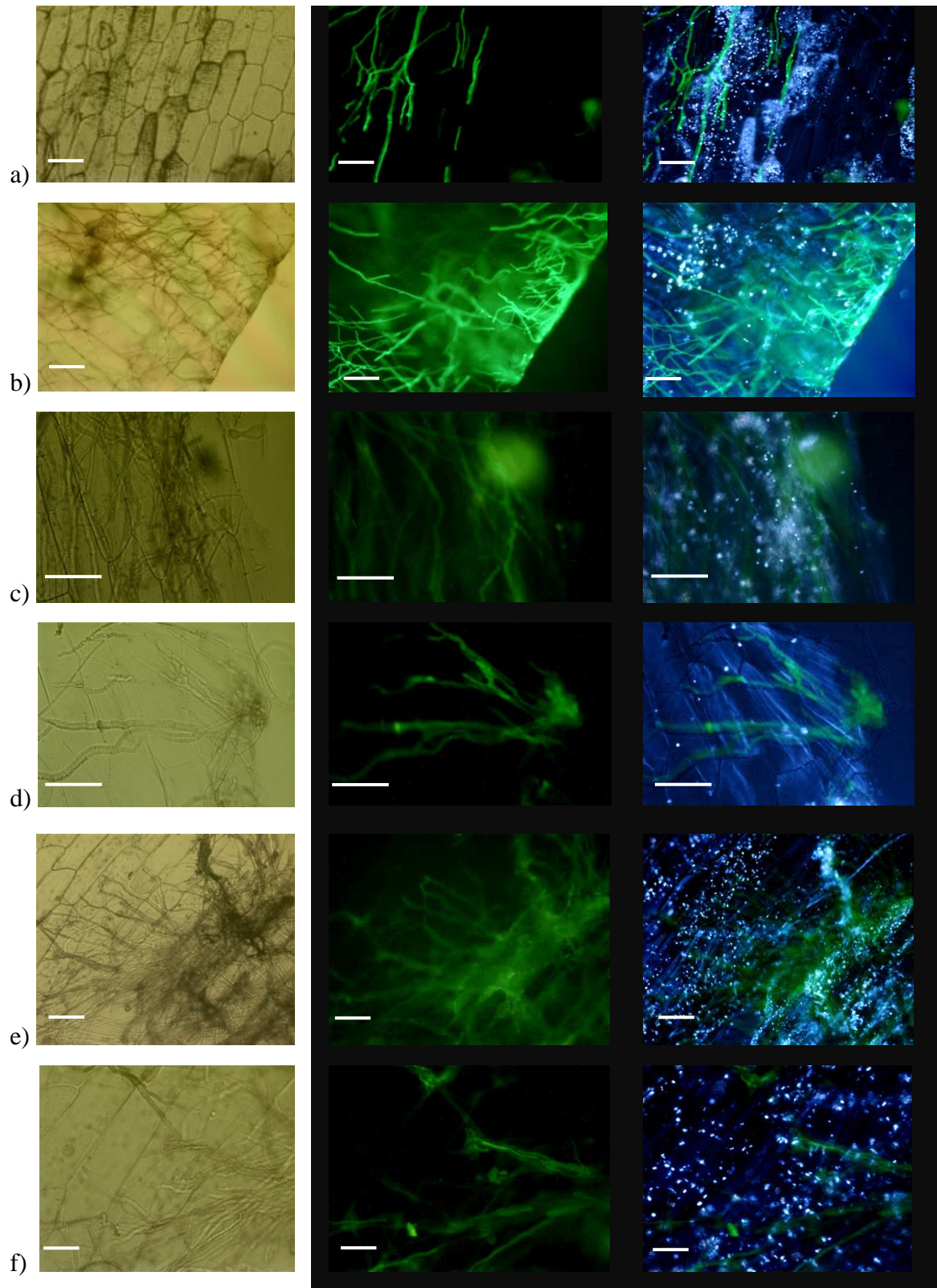


Figure 65. *S. sclerotiorum* transformant infection of onion epidermis.

The top layer of epidermis was observed using a Leica compound microscope, 1 day post inoculation. Column 1: slides viewed under bright field. Column 2: slides observed under GFP fluorescence filter. Column 3: slides viewed under polarised light combined with GFP filter. (a-b) Constitutive GFP 100X magnification. (c-d) SP1b x20. (e-f) SP1e 200x Magnification .Scalebar: 100 μ m.

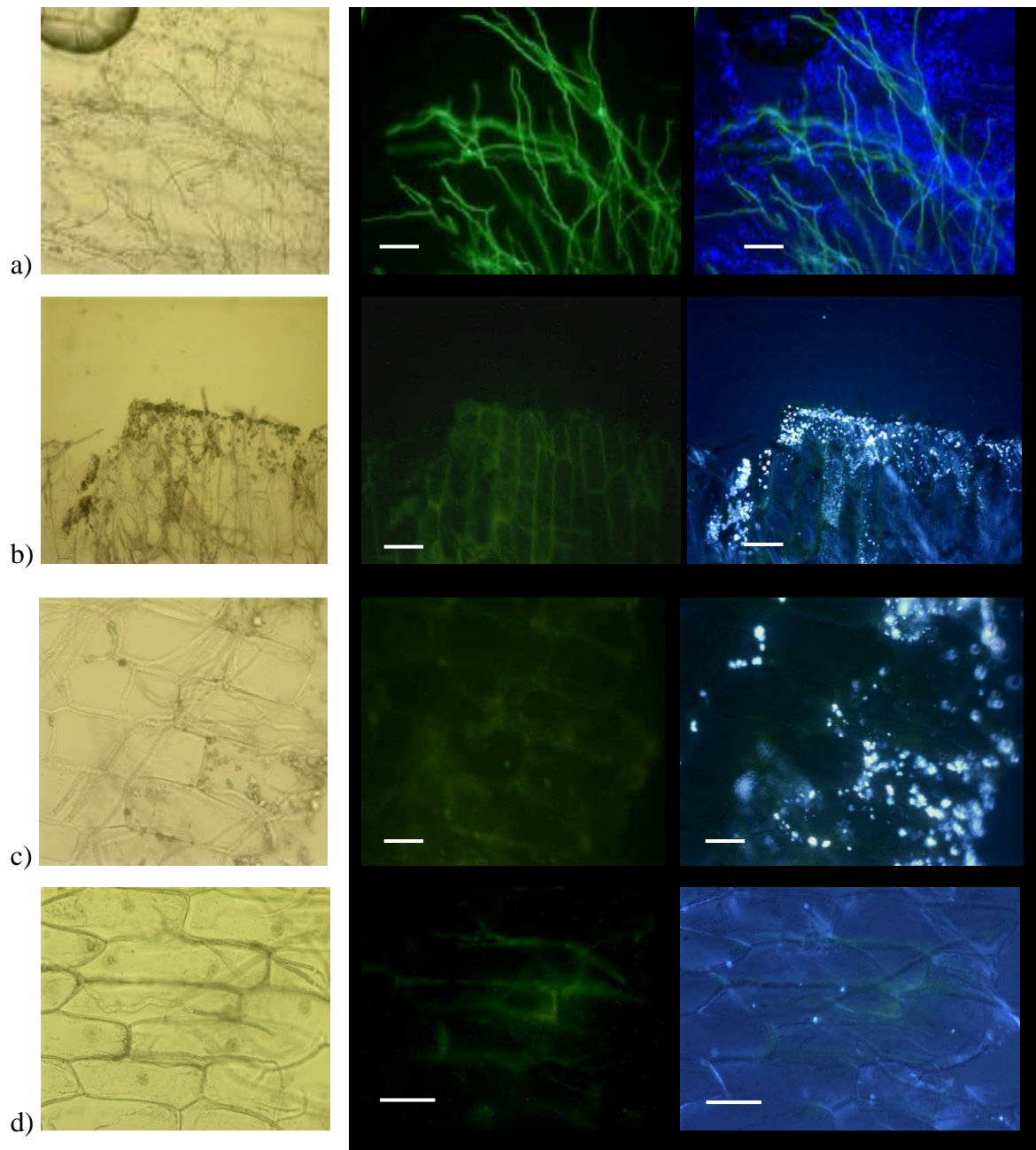


Figure 66. *S. sclerotiorum* transformant infection of onion epidermis, 1 day post inoculation.

The top layer of epidermis was observed using a Leica compound microscope. Column 1: slides viewed under bright field. Column 2: slides observed under GFP fluorescence filter. Column 3: slides viewed under polarised light combined with GFP filter. (a) Constitutive GFP 100x magnification. (b) SP14b 100x magnification. (c-d) GPI2a 200x magnification. Scalebar: 100 μ m.

Table 44: NCBI BlastP result performed after transformants were made.

Protein sequences were blasted against the NCBI database to explore any sequence homology in other fungi. The top hit in another fungal species was recorded.

SP	Gene ID in Broad	Top BlastP Hit	Gene Name	Accession	Expected Value (e- value)	hit-length	align-length	+ve bp	similarity
SP1	SS1G_01003	<i>Botryotinia fuckeliana</i>	-	CCD50509.1	4.57667e ⁻¹³	109	101	51	50%
SP1	SS1G_01003	<i>Trichoderma reesei</i>	-	EGR44794.1	7.46162e ⁻⁵	102	101	50	49%
SP2	SS1G_01749	<i>Botryotinia fuckeliana</i>	BcDW1_9533	CCD48435.1 EMR81869.1	9.79916e ⁻³³	377	143	98	68%
SP3	SS1G_06412	<i>Coniosporium apollinis</i>	-	EON67515.1	5.15112e ⁻⁶	592	171	79	46%
SP 4	SS1G_00564	<i>Fusarium oxysporum</i>	-	EGU73827.1	1.46706e ⁻³³	281	206	108	52%
SP 12	SS1G_10452	<i>Neosartorya fischeri</i>	NFIA_005660	XP_001259100.1 EAW17203.1	2.01735e ⁻⁴⁸	244	198	133	67%
GPI 1	SS1G_03000	<i>Podospora anserina</i>	PODANSg7294	XP_001910257.1 CAP71391.1	8.18751e ⁻¹²	115	78	47	60%
GPI 2	SS1G_04875	<i>Sclerotinia sclerotiorum</i>	SS1G_04875	XP_001593448.1 EDO02399.1	1.46416e ⁻⁵⁸	117	104	104	100%
GPI 3	SS1G_07678	<i>Sclerotinia sclerotiorum</i>	SS1G_07678	XP_001591053.1 EDN91817.1	6.8217e ⁻²⁶	56	56	56	100%

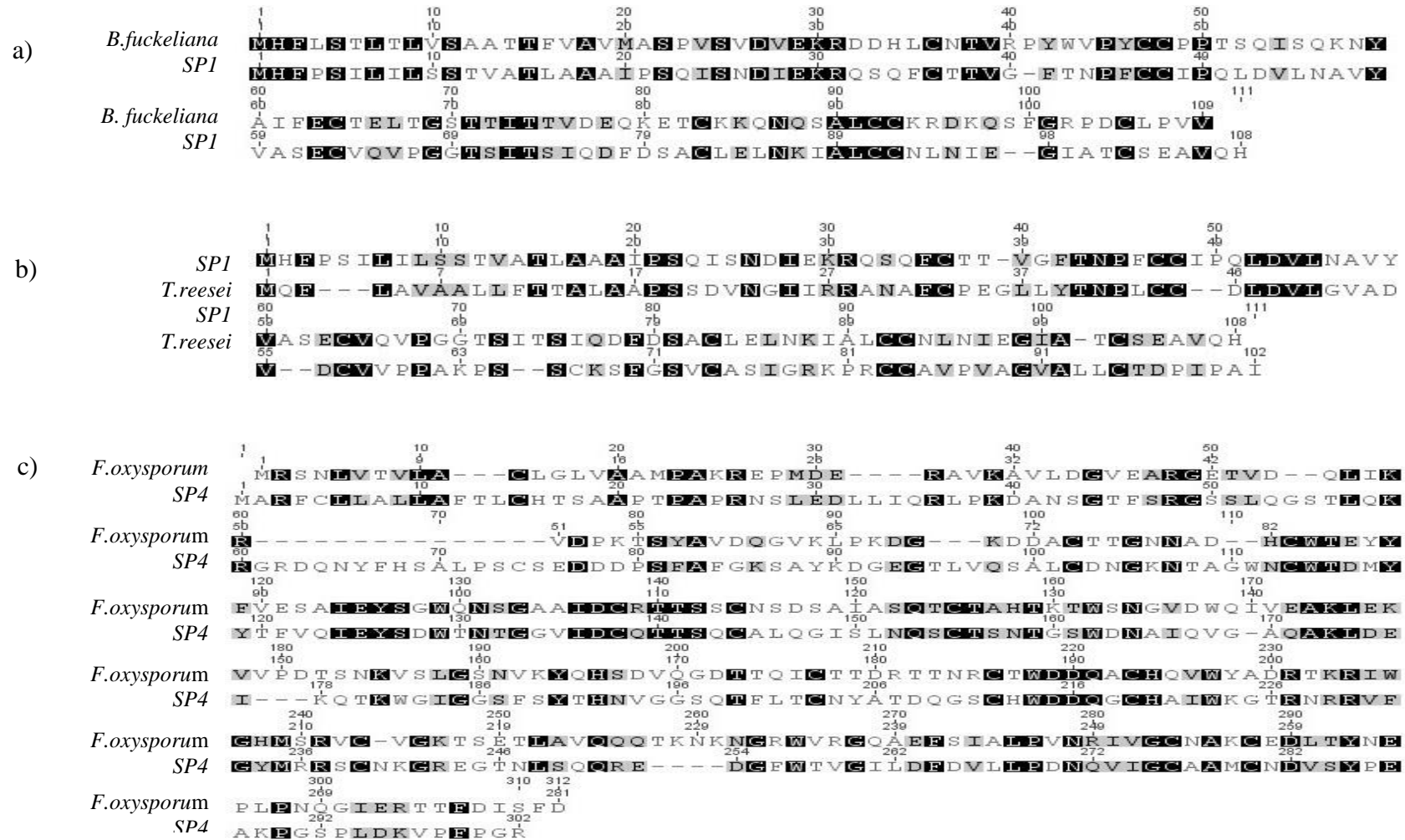


Figure 67. Alignments of successfully integrated SP1 and SP4 protein sequences.

Proteins along with the Blastp top hit homologous sequence found in other fungal species. a) SP1 protein sequence aligned to *B. fuckeliana* homologous sequence ($4.58e^{-13}$). b) SP1 protein sequence aligned to *T. reesei* homologous sequence ($7.46e^{-5}$). b) SP4 protein sequence aligned to *F. oxysporum* homologous sequence ($1.7e^{-33}$).

6.3.9 Updated BlastP results

For completeness, the eight putative protein sequences were subject to a final Blastp search at the end of the analysis (17.05.2013) to explore whether any updated information about homologous protein sequences in any other species had been added to the public domain since the beginning of the study (**Table 44**). Interestingly, SP1 has some homology to a hydrophobin protein sequence found in *Trichoderma reesei* ($7.46e^{-5}$). This protein sequence had some homology with a sequence in *Botryotinia fuckeliana*, the anamorph of *B. cinerea*. However, when these sequences were blasted against the *B. cinerea* genomes there was no homologous sequences found. SP4 had some homology with a sequence in the *Fusarium oxysporum* genome ($1.7E^{-33}$). ClustalW alignments of the *S. sclerotiorum* proteins and the semi homologous protein sequence were created in Geneious (**Figure 67**).

6.4 Discussion

The use of bioinformatics tools to assist in the discovery of novel protein targets which have putative effector functionality has been a success in many fungal and bacterial plant pathogen systems (Brown et al. 2012, do Amaral et al. 2012). Recent studies on the predicted secretomes of fungal pathogens including wheat infecting pathogens, *Fusarium graminearum* and *Mycosphaerella graminicola* provide a valuable resource to further our understanding of how secreted proteins are central to fungal disease development in host plants (Brown et al. 2012, do Amaral et al. 2012). This chapter reports another use of such a valuable resource. Instead of using the described bioinformatics pipeline to find proteins involved in infection, the pipeline has been modified to identify proteins which are unique to *S. sclerotiorum* and can be used as novel detection targets in systems such as lateral flow devices or even in an adapted electrochemical biosensor systems such as the SYield detection system.

6.4.1 The use of a bioinformatics pipeline to select protein targets for pathogen detection

The total secretome of *S. sclerotiorum* was explored to identify those sequences which had a high cysteine content and a WoLF P-SORT score of 18 or above. These are common characteristics in protein sequences which have a high probability of being secreted (Luderer et al. 2002, Horton et al. 2007). Unique targets with these characteristics were then identified if they had no homologous nucleotide or protein sequences in other fungal species. It was of particular importance that there was no homology in the closely related fungal species *B.*

cinerea so that future detection systems could consistently distinguish the two species. GPI anchor containing sequences identified in the total *S. sclerotiorum* secretome but not in the *B.cinerea* genome were also investigated as they are anchored to the extracellular side of the plasma membrane and so could be used as a detection target (Brown and Waneck 1992). A total of eight protein sequences were identified from this bioinformatics study. In this chapter the physical secretion of these proteins was explored using a range of molecular techniques.

6.4.2 Protein expression verification

The transformation work reported in this chapter was carried out during a three month visit to the JRL. Due to the time constraint of this trip only three of the protein detection targets were successfully tagged with a GFP and transformed into *S. sclerotiorum*. Successful integration of the three GFP tagged constructs into *S. sclerotiorum* DNA was shown via southern blot analysis. Growth on solid media for these transformants was comparable to the wild type strain but the inability of SP4 and GPi2 to grow in liquid culture and the production of smaller sclerotia compared to the WT may indicate that the GFP insert may have disabled some developmental abilities in these strains.

After growing the transformants under a number of different conditions, the strongest GFP signals were observed in SP1 and fluorescence was enhanced particularly when grown in a liquid environment. Since this protein has now been shown to have some distant homology with a *Trichoderma reesei* hydrophobin protein sequence and strong GFP signals were observed in the transformant grown in the liquid medium it is tempting to speculate that this protein may have hydrophobin functionality. Hydrophobins are unique fungal proteins found in filamentous fungi and not yeast (Bayry et al. 2012). Two hydrophobin classes have been described based on their hydropathy patterns and solubility characteristics (Wosten 2001). They consist of a diverse group of proteins which have many functions and as a result there is very little sequence conservation. The proteins do however form four disulphide bridges in the mature protein which is formed by eight characteristic cysteine residues (Kwan et al. 2006). The SP1 protein sequence has the characteristic eight cysteines, but it only contains an insignificant PFAM hydrophobin domain. Hydrophobin proteins have a high surfactant activity which is a result of their hydrophilic-hydrophobic arrangement which forms an amphipathic membrane (Wang et al. 2005). This monolayer will self-assemble at interfaces between water and air, water and oil or water and a hydrophobic solid and prevent waterlogging which may hinder gaseous exchange (Bayry et al. 2012). This aids aerial hyphae

to grow through wet environments. Some fungal spores which develop on aerial hyphae have been shown to be waterproofed by a hydrophobin rodlet layer encapsulating the spore and this aids spore dispersal through the air (Bayry et al. 2012). Some hydrophobins play a significant role in fungal attachment which was demonstrated in the basidiomycete *Schizophyllum commune* which will adhere to Teflon via its cell wall hydrophobin, SC3 (Wosten et al. 1994). This hydrophobin was shown to be secreted into fungal growth media when it was purified from both hyphal cell walls and liquid media (Wosten et al. 1993). A similar protocol was used to identify the ABH3 hydrophobin secreted into a liquid medium from the common white button mushroom, *Agaricus bisporus* (Lugones et al. 1998).

Interestingly the Dutch-Elm disease caused by the pathogens *Ophiostoma ulmi* and *O. novo-ulmi* both secrete a hydrophobin toxin, CU (Wosten 2001). It has been suggested that this hydrophobin may be secreted into host xylem and cause plugging of the vesicles by coating air bubbles (Russo et al. 1982). This was proposed because when purified CU was injected into the host plant which caused wilting, increase in leaf respiration, reduction in transpiration and electrolyte loss.

The role of the potential hydrophobin SP1 in this study may in fact be assisting the mycelia escape an aqueous environment (Wosten 2001) by making it easier for hyphae to grow through the liquid. This would explain the much stronger signal mycelium grown in liquid. Less of a GFP signal was observed in this transformant growing on solid media and during the onion epidermis infection but it was still evident suggesting it is just turned on in certain parts of the colony when there may be some difficulty in hyphal development. The lack of expression support in the EST libraries, the RT-qPCR data and the RNA sequencing could be explained by the fungus not being grown fully submerged in liquid. The RT-qPCRs were performed on RNA collected from spores which had been germinated in 1ml of PDB in 12 multiwell plates. This growth assay allows the fungal hyphae to form a floating raft on top of the medium so that the majority of the hyphae remain on top of the liquid rather than submerged. There was also very little liquid left in these small wells after 5 days of growth. In this study, the transformants were grown in 100 ml of YPD sucrose medium in a flask and so agar plugs were fully submerged. Further experimentation is required to look at relative gene expression in transformants submerged and not submerged. The SP1:GFP transformants could also be grown in a submerged liquid environment and then it could be observed whether the GFP signal reduces once the same culture is placed on a solid agar plate for a few days. A

simple gene knock out experiment to determine the significance of this protein when the mutant is grown submerged liquid or floating on top of liquid could also be done to further characterise this protein. Environmental conditions can significantly affect gene expression and so further growth tests will be required to pin point at which other exact point this particular protein is expressed. If this protein truly is secreted in a liquid environment then this protein could be a very good candidate detection target for a liquid sampling system similar to the SYield biosensor. However the biosensor would require the electrochemical assay to be based on antibody recognition rather than enzymatic based recognition. The next logical experiment to explore this possibility would be to raise an antibody against the SP1 protein and used it to show whether the protein was secreted in a liquid environment with the use of a Western blot. Comparisons between the distant related *Trichoderma reesei* hydrophobin and other fungal hydrophobins would be required to ensure any antibody raised against this SP1 would not bind to other hydrophobins.

The SP4 and Gpi2 transformants were more difficult to assess for GFP expression. Signals were very rarely discernible on the solid medium for SP4 and never for GPi2. SP4 had some GFP signal on agar plates covered with lily pollen and slight fluorescence in the onion infection assay suggesting that there may be some compound in plant based tissue which triggers the expression of this protein. GFP fluorescence was only seen weakly in the onion infection assay for Gpi2a. Establishing infection by this transformant was difficult and background autofluorescence made it challenging to distinguish GFP expression. It was observed occasionally tracking along some of the hyphae. There was no support for these two proteins in the EST, RNAseq or RT-qPCR studies, but as with SP1 this might be due to the material being collected at the wrong time or the growing conditions not induces for expression of these particular proteins. Further growth experiments of both the SP4:GFP and GPi2:GFP strains could reveal further information about the expression pattern of these proteins.

6.4.3 GFP as a reporter tag for secreted proteins

GFP has been used in countless studies as a successful reporter strain to explore gene regulation, protein localisation and specific organelle labelling *in vivo* in bacteria, yeast, insects, mammals and plants. This stable protein is 238 amino acids in length absorbs light at maxima of 395 and 475 nm and emits light at a maximum of 508 nm, requiring UV or blue

light and oxygen to cause fluorescence (Lorang et al. 2001). It has been used to tag successfully characterised secreted effector proteins including the *Ustilago maydis* secreted effector, Pep1 (Doehlemaun et al. 2009). It was used in this study to observe whether protein sequences of interest are truly expressed proteins and where they localised within the hyphae. A qualitative comparison of protein expression made between the constitutive GFP transformant and the other transformants was very useful to observe how highly expressed these proteins were under certain conditions. However it still remains unclear as to whether or not these proteins were fully secreted into the extracellular environment. A blurred expression pattern of GFP was sometimes observed in transformants compared to the very defined GFP signals seen along the hyphae of the constitutive GFP transformant. This may be a result of the proteins actually being secreted extracellularly but in very low quantities. It could also be possible that in the case of SP4:GFP and GPi2:GFP, they were secreted in low quantities but the GFP tag may have been cleaved off during extracellular secretion and result in the no GFP fluorescence being observed. This could be further tested by using a GFP specific antibody pull down system to pull out any proteins that were secreted into the growth medium and whether they were still tagged with GFP and secreted into a liquid medium and visualised using a western blot.

In conclusion, this chapter revealed the use of a bioinformatics pipeline to identify fungal secretomes can be used not only to find secreted effector proteins but to look for unique targets of detection for *S. sclerotiorum*. This bioinformatics method could be applied to many other plant pathogens with sequenced genomes. The unique detection targets could then be used to design specific DNA based identification using qPCR and Taqman assays as well as in LFDs if suitable proteins are identified and antibodies could be generated to be used directly in field diagnostic equipment. This chapter also reports the potential characterisation of the novel hydrophobin in *S. sclerotiorum*, SP1. This protein would work specifically well in a liquid detection system as its expression was upregulated when the fungus was submerged in liquid. Providing the electrochemistry of the SYield biosensor could be adjusted to recognise this protein rather than oxalic acid it could prove to be an interesting second choice as a detection target. Further investigation would be required to generate an antibody specific to SP1 to identify that it is truly secreted into a liquid and to explore whether other hydrophobins from other fungal species be detected in such a system. It would need to be truly specific to *S. sclerotiorum* SP1 for it to be of any use in a detection system.

Chapter 7: A comparative investigation into the transcriptomes of wild type and an oxalic acid deficient *S. sclerotiorum* mutant during *in vitro* growth and infection of *Arabidopsis* leaves

7.1 Introduction

The secretion of oxalic acid during early plant infection has been described as the main pathogenicity mechanism for *S. sclerotiorum* disease progression in multiple host species (Maxwell and Lumsden 1970, Magro et al. 1984, Dutton and Evans 1996, Godoy et al. 1990, De 1884). This seemingly simple molecule is responsible for a range of functions including the mediation of pH signalling during the infection process (Rollins and Dickman 2001), and as a result increases the activity of pH dependent enzymes including polygalacturonases, which degrade plant cell walls (Bateman and Beer 1965). Oxalic acid deregulates stomatal guard cell closure (Guimaraes and Stotz 2004), suppresses the plant oxidative burst (Cessna et al. 2000), is an elicitor of plant programmed cell death (Kim et al. 2008) and changes the cellular redox-status of the host plant during infection (Williams et al. 2011).

The biosynthesis of this compound in *S. sclerotiorum* has not been fully characterised. However it is speculated that oxalic acid is produced principally via the tricarboxylic acid cycle (TCA) (Cessna et al. 2000), an essential aerobic pathway which involves many enzymes which metabolise pyruvate and fatty acids to produce acetyl CoA. NADH is the principle end-product which is fed into the electron-transport chain in mitochondria as the main source of electrons. Oxalic acid is generated during this process via the direct hydrolysis of oxaloacetate into acetate and oxalate (Lenz et al. 1976) by the relatively well characterised enzyme oxaloacetate acetylhydrolase (OAH) (EC 3.7.1.1) (Han et al. 2007).

OAH was initially purified from *Aspergillus niger* (Han et al. 2007) and homologues of this protein have been identified in both *S. sclerotiorum* (SS1G_08218) and *B. cinerea* (BC1G_03473). *S. sclerotiorum* mutant strains deficient in this enzyme are unable to produce oxalic acid and its ability to induce disease is severely impaired (Rollins, JA unpublished, Amselem et al. 2011, Kabbage et al. 2013). The *oah* gene deletion mutant (Δoah_1 - KO_2) generated in the Jeffrey Rollins laboratory at the University of Florida, Gainesville, is deficient in oxalic acid production (unpublished data, (Amselem et al. 2011)) and can only cause limited infection if the plant is pre-wounded and a mycelial-agar plug is placed over the wound. A small lesion can be seen surrounding the infection plug but unlike wild type infection, the lesion remains small, the disease is unable to progress

and clear signs of plant defence are visible.

To further our understanding of the role of oxalic acid during infection and its signalling effect on other pathogenicity genes during infection, wild type *S. sclerotiorum* infection of *Arabidopsis thaliana* was compared to the same infection by the OAH deficient strain, Δoah_1-KO_2 . Transcriptome sequencing (RNA-seq) was used to analyse the gene expression of these two strains during an infection time course. In addition, tissue collected from both strains growing *in vitro* was collected for transcriptome analysis to distinguish those genes specifically expressed *in planta*.

7.2 Experimental Procedures

7.2.1 Plant varieties, fungal strains and infection conditions.

Arabidopsis thaliana ecotype *Columbia* (Col) seeds were sown in moist vermiculite potting soil and put in a cold chamber to vernalise for five days. Subsequently, the seedlings were potted up individually and grown up in a controlled environment chamber in a regime of 12 hr day/12hr night light at 22 °C. Fungal infections were carried out after 6 weeks of plant growth, once rosette leaves had fully expanded to approximately 7 cm diameter, but before plant bolting.

Two *S. sclerotiorum* strains were used in this study. The sequenced wild type strain 1980 (WT) and the oxalic acid deficient strain Δoah_1-KO_2 (Δoah). Both were maintained on potato dextrose agar (PDA) plates kept at room temperature. Two days before plant inoculation, Δoah agar plugs were placed onto new PDA plates, to ensure the inoculation plugs could be taken from expanding cultures for plant infection. WT agar plugs were re-plated 24hrs before plant inoculation because the growth rate of the WT strain is faster than the mutant strain.

Expanding cultures harvested for the first time point (T0) were grown on cellophane discs placed on the surface of the PDA plates. This allowed harvesting of the mycelium without the uptake of agar which inhibits the RNA extraction process. Agar plugs with cellophane were not used in the inoculation time course because this prevented the annealing of Δoah strain to the leaves and thus reduced the incidence of plant infection. Mycelium was taken from the edge of the expanding cultures, the same area where the inoculation plugs were cut from. Mycelia was immediately flash frozen in liquid nitrogen and kept at -80 °C.

Twenty-four hours before fungal inoculation, plants were placed in the controlled

environment chamber in smaller, sealed plastic boxes lined with damp paper roll to maintain high humidity within each box. Eight plants were placed in each of the eight boxes and four boxes placed on each shelf in the chamber. The plants were placed in the boxes according to a randomised block design. Representative plants inoculated with either the WT strain, the *Δoah* strain or mock inoculated with an colonised agar plug were selected in each smaller box. The lights were kept on throughout the experiment to reduce the effect of photoresponses by the plant and fungus.

Before inoculation, plants were wounded with a sterile scalpel, making a cut across the centre of the rosette leaves, which included the midvein. A single 0.5 mm² square agar plug was cut from the edge of the expanding culture and placed fungal side down on top of each cut. One strain only was used to infect multiple leaves on a single plant. Twenty-five plants were inoculated with the *Δoah* strain and 15 plants were inoculated with the wild type strain. A further 15 plants were mock inoculated with uncolonised agar plugs.

Leaves were harvested at two stages during fungal infection. The first harvest time point (T1) occurred when a small infection lesion was observed under the agar plug surrounding the cut. The second harvest time point (T2) occurred when the infection lesion had expanded beyond the agar plug. T1 harvest for WT was approximately at 12 hrs post inoculation (hpi) but for the slower growing *Δoah*, this stage of symptom of development was observed at 24 hpi. T2 harvest occurred at 24 and 72 hpi for WT and *Δoah* respectively. Mock inoculated leaves were collected at 12, 24 and 72 hpi.

Material was harvested by detaching leaves from the plant, removing the agar plug and then using a sterile razor blade to cut around the observed lesion, leaving a thin area of green leaf around the lesion. Ten leaf samples infected with the same strain from different plants were pooled into one sample for RNA extraction. Material was immediately flash frozen in liquid nitrogen and stored at -80 °C.

7.2.2 RNA extraction

Frozen leaves were lyophilised and ground into a fine powder using a bead beater with baked 3.2 mm stainless steel beads in 1.8 ml stainless steel vials. RNA was extracted using Qiagen RNeasy mini kit. RNA was sent for quality checking, cDNA library construction and RNA sequencing at the Interdisciplinary Center for Biotechnology Research facility (ICBR), University of Florida.

7.2.3 TruSeq RNA Library Construction (ICBR Experimental procedure)

RNA concentration was determined on a NanoDrop Spectrophotometer (NanoDrop Technologies, Inc) and sample quality was assessed using the Agilent 2100 Bioanalyser (Agilent Technologies, Inc). Two μg of total RNA was used for library construction using Illumina TruSeq RNA sample preparation kit according to manufacturer's protocol. Briefly, poly-A mRNA was enriched from 2 μg of total RNA sample using the polydT oligo-attached magnetic beads. Purified mRNA was then fragmented using divalent cations at 94 °C, followed by first strand cDNA synthesis using reverse transcriptase and random primers. Synthesis of ds cDNA using DNA Polymerase I and RNase H was performed followed by end-repair and dA-tailing. Indexed Illumina adaptors were ligated to each sample. Each library was appropriately barcoded. Finally, the library was enriched by 12 cycles of amplification and purified by Agencourt AMPure beads (Beckman Coulter). TruSeq RNA library construction was performed at the Interdisciplinary Center for Biotechnology Research (ICBR) Gene Expression Core, University of Florida (UF).

7.2.4 Illumina GAIIX Sequencing (ICBR Experimental procedure)

The amplified TruSeq libraries were quantified using the Agilent DNA high-sensitivity kit on an Agilent 2100 Bioanalyzer and qPCR using Bio-Rad CFX 96. Based on the calculated values, the libraries were pooled and diluted to 10 nM and then applied at 9 pM to individual lane of Illumina pair-end flowcell for cluster generation on cBOT (Illumina). Therefore each of the seven flow cells contained an equal mixture of each library. Each library was sequenced for 1x100 bp reads on Illumina GAIIX. Image analysis and base calling were performed using the Illumina Pipeline, where sequence tags were obtained after purity filtering. The Illumina GAIIX sequencing was performed by the NextGen Sequencing Core at UF-ICBR.

7.2.5 Bioinformatics Analysis

David Hughes, Ambrose Andongabo and Keywan Hassani-Pak from the Rothamsted Computation and Systems Biology group assisted on workflow methods, statistical calculation of reads and writing command lines for the following analysis.

The raw RNA sequencing reads were mapped and differential gene expression calculated using the workflow described by Trapnell et al (2012) (Trapnell et al. 2012) using the Galaxy platform (Blankenberg et al. 2010, Giardine et al. 2005, Goecks et al. 2010) which combines the necessary tools required for the analysis (**Figure 68**). The *S.*

sclerotiorum reference genome GTF file for read alignment was downloaded: (http://www.broadinstitute.org/annotation/genome/sclerotinia_sclerotiorum/MultiDownloads.html). The Arabidopsis TAIR reference genome GTF file was downloaded from TAIR (<http://www.arabidopsis.org/>). Quality of reads was calculated using FastQC and determined to be of good quality and did not require trimming before analysis. Tophat2 was used to align the reads for each library to the genome and to find transcript splice-sites. To calculate the correct expression level of each transcript, Cufflinks was used to count the reads that map to each transcript and then normalise this count by each transcript's length. To compare the expression level of a transcript across runs, the counts must be normalised for the total yield of the machine. Cufflinks combines these two steps by assembling the reads into transcripts and calculating the Fragments Per Kilobase of transcript per Million mapped reads (FPKM). Expression levels can be calculated easily as the software simply adds up the expression level of each splice variant. This is possible because FPKM is directly proportional to abundance (Trapnell et al. 2012).

Cufflinks estimates transcript abundance based on how many reads support each transcript, taking into account biases in library preparation protocols. It accepts aligned RNA-Seq reads from Tophat2 and assembles the alignments into a parsimonious set of transcripts. Then it tests for differential expression and regulation in RNA-Seq samples (<http://cufflinks.cbc.umd.edu/index.html>).

Cuffmerge combines all the transcript assemblies together. Some genes with low expression may receive inadequate sequencing depth to allow full reconstruction in each replicate. Merging these replicate assemblies with Cuffmerge was used to recover the complete gene (Trapnell et al. 2012). Cuffdiff then uses the merged transcripts to report genes which were differentially expressed using a rigorous statistical analysis across two or more conditions (Trapnell et al. 2012). CummeRBund package in R version 2.15.3[©] was used to generate graphical representations of the differential gene expression events. General commands followed (http://compbio.mit.edu/cummeRbund/manual_2_0.html) from the user manual to plot graphs.

Blast2go was used to explore the gene annotation and function of the genes with significant gene expression (<http://www.blast2go.com/b2glaunch>) (Conesa et al. 2005). From this interface, the InterPro website was accessed to further explore the IPO entries discovered (<http://www.ebi.ac.uk/interpro>) (Hunter et al. 2012, Quevillon et al. 2005).

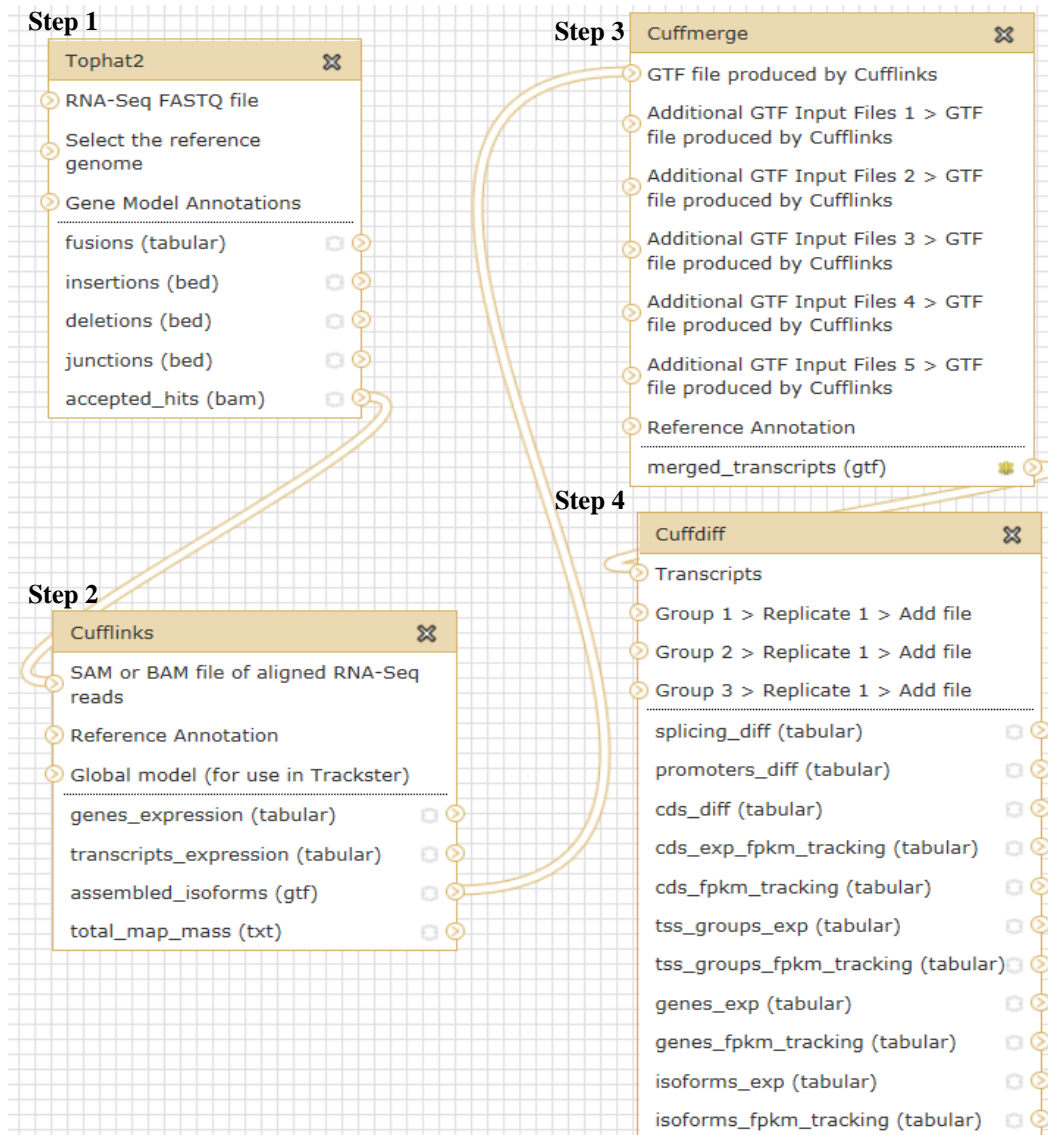


Figure 68: Bioinformatics workflow for RNAseq alignments.

The workflow based on Trapnell et al (2013) (Trapnell et al. 2012) to process the Illumina sequencing data. Tophat2 and Cufflinks (steps 1-2) used to align the reads to the *S. sclerotiorum* genome and calculate Fragments Per Kilobase of transcript per Million mapped reads (FPKM). Cuffmerge (step 3) then merged all files so that differential gene expression could be calculated across the different time points. Cuffdiff (step 4) calculates the statistical significant gene expression events between two or more conditions. Files can then be used in R to generate graphical representation using CummeRbund.

7.3 Results

Financial constraints for this experiment prevented the sequencing of three biological replicates for each condition. Instead, 10 biological replicates per condition were pooled as a single library and sequenced as one replicate. Each library was barcoded and run across all 7 lanes of the Illumina platform, resulting in seven technical replicates for each condition. Due to time constraints, these libraries were recombined for data analysis.

7.3.1 Challenges with using *Δoah* mutant to obtain high quality RNA

A considerable challenge for this experiment was obtaining RNA for the *Δoah* mutant at T2. The infection for this mutant did not progress as fully as the WT sample (**Figure 70**). During WT infection initially a small lesion was evident at 12phi. At 24 hpi the lesion is fully extended around the agar plug (**Figure 70**) and across the leaf. If the infection was left to progress further than 24 hpi, the lesion would expand fully until the leaf was completely colonised and cells are fully lysed. The infection then extends into the stem and base of the plant. This infection course was monitored using trypan blue staining which is a vital stain which stains dead plant cells blue (**Figure 71**). The *Δoah* mutant was capable of causing initial infection symptoms but only if the leaf was wounded. This strain was able to cause an initial expanding lesion around the wounding site however it could not cause a fully expanding lesion. Yellowing of the leaf and a dark green outline around the lesion was observed (**Figure 70**). It is hypothesised that the dark ring around the lesion is the deposition of lignin and this is a result of induced plant defences which would normally be evaded or overpowered by the action of oxalic acid secreted by the fungus. When samples for *Δoah* were collected, the RNA obtained at later time points was constantly degraded, even after setting up the infection course a further two times. As a result only the *Δoah* T0 and T1 libraries were sequenced for this time course. The quality and extent of RNA degradation was assessed using an Agilent 2100 Bioanalyser. Only libraries with RIN values above 6 passed QC and were included in the analysis (**Table 45**).

7.3.2 Calculation of the percentage of reads aligned to each reference genome

Initially the reads were aligned to both the *Arabidopsis* TAIR reference genome as well as the *S. sclerotiorum* reference genome to calculate the percentage of reads which aligned to each genome (**Table 46**). Flagstat was used to calculate this information. This helped to distinguish between any plant transcripts which have conserved homology with

fungal transcripts. The plant reads which aligned to the *S. sclerotiorum* genome were excluded from the fungal aligned datasets so that these reads do not bias the set of fungal FPKM values and subsequent calculation of significant gene expression. A pile up of plant reads were observed to align to the *S. sclerotiorum* genome at Contig 2.35 at positions 5759-5920 and 16241-16398. These transcripts are annotated as ribonucleases. The Mock T2 library which contains only plant material contained 619,886 mapped reads to the fungal genome of which 608,481 mapped to contig 2.35. The Mock T1 library which also contained plant reads contained 378,944 reads which mapped to the fungal genome, of which 371,767 map to just one fungal contig. This group of reads were excluded from the libraries containing both plant and fungal material. Only the libraries containing fungal material were used for the analysis; WT T0, WT T1, WT T2, *Δoah* T0 and *Δoah* T1.

Table 45: RIN values calculated using an Agilent 2100 Bioanalyser.

These libraries had the best RIN values which past quality control checks.

Library	260/280	260/230	Bioanalyser RIN values
Mock T2	2.13	2.3	6.80
Mock T1	2.13	2.5	6.50
<i>Δoah</i> T1	2.18	2.3	7.40
<i>Δoah</i> T0	2.12	1.62	6.70
WT T1	2.15	2.44	7.60
WT T2	2.16	2.44	6.10
WT T0	2.21	2.63	6.40

Table 46: The total reads for each library aligned to both the *A. thaliana* and *S. sclerotiorum* reference genome.

Library name	Material	Total Reads	Mapped reads/plant	Mapped reads/fungi	%Mapped reads/plant	%Mapped reads fungi
Mock T1	Plant	122842668	31547444	378944	25.68	0.31
Mock T2	Plant	227283408	54194299	619886	23.84	0.27
<i>Δoah</i> T0	Fungi	168187016	463319	77792790	0.28	46.25
<i>Δoah</i> T1	Fungi/Plant	295259772	53333467	42774717	18.06	14.49
WT T0	Plant	143689092	526649	68515543	0.37	47.68
WT T1	Fungi/Plant	193495152	25687260	43638284	13.28	22.6
WT T2	Fungi/Plant	159848476	9842378	58671081	6.15	36.7

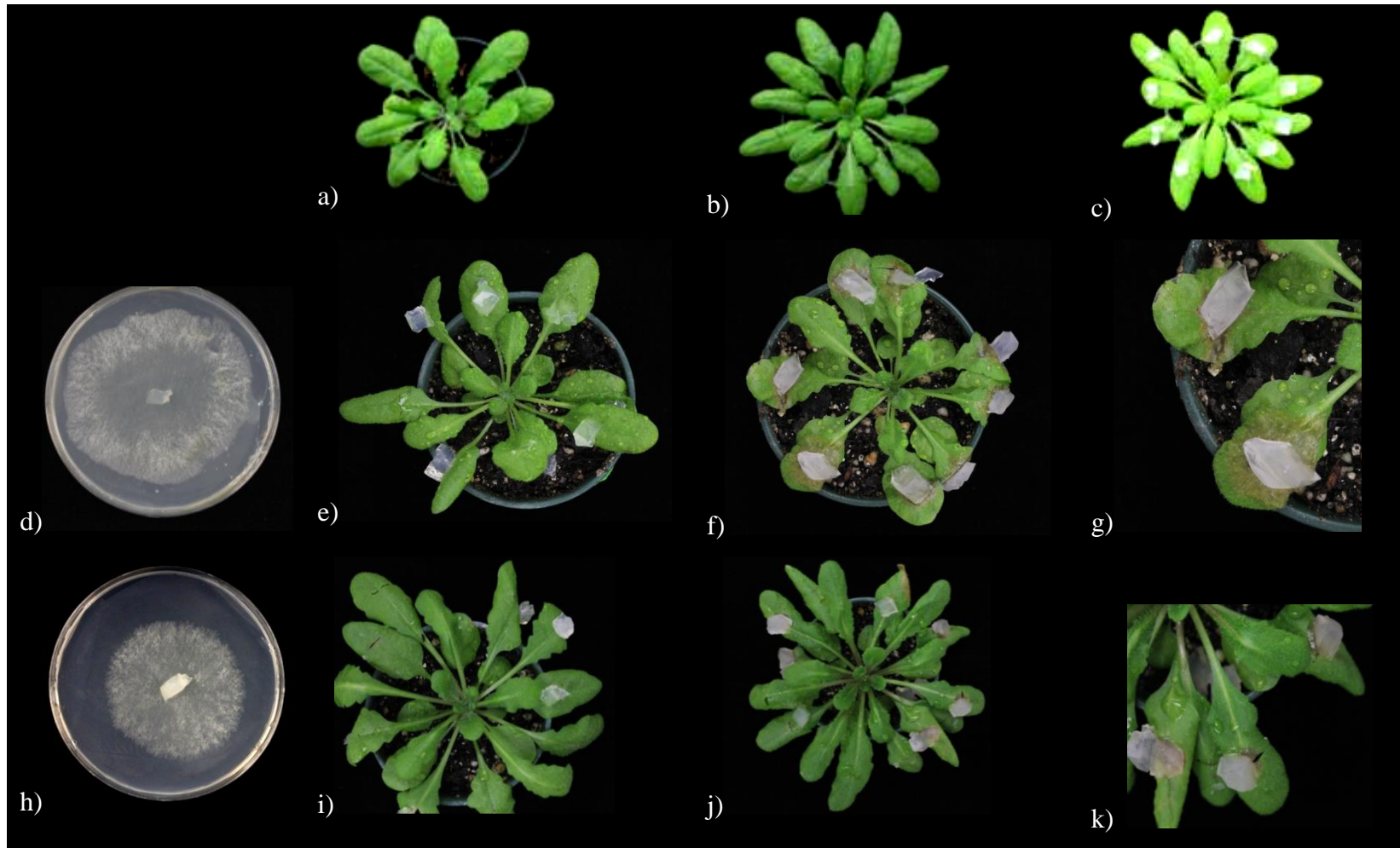


Figure 69: *A. thaliana* infection with *S. sclerotiorum* agar plugs inoculated with WT strain and Δoah strain.

a) *A. thaliana* pre-wounding and pre-infection. b) *A. thaliana* leaves wounded by slitting the leaf with a sterile scalpel. c) Arrangement of agar plugs. d) WT T0 grown on PDA and cellophane. e) Mock T2 (24hpi). f-g) WT T2 (24hr pi). h) Δoah T0 grown on PDA and cellophane. i) Mock T2 (72hpi). j-k) Δoah T2 (72hpi). Panels g and k are close up images of infected leaves from images shown in panels f and j, respectively.

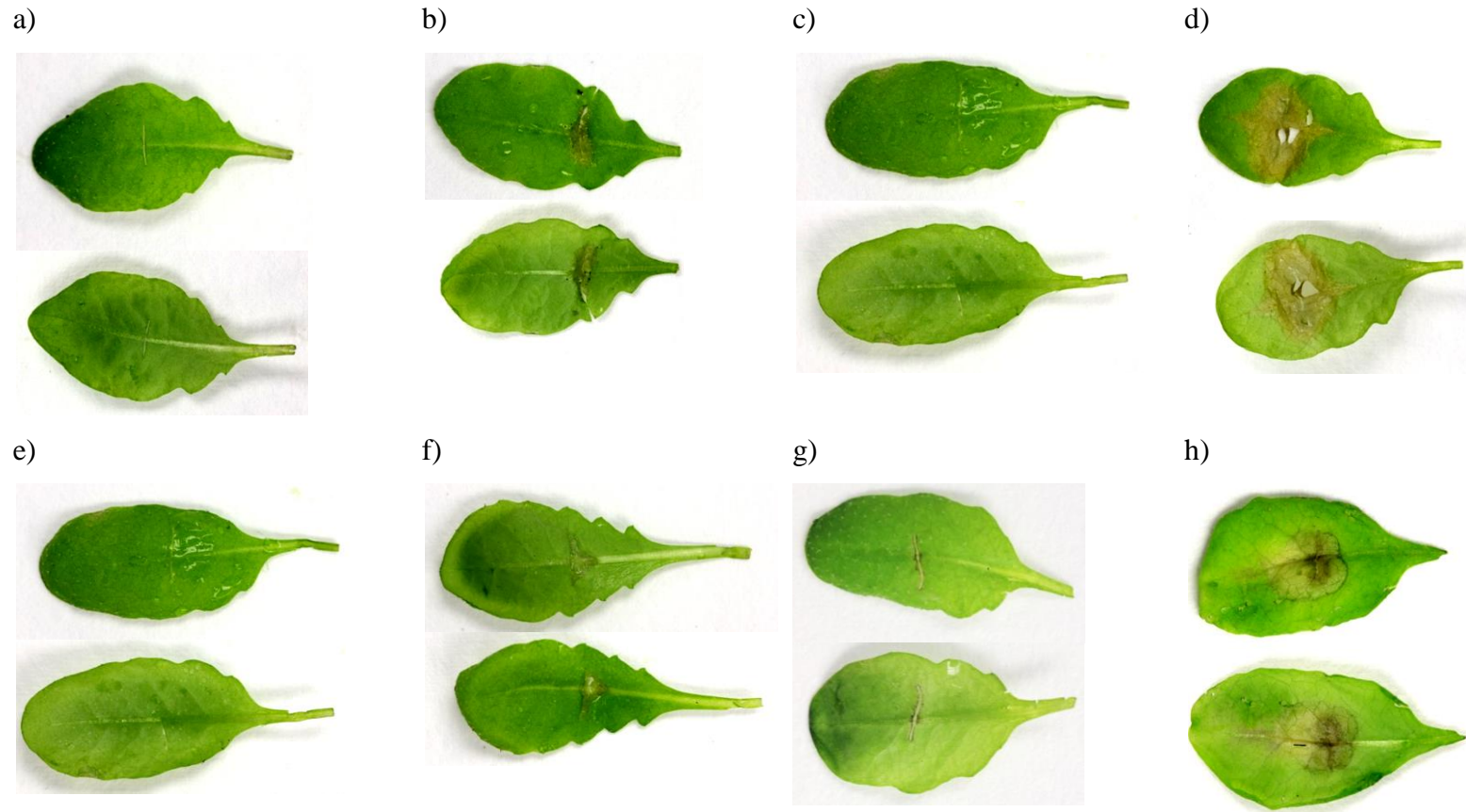


Figure 70: *A. thaliana* leaf infection progression over two time points.

Leaves were inoculated with a PDA agar plug colonised by the wild type strain (WT) or the oxalic acid deficient strain Δoah_1-KO_2 (Δoah). Leaves were mock inoculated with an uncolonised agar plug. RNA was then collected at different time points. a) Mock T1 (12hpi). b) WT T1 (12hpi). c) Mock T2 (24hpi). d) WT T2 (24hpi). e) Mock T1 (26hpi). f) Δoah T1 (26hpi). g) Mock T2 (72hpi). h) Δoah T2 (72hpi), a dark ring was observed around lesion.

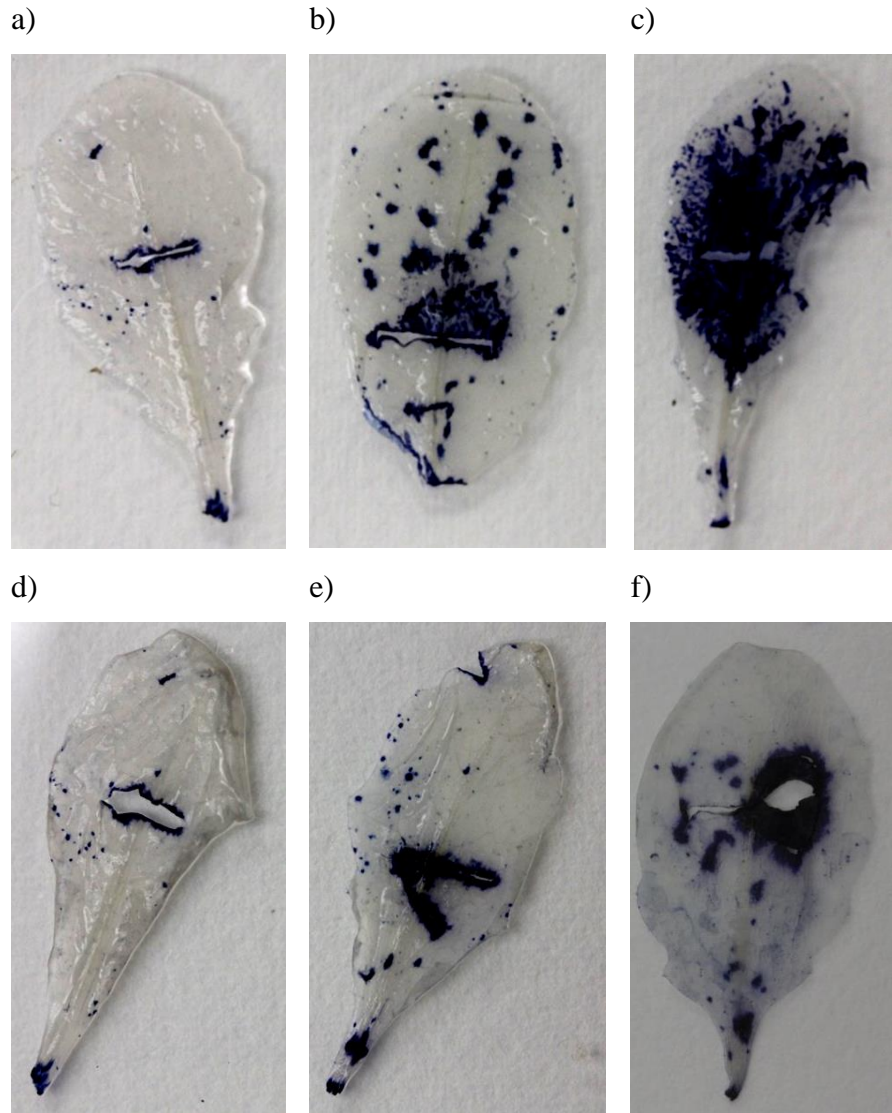


Figure 71: Leaf staining of fungal infection.

A. thaliana ecotype Columbia leaves inoculated with a PDA agar plug colonised by the wild type strain 1980 (WT) or the oxalic acid deficient strain Δoah_1-KO_2 (Δoah). Control leaves were mock inoculated with an uncolonised agar plug. Agar plugs were removed and leaves stained with trypan blue stain. Cells were fixed by soaking leaves in 95% acetone overnight. a) Mock T1 (12hpi). b) WT T1 (12hpi). c) WT 1 T2 (24hpi). d) Mock T1 (24hpi). e) ΔOAH T1 (24hpi). f) ΔOAH T2 (72hpi).

7.3.3 The most abundant transcripts in each library

The number of gene with FPKM values above 100 were calculated and the number of secreted expressed in each library with an FPKM value above 100 was also assessed (Table 47).

Table 47: The most abundant *S. sclerotiorum* transcripts in each RNAseq library

RNAseq Library	No. of genes FPKM >100 in total library	No. of secretome genes FPKM >100
<i>Δoah</i> T1	824	38
<i>Δoah</i> T0	802	52
WT T0	796	52
WT T1	838	56
WT T2	810	57

The top ten genes with the highest FPKM values were analysed in each library This resulted in an overlapping set of 20 genes (Table 48). The hypothetical protein SS1G_00253, with no domain of known function or protein domain, had the highest FPKM abundance in all libraries, however it most likely to be a Ribosomal gene as the gene model may overlap with the ribosomal gene SS1G_00254. Ribosomal subunit genes were also highly expressed in all libraries. Eleven hypothetical proteins were highly expressed which may give clues to other significant genes involved during infection in the WT libraries or those genes which are integral for development.

SS1G_12734, a bZIP transcription factor is involved in dimerising two DNA binding regions (PFAM, PF00170). The antibiotic response gene SS1G_01463 has the highest up regulation *in vitro* which is understandable because antibiotics were used in the PDA to prevent bacterial contamination. It is likely this gene would not be expressed during infection in the field. SS1G_12763, a cyanovirin-n family protein was also expressed highly *in vitro*. These expression patterns are approximately halved *in planta*. This protein domain has shown to have some activity to suppress viruses including the HIV and is expressed in many eukaryotes (Percudani et al. 2005).

SS1G_10335, contains a proteolipid membrane potential modulator domain (PFAM, PF01679). These proteins function to control membrane potential. In eukaryotic organisms, this domain is found in stress-activated mitogen-activated protein kinases.

These proteins are well known to transmit environmental signals that will regulate gene expression to permit the cell to adapt to cellular stress). SS1G_10335 was up regulated *in planta* when there may be more cellular stress experienced by the fungus whilst evading host plant defence.

Table 48: The combined genes with the highest FPKM values from each of the five conditions analysed.

Gene ID	Blast2Go Description	FPKM Value				
		WT T0	WT T1	WT T2	ΔOAH T0	ΔOAH T1
SS1G_00030	predicted protein	1441	4583	1774	3966	16992
SS1G_00126	predicted protein	2548	5045	5422	2484	6301
SS1G_00253	hypothetical protein	78414	128363	68007	85496	37605
SS1G_00544	60s ribosomal protein l39	11631	21119	11707	8491	3143
SS1G_01463	cipc-like antibiotic response protein	20999	10077	9682	12445	2556
SS1G_01771	predicted protein	3302	5654	4689	1864	7273
SS1G_03299	ekda protein	271	415	8955	241	11
SS1G_03582	40s ribosomal protein s29	6547	13249	7133	4640	1733
SS1G_03868	predicted protein	13349	7445	7602	7402	6545
SS1G_05038	40s ribosomal protein s30	8254	11005	7270	6405	2820
SS1G_06999	60s ribosomal protein l29	10064	13413	8431	7643	2278
SS1G_08102	predicted protein	351	1564	2594	1160	11832
SS1G_09040	hypothetical protein	38781	21505	28745	15258	3401
SS1G_09993	predicted protein	11673	1049	4857	15386	898
SS1G_10335	plasma membrane proteolipid 3	1655	7367	8707	3731	7702
SS1G_12734	transcription factor bzip	2414	2821	1863	5439	7033
SS1G_12763	cyanovirin-N family protein	6843	3039	2764	3987	1691
SS1G_13124	predicted protein	6367	3135	1044	7773	6290
SS1G_13356	predicted protein	3048	0	10004	32384	428
SS1G_13910	hypothetical protein	36078	9358	8215	55315	14315

7.3.4 Comparison of significant differential putative secreted protein gene expression events across the different conditions.

The defence response to pathogen infection in *Arabidopsis* would be interesting to analyse, however due to time constraints only the gene expression data for fungal gene expression was analysed during this study. Four comparisons across the libraries aligned to the *S. sclerotiorum* reference genome were analysed to explore the significant changes in gene expression over the time course and between the two strains (**Table 49**). The expression of the putative secreted proteins identified in the *S.sclerotiorum* refined secretome (Chapter 5) was investigated. Only two of the four comparisons exhibited significantly expressed secreted proteins which are discussed in further detail.

Table 49: Four comparisons of libraries analysed and the number of statistically significant gene expression events calculated in each comparison.

Comparison	Libraries compared	Significant* gene expression events	No. of refined secreted protein involved in sig exp events
1	WT T0 vs WT T1 vs WT T2	519	60
2	WT T0 vs Δoah T0	34	4
3	WT T1 vs Δoah T1	12	0
4	Δoah T0 vs Δoah T1	0	0

* The statistical significance of the fold change in gene expression across the different libraries was calculated in Cuffdiff. It uses the Benjamini-Hochberg correction for multiple-testing to determine a False Discovery Rate (FDR) adjusted p-value described as the q-value. The test directly samples from the beta negative binomial model for each transcript in each condition in order to estimate the null distribution of its log fold change under the null hypothesis (<http://cufflinks.cbc.umd.edu/>). There were no biological replicates in the dataset and as a result the statistical testing used variation across the entire dataset to calculate significance however this is not be as powerful as using biological replicates.

7.3.5 Expressed putative secreted proteins

In total, 88 predicted genes identified in the secretome had high expression (> 100FPKM) in at least one of the libraries analysed using RNA sequencing (**Table 50** and **Table 51**). Twenty of these genes had no previous annotation (**Table 50**).

Table 50: The 20 genes with no annotation identified in the secretome which had expression.

No.	Gene ID	<i>oah</i> T0	<i>oah</i> T1	WT T0	WT T1	WT T2
1	SS1G_00263	x*	x	x	x	x
2	SS1G_00849	x	x	x	x	x
3	SS1G_01086	x		x	x	x
4	SS1G_01226	x		x	x	x
5	SS1G_01867	x		x		
6	SS1G_02250	x	x	x	x	x
7	SS1G_02828			x	x	x
8	SS1G_03146	x	x			
9	SS1G_05103	x		x	x	x
10	SS1G_06068	x	x	x	x	x
11	SS1G_07027	x		x	x	x
12	SS1G_07230	x		x	x	x
13	SS1G_08110	x	x	x	x	x
14	SS1G_08907	x			x	x
15	SS1G_09232	x		x	x	x
16	SS1G_11706	x		x	x	x
17	SS1G_12262	x	x	x	x	
18	SS1G_12361	x		x	x	x
19	SS1G_13599			x	x	x
20	SS1G_13764		x	x	x	

*x: The FPKM value for that gene in that library >100.

Table 51: The 68 genes with annotation identified in the secretome which had expression support.

Gene ID	Annotation/ protein domain	<i>oah</i> T0	<i>oah</i> T1	WT T0	WT T1	WT T2
SS1G_00044	ribonuclease	x*				
SS1G_00332	carbohydrate esterase family 8 protein		x	x	x	
SS1G_00458	endo-beta- -glucanase precursor					x
SS1G_00468	carbohydrate esterase family 8 protein			x	x	
SS1G_00730	gmc oxidoreductase		x			
SS1G_00974	extracellular dihydrogeodin oxidase				x	
SS1G_01662	glycoside hydrolase family 1 protein				x	x
SS1G_01776	glycoside hydrolase family 13 protein				x	
SS1G_02495	wsc domain containing protein			x	x	x
SS1G_02857	protease s8 tripeptidyl peptidase				x	x
SS1G_03181	aspartic endopeptidase	x		x	x	x
SS1G_03286	pectin methylesterase	x	x	x	x	x
SS1G_03361	serine peptidase	x	x	x	x	x
SS1G_03518	protease s8 tripeptidyl peptidase	x		x		x
SS1G_03611	predicted protein	x		x		x
SS1G_03647	beta-galactosidase					x
SS1G_03656	secreted protein	x				
SS1G_04085	extracellular cellulase allergen asp f7				x	
SS1G_04200	alpha- -mannosidase family protein	x				
SS1G_04468	glycoside hydrolase family 47 protein	x				

SS1G_04497	glycoside hydrolase family 16 protein	x	x	x	x	x
SS1G_04530	lysophospholipase plb1		x		x	x
SS1G_04592	carbohydrate esterase family 16 protein					x
SS1G_04790	acid phosphatase	x		x	x	x
SS1G_04945	glycoside hydrolase family 7 protein	x	x	x	x	x
SS1G_05337	malate dehydrogenase protein	x				x
SS1G_05449	carboxypeptidase cpds	x		x	x	x
SS1G_05612	prolyl aminopeptidase		x			
SS1G_05832	glycoside hydrolase family 28 protein	x	x	x	x	x
SS1G_06365	extracellular dihydrogeodin oxidase laccase		x			
SS1G_07268	protease s8 tripeptidyl peptidase			x		
SS1G_07554	endo- -beta-xylanase	x	x	x	x	
SS1G_07613	phosphatidylinositol transfer protein	x	x	x	x	x
SS1G_07639	acid phosphatase	x				
SS1G_07655	subtilisin-like protein	x		x	x	x
SS1G_07836	acid protease partial	x		x	x	x
SS1G_08645	fad binding domain-containing protein		x			
SS1G_09020	beta-d-glucan cellobiohydrolase b					x
SS1G_09225	tripeptidyl peptidase a	x		x	x	x
SS1G_09248	hydrophobin					x
SS1G_09268	tripeptidyl-peptidase 1 precursor			x		
SS1G_09270	hydrophobic surface binding protein			x		x
SS1G_09475	serine carboxypeptidase	x	x	x	x	x
SS1G_09782	nuclease s1	x				
SS1G_09866	glycoside hydrolase family 5 protein					x
SS1G_09965	sphingomyelin phosphodiesterase	x		x	x	x
SS1G_10096	ep11 protein	x	x	x	x	x
SS1G_10167	polygalacturonase 1	x	x	x	x	x
SS1G_11126	major royal jelly protein		x			
SS1G_11468	cas1 appressorium specific protein	x			x	x
SS1G_11700	glycoside hydrolase family 18 protein	x				
SS1G_11853	carboxylesterase family protein		x			
SS1G_11912	necrosis and ethylene inducing peptide 2	x				
SS1G_12017	beta- -glucanosyltransferase	x	x	x	x	x
SS1G_12024	cell wall glucanase		x		x	
SS1G_12191	Glycoside hydrolase					x
SS1G_12210	Peptidase	x		x	x	x
SS1G_12413	carboxypeptidase	x		x	x	x
SS1G_12499	carboxypeptidase			x	x	
SS1G_12500	carboxypeptidase	x	x	x	x	x
SS1G_12907	cutinase					x
SS1G_12930	glycoside hydrolase family 17 protein	x	x	x	x	x
SS1G_13199	extracellular aldonolactonase	x	x	x	x	
SS1G_13385	actin patch protein 1				x	x
SS1G_13472	glycoside hydrolase 35	x	x	x	x	x
SS1G_14133	Integrin	x	x		x	x
SS1G_14184	carbohydrate esterase family 4 protein		x			
SS1G_14293	glucose oxidase		x			

*x: The FPKM value for that gene in that library >100.

7.3.6 Comparison of significantly expressed secreted proteins during WT *in vitro* conditions and in planta infection

The WT T0, WT T1 and WT T2 libraries were compared and based on fold changes in gene expression, 519 gene expression events were calculated to be significant across the 3 libraries. Across these significant events, secreted proteins identified in the refined secretome (Chapter 5) were responsible for 60 of these significant events (**Table 52**). The comparison of these libraries highlighted which secreted proteins are specifically involved in WT infection or are constitutively expressed. Out of this group, three sub groups were identified to have similar expression profiles. Group 1 contains genes which had significant up regulation in WT T1 and were down regulated in WT T2 (**Figure 72a**). Group 2 includes genes which were significantly up regulated late in *in planta* infection at WT T2 (**Figure 72b**) and Group 3 included those genes which exhibited high expression *in vitro*, then a reduction in expression during WT T1 and finally an expression increase again during later plant infection stages (**Figure 72c**).

Table 52: Forty secreted proteins identified in the *S. sclerotiorum* refined secretome that account for the 60 statistically significant gene expression events across the comparison of *in vitro* and *in planta* conditions.

Bold Genes denote the most highly expressed genes across the conditions.

Group	Gene ID	Protein domain	FPKM		
			WT T0	WT T1	WTT2
1	SS1G_00974	dihydrogeodin oxidase	45	662	288
1	SS1G_07022	histidine acid phosphatase	14	93	45
1	SS1G_09495	phospholipase	5	132	112
1	SS1G_11912	necrosis and ethylene inducing peptide 2	24	159	108
1	SS1G_13385	actin patch protein 1	13	473	346
2	SS1G_00746	endo- β -mannosidase	2	6	148
2	SS1G_01083	GH 31 protein	1	2	99
2	SS1G_02334	GH 7 protein	22	27	201
2	SS1G_02620	GH 79 protein	11	14	184
2	SS1G_03387	GH 5 protein	1	2	89
2	SS1G_04030	lysophospholipase 1	13	38	106
2	SS1G_04473	extracellular serine-rich protein	4	81	210
2	SS1G_05192	GH65	23	34	137
2	SS1G_05434	gds1-like lipase acylhydrolase	9	13	167
2	SS1G_06426	GH 43 protein	6	6	41
2	SS1G_07749	GH 11 protein	0	0	12
2	SS1G_08163	signal peptide-containing protein	0	13	139
2	SS1G_08634	exo-polygalacturonase	20	20	130
2	SS1G_08695	class III chitinase (GH18)	0	1	9
2	SS1G_09060	subtilisin-like protease	1	1	44
2	SS1G_09866	GH 5 protein	13	51	526
2	SS1G_11922	arabinan endo-1,5- α -L-arabinosidase (GH43)	0	0	17
2	SS1G_12200	glucooligosaccharide oxidase	74	25	152
2	SS1G_12287	predicted protein	0	0	6
2	SS1G_13501	alpha-l-rhamnosidase	29	34	290
2	SS1G_13736	protein rds1	8	21	136
2	SS1G_14133	fg-gap repeat protein	171	658	1764
3	SS1G_00423	ser thr protein phosphatase	91	8	60
3	SS1G_01005	GH 31 protein	5	2	24
3	SS1G_02022	alpha-mannosidase	60	9	99
3	SS1G_03610	carbohydrate esterase family 16 protein	108	43	293
3	SS1G_03611	predicted protein CFEM domain	1315	79	10625
3	SS1G_04468	GH 47 protein	52	7	203
3	SS1G_07230	predicted protein (unique to Ss)	3146	638	3920
3	SS1G_07639	acid phosphatase	50	4	57
3	SS1G_08208	β -mannanase (GH 5)	55	25	179
3	SS1G_09020	cellulose 1,4- β -cellobiosidase	121	17	376
3	SS1G_09270	hydrophobic surface binding protein	3714	191	988
3	SS1G_12083	GH 115 protein	11	2	61
3	SS1G_12907	cutinase	81	61	728

Group 1

This group of putative secreted proteins are specifically up regulated during the change from *in vitro* conditions to early plant infection. They are all down regulated during later plant infection. Apart from the phospholipase (SS1G_09495), the genes identified here are not lipid or cell wall degrading enzymes but instead consist of enzymes that may be more fundamental for the switch between general vegetative growth to infection, or the possible switch between biotrophy and necrotrophy. These may include SS1G_11912, a necrosis and ethylene inducing peptide 2 precursor, which was significantly up regulated and could be important for infection. SS1G_13385, an actin patch protein 1, is not directly involved in de novo lipid synthesis but is a phosphatidate phosphatase that catalyses the conversion of phosphatide to diacylglycerol. SS1G_00974, an extracellular dihydrogeodin oxidase had the highest expression at WT T1 in this group. This enzyme is widespread in fungi and likely involved in phenolic metabolism potentially as a laccase involved in lignin degradation.

Group 2

Many of the secreted proteins up regulated at later points during *in planta* infection are hydrolysing enzymes which are required to breakdown different parts of plant cell walls and other plant substrates. Many of these proteins would be secreted extracellularly to act on plant substrates. Group 2 consists of many Glycoside Hydrolase (GH) domain containing genes which have a role in hydrolysing plant polysaccharides.

SS1G_08163 was identified in the refined secretome as small, cysteine rich secreted protein which is typical of some effector proteins (Bolton et al. 2008b, do Amaral et al. 2012). This gene was expressed only *in planta* highlighting that its induction is during infection. SS1G_07749, containing a GH11 domain, SS1G_08695 a class III chitinase, SS1G_11922, a arabinosidase and SS1G_12287 a hypothetical protein, all have no transcripts detected *in vitro* but were significantly up regulated during later infection.

SS1G_10167 (SsPg1) a polygalacturonase involved in virulence (Dallal Bashi et al. 2012), has very high abundance across all 5 libraries and shows no significant change in expression. Another polygalacturonase (SS1G_08634) was however significantly up regulated later on in the infection course. This is in keeping with other studies as which have demonstrated that other polygalacturonases (SsPg3, SsPg5, or SsPg6) are expressed much later than SsPg1 (Cotton et al. 2003, Li et al. 2004b, Favaron et al. 2004) during infection.

SS1G_14133 was the most highly expressed gene in Group 2. It is a fg-gap repeat

protein which is one of the α subunits of an integrin protein. Integrins are involved in many critical roles including cell structure, cell migration, anchoring cells to the extracellular matrices and carrying signals from the outside to the inside of the cell and vice versa (Zhu et al. 2013). Silencing of this gene (SSITL) resulted in a significant reduction in virulence and initiated strong and rapid defence response in Arabidopsis. It has been suggested that SSITL is an effector protein and plays significant role in the suppression of jasmonic/ethylene (JA/ET) signal pathway (Zhu et al. 2013).

Group 3

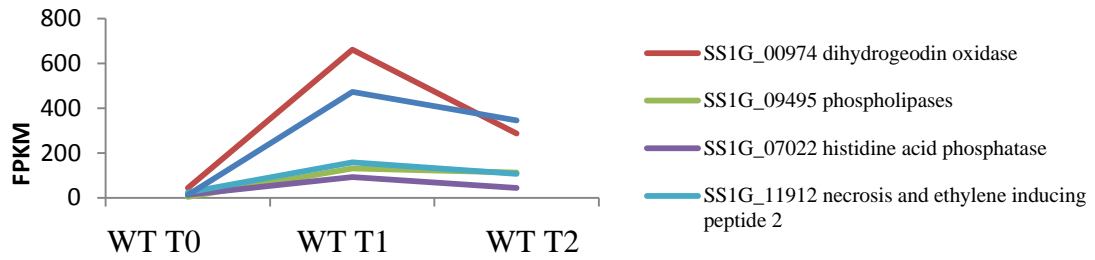
This group of putative secreted proteins show significant expression during the transition from agar plug to 12hpi *A. thaliana* infection. SS1G_03611 had the highest FPKM in WT T2. This protein was identified in the refined secretome as small, cysteine rich secreted proteins which is the protein profile typical of some effector proteins (Bolton et al. 2008b, do Amaral et al. 2012). As described previously, SS1G_03611 has further EST support from in other EST libraries and also contains a CFEM domain which may be important for virulence. SS1G_07230, a protein identified as unique to *S. sclerotiorum* also follows a high expression pattern like SS1G_03611 but is also expressed during culture. This protein has only 63 amino acids in the mature protein but no cysteine residues.

The cutinase SS1G_12907 was significantly up regulated *in planta*. SS1G_07661 a cutinase (Sscuta) which has been implicated in virulence (Dallal Bashi et al. 2012) and shares 52% homology with SS1G_12907 which was identified in this study suggesting that other cutinases may also be required for virulence. In previous studies, 4 cutinase-like enzymes encoded by SS1G_07661 (down regulated *in planta*), SS1G_12709 (lowly expressed), SS1G_13386 (some abundance in WT T2), and SS1G_12907 exhibited 81%, 63%, 58%, and 52% homology respectively to the homologous *B.cinerea* cutinase (BcCUTA).

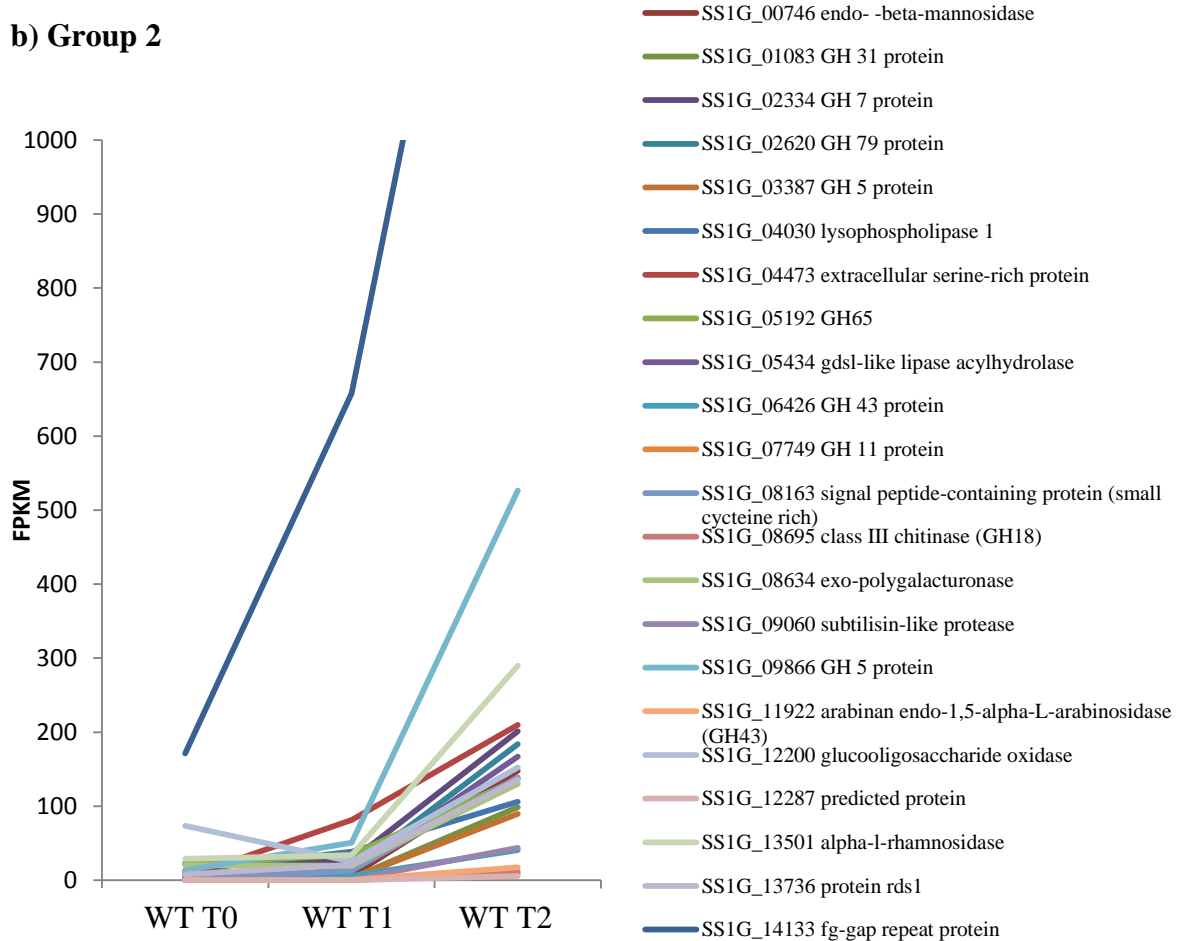
The phosphatases SS1G_07639 and SS1G_00423 are not highly expressed but are required for the specific dephosphorylation of specific phosphoprotein substrates. SS1G_09020 a cellulose 1,4-beta-cellobiosidase was down regulated during the transition from agar to plant most likely because the cellulose and cellotetraose which it hydrolyses were not available during early infection. Instead this gene is up regulated during the later stages of infection once the cellulose has been release after hydrolysis of the cell wall.

The hydrophobic surface binding protein, SS1G_09270, which has been previous isolated from the liquid exudates from sclerotial (Liang et al. 2010), was highly up regulated *in vitro*. This could be a result of growing the fungus aerially on cellophane and therefore may require more surface binding proteins.

a) Group 1



b) Group 2



c) Group 3

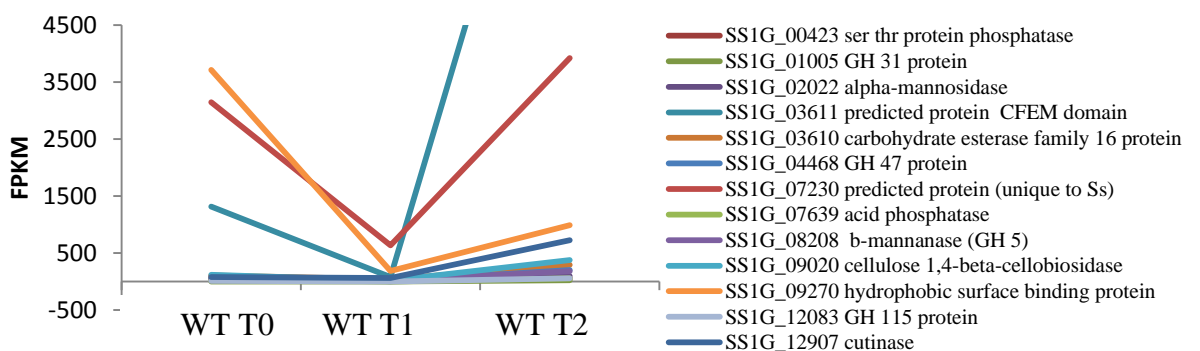


Figure 72: Patterns of secreted protein expression.

Secreted proteins identified in the refined secretome which are divided into three groups based on similar expression profiles across the WT time course. The x-axis represents the time points during infection: 1- WT T0, 2- WT T1, 3- WT T2.

7.3.7 Comparison of significantly expressed secreted proteins during WT and Δoah in vitro conditions

Across all 34 significant gene expression events between WT T1 and Δoah T0 libraries, only four secreted proteins from the refined secretome were identified (**Table 53**). SS1G_02828 was significantly down regulated in the mutant, however with no protein domain information we cannot really speculate on its involvement with oxalic acid. An increase in expression was seen ΔOAH T0 library in the remaining 3 genes. SS1G_04200 contains a glycoside hydrolase domain and is speculated to have alpha-mannosidase activity which hydrolyses alpha mannose. SS1G_04958 which contains a putative Prokumamolisin, activation domain is predicted to have peptidase activity. Finally SS1G_10172 has a phytase-like PFAM domain, which is suggested to have PLC-like phospho-diesterase which hydrolyse phosphodiester bonds.

Table 53: Four secreted proteins identified in the refined secretome with significant gene expression between the in vitro WT and Δoah samples.

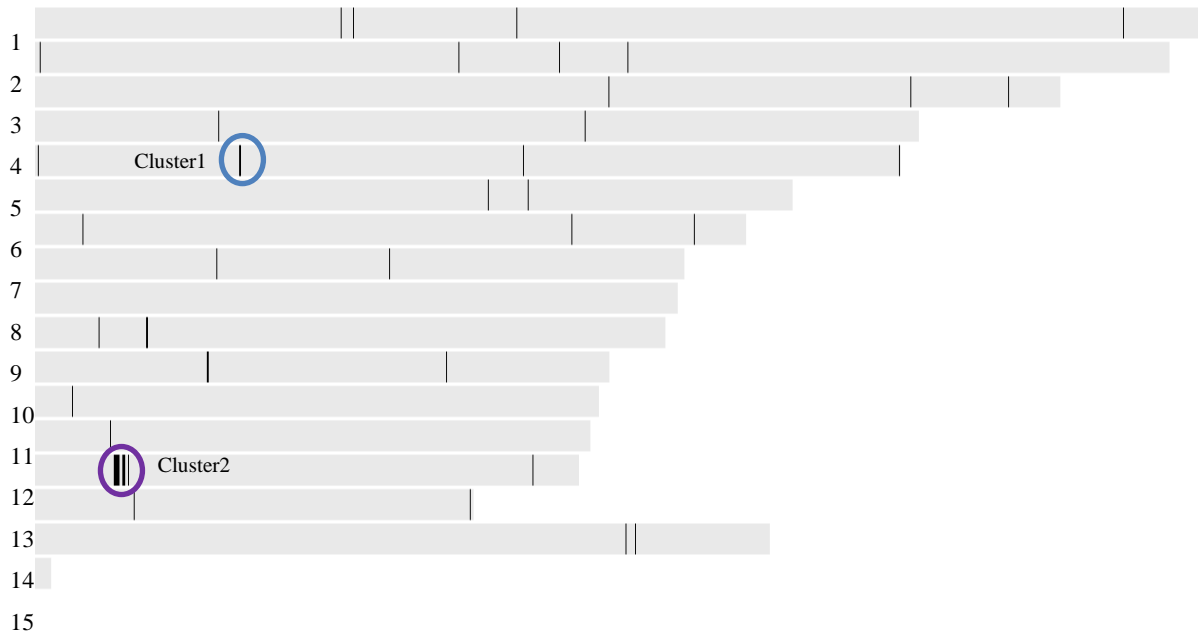
Gene ID	Gene annotation	Length	Cysteine	% Cys	WoLF PSORT	PFAM	WT T0 FPKM	Δoah T0 FPKM
SS1G_02828	Protein	187	4	2.14	extr=21	-	1292.43	16.8366
SS1G_04200	alpha-mannosidase family protein	755	3	0.4	extr=25	07971	3.49278	335.028
SS1G_04958	tripeptidyl-peptidase precursor	567	6	1.06	extr=25	09286	5.11701	188.57
SS1G_10172	Phytase-like	401	4	1	extr=25	13449	15.4866	319.67

7.3.8 The botcinic acid biosynthesis cluster

The 50 genes with highest fold changes, regardless of significance, between the *Δoah* T0 and *Δoah* T1 libraries were investigated. The 50 gene IDs were mapped to the *S. sclerotiorum* genome using Omnimap. This identified a cluster of 10 genes which were up regulated in the fungus during *in planta* infection (**Figure 73a**). The genes all cluster on the 14th chromosome. Three of these genes have cytochrome P450 domains, two exhibit sequence homology with polyketide synthase enzymes and a further two genes were annotated as having possible mono-oxygenase activity. The annotation and close proximity of the genes in the genome is highly suggestive of a gene cluster involved in secondary metabolite synthesis. On closer inspection of this gene cluster, the genes were identified to be homologues to the BcBOA genes in *B.cinerea* genome which have been predicted to be involved in the biosynthetic pathway of botcinic acid (Dalmais et al. 2011).

In the proposed botcinic acid biosynthetic pathway, 17 genes are predicted to be involved in biosynthesis of this phytotoxin (Dalmais et al. 2011). Of these, thirteen homologue genes have been identified in the *S. sclerotiorum* sequenced genome. Both fungi possess two clusters of genes involved in this pathway but their repartitions are different (Dalmais et al. 2011) (**Figure 73b**). What is very interesting about this group of genes in *S. sclerotiorum* is that they are highly expressed under the *Δoah in planta* conditions but had relatively no expression in any of the other 4 libraries (**Table 54**).

a)



b) *Botrytis cinerea* B05.10

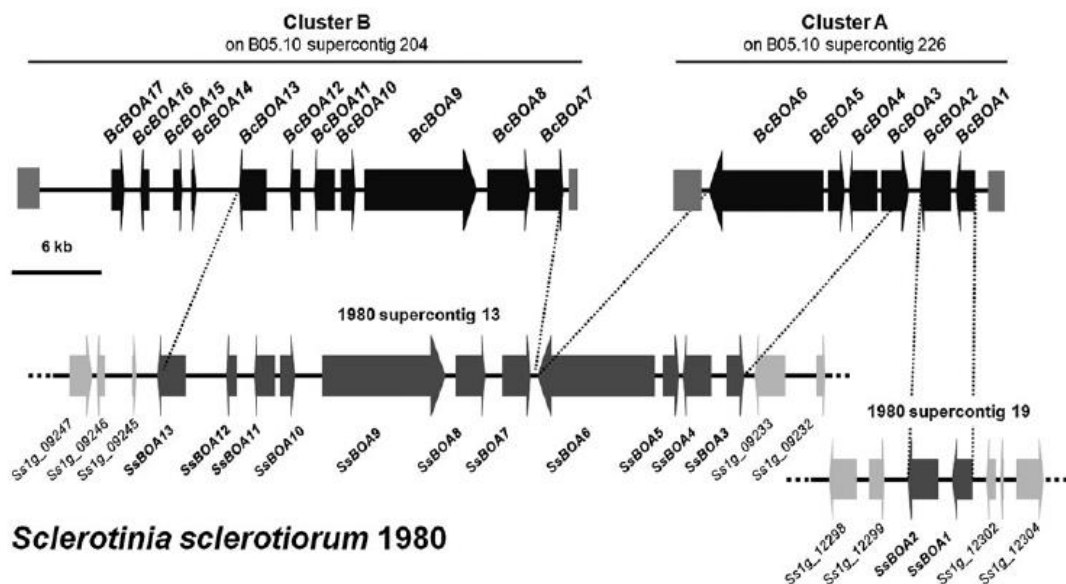


Figure 73: Botcinic acid cluster.

a) The two clusters of genes identified on chromosome 14 which corresponds to the homologue botcinic acid synthesis genes. b) Figure from Dalmais et al. (2011) (Dalmais et al. 2011) which highlights the putative botcinic acid biosynthetic genes. BcBOA genes are part of two clusters in both *B. cinerea* B05.10 and *S. sclerotiorum* sequenced genomes. Black arrows indicate genes that might be involved in botcinic acid biosynthesis in *B. cinerea*. Dark grey arrows in *S. sclerotiorum* indicate the homologue BcBOA genes. Light grey arrows indicate the *S. sclerotiorum* genes that are probably not related to secondary metabolism and the botcinic acid cluster. Grey boxes at the ends of the *B. cinerea* clusters indicate AT-rich regions exhibiting AT contents from 70% to 90%.

Table 54: The *S. sclerotiorum* homologue gene identified in *B. cinerea* which are responsible for the synthesis of botcinic acid.

Cluster	Gene ID		FPKM					Pfam	<i>B. cinerea</i> ID	Ref paper
			<i>Δoah</i> T0	<i>Δoah</i> T1	WT T0	WT T1	WT T2			
1	SS1G_12300	Flavin-binding monooxygenase	1	252	0	0	0	PF00743	BcBOA2 Bc1g_16083	Schumacher et al.(2008)
1	SS1G_12301	monooxygenase-like, NmrA-like family	1	967	1	0	0	PF05368	BcBOA1	Schumacher et al.(2008)
2	SS1G_09234	cytochrome p449	15	1113	1	1	1	PF00067	BcBOA3 Bc1g_16084	Schumacher et al.(2008)
2	SS1G_09235	cytochrome p450	36	1099	3	1	4	PF00067	BcBOA4 Bc1g_16085	Schumacher et al.(2008)
2	SS1G_09236	alcohol dehydrogenase	3	327	0	0	1	PF08240	BcBOA5	Schumacher et al.(2008)
2	SS1G_09237	Reducing polyketide synthase	4	804	0	0	1	PF00109 PF02801 PF00698	BcBOA6 Bc1g_16086 Bc1g_16087	Schumacher et al.(2008)
2	SS1G_09238	cytochrome monooxygenase p450	3	505	0	0	0	PF00067	BcBOA7	Dalmais et al. (2011)
2	SS1G_09239	fad binding domain	3	599	0	1	0	PF01494	BcBOA8 Bc1g_15836	Dalmais et al. (2011)
2	SS1G_09240	polyketide synthase	20	333	7	10	13	PF00109 PF02801 PF00698	BcBOA9 Bc1g_15837 Bc1g_15838 Bc1g_15839	Dalmais et al. (2011)
2	SS1G_09241	thioesterase domain containing protein	1	1005	0	0	0	PF00975	BcBOA10 Bc1g_15840	Dalmais et al. (2011)
2	SS1G_09242	Transferase family	0	108	0	0	0	PF02458	BcBOA11 Bc1g_15841	Dalmais et al. (2011)
2	SS1G_09243	unknown function (no domains found)	1	777	0	0	0	-	BcBOA12 Bc1g_15842	Dalmais et al. (2011)
2	SS1G_09244	fungal Zn(2)-Cys(6) binuclear cluster domain	7	167	1	0	0	PF00172	BcBOA13 Bc1g_15843	Dalmais et al. (2011)

7.3.9 Expression of appressoria associated genes

The expression of genes associated with the development of appressoria that were listed in the genome analysis paper (Amselem et al. 2011) was investigated which revealed that the expression between the mutant and the WT strain were comparable (**Table 55**). As the *oah* mutant has been observed to produce a very low frequency of appressoria, this suggests that there was very little development of apothecia during the WT infection. SS1G_11468 may be induced by thigmotrophic sensing as it highly upregulated in the *oah* T0 library. This gene was also identified in the *S. sclerotiorum* secretome (Chapter 5).

Table 55: The ortholog genes in *S. sclerotiorum* known to be associated with appressoria formation.

The numerical values represent the FPKM calculated for each library.

Gene ID	Proposed function	WT T0	WT T1	WT T2	<i>Δoah</i> T0	<i>Δoah</i> T1
SS1G_00173	uncharacterized	3.1671	9.78576	3.83291	9.12065	9.13484
SS1G_00637	appressorium formation and penetration; PAK protein kinase	112.798	74.2221	74.1364	93.9233	142.959
SS1G_01602	penetration hyphae; autophagy	1594.88	963.326	1040.47	987.626	1544.08
SS1G_01851	appressorium formation; extracellular matrix protein	263.849	97.1984	84.6698	170.006	367.768
SS1G_04934	uncharacterized	96.3784	39.7014	18.0993	53.0418	7.39463
SS1G_05586	appressorium penetration; tetraspanin	112.254	60.2846	67.2887	142.456	56.5463
SS1G_07136	appressorium maturation; steA Transcription factor	97.6622	85.5689	93.2887	133.322	221.061
SS1G_10311	appressorium penetration	244.265	295.718	177.454	54.9693	24.1381
SS1G_11468	uncharacterized	227.984	966.581	392.496	5284.91	7.9385
SS1G_13339	penetration hyphae; carnitine O-acetyl transferase	694.224	495.879	430.443	208.49	156.45
SS1G_14237	uncharacterized	0.700403	3.59151	1.48338	3.64723	0.606049

7.3.10 Expression of documented virulence genes

The expression levels of reported virulence genes and other potential genes identified in the refined *S. sclerotiorum* secretome involved in pathogenesis were investigated across the different conditions (**Table 56**). What is noticeable is that most of the highly expressed proposed virulence genes (SS1G_08218, SS1G_10167, SS1G_00699, SS1G_00263) in the WT libraries are still expressed highly but at much lower transcripts were measured in the corresponding mutant libraries. An exception to this is the *pac1* gene (SS1G_07355) which was up regulated in both Δoah libraries. There was no expression seen for the *oah* gene which confirmed the lack of this enzyme within the mutant.

The identified oxalate decarboxylase proteins which are associated with the breakdown of oxalate (SS1G_08814 and SS1G_10796) had relatively low expression. SS1G_08814 had relatively constant expression throughout the experiment. SS1G_10796 was more highly expressed later on during infection. However expression levels dropped considerably in the mutant libraries.

SS1G_00772 a putative secreted protein containing three LysM domains which had been identified in the *S. sclerotiorum* refined secretome was expressed throughout the infection in both WT and Δoah strains but in relatively low abundance. The other three proteins containing LysM domains were not expressed during this experiment. This gene had higher expression levels *in vitro* then during plant infection, although the LysM genes are often expressed more highly at later points in infection which is something which could be further investigated.

The two NADPH oxidases (SS1G_05661, SS1G_11172) had low expression across all libraries which is surprising as this protein is important for regenerating superoxide which is an important precursor of several reactive oxygen species (ROS), including hydrogen peroxide (Kim et al. 2011). SsSod1, a superoxide dismutase (SS1G_00699) had higher expression in comparison to NADPH oxidase genes, which but was reduced lower in the mutant libraries.

Table 56: Expression of documented virulence genes.

The expression levels of genes documented in the literature or identified in the refined secretome to be potentially involved in virulence of pathogenicity during *S. sclerotiorum* infection. Red denotes genes which were down regulated in the corresponding OAH libraries. Green denotes those genes which were up regulated in the corresponding library.

Gene ID	Documented virulence genes	FPKM				
		WT T0	WT T1	WT T2	Δoah T0	Δoah T1
SS1G_02462	arabinofuranosidase/beta-xylosidase	51	211	495	15	13
SS1G_01788	cna1	193	201	187	135	122
SS1G_00772	LysM domain	73	48	26	38	11
SS1G_12509	LysM domain	0	0	0	0	0
SS1G_12513	LysM domain	0	0	0	1	0
SS1G_03535	LysM domain	1	0	0	1	0
SS1G_08218	OAH	7110	6050	3004	2	12
SS1G_08814	oxalate decarboxylase	22	22	16	16	28
SS1G_10796	oxalate decarboxylase	2	27	29	3	4
SS1G_07355	pac 1	68	120	108	257	440
SS1G_08104	Cutinase	6	31	35	6	72
SS1G_12907	Cutinase	81	61	728	103	18
SS1G_07661	Sscuta	75	25	27	44	60
SS1G_14127	Ss-ggt1	21	19	62	29	16
SS1G_10167	sppg1	16564	11091	6353	10141	5548
SS1G_00699	SsSod1	1887	1518	1332	1739	1195
SS1G_00263	ssv263	17757	14887	10574	14063	2273
SS1G_07626	<i>B.cinerea</i> velvet homologue	45	48	63	58	123
SS1G_05661	NADPH oxidase(Ssnox1)	13	16	20	27	24
SS1G_11172	NADPH oxidase(Ssnox2)	47	43	43	42	15

7.3.11 Polygalacturonase expression

The analysis of the *S. sclerotiorum* refined secretome revealed 17 genes with Glycoside Hydrolase family 28 (GH28) protein domains which are characteristic of polygalacturonases (PGs) (Chapter 5) (**Table 57**). Six of these genes have been identified and characterised as PGs in previous studies ((Li et al. 2004b, Dallal Bashi et al. 2012, Kasza et al. 2004, Cotton et al. 2003). In this experiment, Sspg1 (SS1G_10167) was the most highly expressed PG across all libraries. It was most highly expressed in the *in vitro* libraries and less expressed *in planta*. The expression level of this gene in the ΔOAH libraries was almost half the expression of that in the corresponding WT libraries. SS1G_05832 which contains a GH28 domain but has not been previously characterised as a PG, was the second most highly expressed gene in this data set. SS1G_14449 was also up regulated across all libraries; again the level of expression was higher in the *in vitro* libraries. An interesting observation is the up regulation of SS1G_01009 only in the Δoah *in planta* T1 library, again suggestive of a link between this enzyme and the OAH enzyme specifically. SS1G_06235 and SS1G_07039 have very little or no expression in any of the libraries suggesting that they may be redundant PGs or require other environmental signals to induce expression. SS1G_06235 had no expression in WT libraries and only very low abundance in the Δoah libraries.

From these data, 3 groups of putative polygalacturonases were identified across the WT infection course. Most of the previously characterised endo-PGs are in Group 1 which exhibit the highest expression *in vitro* and then have decreasing expression over time *in planta* (**Figure 74a**). Group 2 consist of other endo-PGs which have expression levels which peak in the WT T1 library suggesting they are principally activated early during infection (**Figure 74b**). Finally Group 3 consists of the exo-PGS which had higher expression levels later during infection (**Figure 74c**).

Table 57: Seventeen *S. sclerotiorum* genes identified in the refined secretome as putative polygalacturonases.

The expression levels in each library are denoted by the FPKM values.

Group	Gene ID	Classified	NCBI	FPKM					
				WT T0	WT T1	WT T2	Δoah T0	Δoah T1	
1	SS1G_02399			56	35	27	31	38	
1	SS1G_04177	Sspg5	AY496277	20	6	6	3	4	
1	SS1G_05832			1 885	1	499	697	939	
1	SS1G_10167	Neutral endo	Sspg1	AF501307	16	11	6	10 141	5 548
				564	091	353			
1	SS1G_11057	Neutral endo	Sspg6	AF501308	6	4	3	14	41
1	SS1G_14449				236	130	133	138	115
2	SS1G_04552				2	7	6	3	12
2	SS1G_07039				5	8	6	5	8
2	SS1G_01009				0	2	0	1	136
2	SS1G_10698	Acid endo	Sspg3	AY312510	58	99	41	75	64
3	SS1G_02553	exo	Xpg2	AY312512	2	1	15	7	1
3	SS1G_03540				40	15	78	57	6
3	SS1G_04207	exo	Xpg1	AY312511	0	0	36	3	0
3	SS1G_08229				3	6	21	2	13
3	SS1G_08634				20	20	130	11	5
3	SS1G_12057				10	6	21	15	15
-	SS1G_06235				0	0	0	2	3

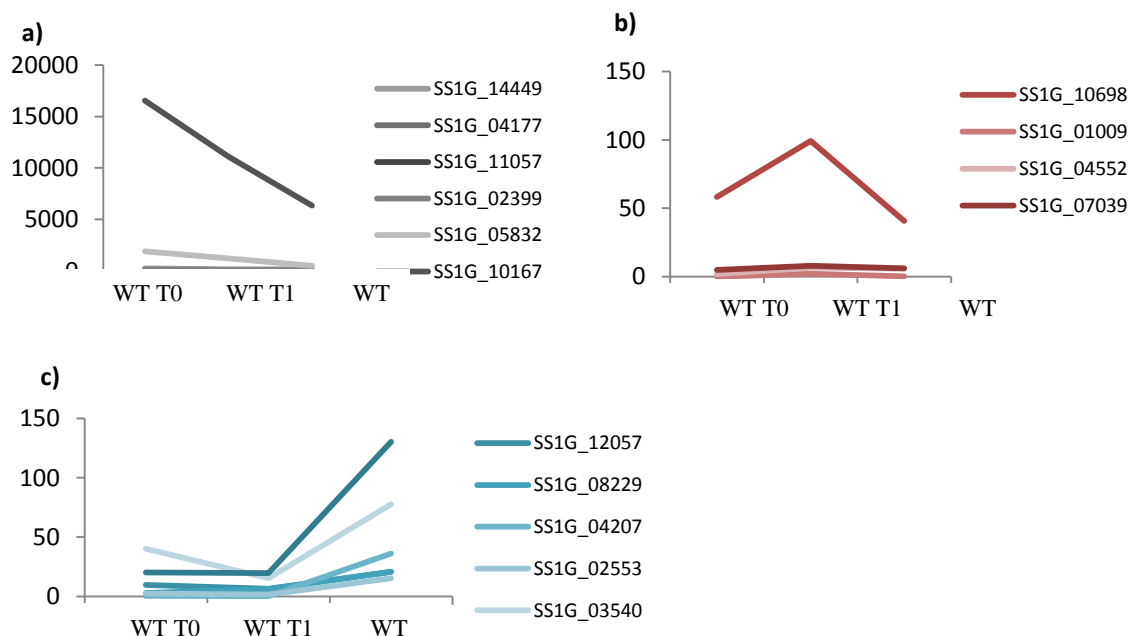


Figure 74: Three subgroups of putative polygalacturonases expressed in during WT *in vitro* and *in planta* condition.

a) Group 1 WT PG expression. b) Group 2 WT PG expression. c) Group 3 WT PG expression.

7.3.12 Genes with similar expression patterns as *oah*

The top 20 genes with most similar expression profiles to oxaloacetate acetylhydrolase (SS1G_08218) across the WT infection course were selected using the ‘mySimilar’ command in R (

Table 58). The aim of this investigation was to monitor which genes were expressed alongside *oah1* and if any of these same genes were down regulated in a similar way to *oah1* in the $\Delta oah1$ libraries. This could be suggestive of co-regulation of important genes linked with OAH function. SS1G_08218 was expressed highly in all three WT conditions but has the highest expression *in vitro*. Out of those 20, only the 15 genes which had FPKM value greater than 100 FPKM in at least one library were analysed. The 15 genes were divided into three groups according to their expression profiles in the Δoah libraries.

Four genes were placed in Group 1 (**Figure 75a**). These genes were considerably down regulated in the Δoah libraries. These include SS1G_14018 a fad binding domain protein, SS1G_09475, a serine carboxypeptidase, SS1G_08795, a succinate fumarate mitochondrial transporter and SS1G_05902, a Sec61beta family domain containing protein may all be directly regulated alongside *oah1*.

In Group 2, expression of genes is up regulated in Δoah *in vitro* library (

Figure 75b). This was observed for SS1G_12839, a pyruvate carboxylase which catalyses the breakdown of pyruvate into oxaloacetate was on the other hand was up regulated in $\Delta oah1$ T0. Other proteins in this group are transporters and transferases.

The third group consists of hypothetical proteins with unknown function, a Git3 glucose receptor (SS1G_07511) and a vesicle coat transport protein (SS1G_14228). These proteins are up regulated in the Δoah T1 library (

Figure 75c).

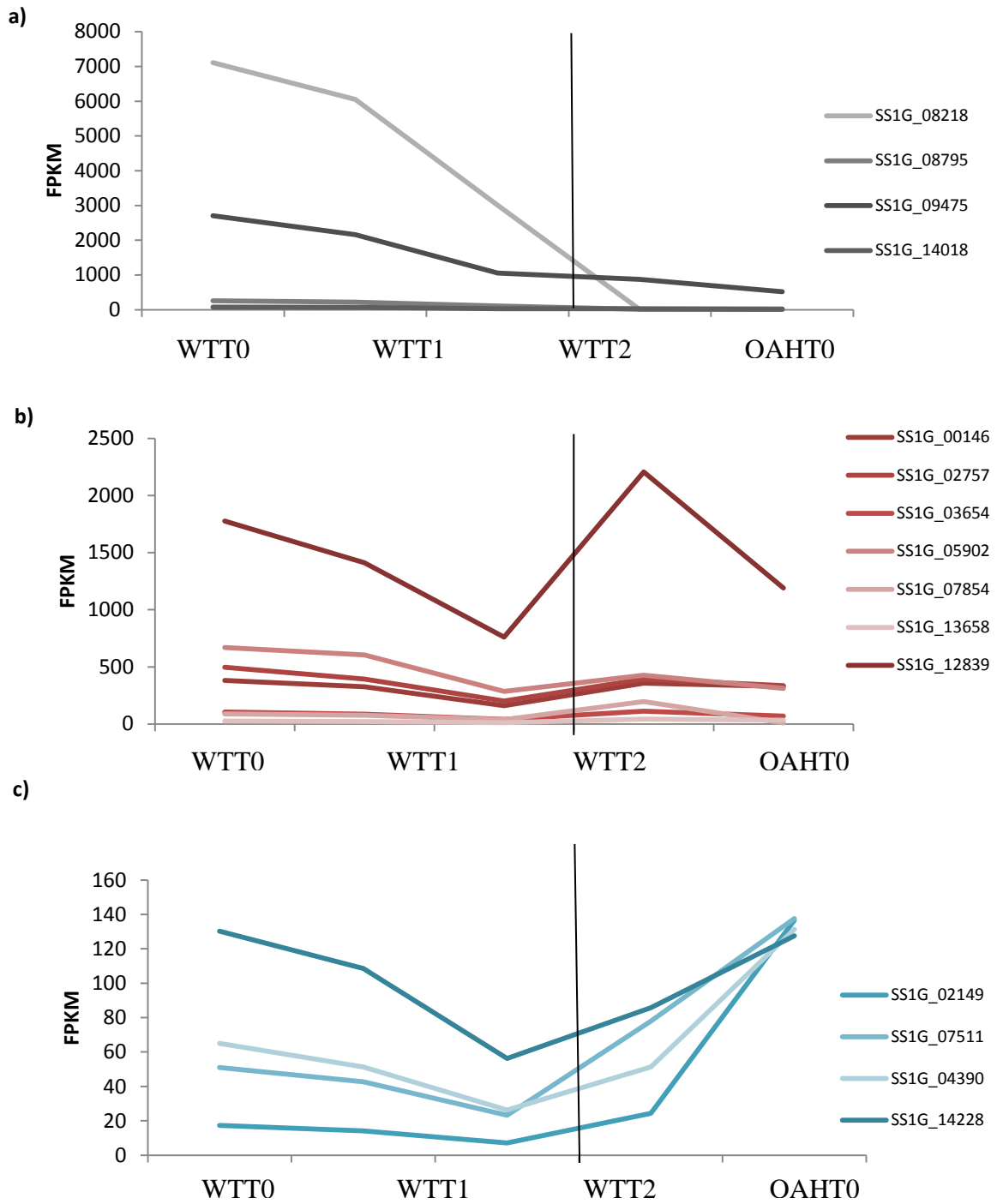


Figure 75: Three groups of genes which exhibited similar expression profiles to *oah*. Genes identified in the WT libraries but have different expression profiles in the OAH libraries. a) Expression is down regulated in the *oah* libraries. b) Expression is up regulated in the *oah1 in vitro* library. c) Expression was up regulated *in planta*.

Table 58: The expression of the top 20 genes with most similar expression profiles to oxaloacetate acetylhydrolase gene across the five libraries.

Group	Name	Function	WT T0	WT T1	WT T2	<i>Δoah</i> T0	<i>Δoah</i> T1	
1	SS1G_08218	oxaloacetate hydrolase	Hydrolyse oxaloacetate into oxalate and acetate.	7110	6050	3004	2	12
1	SS1G_08795	succinate fumarate mitochondrial transporter	Transporter protein within the TCA cycle.	257	217	106	15	9
1	SS1G_09475	serine carboxypeptidase	Peptide hydrolysis, found in the refined secretome.	2704	2163	1056	878	520
1	SS1G_14018	fad binding domain protein	Oxygen oxidoreductase which uses FAD as a co-factor.	79	70	33	30	21
2	SS1G_00146	carbonic anhydrase	Catalyses the hydration of CO ₂ to give bicarbonate and a proton. Provide bicarbonate for metabolic carboxylation reactions and involved in CO ₂ sensing by producing bicarbonate for the activation of adenylyl cyclase.	382	326	161	358	329
2	SS1G_02757	predicted protein	-	497	392	201	392	335
2	SS1G_03654	formate transporter	Formate/nitrate transporters.	105	87	41	113	68
2	SS1G_05902	Sec61beta family domain	Protein-conducting channel transferring polypeptides across the endoplasmic reticulum.	670	604	284	427	312
2	SS1G_07854	Acetyltransferase (GNAT) family	Transferase enzyme that transfers an acetyl group. Possibly to traffic intermediates of the glyoxylate cycle.	89	75	37	197	9
2	SS1G_12839	pyruvate carboxylase	Catalyses the breakdown of pyruvate into oxaloacetate.	1776	1412	761	2206	1190
2	SS1G_13658	1-aminocyclopropane-1-carboxylate synthase	Generates aminocyclopropane-1-carboxylate, a precursor for ethylene.	26	21	11	42	33
3	SS1G_02149	hypothetical protein SS1G_02149	-	17	14	7	24	137
3	SS1G_04390	hypothetical protein SS1G_04390	-	65	51	26	51	131
3	SS1G_07511	G protein-coupled glucose receptor regulating Gpa2	Git3 functions during adenylate cyclase activation.	51	43	23	78	138
3	SS1G_14228	copii-coated vesicle membrane protein	Vesicle coat protein that transports proteins from the rough endoplasmic reticulum to the Golgi apparatus.	130	109	56	86	128

7.4 Discussion

The use of RNA sequencing to monitor the infection process of *S. sclerotiorum* WT and *Δoah* mutant strains in *Arabidopsis* has revealed a wealth of expression data which will improve the community's understanding of this interaction and how oxalic acid may regulate other genes important to the infection process and pathogen development. However due to the lack of finance to sequence biological replicates, the observations made in this chapter would require further validation through repetition of the RNA sequencing or RT-qPCR to explore further a particular gene expression pattern. In future, the technical replicate data which is available for each library will be individually processed through the bioinformatics pipeline to calculate the FPKM values per genes per technical replicate to allow for further statistical analysis of the results.

In total, seven libraries were sequenced using the Illumina RNAseq platform. The changes in the fungal gene expression profiles have been analysed but changes in the expression profile of the plant genes is yet to be analysed. The transcriptome information of the fungal *in vitro* samples (WT T0, *Δoah* T0) and the plant samples infected with the pathogen (WT T1, WT T2, *Δoah*T1) were explored to observe expression of putative secreted proteins, documented virulence genes and proteins with a similar expression profile to *oah* (SS1G_08218). Due to time constraints, the entire set of data has not been fully explored but continues to be analysed by collaborators at the University of Florida.

7.4.1 Genes with the highest abundance

The analysis initially has revealed the 10 most highly expressed genes across the five libraries. These genes predominately include ribosomal proteins was expected as ribosomes are essential for the synthesis of the plethora of proteins and enzymes required for growth and pathogenesis. The most highly expressed gene across all libraries was SS1G_00253 which has no known protein domains or any annotation but is most likely a ribosomal protein. Although still highly expressed in the *Δoah* libraries compared to other genes, SS1G_00253 was expressed at reduced levels suggesting the lack of *oah* and the subsequent reduction in oxalic acid production will affect some of the most important basic growth and metabolism genes. Other housekeeping genes like proteolipid membrane potential modulators and a putative transcription factor bZIP were also highly expressed. Transcription factor bZIP was present in high abundance across all libraries suggesting it regulates general growth and metabolism. The *S. sclerotiorum* genome contains a predicted 345 transcription factors which are responsible for regulating a range of genetic networks and so it is logical that these would be highly up regulated during certain conditions.

Eleven hypothetical proteins with no known protein domains were expressed at high levels across the five libraries. This highlights an abundance of proteins within the two saprotrophic and necrotrophic phases that are expressed at high levels during growth but remains relatively unknown and require further investigation.

7.4.2 Expression of the putative refined secretome

Eighty eight genes identified in the refined secretome were found have an FPKM > 100 in at least one of the RNAseq libraries. This provides further expression support for 20% of the refined secretome. Furthermore, determining the significant expression pattern across different conditions is a very powerful tool to observe important genes involved in specific processes. This allows identification of certain genes that differ in gene expression between different fungal strains as well as looking at changes in the same species over time or during infection. As there were no biological replicates to calculate the variations across gene events, cuffdiff calculated significant expression by taking into account variations across all the different conditions being compared. As a result there were fewer significant events than expected because of the reduced statistical power.

The significant expression of genes from the refined secretome defined in Chapter 5 was investigated across the *in vitro* and *in planta* WT libraries. If these putative secreted proteins have high levels of expression, it provides further validation that these proteins have a function. Forty one putative secreted proteins were responsible for 60 significant gene expression events across WT T0, WT T1 and WT T2. Three subgroups (Group1-3) of these proteins which have similar expression patterns were the subject of further investigation. Group 1 identified genes that were switched on *in planta*. One of the most interesting genes observed with significant expression in Group 1 was SS1G_11912, the putative necrosis and ethylene inducing peptide identified in the refined secretome. This should be investigated further as a homologous protein in *Phytophthora sojae* (PsojNIP) was shown to be expressed during the transition from biotrophy to necrotrophy (Qutob et al. 2002). This is similar to the conditions being investigated here where *S. sclerotiorum* was forced to switch from a non-pathogenic lifecycle on the agar plate to infecting *A. thaliana*. PsojNIP is hypothesised to be a toxin gene that is expressed late during the colonisation of soybean, and facilitates colonisation of host tissue during the necrotrophic phase of infection (Qutob et al. 2002). It has recently been speculated that *S. sclerotiorum* should be re-classified from a necrotroph to a hemibiotroph as observations using different microscopy techniques (Kabbage et al. 2013) and staining during the initiation of pathogenesis, indicate that the WT fungus does not kill host plant cells; there is no

evidence for oxidative stress and fungal growth is observed in living plant tissue. This recent bioimaging study, also revealed the induction of apoptosis necrotrophy which enables the fungus to live off dead cells. Kabbage et al (2013) demonstrated that WT strains induced runaway apoptotic cell death of host plant cells which is associated with a necrotrophic lifestyle, whereas the oxalate deficient A2 mutant strain induces autophagic cell death is associated with a restricted phenotype (Kabbage et al. 2013).

A phospholipase (SS1G_09495) which was significantly up regulated *in planta* requires further investigation. Secreted phospholipases have been implicated in virulence in bacteria for many years and there is evidence that this may also be the case for fungal pathogens. These enzymes hydrolyse one or more ester linkages in glycerophospholipids which are the main components of biological membranes (Ghannoum 2000). It is tempting speculate that the expression of this gene may be directly involved with the expression of the actin patch protein 1 which catalyses the conversion of phosphatide to diacylglycerol. In yeast this protein is thought to play a role in endocytosis (Chae and Carman 2013). Endocytosis has been shown to be important in the filamentous fungus *Aspergillus oryzae* for apical growth and for recycling components which are required for re-transported to the tip region (Higuchi et al. 2009). If the phospholipase is secreted into the plant alongside other lysophospholipase (SS1G_04030) which then break down plant membranes, then the actin patch protein may then be required to recycle plant material via endocytosis.

Twenty-five of the significantly expressed genes across the three libraries are involved in hydrolysis of different plant substrates and most have glycoside hydrolase domains which will hydrolyse plant polysaccharides. Many of the genes in Group 2 were up regulated during the later stages of infection. This was an expected result as at this point the infection lesion across the leaf was observed to have spread considerably and the plant cells would be accessible to the enzymes for hydrolysis.

The most highly expressed protein in Group 2 was SS1G_14133, a putative integrin. Integrins belong to a large family of cell surface protein molecules that act as conserved transmembrane cell-adhesion receptors in a variety of vertebrates, invertebrates (Marcantonio and Hynes 1988) and plants. *Arabidopsis* NDR1 is required for ETI mediated defence and is an integrin. This gene now described as *S. sclerotiorum* integrin-like gene (SSITL) was recently silenced in *S. sclerotiorum* and was shown to be a potential effector and is involved in suppressing host resistance at the early stage of infection (Zhu et al. 2013). Zhu et al (2013) used RT-qPCR to show the expression of this gene during *Arabidopsis* infection peaked at 3hpi. They observed infection up to 12hpi and reported that expression of SS1G_14133 was reduced after 3hpi but remained 120–250 fold higher

than at 0 hpi. The expression of this gene in the RNAseq experiment highlights that this protein may be required later on during infection, after 12hpi.

In Group 3, SS1G_03611, which contains an eight cysteine-containing domain known as a CFEM domain, and SS1G_07230, a protein unique to *S. sclerotiorum*, both had the highest expression values in WT T2. These genes were identified in the refined secretome to have a potential role in pathogenesis and their expression during later infection stages has now been confirmed. CFEM domains have been previously implicated to have potential pathogenicity roles in other fungal pathogens including *M. grisea* (Kulkarni et al. 2003). Significant gene expression events were analysed between WT T0 and Δoah T0 conditions to identify which secreted proteins may vary between the two strains in an *in vitro* environment. On agar plates, Δoah grows at a distinctly slower rate compared with WT. It was hypothesised that large changes in protein expression would be observed between the two. Only 39 genes were significantly different across the two conditions. Four of these were identified as putative secreted proteins. Three of the genes were expressed at much lower levels in the WT strain and are involved in some form hydrolysis. The higher expression of these genes in Δoah libraries could be as a direct effect of lack of oxalic acid *in vitro*. One reason for this that could be that because OA is reduced in the mutant, more proteins need to be expressed to sustain an infection. However, this remains a speculation.

7.4.3 Botcinic acid gene cluster expression

Arguably, the most interesting observation in this investigation was the up regulation of the homologue gene cluster responsible for the biosynthesis of botcinic acid in *B. cinerea* during Δoah *in planta* infection. The up regulation of the gene cluster was not observed during the WT infection. The direct role of botcinic acid, an acetate-derived polyketide (Dalmais et al. 2011), is unclear but has been shown to induce chlorosis and necrosis (Cutler et al. 1996) as well as having antifungal activities (Sakuno et al. 2007). In *B. cinerea* experimental evidence with single and double synthetic mutants suggested that botcinic acid along with the secretion of botrydial acid have redundant roles in virulence (Dalmais et al. 2011). The secretion of this proposed phytotoxin has not previously been associated with *S. sclerotiorum* infection or growth. There was some expression of these genes in the Δoah strain grown on agar plates (Δoah T0) but this was minimal compared with the Δoah T1 expression levels. Although the entire cluster of genes was expressed, without doing the appropriate chemical analysis on the samples, there is no evidence that this compound was synthesised and secreted during infection. However, there was

evidence of chlorosis in *Arabidopsis* leaves infected with Δ OA H compared with WT infected leaves but that could be a result of a variety of plant defence mechanisms induced by the mutant strain which are usually evaded during WT infection (Kabbage et al. 2013).

The homologue *S. sclerotiorum* botcinin acid cluster of genes has been observed to be expressed in WT *S. sclerotiorum* previously during infection cushion or appressoria formation (unpublished data, Jeff Rollins). Appressoria formation is associated a very early point of WT infection, between 3 and 5 hpi. In this study, expression after 12 hpi was the 1st *in planta* time point explored. This may explain the very low transcript abundance or no expression of the cluster observed in the wild type libraries. Another reason for this lack of expression in WT could be that appressoria were not required during this infection course because the leaf was wounded prior to inoculation. The induction of appressoria formation may not be required for wounded leaf penetration because hyphae were observed to grow easily into the wound. The group of genes described to be associated with appressoria formation were analysed for expression, there is evidence of gene expression. However expression levels in both the mutant and the WT are comparable and appressoria formation is has been observed to be reduced in the mutant (unpublished data, Jeff Rollins). This is suggestive that if plant were not wounded the expression of these genes may be higher in the WT.

B. cinerea is a close phylogenetic relative to *S. sclerotiorum* and although they share 84 % of their protein sequences (Amselem et al. 2011) it is plausible that they share biosynthetic pathways that over time may have become specialised in their products or regulation due to the evolution of different infection strategies. In support of this notion, the *S. sclerotiorum* genome does lack four of the seventeen homologue genes from the *B. cinerea* putative biosynthetic pathway so until botcinic acid levels can be quantified during *S. sclerotiorum* infection with the mutant it is difficult to speculate whether this specific phytotoxin is being produced. The secretion of botcinic acid varies between different *B. cinerea* strains (Dalmais et al. 2011) and it is reported that *B. cinerea* produces lower amounts of OA compared with *S. sclerotiorum*. It is very tempting to speculate that there is a direct link between the lack of oxaloacetate acetylhydrolase and subsequent lack of oxalic acid formation which has forced the Δ oah strain to increase the expression of this toxin biosynthetic pathway as its attempt to induce further infection in the absence of its primary virulence factor. To speculate, botcinic acid may be induced when there is low oxalic acid produced in both fungi. In addition there may be variation between different strains of *S. sclerotiorum* that may or may not possess a full pathway and therefore would be unable to produce botcinic acid.

7.4.4 Proposed virulence genes

The expression of *S. sclerotiorum* genes previously reported to be involved in pathogenesis, virulence or infection regulation were compared across the five libraries. This analysis revealed that 10 of the documented virulence genes were down-regulated in the corresponding mutant libraries. Collectively, these data highlight that some virulence factors may be negatively regulated in the absence of oxalic acid and contribute to the restricted infection phenotype of the *Δoah* mutant.

SS1G_00263 (*ssv263*) was the most highly expressed gene in this set and however, expression was markedly reduced in only the *Δoah T1* library. This protein which is unique to *B. cinerea* and *S. sclerotiorum* has been shown not to be involved with saprophytic growth, gene-disrupted mutant strains grew comparably to WT strains on PDA plates (Liang et al. 2013). Instead, when the gene-disrupted strain was used to infect susceptible Canola (*Brassica napus*), infection still occurred but the rate of lesion expansion and the final lesion size were reduced. It is suggested then that this protein is not essential for pathogenicity but affects symptom severity.

Other genes exhibited an increase in expression in the corresponding mutant libraries. This pattern of mis-regulation may result from the lack of pH regulation during infection. Consistent with this hypothesis, the *pac1* gene was considerably up regulated in both *Δoah* conditions. *pac1* is a pH responsive gene which was reported in *A. nidulans* to be positively regulated under alkaline conditions. It actively promotes transcription of alkaline-expressed genes (Rollins 2003). This occurs in accordance with the PacC model from *A. nidulans*, when the a zinc finger DNA-binding domain of the activated Pac1 protein recognises alkaline expressed genes containing multiple copies of a 5'GCCARG-3'binding site situated upstream of their coding sequences (Espeso et al. 1997). Under alkaline conditions this gene is activated and so ensures that only pH responsive genes are activated under the appropriate pH conditions (Espeso et al. 1997). In the *oah* mutant libraries, *pac1* transcripts are more abundant than in the WT libraries, specifically *in planta*. This is an expected result as lack of OAH activity and subsequent lack of secreted oxalic acid would prevent the environment from becoming acidified. In the JRL, soybean leaves infected with WT and *Δoah* strain show different effects on leaf pH. At 4dpi, leaves infected with WT strains are measured at pH 3.55, whereas leaves infected with *Δoah* strain remain at pH5. In this situation, *pac1* transcripts would continue to be generated and the transcription of alkaline regulated genes would occur.

One curious result is the low expression levels of the predicted oxalate decarboxylase encoding genes. These two proteins SS1G_08814 and SS1G_10796 are

predicted to have cupin domains which have been implicated in oxalate decarboxylase activity. These proteins were identified in the refined secretome and it is speculated that these proteins are required to breakdown oxalic acid to regulate the environment pH (Magro et al. 1988). Magro et al (1988) demonstrated that different isolates of *S. sclerotiorum* provided different levels of oxalic acid as well as oxalate decarboxylase and that oxalate decarboxylase functions optimally at acidic pH (Magro et al. 1988). This was shown in for SS1G_10796, which had much lower expression in the mutant libraries which would have a higher environmental pH. A reason for the low abundance could be that this enzyme may be secreted at a later point during infection. Or because it is a secreted enzyme it could have been missed during tissue collection for RNA extraction.

Sscuta, (SS1G_07661) a putative cutinase-encoding gene, had higher expression in the *Δoah in planta* infection possibly because under normal WT infection, oxalate usually helps chelate calcium from plant cells walls making plant substrates more accessible to enzymatic hydrolysis. However without this, the fungal strain may have increased cutinase expression to aid with plant cuticle breakdown. This study suggests that cutinase expression may be higher at an earlier point during infection which has been shown previously (Dallal Bashi et al. 2012) and therefore may already have reduced expression levels before 12hpi. Another putative cutinase appears to have a significant expression increase in WT T2, which suggests that this enzyme has high activity when expanding the infection lesion.

The expression of NADPH oxidases (NOX) and superoxide dismutases (SOD) have been reported to be extremely important during fungal infection. Superoxide generated from NADPH oxidase is converted to hydrogen peroxide via superoxide dismutase (Scott and Eaton 2008). This allows the fungus to suppress host plant oxidative bursts or prevent damage from fungal released free radicals which may damage their own cells. The two NOX genes in *S. sclerotiorum* (*Ssnox1/Ssnox2*) were previously silenced using RNA-interference (RNAi). Tomato plants challenged with *Ssnox1* silenced strains, exhibited an increase in the plant oxidative burst, a decrease in symptom development and this mutant strain was shown to produce less oxalic acid. *Ssnox2* did not affect virulence but the mutant had limited sclerotial production (Xu and Chen 2013). *Ssnox2* did not render the mutant strain non-pathogenic, but it had limited sclerotial production (Kim et al. 2011).

Fungal superoxide dismutases are involved in detoxifying the oxidative burst during pathogenicity by converting superoxide radicals to oxygen and hydrogen peroxide. These can then be removed by catalases and peroxidases (Vallino et al. 2009). It has been

proposed that the secretion of fungal SOD derived hydrogen peroxide may help the fungus to colonise the host plant tissue. In two separate studies which used different *S. sclerotiorum* strains, the superoxide dismutase, *Sssod1*, was deleted. In one study *Sssod1* mutants failed to produce sclerotia and exhibited significantly lower oxalate levels than the WT strain (Veluchamy et al. 2012). In the second study *Sssod1* mutants exhibited normal saprophytic growth and no change in oxalate production (Xu and Chen 2013). Both studies noted that both mutant strains were more sensitive to the oxidative burst.

In this RNAseq investigation, the expression levels of *Ssnox1/2* were unexpectedly low in all libraries although *Ssnox1* did exhibit a small increase in the mutant libraries. *Ssnox2* had nearly double the expression level of *Ssnox1* but decreased in *Δoah* T1 condition. NADPH oxidases, which generate superoxide as a ROS precursor, have been shown to be important in sexual and asexual production in fungi. In the pathogen of rice, *Magnaporthe oryzae*, the ROS generated from these genes facilitates the oxidative cross linking of proteins in appressoria cell walls. This strengthens the appressoria to withstand the cell wall penetration pressure during the beginning of infection (Thines et al. 2000). If the same is true for *S. sclerotiorum*, then the lack of appressoria formation would infection may have a negative effect on NADPH oxidase expression, accounting for the overall low levels of expression.

Sssod1 had much higher expression levels but both levels dropped considerably in the corresponding mutant libraries. The reduction in *Sssod1* transcripts in the mutant libraries from this experiment may support Veluchamy and colleagues (Veluchamy et al. 2012) who assert that *Sssod1* is linked to oxalate production as addition of exogenous oxalate to *Sssod1* mutants partially restores pathogenicity. Secreted oxalate has been described to create a reducing environment around host plant cells ahead of *S. sclerotiorum* which suppresses host defenses. Later on during infection oxidising conditions are induced which induces host plant programmed cell death and allows fungal infection to progress (Williams et al. 2011). In oxalate deficient mutants it has been observed that these strains cannot regulate this redox shift and induce lower *Sssod1* expression.

Kim et al (2011) suggest that *Ssnox1* and *SsSod1* may act in the same pathway as oxalate biosynthesis (Kim et al. 2011). This could be plausible as NADPH oxidase releases NADP⁺ which along with NADH released from the TCA cycle can be transformed into NADPH and NAD⁺ through the oxidation of glyoxylate. This provides the cofactors for ROS production and oxalate biosynthesis. Further analysis of the data is required to find any evidence of this.

7.4.5 Polygalacturonases expression

Polygalacturonases (PGs), or pectinases, are responsible for degrading dicotyledonous plant cells walls, particularly the middle lamella, by hydrolysing the pectic polysaccharide, homogalacturonan. After cutinases, which hydrolyse ester bonds in fatty acids in the plant cuticle, PGs are the next wave of enzymes to be secreted by fungi to carry out cell wall degradation (Baker and Bateman 1978). These enzymes can be classified as either endo-PGs or exo-PGS. The first catalyse the fragmentation and solubilisation of pectic polymers by cleaving the internal bonds of homogalacturonan (Federici et al. 2001) and have been described as indispensable for necrotic lesions developments (Favaron et al. 2004). Exo-PGs cleave the linkages from the non-reducing ends of the pectic polymers (Yadav et al. 2012). Oxalic acid has been linked to the activity of PGs as it has been reported that oxalic acid will make plant cell walls more accessible to PGS as it sequesters calcium ions bound to cell wall pectate. Secondly, oxalate lowers the ambient pH to create an optimum environment for some PG activity (Favaron et al. 2004). During a study of *S. sclerotiorum* infection of soybean hypocotyls, at 24hpi, the pH of the plant was 4.8 with an oxalic acid concentration of 7mM. However at 48 hpi, the oxalate concentration was closer to 50 mM and the pH had decreased to 3.8 (Favaron et al. 2004) highlighting just how the environment changes during disease development.

Oxalic acid does not necessarily regulate the expression of the PG directly. The induction of some PG expression has been shown to be a result of the substrate the fungus is exposed to. Li et al (2004) demonstrated that *sspg3*, *sspg5*, *ssxpg1* (and *sspg1* to a lesser extent) were expressed either when in contact with a pectate substrate or galacturonic acid, which is a pectin monomer and that PG expression was repressed by glucose.

Sspg1 (SS1G_10167), an endo-polygalacturonase has been classified as a significant protein during pathogenesis, and is usually secreted ahead of other PGs including *sspg3*, *sspg5*, *sspg6* (Cotton et al. 2003, Li et al. 2004b). Along with *SsCUTA*, *sspg1* can be induced through thigmotrophic interactions such as being grown on a solid surface (Dallal Bashi et al. 2012). In this experiment *Sspg1* has the highest expression of all PGs and also exhibited the highest abundance *in vitro*. This could be a result of the solid surface it was grown on and potentially the detection of a cellulose disc placed over the PDA which the fungus may have been trying to hydrolyse. *Sspg1* may have reduced abundance in the mutant conditions due to the lack of OA directly as the pH was not optimum. *Sspg6* (SS1G_11057) was expressed at low levels in the WT libraries but increased expression in the mutant libraries along with SS1G_01009. SS1G_11057 constantly behaves as a neutral/alkaline enzyme which would account for the increase in

expression in the absence of OA in the mutant conditions and this may also be true for SS1G_01009.

Another consideration to note is that although previous *in vitro* tests have shown that ambient pH is a major regulator of PGs, it is quite possible that there are other plant signals that are more important than pH during infection or that can substitute for pH during infection. Plant polygalacturonase-inhibiting proteins (PGIPs) which are located in the plant cell wall are also important for regulating fungal PG activity. At low pH values (3.6 - 4), some PGs are only slightly inhibited by PGIPs and so it is suggested that as more OA is secreted and the environment is acidified, the activity of acid PGs will be increased but PGIPs are inhibited (Favaron et al. 2004). This would not be true for the *Δoah* in *planta* infection, so PGIPs may have inhibited other PGs.

7.4.6 Genes with a similar expression pattern as *oah*

Monitoring the expression of genes with a similar expression profiles as *oah* in the WT strain and how this profile changes in the *Δoah* deficient strains is useful to determine which genes may be regulated directly by the activity of *oah* and the subsequent production of oxalic acid.

The genes classified as Group 1 follow the same expression pattern as *oah*, there is little or no expression in the mutant libraries. The transcript fragments that are observed are produced from non-coding sequences of the deleted gene. An interesting observation in this group is a succinate/ fumarate mitochondrial transporter (SS1G_08795). This transporter protein was characterised in yeast (*ACR1*) to be located in the inner membranes of yeast mitochondria that connects the intermediate made in metabolic cycles or the anaplerotic steps of succinate biosynthesis by the glyoxylate cycle in the cytosol which then feeds into the tricarboxylic acid. In the TCA cycle it is required for electron transfer by complex II (succinate dehydrogenase: ubiquinone reductase). If *ACR1* is disrupted, the anaplerotic replenishment of oxaloacetate would be prevented and the tricarboxylic acid cycle blocked (Palmieri et al. 1997). In this case, the loss of *oah* could potentially reduce some metabolic intermediates which feed back into the cycle. This may cause the reduced growth rate observed on the agar plates.

The serine carboxypeptidase identified in the secretome had reduced expression in the mutant libraries as it is generally an acid acting enzyme. Some proteases have been identified as effectors in some pathogenic fungi (van Esse et al. 2008) and so should be further investigated for effector function. The presence of oxalic acid may also be important for protease activity during infection as this is an acid- acting enzyme.

In Group 2, the pyruvate carboxylase (SS1G_12839) has a higher expression value in the *Δoah* T0 library. This enzyme catalysed the breakdown of pyruvate into oxaloacetate in the TCA cycle. If the anaplerotic replenishment of intermediates within the mutant mitochondrion is disrupted, the *Δoah* strain may induce increased expression of some other enzyme within the metabolic pathways to try restore the balance. In this case the lack of acetate released from the breakdown of oxaloacetate which is required for citrate formation, may induce the increase in pyruvate carboxylase which can generate more acetate substrates.

Generally there appears to be a change in many proteins controlling transport of proteins round the cell or transporters of intermediates within of the TCA cycle. This is understandable *oah* is a vital to generate the supply of acetate within the cycle. Without this enzyme the fungus will need to change the regulation of other enzymes which can restore intermediate supply to continue growth of fungus.

Overall, RNAseq is rapidly becoming the norm for genome annotation and transcriptomic analysis as it enables the user to identify all the functional expressed genes within an organism under a certain condition. In this experiment, the RNAseq was used to identify how the expression of a *S. sclerotiorum* strain deficient in its main pathogenicity factor, oxalic acid, would compare to the wild type. It is evident that there are extreme changes in the expression profiles of important genes involved in virulence as a direct result of the lack of OAH activity and subsequent secretion of OA. However the ability of the strain to continue to grow normally *in vitro* suggests that OA principally acts to indirectly regulate other genes for disease progression. It is also clear that it is not only OA which is important during infection but this study has highlighted some other genes which need further investigation into potential roles as effector proteins or contributors to virulence. This data has also provided expression evidence for many of the putative secreted proteins described in Chapter 5 whose expression had not been previously reported and will help the community further their understanding of the control of oxalic acid and other factors as facilitators of infection.

Chapter 8: General Discussion

The major scientific findings revealed by this interdisciplinary study are discussed below. The future prospects of the SYield consortium and how this detection system could be applied to other sectors are also explored. In addition, previously unknown aspects of *S. sclerotiorum* biology are defined and how these new discoveries relate to the wider implications of disease control in UK agriculture will be discussed.

8.1 Summary of key findings and developments

- **The development of a compatible biological matrix to be used within a biosensor for the detection of *S. sclerotiorum***

The SYield consortium, as a whole, developed an electrochemical biosensor, coupled with an air sampler which is capable of measuring the oxalic acid production from *S. sclerotiorum* ascospores sampled into the device. The work in this Ph.D. project established a biological matrix, compatible with a carbon based electrochemical biosensor which induces rapid growth of the fungus and also induces measurable amounts oxalic acid secretion. A liquid medium as opposed to a solid medium proved to be the best system to use within the biosensor. Sabouraud Dextrose Broth (SDB) with a micronutrient base at pH5 induces rapid spore germination and increased concentrations of OA secreted by the fungus significantly when compared to other nutrient media tested (Chapter 3). The medium is compatible with a potentiometric based electrochemical biosensor optimised to measure the oxidation of secreted OA by the enzyme, oxalate oxidase. This medium has been successfully field trialled using manual spore traps as well as the automated biosensor (results not described), in oilseed rape fields (Chapter 4).

- **Oxalic acid concentrations produced does not correlate with the original spore number used**

For disease modelling purposes, relating spore number to oxalate concentrations measured by the electrochemical biosensor was anticipated, however the research revealed that this is not possible. Oxalic acid production is not consistently positively correlated with either ascospore number or fungal biomass (Chapter 3). What was consistently revealed was that larger spore doses (>1000 spores/sample) will lead to the secretion of measurable levels of OA after three days of sample incubation compared

with four days of incubation following seeding the cultures with smaller spore doses. This information could be incorporated into future incubation times for the biosensor.

- **The identification of the fungal species present in an air sample collected from UK oilseed rape fields**

The fungal species present in an air sample collected in UK oilseed rape fields was assessed using culturing methods, physical taxonomic identification and sequencing of the ITS4/5 regions of the fungal genome (Chapter 4). These species include some potential inhibitors of *S. sclerotiorum* growth including *Trichoderma spp*, *Epicoccum nigrum* and *Alternaria spp*. The oxalic acid producers *Botrytis cinerea* was isolated from the samples.

- **Production methods for larger *S. sclerotiorum* sclerotia**

Carrot agar was discovered to be an optimum medium for the production of enlarged sclerotia from a variety of isolates from different geographical regions. This also resulted in an increase in the production of apothecia production. This new method of sclerotia production increase the numbers of ascospores harvested for experimentation (Chapter 2).

- **Identification of putative secreted proteins which may play a role in *S. sclerotiorum* pathogenicity**

The prediction of the *S. sclerotiorum* secretome identified a number of candidate genes which could be involved during infection and which may work alongside secreted oxalic acid to cause infection (Chapter 5). The analysis has also generated further annotations for genes which previously had no annotation on the publically available genome.

- **Identification of secreted proteins to be used as potential detection targets in other nucleic acid or antibody based diagnostic systems.**

The analysis of the predicted secretome revealed a handful of genes which are unique to *S. sclerotiorum* and which could be used in diagnostics for this species. Expression studies using GFP expression constructs highlighted one protein in particular (SP1) which is potentially a very applicable target protein. SP1 could be used as a detection target when the fungus is grown in liquid culture which could be applied to the SYield biosensor (Chapter 6). However, this approach would require the use of modified electrochemistry incorporating a stabilised antibody rather than an enzyme.

- **The absence of the oxaloacetate acetylhydrolase (OAH) gene in *S. sclerotiorum* causes significant changes in gene expression and resulted in reduced pathogenicity during infection.**

The intercomparative study of the wild-type and *oah* deletion strain transcriptome revealed likely genes which are significantly down regulated in the *oah* deletion strain which could have potential roles in pathogenicity and / or are regulated in a similar pattern as the *oah* gene. These may contribute to the mechanism(s) of infection which has been well described to be regulated by oxalic acid and pH (Chapter 7).

- **The predicted secretome has transcriptional evidence which supports the expression of many of the putative secreted proteins.**

RNA sequencing of the wild-type *S. sclerotiorum* strain has provided transcriptional support for some of the 432 genes predicted in the secretome. This is useful to the community who can use this evidence for further investigation into genes of interest.

- **Up regulation of Botcinic acid metabolic genes in OA deficient strains**

The transcriptome study (Chapter 7) revealed the up regulation of the polyketide biosynthetic pathway of botcinic acid in the oxalic acid deficient mutant which is normally associated with the closely related species *B. cinerea* and not *S. sclerotiorum*. This is potential evidence of a redundant pathway in *S. sclerotiorum*. Further investigation is required to determine whether the lower amounts of OA produced by *B. cinerea* induces the production of Botcinic acid and so could account for the up regulation of this pathway within the oxalic acid deficient *S. sclerotiorum* mutant.

8.2 Development of a robust method for ascospore production

It is worth commenting that the use of carrot agar to induce production of large sclerotia (Chapter 2) and subsequent viable apothecia production should be adopted as a new method of sclerotia production within the community to ensure reliable ascospores production. It would also be worth investigating whether other sclerotia producing fungi respond to carrot agar in the same way. This could be further investigated as there may be some compound with the carrot root which is able to induce certain developmental stages within fungi. This has been seen in *Fusarium graminearum*, which will form perithecia when the fungus is routinely grown on carrot agar which the closely related *Fusarium culmorum* has not been observed to do (Cavinder et al. 2012).

8.3 Advances in Decision Support Systems for monitoring *S. sclerotiorum* disease outbreaks and the future of the SYield biosensor

Since the manual testing of the Sabouraud dextrose broth nutrient medium and the monitoring of the newly developed spore sampling machinery in the 2012 field trials, an automated biosensor that can detect oxalic acid secreted from *S. sclerotiorum* ascospores has been developed. This device sampled a defined volume of air over a pre-determined time interval of twelve hours. There is no doubt that this is the only device of its type in the world. Most detection devices require some form of human handling to obtain the biological sample and carry out the diagnostic test either in the field or in a laboratory and then process the data. Whereas this device situated in the field or at another location in the agricultural landscape is capable of sampling air, incubating the air sample and carrying out the electrochemical test four days after the sample was taken, all without any human interference required. This device has been compared to a 'lab in a box'. The device can also relay the information to a central processing unit (CPU). The device has its own meteorological station attached and this information can also be relayed to the same CPU for processing.

The future of this system relies now on being able to compile the real time oxalic acid measurements with the meteorological data to develop a real time disease risk assessment and provide valuable spray window(s) for farmers. Currently the meteorological data collected from this project is being fed into an existing model designed by modellers based in Syngenta, France. The RAISO-Sclero prediction model, combines current *S. sclerotiorum* prediction models, but also uses soil conditions and humidity at ground level, which dictates the release of the ascospores that spread the infection to the crop (Clarke 2012). This model would have successfully predicted the risk of a *S. sclerotiorum* outbreak in 2008 and subsequently crops could have been better protected against infection (unpublished data). The real-time spore information obtained from the SYield biosensor will substantiate the predictions made by the RAISO-sclero model. However there is still a need to relate the oxalic acid information to a disease risk factor. Even though there are spores in the air, which the biosensor will detect, there are other important factors which affect whether disease formation will subsequently occur. For example, petal stick is an important factor in governing whether there will be disease outbreak. As described previously (Chapter 1), germinating ascospores need to land on a petal or other senescing tissue (Lumsden 1979, Bolton et al. 2006). Only colonised petal tissue which falls and sticks to healthy tissue will induce disease. If it is too dry, petals fall to the floor. If it is too wet, the petals are washed off the plant. Therefore measuring the

fine balance between the two environmental conditions may be a key factor to work into the disease model. Suggestions have been made that using video technology to monitor petal stick may be useful to incorporate into the biosensor device. Combining positive events from the oxalic acid biosensor, meteorological data and petal stick monitoring may be the best formula for predicting disease risks.

Further research into the locations of the sensor nodes is vital in establishing an efficient network system. From this study, it is evident that the sampling system can sample ascospores which are released from apothecia a few meters away from the device. It is also understood that DNA from ascospores can be detected on rooftops, but further field trialling of the automated biosensor is necessary to determine whether placing biosensor device on rooftops is suitable for ascospores capture and subsequent oxalic acid detection. Current thinking is that a reliable biosensor device placed on a rooftop will give a more diluted sample of spores, but from a larger area than a sensor placed in an oilseed rape field. Placing the device on a rooftop may also be better for assessing whether ascospores are moving into the region from sources of inoculum further afield. Whether the fungal community changes in air samples collected on rooftops also needs further investigation. Other species might be identified which pose more significant threats to either inhibit *S. sclerotiorum* growth or oxalic acid production, than the species already identified within air samples from oilseed rape fields in Chapter 4. Chemicals or pollutants present in the air at roof height may also affect the behaviour of the spore samples in the biosensor.

The business model for the biosensor is an extremely important part of the project which requires further attention to ensure this detection system becomes accessible to growers. It remains to be decided who will maintain the sensor network, collate the real time information and how will it pay for itself. The Decision Support Systems are usually available free online. Growers have to supply some information including crop variety and location and a risk factor will be available. It's then up to the grower to decide whether to spray and use that particular company's product. The SYield biosensor network would need monitoring, maintenance and the cost of the biosensor devices would also need to be covered. A possible model is that growers could buy into the network information. However, the system would require years of field testing to ensure that the predictions are accurate for growers to trust the outputs generated.

There is the possibility that this device could be modified not only to detect other species of fungi but to be used in sectors other than agriculture. In its current design the device could be used to detect *S. sclerotiorum* in other host crops including soybean,

sunflower, carrot and lettuce. *B. cinerea*, the pathogen responsible for grey mould on a variety of vegetables, strawberries and grapes in vineyards, is also a producer of oxalic acid and its airborne conidia have been captured using Burkard seven day wax traps in previous studies (Blanco et al. 2006). For the device to be suitable as a detection device for grey mould, several features would need to be verified for successful detection. The work in this Ph.D. project revealed that *B. cinerea* conidia produce OA when seeded into SDB medium in laboratory assays. Further testing is required to ensure that air sampled *B. cinerea* conidia behave in a similar manner to *S. sclerotiorum* ascospores. This work also showed that *B. cinerea* conidia produced lower amounts of OA compared with *S. sclerotiorum*. It would need to be verified that lower amounts of OA were still detected within the device. In addition, the spray window supplied by the detection device would need to be tested to ensure it provides enough time for control measures to be taken.

The automation aspect of the SYield device is attractive to both growers and plant pathology researchers. The ability to use electrochemical assays with antibodies as bioreceptors, could be invaluable in further investigations and detection systems. For example, the stabilisation of commonly used antibodies, already commercially available, which detects airborne pathogens within this electrochemical system would enable the device to be used as a detection tool for a range of other pathogenic species. This system may be of benefit for border control and plant disease inspectors to monitor the influx of airborne spores and hence potential phytopathogens from other countries. Outbreaks of fungal diseases which release airborne spores could be monitored more closely. For example, new information could be learnt on the wind dispersal pattern of the spores of *Chalara fraxinea*, the devastating causal agent of Ash Die Back which has spread from Poland to the UK over the last two decades (Kowalski and Holdenrieder 2009). If protein/nucleic or metabolite detection targets could be developed for other fungal pathogens, then this device would be best adapted to detect rusts, powdery mildew, and other downy mildew diseases which produce huge numbers of airborne spores. This is particularly attractive for species where the spores can be dispersed for hundreds of kilometers as a direct result of windborne spore movement (**Figure 76**) (Brown and Hovmoller 2002). *Puccinia triticina*, a rust of wheat which can account for 14% loss of winter wheat yields (Bolton et al. 2008a) is a major problem on UK wheat as well as globally. This detection system could be used to detect the wind dispersed urediniospores which can be dispersed hundreds of kilometers from their source plant (Bolton et al. 2008a). One study showed how the rust uredospores of *Hemileia vastatrix* may have been carried from the coffee plantations in Angola via Transatlantic winds to Bahia in Brazil in the 1960s (Bowden et

al. 1971). Antibodies are currently available for the detection of wind dispersed spores of the bacterial pathogen *Erwinia amylovora* (Roberts et al. 1998). A detection system could be used within greenhouse environments to monitor this pathogen. If the agricultural community is to secure food production for 9.6 billion people, it is essential that more stringent monitoring and containment programmes for emerging fungal disease are put in place.

Industrial sectors other than agriculture could also benefit from the novel technology developed within the SYield project. For example, an automated device could be used in the biosecurity sector to monitor the incidence of fungal or bacterial biosecurity hazards. An indoor monitoring system for fungi harmful to humans or farm animals is also a large sector where this automated detection systems is required. This technology could be transferred to monitor asthma causing pathogens like *Penicillium* or *Aspergillus* and *Cladosporium* spores which has the potential to cause atopy or allegergenic hypersensitivity and respiratory allergies, respectively (Garrett et al. 1998). Monoclonal antibodies (MAbs) against *Aspergillus fumigatus* are available which could be used in such a detection system (Stynen et al. 1992).

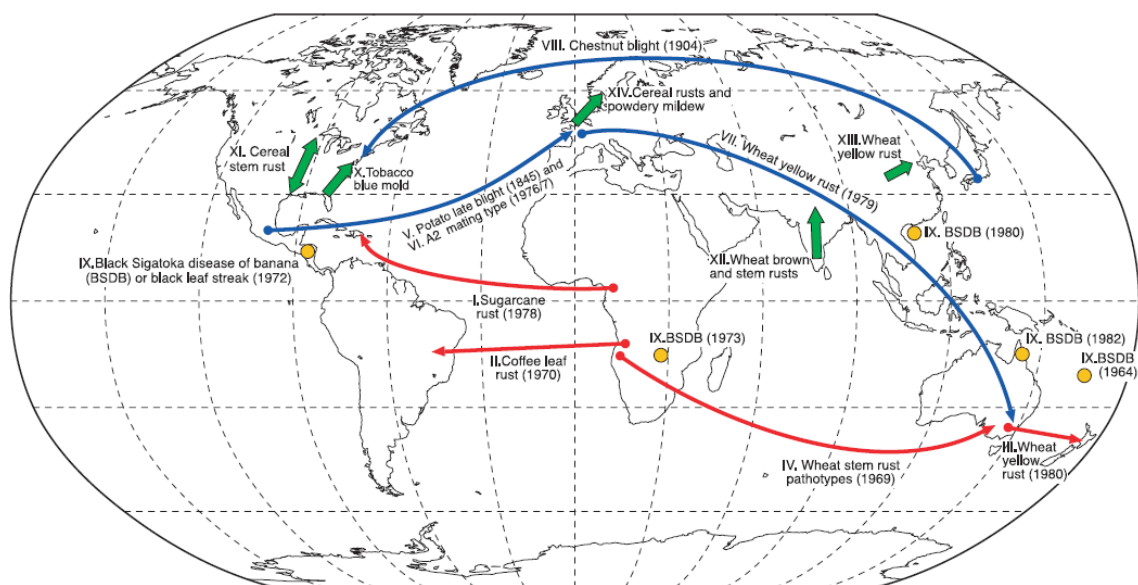


Figure 76: Spore dispersal events of fungal pathogens.

Taken from (Brown and Hovmoller 2002). Red and blue arrows indicate invasions of new territories (first year recorded in brackets). Red arrows indicate dispersal that probably occurred by direct movement of airborne. Blue arrows indicate pathogens that were probably transported to the new territory in infected plant material or by people and spread thereafter as airborne spores. Orange circles indicate the worldwide spread of black Sigatoka disease of banana. Green arrows indicate periodic migrations of airborne spores in extinction-recolonisation cycle. Background world map © C. Lukinbeal, Southern Connecticut State University, New Haven, Connecticut.

8.4 Advances in pathogenomics

Pathogenomics is an extremely important area of research in determining how plant pathogens infect their plant hosts. This area of research can contribute to control strategies for pathogens which will ultimately help growers and farmers secure greater yields. Advances in genomics and the ease in sequencing genomes has made the identification and understanding of molecular mechanisms underpinning infection by different types of pathogens i.e. virus, bacteria, fungi, oomycetes and nematode, much more accessible. This type of research aims to discover potential targets for chemical control of diseases using well designed spray management programmes. Likewise, this information is important to plant breeders who want to develop pathogen resistant cultivars, by using the corresponding pathogen effector sequences as screening tools (Goodwin et al. 2011, Kaemper et al. 2006). This new technology can also be used to improve the isolation of bioproducts within industry as fungal fermentation plays a significant role in the food and drink sector as well as biofuel production. Since the first publication of the brewers yeast *Saccharomyces cerevisiae* genome in 1996 (Goffeau et al. 1996), 269 subsequent fungal genomes are publically available on the NCBI Fungi Blast website. We are now in the age of multi-isolate genome sequencing. The genomes of multiple isolates of a single species can be sequenced cost-effectively and this allows researchers to pull out truly conserved regions of a species' genome or the regions which are highly variable. This information is helping researchers identify *R* genes and effectors in fungal pathogens. For example one study revealed interesting new biology including the dispensable chromosomes 'the dispensome' of the wheat infecting fungus *Mycosphaerella graminicola* (Goodwin et al. 2011). Another pathogenomic study revealed that the tomato gene encoding Ve1, which encodes a receptor like protein, (RLP) and confers resistance against *Verticillium* wilt fungi can be transferred to an *Arabidopsis* host plant where it remains fully functional against race 1 of *Verticillium* (Fradin et al. 2011). This example highlights how there is race specific transfer of *R* genes across species boundaries, however this transfer of genetic information is usually successful between phylogenetically related donor and recipient species (Fradin et al. 2011, Hammond-Kosack and Rudd 2008).

Publically available microbial genomes and their current annotation allow research communities to explore genomes with ease to identify potentially homologous mechanisms of infection by comparing the predicted gene repertoire of different fungal species with similar or dissimilar lifestyles. The Next Generation Sequencing (NGS) methods and bioinformatics tools now available to researchers have made this previously perplexing area of research very accessible to molecular biologists. In addition, this deluge of new

data has facilitated the cross disciplinary communication between biologist and bioinformatician to drive the era of genomics forward and allow biologists to have more control of gene annotation.

Full genome transcriptomics including RNA sequencing is rapidly superceding traditional NGS and array based platforms. Transcriptome analysis is extremely powerful in generating large datasets of gene expression data for different biological scenarios, for example, at various life stages or phases of growth *in planta*. It will not be long before the cost of RNA sequencing will be so economic that time consuming qPCR to explore the expression of single to a few genes will be outdated. The ability to sequence an entire species' transcriptome is also fast becoming the way to map genomes *de novo*, *i.e.* without the need to assemble a reference genome. If enough RNA can be collected from a range of different life stages and under different treatments, then biologists can determine the genes which are non-redundant and how they interact under different conditions. This type of data is extremely useful when placing genes in pathways and/or closely regulated networks. With so many large datasets now arising from transcriptional studies, the problem is currently not how to obtain the data but instead it is how to manage such large datasets and deciding on the best method to use to construct possible molecular pathways and identify the relationships between different clusters of co-expressed genes. Bioinformatics programmes such as Galaxy which was used within this work (Chapter 5), allow biologists with no experience of software programming, to run pre-prescribed bioinformatics and statistical pipelines on the raw RNAseq data to find significant biological relationships. The most significant problems with this new era of technology is developing a standardised method that research communities across the world can use to determine the statistically correct changes in gene expression across libraries. What's more, an improvement in experimental design is required to order to be able to obtain the most from these large dataset. In this study, the cost restricted the number of biological replicate samples to be sequenced which severely restricted the amount of analysis which can be performed on the dataset. Future studies should incorporate at least three biological replicates to determine general gene expression trends.

8.5 Advances in the understanding of *S. sclerotiorum* biology through genomics

This study has not only looked at the aerobiology of *S. sclerotiorum* ascospores release and detection within an oilseed rape system but aimed to discover new targets for detection other than oxalic acid and how other genes potentially contribute to infection mechanisms alongside the production of oxalic acid though the use of modern genomic

technologies.

The use of a pre-existing bioinformatics pipeline to predict the *S. sclerotiorum* secretome and identify detection targets has proved to be successful. The use of GFP constructs fused to the protein targets successfully revealed that the targets chosen could potentially be used in detection devices. Unfortunately due to time constraints further work was not carried out to isolate these secreted GFP fused proteins in culture medium through the use of pull down antibodies. However this could be carried out in the future. This same analysis using fungal secretome prediction could now be applied to other fungal genomes to look for detection targets.

The combined secretome and RNA sequencing studies will provide the *Sclerotinia* research community with a valuable genomic resource that they can now exploit to investigate interesting *S. sclerotiorum* biology. The secretome prediction would not have been enough on its own, but alongside the RNAseq data the genes of specific interest have some support.

The use of RNA sequencing provided some expression support for some of the 432 genes predicted in the secretome. In total, 88 predicted genes identified in the secretome had high expression (> 100FPKM) in at least one of the libraries analysed using RNA sequencing (Chapter 7). Twenty of these genes had no previous annotation (Chapter 7). It is challenging to assign functions to any unannotated genes in the secretome, but the expression detected in certain libraries provides some evidence suggesting which stage specific genes were expressed, for example, *in planta* or *in vitro* or during later stage of plant infection.

The RNAseq study was the first of its kind to compare the transcriptome of the *oah1* knock out strain and the wild type strain *in vitro* and during infection of *Arabidopsis*. Originally this comparison aimed to deliver further insights into which genes were up- or down-regulated alongside or as a result of the expression of *oah1* gene. A few candidate genes have been identified. However it was extremely challenging to pull this aspect of biology out of the data in the time available. Further analysis of the dataset is required to identify the sub-set of genes co-regulated with *oah* gene compared to those directly induced or suppressed as a result of the production of OA.

Future studies could use gene the gene deletion technology to explore candidate genes identified in this secretome and RNAseq study to determine their gene function during infection and development of the fungus. This would provide further supporting evidence for the genes predicted in the secretome. Candidate genes including SS1G_08163 which was identified in the refined secretome as small, cysteine rich secreted proteins

which is typical of some effector proteins (do Amaral et al. 2012, Bolton et al. 2008b). This gene was expressed only *in planta* highlighting that its induction is during infection. SS1G_03611 had the highest expression during later infection. This protein was also identified in the refined secretome as small, cysteine rich secreted. This protein contains a CFEM domain which may be important for virulence (Kulkarni et al. 2003). Both these genes need further investigation to determine whether they are effector proteins.

The group of genes which had similar expression profiles to the *oah* gene in the wild-type *S. sclerotiorum* libraries should also be investigated further to explore whether they are directly regulated by this gene or the subsequent secretion of oxalic acid to further the infection model. These include SS1G_14018 a fad binding domain protein, SS1G_09475, a serine carboxypeptidase, SS1G_08795, a succinate fumarate mitochondrial transporter and SS1G_05902, a Sec61beta family domain containing protein.

An improved RNA sequencing study would incorporate three biological replicates per treatment. This would allow more power to calculate statistically significant gene expression events. Secondly RNA sequencing for earlier time points during infection may also reveal other effector gene candidates that are expressed very early on during infection. For example the ortholog (SS1G_08569) (Kabbage et al. 2013) of the *Ustilago maydis* effector *Cmu1*, which codes for a secreted chorismate mutase is required to maintain biotrophy during the establishment of smut infections (Djamei et al. 2011). Therefore, the *S. sclerotiorum* homologue of *Cmu1* may have higher level of expression during earlier time points. Leaf tissue would need to be collected without visible disease symptoms, and therefore obtaining sufficient fungal biomass at this stage would be very challenging.

Another important aspect which requires further investigation is whether *S. sclerotiorum* appressoria were formed when plants were wounded. The appressoria are extremely important infection cushions which allow the fungal hyphae to penetrate through the plant cuticle directly (Hegedus and Rimmer 2005). The expression of genes related to appressoria development is dependent on highly conserved Mitogen activated protein kinase (MAP kinase) and cAMP-dependent signal transduction pathways (Amselem et al. 2011). Growing mycelium on cellophane for the *in vitro* time points would have reduced the number of appressoria present in the sample, because appressoria only develop when a plate is fully colonised (Jeffrey Rollins, unpublished data). The *oah1* mutant produces appressoria in low frequency compared with the wild-type. It is likely that fewer of these structures would have developed during infection because the mycelium would have easily been able to grow through pre-wounded plant tissue, without needing to penetrate the cuticle. The expression of the appressoria related genes (Amselem et al. 2011) in both the

mutant and WT strains, *in planta* and during infection was comparable which is suggestive that there was lower appressoria developed by the WT strain during infection. The lower incidence of appressoria will clearly change the expression profile of this fungus and therefore may also determine whether some of the genes identified in the secretome were present or not. This may also be important when using the secretome to identify detection targets for *S. sclerotiorum* within the biosensor system. This set of appressoria related genes and other thigmotrophic-response genes would not be expected to be expressed in a liquid medium and so gene expression would be very different in this environment. A future RNA sequencing study is therefore required to assess how the secretome expression of mycelium changes in a liquid medium in the biosensor device compared with expression on a medium surface or *in planta*. This experimental design would also aid in the classification of genes not currently either identified or confirmed to be present in the genome through expression studies.

There is a further debate regarding the expression profile differences between germinating spores and infection plugs. The biosensor is designed to sample wind dispersed ascospores which then grown in a liquid medium whereas this RNA study explored infection by agar plugs containing mycelium. This may change the expression of the secretome gene set. It would be useful to carry out another RNAseq experiment which compares the two types of infection and then determine what other putative secreted protein may also be candidate for detection when spores are grown in a liquid environment rather than on the plate or during plant infection. Again this would be technically challenging as earlier time points would be required and obtaining sufficient fungal biomass would be tricky.

Originally the biosensor matrix in which the *S. sclerotiorum* ascospores would grow in was going to be a solid surface. However after much experimentation, the liquid system work better for quantifying oxalic acid quantification as well as being compatible with the electrochemistry. This may also be beneficial as growing the fungus in a liquid keeps the fungus in a saprotrophic phase and prevents the expression of any thigmotrophic responses including appressoria formation which could damage the biosensor and make the system less predictable. **Figure 77** highlights how the infection response of *S. sclerotiorum* varies when infecting wounded and intact leaves and how these responses differ quite considerably when seeding liquid cultures with ascospores. Again this highlights that keeping the fungus in a basal infection state in liquid medium would reduce an increase in other response which are less predictable than pure development of a saprotrophic phase.

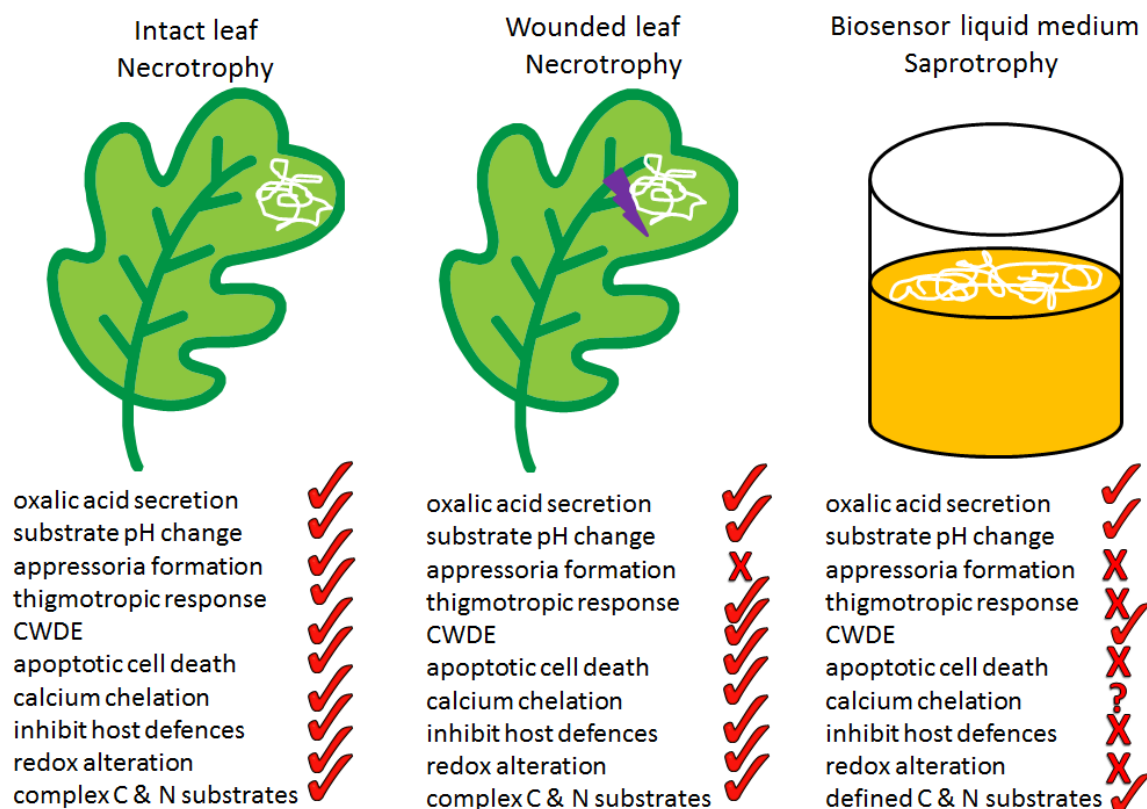


Figure 77: Comparison of *in planta* and *in vitro* infection/ growth of *S. sclerotiorum*.

Comparison of the responses observed during *S. sclerotiorum* early infection of intact and wounded leaves of oilseed as well as the response observed when ascospores are seeded the liquid medium in the SYield biosensor.

In conclusion this study has embraced the use of modern genomic techniques including sequencing and bioinformatics to explore the infection biology of the pathogen *S. sclerotiorum*. This study has generated a wealth of expression data which will be useful to the *S. sclerotiorum* community. The methods described in this study can also be followed by researchers investigating similar aspects of molecular biology of other fungal pathogens. Not only will this allow them to investigate interesting aspects of science but develop tools which can truly be used to develop control strategies for these devastating pathogens. If uncontrolled, these pathogens aim to challenge high yields of food production which are becoming more and more valuable as the population grows. The tools described in this study allow the selection of appropriate detection target (protein or nucleic) to allow the monitoring of pathogens either within an agricultural industry or by plant health inspectors who monitor emerging diseases which threaten our countryside and farms. The technology from the SYield biosensor could also be potentially used within

other sectors including medical and biosecurity industries. The success of SYield detection system was reliant on the exploration and validation of important aspects of molecular and aero-biology which have now been demonstrated across this project.

List of References

- Akyildiz, I. F., Su, W., Sankarasubramaniam, Y. and Cayirci, E. (2002) 'Wireless sensor networks: a survey', *Computer Networks*, 38(4), 393-422.
- Amador, C. E., J.P.; Nunes, M.C.; (2008)
'<http://www.asabe.org/meetings/food2008/index.htm>',
- Amselem, J., Cuomo, C. A., van Kan, J. A. L., Viaud, M., Benito, E. P., Couloux, A., Coutinho, P. M., de Vries, R. P., Dyer, P. S., Fillinger, S., Fournier, E., Gout, L., Hahn, M., Kohn, L., Lapalu, N., Plummer, K. M., Pradier, J.-M., Quevillon, E., Sharon, A., Simon, A., ten Have, A., Tudzynski, B., Tudzynski, P., Wincker, P., Andrew, M., Anthouard, V., Beever, R. E., Beffa, R., Benoit, I., Bouzid, O., Brault, B., Chen, Z., Choquer, M., Collemare, J., Cotton, P., Danchin, E. G., Da Silva, C., Gautier, A., Giraud, C., Giraud, T., Gonzalez, C., Grossetete, S., Gueldener, U., Henrissat, B., Howlett, B. J., Kodira, C., Kretschmer, M., Lappartient, A., Leroch, M., Levis, C., Mauceli, E., Neuveglise, C., Oeser, B., Pearson, M., Poulain, J., Poussereau, N., Quesneville, H., Rasclé, C., Schumacher, J., Segurens, B., Sexton, A., Silva, E., Sirven, C., Soanes, D. M., Talbot, N. J., Templeton, M., Yandava, C., Yarden, O., Zeng, Q., Rollins, J. A., Lebrun, M.-H. and Dickman, M. (2011) 'Genomic Analysis of the Necrotrophic Fungal Pathogens *Sclerotinia sclerotiorum* and *Botrytis cinerea*', *Plos Genetics*, 7(8).
- Antoniw, J., Beacham, A. M., Baldwin, T. K., Urban, M., Rudd, J. J. and Hammond-Kosack, K. E. (2011) 'OmniMapFree: A unified tool to visualise and explore sequenced genomes', *Bmc Bioinformatics*, 12.
- Australia, Canola association of Australia. (2008)
'http://www.icf.org.au/proj_f/pdf/Sclerotinia%20report.pdf'.
- Baggio, A. (2005) 'Wireless sensor networks in precision agriculture (Workshop)', paper presented at *RealWSN'05*, Stolckhom, Sweden,
- Baker, C. J. and Bateman, D. F. (1978) 'Cutin degradation by plant pathogenic fungi', *Phytopathology*, 68(11), 1577-1584.
- Balion, C. M. and Thibert, R. J. (1994) 'Determination of oxalate by luminol chemiluminescence', *Clinical Chemistry*, 40(6), 1096-1097.
- Balmforth, A. J. and Thomson, A. (1984) 'Isolation and characterization of glyoxylate dehydrogenase from the fungus *Sclerotium-rolfsii*', *Biochemical Journal*, 218(1), 113-118.
- Bartlett, D. W., Clough, J. M., Godwin, J. R., Hall, A. A., Hamer, M. and Parr-Dobrzanski, B. (2002) 'The strobilurin fungicides', *Pest Management Science*, 58, 649-662.
- Bateman, D. F. and Beer, S. V. (1965) 'Simultaneous production and synergistic action of oxalic acid and polygalacturonase during pathogenesis by *Sclerotium rolfsii*', *Phytopathology*, 55(2), 204-&.

- Bayry, J., Aïmanianda, V., Guijarro, J. I., Sunde, M. and Latge, J.-P. (2012) 'Hydrophobins-Unique Fungal Proteins', *PLoS Pathogens*, 8(5).
- Birch, P. R. J., Rehmany, A. P., Pritchard, L., Kamoun, S. and Beynon, J. L. (2006) 'Trafficking arms: Oomycete effectors enter host plant cells', *Trends in Microbiology*, 14(1), 8-11.
- Blanco, C., de los Santos, B. and Romero, F. (2006) 'Relationship between concentrations of *Botrytis cinerea* conidia in air, environmental conditions, and the incidence of grey mould in strawberry flowers and fruits', *European Journal of Plant Pathology*, 114(4), 415-425.
- Blankenberg, D., Von Kuster, G., Coraor, N., Ananda, G., Lazarus, R., Mangan, M., Nekrutenko, A. and Taylor, J. (2010) 'Galaxy: a web-based genome analysis tool for experimentalists', *Current protocols in molecular biology / edited by Frederick M. Ausubel*. Chapter 19, Unit 19.10.1-21.
- Boer, P., Vanleersum, L. and Endeman, H. J. (1984) 'Determination of plasma oxalate with oxalate oxidase', *Clinica Chimica Acta*, 137(1), 53-60.
- Boland, G. J. and Hall, R. (1994) 'Index of plant hosts of *Sclerotinia sclerotiorum*', *Canadian Journal of Plant Pathology-Revue Canadienne De Phytopathologie*, 16(2), 93-108.
- Bolton, M. D., Kolmer, J. A. and Garvin, D. F. (2008a) 'Wheat leaf rust caused by *Puccinia triticina*', *Molecular Plant Pathology*, 9(5), 563-575.
- Bolton, M. D., Thomma, B. and Nelson, B. D. (2006) '*Sclerotinia sclerotiorum* (Lib.) de Bary: biology and molecular traits of a cosmopolitan pathogen', *Molecular Plant Pathology*, 7(1), 1-16.
- Bolton, M. D., van Esse, H. P., Vossen, J. H., de Jonge, R., Stergiopoulos, I., Stulemeijer, I. J. E., van den Berg, G. C. M., Borrás-Hidalgo, O., Dekker, H. L., de Koster, C. G., de Wit, P. J. G. M., Joosten, M. H. A. J. and Thomma, B. P. H. J. (2008b) 'The novel *Cladosporium fulvum* lysin motif effector Ecp6 is a virulence factor with orthologues in other fungal species', *Molecular Microbiology*, 69(1), 119-136.
- Bowden, J., Gregory, P. H. and Johnson, C. G. (1971) 'Possible wind transport of coffee leaf rust across atlantic ocean', *Nature*, 229(5285), 500-&.
- Bowen, J. K., Mesarich, C. H., Rees-George, J., Cui, W., Fitzgerald, A., Win, J., Plummer, K. M. and Templeton, M. D. (2009) 'Candidate effector gene identification in the ascomycete fungal phytopathogen *Venturia inaequalis* by expressed sequence tag analysis', *Molecular Plant Pathology*, 10(3), 431-448.
- BROAD, Institute .
'(http://www.broadinstitute.org/annotation/genome/sclerotinia_sclerotiorum/MultiHome.html)',
- Brown, D. and Wanek, G. L. (1992) 'Glycosyl-phosphatidylinositol anchored membrane-proteins', *Journal of the American Society of Nephrology*, 3(4), 895-906.

- Brown, J. K. M. and Hovmoller, M. S. (2002) 'Epidemiology - Aerial dispersal of pathogens on the global and continental scales and its impact on plant disease', *Science*, 297(5581), 537-541.
- Brown, N. A., Antoniw, J. and Hammond-Kosack, K. E. (2012) 'The Predicted Secretome of the Plant Pathogenic Fungus *Fusarium graminearum*: A Refined Comparative Analysis', *Plos One*, 7(4).
- Candresse, T., Lot, H., German-Retana, S., Krause-Sakate, R., Thomas, J., Souche, S., Delaunay, T., Lanneau, M. and Le Gall, O. (2007) 'Analysis of the serological variability of Lettuce mosaic virus using monoclonal antibodies and surface plasmon resonance technology', *Journal of General Virology*, 88, 2605-2610.
- Cantarel, B. L., Coutinho, P. M., Rancurel, C., Bernard, T., Lombard, V. and Henrissat, B. (2009) 'The Carbohydrate-Active EnZymes database (CAZy): an expert resource for Glycogenomics', *Nucleic Acids Research*, 37, D233-D238.
- Carbone, I., Anderson, J. B. and Kohn, L. M. (1999) 'Patterns of descent in clonal lineages and their multilocus fingerprints are resolved with combined gene genealogies', *Evolution*, 53(1), 11-21.
- Carisse, O., McCartney, H. A., Gagnon, J. A. and Brodeur, L. (2005) 'Quantification of airborne inoculum as an aid in the management of leaf blight of onion caused by *Botrytis squamosa*', *Plant Disease*, 89(7), 726-733.
- Cavener, D. R. (1992) 'GMC oxidoreductases - a newly defined family of homologous proteins with diverse catalytic activities', *Journal of Molecular Biology*, 223(3), 811-814.
- Cavinder, B., Sikhakolli, U., Fellows, K. M. and Trail, F. (2012) 'Sexual development and ascospore discharge in *Fusarium graminearum*', *Journal of visualized experiments : JoVE*, (61).
- Cessna, S. G., Sears, V. E., Dickman, M. B. and Low, P. S. (2000) 'Oxalic acid, a pathogenicity factor for *Sclerotinia sclerotiorum*, suppresses the oxidative burst of the host plant', *Plant Cell*, 12(11), 2191-2199.
- Chae, M. and Carman, G. M. (2013) 'Characterization of the Yeast Actin Patch Protein App1p Phosphatidate Phosphatase', *Journal of Biological Chemistry*, 288(9), 6427-6437.
- Cheng, V., Stotz, H. U., Hippchen, K. and Bakalinsky, A. T. (2007) 'Genome-wide screen for oxalate-sensitive mutants of *Saccharomyces cerevisiae*', *Applied and Environmental Microbiology*, 73(18), 5919-5927.
- Clark, L. C. and Lyons, C. (1962) 'Electrode systems for continuous monitoring in cardiovascular surgery', *Annals of the New York Academy of Sciences*, 102(1), 29-&.
- Clark, M. F. and Adams, A. N. (1977) 'Characteristics of microplate method of enzyme-linked immunosorbent assay for the detection of plant-viruses', *Journal of General Virology*, 34(MAR), 475-483.

- Clarke, A. (2012) 'Prediction model gives optimum fungicide timing for *Sclerotinia*', [online], available: <http://www.fwi.co.uk/articles/29/02/2012/131667/prediction-model-gives-optimum-fungicide-timing-for.html>
- Clarkson, J. P., Coventry, E., Kitchen, J., Carter, H. E. and Whipps, J. M. (2013) 'Population structure of *Sclerotinia sclerotiorum* in crop and wild hosts in the UK', *Plant Pathology*, 62(2), 309-324.
- Clarkson, J. P., Phelps, K., Whipps, J. A., Young, C. S., Smith, J. A. and Watling, M. (2007) 'Forecasting sclerotinia disease on lettuce: A predictive model for carpogenic germination of *Sclerotinia sclerotiorum* sclerotia', *Phytopathology*, 97(5), 621-631.
- Colmenares, A. J., Aleu, J., Duran-Patron, R., Collado, I. G. and Hernandez-Galan, R. (2002) 'The putative role of botrydial and related metabolites in the infection mechanism of *Botrytis cinerea*', *Journal of Chemical Ecology*, 28(5), 997-1005.
- Conesa, A., Gotz, S., Garcia-Gomez, J. M., Terol, J., Talon, M. and Robles, M. (2005) 'Blast2GO: a universal tool for annotation, visualization and analysis in functional genomics research', *Bioinformatics*, 21(18), 3674-3676.
- Copeland, R. A. (1996) *Enzymes: A practical introduction to structure, mechanism, and data analysis*, VCH Publishers.
- Cotton, P., Kasza, Z., Bruel, C., Rasclé, C. and Fevre, M. (2003) 'Ambient pH controls the expression of endopolygalacturonase genes in the necrotrophic fungus *Sclerotinia sclerotiorum*', *Fems Microbiology Letters*, 227(2), 163-169.
- Culbertson, B. J., Furumo, N. C. and Daniel, S. L. (2007a) 'Impact of nutritional supplements and monosaccharides on growth, oxalate accumulation, and culture pH by *Sclerotinia sclerotiorum*', *Fems Microbiology Letters*, 270(1), 132-138.
- Culbertson, B. J., Krone, J., Gatebe, E., Furumo, N. C. and Daniel, S. L. (2007b) 'Impact of carbon sources on growth and oxalate synthesis by the phytopathogenic fungus *Sclerotinia sclerotiorum*', *World Journal of Microbiology & Biotechnology*, 23(10), 1357-1362.
- Cutler, H. G., Jacyno, J. M., Harwood, J. S., Dulik, D., Goodrich, P. D. and Roberts, R. G. (1993) 'Botcinolide - a biologically-active natural product from botrytis-cinerea', *Bioscience Biotechnology and Biochemistry*, 57(11), 1980-1982.
- Cutler, H. G., Parker, S. R., Ross, S. A., Crumley, F. G. and Schreiner, P. R. (1996) 'Homobotcinolide: A biologically active natural homolog of botcinolide from *Botrytis cinerea*', *Bioscience Biotechnology and Biochemistry*, 60(4), 656-658.
- Dallal Bashi, Z., Rimmer, S. R., Khachatourians, G. G. and Hegedus, D. D. (2012) 'Factors governing the regulation of *Sclerotinia sclerotiorum* cutinase A and polygalacturonase 1 during different stages of infection', *Canadian Journal of Microbiology*, 58(5), 605-16.
- Dalmaï, B., Schumacher, J., Moraga, J., Le Pêcheur, P., Tudzynski, B., Gonzalez Collado, I. and Viaud, M. (2011) 'The *Botrytis cinerea* phytotoxin botcinic acid requires two polyketide synthases for production and has a redundant role in virulence with botrydial', *Molecular Plant Pathology*, 12(6), 564-579.

- De, B. (1884) " *Vergleichende Morphologie und Biologie de Pilze, Mycetozen und Bacterien,* " " *Vergleichende Morphologie und Biologie de Pilze, Mycetozen und Bacterien,* " .
- de Vrije, T., Antoine, N., Buitelaar, R. M., Bruckner, S., Dissevelt, M., Durand, A., Gerlagh, M., Jones, E. E., Luth, P., Oostra, J., Ravensberg, W. J., Renaud, R., Rinzema, A., Weber, F. J. and Whipps, J. M. (2001) 'The fungal biocontrol agent *Coniothyrium minitans*: production by solid-state fermentation, application and marketing', *Applied Microbiology and Biotechnology*, 56(1-2), 58-68.
- Delgado-Jarana, J., Moreno-Mateos, M. A. and Benitez, T. (2003) 'Glucose uptake in *Trichoderma harzianum*: Role of gtt1', *Eukaryotic Cell*, 2(4), 708-717.
- Djamei, A., Schipper, K., Rabe, F., Ghosh, A., Vincon, V., Kahnt, J., Osorio, S., Tohge, T., Fernie, A. R., Feussner, I., Feussner, K., Meinicke, P., Stierhof, Y.-D., Schwarz, H., Macek, B., Mann, M. and Kahmann, R. (2011) 'Metabolic priming by a secreted fungal effector', *Nature*, 478(7369), 395-+.
- do Amaral, A. M., Antoniw, J., Rudd, J. J. and Hammond-Kosack, K. E. (2012) 'Defining the Predicted Protein Secretome of the Fungal Wheat Leaf Pathogen *Mycosphaerella graminicola*', *Plos One*, 7(12).
- Doehlemann, G., van der Linde, K., Amann, D., Schwammbach, D., Hof, A., Mohanty, A., Jackson, D. and Kahmann, R. (2009) 'Pep1, a Secreted Effector Protein of *Ustilago maydis*, Is Required for Successful Invasion of Plant Cells', *PLoS Pathogens*, 5(2).
- Donaghy, J. and McKay, A. M. (1992) 'Extracellular carboxylesterase activity of fusarium-graminearum', *Applied Microbiology and Biotechnology*, 37(6), 742-744.
- Doubayashi, D., Ootake, T., Maeda, Y., Oki, M., Tokunaga, Y., Sakurai, A., Nagaosa, Y., Mikami, B. and Uchida, H. (2011) 'Formate Oxidase, an Enzyme of the Glucose-Methanol-Choline Oxidoreductase Family, Has a His-Arg Pair and 8-Formyl-FAD at the Catalytic Site', *Bioscience Biotechnology and Biochemistry*, 75(9), 1662-1667.
- Durman, S. B., Menendez, A. B. and Godeas, A. M. (2005) 'Variation in oxalic acid production and mycelial compatibility within field populations of *Sclerotinia sclerotiorum*', *Soil Biology & Biochemistry*, 37(12), 2180-2184.
- Dutton, M. V. and Evans, C. S. (1996) 'Oxalate production by fungi: Its role in pathogenicity and ecology in the soil environment', *Canadian Journal of Microbiology*, 42(9), 881-895.
- Eisenhaber, B., Schneider, G., Wildpaner, M. and Eisenhaber, F. (2004) 'A sensitive predictor for potential GPI lipid modification sites in fungal protein sequences and its application to genome-wide studies for *Aspergillus nidulans*, *Candida albicans*, *Neurospora crassa*, *Saccharomyces cerevisiae* and *Schizosaccharomyces pombe*', *Journal of Molecular Biology*, 337(2), 243-253.
- Elad, Y. (2000) '*Trichoderma harzianum* T39 preparation for biocontrol of plant diseases - Control of *Botrytis cinerea*, *Sclerotinia sclerotiorum* and *Cladosporium fulvum*', *Biocontrol Science and Technology*, 10(4), 499-507.

- Emanuelsson, O., Brunak, S., von Heijne, G. and Nielsen, H. (2007) 'Locating proteins in the cell using TargetP, SignalP and related tools', *Nature Protocols*, 2(4), 953-971.
- Emanuelsson, O., Nielsen, H., Brunak, S. and von Heijne, G. (2000) 'Predicting subcellular localization of proteins based on their N-terminal amino acid sequence', *Journal of Molecular Biology*, 300(4), 1005-1016.
- Espeso, E. A., Tilburn, J., Sanchez-Pulido, L., Brown, C. V., Valencia, A., Arst, H. N. and Penalva, M. A. (1997) 'Specific DNA recognition by the *Aspergillus nidulans* three zinc finger transcription factor PacC', *Journal of Molecular Biology*, 274(4), 466-480.
- Evans, N., Welham, S. J., Antoniow, J. F. and Fitt, B. D. L. (2006) 'Development and uptake of a scheme for predicting risk of severe light leaf spot on oilseed rape', *Outlooks on Pest Management*, 17(6), 243-245.
- Favaron, F., Sella, L. and D'Ovidio, R. (2004) 'Relationships among endopolygalacturonase, oxalate, pH, and plant polygalacturonase-inhibiting protein (PGIP) in the interaction between *Sclerotinia sclerotiorum* and soybean', *Molecular Plant-Microbe Interactions*, 17(12), 1402-1409.
- Federici, L., Caprari, C., Mattei, B., Savino, C., Di Matteo, A., De Lorenzo, G., Cervone, F. and Tsernoglou, D. (2001) 'Structural requirements of endopolygalacturonase for the interaction with PGIP (polygalacturonase-inhibiting protein)', *Proceedings of the National Academy of Sciences of the United States of America*, 98(23), 13425-13430.
- Fitt, B. D. L., Brun, H., Barbetti, M. J. and Rimmer, S. R. (2006) 'World-wide importance of phoma stem canker (*Leptosphaeria maculans* and *L. biglobosa*) on oilseed rape (*Brassica napus*)', *European Journal of Plant Pathology*, 114(1), 3-15.
- Fitt, B. D. L., Gladders, P., Turner, J. A., Sutherland, K. G., Welham, S. J. and Davies, J. M. L. (1997) 'Prospects for developing a forecasting scheme to optimise use of fungicides for disease control on winter oilseed rape in the UK', *Aspects of Applied Biology*, (48), 135-142.
- Flor, H. H. (1971) 'Current status of gene-for-gene concept', *Annual Review of Phytopathology*, 9, 275-&.
- Fradin, E. F., Abd-El-Haliem, A., Masini, L., van den Berg, G. C. M., Joosten, M. H. A. J. and Thomma, B. P. H. J. (2011) 'Interfamily Transfer of Tomato Ve1 Mediates *Verticillium* Resistance in *Arabidopsis*', *Plant Physiology*, 156(4), 2255-2265.
- FRAG-UK '<http://www.pesticides.gov.uk/rags.asp?id=644>', [online], available: [accessed
- Freeman, J., Ward, E., Calderon, C. and McCartney, A. (2002) 'A polymerase chain reaction (PCR) assay for the detection of inoculum of *Sclerotinia sclerotiorum*', *European Journal of Plant Pathology*, 108(9), 877-886.
- Garrett, M. H., Rayment, P. R., Hooper, M. A., Abramson, M. J. and Hooper, B. M. (1998) 'Indoor airborne fungal spores, house dampness and associations with environmental factors and respiratory health in children', *Clinical and Experimental Allergy*, 28(4), 459-467.

- Gehring, A. G., Crawford, C. G., Mazonko, R. S., VanHouten, L. J. and Brewster, J. D. (1996) 'Enzyme-linked immunomagnetic electrochemical detection of *Salmonella typhimurium*', *Journal of Immunological Methods*, 195(1-2), 15-25.
- Gelot, M. A., Lavoue, G., Belleville, F. and Nabet, P. (1980) 'Determination of oxalates in plasma and urine using gas-chromatography', *Clinica Chimica Acta*, 106(3), 279-285.
- Ghannoum, M. A. (2000) 'Potential role of phospholipases in virulence and fungal pathogenesis', *Clinical Microbiology Reviews*, 13(1), 122-+.
- Giardine, B., Riemer, C., Hardison, R. C., Burhans, R., Elnitski, L., Shah, P., Zhang, Y., Blankenberg, D., Albert, I., Taylor, J., Miller, W., Kent, W. J. and Nekrutenko, A. (2005) 'Galaxy: A platform for interactive large-scale genome analysis', *Genome Research*, 15(10), 1451-1455.
- Gimenez-Ibanez, S., Ntoukakis, V. and Rathjen, J. P. (2009) 'The LysM receptor kinase CERK1 mediates bacterial perception in *Arabidopsis*', *Plant signaling & behavior*, 4(6), 539-41.
- Godfrey, D., Bohlenius, H., Pedersen, C., Zhang, Z., Emmersen, J. and Thordal-Christensen, H. (2010) 'Powdery mildew fungal effector candidates share N-terminal Y/F/WxC-motif', *Bmc Genomics*, 11.
- Godoy, G., Steadman, J. R., Dickman, M. B. and Dam, R. (1990) 'Use of mutants to demonstrate the role of oxalic acid in pathogenicity of *Sclerotinia sclerotiorum* on *Phaseolus vulgaris*', *Physiological and Molecular Plant Pathology*, 37(3), 179-191.
- Goecks, J., Nekrutenko, A., Taylor, J. and Galaxy, T. (2010) 'Galaxy: a comprehensive approach for supporting accessible, reproducible, and transparent computational research in the life sciences', *Genome Biology*, 11(8).
- Goffeau, A., Barrell, B. G., Bussey, H., Davis, R. W., Dujon, B., Feldmann, H., Galibert, F., Hoheisel, J. D., Jacq, C., Johnston, M., Louis, E. J., Mewes, H. W., Murakami, Y., Philippsen, P., Tettelin, H. and Oliver, S. G. (1996) 'Life with 6000 genes', *Science*, 274(5287), 546-&.
- Goodwin, S. B., Ben M'Barek, S., Dhillon, B., Wittenberg, A. H. J., Crane, C. F., Hane, J. K., Foster, A. J., Van der Lee, T. A. J., Grimwood, J., Aerts, A., Antoniw, J., Bailey, A., Bluhm, B., Bowler, J., Bristow, J., van der Burgt, A., Canto-Canche, B., Churchill, A. C. L., Conde-Ferraz, L., Cools, H. J., Coutinho, P. M., Csukai, M., Dehal, P., De Wit, P., Donzelli, B., van de Geest, H. C., van Ham, R. C. H. J., Hammond-Kosack, K. E., Henrissat, B., Kilian, A., Kobayashi, A. K., Koopmann, E., Kourmpetis, Y., Kuzniar, A., Lindquist, E., Lombard, V., Maliepaard, C., Martins, N., Mehrabi, R., Nap, J. P. H., Ponomarenko, A., Rudd, J. J., Salamov, A., Schmutz, J., Schouten, H. J., Shapiro, H., Stergiopoulos, I., Torriani, S. F. F., Tu, H., de Vries, R. P., Waalwijk, C., Ware, S. B., Wiebenga, A., Zwieters, L.-H., Oliver, R. P., Grigoriev, I. V. and Kema, G. H. J. (2011) 'Finished Genome of the Fungal Wheat Pathogen *Mycosphaerella graminicola* Reveals Dispensome Structure, Chromosome Plasticity, and Stealth Pathogenesis', *Plos Genetics*, 7(6).

- Guimaraes, R. L. and Stotz, H. U. (2004) 'Oxalate production by *Sclerotinia sclerotiorum* deregulates guard cells during infection', *Plant Physiology*, 136(3), 3703-3711.
- Halaouli, S., Asther, M., Sigoillot, J. C., Hamdi, M. and Lomascolo, A. (2006) 'Fungal tyrosinases: new prospects in molecular characteristics, bioengineering and biotechnological applications', *Journal of Applied Microbiology*, 100(2), 219-232.
- Hambleton, S., Walker, C. and Kohn, L. M. (2002) 'Clonal lineages of *Sclerotinia sclerotiorum* previously known from other crops predominate in 1999-2000 samples from Ontario and Quebec soybean', *Canadian Journal of Plant Pathology-Revue Canadienne De Phytopathologie*, 24(3), 309-315.
- Hammel, K. E., Mozuch, M. D., Jensen, K. A. and Kersten, P. J. (1994) 'H₂O₂ recycling during oxidation of the arylglycerol beta-aryl ether lignin structure by lignin peroxidase and glyoxal oxidase', *Biochemistry*, 33(45), 13349-13354.
- Hammond-Kosack, K. E. and Rudd, J. J. (2008) 'Plant resistance signalling hijacked by a necrotrophic fungal pathogen', *Plant signaling & behavior*, 3(11), 993-5.
- Han, Y., Joosten, H.-J., Niu, W., Zhao, Z., Mariano, P. S., McCalman, M., van Kan, J., Schaap, P. J. and Dunaway-Mariano, D. (2007) 'Oxaloacetate hydrolase, the C-C bond lyase of oxalate secreting fungi', *Journal of Biological Chemistry*, 282(13), 9581-9590.
- Hegedus, D. D. and Rimmer, S. R. (2005) '*Sclerotinia sclerotiorum*: When "to be or not to be" a pathogen?', *Fems Microbiology Letters*, 251(2), 177-184.
- Heger, A. and Holm, L. (2000) 'Rapid automatic detection and alignment of repeats in protein sequences', *Proteins-Structure Function and Genetics*, 41(2), 224-237.
- HGCA '<http://www.hgca.com/content.template/0/0/Home/Home/Home.msp>'.
- Higuchi, Y., Arioka, M. and Kitamoto, K. (2009) 'Endocytic recycling at the tip region in the filamentous fungus *Aspergillus oryzae*', *Communicative & integrative biology*, 2(4), 327-8.
- Horton, P., Park, K.-J., Obayashi, T., Fujita, N., Harada, H., Adams-Collier, C. J. and Nakai, K. (2007) 'WoLF PSORT: protein localization predictor', *Nucleic Acids Research*, 35, W585-W587.
- Huang, H. C., Bremer, E., Hynes, R. K. and Erickson, R. S. (2000) 'Foliar application of fungal biocontrol agents for the control of white mold of dry bean caused by *Sclerotinia sclerotiorum*', *Biological Control*, 18(3), 270-276.
- Huang, H. C. and Kozub, G. C. (1991) 'Temperature requirements for carpogenic germination of sclerotia of *Sclerotinia-sclerotiorum* isolates of different geographic origin', *Botanical Bulletin of Academia Sinica*, 32(4), 279-286.
- Hunter, S., Jones, P., Mitchell, A., Apweiler, R., Attwood, T. K., Bateman, A., Bernard, T., Binns, D., Bork, P., Burge, S., de Castro, E., Coggill, P., Corbett, M., Das, U., Daugherty, L., Duquenne, L., Finn, R. D., Fraser, M., Gough, J., Haft, D., Hulo, N., Kahn, D., Kelly, E., Letunic, I., Lonsdale, D., Lopez, R., Madera, M., Maslen, J., McAnulla, C., McDowall, J., McMenamin, C., Mi, H., Mutowo-Muellenet, P., Mulder,

- N., Natale, D., Orengo, C., Pesseat, S., Punta, M., Quinn, A. F., Rivoire, C., Sangrador-Vegas, A., Selengut, J. D., Sigrist, C. J. A., Scheremetjew, M., Tate, J., Thimmajananathan, M., Thomas, P. D., Wu, C. H., Yeats, C. and Yong, S.-Y. (2012) 'InterPro in 2011: new developments in the family and domain prediction database', *Nucleic Acids Research*, 40(D1), D306-D312.
- Inbar, J., Menendez, A. and Chet, I. (1996) 'Hyphal interaction between *Trichoderma harzianum* and *Sclerotinia sclerotiorum* and its role in biological control', *Soil Biology & Biochemistry*, 28(6), 757-763.
- Innes, J. (2010) '<http://www.jic.ac.uk/Corporate/about/publications/EconomicImpact.pdf>',
- Islam, M. S., Haque, M. S., Islam, M. M., Emdad, E. M., Halim, A., Hossen, Q. M. M., Hossain, M. Z., Ahmed, B., Rahim, S., Rahman, M. S., Alam, M. M., Hou, S., Wan, X., Saito, J. A. and Alam, M. (2012) 'Tools to kill: Genome of one of the most destructive plant pathogenic fungi *Macrophomina phaseolina*', *Bmc Genomics*, 13.
- Johnsson, B., Lofas, S. and Lindquist, G. (1991) 'Immobilization of proteins to a carboxymethyl-dextran modified gold surface for biospecific interaction analysis in Surface-Plasmon Resonance sensors', *Analytical Biochemistry*, 198(2), 268-277.
- Jones, J. D. G. and Dangl, J. L. (2006) 'The plant immune system', *Nature*, 444(7117), 323-329.
- Jurick, W. M., Dickman, M. B. and Rollins, J. A. (2004) 'Characterization and functional analysis of a cAMP-dependent protein kinase A catalytic subunit gene (*pka1*) in *Sclerotinia sclerotiorum*', *Physiological and Molecular Plant Pathology*, 64(3), 155-163.
- Kabbage, M., Williams, B. and Dickman, M. B. (2013) 'Cell Death Control: The Interplay of Apoptosis and Autophagy in the Pathogenicity of *Sclerotinia sclerotiorum*', *PLoS Pathogens*, 9(4).
- Kaemper, J., Kahmann, R., Boelker, M., Ma, L.-J., Brefort, T., Saville, B. J., Banuett, F., Kronstad, J. W., Gold, S. E., Mueller, O., Perlin, M. H., Woesten, H. A. B., de Vries, R., Ruiz-Herrera, J., Reynaga-Pena, C. G., Snetselaar, K., McCann, M., Perez-Martin, J., Feldbruegge, M., Basse, C. W., Steinberg, G., Ibeas, J. I., Holloman, W., Guzman, P., Farman, M., Stajich, J. E., Sentandreu, R., Gonzalez-Prieto, J. M., Kennell, J. C., Molina, L., Schirawski, J., Mendoza-Mendoza, A., Greilinger, D., Muench, K., Roessel, N., Scherer, M., Vranes, M., Ladendorff, O., Vincon, V., Fuchs, U., Sandrock, B., Meng, S., Ho, E. C. H., Cahill, M. J., Boyce, K. J., Klose, J., Klosterman, S. J., Deelstra, H. J., Ortiz-Castellanos, L., Li, W., Sanchez-Alonso, P., Schreier, P. H., Haeuser-Hahn, I., Vaupel, M., Koopmann, E., Friedrich, G., Voss, H., Schlueter, T., Margolis, J., Platt, D., Swimmer, C., Gnrke, A., Chen, F., Vysotskaia, V., Mannhaupt, G., Gueldener, U., Muensterkoetter, M., Haase, D., Oesterheld, M., Mewes, H.-W., Mauceli, E. W., DeCaprio, D., Wade, C. M., Butler, J., Young, S., Jaffe, D. B., Calvo, S., Nusbaum, C., Galagan, J. and Birren, B. W. (2006) 'Insights from the genome of the biotrophic fungal plant pathogen *Ustilago maydis*', *Nature*, 444(7115), 97-101.
- Kamoun, S. (2003) 'Molecular genetics of pathogenic Oomycetes', *Eukaryotic Cell*, 2(2), 191-199.

- Kasza, Z., Vagvolgyi, C., Fevre, M. and Cotton, P. (2004) 'Molecular characterization and in planta detection of *Sclerotinia sclerotiorum* endopolygalacturonase genes', *Current Microbiology*, 48(3), 208-213.
- Kawabe, M., Onokubo, A. O., Arimoto, Y., Yoshida, T., Azegami, K., Teraoka, T. and Arie, T. (2011) 'GMC oxidoreductase, a highly expressed protein in a potent biocontrol agent *Fusarium oxysporum* Cong:1-2, is dispensable for biocontrol activity', *Journal of General and Applied Microbiology*, 57(4), 207-217.
- Khuri, S., Bakker, F. T. and Dunwell, J. M. (2001) 'Phylogeny, function, and evolution of the cupins, a structurally conserved, functionally diverse superfamily of proteins', *Molecular Biology and Evolution*, 18(4), 593-605.
- Kim, H.-j., Chen, C., Kabbage, M. and Dickman, M. B. (2011) 'Identification and Characterization of *Sclerotinia sclerotiorum* NADPH Oxidases', *Applied and Environmental Microbiology*, 77(21), 7721-7729.
- Kim, K. S., Min, J.-Y. and Dickman, M. B. (2008) 'Oxalic acid is an elicitor of plant programmed cell death during *Sclerotinia sclerotiorum* disease development', *Molecular Plant-Microbe Interactions*, 21(5), 605-612.
- Kimura, M., Tokai, T., Matsumoto, G., Fujimura, M., Hamamoto, H., Yoneyama, K., Shibata, T. and Yamaguchi, I. (2003) 'Trichothecene nonproducer *Gibberella* species have both functional and nonfunctional 3-O-acetyltransferase genes', *Genetics*, 163(2), 677-684.
- Kohlbecker, G. and Butz, M. (1981) 'Direct spectrophotometric determination of serum and urinary oxalate with oxalate oxidase', *Journal of Clinical Chemistry and Clinical Biochemistry*, 19(11), 1103-1106.
- Kohn, L. M. (1979) 'Monographic revision of the genus *Sclerotinia*', *Mycotaxon*, 9(2), 365-444.
- Kowalski, T. and Holdenrieder, O. (2009) 'Pathogenicity of *Chalara fraxinea*', *Forest Pathology*, 39(1), 1-7.
- Kulkarni, R. D., Kelkar, H. S. and Dean, R. A. (2003) 'An eight-cysteine-containing CFEM domain unique to a group of fungal membrane proteins', *Trends in Biochemical Sciences*, 28(3), 118-121.
- Kutchan, T. M. and Dittrich, H. (1995) 'Characterization and mechanism of the berberine bridge enzyme, a covalently flavinylated oxidase of benzophenanthridine alkaloid biosynthesis in plants', *Journal of Biological Chemistry*, 270(41), 24475-24481.
- Kwan, A. H. Y., Winefield, R. D., Sunde, M., Matthews, J. M., Haverkamp, R. G., Templeton, M. D. and Mackay, J. P. (2006) 'Structural basis for rodlet assembly in fungal hydrophobins', *Proceedings of the National Academy of Sciences of the United States of America*, 103(10), 3621-3626.
- Lagunas, R. (1993) 'Sugar-transport in *Saccharomyces cerevisiae*', *Fems Microbiology Reviews*, 104(3-4), 229-242.

- Lamberski, J. A., Thompson, N. E. and Burgess, R. R. (2006) 'Expression and purification of a single-chain variable fragment antibody derived from a polyol-responsive monoclonal antibody', *Protein Expression and Purification*, 47(1), 82-92.
- Lenz, H., Wunderwald, P. and Eggerer, H. (1976) 'Partial-purification and some properties of oxalacetase from *Aspergillus niger*', *European Journal of Biochemistry*, 65(1), 225-236.
- Leroch, M., Mernke, D., Koppenhoefer, D., Schneider, P., Mosbach, A., Doehlemann, G. and Hahn, M. (2011) 'Living Colors in the Gray Mold Pathogen *Botrytis cinerea*: Codon-Optimized Genes Encoding Green Fluorescent Protein and mCherry, Which Exhibit Bright Fluorescence', *Applied and Environmental Microbiology*, 77(9), 2887-2897.
- Levasseur, A., Saloheimo, M., Navarro, D., Andberg, M., Pontarotti, P., Kruus, K. and Record, E. (2010) 'Exploring laccase-like multicopper oxidase genes from the ascomycete *Trichoderma reesei*: a functional, phylogenetic and evolutionary study', *Bmc Biochemistry*, 11.
- Li, R. G., Rimmer, R., Buchwaldt, L., Sharpe, A. G., Seguin-Swartz, G., Coutu, C. and Hegedus, D. D. (2004a) 'Interaction of *Sclerotinia sclerotiorum* with a resistant *Brassica napus* cultivar: expressed sequence tag analysis identifies genes associated with fungal pathogenesis', *Fungal Genetics and Biology*, 41(8), 735-753.
- Li, R. G., Rimmer, R., Buchwaldt, L., Sharpe, A. G., Seguin-Swartz, G. and Hegedus, D. D. (2004b) 'Interaction of *Sclerotinia sclerotiorum* with *Brassica napus*: cloning and characterization of endo- and exo-polygalacturonases expressed during saprophytic and parasitic modes', *Fungal Genetics and Biology*, 41(8), 754-765.
- Li, Y., Zhang, Y. and Li, B. (1994) 'Study on the disseminating distance of ascospore of sunflower stem rot fungus', *Plant Protection*, 20(1), 12-13.
- Liang, Y., Strelkov, S. E. and Kav, N. N. V. (2010) 'The Proteome of Liquid Sclerotial Exudates from *Sclerotinia sclerotiorum*', *Journal of Proteome Research*, 9(6), 3290-3298.
- Liang, Y., Yajima, W., Davis, M. R., Kav, N. N. V. and Strelkov, S. E. (2013) 'Disruption of a gene encoding a hypothetical secreted protein from *Sclerotinia sclerotiorum* reduces its virulence on canola (*Brassica napus*)', *Canadian Journal of Plant Pathology*, 35(1), 46-55.
- Lithourgidis, A. S., Roupakias, D. G. and Tzavella-Klonari, K. (2007) 'Stem rot disease incidence on faba beans in an artificially infested field', *Journal of Plant Diseases and Protection*, 114(3), 120-125.
- Lorang, J. M., Tuori, R. P., Martinez, J. P., Sawyer, T. L., Redman, R. S., Rollins, J. A., Wolpert, T. J., Johnson, K. B., Rodriguez, R. J., Dickman, M. B. and Ciuffetti, L. M. (2001) 'Green fluorescent protein is lighting up fungal biology', *Applied and Environmental Microbiology*, 67(5), 1987-1994.

- Lowe, R., Jubault, M., Canning, G., Urban, M. and Hammond-Kosack, K. E. (2012) 'The Induction of Mycotoxins by Trichothecene Producing *Fusarium* Species' in Bolton, M. D. and Thomma, B., eds., *Plant Fungal Pathogens: Methods and Protocols*, 439-455.
- Lu, G. (2003) 'Engineering *Sclerotinia sclerotiorum* resistance in oilseed crops', *African Journal of Biotechnology*, 2(12 Cited December 31, 2003), 509-516.
- Luderer, R., De Kock, M. J. D., Dees, R. H. L., De Wit, P. and Joosten, M. (2002) 'Functional analysis of cysteine residues of ECP elicitor proteins of the fungal tomato pathogen *Cladosporium fulvum*', *Molecular Plant Pathology*, 3(2), 91-95.
- Lugones, L. G., Wosten, H. A. B. and Wessels, J. G. H. (1998) 'A hydrophobin (ABH3) specifically secreted by vegetatively growing hyphae of *Agaricus bisporus* (common white button mushroom)', *Microbiology-Uk*, 144, 2345-2353.
- Lumsden, R. D. (1979) 'Histology and physiology of pathogenesis in plant diseases caused by *Sclerotinia* species', *Phytopathology*, 69(8), 890-896.
- Magarey, R. D., Sutton, T. B. and Thayer, C. L. (2005) 'A simple generic infection model for foliar fungal plant pathogens', *Phytopathology*, 95(1), 92-100.
- Magro, P., Marciano, P. and Dilenza, P. (1984) 'Oxalic acid production and its role in pathogenesis of *Sclerotinia sclerotiorum*', *Fems Microbiology Letters*, 24(1), 9-12.
- Magro, P., Marciano, P. and Dilenza, P. (1988) 'Enzymatic oxalate decarboxylation in isolates of *Sclerotinia sclerotiorum*', *Fems Microbiology Letters*, 49(1), 49-52.
- Marcantonio, E. E. and Hynes, R. O. (1988) 'Antibodies to the conserved cytoplasmic domain of the integrin beta-1-subunit react with proteins in vertebrates, invertebrates, and fungi', *Journal of Cell Biology*, 106(5), 1765-1772.
- Marciano, P., Magro, P. and Favaron, F. (1989) '*Sclerotinia sclerotiorum* growth and oxalic acid production on selected culture media', *Fems Microbiology Letters*, 61(1-2), 57-59.
- Marshall, R., Kombrink, A., Motteram, J., Loza-Reyes, E., Lucas, J., Hammond-Kosack, K. E., Thomma, B. P. H. J. and Rudd, J. J. (2011) 'Analysis of Two in Planta Expressed LysM Effector Homologs from the Fungus *Mycosphaerella graminicola* Reveals Novel Functional Properties and Varying Contributions to Virulence on Wheat', *Plant Physiology*, 156(2), 756-769.
- Matson, P. A. and Vitousek, P. M. (2006) 'Agricultural intensification: Will land spared from farming be land spared for nature?', *Conservation Biology*, 20(3), 709-710.
- Maxwell, D. P. and Lumsden, R. D. (1970) 'Oxalic acid production by *Sclerotinia sclerotiorum* in infected bean and in culture.', *Phytopathology*, 60(9), 1395-&.
- Miki, K., Tsuchida, T., Kawagoe, M., Kinoshita, H. and Ikeda, T. (1994) 'Bioelectrocatalysis at the yeast cell-immobilized electrode with mediators', *Denki Kagaku*, 62(12), 1249-1250.

- Miyamoto, S., Murakami, T., Saito, A. and Kimura, J. (1991) 'Development of an amperometric alcohol sensor based on immobilized alcohol-dehydrogenase and entrapped NAD⁺', *Biosensors & Bioelectronics*, 6(7), 563-567.
- Mueller, O., Schreier, P. H. and Uhrig, J. F. (2008) 'Identification and characterization of secreted and pathogenesis-related proteins in *Ustilago maydis*', *Molecular Genetics and Genomics*, 279(1), 27-39.
- Muhammad-Tahir, Z. and Alocilja, E. C. (2003) 'Fabrication of a disposable biosensor for *Escherichia coli* O157 : H7 detection', *Ieee Sensors Journal*, 3(4), 345-351.
- Muhammad-Tahir, Z. and Alocilja, E. C. (2004) 'A disposable biosensor for pathogen detection in fresh produce samples', *Biosystems Engineering*, 88(2), 145-151.
- Nations, United Nations. (2013) 'World Population Prospects: The 2012 Revision', [online], (<http://esa.un.org/wpp/>)
- Niderman, T., Genetet, I., Bruyere, T., Gees, R., Stintzi, A., Legrand, M., Fritig, B. and Mosinger, E. (1995) 'Pathogenesis-related pr-1 proteins are antifungal - isolation and characterization of 3 14-kilodalton proteins of tomato and of a basic pr-1 of tobacco with inhibitory activity against *phytophthora infestans*', *Plant Physiology*, 108(1), 17-27.
- Nierman, W. C., Pain, A., Anderson, M. J., Wortman, J. R., Kim, H. S., Arroyo, J., Berriman, M., Abe, K., Archer, D. B., Bermejo, C., Bennett, J., Bowyer, P., Chen, D., Collins, M., Coulsen, R., Davies, R., Dyer, P. S., Farman, M., Fedorova, N., Feldblyum, T. V., Fischer, R., Fosker, N., Fraser, A., Garcia, J. L., Garcia, M. J., Goble, A., Goldman, G. H., Gomi, K., Griffith-Jones, S., Gwilliam, R., Haas, B., Haas, H., Harris, D., Horiuchi, H., Huang, J., Humphray, S., Jimenez, J., Keller, N., Khouri, H., Kitamoto, K., Kobayashi, T., Konzack, S., Kulkarni, R., Kumagai, T., Lafton, A., Latge, J. P., Li, W. X., Lord, A., Majoros, W. H., May, G. S., Miller, B. L., Mohamoud, Y., Molina, M., Monod, M., Mouyna, I., Mulligan, S., Murphy, L., O'Neil, S., Paulsen, I., Penalva, M. A., Perteza, M., Price, C., Pritchard, B. L., Quail, M. A., Rabbinowitsch, E., Rawlins, N., Rajandream, M. A., Reichard, U., Renauld, H., Robson, G. D., de Cordoba, S. R., Rodriguez-Pena, J. M., Ronning, C. M., Rutter, S., Salzberg, S. L., Sanchez, M., Sanchez-Ferrero, J. C., Saunders, D., Seeger, K., Squares, R., Squares, S., Takeuchi, M., Tekaia, F., Turner, G., de Aldana, C. R. V., Weidman, J., White, O., Woodward, J., Yu, J. H., Fraser, C., Galagan, J. E., Asai, K., Machida, M., Hall, N., Barrell, B. and Denning, D. W. (2005) 'Genomic sequence of the pathogenic and allergenic filamentous fungus *Aspergillus fumigatus*', *Nature*, 438(7071), 1151-1156.
- Nugaeva, N., Gfeller, K. Y., Backmann, N., Dueggelin, M., Lang, H. P., Guentherodt, H.-J. and Hegner, M. (2007) 'An antibody-sensitized microfabricated cantilever for the growth detection of *Aspergillus niger* spores', *Microscopy and Microanalysis*, 13(1), 13-17.
- OECD-FAO Agricultural Outlook 2012-2021, (2012) (<http://www.oecd.org/site/oecd-faoagriculturaloutlook/>).
- Oerke, E. C. (2006) 'Crop losses to pests', *Journal of Agricultural Science*, 144, 31-43.

- Oerke, E. C. and Dehne, H. W. (2004) 'Safeguarding production - losses in major crops and the role of crop protection', *Crop Protection*, 23(4), 275-285.
- Ortiz-Bermudez, P., Srebotnik, E. and Hammel, K. E. (2003) 'Chlorination and cleavage of lignin structures by fungal chloroperoxidases', *Applied and Environmental Microbiology*, 69(8), 5015-5018.
- Palmieri, L., Lasorsa, F. M., DePalma, A., Palmieri, F., Runswick, M. J. and Walker, J. E. (1997) 'Identification of the yeast ACR1 gene product as a succinate-fumarate transporter essential for growth on ethanol or acetate', *Febs Letters*, 417(1), 114-118.
- Palumbi, S. R. (2001) 'Evolution - Humans as the world's greatest evolutionary force', *Science*, 293(5536), 1786-1790.
- Parker, M., McDonald, M. R. and Boland, G. J. (2009) 'Detecting ascospores of *Sclerotinia sclerotiorum* in carrot crops in Ontario - prelude to regional level forecasting of sclerotinia rot of carrot', *Canadian Journal of Plant Pathology-Revue Canadienne De Phytopathologie*, 31(1), 153-153.
- Percudani, R., Montanini, B. and Ottonello, S. (2005) 'The anti-HIV cyanovirin-N domain is evolutionarily conserved and occurs as a protein module in eukaryotes', *Proteins-Structure Function and Bioinformatics*, 60(4), 670-678.
- Phalan, B., Onial, M., Balmford, A. and Green, R. E. (2011) 'Reconciling Food Production and Biodiversity Conservation: Land Sharing and Land Sparing Compared', *Science*, 333(6047), 1289-1291.
- Pierson, P. E. and Rhodes, L. H. (1992) 'Effect of culture medium on the production of oxalic acid by *Sclerotinia trifoliorum*.', *Mycologia*, 84(3), 467-469.
- Pijls, C. F. N., Shaw, M. W. and Parker, A. (1994) 'A rapid test to evaluate in-vitro sensitivity of *Septoria tritici* to flutriafol, using a microtitre plate reader', *Plant Pathology*, 43(4), 726-732.
- Pingali, P. L. (2012) 'Green Revolution: Impacts, limits, and the path ahead', *Proceedings of the National Academy of Sciences of the United States of America*, 109(31), 12302-12308.
- Plessner, O., Klapatch, T. and Guerinot, M. L. (1993) 'Siderophore utilization by *Bradyrhizobium japonicum*', *Applied and Environmental Microbiology*, 59(5), 1688-1690.
- Postnote, P. o. o. S. a. T. (2009) '<http://www.parliament.uk/documents/post/postpn336.pdf>', [online].
- Quevillon, E., Silventoinen, V., Pillai, S., Harte, N., Mulder, N., Apweiler, R. and Lopez, R. (2005) 'InterProScan: protein domains identifier', *Nucleic Acids Research*, 33, W116-W120.
- Qutob, D., Kamoun, S. and Gijzen, M. (2002) 'Expression of a *Phytophthora sojae* necrosis-inducing protein occurs during transition from biotrophy to necrotrophy', *Plant Journal*, 32(3), 361-373.

- Rassam, M. and Laing, W. (2005) 'Variation in ascorbic acid and oxalate levels in the fruit of *Actinidia chinensis* tissues and genotypes', *Journal of Agricultural and Food Chemistry*, 53(6), 2322-2326.
- Ray, D. M., ND. West, PC. Foley, JA. (2013) 'Yield Trends Are Insufficient to Double Global Crop Production by 2050', *Plos One*, 8(6).
- Rigden, D. J. (2008) 'The histidine phosphatase superfamily: structure and function', *Biochemical Journal*, 409, 333-348.
- Riou, C., Freyssinet, G. and Fevre, M. (1991) 'Production of Cell Wall-Degrading Enzymes by the Phytopathogenic Fungus *Sclerotinia sclerotiorum*', *Applied and Environmental Microbiology*, 57(5), 1478-1484.
- Roberts, R. G., Hale, C. N., van der Zwet, T., Miller, C. E. and Redlin, S. C. (1998) 'The potential for spread of *Erwinia amylovora* and fire blight via commercial apple fruit; a critical review and risk assessment', *Crop Protection*, 17(1), 19-28.
- Rogers, S. L., Atkins, S. D. and West, J. S. (2009) 'Detection and quantification of airborne inoculum of *Sclerotinia sclerotiorum* using quantitative PCR', *Plant Pathology*, 58(2), 324-331.
- Rollins, J. A. (2003) 'The *Sclerotinia sclerotiorum* pac1 gene is required for sclerotial development and virulence', *Molecular Plant-Microbe Interactions*, 16(9), 785-795.
- Rollins, J. A. and Dickman, M. B. (2001) 'PH signaling in *Sclerotinia sclerotiorum*: Identification of a pacC/RIM1 Homolog', *Applied and Environmental Microbiology*, 67(1), 75-81.
- Ruijter, G. J. G., van de Vondervoort, P. J. I. and Visser, J. (1999) 'Oxalic acid production by *Aspergillus niger*: an oxalate-non-producing mutant produces citric acid at pH 5 and in the presence of manganese', *Microbiology-Uk*, 145, 2569-2576.
- Ruiz-Garcia, L., Lunadei, L., Barreiro, P. and Robla, J. I. (2009) 'A Review of Wireless Sensor Technologies and Applications in Agriculture and Food Industry: State of the Art and Current Trends', *Sensors*, 9(6), 4728-4750.
- Russell, P. E. (2005) 'A century of fungicide evolution', *Journal of Agricultural Science*, 143, 11-25.
- Russo, P. S., Blum, F. D., Ipsen, J. D., Abulhajj, Y. J. and Miller, W. G. (1982) 'The surface-activity of the phytotoxin cerato-ulmin', *Canadian Journal of Botany-Revue Canadienne De Botanique*, 60(8), 1414-1422.
- Sakuno, E., Tani, H. and Nakajima, H. (2007) '2-epi-Botcinin A and 3-O-acetylbotcinic acid from *Botrytis cinerea*', *Bioscience Biotechnology and Biochemistry*, 71(10), 2592-2595.
- Scarboro.Ga (1970a) 'Sugar transport in *Neurospora crassa*', *Journal of Biological Chemistry*, 245(7), 1694-&.

- Scarboro.Ga (1970b) 'Sugar transport in *Neurospora crassa*. 2. A second glucose transport system', *Journal of Biological Chemistry*, 245(15), 3985-&.
- Schneide.Rp and Wiley, W. R. (1971) 'Regulation fo sugar transport in *Neurospora crassa*', *Journal of Bacteriology*, 106(2), 487-&.
- Schwille, P. O., Manoharan, M., Rumenapf, G., Wolfel, G. and Berens, H. (1989) 'Oxalate measurement in the picomol range by ion chromatography values in fasting plasma and urine of controls and patients with idiopathic calcium urolithiasis', *Journal of Clinical Chemistry and Clinical Biochemistry*, 27(2), 87-96.
- Scott, B. and Eaton, C. J. (2008) 'Role of reactive oxygen species in fungal cellular differentiations', *Current Opinion in Microbiology*, 11(6), 488-493.
- Shimizu, T., Nakano, T., Takamizawa, D., Desaki, Y., Ishii-Minami, N., Nishizawa, Y., Minami, E., Okada, K., Yamane, H., Kaku, H. and Shibuya, N. (2010) 'Two LysM receptor molecules, CEBiP and OsCERK1, cooperatively regulate chitin elicitor signaling in rice', *Plant Journal*, 64(2), 204-214.
- Skidgel, R. A. and Erdos, E. G. (1998) 'Cellular carboxypeptidases', *Immunological Reviews*, 161, 129-141.
- Skottrup, P., Nicolaisen, M. and Justesen, A. F. (2007) 'Rapid determination of *Phytophthora infestans* sporangia using a surface plasmon resonance immunosensor', *Journal of Microbiological Methods*, 68(3), 507-515.
- Skottrup, P. D., Nicolaisen, M. and Justesen, A. F. (2008) 'Towards on-site pathogen detection using antibody-based sensors', *Biosensors & Bioelectronics*, 24(3), 339-348.
- Smith, D. L., Hollowell, J. E., Isleib, T. G. and Shew, B. B. (2007) 'A site-specific, weather-based disease regression model for *Sclerotinia* blight of peanut', *Plant Disease*, 91(11), 1436-1444.
- Society, The Royal Society. (2009) Reaping the benefits: Science and the sustainable intensification of global agriculture., (<http://royalsociety.org/policy/publications/2009/reaping-benefits/>).
- SolerRivas, C., Arpin, N., Olivier, J. M. and Wichers, H. J. (1997) 'Activation of tyrosinase in *Agaricus bisporus* strains following infection by *Pseudomonas tolaasii* or treatment with a tolaasin-containing preparation', *Mycological Research*, 101, 375-382.
- Steadman, J. R., Marcinkowska, J. and Rutledge, S. (1994) 'A semi-selective medium for isolation of *Sclerotinia sclerotiorum* ', *Canadian Journal of Plant Pathology-Revue Canadienne De Phytopathologie*, 16(1), 68-70.
- Stergiopoulos, I. and de Wit, P. J. G. M. (2009) 'Fungal Effector Proteins' in *Annual Review of Phytopathology*, 233-263.
- Stynen, D., Sarfati, J., Goris, A., Prevost, M. C., Lesourd, M., Kamphuis, H., Darras, V. and Latge, J. P. (1992) 'Rat monoclonal-antibodies against *Aspergillus galactomannan*', *Infection and Immunity*, 60(6), 2237-2245.

- Thines, E., Weber, R. W. S. and Talbot, N. J. (2000) 'MAP kinase and protein kinase A-dependent mobilization of triacylglycerol and glycogen during appressorium turgor generation by *Magnaporthe grisea*', *Plant Cell*, 12(9), 1703-1718.
- Tilman, D., Balzer, C., Hill, J. and Befort, B. L. (2011) 'Global food demand and the sustainable intensification of agriculture', *Proceedings of the National Academy of Sciences of the United States of America*, 108(50), 20260-20264.
- Tilman, D., Cassman, K. G., Matson, P. A., Naylor, R. and Polasky, S. (2002) 'Agricultural sustainability and intensive production practices', *Nature*, 418(6898), 671-677.
- Torrance, L., Ziegler, A., Pittman, H., Paterson, M., Toth, R. and Eggleston, I. (2006) 'Oriented immobilisation of engineered single-chain antibodies to develop biosensors for virus detection', *Journal of Virological Methods*, 134(1-2), 164-170.
- Trapnell, C., Roberts, A., Goff, L., Pertea, G., Kim, D., Kelley, D. R., Pimentel, H., Salzberg, S. L., Rinn, J. L. and Pachter, L. (2012) 'Differential gene and transcript expression analysis of RNA-seq experiments with TopHat and Cufflinks', *Nature Protocols*, 7(3), 562-578.
- Turner, A. P. F. (2000) 'Biochemistry - Biosensors sense and sensitivity', *Science*, 290(5495), 1315-1317.
- Twengstrom, E. and Sigvald, R. (1993) 'Forecasting *Sclerotinia* stem rot using meteorological and field specific data', *SP Rapport*, (7), 211-216.
- Twengstrom, E. and Sigvald, R. (1996) '*Sclerotinia* stem rot in spring sown rapeseed - evaluation of a forecasting method', *37th Swedish Crop Protection Conference, Uppsala, Sweden, 26-27 January, 1996. Agriculture - pests, diseases and weeds.*, 77-84.
- Twengstrom, E., Sigvald, R., Svensson, C. and Yuen, J. (1998) 'Forecasting *Sclerotinia* stem rot in spring sown oilseed rape', *Crop Protection*, 17(5), 405-411.
- Tyler, B. M. (2009) 'Entering and breaking: virulence effector proteins of oomycete plant pathogens', *Cellular Microbiology*, 11(1), 13-20.
- Vallino, M., Martino, E., Boella, F., Murat, C., Chiapello, M. and Perotto, S. (2009) 'Cu,Zn superoxide dismutase and zinc stress in the metal-tolerant ericoid mycorrhizal fungus *Oidiodendron maius* Zn', *Fems Microbiology Letters*, 293(1), 48-57.
- van Esse, H. P., van't Klooster, J. W., Bolton, M. D., Yadeta, K. A., van Baarlen, P., Boeren, S., Vervoort, J., de Wit, P. J. G. M. and Thomma, B. P. H. J. (2008) 'The *Cladosporium fulvum* virulence protein Avr2 inhibits host proteases required for basal defense', *Plant Cell*, 20(7), 1948-1963.
- van Kan, J. A. L. (2005) 'Infection strategies of *Botrytis cinerea*' in Marissen, N., VanDoorn, W. G. and VanMeeteren, U., eds., *Proceedings of the Viiiith International Symposium on Postharvest Physiology of Ornamental Plants*, 77-89.
- Vega, R. R., Corsini, D. and Letourne, D. (1970) 'Nonvolatile organic acids produced by *Sclerotinia sclerotiorum* in synthetic liquid media', *Mycologia*, 62(2), 332-&.

- Veluchamy, S., Williams, B., Kim, K. and Dickman, M. B. (2012) 'The CuZn superoxide dismutase from *Sclerotinia sclerotiorum* is involved with oxidative stress tolerance, virulence, and oxalate production', *Physiological and Molecular Plant Pathology*, 78, 14-23.
- Velusamy, V., Arshak, K., Korostynska, O., Oliwa, K. and Adley, C. (2010) 'An overview of foodborne pathogen detection: In the perspective of biosensors', *Biotechnology Advances*, 28(2), 232-254.
- Wang, C. and St. Leger, R. J. (2007) 'The MAD1 adhesin of *Metarhizium anisopliae* links adhesion with blastospore production and virulence to insects, and the MAD2 adhesin enables attachment to plants', *Eukaryotic Cell*, 6(5), 808-816.
- Wang, J. (2008) 'Electrochemical Glucose Biosensors', *American Chemical Society*, 108, 814-825.
- Wang, X., Shi, F. X., Wosten, H. A. B., Hektor, H., Poolman, B. and Robillard, G. T. (2005) 'The SC3 hydrophobin self-assembles into a membrane with distinct mass transfer properties', *Biophysical Journal*, 88(5), 3434-3443.
- Ward, E., Foster, S. J., Fraaije, B. A. and McCartney, H. A. (2004) 'Plant pathogen diagnostics: immunological and nucleic acid-based approaches', *Annals of Applied Biology*, 145(1), 1-16.
- White, T. J., Bruns, T., Lee, S. and Taylor, J. (1990) Amplification and direct sequencing of fungal ribosomal rna genes for phylogenetics, innis, m. A., et al.
- Williams, B., Kabbage, M., Kim, H. J., Britt, R. and Dickman, M. B. (2011) 'Tipping the Balance: *Sclerotinia sclerotiorum* Secreted Oxalic Acid Suppresses Host Defenses by Manipulating the Host Redox Environment', *PLoS Pathogens*, 7(6).
- Wojtaszek, P. (1997) 'Oxidative burst: An early plant response to pathogen infection', *Biochemical Journal*, 322, 681-692.
- Wosten, H. A. B. (2001) 'Hydrophobins: Multipurpose proteins', *Annual Review of Microbiology*, 55, 625-646.
- Wosten, H. A. B., Devries, O. M. H. and Wessels, J. G. H. (1993) 'Interfacial self-assembly of a fungal hydrophobin into a hydrophobic rodlet layer', *Plant Cell*, 5(11), 1567-1574.
- Wosten, H. A. B., Schuren, F. H. J. and Wessels, J. G. H. (1994) 'Interfacial self-assembly of a hydrophobin into an amphipathic protein membrane mediates fungal attachment to hydrophobic surfaces', *Embo Journal*, 13(24), 5848-5854.
- Xu, L. and Chen, W. (2013) 'Random T-DNA Mutagenesis Identifies a Cu/Zn Superoxide Dismutase Gene as a Virulence Factor of *Sclerotinia sclerotiorum*', *Molecular plant-microbe interactions : MPMI*, 26(4), 431-41.
- Yadav, S., Anand, G., Dubey, A. K. and Yadav, D. (2012) 'Purification and characterization of an exo-polygalacturonase secreted by *Rhizopus oryzae* MTCC 1987 and its role in retting of *Crotalaria juncea* fibre', *Biologia*, 67(6), 1069-1074.

- Yajima, W. and Kay, N. N. V. (2006) 'The proteome of the phytopathogenic fungus *Sclerotinia sclerotiorum*', *Proteomics*, 6(22), 5995-6007.
- Yamashita, N., Motoyoshi, T. and Nishimura, A. (2000) 'Molecular cloning of the isoamyl alcohol oxidase-encoding gene (mreA) from *Aspergillus oryzae*', *Journal of Bioscience and Bioengineering*, 89(6), 522-527.
- Yang, L. J., Ruan, C. M. and Li, Y. B. (2001) 'Rapid detection of *Salmonella typhimurium* in food samples using a bienzyme electrochemical biosensor with flow injection', *Journal of Rapid Methods and Automation in Microbiology*, 9(4), 229-240.
- Zeza, F., Pascale, M., Mule, G. and Visconti, A. (2006) 'Detection of *Fusarium culmorum* in wheat by a surface plasmon resonance-based DNA sensor', *Journal of Microbiological Methods*, 66(3), 529-537.
- Zhou, T., Reeleder, R. D. and Sparace, S. A. (1991) 'Interactions between *Sclerotinia sclerotiorum* and *Epicoccum purpurascens*', *Canadian Journal of Botany-Revue Canadienne De Botanique*, 69(11), 2503-2510.
- Zhu, W., Wei, W., Fu, Y., Cheng, J., Xie, J., Li, G., Yi, X., Kang, Z., Dickman, M. B. and Jiang, D. (2013) 'A Secretory Protein of Necrotrophic Fungus *Sclerotinia sclerotiorum* That Suppresses Host Resistance', *Plos One*, 8(1).

Appendices

Appendix 1: The 432 genes which make up the refined *S. sclerotiorum* secretome.

Gene no.	Broad ID	Length	numcs	%C	WoLFPSORT	Annotation	PFAM/ IPR no.
1	SS1G_00040	385	8	2.08	extr=26	pectin lyase a precursor	544
2	SS1G_00044	341	12	3.52	extr=26	ribonuclease t2	445
3	SS1G_00173	362	8	2.21	extr=23	gas1-like protein	IPR021476
4	SS1G_00233	639	24	3.76	extr=24	autophagy related lipase	8702
5	SS1G_00238	312	1	0.32	extr=27	pectate lyase a	544
6	SS1G_00263	135	4	2.96	extr=21	predicted protein	-
7	SS1G_00265	597	38	6.37	extr=26	CEF 4 protein	1522
8	SS1G_00271	603	5	0.83	extr=26	glutamyl-trna amidotransferase	1425
9	SS1G_00332	369	4	1.08	extr=27	CEF 8 protein	1095
10	SS1G_00423	659	14	2.12	extr=23	ser thr protein phosphatase family protein	IPR004843
11	SS1G_00458	371	5	1.35	extr=26	endo-beta- precursor -glucanase	150
12	SS1G_00468	331	1	0.3	extr=26	CEF 8 protein	1095
13	SS1G_00501	228	2	0.88	extr=27	GHF 12 protein	1670
14	SS1G_00505	696	9	1.29	extr=26	alpha- -	7971
15	SS1G_00513	293	5	1.71	extr=25	predicted protein	-
16	SS1G_00514	252	2	0.79	extr=26	GHF 26 protein	IPR013781; IPR017853; IPR022790
17	SS1G_00534	91	8	8.79	extr=20	predicted protein	-
18	SS1G_00564	283	12	4.24	extr=27	predicted protein	-
19	SS1G_00604	168	1	0.6	extr=20	urease accessory protein	IPR002639
20	SS1G_00624	462	4	0.87	extr=25	aspartic-type endopeptidase	26
21	SS1G_00642	545	34	6.24	extr=26	chitin binding protein	1522
22	SS1G_00730	606	4	0.66	extr=25	gmc oxidoreductase	73,205,199
23	SS1G_00746	420	8	1.9	extr=26	endo- -beta-mannosidase	15,000,734
24	SS1G_00768	104	4	3.85	extr=25	predicted protein	-
25	SS1G_00772	554	27	4.87	extr=26	domain protein	IPR002482
26	SS1G_00773	1690	57	3.37	extr=23	class v	704
27	SS1G_00849	134	4	2.99	extr=27	predicted protein	-
28	SS1G_00877	527	4	0.76	extr=27	lipase 4	135
29	SS1G_00891	394	12	3.05	extr=26	GHF 5 protein	15,000,734
30	SS1G_00892	402	9	2.24	extr=26	GHF 6 protein	73,401,341
31	SS1G_00974	561	10	1.78	extr=24	extracellular dihydrogeodin oxidase	3,940,773,10 7,732
32	SS1G_00978	495	24	4.85	extr=22	wsc domain protein	182,209,362
33	SS1G_01003	89	8	8.99	extr=25	predicted protein	-
34	SS1G_01005	887	8	0.9	extr=20	GHF 31 protein	1055
35	SS1G_01009	355	9	2.54	extr=27	polygalacturonase 2	295
36	SS1G_01081	699	1	0.14	extr=26	thermophilum	19,906,628
37	SS1G_01083	976	9	0.92	extr=26	GHF 31 protein	1055
38	SS1G_01086	135	2	1.48	extr=25	predicted protein	-
39	SS1G_01107	166	8	4.82	extr=27	predicted protein	-
40	SS1G_01116	532	11	2.07	extr=27	isoamyl alcohol oxidase	1565
41	SS1G_01226	144	10	6.94	extr=27	predicted protein	-
42	SS1G_01235	166	4	2.41	extr=23	predicted protein	-
43	SS1G_01262	390	3	0.77	extr=24	serine-rich protein	IPR013781; IPR017853; IPR024655
44	SS1G_01325	30	1	3.33	extr=23	predicted protein	-
45	SS1G_01373	228	5	2.19	extr=26	carbohydrate-binding module family 1 protein	734
46	SS1G_01378	487	22	4.52	extr=25	wsc domain protein	182,209,362
47	SS1G_01384	522	0	0	extr=18	predicted protein	-
48	SS1G_01389	251	5	1.99	extr=27	polysaccharide lyase family 7 protein	8787
49	SS1G_01426	218	12	5.5	extr=26	predicted protein	-
50	SS1G_01428	395	25	6.33	extr=25	pan domain containing protein	IPR003014
51	SS1G_01472	560	5	0.89	extr=21	lipase 2	135
52	SS1G_01576	581	2	0.34	extr=26	tyrosinase protein	264
53	SS1G_01587	734	58	7.9	extr=25	predicted protein	-
54	SS1G_01662	578	6	1.04	extr=26	GHF 1 protein	232

55	SS1G_01749	401	15	3.74	extr=20	predicted protein	-
56	SS1G_01776	427	8	1.87	extr=25	GHF 13 protein	12,809,260
57	SS1G_01811	454	3	0.66	extr=25	gmc oxidoreductase	73,205,199
58	SS1G_01828	307	18	5.86	extr=26	GHF 45 protein	73,402,015
59	SS1G_01838	252	4	1.59	extr=25	GHF 61 protein	3443
60	SS1G_01867	102	6	5.88	extr=23	predicted protein	-
61	SS1G_01966	210	6	2.86	extr=18	predicted protein	-
62	SS1G_02003	306	18	5.88	extr=27	GHF 25 protein	-
63	SS1G_02014	408	10	2.45	extr=27	predicted protein	-
64	SS1G_02022	825	10	1.21	extr=21	alpha- -mannosidase family	7971
65	SS1G_02025	232	8	3.45	extr=23	predicted protein	-
66	SS1G_02038	233	2	0.86	extr=26	aspergillopepsin-2 heavy chain (secreted protein)	1828
67	SS1G_02068	146	8	5.48	extr=26	predicted protein	-
68	SS1G_02119	567	8	1.41	extr=26	fad binding domain protein	156,508,031
69	SS1G_02250	224	0	0	extr=27	predicted protein	-
70	SS1G_02334	487	20	4.11	extr=26	GHF 7 protein	73,400,840
71	SS1G_02345	124	7	5.65	extr=27	predicted protein	-
72	SS1G_02347	372	4	1.08	extr=23	alpha- -glucanase mutanase	3659
73	SS1G_02369	333	6	1.8	extr=27	xyloglucan-specific endo-beta- -glucanase a	1670
74	SS1G_02399	522	10	1.92	extr=26	rhamnogalacturonase b	295
75	SS1G_02495	557	5	0.9	extr=22	wsc domain containing protein	141
76	SS1G_02522	265	27	10.19	extr=23	predicted protein	-
77	SS1G_02553	270	7	2.59	extr=26	GHF 28 protein	295
78	SS1G_02600	391	1	0.26	extr=18	predicted protein	-
79	SS1G_02612	521	3	0.58	extr=27	GHF 79 protein	-
80	SS1G_02620	465	5	1.08	extr=25	GHF 79 protein	-
81	SS1G_02655	341	2	0.59	extr=21	heme steroid binding protein	173
82	SS1G_02690	101	0	0	extr=21	predicted protein	-
83	SS1G_02703	384	7	1.82	extr=21	serum paraoxonase arylesterase	-
84	SS1G_02708	290	3	1.03	extr=27	CEF 16 protein	IPR001087; IPR013831
85	SS1G_02714	381	1	0.26	extr=27	predicted protein	-
86	SS1G_02781	990	6	0.61	extr=25	GHF 35 protein	130,110,435
87	SS1G_02790	508	8	1.57	extr=24	3-phytase a	328
88	SS1G_02800	57	6	10.53	extr=20	predicted protein	-
89	SS1G_02812	581	8	1.38	extr=23	predicted protein	-
90	SS1G_02828	187	4	2.14	extr=21	predicted protein	-
91	SS1G_02857	659	9	1.37	extr=24	protease s8 tripeptidyl peptidase	9286
92	SS1G_03029	498	5	1	extr=27	fad-	1565
93	SS1G_03041	227	4	1.76	extr=26	GHF 61 protein	3443
94	SS1G_03080	226	3	1.33	extr=25	necrosis and ethylene inducing peptide 1 precursor	5630
95	SS1G_03084	170	2	1.18	extr=25	predicted protein	-
96	SS1G_03146	174	3	1.72	extr=21	predicted protein	-
97	SS1G_03160	541	18	3.33	extr=24	autophagy related lipase	1764
98	SS1G_03181	385	2	0.52	extr=26	aspartic endopeptidase pep1	26
99	SS1G_03214	510	11	2.16	extr=25	predicted protein	IPR003014
100	SS1G_03221	965	3	0.31	extr=21	duf1620	7774
101	SS1G_03268	1020	27	2.65	extr=25	predicted protein	-
102	SS1G_03276	229	1	0.44	extr=20	kelch repeat-containing protein	1344
103	SS1G_03286	324	1	0.31	extr=26	pectin methylesterase	1095
104	SS1G_03326	338	4	1.18	extr=25	scp-like extracellular protein	188
105	SS1G_03361	517	7	1.35	extr=25	serine	5577
106	SS1G_03385	529	9	1.7	extr=24	alpha-amylase a type-1 2	12,809,260
107	SS1G_03387	568	6	1.06	extr=25	GHF 5 protein	1,500,073,40 3,442
108	SS1G_03420	305	1	0.33	extr=26	class iii	-
109	SS1G_03518	600	8	1.33	extr=27	protease s8 tripeptidyl peptidase	9286
110	SS1G_03523	156	0	0	extr=25	hydrophobic surface binding protein a	IPR021054
111	SS1G_03537	88	3	3.41	extr=26	predicted protein	-
112	SS1G_03540	414	10	2.42	extr=23	GHF 28 protein	295
113	SS1G_03576	377	5	1.33	extr=21	pepsinogen c protein	26
114	SS1G_03602	599	2	0.33	extr=22	alpha-l-arabinofuranosidase a	6964
115	SS1G_03610	285	2	0.7	extr=24	CEF 16 protein	657
116	SS1G_03611	101	8	7.92	extr=21	predicted protein	IPR008427
117	SS1G_03618	262	6	2.29	extr=26	endo- -beta-xylanase	457
118	SS1G_03629	415	2	0.48	extr=26	aspartyl partial	26
119	SS1G_03647	994	2	0.2	extr=25	beta-galactosidase	130,110,435
120	SS1G_03653	368	9	2.45	extr=23	predicted protein	-

121	SS1G_03656	186	4	2.15	extr=26	secreted protein	9352
122	SS1G_03721	177	3	1.69	extr=19	predicted protein	-
123	SS1G_03744	181	0	0	extr=24	predicted protein	-
124	SS1G_03795	319	10	3.13	extr=26	ribonuclease t2	445
125	SS1G_03803	354	7	1.98	extr=25	extracellular cellulase allergen asp f7-	-
126	SS1G_03897	106	8	7.55	extr=26	predicted protein	-
127	SS1G_03941	533	6	1.13	extr=26	eukaryotic aspartyl protease	26
128	SS1G_04030	520	11	2.12	extr=26	lysophospholipase 1	1735
129	SS1G_04085	284	7	2.46	extr=23	extracellular cellulase allergen asp f7-	3330
130	SS1G_04095	264	7	2.65	extr=27	rhamnogalacturonan acylesterase	657
131	SS1G_04116	432	4	0.93	extr=20	purine nucleoside	6516
132	SS1G_04177	361	8	2.22	extr=26	endopolygalacturonase 5	295
133	SS1G_04196	580	7	1.21	extr=24	multicopper like protein	3,940,773,107,732
134	SS1G_04200	755	3	0.4	extr=25	alpha- -mannosidase family protein	7971
135	SS1G_04207	420	10	2.38	extr=23	polygalacturonase partial	295
136	SS1G_04312	1162	7	0.6	extr=26	predicted protein	-
137	SS1G_04382	185	8	4.32	extr=26	predicted protein	-
138	SS1G_04468	506	2	0.4	extr=25	GHF 47 protein	1532
139	SS1G_04473	738	8	1.08	extr=27	predicted protein	-
140	SS1G_04497	368	5	1.36	extr=24	GHF 16 protein	722
141	SS1G_04519	206	12	5.83	extr=23	predicted protein	-
142	SS1G_04530	629	9	1.43	extr=26	lysophospholipase plb1	1735
143	SS1G_04541	684	5	0.73	extr=24	alpha-l-rhamnosidase	5592
144	SS1G_04552	376	9	2.39	extr=25	extracellular exo-	295
145	SS1G_04588	267	0	0	extr=22	hva22 family tb2 dpl protein	3134
146	SS1G_04592	320	4	1.25	extr=27	CEF 16 protein	IPR001087; IPR013831
147	SS1G_04611	127	4	3.15	extr=21	predicted protein	-
148	SS1G_04618	137	8	5.84	extr=22	predicted protein	-
149	SS1G_04639	367	7	1.91	extr=24	l-sorbose dehydrogenase	IPR011042; IPR012938
150	SS1G_04662	511	8	1.57	extr=27	alpha-galactosidase precursor	A 65,202,065
151	SS1G_04664	257	3	1.17	extr=26	cell surface spherulin 4-like protein	IPR021986
152	SS1G_04725	569	2	0.35	extr=25	tyrosinase	264
153	SS1G_04766	192	4	2.08	extr=24	-like cupin protein	-
154	SS1G_04786	379	14	3.69	extr=26	carbohydrate-binding module family 18 protein	-
155	SS1G_04790	419	5	1.19	extr=22	acid phosphatase	328
156	SS1G_04850	440	7	1.59	extr=25	GHF 76 protein	3663
157	SS1G_04857	122	8	6.56	extr=26	predicted protein	-
158	SS1G_04871	309	2	0.65	extr=25	predicted protein	-
159	SS1G_04881	348	0	0	extr=19	protein	13343
160	SS1G_04885	197	0	0	extr=27	amine flavin-containing superfamily	89,003,486
161	SS1G_04898	791	11	1.39	extr=26	glycosyl hydrolase	1522
162	SS1G_04923	380	12	3.16	extr=25	predicted protein	-
163	SS1G_04934	223	4	1.79	extr=25	cas1 appressorium specific protein	IPR021476
164	SS1G_04945	571	23	4.03	extr=24	GHF 7 protein	840
165	SS1G_04946	501	4	0.8	extr=25	predicted protein	-
166	SS1G_04958	567	6	1.06	extr=25	tripeptidyl-peptidase 1 precursor	9286
167	SS1G_05013	300	5	1.67	extr=23	predicted protein	-
168	SS1G_05073	274	6	2.19	extr=26	hypothetical protein SS1G_05073	-
169	SS1G_05103	83	6	7.23	extr=22	predicted protein	-
170	SS1G_05192	870	5	0.57	extr=26	glycosyl hydrolase family 65 protein	3632
171	SS1G_05337	206	4	1.94	extr=27	malate dehydrogenase protein	IPR021851
172	SS1G_05368	783	7	0.89	extr=25	GHF 3 protein	93,301,915
173	SS1G_05434	389	2	0.51	extr=25	gds1-like lipase acylhydrolase	657
174	SS1G_05449	544	6	1.1	extr=22	carboxypeptidase cpds	450
175	SS1G_05454	1742	63	3.62	extr=21	glycosyl hydrolases family 18 protein	18,700,704
176	SS1G_05493	558	10	1.79	extr=27	tannase subunit	7519
177	SS1G_05494	1138	26	2.28	extr=27	wsc domain-containing protein	18,220,441,506,933
178	SS1G_05569	144	3	2.08	extr=26	predicted protein	-

179	SS1G_05609	314	2	0.64	extr=22	enoyl- hydratase isomerase	378
180	SS1G_05612	450	4	0.89	extr=27	prolyl aminopeptidase (secreted protein)	12697
181	SS1G_05677	520	1	0.19	extr=25	gmc oxidoreductase	73,205,199
182	SS1G_05775	396	5	1.26	extr=25	GHF 5 protein	150
183	SS1G_05784	557	14	2.51	extr=27	glucan endo- -alpha-glucosidase agn1	3659
184	SS1G_05794	311	0	0	extr=25	six-bladed beta-propeller -like protein	-
185	SS1G_05827	160	2	1.25	extr=24	predicted protein	-
186	SS1G_05832	436	11	2.52	extr=26	GHF 28 protein	295
187	SS1G_05917	336	11	3.27	extr=26	predicted protein	-
188	SS1G_05925	414	5	1.21	extr=27	aromatic peroxygenase	1328
189	SS1G_05996	253	3	1.19	extr=20	carbonic anhydrase	194
190	SS1G_06009	395	4	1.01	extr=22	predicted protein	-
191	SS1G_06037	402	6	1.49	extr=27	exo-beta- -glucanase	150
192	SS1G_06068	73	10	13.7	extr=27	predicted protein	-
193	SS1G_06119	176	0	0	extr=23	hypothetical protein SS1G_06119	13577
194	SS1G_06230	162	0	0	extr=27	cupin family protein	6172
195	SS1G_06235	447	2	0.45	extr=24	endo-rhamnogalacturonase f	295
196	SS1G_06264	800	8	1	extr=26	cellobiose dehydrogenase	73,205,199
197	SS1G_06333	488	8	1.64	extr=27	histidine acid phosphatase	328
198	SS1G_06349	338	3	0.89	extr=26	nucleoside hydrolase	1156
199	SS1G_06365	550	6	1.09	extr=25	extracellular dihydrogeodin oxidase laccase	3,940,773,10 7,732
200	SS1G_06412	237	7	2.95	extr=18	predicted protein	
201	SS1G_06426	863	1	0.12	extr=27	predicted protein	
202	SS1G_06534	252	6	2.38	extr=26	a chain fusarium oxysporum trypsin at atomic resolution	89
203	SS1G_06653	372	0	0	extr=24	GHF 65	
204	SS1G_06695	424	5	1.18	extr=22	fad dependent oxidoreductase	1266
205	SS1G_06742	232	4	1.72	extr=25	scp-like extracellular protein	188
206	SS1G_06747	134	1	0.75	extr=23	predicted protein	
207	SS1G_06817	281	1	0.36	extr=23	predicted protein	
208	SS1G_06890	262	0	0	extr=23	predicted protein	
209	SS1G_06942	507	6	1.18	extr=23	cupredoxin (secreted protein)	-
210	SS1G_07015	248	4	1.61	extr=26	malate dehydrogenase	IPR021851
211	SS1G_07022	434	8	1.84	extr=25	histidine acid phosphatase	328
212	SS1G_07027	155	6	3.87	extr=26	predicted protein	
213	SS1G_07039	414	10	2.42	extr=26	rhamnogalacturonase b	295
214	SS1G_07093	383	4	1.04	extr=26	alpha beta-hydrolase	12697
215	SS1G_07162	867	8	0.92	extr=27	beta	93,301,915
216	SS1G_07183	173	4	2.31	extr=25	predicted protein	
217	SS1G_07184	533	2	0.38	extr=26	GHF 32 protein	251
218	SS1G_07224	322	0	0	extr=18	predicted protein	
219	SS1G_07230	63	0	0	extr=25	predicted protein	
220	SS1G_07268	651	9	1.38	extr=18	protease s8 tripeptidyl peptidase	9286
221	SS1G_07393	761	9	1.18	extr=26	GHF 55 protein	12708
222	SS1G_07491	121	7	5.79	extr=25	predicted protein	
223	SS1G_07498	434	0	0	extr=25	glucose-methanol-choline oxidoreductase	73,205,199
224	SS1G_07526	353	3	0.85	extr=26	predicted protein	
225	SS1G_07532	188	2	1.06	extr=27	predicted protein	
226	SS1G_07554	261	5	1.92	extr=24	endo- -beta-xylanase	734
227	SS1G_07571	333	3	0.9	extr=27	predicted protein	
228	SS1G_07579	590	6	1.02	extr=27	isoamyl alcohol	156,508,031
229	SS1G_07613	153	4	2.61	extr=20	phosphatidylglycerol phosphatidylinositol transfer protein	2221
230	SS1G_07639	374	0	0	extr=25	acid phosphatase	4185
231	SS1G_07655	569	9	1.58	extr=26	subtilisin-like protein	9286
232	SS1G_07656	327	4	1.22	extr=26	GHF 61 protein	3443
233	SS1G_07661	182	4	2.2	extr=21	cutinase	1083
234	SS1G_07749	203	0	0	extr=25	GHF 11 protein	457
235	SS1G_07780	206	4	1.94	extr=23	predicted protein	
236	SS1G_07836	234	2	0.85	extr=24	acid protease partial	1828
237	SS1G_07837	263	0	0	extr=27	predicted protein	
238	SS1G_07847	798	11	1.38	extr=21	beta-d-glucoside glucohydrolase	7,340,093,30 1,915
239	SS1G_07863	837	6	0.72	extr=26	cellobiose dehydrogenase	73,205,199
240	SS1G_07928	210	8	3.81	extr=24	transmembrane alpha-helix domain-containing protein	1822
241	SS1G_07942	373	6	1.61	extr=27	polysaccharide lyase family 1	544

						protein	
242	SS1G_08104	280	14	5	extr=26	acetyl xylan esterase	73,401,083
243	SS1G_08110	171	4	2.34	extr=27	predicted protein	
244	SS1G_08128	71	11	15.49	extr=21	predicted protein	5980
245	SS1G_08163	69	8	11.59	extr=22	predicted protein	
246	SS1G_08208	379	4	1.06	extr=27	a chain the 3-d structure of a trichoderma reesei b-mannanase from GHF 5	150
247	SS1G_08229	422	11	2.61	extr=27	GHF 28 protein	295
248	SS1G_08361	563	11	1.95	extr=25	tannase subunit	7519
249	SS1G_08493	417	20	4.8	extr=26	GHF 61 protein	3443
250	SS1G_08528	296	8	2.7	extr=20	major allergen asp f 2-like protein	13933
251	SS1G_08542	445	4	0.9	extr=27	predicted protein	
252	SS1G_08548	328	3	0.91	extr=25	six-bladed beta-propeller -like protein	-
253	SS1G_08566	204	4	1.96	extr=22	predicted protein	
254	SS1G_08621	263	4	1.52	extr=21	nuclease s1	2265
255	SS1G_08634	419	8	1.91	extr=24	extracellular exo-	295
256	SS1G_08644	440	4	0.91	extr=24	lipase 3	3583
257	SS1G_08645	464	3	0.65	extr=27	fad binding domain-containing protein	1565
258	SS1G_08695	398	8	2.01	extr=26	class iii	70,400,734
259	SS1G_08698	393	11	2.8	extr=27	mg2+ transporter protein	IPR000772
260	SS1G_08706	113	4	3.54	extr=26	barwin-like endoglucanase	3330
261	SS1G_08790	195	0	0	extr=22	predicted protein	
262	SS1G_08814	433	1	0.23	extr=23	oxalate decarboxylase	1,900,105,007,883
263	SS1G_08858	337	8	2.37	extr=21	deuterolysin metalloprotease	2102
264	SS1G_08889	719	8	1.11	extr=26	glutaminase	8760
265	SS1G_08892	268	18	6.72	extr=26	predicted protein	
266	SS1G_08894	384	6	1.56	extr=27	alpha beta-hydrolase	12697
267	SS1G_08907	496	11	2.22	extr=27	predicted protein	
268	SS1G_08917	242	1	0.41	extr=20	beta- -glucan boisynthesis protein	5390
269	SS1G_09000	898	14	1.56	extr=25	carbohydrate-binding -like protein	10528
270	SS1G_09020	434	18	4.15	extr=26	-beta-d-glucan cellobiohydrolase b	840
271	SS1G_09050	435	22	5.06	extr=24	predicted protein	
272	SS1G_09060	916	5	0.55	extr=25	subtilisin-like protease	82
273	SS1G_09129	575	11	1.91	extr=22	GHF 1 protein	232
274	SS1G_09130	297	4	1.35	extr=25	-	13668
275	SS1G_09143	366	0	0	extr=19	amidohydrolase 2	4909
276	SS1G_09169	859	11	1.28	extr=25	predicted protein	
277	SS1G_09175	108	10	9.26	extr=22	predicted protein	
278	SS1G_09193	219	1	0.46	extr=19	isochorismatase family	857
279	SS1G_09196	114	0	0	extr=20	predicted protein	
280	SS1G_09216	806	11	1.36	extr=27	GHF 55 protein	12708
281	SS1G_09219	342	2	0.58	extr=26	major royal jelly protein	3022
282	SS1G_09225	574	6	1.05	extr=25	tripeptidyl peptidase a	9286
283	SS1G_09232	190	4	2.11	extr=25	predicted protein	
284	SS1G_09248	76	8	10.53	extr=19	hydrophobin	6766
285	SS1G_09250	252	3	1.19	extr=25	iron-sulfur cluster-binding rieske family domain protein	1670
286	SS1G_09251	303	8	2.64	extr=26	GHF 61 protein	73,403,443
287	SS1G_09268	613	6	0.98	extr=26	tripeptidyl-peptidase 1 precursor	9286
288	SS1G_09270	157	1	0.64	extr=27	hydrophobic surface binding protein a protein	IPR021054
289	SS1G_09363	306	8	2.61	extr=22	predicted protein	
290	SS1G_09365	399	5	1.25	extr=27	endo-beta- -	150
291	SS1G_09366	754	4	0.53	extr=20	GHF 3 protein	93,301,915
292	SS1G_09475	534	6	1.12	extr=27	serine carboxypeptidase	450
293	SS1G_09495	381	1	0.26	extr=24	paf acetylhydrolase family protein	3403
294	SS1G_09693	133	4	3.01	extr=27	predicted protein	
295	SS1G_09782	267	4	1.5	extr=25	nuclease s1	2265
296	SS1G_09841	206	4	1.94	extr=26	predicted protein	IPR018620
297	SS1G_09844	189	4	2.12	extr=27	predicted protein	
298	SS1G_09861	588	14	2.38	extr=22	GHF 71 protein	
299	SS1G_09866	403	5	1.24	extr=25	GHF 5 protein	150
300	SS1G_09882	136	1	0.74	extr=23	predicted protein	
301	SS1G_09909	713	2	0.28	extr=25	oligopeptidase family protein	32,605,448
302	SS1G_09959	447	10	2.24	extr=26	histidine acid phosphatase	328

303	SS1G_09965	612	15	2.45	extr=24	sphingomyelin phosphodiesterase	IPR004843; IPR008139; IPR011160;
304	SS1G_09982	203	4	1.97	extr=21	clock-controlled protein 6	-
305	SS1G_10038	562	7	1.25	extr=27	GHF 20 protein	728
306	SS1G_10071	361	6	1.66	extr=26	pectin lyase	544
307	SS1G_10078	518	8	1.54	extr=22	oxidase-like protein	1328
308	SS1G_10082	107	2	1.87	extr=19	predicted protein	
309	SS1G_10092	207	0	0	extr=26	endo- -beta-xylanase	457
310	SS1G_10096	119	4	3.36	extr=24	epl1 protein	7249
311	SS1G_10104	203	4	1.97	extr=20	predicted protein	
312	SS1G_10165	311	3	0.96	extr=27	CEF 8 protein	1095
313	SS1G_10167	360	8	2.22	extr=27	polygalacturonase 1	295
314	SS1G_10172	401	4	1	extr=25	outer membrane autotransporter protein	13449
315	SS1G_10266	414	5	1.21	extr=27	predicted protein	
316	SS1G_10452	174	8	4.6	extr=26	predicted protein	
317	SS1G_10482	322	4	1.24	extr=24	lysophospholipase a	IPR001087; IPR013831;
318	SS1G_10581	82	2	2.44	extr=19	predicted protein	
319	SS1G_10683	405	4	0.99	extr=27	aldose 1-epimerase	1263
320	SS1G_10698	466	16	3.43	extr=27	polygalacturonase 3	295
321	SS1G_10796	482	1	0.21	extr=27	oxalate decarboxylase	19,007,883
322	SS1G_10842	965	5	0.52	extr=26	predicted protein	IPR001944;
323	SS1G_10845	368	5	1.36	extr=24	GHF 12 protein	-
324	SS1G_10867	381	4	1.05	extr=25	glycosyl hydrolase	3663
325	SS1G_10875	516	2	0.39	extr=26	carboxylesterase	135
326	SS1G_10949	600	5	0.83	extr=23	glucose oxidase	73,205,199
327	SS1G_10956	96	5	5.21	extr=25	predicted protein	
328	SS1G_11057	349	8	2.29	extr=26	polygalacturonase partial	295
329	SS1G_11065	190	5	2.63	extr=18	predicted protein	
330	SS1G_11108	355	4	1.13	extr=24	predicted protein	
331	SS1G_11120	343	9	2.62	extr=24	predicted protein	
332	SS1G_11126	397	5	1.26	extr=27	major royal jelly protein	3022
333	SS1G_11189	403	4	0.99	extr=27	carboxypeptidase a2	246
334	SS1G_11202	648	6	0.93	extr=20	predicted protein	
335	SS1G_11223	258	2	0.78	extr=25	predicted protein	
336	SS1G_11239	613	16	2.61	extr=26	wsc domain containing protein	182,209,362
337	SS1G_11366	460	5	1.09	extr=19	vacuolar protease a	26
338	SS1G_11382	655	11	1.68	extr=25	carboxypeptidase s1	450
339	SS1G_11412	352	1	0.28	extr=26	quercetin -dioxygenase	IPR011051; IPR013096; IPR014710
340	SS1G_11468	232	2	0.86	extr=23	cas1 appressorium specific protein	IPR021476
341	SS1G_11499	197	2	1.02	extr=19	GHF 16 protein	IPR000757; IPR008985; IPR013320;
342	SS1G_11535	775	7	0.9	extr=26	GHF 95 protein	-
343	SS1G_11585	333	2	0.6	extr=26	arabinogalactan endo- -beta-galactosidase	7745
344	SS1G_11673	108	7	6.48	extr=18	predicted protein	-
345	SS1G_11693	188	4	2.13	extr=18	predicted protein	
346	SS1G_11700	414	1	0.24	extr=24	GHF 18 protein	704
347	SS1G_11703	101	0	0	extr=21	gpi transamidase component gpi16	4113
348	SS1G_11706	59	5	8.47	extr=26	predicted protein	
349	SS1G_11765	521	4	0.77	extr=23	alpha- -glucanase	3659
350	SS1G_11853	547	5	0.91	extr=26	carboxylesterase family protein	13,507,859
351	SS1G_11912	224	5	2.23	extr=26	necrosis and ethylene inducing peptide 2 precursor	5630
352	SS1G_11922	302	4	1.32	extr=26	extracellular endo- -alpha-l-	4616
353	SS1G_11927	637	10	1.57	extr=27	carbohydrate-binding module family 20 protein	3,940,773,10 7,732
354	SS1G_11930	508	6	1.18	extr=26	para-nitrobenzyl esterase	135
355	SS1G_11988	659	5	0.76	extr=24	choline dehydrogenase	73,205,199
356	SS1G_11992	238	4	1.68	extr=26	rhamnogalacturonan acetyltransferase	657
357	SS1G_12017	515	14	2.72	extr=26	beta- -glucanosyltransferase	319,807,983
358	SS1G_12024	454	5	1.1	extr=23	cell wall glucanase	IPR000490; IPR013781; IPR017853;
359	SS1G_12052	226	11	4.87	extr=23	predicted protein	
360	SS1G_12057	434	9	2.07	extr=26	extracellular exo-	295
361	SS1G_12059	297	5	1.68	extr=25	endoglucanase ii	3443

362	SS1G_12083	1130	3	0.27	extr=26	GHF 115 protein	
363	SS1G_12191	336	6	1.79	extr=27	endo- -beta-	331
364	SS1G_12198	593	5	0.84	extr=24	gmc oxidoreductase	73,205,199
365	SS1G_12200	554	7	1.26	extr=26	glucooligosaccharide oxidase	156,508,031
366	SS1G_12210	609	9	1.48	extr=23	-	9286
367	SS1G_12262	338	3	0.89	extr=26	predicted protein	
368	SS1G_12263	471	9	1.91	extr=27	protein tos1 precursor	1,028,710,290
369	SS1G_12287	257	15	5.84	extr=19	predicted protein	
370	SS1G_12320	560	6	1.07	extr=18	GHF 16 protein	IPR000757; IPR008985; IPR013320
371	SS1G_12336	275	7	2.55	extr=22	chitin binding	IPR004302
372	SS1G_12361	166	4	2.41	extr=27	predicted protein	
373	SS1G_12365	188	4	2.13	extr=18	predicted protein	
374	SS1G_12383	457	8	1.75	extr=24	histidine acid	328
375	SS1G_12413	457	9	1.97	extr=26	carboxypeptidase s1	450
376	SS1G_12499	568	9	1.58	extr=18	carboxypeptidase s1	450
377	SS1G_12500	531	11	2.07	extr=22	carboxypeptidase y	450
378	SS1G_12509	429	24	5.59	extr=23	domain protein	IPR002482; IPR018392;
379	SS1G_12513	342	17	4.97	extr=26	domain-containing protein	IPR018392
380	SS1G_12609	257	1	0.39	extr=20	sterigmatocystin biosynthesis peroxidase stcc protein	1328
381	SS1G_12648	134	8	5.97	extr=26	predicted protein	
382	SS1G_12721	43	2	4.65	extr=24	predicted protein	
383	SS1G_12724	448	6	1.34	extr=26	-	
384	SS1G_12765	447	11	2.46	extr=26	CEF 15 protein	IPR000254
385	SS1G_12907	223	4	1.79	extr=27	cutinase	1083
386	SS1G_12917	374	12	3.21	extr=26	uncharacterized serine-rich protein	1822
387	SS1G_12927	151	3	1.99	extr=21	predicted protein	
388	SS1G_12930	276	5	1.81	extr=25	GHF 17 protein	332
389	SS1G_12937	389	6	1.54	extr=26	glycosyl hydrolase	3663
390	SS1G_12938	537	3	0.56	extr=26	extracellular proline-serine rich protein	##### ##### ##
391	SS1G_12961	78	0	0	extr=18	predicted protein	
392	SS1G_13035	161	0	0	extr=27	predicted protein	
393	SS1G_13036	705	9	1.28	extr=26	multicopper oxidase	3,940,773,107,732
394	SS1G_13115	360	7	1.94	extr=27	predicted protein	
395	SS1G_13126	129	8	6.2	extr=20	predicted protein	
396	SS1G_13199	394	3	0.76	extr=25	extracellular aldonolactonase	10282
397	SS1G_13255	822	6	0.73	extr=27	GHF 3 protein	93,301,915
398	SS1G_13277	327	4	1.22	extr=27	serine-threonine rich	-
399	SS1G_13364	610	3	0.49	extr=25	tyrosinase	264
400	SS1G_13371	203	4	1.97	extr=20	predicted protein	
401	SS1G_13385	501	2	0.4	extr=21	actin patch protein 1	9949
402	SS1G_13386	238	4	1.68	extr=27	cutinase	1083
403	SS1G_13394	167	6	3.59	extr=18	predicted protein	
404	SS1G_13472	537	8	1.49	extr=26	alpha-	12,809,260
405	SS1G_13501	661	3	0.45	extr=25	alpha-l-rhamnosidase	5592
406	SS1G_13589	394	7	1.78	extr=26	plc-like phosphodiesterase protein	-
407	SS1G_13599	401	13	3.24	extr=26	predicted protein	
408	SS1G_13668	177	4	2.26	extr=26	predicted protein	
409	SS1G_13682	754	3	0.4	extr=19	predicted protein	-
410	SS1G_13732	510	36	7.06	extr=24	predicted protein	-
411	SS1G_13736	508	5	0.98	extr=26	protein rds1	13668
412	SS1G_13764	271	3	1.11	extr=23	predicted protein	-
413	SS1G_13809	603	11	1.82	extr=27	glucoamylase p	68,600,723
414	SS1G_13860	317	15	4.73	extr=25	GHF 45 protein	2015
415	SS1G_13881	179	2	1.12	extr=27	chlorogenic acid esterase precursor	135
416	SS1G_13935	512	17	3.32	extr=27	ibr domain-containing protein	5730
417	SS1G_13965	97	2	2.06	extr=25	predicted protein	-
418	SS1G_13982	519	6	1.16	extr=26	triacylglycerol lipase	135
419	SS1G_14007	151	3	1.99	extr=25	predicted protein	-
420	SS1G_14041	207	0	0	extr=25	predicted protein	-
421	SS1G_14133	285	0	0	extr=25	fg-gap repeat	-
422	SS1G_14160	345	5	1.45	extr=26	GHF 61 protein	3443
423	SS1G_14184	224	30	13.39	extr=27	CEF 4 protein	IPR000254; IPR001002; IPR018371

424	SS1G_14237	283	6	2.12	extr=24	gas1-like protein	-
425	SS1G_14289	278	6	2.16	extr=26	CEF 16 protein	734
426	SS1G_14293	573	1	0.17	extr=26	glucose oxidase	73,205,199
427	SS1G_14321	364	3	0.82	extr=26	gpi anchored	775
428	SS1G_14379	188	4	2.13	extr=18	predicted protein	-
429	SS1G_14441	525	7	1.33	extr=27	triacylglycerol lipase	135
430	SS1G_14449	395	10	2.53	extr=26	extracellular exo-	295
431	SS1G_14497	661	7	1.06	extr=24	GHF 76 protein	3663
432	SS1G_14515	45	0	0	extr=20	predicted protein	-

Appendix 2: The 499 genes which make up the refined *B.cinerea* secretome

Gene no.	Refined Secretome	maturelen	% C	numcs	WoLF P-SORT	PFAM
1	BC1T_00003	302	1.32	4	extr=26	-
2	BC1T_00109	265	0.38	1	extr=26	12138
3	BC1T_00198	495	1.01	5	extr=23	06824
4	BC1T_00226	414	0.48	2	extr=25	-
5	BC1T_00230	361	1.66	6	extr=27	00295
6	BC1T_00233	568	2.29	13	extr=23	-
7	BC1T_00240	640	1.41	9	extr=23	00295,04063
8	BC1T_00245	770	0.39	3	extr=27	07971
9	BC1T_00246	162	1.85	3	extr=19	-
10	BC1T_00279	367	0.82	3	extr=26	-
11	BC1T_00308	309	2.27	7	extr=24	00657
12	BC1T_00376	502	0.6	3	extr=27	01735
13	BC1T_00384	489	1.02	5	extr=24	00450
14	BC1T_00409	371	1.62	6	extr=25	00722
15	BC1T_00448	699	1.14	8	extr=27	-
16	BC1T_00455	510	0.39	2	extr=25	01532
17	BC1T_00514	163	2.45	4	extr=25	-
18	BC1T_00529	211	3.32	7	extr=26	-
19	BC1T_00545	423	0.95	4	extr=27	00026
20	BC1T_00572	253	1.19	3	extr=25	-
21	BC1T_00576	331	0.91	3	extr=26	00331
22	BC1T_00594	230	0.87	2	extr=26	01670
23	BC1T_00617	329	0.61	2	extr=27	01095
24	BC1T_00639	522	1.92	10	extr=25	07519
25	BC1T_00642	406	1.23	5	extr=27	00150
26	BC1T_00689	659	2.12	14	extr=26	-
27	BC1T_00750	497	1.01	5	extr=27	00135,07859
28	BC1T_00837	152	1.32	2	extr=19	-
29	BC1T_00878	489	0.82	4	extr=26	01425
30	BC1T_00896	135	2.96	4	extr=23	-
31	BC1T_00912	312	0.32	1	extr=25	00544
32	BC1T_00922	126	3.17	4	extr=24	03443
33	BC1T_00958	200	3.5	7	extr=18	-
34	BC1T_00960	167	2.4	4	extr=22	-
35	BC1T_00977	157	0	0	extr=26	12296
36	BC1T_00978	568	1.06	6	extr=22	09286
37	BC1T_00991	342	0.88	3	extr=20	00248
38	BC1T_01000	335	2.99	10	extr=25	00264
39	BC1T_01008	376	1.06	4	extr=25	01670
40	BC1T_01012	80	10	8	extr=20	06766
41	BC1T_01015	122	3.28	4	extr=26	-
42	BC1T_01016	183	2.19	4	extr=25	-
43	BC1T_01026	575	1.04	6	extr=26	09286
44	BC1T_01031	342	0.58	2	extr=26	03022
45	BC1T_01033	788	1.27	10	extr=26	12708
46	BC1T_01059	236	8.47	20	extr=25	-
47	BC1T_01064	850	1.29	11	extr=23	-
48	BC1T_01073	706	1.42	10	extr=22	09286
49	BC1T_01077	33	0	0	extr=21	-
50	BC1T_01080	225	0.44	1	extr=18	12138
51	BC1T_01152	461	1.08	5	extr=26	-

52	BC1T_01204	800	4	32	extr=27	00187,07250,09118
53	BC1T_01234	356	1.4	5	extr=25	00295
54	BC1T_01286	225	0.89	2	extr=26	00450
55	BC1T_01367	468	2.14	10	extr=22	12697
56	BC1T_01393	170	0	0	extr=26	13577
57	BC1T_01397	212	0.94	2	extr=24	00026
58	BC1T_01444	70	14.3	10	extr=25	-
59	BC1T_01472	305	1.31	4	extr=22	-
60	BC1T_01612	232	3.02	7	extr=26	-
61	BC1T_01615	567	1.76	10	extr=26	07519
62	BC1T_01617	453	2.21	10	extr=27	00295
63	BC1T_01628	423	0.95	4	extr=20	01328
64	BC1T_01630	656	0.91	6	extr=22	00732,05199
65	BC1T_01674	278	2.52	7	extr=24	03067
66	BC1T_01719	807	0.99	8	extr=26	00732,05199
67	BC1T_01778	470	2.34	11	extr=27	00331,00734
68	BC1T_01789	594	0.84	5	extr=26	00732,05199
69	BC1T_01794	421	0.95	4	extr=26	00026
70	BC1T_01803	632	1.42	9	extr=23	09286
71	BC1T_01872	328	1.22	4	extr=25	-
72	BC1T_01874	475	1.89	9	extr=22	10287,10290
73	BC1T_01886	61	3.28	2	extr=18	-
74	BC1T_01896	316	5.06	16	extr=23	-
75	BC1T_01923	458	0.44	2	extr=27	00295
76	BC1T_02003	353	1.98	7	extr=24	00295
77	BC1T_02011	310	1.29	4	extr=26	-
78	BC1T_02012	247	2.43	6	extr=25	-
79	BC1T_02016	504	0.79	4	extr=24	00135
80	BC1T_02021	606	0.66	4	extr=25	00732,05199
81	BC1T_02036	332	1.2	4	extr=26	00150
82	BC1T_02060	143	4.2	6	extr=25	-
83	BC1T_02163	119	3.36	4	extr=26	07249
84	BC1T_02314	487	1.23	6	extr=25	00328
85	BC1T_02333	379	4.22	16	extr=26	00686
86	BC1T_02364	759	0.53	4	extr=21	00933,01915,14310
87	BC1T_02365	400	1.25	5	extr=27	-
88	BC1T_02388	203	3.94	8	extr=23	-
89	BC1T_02410	989	0.61	6	extr=26	01301,10435,13363,13364
90	BC1T_02480	41	0	0	extr=19	-
91	BC1T_02486	516	1.94	10	extr=26	07519
92	BC1T_02487	504	0.4	2	extr=27	00135
93	BC1T_02492	386	0.78	3	extr=23	11790
94	BC1T_02541	252	1.59	4	extr=20	03443
95	BC1T_02591	431	1.62	7	extr=22	02065
96	BC1T_02623	402	2.24	9	extr=27	00128,09260
97	BC1T_02643	122	6.56	8	extr=25	-
98	BC1T_02676	102	7.84	8	extr=27	-
99	BC1T_02701	117	8.55	10	extr=22	-
100	BC1T_02702	328	0.3	1	extr=25	-
101	BC1T_02714	321	5.61	18	extr=27	-
102	BC1T_02731	737	1.22	9	extr=27	12708
103	BC1T_02738	594	2.36	14	extr=22	03659
104	BC1T_02740	403	1.24	5	extr=22	-
105	BC1T_02755	224	0.89	2	extr=27	-
106	BC1T_02790	232	0.86	2	extr=22	01828
107	BC1T_02834	151	5.3	8	extr=19	-
108	BC1T_02944	569	1.58	9	extr=26	09286
109	BC1T_02965	419	0.24	1	extr=18	04185
110	BC1T_02986	149	2.68	4	extr=26	02221
111	BC1T_03038	238	2.1	5	extr=21	00734
112	BC1T_03045	116	0.86	1	extr=26	02089
113	BC1T_03065	41	0	0	extr=24	-
114	BC1T_03070	372	0.54	2	extr=27	00026
115	BC1T_03086	562	1.96	11	extr=22	07519
116	BC1T_03097	480	1.04	5	extr=26	00135
117	BC1T_03179	764	0.79	6	extr=24	00933,01915,14310

118	BCIT_03205	205	0	0	extr=24	-
119	BCIT_03220	910	0.77	7	extr=24	00732,05199
120	BCIT_03298	177	0.56	1	extr=25	-
121	BCIT_03406	256	0.39	1	extr=25	01328
122	BCIT_03412	28	0	0	extr=19	-
123	BCIT_03464	422	2.61	11	extr=27	00295
124	BCIT_03557	186	2.15	4	extr=26	07510
125	BCIT_03560	396	2.27	9	extr=25	-
126	BCIT_03567	994	0.2	2	extr=25	01301,10435,13363,13364
127	BCIT_03579	413	0.48	2	extr=26	00026
128	BCIT_03590	262	2.29	6	extr=26	00457,00734
129	BCIT_03591	63	9.52	6	extr=19	-
130	BCIT_03596	123	0.81	1	extr=23	-
131	BCIT_03619	425	2.35	10	extr=26	00295
132	BCIT_03710	553	1.63	9	extr=25	00450
133	BCIT_03711	531	2.07	11	extr=23	00450,05388
134	BCIT_03813	482	0.21	1	extr=24	00190,07883
135	BCIT_03849	284	2.46	7	extr=26	-
136	BCIT_03859	351	1.14	4	extr=24	01301
137	BCIT_03881	383	1.04	4	extr=23	03663
138	BCIT_03886	516	0.39	2	extr=26	00135
139	BCIT_03951	809	8.03	65	extr=25	-
140	BCIT_03976	546	1.47	8	extr=25	08386
141	BCIT_03977	166	2.41	4	extr=20	-
142	BCIT_04043	593	0.34	2	extr=25	00732,05199
143	BCIT_04089	235	0.43	1	extr=25	-
144	BCIT_04092	511	0.2	1	extr=26	00264
145	BCIT_04114	176	1.14	2	extr=18	-
146	BCIT_04233	389	1.03	4	extr=26	01263
147	BCIT_04246	412	3.64	15	extr=27	00295
148	BCIT_04267	189	0.53	1	extr=24	-
149	BCIT_04280	41	7.32	3	extr=21	-
150	BCIT_04347	174	3.45	6	extr=20	-
151	BCIT_04368	218	0	0	extr=27	-
152	BCIT_04506	84	15.5	13	extr=27	-
153	BCIT_04515	364	1.65	6	extr=25	-
154	BCIT_04521	143	5.59	8	extr=25	-
155	BCIT_04660	132	6.06	8	extr=26	-
156	BCIT_04810	250	2.4	6	extr=26	00089
157	BCIT_04919	368	0.27	1	extr=24	03403
158	BCIT_04935	265	10.2	27	extr=27	-
159	BCIT_04947	295	1.02	3	extr=23	03663
160	BCIT_04955	518	1.16	6	extr=24	00141
161	BCIT_04994	480	1.67	8	extr=26	05270,09206
162	BCIT_05010	551	1.09	6	extr=26	01412
163	BCIT_05033	217	1.38	3	extr=26	14021
164	BCIT_05056	191	1.05	2	extr=27	-
165	BCIT_05076	353	0.85	3	extr=25	-
166	BCIT_05134	128	6.25	8	extr=25	-
167	BCIT_05199	188	2.13	4	extr=20	01083
168	BCIT_05442	306	1.31	4	extr=27	-
169	BCIT_05455	343	2.04	7	extr=26	00704
170	BCIT_05478	180	1.11	2	extr=18	-
171	BCIT_05479	112	1.79	2	extr=20	-
172	BCIT_05488	392	0.26	1	extr=24	05426
173	BCIT_05517	549	1.64	9	extr=27	01565,08031
174	BCIT_05539	720	3.19	23	extr=26	03659
175	BCIT_05542	277	2.17	6	extr=27	-
176	BCIT_05576	248	2.82	7	extr=26	11790
177	BCIT_05590	71	0	0	extr=18	-
178	BCIT_05646	163	2.45	4	extr=25	-
179	BCIT_05658	114	0	0	extr=25	-
180	BCIT_05765	758	1.32	10	extr=22	09286
181	BCIT_05866	87	6.9	6	extr=24	-
182	BCIT_05885	357	1.96	7	extr=26	-
183	BCIT_05925	301	1.99	6	extr=24	-

184	BCIT_05961	258	2.33	6	extr=23	00295
185	BCIT_05976	142	1.41	2	extr=24	-
186	BCIT_05986	419	0.48	2	extr=23	01565
187	BCIT_06005	40	2.5	1	extr=21	-
188	BCIT_06019	121	5.79	7	extr=22	-
189	BCIT_06035	499	4.41	22	extr=26	00734,00840
190	BCIT_06114	334	2.4	8	extr=24	11327
191	BCIT_06211	119	3.36	4	extr=25	-
192	BCIT_06237	383	1.04	4	extr=24	01425
193	BCIT_06274	174	1.72	3	extr=27	01083
194	BCIT_06310	226	1.33	3	extr=24	05630
195	BCIT_06314	160	1.25	2	extr=24	-
196	BCIT_06328	625	0.48	3	extr=27	05592
197	BCIT_06334	499	1.2	6	extr=26	01565
198	BCIT_06369	239	1.67	4	extr=27	01083
199	BCIT_06380	79	0	0	extr=22	00795
200	BCIT_06463	531	1.51	8	extr=25	00128,09260
201	BCIT_06509	466	6.01	28	extr=25	01522
202	BCIT_06546	440	2.05	9	extr=25	02065
203	BCIT_06727	153	0	0	extr=18	12296
204	BCIT_06769	525	2.29	12	extr=25	-
205	BCIT_06815	912	2.96	27	extr=25	-
206	BCIT_06836	505	0.59	3	extr=24	00082,05922
207	BCIT_06840	217	0.46	1	extr=27	01095
208	BCIT_06893	493	1.22	6	extr=19	00067
209	BCIT_07052	217	5.53	12	extr=23	03211
210	BCIT_07058	473	1.69	8	extr=25	03659
211	BCIT_07073	204	1.96	4	extr=26	11937
212	BCIT_07101	835	0.6	5	extr=27	05592
213	BCIT_07110	784	0.89	7	extr=24	00933,01915,14310
214	BCIT_07149	544	1.1	6	extr=25	00450
215	BCIT_07160	273	2.2	6	extr=25	-
216	BCIT_07173	232	1.72	4	extr=26	-
217	BCIT_07175	83	7.23	6	extr=27	-
218	BCIT_07215	582	1.2	7	extr=25	00728
219	BCIT_07220	541	1.48	8	extr=25	10528
220	BCIT_07275	735	0.95	7	extr=23	-
221	BCIT_07314	266	0.75	2	extr=19	-
222	BCIT_07319	760	1.18	9	extr=26	12708
223	BCIT_07326	326	0	0	extr=21	-
224	BCIT_07477	40	2.5	1	extr=19	-
225	BCIT_07482	468	0.64	3	extr=23	01565
226	BCIT_07483	433	0.92	4	extr=27	03583
227	BCIT_07521	386	0.52	2	extr=26	00026
228	BCIT_07527	367	1.63	6	extr=27	00544
229	BCIT_07558	353	0.28	1	extr=18	04488
230	BCIT_07577	61	1.64	1	extr=23	-
231	BCIT_07608	289	0.69	2	extr=25	13668
232	BCIT_07611	73	11	8	extr=20	-
233	BCIT_07620	556	0.54	3	extr=20	01019
234	BCIT_07622	759	0.92	7	extr=26	00933,01915,14310
235	BCIT_07637	539	1.11	6	extr=27	00135
236	BCIT_07653	307	1.63	5	extr=24	03443
237	BCIT_07658	356	1.12	4	extr=25	03443
238	BCIT_07770	492	1.22	6	extr=22	02225,04389
239	BCIT_07778	457	1.53	7	extr=25	-
240	BCIT_07794	822	1.09	9	extr=26	00732,05199
241	BCIT_07820	528	1.7	9	extr=24	00128,09260
242	BCIT_07822	580	0.34	2	extr=25	00150,03442
243	BCIT_07854	281	0	0	extr=25	-
244	BCIT_07899	218	1.83	4	extr=26	01083
245	BCIT_07945	299	2.68	8	extr=27	00722
246	BCIT_07949	211	5.69	12	extr=26	-
247	BCIT_07950	312	9.29	29	extr=23	-
248	BCIT_07951	395	6.08	24	extr=24	-
249	BCIT_07974	289	1.38	4	extr=27	00135,07859

250	BCIT_08033	349	2.29	8	extr=26	00295
251	BCIT_08058	220	1.82	4	extr=21	-
252	BCIT_08063	352	1.14	4	extr=26	-
253	BCIT_08101	329	0.3	1	extr=19	-
254	BCIT_08106	365	2.47	9	extr=25	-
255	BCIT_08110	403	1.24	5	extr=27	03022
256	BCIT_08253	563	1.78	10	extr=26	07519
257	BCIT_08280	223	1.79	4	extr=21	00188
258	BCIT_08308	371	3.23	12	extr=26	01822,11790
259	BCIT_08314	211	2.37	5	extr=26	01083
260	BCIT_08354	602	1.5	9	extr=26	09286
261	BCIT_08363	78	12.8	10	extr=26	-
262	BCIT_08370	284	1.76	5	extr=23	00332
263	BCIT_08372	636	0.31	2	extr=24	06964
264	BCIT_08393	384	1.04	4	extr=25	00026
265	BCIT_08414	153	2.61	4	extr=26	-
266	BCIT_08442	155	3.87	6	extr=25	-
267	BCIT_08544	522	4.6	24	extr=22	01822,09362
268	BCIT_08574	264	1.89	5	extr=27	08787
269	BCIT_08580	147	4.08	6	extr=25	-
270	BCIT_08585	487	4.52	22	extr=26	01822,09362
271	BCIT_08615	825	0.24	2	extr=26	-
272	BCIT_08635	189	2.12	4	extr=26	-
273	BCIT_08638	202	1.98	4	extr=25	-
274	BCIT_08658	403	0.99	4	extr=25	00246
275	BCIT_08692	199	3.02	6	extr=27	03443
276	BCIT_08735	132	3.79	5	extr=27	07249
277	BCIT_08748	476	0.84	4	extr=26	-
278	BCIT_08749	189	0.53	1	extr=18	-
279	BCIT_08751	189	0.53	1	extr=18	-
280	BCIT_08755	523	1.15	6	extr=27	00686,00723
281	BCIT_08757	584	1.71	10	extr=25	08450
282	BCIT_08801	685	0.29	2	extr=23	-
283	BCIT_08831	653	1.68	11	extr=25	00450
284	BCIT_08904	293	0.34	1	extr=26	-
285	BCIT_08911	37	2.7	1	extr=19	-
286	BCIT_08924	264	0.76	2	extr=25	00722
287	BCIT_08931	230	0.87	2	extr=24	11327
288	BCIT_08975	771	0.91	7	extr=26	-
289	BCIT_08989	438	2.28	10	extr=27	01341
290	BCIT_08990	392	3.06	12	extr=26	00150,00734
291	BCIT_09000	272	0	0	extr=23	00544
292	BCIT_09013	551	0.73	4	extr=26	00135
293	BCIT_09029	389	1.03	4	extr=21	00491
294	BCIT_09054	133	3.01	4	extr=26	-
295	BCIT_09084	122	6.56	8	extr=24	-
296	BCIT_09106	308	0.65	2	extr=24	-
297	BCIT_09121	563	1.24	7	extr=24	00135,07859
298	BCIT_09122	322	0	0	extr=21	-
299	BCIT_09146	789	1.52	12	extr=26	01522
300	BCIT_09180	336	2.38	8	extr=24	02102
301	BCIT_09190	613	1.14	7	extr=26	01565,08031
302	BCIT_09210	360	1.39	5	extr=25	00150
303	BCIT_09240	433	0.23	1	extr=25	00190,07883
304	BCIT_09364	414	0.72	3	extr=24	01328
305	BCIT_09391	518	0.58	3	extr=26	00135
306	BCIT_09495	490	2.04	10	extr=27	07519
307	BCIT_09564	526	1.33	7	extr=26	05577
308	BCIT_09565	393	1.02	4	extr=25	05577
309	BCIT_09594	303	1.65	5	extr=27	00188
310	BCIT_09613	315	0	0	extr=18	03345
311	BCIT_09644	538	1.12	6	extr=25	00135
312	BCIT_09656	494	0.4	2	extr=25	-
313	BCIT_09657	310	1.29	4	extr=21	-
314	BCIT_09694	527	1.33	7	extr=27	00135,07859
315	BCIT_09789	519	0.39	2	extr=19	-

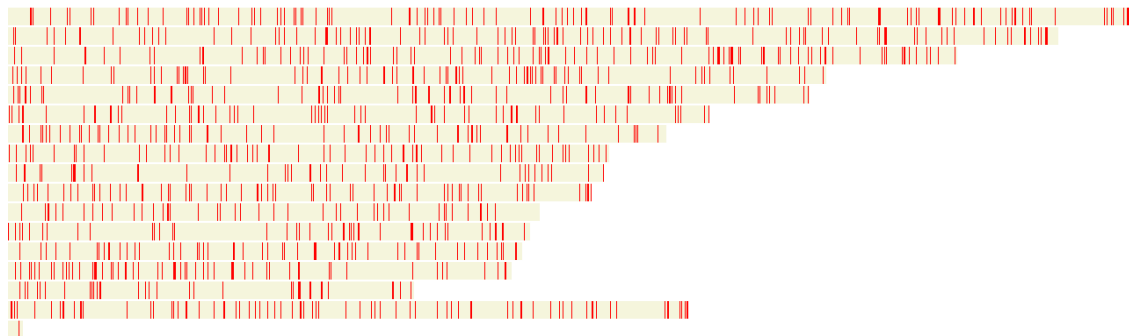
316	BCIT_09791	436	0.92	4	extr=27	-
317	BCIT_09803	291	1.37	4	extr=25	-
318	BCIT_09829	312	2.88	9	extr=25	-
319	BCIT_09883	399	1.5	6	extr=25	12697
320	BCIT_09892	341	2.93	10	extr=27	09792
321	BCIT_09968	140	5	7	extr=23	-
322	BCIT_09991	873	1.72	15	extr=24	-
323	BCIT_09997	575	1.04	6	extr=25	01425
324	BCIT_10075	363	0.83	3	extr=20	04909
325	BCIT_10091	493	1.22	6	extr=26	00135,07859
326	BCIT_10095	504	0.79	4	extr=26	13668
327	BCIT_10164	327	0.92	3	extr=22	00300
328	BCIT_10221	868	0.92	8	extr=26	00933,01915,14310
329	BCIT_10229	333	2.4	8	extr=23	03211
330	BCIT_10231	867	0.92	8	extr=27	00933,01915,14310
331	BCIT_10246	173	2.31	4	extr=26	-
332	BCIT_10247	493	0.41	2	extr=25	00251
333	BCIT_10306	223	1.79	4	extr=25	05630
334	BCIT_10322	301	1.33	4	extr=26	04616
335	BCIT_10329	648	1.54	10	extr=27	00394,07731,07732
336	BCIT_10341	447	0.22	1	extr=25	02156
337	BCIT_10379	369	3.25	12	extr=26	-
338	BCIT_10381	1147	1.39	16	extr=25	-
339	BCIT_10397	394	1.52	6	extr=26	-
340	BCIT_10445	70	4.29	3	extr=24	-
341	BCIT_10462	114	1.75	2	extr=20	-
342	BCIT_10466	429	2.33	10	extr=26	-
343	BCIT_10473	713	0.84	6	extr=26	-
344	BCIT_10475	392	1.53	6	extr=27	-
345	BCIT_10486	488	0.61	3	extr=25	-
346	BCIT_10695	310	2.58	8	extr=26	-
347	BCIT_10768	365	1.1	4	extr=26	00775
348	BCIT_10788	476	0	0	extr=26	00732,05199
349	BCIT_10789	302	0.66	2	extr=26	03664
350	BCIT_10791	298	2.68	8	extr=24	13933
351	BCIT_10797	498	0.6	3	extr=27	04616
352	BCIT_10827	694	0.43	3	extr=24	08760
353	BCIT_10861	95	4.21	4	extr=22	-
354	BCIT_10872	338	0.59	2	extr=25	12006
355	BCIT_10880	434	4.15	18	extr=26	00840
356	BCIT_11080	191	0	0	extr=24	-
357	BCIT_11115	438	0.91	4	extr=23	01055,13802
358	BCIT_11134	279	2.15	6	extr=24	01975
359	BCIT_11139	504	0.99	5	extr=24	13449
360	BCIT_11143	362	2.21	8	extr=27	00295
361	BCIT_11144	311	0.96	3	extr=26	01095
362	BCIT_11259	64	0	0	extr=18	-
363	BCIT_11266	571	1.23	7	extr=24	00394,07731,07732
364	BCIT_11288	365	0.82	3	extr=24	01156
365	BCIT_11302	309	0.32	1	extr=20	13668
366	BCIT_11306	487	1.64	8	extr=25	00328
367	BCIT_11403	95	9.47	9	extr=27	-
368	BCIT_11407	405	0.25	1	extr=25	00704
369	BCIT_11439	620	0.97	6	extr=27	00933,01915,14310
370	BCIT_11503	80	7.5	6	extr=22	-
371	BCIT_11556	638	1.1	7	extr=19	01565,08031
372	BCIT_11606	137	1.46	2	extr=26	-
373	BCIT_11690	367	2.18	8	extr=24	00544
374	BCIT_11698	340	2.94	10	extr=26	00445
375	BCIT_11751	434	1.84	8	extr=24	00328
376	BCIT_11795	263	1.52	4	extr=27	11937
377	BCIT_11826	387	3.62	14	extr=26	-
378	BCIT_11835	451	0.89	4	extr=25	00328
379	BCIT_11891	146	0.68	1	extr=26	-
380	BCIT_11898	275	1.82	5	extr=25	00332
381	BCIT_11909	392	3.06	12	extr=26	00295

382	BCIT_11941	201	2.49	5	extr=21	-
383	BCIT_12003	127	4.72	6	extr=21	-
384	BCIT_12117	562	0.89	5	extr=26	00732,05199
385	BCIT_12131	229	0	0	extr=25	03636
386	BCIT_12132	981	0.51	5	extr=25	03632,03636
387	BCIT_12138	558	0.36	2	extr=27	06964
388	BCIT_12139	523	0.76	4	extr=27	00135
389	BCIT_12145	618	0.81	5	extr=26	00754,09118
390	BCIT_12157	379	0.79	3	extr=22	00491
391	BCIT_12169	119	5.04	6	extr=23	-
392	BCIT_12171	340	1.76	6	extr=26	-
393	BCIT_12174	486	0.62	3	extr=24	05426
394	BCIT_12229	1132	0.62	7	extr=26	-
395	BCIT_12249	493	0.61	3	extr=26	00135
396	BCIT_12292	519	1.16	6	extr=22	-
397	BCIT_12343	916	0.55	5	extr=27	00082,06280
398	BCIT_12374	170	2.35	4	extr=26	-
399	BCIT_12379	277	5.05	14	extr=25	01083
400	BCIT_12449	414	1.21	5	extr=26	01328
401	BCIT_12450	371	0	0	extr=27	-
402	BCIT_12455	335	3.28	11	extr=26	-
403	BCIT_12478	397	1.26	5	extr=25	00150
404	BCIT_12517	364	1.65	6	extr=26	00544
405	BCIT_12522	671	2.09	14	extr=26	-
406	BCIT_12525	408	0.74	3	extr=27	01328
407	BCIT_12529	106	1.89	2	extr=21	-
408	BCIT_12537	486	1.03	5	extr=25	01565
409	BCIT_12619	294	2.04	6	extr=26	11327
410	BCIT_12627	452	2.43	11	extr=26	03856
411	BCIT_12680	212	1.42	3	extr=27	-
412	BCIT_12725	156	0	0	extr=18	12296
413	BCIT_12732	121	2.48	3	extr=18	-
414	BCIT_12747	86	9.3	8	extr=25	-
415	BCIT_12753	166	4.82	8	extr=24	-
416	BCIT_12766	157	1.27	2	extr=27	-
417	BCIT_12776	596	1.01	6	extr=26	09286
418	BCIT_12793	886	2.37	21	extr=27	-
419	BCIT_12859	975	0.82	8	extr=27	01055
420	BCIT_12867	169	1.78	3	extr=27	-
421	BCIT_12914	519	1.93	10	extr=26	01735
422	BCIT_12927	210	1.9	4	extr=26	-
423	BCIT_12931	161	1.24	2	extr=21	-
424	BCIT_12932	568	1.76	10	extr=26	07519
425	BCIT_13123	254	0	0	extr=27	00657,13472
426	BCIT_13137	438	2.05	9	extr=21	00295
427	BCIT_13139	305	1.64	5	extr=25	03443
428	BCIT_13153	1140	0.35	4	extr=27	-
429	BCIT_13158	307	0.98	3	extr=19	-
430	BCIT_13289	185	4.32	8	extr=25	-
431	BCIT_13367	148	1.35	2	extr=23	00295
432	BCIT_13386	590	0.51	3	extr=25	00732,05199
433	BCIT_13445	623	0.96	6	extr=24	-
434	BCIT_13543	341	0.59	2	extr=25	-
435	BCIT_13645	203	0	0	extr=23	00457
436	BCIT_13659	1110	4.23	47	extr=25	03659
437	BCIT_13714	407	1.97	8	extr=26	00135
438	BCIT_13815	548	1.82	10	extr=26	07519
439	BCIT_13846	30	0	0	extr=21	-
440	BCIT_13855	446	1.35	6	extr=26	-
441	BCIT_13862	335	4.48	15	extr=26	02015
442	BCIT_13879	68	11.8	8	extr=22	-
443	BCIT_13881	338	0.3	1	extr=25	-
444	BCIT_13903	565	1.42	8	extr=23	00884
445	BCIT_13938	366	0	0	extr=26	-
446	BCIT_13960	548	0.91	5	extr=27	00135,07859
447	BCIT_13970	409	2.44	10	extr=26	00295

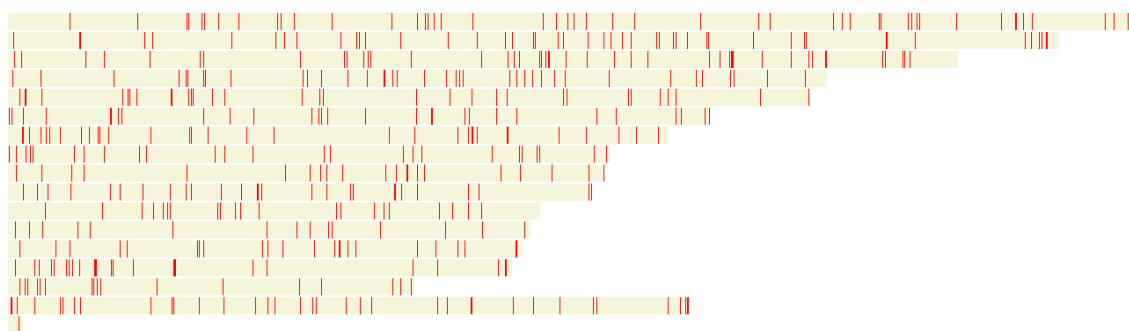
448	BC1T_14009	238	1.68	4	extr=25	-
449	BC1T_14012	659	0.76	5	extr=24	00732,05199
450	BC1T_14014	261	0	0	extr=24	-
451	BC1T_14030	515	2.72	14	extr=27	03198,07983
452	BC1T_14101	364	1.1	4	extr=26	00246
453	BC1T_14129	143	1.4	2	extr=27	-
454	BC1T_14136	68	2.94	2	extr=24	-
455	BC1T_14153	239	1.67	4	extr=25	01828
456	BC1T_14154	208	0	0	extr=24	-
457	BC1T_14164	852	0.94	8	extr=24	00933,01915,14310
458	BC1T_14177	504	1.39	7	extr=26	08031
459	BC1T_14299	330	2.12	7	extr=24	-
460	BC1T_14317	248	2.02	5	extr=26	00445
461	BC1T_14330	553	1.27	7	extr=26	00732,05199
462	BC1T_14348	181	0.55	1	extr=26	-
463	BC1T_14349	692	1.3	9	extr=25	00394,07731,07732
464	BC1T_14398	314	2.23	7	extr=24	01266
465	BC1T_14415	220	3.18	7	extr=24	01083
466	BC1T_14418	148	0	0	extr=20	-
467	BC1T_14469	394	2.54	10	extr=25	-
468	BC1T_14481	231	3.46	8	extr=26	-
469	BC1T_14501	208	1.92	4	extr=25	-
470	BC1T_14535	98	2.04	2	extr=23	-
471	BC1T_14570	432	0.46	2	extr=23	00388
472	BC1T_14591	444	1.8	8	extr=26	00450
473	BC1T_14698	554	1.44	8	extr=23	-
474	BC1T_14702	581	3.96	23	extr=23	00840
475	BC1T_14711	223	1.79	4	extr=26	11327
476	BC1T_14714	333	0.6	2	extr=22	00710
477	BC1T_14733	239	0	0	extr=26	-
478	BC1T_14944	399	2.01	8	extr=26	00704,00734
479	BC1T_14954	113	3.54	4	extr=23	03330
480	BC1T_14974	494	1.01	5	extr=25	00141
481	BC1T_14990	644	0.62	4	extr=26	00264
482	BC1T_15017	229	2.62	6	extr=21	03443
483	BC1T_15041	270	1.11	3	extr=24	10282
484	BC1T_15095	125	0	0	extr=23	-
485	BC1T_15118	381	2.1	8	extr=25	00295
486	BC1T_15341	105	1.9	2	extr=24	-
487	BC1T_15524	358	6.15	22	extr=27	-
488	BC1T_15542	175	2.29	4	extr=26	-
489	BC1T_15641	656	0.76	5	extr=25	00930
490	BC1T_15643	258	1.55	4	extr=24	02265
491	BC1T_15646	180	6.11	11	extr=19	-
492	BC1T_15663	672	0.3	2	extr=25	00326,05448
493	BC1T_15784	409	3.91	16	extr=26	03856
494	BC1T_15977	388	3.87	15	extr=24	-
495	BC1T_16006	189	0	0	extr=26	01161
496	BC1T_16107	76	13.2	10	extr=24	-
497	BC1T_16127	419	0.95	4	extr=25	00135
498	BC1T_16238	296	1.01	3	extr=26	-
499	BC1T_16413	58	1.72	1	extr=27	-

Appendix 3: Secretome sequence sets mapped across the *S. sclerotiorum* refined secretome.

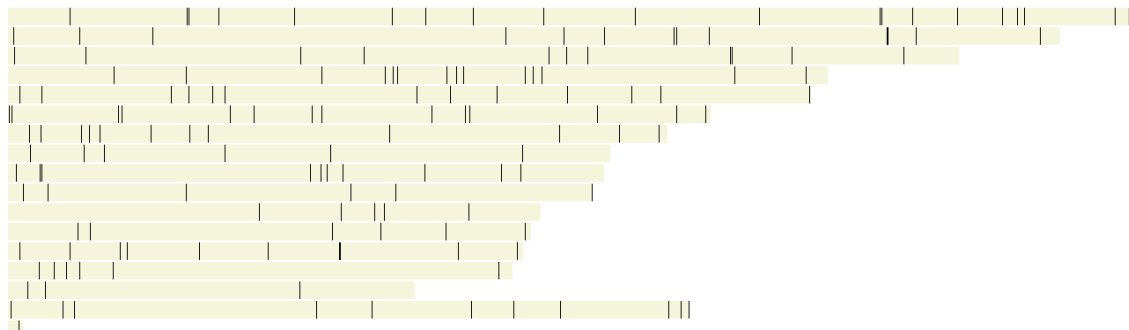
a) The secretome (1060 genes)



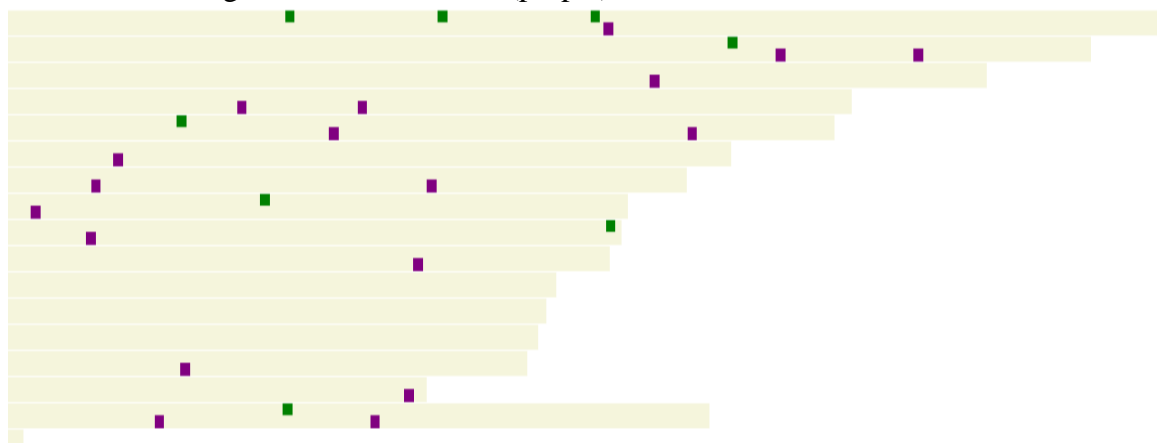
b) Refined secretome (432 genes):



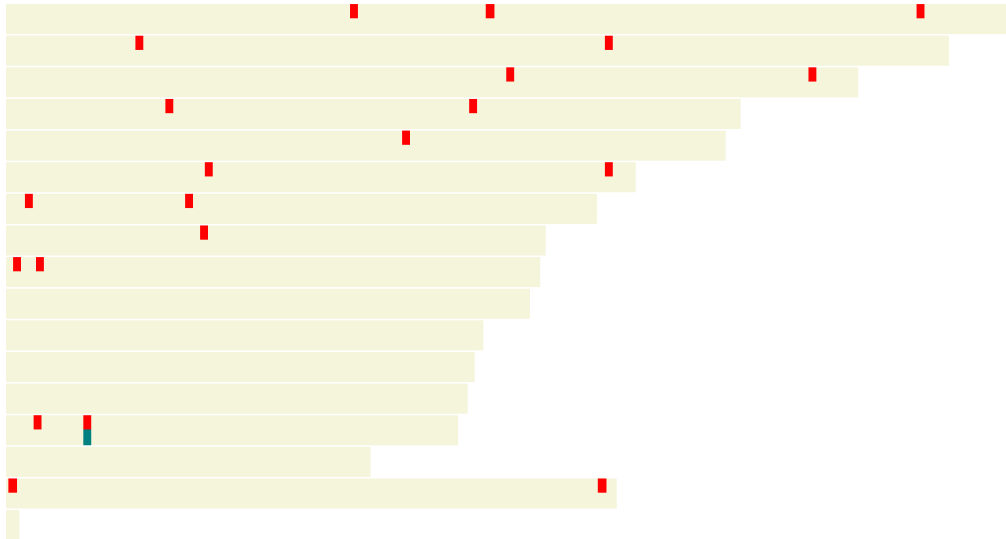
c) 122 unannotated sequences:



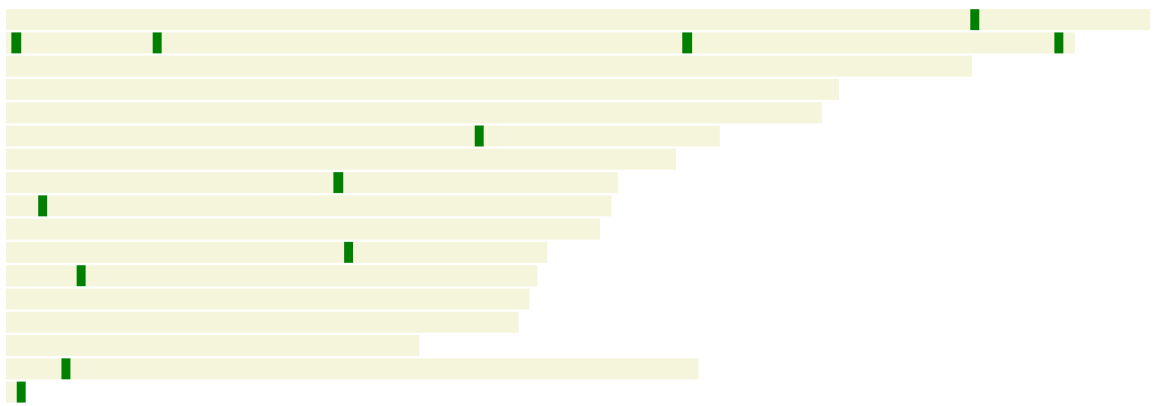
d) 8 secreted proteins with Y/F/WxC motifs (green) and 21 secreted proteins containing RxLR dEER motifs (purple).



- e) Small, cysteine rich proteins mapped across the *S.sclerotiorum* genome (red). No proteins were mapped onto the chromosome 10, 11, 12, 13 and 15. Hydrophobin domain protein SS1G_09248 mapped in blue.



- f) 12 Genes in the refined secretome unique only to *S.sclerotiorum*.



- g) Distribution of the 30 gene sequences found only in *S.sclerotiorum* and *B.cinerea*



Appendix 4.1: Plant polysaccharide degrading proteins

Gene No.	Gene ID	Interpro accession	Annotation	PFAM	Annotation from EST library in BROAD
1	SS1G_03602	IPR010720	Alpha-L-arabinofuranosidase, C-terminal	6964	alpha-N-arabinofuranosidase A precursor
2	SS1G_07661	IPR000675	Cutinase	1083	cutinase
3	SS1G_08104	IPR000675	Cutinase	1083	acetyl xylan esterase
4	SS1G_12907	IPR000675	Cutinase	1083	cutinase
5	SS1G_13386	IPR000675	Cutinase	1083	cutinase
6	SS1G_13809	IPR011613	GHF15	723	glucoamylase precursor
7	SS1G_07162	IPR002772	GHF3 C-terminal domain	1915	beta-glucosidase 1 precursor
8	SS1G_07847	IPR002772	GHF3 C-terminal domain	1915	beta-glucosidase 2 precursor
9	SS1G_09366	IPR002772	GHF3 C-terminal domain	1915	periplasmic beta-glucosidase precursor
10	SS1G_13255	IPR002772	GHF3 C-terminal domain	1915	beta-glucosidase 1 precursor
11	SS1G_00892	IPR016288	GHF6	1341	exoglucanase-6A precursor
12	SS1G_04541	IPR008902	GHF78	5592	hypothetical protein similar to alpha-L-rhamnosidase A
13	SS1G_13501	IPR008902	GHF78	5592	hypothetical protein similar to alpha-rhamnosidase
14	SS1G_04662	IPR000111	Glycoside hydrolase, clanGH-D	2065	alpha-galactosidase A precursor
15	SS1G_12191	IPR001000	GHF10	331	endo-1,4-beta-xylanase C precursor
16	SS1G_03618	IPR001137	GHF11	457	endo-1,4-beta-xylanase B precursor
17	SS1G_07749	IPR001137	GHF11	457	endo-1,4-beta-xylanase B
18	SS1G_10092	IPR001137	GHF11	457	endo-1,4-beta-xylanase B
19	SS1G_00501	IPR002594	GHF12	1670	endoglucanase A precursor
20	SS1G_02369	IPR002594	GHF12	1670	endoglucanase A precursor
21	SS1G_09250	IPR002594	GHF12	1670	hypothetical protein similar to iron-sulfur cluster-binding protein
22	SS1G_12024	IPR000490	GHF17	332	hypothetical protein similar to mannoprotein MP65
23	SS1G_12930	IPR000490	GHF17	332	glucan 1,3-beta-glucosidase precursor
24	SS1G_01009	IPR000743	GHF28	295	polygalacturonase precursor
25	SS1G_02399	IPR000743	GHF28	295	hypothetical protein similar to rhamnogalacturonan hydrolase
26	SS1G_02553	IPR000743	GHF28	295	hypothetical protein similar to exo-rhamnogalacturonase B
27	SS1G_03540	IPR000743	GHF28	295	hypothetical protein similar to exo-rhamnogalacturonase B
28	SS1G_04177	IPR000743	GHF28	295	polygalacturonase 5
29	SS1G_04207	IPR000743	GHF28	295	polygalacturonase precursor
30	SS1G_04552	IPR000743	GHF28	295	polygalacturonase precursor
31	SS1G_05832	IPR000743	GHF28	295	polygalacturonase precursor
32	SS1G_06235	IPR000743	GHF28	295	hypothetical protein similar to rhamnogalacturonase
33	SS1G_07039	IPR000743	GHF28	295	hypothetical protein similar to rhamnogalacturonan hydrolase
34	SS1G_08229	IPR000743	GHF28	295	hypothetical protein similar to rhamnogalacturonase A precursor
35	SS1G_08634	IPR000743	GHF28	295	exopolygalacturonase precursor
36	SS1G_10167	IPR000743	GHF28	295	polygalacturonase precursor
37	SS1G_10698	IPR000743	GHF28	295	polygalacturonase precursor
38	SS1G_11057	IPR000743	GHF28	295	polygalacturonase precursor
39	SS1G_12057	IPR000743	GHF28	295	polygalacturonase precursor
40	SS1G_14449	IPR000743	GHF28	295	exo-polygalacturonase
41	SS1G_01005	IPR000322	GHF31	1055	alpha-glucosidase precursor
42	SS1G_01083	IPR000322	GHF31	1055	alpha-glucosidase precursor
43	SS1G_02781	IPR001944	GHF35	1301	hypothetical protein similar to beta-galactosidase

44	SS1G_03647	IPR001944	GHF35		1301	hypothetical protein similar to beta-galactosidase
45	SS1G_10842	IPR001944	GHF35		1301	hypothetical protein similar to beta-galactosidase
46	SS1G_11922	IPR006710	GHF43		4616	hypothetical protein similar to endo-1,5-alpha-L-arabinase
47	SS1G_01828	IPR000334	GHF45		2015	endoglucanase-5
48	SS1G_13860	IPR000334	GHF45		2015	endoglucanase-5
49	SS1G_04468	IPR001382	GHF47		1532	hypothetical protein similar to mannosidase MsdS
50	SS1G_00458	IPR001547	GHF5		150	endoglucanase precursor
51	SS1G_00746	IPR001547	GHF5		150	hypothetical protein similar to mannanase
52	SS1G_00891	IPR001547	GHF5		150	hypothetical protein similar to endoglucanase III
53	SS1G_03387	IPR001547	GHF5		150	endoglucanase E precursor
54	SS1G_05775	IPR001547	GHF5		150	glucan 1,3-beta-glucosidase precursor
55	SS1G_06037	IPR001547	GHF5		150	glucan 1,3-beta-glucosidase precursor
56	SS1G_08208	IPR001547	GHF5		150	hypothetical protein similar to endo-beta-1,4-mannanase
57	SS1G_09365	IPR001547	GHF5		150	glucan 1,3-beta-glucosidase precursor
58	SS1G_09866	IPR001547	GHF5		150	hypothetical protein similar to beta-1,6-galactanase
59	SS1G_01838	IPR005103	GHF61		3443	hypothetical protein similar to endoglucanase IV precursor
60	SS1G_03041	IPR005103	GHF61		3443	hypothetical protein similar to Cel61b
61	SS1G_07656	IPR005103	GHF61		3443	conserved hypothetical protein
62	SS1G_08493	IPR005103	GHF61		3443	conserved hypothetical protein
63	SS1G_09251	IPR005103	GHF61		3443	hypothetical protein similar to endoglucanase II
64	SS1G_12059	IPR005103	GHF61		3443	hypothetical protein similar to endoglucanase B
65	SS1G_14160	IPR005103	GHF61		3443	hypothetical protein similar to endoglucanase IV
66	SS1G_05192	IPR005195	GHF65, catalytic	central	3632	hypothetical protein similar to glycosyl hydrolase family 65 protein
67	SS1G_02334	IPR001722	GHF7		840	exoglucanase I precursor
68	SS1G_04945	IPR001722	GHF7		840	exoglucanase I precursor
69	SS1G_09020	IPR001722	GHF7		840	exoglucanase I precursor
70	SS1G_02347	IPR005197	GHF71		3659	hypothetical protein similar to mutanase
71	SS1G_05784	IPR005197	GHF71		3659	hypothetical protein similar to alpha-1,3-glucanase
72	SS1G_09861	IPR005197	GHF71		3659	hypothetical protein similar to alpha-1,3-glucanase
73	SS1G_11765	IPR005197	GHF71		3659	hypothetical protein similar to mutanase
74	SS1G_04850	IPR005198	GHF76		3663	mannan endo-1,6-alpha-mannosidase DCW1 precursor
75	SS1G_10867	IPR005198	GHF76		3663	hypothetical protein similar to glycosyl hydrolase
76	SS1G_12937	IPR005198	GHF76		3663	hypothetical protein similar to glycosyl hydrolase
77	SS1G_14497	IPR005198	GHF76		3663	mannan endo-1,6-alpha-mannosidase DCW1 precursor
78	SS1G_11585	IPR011683	Glycosyl hydrolase family 53		7745	hypothetical protein similar to arabinogalactan endo-1,4-beta-galactosidase
79	SS1G_00505	IPR012939	Glycosyl hydrolase family 92		7971	conserved hypothetical protein
80	SS1G_02022	IPR012939	Glycosyl hydrolase family 92		7971	conserved hypothetical protein
81	SS1G_04200	IPR012939	Glycosyl hydrolase family 92		7971	hypothetical protein similar to alpha-1,2-mannosidase family protein
82	SS1G_01776	IPR006047	Glycosyl hydrolase, family 13, catalytic domain		128	alpha-amylase I precursor
83	SS1G_03385	IPR006047	Glycosyl hydrolase, family 13, catalytic domain		128	alpha-amylase precursor

84	SS1G_13472	IPR006047	Glycosyl hydrolase, family 13, catalytic domain	128	alpha-amylase A type-3 precursor
85	SS1G_02708	IPR001087	Lipase, GDSL	657	conserved hypothetical protein)
86	SS1G_03610	IPR001087	Lipase, GDSL	657	conserved hypothetical protein
87	SS1G_04095	IPR001087	Lipase, GDSL	657	rhamnogalacturonan acetylsterase precursor
88	SS1G_04592	IPR001087	Lipase, GDSL	657	conserved hypothetical protein)
89	SS1G_10482	IPR001087	Lipase, GDSL	657	conserved hypothetical protein
90	SS1G_14289	IPR001087	Lipase, GDSL	657	conserved hypothetical protein
91	SS1G_00040	IPR002022	Pectate lyase/Amb allergen	544	pectin lyase A precursor
92	SS1G_00238	IPR002022	Pectate lyase/Amb allergen	544	pectin lyase A precursor
93	SS1G_07942	IPR002022	Pectate lyase/Amb allergen	544	pectin lyase A precursor
94	SS1G_10071	IPR002022	Pectate lyase/Amb allergen	544	pectin lyase A precursor

GHF: Glycoside Hydrolase Family

Appendix 4.2: Lipid degrading proteins

	Gene ID	Interpro accession	Annotation	PFAM
1	SS1G_00877	IPR002018	Carboxylesterase, type B	00135
2	SS1G_01472	IPR002018	Carboxylesterase, type B	00135
3	SS1G_10875	IPR002018	Carboxylesterase, type B	00135
4	SS1G_11853	IPR002018	Carboxylesterase, type B	00135
5	SS1G_11930	IPR002018	Carboxylesterase, type B	00135
6	SS1G_13881	IPR002018	Carboxylesterase, type B	00135
7	SS1G_13982	IPR002018	Carboxylesterase, type B	00135
8	SS1G_14441	IPR002018	Carboxylesterase, type B	00135
9	SS1G_02708	IPR001087	Lipase, GDSL	00657
10	SS1G_03610	IPR001087	Lipase, GDSL	00657
11	SS1G_04095	IPR001087	Lipase, GDSL	00657
12	SS1G_04592	IPR001087	Lipase, GDSL	00657
13	SS1G_10482	IPR001087	Lipase, GDSL	00657
14	SS1G_14289	IPR001087	Lipase, GDSL	00657
15	SS1G_07661	IPR000675	Cutinase	01083
16	SS1G_08104	IPR000675	Cutinase	01083
17	SS1G_12907	IPR000675	Cutinase	01083
18	SS1G_13386	IPR000675	Cutinase	01083
19	SS1G_00332	IPR000070	Pectinesterase, catalytic	01095
20	SS1G_00468	IPR000070	Pectinesterase, catalytic	01095
21	SS1G_03286	IPR000070	Pectinesterase, catalytic	01095
22	SS1G_10165	IPR000070	Pectinesterase, catalytic	01095
23	SS1G_04030	IPR002642	Lysophospholipase, catalytic domain	01735
24	SS1G_04530	IPR002642	Lysophospholipase, catalytic domain	01735
25	SS1G_00233	IPR002921	Lipase, class 3	01764
26	SS1G_03160	IPR002921	Lipase, class 3	01764

27	SS1G_08644	IPR005152	Lipase, secreted	03583
28	SS1G_07639	IPR007312	Phosphoesterase	04185
29	SS1G_05493	IPR011118	Tannase/feruloyl esterase	07519
30	SS1G_08361	IPR011118	Tannase/feruloyl esterase	07519

Appendix 4.3: Protein degrading proteins

	Gene ID	Interpro accession	Annotation	PFAM
1	SS1G_00624	IPR001461	Peptidase A1	00026
2	SS1G_03181	IPR001461	Peptidase A1	00026
3	SS1G_03576	IPR001461	Peptidase A1	00026
4	SS1G_03629	IPR001461	Peptidase A1	00026
5	SS1G_03941	IPR001461	Peptidase A1	00026
6	SS1G_11366	IPR001461	Peptidase A1	00026
7	SS1G_03518	IPR000209	Peptidase S8/S53 domain	00082
8	SS1G_04958	IPR000209	Peptidase S8/S53 domain	00082
9	SS1G_07655	IPR000209	Peptidase S8/S53 domain	00082
10	SS1G_09060	IPR000209	Peptidase S8/S53 domain	00082
11	SS1G_09225	IPR000209	Peptidase S8/S53 domain	00082
12	SS1G_09268	IPR000209	Peptidase S8/S53 domain	00082
13	SS1G_12210	IPR000209	Peptidase S8/S53 domain	00082
14	SS1G_06534	IPR001254	Peptidase S1	00089
15	SS1G_11189	IPR000834	Peptidase M14, carboxypeptidase A	00246
16	SS1G_09909	IPR001375	Peptidase S9, prolyl oligopeptidase, catalytic domain	00326
17	SS1G_05449	IPR001563	Peptidase S10, serine carboxypeptidase	00450
18	SS1G_09475	IPR001563	Peptidase S10, serine carboxypeptidase	00450
19	SS1G_11382	IPR001563	Peptidase S10, serine carboxypeptidase	00450
20	SS1G_12413	IPR001563	Peptidase S10, serine carboxypeptidase	00450
21	SS1G_12499	IPR001563	Peptidase S10, serine carboxypeptidase	00450
22	SS1G_12500	IPR001563	Peptidase S10, serine carboxypeptidase	00450
23	SS1G_02038	IPR000250	Peptidase G1	01828
24	SS1G_07836	IPR000250	Peptidase G1	01828
25	SS1G_08858	IPR001384	Peptidase M35, deuterolysin	02102
26	SS1G_11189	IPR003146	Proteinase inhibitor, carboxypeptidase propeptide	02244
27	SS1G_12500	IPR008442	Propeptide, carboxypeptidase Y	05388
28	SS1G_03361	IPR008758	Peptidase S28	05577
29	SS1G_09060	IPR010435	Peptidase S8A, DUF1034 C-terminal	06280
30	SS1G_02857	IPR015366	Peptidase S53, propeptide	09286
31	SS1G_03518	IPR015366	Peptidase S53, propeptide	09286
32	SS1G_04958	IPR015366	Peptidase S53, propeptide	09286
33	SS1G_07268	IPR015366	Peptidase S53, propeptide	09286
34	SS1G_07655	IPR015366	Peptidase S53, propeptide	09286

35	SS1G_09225	IPR015366	Peptidase S53, propeptide	09286
36	SS1G_09268	IPR015366	Peptidase S53, propeptide	09286
37	SS1G_12210	IPR015366	Peptidase S53, propeptide	09286

Appendix 5: The proteomes used in the cross species comparison.

No.	Species name	Fasta file of proteome downloaded
1	Acremonium alcalophilum	Acral2_GeneCatalog_proteins_20110414.aa.fasta
2	Albugo laibachii	Albugo_laibachii.ENA1.16.pep.all.fasta
3	Alternaria brassicicola	Alternaria_brassicicola_proteins.fasta
4	Aspergillus Comparative	aspergillus_clavatus_1_proteins.fasta
5	Aspergillus Comparative	aspergillus_flavus_2_proteins.fasta
6	Aspergillus Comparative	aspergillus_fumigatus_1_proteins.fasta
7	Aspergillus Comparative	aspergillus_nidulans_fgsc_a4_1_proteins.fasta
8	Aspergillus Comparative	aspergillus_niger_1_proteins.fasta
9	Aspergillus Comparative	aspergillus_oryzae_1_proteins.fasta
10	Aspergillus Comparative	aspergillus_terreus_1_proteins.fasta
11	Aspergillus Comparative	Aspnid1_GeneCatalog_proteins_20110130.aa.fasta
12	Aspergillus niger	Aspergillus_niger_v3_FilteredModels_proteins.fasta
13	Aureobasidium pullulans	Aurpu2p4.representatives.fasta
14	Batrachochytrium dendrobatidis	batrachochytrium_dendrobatidis_1_proteins.fasta
15	Batrachochytrium dendrobatidis	Batde5_best_proteins.fasta
16	Baudoinia compniacensis	Baucol_GeneCatalog_proteins_20110511.aa.fasta
17	Bjerkandera adusta	Bjead1_1_GeneCatalog_proteins_20110614.aa.fasta
18	Blastomyces dermatitidis	blastomyces_dermatitidis_atcc_18188_1_proteins.fasta
19	Blastomyces dermatitidis	blastomyces_dermatitidis_er-3_1_proteins.fasta
20	Blastomyces dermatitidis	blastomyces_dermatitidis_slh14081_1_proteins.fasta
21	Blumeria graminis	bgh_dh14_v3.0_peptides.fasta
22	Botryosphaeria dothidea	Botdo1_GeneCatalog_proteins_20111003.aa.fasta
23	Botryotinia fuckeliana	Botryotinia_fuckeliana.BotFuc_Aug2005.16.pep.all.fasta
24	Botrytis cinerea	botrytis_cinerea_b05.10_1_proteins.fasta
25	Botrytis cinerea	botrytis_cinerea_b05.10_vankan_1_proteins.fasta
26	Botrytis cinerea	botrytis_cinerea_t4_1_proteins.fasta
27	Botrytis Cinerea	botrytis_cinerea_1_proteins.fasta
28	Botrytis cinerea	Botci1_GeneCatalog_proteins_20110903.aa.fasta
29	Caenorhabditis elegans	c_elegans_WS234_protein.fasta
30	Candida	candida_albicans_sc5314_assembly_21_1_proteins.fasta
31	Candida	candida_albicans_wo1_1_proteins.fasta
32	Candida	candida_guilliermondii_1_proteins.fasta
33	Candida	candida_lusitaniae_1_proteins.fasta
34	Candida	candida_parapsilosis_1_proteins.fasta
35	Candida	candida_tropicalis_3_proteins.fasta
36	Candida	debaryomyces_hansenii_1_proteins.fasta
37	Candida	lodderomyces_elongisporus_1_proteins.fasta
38	Candida Genome	C_dubliniensis_CD36_orf_trans_all.fasta
39	Candida Genome	C_glabrata_CBS138_version_s02-m01-r13_orf_trans_all.fasta
40	Cercospora zae-maydis	Cerzm1_GeneCatalog_proteins_20111029.aa.fasta
41	Chaetomium globosum	chaetomium_globosum_1_proteins.fasta
42	Chaetomium globosum	Chagl_1_GeneModels_BroadGeneModels_aa.fasta
43	Coccidioides group	coccidioides_immitis_h538.4_1_proteins.fasta
44	Coccidioides group	coccidioides_immitis_rmscc_2394_1_proteins.fasta
45	Coccidioides group	coccidioides_immitis_rmscc_3703_1_proteins.fasta
46	Coccidioides group	coccidioides_immitis_rs_3_proteins.fasta
47	Cochliobolus heterostrophus	CocheC4_1_GeneCatalog_proteins_20110824.aa.fasta
48	Cochliobolus heterostrophus	CocheC5_3_GeneCatalog_proteins_20110901.aa.fasta
49	Cochliobolus sativus	Cocsa1_GeneCatalog_proteins_20110610.aa.fasta
50	Colletotrichum	colletotrichum_graminicola_m1.001_1_proteins.fasta
51	Colletotrichum	colletotrichum_higginsianum_imi_349063_1_proteins.fasta
52	Coprinopsis cinerea	coprinopsis_cinerea_okayama7#130_3_proteins.fasta
53	Coprinopsis cinerea	laccaria_bicolor_s238n-h82_1_proteins.fasta
54	Cryphonectria parasitica	Cparasiticav2.GeneCatalog20091217.proteins.fasta
55	Cryptococcus neoformans var. grubii	Cryptococcus_neoformans_H99.proteins.fasta
56	Cryptococcus neoformans var. grubii	cryptococcus_neoformans_grubii_h99_2_proteins.fasta
57	Dermatophyte Comparative	microsporium_canis_cbs_113480_1_proteins.fasta
58	Dermatophyte Comparative	microsporium_gypseum_cbs_118893_1_proteins.fasta

59	Dermatophyte Comparative	trichophyton_equinum_cbs127.97_1_proteins.fasta
60	Dermatophyte Comparative	trichophyton_rubrum_cbs_118892_2_proteins.fasta
61	Dermatophyte Comparative	trichophyton_tonsurans_1_proteins.fasta
62	Dothistroma septosporum	Dotse1_GeneCatalog_proteins_20100818.aa.fasta
63	Drosophila melanogaster	dmel-all-translation-r5_48.fasta
64	Fomitiporia mediterranea	Fomme1_GeneCatalog_proteins_20101122.aa.fasta
65	Fusarium Comparative	fusarium_graminearum_ph-1_3_proteins.fasta
66	Fusarium Comparative	fusarium_oxysporum_f_sp_lycopersici_4287_2_proteins.fasta
67	Fusarium Comparative	fusarium_verticillioides_7600_3_proteins.fasta
68	Fusarium graminearum	Fusgr1_GeneCatalog_proteins_20110524.aa.fasta
69	Fusarium oxysporum	Fusox1_GeneCatalog_proteins_20110522.aa.fasta
70	Fusarium solani Nectria haematococca	Necha2_best_proteins.fasta
71	Geomyces destructans	geomyces_destructans_20631-21_1_proteins.fasta
72	Histoplasma capsulatum	histoplasma_capsulatum_g186ar_2_proteins.fasta
73	Histoplasma capsulatum	histoplasma_capsulatum_h143_2_proteins.fasta
74	Histoplasma capsulatum	histoplasma_capsulatum_h88_2_proteins.fasta
75	Histoplasma capsulatum	histoplasma_capsulatum_nam1_1_proteins.fasta
76	Hyaloperonospora arabidopsidis	Hyaloperonospora_arabidopsidis.HyaAraEmoy2_2.0.16.pep.all.fasta
77	Hysterium pulicare	Hyspu1_GeneCatalog_proteins_20110209.aa.fasta
78	Laccaria bicolor	Lacbi2_GeneCatalog_proteins_20110203.aa.fasta
79	Leptosphaeria maculans	Lepmu1_GeneCatalog_proteins_20110301.aa.fasta
80	Magnaporthe comparative	gaemannomyces_graminis_var_tritici_r3-111a-1_1_proteins.fasta
81	Magnaporthe comparative	magnaporthe_oryzae_70-15_8_proteins.fasta
82	Magnaporthe comparative	magnaporthe_poae_atcc_64411_1_proteins.fasta
83	Magnaporthe grisea	magnaporthe_grisea_m_oryzae_70-15_6_proteins.fasta
84	Magnaporthe grisea	Maggr1_GeneCatalog_proteins_20110524.aa.fasta
85	Melampsora laricis-populina	Mlaricis_populina.FrozenGeneCatalog_20110215.proteins.fasta
86	Meloidogyne hapla	Meloidogyne_hapla.fasta
87	Meloidogyne incognita	Meloidogyne_incognita.fasta
88	Mucor circinelloides	Mucor_circinelloides_v2_filtered_proteins.fasta
89	Mycosphaerella fijiensis	Mfijiensis_v2.FrozenGeneCatalog_20100402.proteins.fasta
90	Mycosphaerella graminicola	Mgraminiclav2.FilteredModels1.proteins.fasta
91	Mycosphaerella graminicola	Mgraminiclav2.FrozenGeneCatalog20080910.proteins.fasta
92	Myzus persicae	aphibase_2.1_pep_with_product.fasta
93	Neurospora crassa	neurospora_crassa_or74a_finished_10_proteins.fasta
94	Neurospora crassa	Neurospora_crassa.proteins.fasta
95	Neurospora discreta	Ndiscreta.FilteredModels2.proteins.fasta
96	Neurospora tetrasperma	N.tetrasperma_matA_v2_FilteredModels.proteins.fasta
97	Neurospora tetrasperma	Ntetrasperma_mata.FilteredModels1.proteins.fasta
98	Origins of Multicellularity	allomyces_macrognus_atcc_38327_3_proteins.fasta
99	Origins of Multicellularity	spizellomyces_punctatus_daom_br117_1_proteins.fasta
100	Paracoccidioides brasiliensis	paracoccidioides_brasiliensis_pb01_1_proteins.fasta
101	Paracoccidioides brasiliensis	paracoccidioides_brasiliensis_pb03_1_proteins.fasta
102	Paracoccidioides brasiliensis	paracoccidioides_brasiliensis_pb18_1_proteins.fasta
103	Penicillium chrysogenum	Pench1_GeneCatalog_proteins_20120123.aa.fasta
104	Phanerochaete chrysosporium	BestModels2.1.proteins.fasta
105	Phytophthora infestans	Phytophthora_infestans.ASM14294v1.16.pep.all.fasta
106	Phytophthora infestans	phytophthora_infestans_t30-4_1_proteins.fasta
107	Phytophthora ramorum	Phytophthora_ramorum.ASM14973v1.16.pep.all.fasta
108	Phytophthora sojae	Phytophthora_sojae.ASM14975v1.16.pep.all.fasta
109	Puccinia graminis	Puccinia_graminis.proteins.fasta
110	Puccinia Group	puccinia_graminis_f_sp_tritici_2_proteins.fasta
111	Puccinia Group	puccinia_triticina_1-1_bbbd_race_1_1_proteins.fasta
112	Punctularia strigosozonata	Punst1_GeneCatalog_proteins_20101026.aa.fasta
113	Pyrenophora teres f. teres	Pyrrt1_GeneCatalog_proteins_20110408.aa.fasta
114	Pyrenophora tritici-repentis	Pyrenophora_tritici_repentis_proteins.fasta
115	Pyrenophora tritici-repentis	pyrenophora_tritici-repentis_1_proteins.fasta
116	Pythium ultimum	Pythium_ultimum.pug.16.pep.all.fasta
117	Rhizopus oryzae	rhizopus_oryzae_3_proteins.fasta
118	Rhytidhysterium rufulum	Rhyru1_GeneCatalog_proteins_20110209.aa.fasta
119	Saccharomyces cerevisiae	saccharomyces_cerevisiae_rm11-1a_1_proteins.fasta
120	Schizosaccharomyces group	schizosaccharomyces_cryophilus_oy26_3_proteins.fasta
121	Schizosaccharomyces group	schizosaccharomyces_japonicus_yfs275_4_proteins.fasta
122	Schizosaccharomyces group	schizosaccharomyces_octosporus_5_proteins.fasta

123	Schizosaccharomyces group	schizosaccharomyces_pombe_972h-_2_proteins.fasta
124	Sclerotinia sclerotiorum	Sclerotinia_sclerotiorum.ASM14694v1.16.pep.all.fasta
125	Sclerotinia sclerotiorum	sclerotinia_sclerotiorum_2_proteins.fasta
126	Sclerotinia sclerotiorum	Scpsc1_GeneCatalog_proteins_20110903.aa.fasta
127	Septoria musiva	Sepmu1_GeneCatalog_proteins_20100915.aa.fasta
128	Septoria populiicola	Seppo1_GeneCatalog_proteins_20110720.aa.fasta
129	Serpula lacrymans	Serpula_lacrymans_S7_3_v2.proteins.fasta
130	Serpula lacrymans	SerlaS7_9_2_GeneCatalog_proteins_20110916.aa.fasta
131	Setosphaeria turcica	Settu1_GeneCatalog_proteins_20110305.aa.fasta
132	Sporisorium reilianum	Sreilianum_prot.fasta
133	Sporotrichum thermophile	Spoth2_GeneCatalog_proteins_20101221.aa.fasta
134	Stagonospora nodorum	phaeosphaeria_nodorum_1_proteins.fasta
135	Stagonospora nodorum	Stano2_GeneCatalog_proteins_20110506.aa.fasta
136	Thielavia terrestris	Thite2_GeneCatalog_proteins_20101221.aa.fasta
137	Trametes versicolor	Trave1_GeneCatalog_proteins_20101111.aa.fasta
138	Trichoderma asperellum	Trias1_GeneCatalog_proteins_20120305.aa.fasta
139	Trichoderma atroviride	Tatroviridev2_FrozenGeneCatalog_20100319.proteins.fasta
140	Trichoderma citrinoviride	Trici1_GeneCatalog_proteins_20120925.aa.fasta
141	Trichoderma harzianum	Triha1_GeneCatalog_proteins_20120306.aa.fasta
142	Trichoderma longibrachiatum	Trilo1_GeneCatalog_proteins_20120926.aa.fasta
143	Trichoderma reesei	TriREUTC30_1_GeneCatalog_proteins_20110526.aa.fasta
144	Trichoderma reesei	TreeseiV2_FilteredModelsv2.0.proteins.fasta
145	Trichoderma reesei	TreeseiV2_FrozenGeneCatalog20081022.proteins.fasta
146	Trichoderma virens	Tvirens_v2.FrozenGeneCatalog_20100318.proteins.fasta
147	Tuber melanosporum from Genoscope	Tubme1_GeneCatalog_proteins_20111120.aa.fasta
148	Uncinocarpus reesii	uncinocarpus_reesii_2_proteins.fasta
149	Ustilago maydis	Ustilago_maydis.proteins.fasta
150	Ustilago maydis	ustilago_maydis_1_proteins.fasta
151	Verticillium dahliae	Verda1_GeneCatalog_proteins_20110524.aa.fasta
152	Verticillium group	verticillium_albo-atrum_vams.102_1_proteins.fasta
153	Verticillium group	verticillium_dahliae_vdls.17_1_proteins.fasta
154	Wolfiporia cocos	Wolco1_GeneCatalog_proteins_20100915.aa.fasta

Appendix 6: The cross species comparison between the 432 protein sequences in the *S. sclerotiorum* refined secretome and the homologous

No. of genes in common with Ss secretome (e-100)	No. of genes in common with Ss secretome (e-5)	Species name	King	Phylum	Class	Lifestyle	Oxalate producer	Host species	No of plant hosts	No seqs in genome
369	433	<i>Sclerotinia sclerotiorum</i>	Fung	Asco	Leotio	Plant path	OA	Non Cereal Monocot /Dicot	Many	14503
369	433	<i>Sclerotinia sclerotiorum</i>	Fung	Asco	Leotio	Plant path	OA	Non Cereal Monocot /Dicot	Many	
269	399	<i>Botrytis cinerea</i>	Fung	Asco	Leotio	Plant path	OA	Non Cereal Monocot /Dicot	Many	
261	399	<i>Botryotinia fuckeliana</i>	Fung	Asco	Leotio	Plant path	OA	Non Cereal Monocot /Dicot	Many	
261	399	<i>Botrytis cinerea</i>	Fung	Asco	Leotio	Plant path	OA	Non Cereal Monocot /Dicot	Many	
261	399	<i>Botrytis cinerea</i>	Fung	Asco	Leotio	Plant path	OA	Non Cereal Monocot /Dicot	Many	16448
261	399	<i>Botrytis cinerea</i>	Fung	Asco	Leotio	Plant path	OA	Non Cereal Monocot /Dicot	Many	14998
267	398	<i>Botrytis cinerea</i>	Fung	Asco	Leotio	Plant path	OA	Non Cereal Monocot /Dicot	Many	
282	387	<i>Sclerotinia sclerotiorum</i>	Fung	Asco	Leotio	Plant path	OA	Non Cereal Monocot /Dicot	Many	5131
140	331	<i>Botryosphaeria dothidea</i>	Fung	Asco	Doth	Plant path		Dicot	Woody species	9555
113	323	<i>Colletotrichum graminicola</i>	Fung	Asco	Sord	Plant path	OA	Dicot	Many	12250
84	321	<i>Alternaria brassicicola</i>	Fung	Asco	Doth	Plant path		Dicot	Many	10688
134	319	<i>Hysterium pulicare</i>	Fung	Asco	Doth	Saprophytic			Woody species	9251
103	318	<i>Colletotrichum higginsianum</i>	Fung	Asco	Sord	Plant path		Cereal Monocot/ Dicot	Few	12006
101	317	<i>Cochliobolus heterostrophus</i>	Fung	Asco	Doth	Plant path		Cereal Monocot/ Dicot	Few	9910
100	317	<i>Cochliobolus heterostrophus</i>	Fung	Asco	Doth	Plant path		Cereal Monocot/ Dicot	Many	12720
103	317	<i>Pyrenophora teres</i>	Fung	Asco	Doth	Plant path		Cereal Monocot	Few	11538
95	316	<i>Stagonospora nodorum</i>	Fung	Asco	Doth	Plant path		Monocot	Many	9110
95	316	<i>Stagonospora nodorum</i>	Fung	Asco	Doth	Plant path		Monocot	Many	12379
93	316	<i>Cochliobolus sativus</i>	Fung	Asco	Doth	Plant path		Monocot	Many	13336
98	315	<i>Setosphaeria turcica</i>	Fung	Asco	Doth	Plant path		Cereal Monocot	Few	16257
95	313	<i>Fusarium oxysporum</i>	Fung	Asco	Sord	Plant path/ animal path	OA	Monocot/Dicot	Many	13322
95	313	<i>Fusarium oxysporum</i>	Fung	Asco	Sord	Plant path/ animal path	OA	Dicot	Many	17701
84	310	<i>Leptosphaeria maculans</i>	Fung	Asco	Doth	Plant path		Dicot	Many	23132
134	310	<i>Cryphonectria parasitica</i>	Fung	Asco	Sord	Plant path		Dicot - Tree	Many	13342
98	308	<i>Pyrenophora tritici-repentis</i>	Fung	Asco	Doth	Plant path		Cereal Monocot	Many	12169
118	308	<i>Rhizidhysterium rufulum</i>	Fung	Asco	Doth	Saprophytic /Plant path	OA		Many	17459
115	308	<i>Aspergillus flavus</i>	Fung	Asco	Euro	Saprophytic	/	OA	Many	12587

						animal path				
98	308	<i>Pyrenophora tritici-repentis</i>	Fung	Asco	Doth	Plant path		Cereal Monocot	Many	11799
95	308	<i>Fusarium verticillioides</i>	Fung	Asco	Sord	Plant path		Cereal Monocot/Dicot	Many	17708
89	307	<i>Gaeumannomyces graminis</i>	Fung	Asco	Sord	Plant Path		Cereal Monocot	Many	
86	306	<i>Magnaporthe grisea</i>	Fung	Asco	Sord	Plant path		Monocot	Many	5799
86	306	<i>Magnaporthe grisea</i>	Fung	Asco	Sord	Plant path		Monocot	Many	11054
92	305	<i>Fusarium solani</i>	Fung	Asco	Sord	Plant path		Dicot	Many	
90	304	<i>Fusarium graminearum</i>	Fung	Asco	Sord	Plant path		Cereal Monocot	Few	13321
90	304	<i>Fusarium graminearum</i>	Fung	Asco	Sord	Plant path		Monocot/Dicot	Many	11333
82	303	<i>Verticillium dahliae</i>	Fung	Asco	Sord	Plant path		Dicot	Many	10535
82	303	<i>Verticillium dahliae</i>	Fung	Asco	Sord	Plant path		Dicot	Many	10220
85	302	<i>Magnaporthe oryzae</i>	Fung	Asco	Sord	Plant path		Cereal Monocot	Few	11054
114	302	<i>Aspergillus oryzae</i>	Fung	Asco	Euro	Saprophytic			Many	
89	300	<i>Cercospora zea-maydis</i>	Fung	Asco	Doth	Plant path		Cereal Monocot	Few	6258
108	298	<i>Aspergillus terreus</i>	Fung	Asco	Euro	Saprophytic animal path	/		Many	12063
115	297	<i>Aspergillus fumigatus</i>	Fung	Asco	Euro	Saprophytic animal path	/	OA	Many	9887
106	296	<i>Penicillium chrysogenum</i>	Fung	Asco	Euro	Saprophytic				
67	296	<i>verticillium albo-atrum</i>	Fung	Asco	Sord	Plant path		Dicot	Many	6522
121	295	<i>Aspergillus niger</i>	Fung	Asco	Euro	Saprophytic animal path	/	OA		8592
107	292	<i>Aspergillus nidulans</i>	Fung	Asco	Euro	Saprophytic				10560
106	292	<i>Aspergillus nidulans</i>	Fung	Asco	Euro	Saprophytic				10406
82	292	<i>Chaetomium globosum</i>	Fung	Asco	Sord	Saprophytic animal path	/			12020
82	292	<i>Chaetomium globosum</i>	Fung	Asco	Sord	Saprophytic animal path	/			11124
99	290	<i>Mycosphaerella fijiensis</i>	Fung	Asco	Doth	Plant path		Dicot	Few	8907
76	289	<i>Neurospora crassa</i>	Fung	Asco	Sord	Saprophytic				15707
76	289	<i>Neurospora crassa</i>	Fung	Asco	Sord	Saprophytic				9907
95	288	<i>Dothistroma septosporum</i>	Fung	Asco	Doth	Plant path		Dicot	One (pine species)	6312
75	287	<i>Neurospora tetrasperma</i>	Fung	Asco	Sord	Saprophytic				10380
75	287	<i>Neurospora tetrasperma</i>	Fung	Asco	Sord	Saprophytic				9948
68	287	<i>Magnaporthe poae</i>	Fung	Asco	Sord	Plant path		Cereal Monocot	Few	12991
89	286	<i>Trichoderma virens</i>	Fung	Asco	Sord	Saprophytic animal path	/			9143
92	285	<i>Trichoderma atroviride</i>	Fung	Asco	Sord	Saprophytic				9813
92	285	<i>Trichoderma asperellum</i>	Fung	Asco	Sord	Saprophytic				
90	284	<i>Trichoderma harzianum</i>	Fung	Asco	Sord	Saprophytic				
87	283	<i>Mycosphaerella graminicola</i>	Fung	Asco	Doth	Plant path		Cereal Monocot	Few	13107
87	283	<i>Mycosphaerella graminicola</i>	Fung	Asco	Doth	Plant path		Cereal Monocot	Few	10933

72	279	<i>Neurospora discreta</i>	Fung	Asco	Sord	Saprophytic				9907
92	279	<i>Thielavia terrestris</i>	Fung	Asco	Sord	Saprophytic				12380
77	275	<i>Sporotrichum thermophile</i>	Fung	Asco	Sord	Saprophytic				8804
82	274	<i>Aspergillus clavatus</i>	Fung	Asco	Euro	Saprophytic / animal path	OA		Many	9120
78	274	<i>Trichoderma reesei</i>	Fung	Asco	Sord	Saprophytic				9852
78	274	<i>Trichoderma reesei</i>	Fung	Asco	Sord	Saprophytic				9129
90	272	<i>Septoria musiva</i>	Fung	Asco	Doth	Plant path		Dicot	Few	14503
80	272	<i>Trichoderma reesei</i>	Fung	Asco	Sord	Saprophytic				11863
92	267	<i>Septoria populicola</i>	Fung	Asco	Doth	Plant path		Dicot	Few	10233
99	267	<i>Aspergillus niger</i>	Fung	Asco	Euro	Saprophytic / animal path / plant path				10680
78	266	<i>Trichoderma citrinoviride</i>	Fung	Asco	Sord	Saprophytic				
96	263	<i>Baudoinia compniacensis</i>	Fung	Asco	Doth	Saprophytic				8732
75	262	<i>Trichoderma longibrachiatum</i>	Fung	Asco	Sord	Saprophytic				
51	262	<i>Punctularia strigosozonata</i>	Fung	Basid	Agaric	Saprophytic				11630
36	255	<i>Serpula lacrymans</i>	Fung	Basid	Agaric	Saprophytic				9739
36	255	<i>Serpula lacrymans</i>	Fung	Basid	Agaric	Saprophytic				14495
52	242	<i>Trametes versicolor</i>	Fung	Basid	Agaric	Saprophytic				
43	240	<i>Bjerkandera adusta</i>	Fung	Basidio	Agarico	Plant patho		Dicot	Many (Woody species)	
55	240	<i>Acremonium alcalophilum</i>	Fung	Asco	Sord	Saprophytic				9521
42	235	<i>Phanerochaete chrysosporium</i>	Fung	Basid	Agaric	Saprophytic				
48	232	<i>Fomitiporia mediterranea</i>	Fung	Basid	Agaric	Saprophytic			Few	12580
24	229	<i>Coprinopsis cinerea</i>	Fung	Basid	Agaric	Saprophytic				
52	224	<i>Geomyces destructans</i>	Fung	Asco	Leotiomyces	Animal path				
40	215	<i>Wolfiporia cocos</i>	Fung	Basid	Agaric	Saprophytic				10535
29	213	<i>Laccaria bicolor</i>	Fung	Basid	Agaric	Plant mutualist		Ectomycorrhizal		18204
35	212	<i>Tuber melanosporum</i>	Fung	Asco	Peziz	Plant mutualist		Dicot	Few	8521
28	209	<i>Coprinopsis cinerea</i>	Fung	Basid	Agaric	Saprophytic				16150
133	208	<i>Aureobasidium pullulans</i>	Fung	Asco	Doth	Saprophytic / animal path			Many	
47	201	<i>Blastomyces dermatitidis</i>	Fung	Asco	Asco	Saprophytic / animal path			Mammals	10513
20	200	<i>Melampsora laricis-populina</i>	Fung	Basidio	Urediniomycetes	Plant path (rust)		Dicot (poplar)	Few	
20	198	<i>Sporisorium reilianum</i>	Fung	Basidio	Microbotryomycetes	Plant Path		Cereal Monocot	Few	

43	196	<i>Blastomyces dermatitidis</i>	Fung	Asco	Asco	Animal path				9522
46	195	<i>Blastomyces dermatitidis</i>	Fung	Asco	Asco	Saprophytic animal path	/			10089
41	186	<i>Coccidioides immitis</i>	Fung	Asco	Euas	Saprophytic animal path	/			10463
39	186	<i>Coccidioides immitis</i>	Fung	Asco	Euas	Saprophytic animal path	/			10593
42	185	<i>Uncinocarpus reesii</i>	Fung	Asco	Euro	Saprophytic				7496
20	185	<i>Ustilago maydis</i>	Fung	Basid	Ustil	Plant path		Cereal Monocot	Few	7798
20	185	<i>Ustilago maydis</i>	Fung	Basid	Ustil	Plant path		Cereal Monocot	Few	6522
55	183	<i>Blumeria graminis</i>	Fung	Asco	Leotio	Plant path		Cereal Monocot	One (wheat with some grasses)	
23	182	<i>Puccinia graminis</i>	Fung	Basid	Pucc	Plant path		Cereal Monocot	Few	20534
40	181	<i>Paracoccidioides brasiliensis</i>	Fung	Asco	Euro	Saprophytic animal path	/			9136
45	181	<i>Histoplasma capsulatum</i>	Fung	Asco	Asco	Saprophytic animal path	/			14650
31	180	<i>Coccidioides immitis</i>	Fung	Asco	Euas	Saprophytic animal path	/			10408
38	180	<i>Paracoccidioides brasiliensis</i>	Fung	Asco	Euro	Saprophytic animal path	/			11192
34	178	<i>Coccidioides immitis</i>	Fung	Asco	Euas	Saprophytic animal path	/		Few	11124
41	178	<i>Histoplasma capsulatum</i>	Fung	Asco	Asco	Saprophytic animal path	/			9428
38	177	<i>Paracoccidioides brasiliensis</i>	Fung	Asco	Euro	Saprophytic animal path	/			7876
45	176	<i>Histoplasma capsulatum</i>	Fung	Asco	Asco	Saprophytic animal path	/			9233
22	175	<i>Puccinia graminis</i>	Fung	Basid	Pucc	Plant path		Cereal Monocot	Many	18140
41	173	<i>Trichophyton equinum</i>	Fung	Asco	Euro	Saprophytic				
42	172	<i>Microsporum canis</i>	Fung	Asco	Euro	Saprophytic animal path	/			
47	171	<i>Microsporum gypseum</i>	Fung	Asco	Euro	Saprophytic animal path	/			
43	171	<i>Trichophyton rubrum</i>	Fung	Asco	Euro	Saprophytic				
41	171	<i>Trichophyton tonsurans</i>	Fung	Asco	Euro	Saprophytic				
42	171	<i>Histoplasma capsulatum</i>	Fung	Asco	Asco	Saprophytic animal path	/			9532
14	170	<i>Puccinia triticina</i>	Fung	Basid	Pucc	Plant path				15979
7	155	<i>Phytophthora ramorum</i>	Chromal	Heterokontophyta	Oomycota	Plant Path		Dicot	Many	
6	154	<i>Phytophthora sojae</i>	Chromal	Heterokontophyta	Oomycota	Plant Path		Dicot (soy and lupins)	Few	

4	152	<i>Phytophthora infestans</i>	Chromal	Heterokontophyta	Oomycota	Plant path		Dicot	Many	8741
4	152	<i>Phytophthora infestans</i>	Chromal	Heterokontophyta	Oomycota	Plant path		Dicot	Many	8741
9	138	<i>Spizellomyces punctatus</i>	Fung	Chytrid	Chytrid	Saprophytic				
10	134	<i>Cryptococcus neoformans</i>	Fung	Basid	Agaric	Saprophytic animal path	/			11609
10	134	<i>Cryptococcus neoformans</i>	Fung	Basid	Agaric	Saprophytic animal path	/			6967
7	131	<i>Rhizopus oryzae</i>	Fung	Mucor		Saprophytic				12169
4	128	<i>Hyaloperonospora arabidopsidis</i>	Eukary	Heterokontanophyta	Oomycete	Plant Pathogen		Dicot	One (arabidopsis)	
6	127	<i>Pythium ultimum</i>	Chromal veolata	Heterokontophyta	Oomycota	Plant path		Cereal Monocot-Dicot	Many	
9	125	<i>Mucor circinelloides</i>	Fung	Zygo	Zygo	Plant path		Dicot	Few	
10	103	<i>Debaryomyces hansenii</i> (<i>Candida famata</i>)	Fung	Asco	Sacc	Saprophytic animal path	/			
3	99	<i>Albugo laibachii</i>	Chrom	Heterokontophyta	Oomycete	Plant path		Dicot	one (arabidopsis)	
4	94	<i>Candida guilliermondii</i>	Fung	Asco	Sacc	Saprophytic animal path	/			5235
11	88	<i>Candida dubliniensis</i>	Fung	Asco	Sacc	Saprophytic animal path	/			
5	87	<i>Candida tropicalis</i>	Fung	Asco	Sacc	Saprophytic animal path	/			5733
0	87	<i>Allomyces macrogynus</i>	Fung	Blasto	Blasto	saprophytic				
8	85	<i>Candida parapsilosis</i>	Fung	Asco	Sacc	Saprophytic animal path	/			5941
4	85	<i>Saccharomyces cerevisiae</i>	Fung	Asco	Sacc	Saprophytic				12117
9	84	<i>Candida albicans</i>	Fung	Asco	Sacc	Saprophytic animal path	/			16447
9	84	<i>Candida albicans</i>	Fung	Asco	Sacc	Saprophytic animal path	/			6017
6	84	<i>Candida lusitanae</i>	Fung	Asco	Sacc	Saprophytic animal path	/			5920
2	81	<i>Batrachochytrium dendrobatidis</i>	Fung	Chytrid	Chytrid	Saprophytic animal path	/		Many amphibians	11197
0	80	<i>Myzus persicae</i>	Animalia	Arthropoda	Insecta	Plant Pest		Dicot	Many	
5	77	<i>Candida (lodderomyces elongisporus)</i>	Fung	Asco	Sacc	Saprophytic animal path	/			
1	76	<i>Batrachochytrium dendrobatidis</i>	Fung	Chytrid	Chytrid	Saprophytic animal path	/			8818
5	76	<i>Schizosaccharomyces pombe</i>	Fung	Asco	Schiz	Saprophytic				4924
0	74	<i>Drosophila melanogaster</i>	Animalia	Arthropoda	Insecta	Plant Pest		Dicot (fruit)	Many	
0	71	<i>Caenorhabditis elegans</i>	Animal	Nematoda	Chromador	Bacterial				

					ea	pathogen			
6	69	<i>Schizosaccharomyces japonicus</i>	Fung	Asco	Schiz	Saprophytic			5178
6	64	<i>Schizosaccharomyces cryophilus</i>	Fung	Asco	Schiz	Saprophytic			5381
6	64	<i>Schizosaccharomyces octosporus</i>	Fung	Asco	Schiz	Saprophytic			4868
4	61	<i>Candida glabrata</i>	Fung	Asco	Sacc	Saprophytic / animal path			
0	58	<i>Meloidogyne incognita</i>	Animalia	Nemat		Plant path			13072
0	55	<i>Meloidogyne hapla</i>	Animalia	Nemat		Plant path			12329

Appendix 7: Field Trials results 2011.

Comparison between the presence of *S. sclerotiorum* DNA obtained from Burkard 7 day traps and the presence of OA in medium incubated field samples. 0= no detection , 1= positive detection.

Date	Spectrophotometer OA event	Ss DNA	Date	Spectrophotometer OA event	Ss DNA
7.4.2011	0	0	19.5.2011	0	1
8.4.2011	0	0	20.5.2011	1	1
9.4.2011	0	1	21.5.2011	0	1
10.4.11	0	1	22.5.2011	1	1
11.4.2011	0	1	23.5.2011	0	1
12.4.2011	0	1	24.5.2011	0	1
13.4.2011	0	1	25.5.2011	0	1
14.4.2011	0	1	26.5.2011	0	1
15.4.2011	0	1	27.5.2011	0	1
16.4.2011	0	0	28.5.2011	0	1
17.4.2011	0	0	29.5.2011	0	1
18.4.2011	1	0	30.5.2011	0	1
19.4.2011	0	1	31.5.2011	0	1
20.4.2011	0	1	1.6.2011	0	1
21.4.2011	0	0	2.6.2011	0	1
22.4.2011	0	0	3.6.2011	0	1
23.4.2011	0	1	4.6.2011	0	1
24.4.2011	0	0	5.6.2011	0	1
25.4.2011	0	0	6.6.2011	0	1
26.4.2011	0	0	7.6.2011	1	1
27.4.2011	1	0	8.6.2011	0	1
28.4.2011	0	0	9.6.2011	0	1
29.4.2011	0	0	10.6.2011	0	1
30.4.2011	0	0	11.6.2011	0	1
1.5.2011	0	0	12.6.2011	0	1
2.5.2011	0	0	13.6.2011	0	1
3.5.2011	0	0	14.6.2011	0	-
4.5.2011	0	0	15.6.2011	1	-
5.5.2011	0	0	16.6.2011	0	-
6.5.2011	1	0	17.6.2011	0	-
7.5.2011	0	1	18.6.2011	0	-
8.5.2011	0	0	19.6.2011	1	-
9.5.2011	0	1	20.6.2011	0	-
10.5.2011	0	1	21.06.2011	0	-
11.5.2011	1	1	22.06.2011	0	1
12.5.2011	0	0	23.06.2011	0	1
13.5.2011	0	1	24.06.2011	0	1

14.5.2011	0	1	25.06.2011	0	1
15.5.2011	0	1	26.06.2011	0	1
16.5.2011	0	0	27.06.2011	0	1
17.5.2011	0	1	28.06.2011	0	1
18.5.2011	0	1			

Appendix 8: Field Trial results 2012.

Comparison between the presence of *S. sclerotiorum* DNA obtained from Burkard 7 day traps and detection of OA in medium incubated field samples using electrochemical and spectrophotometer methods of detection. 0= no detection , 1= positive detection.

Date	HRP Electrode	PB electrode	Spectrophotometer	Ss DNA
04/04/2012	0	0	0	1
05/04/2012	0	0	0	0
06/04/2012	0	0	0	1
07/04/2012	0	0	0	1
08/04/2012	0	0	0	1
09/04/2012	0	0	0	1
10/04/2012	1	1	0	1
11/04/2012	0	0	0	1
12/04/2012	0	0	0	1
13/04/2012	0	0	0	1
14/04/2012	0	0	0	1
15/04/2012	0	0	0	1
16/04/2012	0	0	0	1
17/04/2012	1	1	0	1
18/04/2012	0	0	0	1
19/04/2012	0	0	0	1
20/04/2012	0	0	0	1
21/04/2012	0	0	0	1
22/04/2012	0	0	0	1
23/04/2012	0	0	0	0
24/04/2012	1	0	0	1
25/04/2012	1	0	0	1
26/04/2012	0	0	0	1
27/04/2012	0	0	0	1
28/04/2012	1	0	0	1
29/04/2012	1	0	0	1
30/04/2012	1	1	1	0
01/05/2012	0	0	0	1
02/05/2012	0	0	0	0
03/05/2012	1	1	0	1
04/05/2012	1	1	1	1
05/05/2012	0	0	0	1
06/05/2012	1	1	1	1
07/05/2012			1	1
08/05/2012	1	1	1	1
09/05/2012	1	1	1	1
10/05/2012	1	1	1	1
11/05/2012	1	1	1	1
12/05/2012	1	1	1	1
14/05/2012	1	1	1	1
15/05/2012	1	1	1	1
16/05/2012	1	1	1	1
17/05/2012	1	1	1	1

18/05/2012	1	1	1	1
19/05/2012	1	1	1	1
20/05/2012	0	0	0	1
21/05/2012	1	1	1	1
22/05/2012	0	0	1	1
23/05/2012	1	1	1	1
24/05/2012	1	1	1	1
25/05/2012	1	1	1	1
27/05/2012	1	1	1	1
28/05/2012	0	0	1	1
29/05/2012	0	0	0	1
30/05/2012	1	1	1	1
31/05/2012	0	0	1	1
01/06/2012	0	0	1	1
06/06/2012	1	1	0	1